MONASH University

The Association Between Epicardial Adipose Tissue and Coronary Plaque Characteristics: Insights from Computed Tomography Coronary Angiography

DR NITESH NERLEKAR

MBBS (Hons), MPH, FRACP

A thesis submitted for the degree of *Doctor of Philosophy* at
Monash University in 2018.

Monash Cardiovascular Research Centre, Department of Medicine, School of Clinical Sciences at Monash, Faculty of Medicine, Nursing & Health Science

Copyright notice

Notice 1

Notice 2

© Nitesh Nerlekar (2018).

I certify that I have made all reasonable efforts to secure copyright permissions for third-party content included in this thesis and have not knowingly added copyright content to my work without the owner's permission.

TABLE OF CONTENTS

ABBREVIATIONS

ACS	Acute Coronary Syndrome
BMI	Body Mass Index
CP	Calcified Plaque
CTCA	Computed Tomography Coronary Angiography
CE	Contrast Enhanced
CACS	Coronary Artery Calcium Score
CAD	Coronary Artery Disease
DD	Diastolic Dysfunction
EAT	Epicardial Adipose Tissue
EATd	Epicardial Adipose Tissue Density
EATt	Epicardial Adipose Tissue Thickness
EATv	Epicardial Adipose Tissue Volume
FFA	Free Fatty Acids
HR	Hazard Ratio
HRP	High-Risk Plaque
HU	Hounsfield Units
IVUS	Intravascular Ultrasound
LV	Left Ventricle
LoA	Limits Of Agreement
LAP	Low Attenuation Plaque
MRI	Magnetic Resonance Imaging
MACE	Major Adverse Cardiovascular Events
NCT	Non-Contrast CT
NCP	Non-Calcified Plaque
OR	Odds Ratio
OCT	Optical Coherence Tomography
PCAT	Pericoronary Adipose Tissue
PVAT	Perivascular Adipose Tissue
SAT	Subcutaneous Adipose Tissue
TCFA	Thin-capped Fibroatheroma
TTE	Transthoracic Echocardiography
VAT	Visceral Adipose Tissue

ABSTRACT

Coronary artery disease (CAD) remains the largest single cause of death in Australia. Atherosclerosis is the underlying mechanism that leads to CAD and has a dynamic, complex pathophysiology often regarded as a chronic inflammatory disorder. Atherosclerosis results in the formation of plaques within the arterial wall. These plaques often remain clinically silent until a surface rupture or endothelial erosion occurs that results in thrombus formation and potential luminal occlusion. This manifestation of CAD is referred to as an acute coronary syndrome (ACS) which is the most hazardous presentation of CAD. There are certain features within coronary plaques that are thought to portend future ACS and may represent part of the spectrum of CAD, although it remains uncertain what potentiates these high-risk plaques. Intracoronary imaging techniques have allowed characterisation of these plaques but is prohibitive for routine application in patients due to their invasive nature. The use of non-invasive imaging methods such as computed tomography coronary angiography (CTCA) has emerged as a feasible and useful method to evaluate coronary plaque with low risk. Burgeoning development in automated software allows CTCA to visualise and quantify coronary plaque characteristics and composition with good correlation to invasive methods.

There is growing interest that obesity may influence plaque vulnerability due to a recognised association with adiposity and inflammation. Obesity is most often regarded as an elevation in the body mass index (BMI), a simple bedside calculation. Commonly used cardiac risk models, such as the Framingham Risk Score, include the components of age, hypertension, cholesterol levels, diabetes and smoking. However, elevated BMI and its surrogate markers are not included. This may stem from the concept of the obesity paradox, whereby some studies have suggested a protective effect of elevated BMI for future prognosis. However, BMI misclassifies true body fat percentage and may not be representative of dysfunctional adipose tissue. There are high levels of pro-inflammatory adipokines inherent in adipose tissue which are also implicated in atherosclerosis. Epicardial adipose tissue (EAT) surrounds the myocardium and coronary arteries and may, through vasocrine or paracrine signalling, result in atherosclerotic plaque modulation. EAT is only modestly correlated with BMI and therefore may be the suitable culprit linking ‘obesity’ and atherosclerosis.

In this thesis, our aims were to assess the use of CTCA to feasibly assess EAT, and its association with coronary artery plaque characteristics and composition.

The introductory chapter of this thesis covers a broad outline of the epidemiologic impact of obesity and its controversial association with cardiovascular disease. This builds the hypothesis that EAT as a visceral adipose tissue store unique to the heart, has prime pathogenic potential for CAD and cardiac dysfunction. We also discuss the current lack of standardisation of EAT measurement methods and their respective limitations, as well as the current understanding of cardiac disease associations with EAT. A portion of this extensive literature review will be submitted for consideration as a review article.

Chapter 2 and 3 are meta-analyses specific to the association between EAT and firstly high-risk plaque features, and secondly cardiovascular structure and function. This allows a comprehensive understanding of the current evidence pertaining to the widespread effects of EAT both at a coronary and structural level. We demonstrate that EAT is significantly associated with high-risk plaque characteristics, although is better demonstrated only when full-volume EAT is measured compared to a linear thickness measure on echocardiography. We therefore evaluated the effects of volumetric CT studies and their association with myocardial parameters and report that there is a definite association with increased EAT and diastolic dysfunction, a moderate effect on chamber geometry but little effect on systolic function. In Chapter 4, we present a complex meta-analysis looking at qualitative plaque characterisation and its association with prognosis. This importantly describes that there is a clear spectrum of coronary plaque with increasing risk based on composition with qualitative high-risk plaques and non-calcified plaques presenting the greatest risk, and calcified plaques potentially describing a more quiescent coronary tree.

In chapter 5 and 6 we describe original methodologic studies of EAT measurement. In chapter 5 we described patients undergoing transthoracic linear thickness measurements of EAT compared to complete volumetric EAT on CT and confirm significant superiority and feasibility of EAT measures by CT which should remain the preferred imaging strategy. In chapter 6, we review inter-vendor and inter-scan comparisons of CT to assess software differences and influence of CT scan parameters (contrast vs. non-contrast) on the EAT volume and

density results. This allowed us to understand which software platform is reproducible and reliable to therefore be employed for all our other prospective studies.

In chapter 7 we present results of the natural history of EAT in a long-term cohort of patients with non-obstructive coronary disease. This identified that EAT volume and density significantly increase and decrease respectively at approximately 5-year follow-up and no other cardiac risk factors appear to have an influence on the change in EAT, in particular BMI. This demonstrates that EAT is a potential independent factor and given its association with cardiac disease, may not simply be a surrogate for risk.

In chapter 8, we present the results of a cross-sectional study evaluating EAT volume and density and the association with high risk plaque features, both qualitatively and quantitatively. This was performed in patients with non-obstructive disease which represent the majority of patients undergoing CTCA. We demonstrate that EAT volume, but not density is significantly, independently associated with quantified high-risk plaque features of necrotic-core and fibrofatty plaque volumes, but not with more stable phenotypes of fibrous and calcified plaque. This lends to the association that EAT may influence the dynamic nature of atherosclerotic plaque.

Finally, we present our future directions whereby we plan to investigate the peri-coronary adipose tissue attenuation, a novel potential imaging biomarker of vascular inflammation to further refine association with coronary plaque and dysfunctional adipose tissue.

In conclusion, we have demonstrated that EAT may be an independent risk factor for cardiac disease that is not modulated by other cardiovascular risk factors. It is reliably and preferably measured using full volumetric CT imaging rather than echocardiography and there is a clear relationship between EAT and high-risk plaque parameters, qualitatively and quantitatively. Therefore, it may be the culprit linking adiposity, inflammation and cardiovascular disease rather than BMI, and represents a potential novel therapeutic target.

Declaration

This declaration is to be included in a standard thesis. Students should reproduce this section in their thesis verbatim.

This thesis contains no material which has been accepted for the award of any other degree or diploma at any university or equivalent institution and that, to the best of my knowledge and belief, this thesis contains no material previously published or written by another person, except where due reference is made in the text of the thesis.

Signature:

Print Name:

Date:

PUBLICATIONS DURING CANDIDATURE

Publications directly related to thesis: completed and published

1. NERLEKAR N, Brown AJ, Muthalaly RG, Talman A, Hettige T, Cameron JD, Wong DTL;
   The Association of Epicardial Adipose Tissue and High Risk Plaque Characteristics: A Systematic Review and Meta-Analysis;
   Journal of the American Heart Association 2017 Aug 23;(6)8

2. NERLEKAR N, Muthalaly RG, Wong NC, Thakur U, Wong DT, Brown AJ, Marwick TH
   Association of Volumetric Epicardial Adipose Tissue Quantification and Cardiac Structure and Function
   Journal of the American Heart Association 2018; Nov 21

3. NERLEKAR N, Ha FJ, Cheshire C, Rashid H, Cameron JD, Wong DT, Seneviratne S, Brown AJ.
   Computed Tomographic Coronary Angiography-Derived Plaque Characteristics Predict Major Adverse Cardiovascular Events.
   Circulation: Cardiovascular Imaging. 2018 Jan;11(1):e006973

4. NERLEKAR N, Baey YW, Brown AJ, Muthalaly RG, Dey D, Tamarapoo B, Cameron JD, Marwick TH, Wong DTL;
   Poor Correlation, Reproducibility, and Agreement Between Volumetric vs. Linear Epicardial Adipose Tissue Measurement: A 3D Computed Tomography vs. 2D Echocardiography Comparison.
   JACC Cardiovascular Imaging 2018; Jul;11(7)1035-1036

Publications directly related to thesis: submitted and under review

5. NERLEKAR N, Thakur U, Muthalaly RG, Talman A, Dey D, Brown AJ, Wu AIY, Seneviratne SK, Cameron JD, Wong DT;
   Inter-software and Inter-scan Variability in Measurement of Epicardial Adipose Tissue: A Three-way Comparison of a Research specific, A Freeware and a Coronary Application Software Platform.
   Submitted to **Radiology**

6. NERLEKAR N, Thakur U, Koh S, Lin A, Potter E, Muthalaly RG, Rashid H, Cameron JD, Dey D, Wong DT;
   The Natural History of Epicardial Adipose Tissue Volume and Attenuation: A Long-term Prospective Cohort Follow Up Study
   Submitted to **Nature Scientific Reports**

7. NERLEKAR N, Thakur U, Koh S, Lin A, Potter E, Muthalaly RG, Ihdayhid AR, Cameron JD, Dey D, Wong DT;
   Epicardial Adipose Tissue Volume but not Density is associated with High Risk Plaque Composition on Coronary Computed Tomography Angiography in patients with non-obstructive coronary artery disease
   Submitted to **Cardiovascular Diabetology**

Publications completed during candidature not directly related to thesis

8. NERLEKAR N, Ha FJ, Verma KP, Bennett MR, Cameron JD, Meredith IT, Brown AJ;
   Percutaneous Coronary Intervention Using Drug-Eluting Stents versus Coronary Artery Bypass Grafting for Unprotected Left Main Coronary Artery Stenosis- A Meta-Analysis of Randomised Trials;
   Circulation: Cardiovascular Interventions 2016 Dec;9(12)

9. NERLEKAR N, Cheshire CJ, Verma KP, Ihdayhid AR, McCormick LM, Cameron JD, Bennett MR, Malaiapan Y, Meredith IT, Brown AJ;
   Intravascular Ultrasound Guidance improves clinical outcomes during implantation of both first and second-generation drug-eluting stents.
   Eurointervention 2017 Jan; 12(**13**): 1632-42

10. NERLEKAR N, Ko BS, Nasis A, Cameron JD, Leung M, Brown AJ, Wong DTL, Ngu PJ, Troupis JM, Seneviratne SK;
    Impact of Heart Rate on diagnostic accuracy of second generation 320-detector computed tomography coronary angiography.
    Cardiovasc Diagn Therapy 2017 Jun;7(3):296-304

11. NERLEKAR N, Mulley W, Rehmani H, Ramkumar S, Cheng K, Vasanthakumar SA, Rashid H, Barton T, Nasis A, Meredith IT, Moir S, Mottram PM.
Feasibility of Exercise Stress Echocardiography for Cardiac Risk Assessment in Chronic Kidney Disease Patients Prior To Renal Transplantation.
Clinical Transplantation 2016 Oct;30(10):1209-1215

12. NERLEKAR N, Harper RW; *Canakinumab for Atherosclerotic Disease.*
The New England Journal of Medicine 2018 Jan 11;378(2):199

13. NERLEKAR N, Peverill RE; *Confusion regarding the meaning of the term left ventricular filling pressure given the non-equivalence of left ventricular end-diastolic pressure and mean left atrial pressure*
American Heart Journal 2017; Feb;196

14. NERLEKAR N, Nasis A
CT Coronary Angiography in Kidney Transplant Candidates.
JACC: **Cardiovascular Imaging** 2016 Mar;9(3):328-9

15. NERLEKAR N, Narayan O, Sapontis J, Stokes M, Vasanthakumar SA, Mottram PM, Harper RW. *Percutaneous closure of three atrial septal defects with three interleaved atrial septal occluders in an adult patient.*
International Journal of Cardiology. 2016 Apr 15;209:7-8.

16. Muthalaly R, NERLEKAR N, Kwong R, Nasis A
Magnetic Resonance Imaging in patients with cardiac implantable electronic devices
Radiology 2018: Nov;289(2):281-292

17. Mirzaee S, Thein OM, Nogic J, NERLEKAR N, Nasis A, Brown AJ
The effect of combined ezetimibe and statin therapy versus statin therapy alone on coronary plaque volume assessed by intravascular ultrasound
J Clin Lipidol 2018; Sept-Oct; 12(5):1133-1140

18. Ihdayhid AR, Sakaguchi T, Linde JJ, Sorgaard MH, Kofoed KF, Fujisawa Y, Hislop-Jambrich J, NERLEKAR N, Cameron JD, Munnur RK, Crosset M, Wong DT, Seneviratne SK, Ko BS
Performance of computer tomography-derived fractional flow reserve using reduced-order modelling and static computed tomography stress myocardial perfusion imaging for detection of haemodynamically significant coronary stenosis
Eur Heart J Cardiovasc Imaging 2018; Nov 1;19(11):1234-1243

19. Munnur RK, Cameron JD, McCormick LM, Psaltis PJ, NERLEKAR N, Ko BS, Meredith IT, Seneviratne SK, Wong DTL
Diagnostic accuracy of ASLA Score, a novel CT angiographic index, and aggregate plaque volume in the assessment of functional significance of coronary stenosis
International Journal of Cardiology 2018; Nov 1;270:343-348

20. Nogic J, Baey YW, NERLEKAR N, Ha FJ, Cameron JD, Nasis A, West NEJ, Brown AJ
Polymer-free versus permanent polymer coated drug eluting stents for the treatment of coronary artery disease
Journal of Interventional Cardiology 2018; Oct;31(5):608-616

21. Koshy AN, Sajeev JK, NERLEKAR N, Brown AJ, Rajakariar K, Zureik M, Wong MC, Roberts L, Street M, Cooke J, The AW
International Journal of Cardiology 2018; Sep 1;266:124-127

22. Koshy AN, Sajeev JK, NERLEKAR N, Brown AJ, Rajakariar K, Zureik M, Wong MC, Roberts L, Street M, Cooke J, Teh AW
Use of photoplethysmography for heart rate estimation among inpatients
Internal Medicine Journal 2018; May;48(587-591)

23. Ha FJ, Nogic J, Montone RA, Cameron JD, NERLEKAR N, Brown AJ.
Drug eluting versus bare metal stents for percutaneous coronary intervention of saphenous vein graft lesions.
Cardiovasc Revasc Med 2018 Apr 3

24. Rashid HN, Gooley RP, NERLEKAR N, Ihdayhid AR, McCormick LM, Nasis A, Cameron JD, Brown AJ.
Bioprosthetic aortic valve leaflet thrombosis detected by multidetector computed tomography is associated with adverse cerebrovascular events: a meta-analysis of observational studies.
EuroIntervention. **2017** Dec 12

25. Rashid HN, McCormick LM, Talman AH, Ihdayhid AR, NERLEKAR N, Amiruddin AS, Cameron J, Nasis A, Meredith IT, Gooley RP.
Effect of aorto-ventricular angulation on procedural success in transcatheter aortic valve replacements with the Lotus Valve system.
Catheter Cardiovasc Intervention. **2017** Dec 6

26. Ha FJ, NERLEKAR N, Cameron JD, Bennett MR, Meredith IT, West NE, Brown AJ;
Midterm Safety and Efficacy of ABSORB Bioresorbable Vascular Scaffold versus Everolimus Eluting Metallic Stent: An Updated Meta-analysis.
JACC Cardiovascular Intervention 2017 Feb 13;10(3):308-310

27. Muthalaly RG, NERLEKAR N, Wong DT, Cameron JD, Seneviratne SK, Ko BS;
Epicardial adipose tissue and myocardial ischemia as detected by computed tomography perfusion imaging and invasive fractional flow reserve.
Journal of Cardiovasc Computed Tomography 2017 Jan-Feb;11(1):46-53

28. Tung MK, Ramkumar S, Cameron JD, Pang B, NERLEKAR N, Kotschet E, Alison J;
Retrospective Cohort Study Examining Reduced Intensity and Duration of Anticoagulation and Antiplatelet Therapy following Left Atrial Appendage Occlusion with the WATCHMAN device.
Heart Lung Circ 2017 May;26(5):477-485

29. Brown AJ, Teng Z, Calvert PA, Rajani NK, Hennessy O, NERLEKAR N, Obaid DR, Costopoulos C, Huang Y, Hoole SP, Goddard M, West NE, Gillard JH, Bennett MR.
Plaque Structural Stress Estimations Improve Prediction of Future Major Adverse Cardiovascular Events After Intracoronary Imaging.
Circulation: Cardiovascular Imaging 2016 Jun;9(6).

30. Nogic J, NERLEKAR N, Nasis A.
Anomalous Coronary Arteries on Computer Tomography Angiography: A Pictorial Review.
Current Cardiovascular Imaging Reports 2017; 10(35)

31. Nogic J, McCormick LM, Francis R, NERLEKAR N, Jaworski C, West NEJ, Brown AJ.
Novel bioabsorbable polymer and polymer-free metallic drug-eluting stents.
Journal of Cardiology 2018; In Press.

32. Ha FJ, Giblett JP, NERLEKAR N, Cameron JD, Meredith IT, West NEJ, Brown AJ.
Optical Coherence Tomography Guided Percutaneous Coronary Intervention.
Heart Lung Circulation 2017 Aug 4:

33. Stokes MB, NERLEKAR N, Moir S, Teo KS.
The evolving role of cardiac magnetic resonance imaging in the assessment of cardiovascular disease.
Australian Family Physician 2016 Oct;45(10):761-764

34. Munnur RK, NERLEKAR N, Wong DT.
Imaging of coronary atherosclerosis in various susceptible groups.
Cardiovascular Diagnosis and Therapy 2016 Aug;6(4):382-95

35. Wald A, Cochrane A, Blecher G, NERLEKAR, B.
Windsock in the heart.
Emerg Med Australas. 2017 Nov 17

36. Muthalaly RG, NERLEKAR N, Brown AJ;
Percutaneous coronary intervention for stable angina in ORBITA
The Lancet 2018 Jul 7;392(10141):25-26

AWARDS AND SCHOLARSHIPS DURING CANDIDATURE

Post-graduate Scholarship – combined National Health and Medical Research Council and National Heart Foundation (NHMRC/NHF): 2016-2018

Clinical Academic Scholarship Award, Monash Health: 2016-2018

American College of Cardiology and Cardiac Society of Australia and New Zealand travelling fellowship award: 2017

Winner – Monash Translational Research: Best Presentation: 2017

Winner – School of Clinical Sciences and Monash University: 3-Minute Thesis Best Presentation 2017

Thesis including published works declaration

I hereby declare that this thesis contains no material which has been accepted for the award of any other degree or diploma at any university or equivalent institution and that, to the best of my knowledge and belief, this thesis contains no material previously published or written by another person, except where due reference is made in the text of the thesis.

This thesis includes *4* original papers published in peer reviewed journals and *3* submitted publications. The core theme of the thesis is *the association of epicardial adipose tissue and coronary plaque characteristics.* The ideas, development and writing up of all the papers in the thesis were the principal responsibility of myself, the student, working within the *Monash Cardiovascular Research Centre* under the supervision of *Associate Professor Dennis Wong.*

The inclusion of co-authors reflects the fact that the work came from active collaboration between researchers and acknowledges input into team-based research.

In the case of *chapters 1-8* my contribution to the work involved the following:

Thesis Chapter	**Publication Title**	**Status** *(published, in press, accepted or returned for revision, submitted)*	**Nature and % of student contribution**	**Co-author name(s) Nature and % of Co-author's contribution***	**Co-author(s), Monash student Y/N***
2	***Epicardial Adipose Tissue and High Risk Coronary Plaque***	Accepted	80%. Concept and collecting data, statistical analysis, manuscript writing	All authors provided input to manuscript through either data collection, mansucript review and editing totalling 20% of contribution 1) Adam J Brown 2) Rahul G Muthalaly 3) Andrew Talman 4) Thushan Hettige 5) James D Cameron 6) Dennis T Wong	Yes
3	***Association of Volumetric Epicardial Adipose Tissue Quantification and Cardiac Structure and Function***	Accepted	70%. Concept and collecting data, statistical analysis, manuscript writing	All authors provided input to manuscript through either data collection, mansucript review and editing totalling 30% of contribution 1) Rahul G Muthalaly 2) Nathan Wong 3) Udit Thakur 4) Dennis T Wong 5) Adam J Brown 6) Thomas H Marwick	Yes
4	***Computed Tompographic Coronary Angiography Derived Plaque Characteristics Predict Major Adverse***	Accepted	70%. Concept and collecting data, statistical analysis, manuscript writing	All authors provided input to manuscript through either data collection, mansucript review and editing totalling 30% of contribution 1) Francis J Ha 2) Caitlin Cheshire	Yes

	Cardiovascular Events			3) Hashrul Rashid 4) James D Cameron 5) Dennis T Wong 6) Sujith Seneviratne 7) Adam J Brown	Yes
5	***Poor Correlation, Reproducibility and Agreement Between Volumetric vs. Linear Epicardial Adipose Tissue Measurement***	Accepted	80%. Concept and collecting data, statistical analysis, manuscript writing	All authors provided input to manuscript through either data collection, mansucript review and editing totalling 20% of contribution 1) Yi-Wei Baey 2) Adam J Brown 3) Rahul G Muthalaly 4) Damini Dey 5) Balaji Tamarappoo 6) James D Cameron 7) Thomas H Marwick 8) Dennis T Wong	No
6	**Inter-software and Inter-scan Variability in Measurement of Epicardial Adipose Tissue: A Three-way Comparison of a Research specific, A Freeware and a Coronary Application Software Platform**	Submitted	80%. Concept and collecting data, statistical analysis, manuscript writing	All authors provided input to manuscript through either data collection, mansucript review and editing totalling 20% of contribution 1) Udit Thakur 2) Rahul G Muthalaly 3) Andrew Talman 4) Damini Dey 5) Adam J Brown 6) Angel IY Wu 7) Sujith K Seneviratne 8) James D Cameron 9) Dennis T Wong	Yes
7	***The Natural History of Epicardial Adipose Tissue Volume and Attenuation: A Long-term Prospective Cohort Follow Up Study***	Submitted	80%. Concept and collecting data, statistical analysis, manuscript writing	All authors provided input to manuscript through either data collection, mansucript review and editing totalling 20% of contribution 1) Udit Thakur 2) Samuel Koh 3) Andrew Lin 4) Elizabeth Potter 5) Rahul G Muthalaly 6) Hashrul Rashid 7) James D Cameron 8) Damini Dey 9) Dennis T Wong	Yes Yes Yes
8	***Epicardial Adipose Tissue Volume but not Denisty is associated with High Risk Plaque Composition on Coronary Computed***	Submitted	70%. Concept and collecting data, statistical analysis, manuscript writing	All authors provided input to manuscript through either data collection, mansucript review and editing totalling 30% of contribution 1) Udit Thakur 2) Samuel Koh 3) Andrew Lin 4) Elizabeth Potter	Yes Yes

	Tomography Angiography in patients with non-obstructive coronary artery disease			5) Rahul G Muthalaly 6) Abdul-Rahman Ihdayhid 7) James D Cameron 8) Damini Dey 9) Dennis T Wong	Yes

**If no co-authors, leave fields blank*

I have renumbered sections of submitted or published papers in order to generate a consistent presentation within the thesis.

Student signature: **Date: 22/11/2018**

The undersigned hereby certify that the above declaration correctly reflects the nature and extent of the student's and co-authors' contributions to this work. In instances where I am not the responsible author I have consulted with the responsible author to agree on the respective contributions of the authors.

Main Supervisor signature: **Date: 22/11/2018**

ACKNOWLEDGEMENTS

Submission of this thesis comes with great anxiety and relief, but also a tremendous sense of accomplishment. The only way I can think of how to describe the journey of this PhD is to compare it to the 1966 cinematic masterpiece, The Good, The Bad and The Ugly. This film, a personal favourite, is an epic, technicolour classic that appears almost interminable, yet filled with moments of high tension and drama, and is at times whimsical before ultimately concluding in an ecstatic triumph of success from perseverance. I have emerged, battle hardened from journal rejections, failed hypotheses and being pipped at the post by other research groups, to become a more balanced, rational and resourceful researcher. But this metamorphosis could only result from the monumental support I have received from others who I must graciously thank in this acknowledgement preamble.

Firstly, to my supervisors, Associate Professor Dennis Wong and Professor James Cameron. Dennis, we have worked together since I was a registrar and more than half of my published papers are associated with you. From the intense foosball stand-offs and the bubbling Perrier, we have had some terrific memories socially, a critical component of the success in our research together. I thank you for allowing me to become an independent researcher and explore my ideas and whims. Jim, your fatherly advice and support in the department is immeasurable and I am grateful for providing me with all the resources I needed without question.

To Professor Tom Marwick, I chased you around varying conferences for several years working up the courage to collaborate with an academic of your calibre. I thank you for your selfless mentorship and guidance. To Dr Adam Brown, thank you for making me discover my love for research once again. In a moment of deep despair, you extended a hand and continued to push me to cultivate my statistical knowledge. I look forward to many future collaborations and a long-lasting friendship. To Dr Abdul Ihdayhid, your effusive intelligence and humility are characteristics I can only wish to achieve.

Thank you for reviewing my work with fine detail and encouraging me to be the best I can be. To Dr Colin Machado, the morning daily coffee routine, and ritual afternoon phone calls were an escape from reality with the perfect recipe of humour, melancholy and nostalgia. To Dr Udit Thakur, a late entry into the arena but invaluable in your incomparable work ethic and media provision. We will have many more tennis and cricket escapades. To Dr Rahul Muthalaly, you once called me your mentor, but I feel I learned more from you. Thank you for keeping me feeling young and being my statistical bouncing board. To Dr Damini Dey at Cedar Sinai, thank you for providing your software and support whch has been the backbone of all my research projects. I look forward to an ongoing and fruitful collaboration.

I also thank the numerous residents, registrars and staff that assisted in patient recruitment and data collection and were patient with the disruptions to workflow!

I thank my parents and my sister. You have always been my biggest fans and though it has been challenging to keep consistent contact in this time, you have pushed me to see this through. To my son Thomas. You entered this world as I entered the PhD arena. Tears fill my eyes thinking of the sacrifices made and time lost when I could have been playing trains with you instead. You are already my best friend and every second spent together feels like a lifetime of happiness. Finally, to my beloved wife Sarah. You've stuck by me for 14 years. You always 'kept it real' and brought me back to earth when there was a danger of egotistically driven cranial insufflation. Thank you for grounding me, at times for surrendering your career so I could embrace mine, and for giving us the gift of our beautiful baby boy. You prove the adage that behind every successful man is an even more successful woman.

Now it's time to start living our lives.

CHAPTER 1:

ADIPOSITY AND CARDIOVASCULAR DISEASE: A COMPREHENSIVE REVIEW OF THE LITERATURE

Adiposity and coronary plaque

Obesity is often considered to be an elevation in body mass index (BMI), a physical measure that aims to reflect body fat. However, patients may have significantly active adipose tissue without a definite elevation in BMI which may be influenced by muscle and bone mass[1]. Therefore, the term obesity should not simply be regarded as elevated BMI, but rather as a reflection of potentially pathogenic adipose tissue. Obesity may act as an intermediary to affect the development of metabolic disturbances such as hyperinsulinaemia, dyslipidaemia and hypertension, all of which are established factors for atherogenesis. However, adipose tissue contains a variety of humoral factors that may all contribute to atherogenesis, suggesting that obesity itself may have an effect on the development of atherosclerosis. Various cytokines have been isolated to adipose tissue and may have deleterious effects on the vascular intima. Increased visceral fat mass results from adipocyte hypertrophy and hyperplasia of adipocyte precursors which causes release of chemotactic factors such as monocyte chemoattractant protein-1 (MCP-1). This causes migration of monocytes into visceral adipose tissue (VAT) and promotes differentiation to macrophages[2]. Multiple factors result in blood monocyte chemotaxis including adipocyte apoptosis, increased lipolysis, local free fatty acids (FFA), reactive oxygen species and tissue hypoxia[3]. Leptin is one of the key cytokines secreted specifically by adipose tissue and several basic science studies have demonstrated the influence it has on the promotion of atherosclerosis. Adiponectin is another vital cytokine produced abundantly in adipose tissue. This factor is significantly reduced in obese subjects and may indeed explain the propensity for obese subjects to have a greater burden of atherosclerosis due to lack of an innate protective factor. It has been suggested that TNF-alpha, another cytokine secreted in adipose tissue, may cause inhibition of adiponectin leading to these biochemical abnormalities, as well as reduced glucose transport, reduced FFA uptake and re-esterification and increased lipolysis[4]. Other important cytokines released from adipose tissue and promote atherosclerosis include Adipocyte Fatty Acid Binding Protein, Plasminogen Activator Inhibtor-1 and Resistin **(Table 1).**

Table 1: Adipokines and association action with atherogenesis (Adapted from Fitzgibbons et al.[5])

Adipokine	Actions associated with atherosclerosis
Leptin	• Enhanced migration and proliferation of vascular smooth muscle cell • Promoting neointimal formation after arterial injury • Increased fatty acid oxidation

	• Increased secretion of inflammatory cytokines • Procoagulant and prothrombotic properties
Adiponectin	• Enhanced nitric oxide production • Anti-inflammatory effect: inhibition of NF-kB, upregulation of IL-10 and tissue inhibitor of metalloproteinase-1 • Promoting proliferation of smooth muscle cell • Improvement of insulin sensitivity • Prevention of apoptosis in endothelial cell
Resistin	• Upregulation of inflammatory cytokines and adhesion molecules • Promoting proliferation and migration of smooth muscle cell
Plasminogen activator inhibitor-1	• Decreased fibrinolytic activity through inhibition of urokinase-type plasminogen activator and tissue-type plasminogen activator
TNF-alpha	• Recruitment of monocytes • Enhanced accumulation of LDL • Diminished insulin sensitivity
Adipocyte fatty-acid binding protein	• Diminished insulin sensitivity • Increased secretion of inflammatory cytokines
Visfatin	• Increase in HDL • Promoting angiogenesis • Promoting proliferation of endothelial cell • Promoting growth of smooth muscle cell
Apelin	• Endothelium-dependent vasodilatation by increased NO production • Inhibition of inflammatory cytokines • Increased cardiomyocyte contractility • Reduction of myocardial infarction size
Omentin	• Inhibition of TNF-alpha • Inhibition of lymphocyte adhesion to vascular cells • Inhibition of endothelial cell migration • Inhibition of angiogenesis
Chemerin	• Inducing endothelial angiogenesis • Inducing NO synthesis

The prevalence of obesity and its cost on the health care system continues to rise with 70% of adult males and 56% of adult females being in the overweight/obese range[6]. Obesity increases all-cause mortality and its rising prevalence continues to place a large financial burden on national health[7]. Coronary artery disease (CAD) is the single largest cause of death in Australia (representative of 15% of all deaths) and contributes to disability, poor quality of life and high health care costs[8]. There has been significant improvement in mortality outcomes of CAD, especially through the use of prescribed medical therapy and primary care management of typical cardiovascular risk factors[9]. Traditional risk calculators for the development of acute coronary syndromes incorporate such risk factors as age, gender, blood pressure, smoking status and lipid biomarkers[10]; however

obesity does not feature as a predictor of CAD in these assessments. There are well-established links with overweight/obesity being an independent risk factor for CAD and indeed practice guidelines for those with CAD recommend achievement of a BMI (calculated as body weight in kilograms divided by the height in metres squared) of less than 25kg/m^2 [11].

There is a strong association between obesity and cardiovascular mortality[12] independent of and in addition to the major traditional CAD risk factors. Furthermore, longitudinal studies have shown that obesity independently predicts CAD[13]. In fact, a large retrospective study evaluating the decrease in deaths from CAD in the United States revealed that over a 20-year period, the reductions in mortality were offset by significant increases in BMI[9].

Despite this, there is conflicting data as to whether an elevated BMI confers a greater risk of acute coronary syndrome and there may in fact be a protective benefit of an increased BMI in those with CAD for long-term mortality. Furthermore, the effect of weight loss in obese patients is controversial with some studies reporting worse outcomes – the so called 'obesity paradox' – however much of this data is from non-randomized observational analyses that don't differentiate between intentional monitored weight loss and passive changes in weight which may occur in the setting of other illness**.** A large systematic review assessing the effect of purposeful weight loss in CAD patients showed a significant reduction in cardiovascular events compared to observational loss of weight[14]. Additionally, at a coronary artery stenosis level a randomised study performing serial coronary angiography on patients with established CAD showed significant atherosclerotic regression with comprehensive lifestyle management[15].

Obesity paradox

There remains contention of whether obesity alone is a factor for CAD or whether it acts as a mediator by contributing to various atherosclerotic risk factors including hypertension, diabetes, the metabolic syndrome and dyslipidaemia:

Table 2: Mechanisms by which obesity increases CAD risk factors.

Risk Factor	Mechanism
Hypertension	Production of angiotensin
	Increase in circulating blood volume
	Increase in total peripheral resistance
Diabetes mellitus and metabolic syndrome	Dietary indiscretion that leads to obesity
	Endocrine activity of adipose tissue
	Increased clotting factors: fibrinogen, von Willebrand factor, factors VII and VIII
	Increased leptin
	Increased tumour necrosis factor-alpha
	Endothelial dysfunction
	Decreased insulin-mediated vasodilation
	Increased insulin-mediated renal sodium absorption
	Insulin-related sympathetic nervous system stimulation
	Increased vasoconstriction related to elevated circulating free fatty acids
	Increased risk of dyslipidaemia
	Increased risk of renal dysfunction
Dyslipidaemia	Low levels of high-density lipoprotein cholesterol
	High levels of triglycerides
	High levels of low-density lipoprotein cholesterol
	Elevated total cholesterol

Reproduced from Jahangir et al with permission[16]

The obesity paradox also shrouds controversy over the association of obesity and cardiovascular disease. Large scale epidemiologic data has demonstrated that despite an increased risk of developing CAD, in those with established cardiovascular disease the overweight or mildly obese patients have a reduced or similar prognosis compared to normal weight individuals as based on BMI[17]. This association appears to be present particularly in the heart failure and atrial fibrillation population, although data is also seen in those with CAD. The obesity paradox has been seen in hospital registry studies, revascularised cohorts, post coronary artery bypass groups, emergency department patients and high-risk patients undergoing non-invasive stress imaging. In a 50,000-patient study of ST-elevation myocardial infarction, patients with BMI 30-35kg/m^2 had the lowest mortality compared to other BMI groups and in another study with solely acute coronary syndrome (ACS) patients, those with BMI >40kg/m_2 had a lower mortality than those <40kg/m^2 [16].

Figure 1: Association of mortality by BMI groups

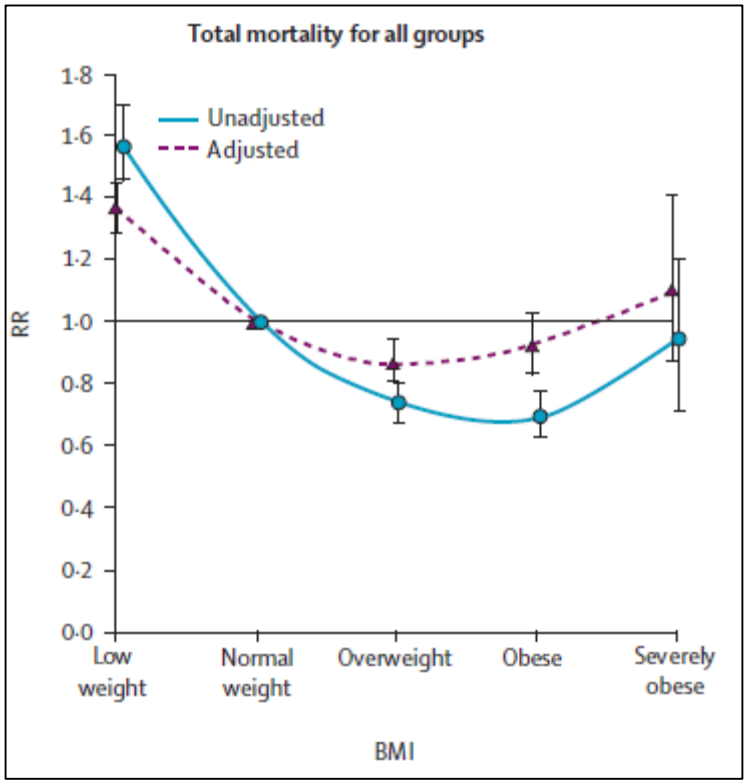

Demonstration of the 'J' curve of increasing weight categories by body mass index and a reduction in total mortality – the so-called obesity paradox. Values below a RR (relative risk) of 1 represent a relative reduction in the outcome of mortality.
Adapted from Romero-Corral et al with permission from Elsevier[17]

And in a large meta-analysis of 250,000 patients, the 'J' curve of protective benefit of overweight or obesity for all mortality was seen in patients with ACS , undergoing PCI or CABG (**Figure 1**) [17].

Several potential mechanisms for the obesity paradox have been put forward. Adiposity from a positive caloric intake may result in atherogenic adipose tissue resulting cardiac disease. However, in times of negative caloric balance as occurs in a cardiovascular effect, adipose tissue may respond with enhanced or protective function to improve clinical outcomes. Patients with more adipose tissue generally have a greater muscle strength which has been associated with better prognosis. Patients with a high BMI may be more aggressively investigated or treated than normal weight counterparts due to perceptions of the negative disease associations with elevated BMI. Importantly, BMI may actually be a poor reflection of a patient's adiposity, particularly adipose tissue that is metabolically more active, with up to 60% of patients misclassified when body-fat percentage is used a reference marker[18].

BMI is the most often reported clinical marker for obesity due to its ease of calculation, however, there are several studies that demonstrate that it is inaccurate in comparison to markers such as waist circumference, waist to hip ratio or body fat percentage. Therefore, body distribution of fat may actually be a more representative and appropriate measurement in considering the risk of obesity and subsequent disease. This has been demonstrated in patients who are considered to be obese based on an elevated BMI who have no metabolic complications, the so-called metabolically healthy obese patient[19-24]. Therefore, BMI at a population level may be beneficial in describing changes in clinical adiposity, but may not discriminate risk at an individual level. As mentioned this may be an explanation for the possible results seen in the obesity paradox. In a large epidemiologic study of >25000 patients, it was seen that BMI was a poor reflection of future myocardial infarction with other markers of obesity including waist-to-hip ratio or waist circumference representing independent effects on future ACS adjusted for traditional risk factors, age and sex [25] (**Figure 2**).

Figure 2: Association of body fat parameters and risk of myocardial infarction

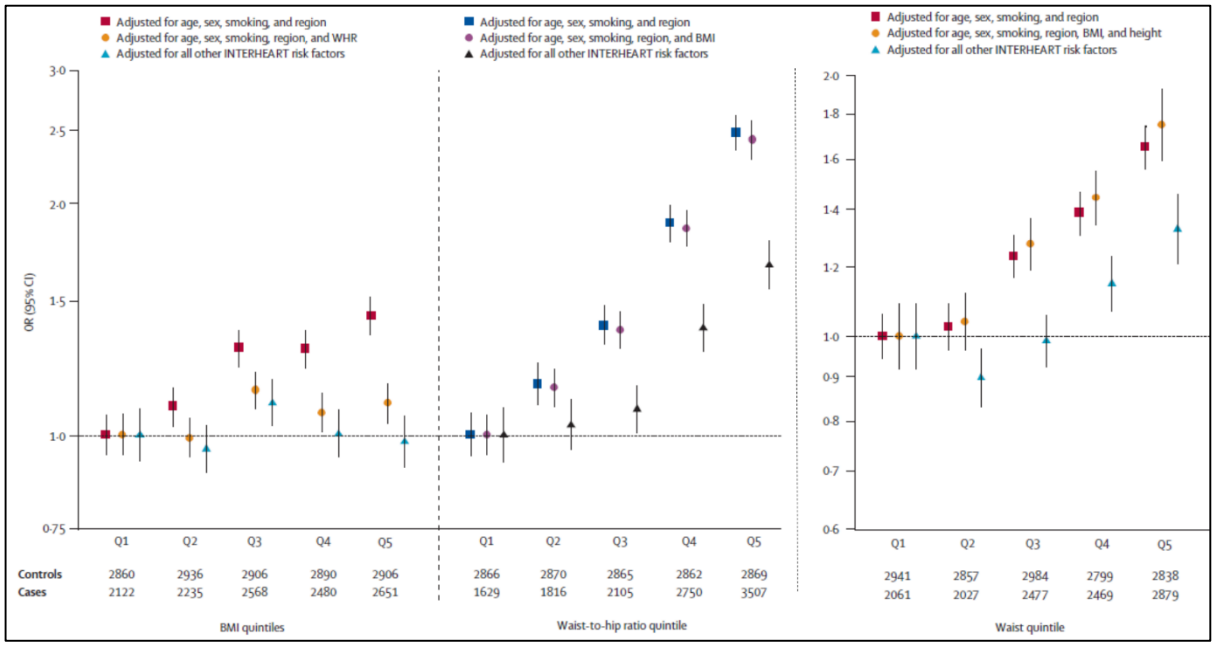

Left panel demonstrates reducing risk of BMI with myocardial infarction risk with adjustment for other cardiovascular risk factors (left panel); Measures of body fat distribution waist-hip ratio (middle) and waist quintile (right) demonstrate increasing risk despite adjustment.
Adapted from Yusuf et al. The Lancet with permission[25]

These results highlight the possibility of body fat distribution having an independent effect on coronary atherosclerosis, in particular abdominal fat which comprises visceral and subcutaneous adipose tissue (**Figure 3**). Further metabolic study has demonstrated that VAT is highly metabolically active and there are three major theories proposed to explain its effect on metabolic/vascular complications[1]:

1. The portal free fatty acid model suggests that an uninterrupted overflow of FFA from VAT exposes the liver to high concentrations (fatty liver) leading to impaired hepatic metabolism, including changes in insulin production, reduced degradation of apolipoprotein leading to elevated triglycerides and increased glucose production leading to type 2 diabetes.
2. The endocrine function of VAT with the rich inflammatory milieu of adipokines which are involved in atherogenesis and found in ruptured atherosclerotic plaques. This is promoted by a larger number of macrophages seen in hypertrophied adipose tissue that are a source of TNF-alpha, interleukins and drive C-reactive protein production.
3. Ectopic adipose tissue: It is suggested that surplus fat may be stored in undesirable sites such as liver, heart, pancreas and skeletal muscle and retain the high metabolic function of VAT to result in systemic circulation of adipokines and therefore further vascular damage.

Figure 3: Pathophysiologic mechanisms of adipose tissue and plaque

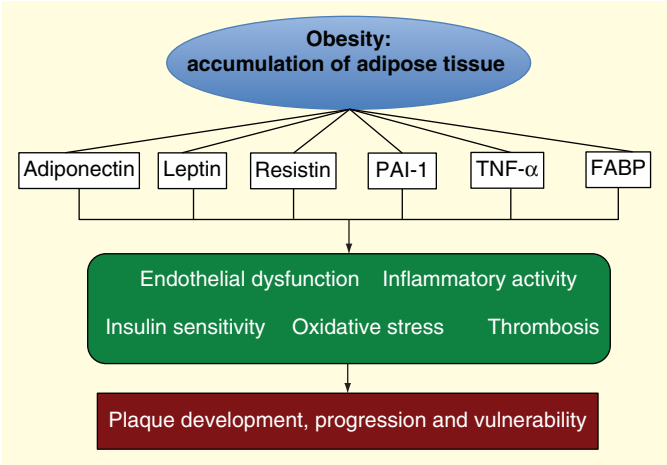

Suggested pathophysiology of obesity (dysfunctional adipose tissue) with abundant adipokines and the effects leading to plaque instability. Reproduced from Kataoka et al with permission [5]

It is known that the heart has a natural adipose store known as epicardial adipose tissue. It has not been proven that this is an ectopic depot from surplus fat, but it may be that it enlarges under such circumstances. EAT is a visceral adipose store for the heart and encases the coronaries whilst being in continuum with as well as invading the adjacent myocardium[26]. Therefore, it is suitable anatomic substrate for adipokine migration into the coronary vasculature or myocardium to affect coronary atherogenesis, ischaemia and cardiac function.

Studies evaluating obesity and coronary plaque characteristics have predominantly utilized intracoronary imaging techniques. These techniques are considered the reference standard in plaque assessment due to the high spatial resolution that allows micrometre characterization of plaque thickness. However routine applicability is not possible with this method due to the invasive nature. Computed tomography coronary angiography (CTCA) is an alternative non-invasive imaging modality that has shown promise in plaque characterization with specific high-risk features that associate with future prognosis [27]. There is good diagnostic agreement with intracoronary plaque assessment and CT evaluation [28]. Hallmarks of higher risk plaques include plaques with necrotic core and thin-capped fibroatheromas, both of which have been seen in culprit and non-culprit vessels of patients presenting with acute coronary syndromes [29]. Such high-risk plaques have been sought for diagnosis non-invasively as means of risk stratification in patients and include low attenuation plaque, napkin ring sign, spotty calcification and positive vessel remodelling [30].

Acute coronary syndrome and Plaque

Histopathologic assessment has demonstrated that the majority of patients with ACS have luminal thrombosis most frequently caused by plaque rupture, followed by plaque erosion and finally calcified nodules[29]. The features of ruptured plaques include large plaque volumes as well as necrotic cores covered by thin fibrous caps often inflamed with monocyte-macrophage infiltration[31]. Plaques prone to rupture share similar characteristics except the thin-capped fibroatheromas (TCFA) have yet to rupture and these lesions are referred to as "vulnerable" plaques or high-risk plaques (HRP). HRP can be detected invasively using methods such as intravascular ultrasound (IVUS) [32] and optical coherence tomography (OCT) [33] or non-invasively with CTCA[27].

Pathological analysis has demonstrated that 60% of acute thrombi found in patients who died from sudden cardiac death resulted from ruptured TCFAs [34]. Additionally, there is robust data to indicate that non-culprit arteries in ACS contain vulnerable plaque that is of prognostic significance [35-37] and nascent evidence that obese patients are more likely to have a greater proportion of vulnerable plaque than non-obese controls irrespective of differing clinical characteristics[5, 38]. Epicardial fat, the visceral fat depot surrounding the coronary vasculature that is abundant in pro-atherogenic cytokines has also shown independent association with the presence of high risk plaque in both stable and ACS patients[39, 40].

Vulnerable plaques however have been shown to change on serial follow up with potential loss of their vulnerable characteristics and development of new plaques within adjacent areas suggesting a dynamic metabolic process [41]. Additionally, there is no evidence demonstrating a benefit of treatment of these individual lesions or the patients themselves. However, these high-grade lesions are likely to represent a marker of significant atherosclerotic disease burden within the coronary tree for which there is evidence to suggest an incremental risk of cardiovascular events [42-44]. Coupled with markers of metabolic activity such as high sensitivity C-reactive protein, an assessment of plaque volume and vulnerable plaque features and their relative change with weight loss may provide insight into the development of further acute coronary events. It has recently been demonstrated that the rate of epicardial coronary disease progression is independently associated with clinical outcomes in patients undergoing serial IVUS evaluation [45].

The serial use of modalities such as IVUS and OCT to assess plaque is not feasible given the risks associated with an invasive study. In a recent meta-analysis[46], compared to IVUS, CTCA was found to only slightly overestimate luminal area (0.46mm^2 or by 6.7%; p = 0.005), while there were no significant differences in plaque area (0.09mm^2; p = 0.88) and volume (5.3mm^3; p = 0.21). Serial quantification of plaque volume using CTCA is also feasible, as shown by one study that compared interval changes in total plaque volume over a 12-month period in patients receiving lipid-lowering medication with those who did not[47].

CTCA has established itself as a non-invasive modality for assessment of suspected CAD with high sensitivity and negative predictive value for detecting coronary artery stenosis[48]. The full scope of CTCA has yet to be explored, especially with respect to serial imaging and monitoring the temporal change of coronary atherosclerotic plaque. This is partly due to the radiation dose (13-18 millisieverts) of CTCA scans on older generation multidetector computed tomography (MDCT). However, the reduction in radiation dose by voltage/current modulation, prospective gating, adaptive iterative reconstruction and limited volume scanning has now rendered serial imaging more acceptable. Local institutional data demonstrated that image quality acquired on a 2nd generation 320-MDCT scanner is excellent when patient heart rate is well-controlled (heart rate <65 bpm) with low radiation exposure (mean of 2.1 millisieverts) despite a mean BMI of 28.3 ± 0.8[49]. CTCA permits the assessment of coronary atherosclerotic plaque morphology, composition and positive remodelling in good agreement with IVUS[50]. In addition, studies have also demonstrated that qualitative

vulnerable plaque features can be detected on CTCA and this has been correlated with IVUS and OCT. These features include 1) positive remodelling, 2) low attenuation plaque, 3) spotty calcification and 4) napkin ring sign **(Figure 4)**. More recently observational studies have demonstrated that patients with vulnerable plaques detected on CTCA are more likely to develop ACS on medium term follow up[27]. In those with diagnosed ACS, the highest risk of a repeat event is within the first 6-12 months with incidence ranging from 6-15%[32].

Figure 4: CT features of high-risk (vulnerable) plaques

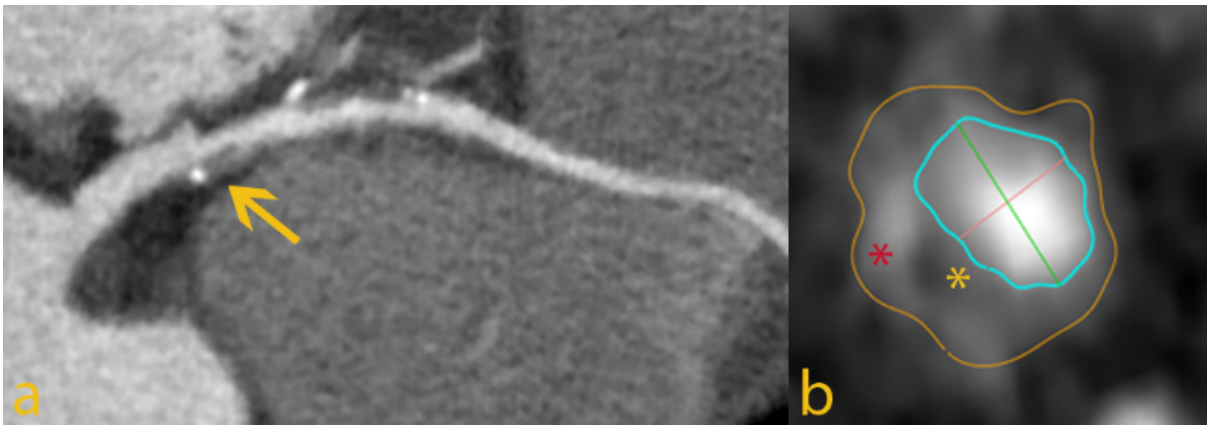

Vulnerable plaque features a) Yellow arrow indicating plaque with positive remodelling, low attenuation plaque and spotty calcification b) Napkin ring sign. Yellow asterisks indicating low attenuation plaque (lipid pool) surrounded by fibrous plaque

Qualitative plaque assessment, particularly with high-risk plaques have a dichotomous assessment and this may not be adequate in characterising the overall risk continuum of atherosclerosis which has demonstrated that greater plaque volumes and extent associate with worse outcome[45]. There has been increasing interest in non-invasive quantifiable characteristics of HRP rather than simply qualitative observations with the rapid developments in automated tracking software. Whilst IVUS remains the reference standard, it is not ideal due to its invasive nature. Correlation on co-registered datasets of IVUS and CT have identified suitable thresholds to describe various plaque subtypes based on specifically derived Hounsfield unit (HU) thresholds [51]. As such, CTCA can now feasibly and reliably identify traditional IVUS features such as necrotic core and fibro-fatty plaque, which are considered to be HRP, and fibrous and calcified plaques which are considered to be of lesser risk. The prognostic utility of plaque was recently described a landmark nested case-control study, the multicentre ICONIC trial (Incident Coronary Syndromes Identified by Computed Tomography) which reported that patients with future ACS had a significantly larger volume of high risk plaque (necrotic core, or fibrofatty plaque) compared to non-ACS controls[52]. No difference was seen in fibrous plaque or calcified plaque volumes.

There remains uncertainty as to absolute volumes or indexed volumes in terms of a population normal reference range for these parameters. Nonetheless, this enhanced level of plaque interrogation via a non-invasive method is likely to become the preferred reporting modality for plaque associations with investigative parameters.

Epicardial Adipose Tissue

Basic Anatomy

Visceral adipose tissue is particularly felt to have a strong association with metabolic abnormalities, atherosclerosis and subsequent acute coronary syndrome [25, 53-55]. Epicardial adipose tissue is the true visceral fat depot of the heart and makes up approximately 20% of the total cardiac mass and covers 80% of the cardiac surface [56], particularly within the atrioventricular and intraventricular grooves and along the free wall of the right ventricle [57, 58]. EAT is thought to originate from the splanchnic mesoderm, but some evidence suggests development from mesenchymal transformation of cells in the myocardium [59, 60]. It shares the same microcirculation as the myocardium with supply from the coronary arteries that it encases without any fascial barrier. EAT lies above the myocardium and within the visceral pericardial layer. This differentiates it from paracardial fat, or intrathoracic fat which lies superior to the parietal pericardium and has a different embryologic genesis (**Figure 5**). Pericardial adipose tissue is regarded as the summation of epicardial and paracardial fat. Both EAT and intra-abdominal fat originate from brown adipose tissue during embryogenesis [61]. EAT and VAT have shown strong correlation with each other, rather than with simple clinical measures of adiposity alone. Autopsy studies have shown that the ratio of EAT to LV mass is higher in the right ventricle and interestingly, the ratio of EAT to ventricular mass is constant in normal, ischaemic and hypertrophied hearts[57].

Figure 5: Epicardial adipose tissue anatomy

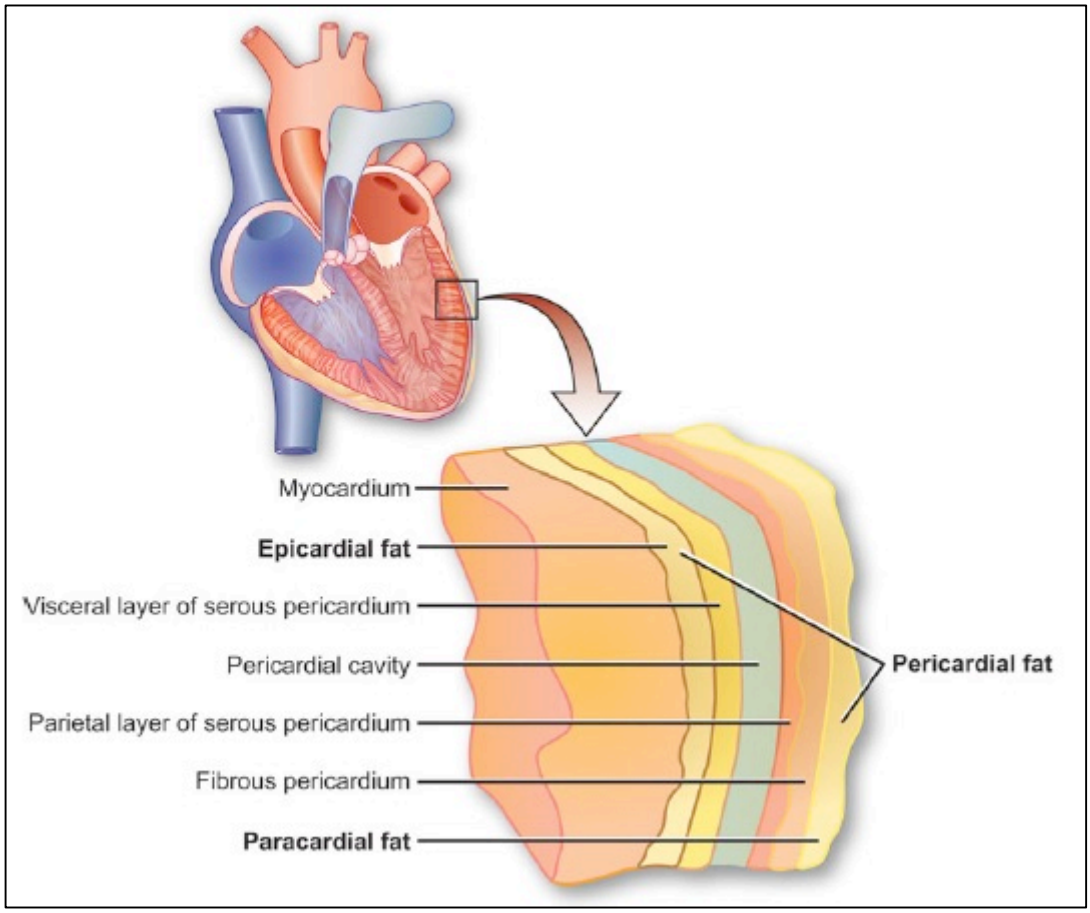

Epicardial fat anatomy demonstrating that epicardial fat is directly apposing the myocardium within the pericardial sac; paracardial fat lies above the fibrous pericardium and the combination of epicardial and paracardial fat is pericardial fat.
Reproduced from Wong et al with permission[62]

Function

There are several potential protective physiologic functions of EAT (**Table 3**). It is thought to provide mechanical support to the coronary arteries during myocardial contraction as well as space for arterial expansion during early atherosclerosis [63, 64]. EAT has a high rate of lipogenesis and free fatty acid (FFA) metabolism as seen in animal models, which may be of benefit in times of increased cardiac stress for extra energy release, or indeed act as a storage depot in times of FFA excess, although this has not been robustly investigated. Additionally, EAT secretes anti-inflammatory cytokines such as adiponectin, adrenomedullin and omentin which have anti-atherogenic effects, as well as regulating vascular tone and cardiac contractility and remodelling [65-70]. It is hypothesized that due to the thermogenic genes expressed in EAT which are associated with brown adipose tissue, it serves to provide direct heat to the myocardium for protection during hypoxia or

hypothermia. Interestingly, there is an association of angiogenesis stimulation with resultant development of collateral circulation in those with obstructive CAD that is seen in patients with excess EAT [71].

Table 3: Vasoprotective factors from EAT.

Factor	Effects
Adiponectin	▪ Endothelium-independent vasodilation ▪ Inhibition of vascular smooth muscle proliferation in vivo and in vitro via an AMPK-dependent pathway ▪ Prevents monocyte adhesion to HAECs ▪ Activation of local eNOS function by stimulatory phosphorylation and increased BH4 production
Leptin	▪ Endothelium-dependent dilation of conduit arteries
Omentin-1	▪ EAT and plasma levels of omentin are reduced in diabetic patients ▪ Recombinant omentin prevented the inhibitory effects of CM-EAT-DM on contraction of ARVC and insulin-stimulated Akt-Ser473 phosphorylation
Nitric oxide	▪ Endothelium-dependent vasodilation
PAME	▪ Vasodilation via direct stimulation of VSMC potassium channels
PGI2	▪ PVAT-derived prostacylin may inhibit endothelial dysfunction by impairing acetylcholine-induced vasoconstriction

EAT indicates epicardial adipose tissue; PVAT, perivascular adipose tissue; AMPK, adenosine monophosphate–activated protein kinase; HAEC, human aortic endothelial cell; eNOS, endothelial nitric oxide synthetase; BH4, tetrahydrobiopterin; CM-EAT-DM, conditioned media from epicardial adipose of diabetic patients; ARVC, adult rat ventricular cardiomyocyte; PAME, palmitic acid methyl ester; VSMC, vascular smooth muscle cell; PGI2, prostacyclin.
Reproduced from Fitzgibbons et al. (open access) [4]

However, the presence of numerous pro-inflammatory and pro-atherogenic cytokines within EAT may lead to a potential imbalance of harmful vs. protective cytokines and disruption of myocardial function. EAT is rich in inflammatory mediators as compared to subcutaneous tissue as seen in patients referred for coronary artery bypass grafting, and the levels seen are higher than that in the systemic circulation [72]. Specifically, there were higher levels of monocyte chemotactic protein-1, interlukin-1β (IL-1β), IL-6, IL-6sR and TNF-alpha [63]). Higher levels of these molecules are seen in patients with coronary artery disease or heart failure. It is uncertain whether the trigger for the imbalance of cytokines is a cause of the pathology or a consequence, and a potential reciprocal or bidirectional role has been proposed ([63]. Due to its anatomic proximity to the adjacent myocardium and lack of fascial barrier with the epicardial coronary arteries, it is postulated that there may be paracrine or vasocrine signalling of cytokines between the surrounding fat and the underlying arterial wall [73]. This suggested pathophysiology is analogous to the visceral intra-abdominal adipose tissue surrounding the portal circulation

that is purported to influence the development of hepatic steatosis[1]. It has been demonstrated that increased EAT volume is related to both the extent and lesion severity of coronary stenosis ([74] and contains a greater amount of inflammatory cytokines compared to serum circulating levels and subcutaneous adipose stores [72]). The apposition of EAT with the arterial adventitia lends itself to the "outside-in" hypothesis of atherosclerosis, whereby the inflammatory milieu of EAT leads to vascular inflammation of the adventitia progressing inward to the intima leading to plaque formation. Therefore, it is possible that cellular cross-talk may lead to the development of plaque characteristics considered to be of high risk due to their association with major adverse cardiovascular events. It has also been reported that high EAT levels are associated with mortality, although it remains unclear whether these are specifically related to preceding cardiovascular events[75]. Furthermore, protective adipokines such as adiponectin which has demonstrated anti-inflammatory and anti-atherogenic properties are nearly 40% lower in the EAT of patients with CAD compared to healthy controls[76].

Table 4: Pathological factors released from EAT.

Factor	Effects
Activin A	▪ Increased fibrosis of rat atrial myocytes treated with conditioned media in vitro ▪ Cardiodepressant effect on ARVCs in vitro by reducing expression of SERCA2a
Angiopoietin	▪ Cardiodepressant effect on ARVCs in vitro by reducing expression of SERCA2a
Angptl-2	▪ Promotes adventitial inflammation in vivo
Angiotensin II	▪ Increased vasoconstriction of aortic rings, blocked by incubation with ATIIR blocker
Calpastatin/CAST	▪ Protein is a partial agonist for intracellular domains of Cav1.2 ▪ Dose-dependently increases coronary arterial contractions like PVAT
Chemerin/RARRES2	▪ May directly stimulate vasoconstriction by binding to ChemR23, which is found on VSMCs
Complement component 3	▪ Stimulates differentiation and migration of adventitial myofibroblasts
Leptin	▪ Local leptin levels may promote neointima formation independently of obesity or inflammation
IL-6, MCP-1, PAI-1, GROa, sICAM-1, sIL-6R, RANTES	▪ Conditioned media from patients with CAD increased THP1 monocyte adhesion and migration in vitro
Resistin	▪ Stimulates endothelial cell permeability in vitro
Secretory type II phospholipase A2	▪ Promotes formation of inflammatory lipid mediators in EAT

TNFa	▪ Loss of vasodilator effect of PVAT; likely due to downregulation of NOS by TNFa
VEGF	▪ VEGF expression was increased in the VAT and EAT of diabetic patients and stimulated greater proliferation ▪ of VSMCs in vitro
Visfatin	▪ Stimulation of vascular smooth muscle proliferation in vitro

EAT indicates epicardial adipose tissue; PVAT, perivascular adipose tissue; ARVC, adult rat ventricular cardiomyocyte; SERCA2, sarcoplasmic reticulum Ca2+ ATPase; ATIIR, angiotensin II receptor; CAST, ; ChemR23, Chemerin receptor 23; VSMC, vascular smooth muscle cell; IL-6, interleukin 6; MCP-1, monocyte chemoattractant protein-1; PAI-1, plasminogen activator inhibitor-1; GROa, growth-regulated oncogene a; sICAM-1, soluble intercellular adhesion molecule 1; sIL-6R, soluble IL-6 receptor; RANTES, Regulated on Activation, Normal T cell Expressed and Secreted; CAD, coronary artery disease; THP1, Human acute monocytic leukaemia cell line; TNFa, tumour necrosis factor a; NOS, nitric oxide synthase; VEGF, vascular endothelial growth factor; VAT, visceral adipose tissue.
Reproduced from Fitzgibbons et al. (open access) [4]

Figure 6: Proposed mechanisms of epicardial adipokines and atherogenesis

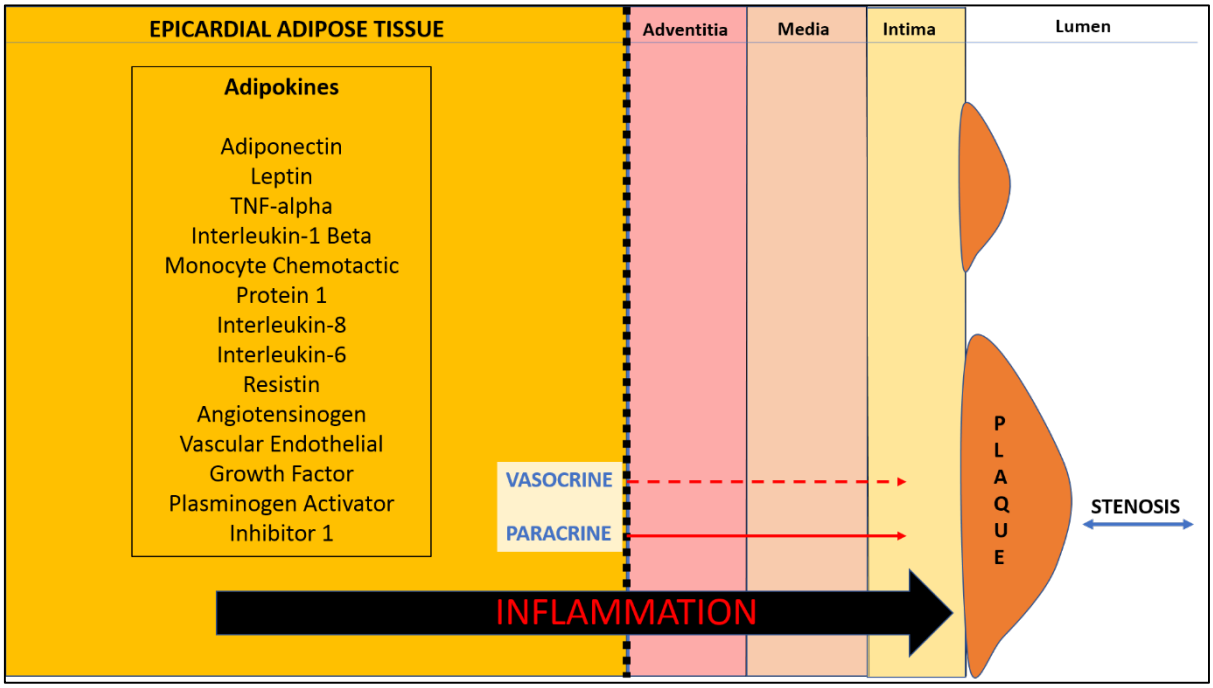

Proposed mechanisms in which epicardial adipokines may access underlying atheroma to play a role in coronary atherogenesis. (I) Paracrine signalling: adipokines directly diffuse through layers of the arterial wall; (II) vasocrine signalling: adipokines transverse through the vessel adventitial vasa vasorum to the lumen. The adipokines are transported downstream to react with cells in the intima and media around atherosclerotic plaques. The overarching inflammatory nature of these cytokines may explain the inflammation hypothesis of atherosclerosis.

The pathophysiology surrounding these adipokines has not been well established. There is belief that radical oxygen species are generated in response to regional ischemia and depressed myocardial function, which in turn activate oxidant-sensitive inflammatory signals in the adipose tissue [77]. Additionally, the presence of TNF-alpha may amplify vascular inflammation through apoptosis and neovascularization resulting in plaque vulnerability and instability [63]. Arterial homeostasis may also be significantly altered by periadventitial presence

of cytokines which cause localized vasospasm and coronary intimal thickening [78, 79]. **Figure 6** represents the potential mechanism and inciting adipokines that may result in atherogenesis.

Measurement of EAT

EAT has been widely studied in cardiovascular research, however there remains no endorsed guideline on the approach to measurement. EAT may be measured non-invasively by a linear thickness measure on echocardiography, CT or MRI; or volumetrically by CT or MRI. Several studies have utilized transthoracic echocardiography, usually in the parasternal long axis view, of the fat adjacent to the right ventricular outflow tract in a plane parallel to the aortic annulus[80] (**Figure 7**). This method however is limited by the single plane assessment, and the effects of probe angulation on two-dimensional linear measurements. Furthermore, a single measurement may under or over-represent the totality of EAT around the heart and therefore even single slice area measurements on CT or MRI may be inappropriate. Correlations of EAT thickness vs volume or mass have shown modest association at best [81, 82] and intuitively, volumetric assessment of EAT would appear to be the most appropriate measurement for complete EAT quantification, despite a longer post-processing time. This may be performed by both MRI or cardiac CT. Studies have included both CT-angiography and non-contrast cardiac CT scans for EAT measurement, however the contrast administration within the lumen may theoretically cause blooming artefact and therefore under-represent the volume of EAT. MRI is limited in its availability and patient factors including ability to breath-hold, but provides a radiation free alternative. MRI has reduced diagnostic sensitivity for coronary artery disease and therefore EAT by CT may be more appropriate in considering associations with CAD. There is no comparative studies of imaging and autopsy measures of EAT, possibly because not all EAT can be removed from the myocardium at post-mortem to obtain exact weight comparisons. Therefore, wide variability is seen in values obtained from studies, making it challenging for clinicians to make decisions with the quantification of EAT.

The Hounsfield unit scale is a quantitative scale to describe radiodensity on CT imaging. In comparison to autopsy studies, the mean attenuation of adipose tissue on CT has been reported at a mean of -105 HU. However, the true attenuation may be dispersed due to volume averaging and beam hardening with contrast administration[83, 84]. The upper threshold level appears to hold a greater effect on the quantification value, and -

30 HU has generally been considered a reference standard. Differences in scan protocol, kV, slice measurement and post-processing software all may have theoretical influence on the value and within laboratory standardization is probably needed. In one study reviewing technical parameters associated with EAT measurement, Bucher et al [85] reconstructed CT datasets that had both contrast and non-contrast enhanced CTs performed throughout the cardiac cycle. Data was analysed at varying upper level threshold of -15, -30, -45 HU in CT at diastole, systole and non-contrast CT. This demonstrated consistently higher non-contrast CT EAT values with little difference between cardiac cycle timing for CTCA. The difference in EAT value CTCA and non-contrast CT at each threshold reduced with change in the upper limit, ~60mL at -15HU, ~40mL at -30HU and ~25mL at -45HU. Interestingly, the -15HU value compared favourably with the -45HU non-contrast CT value. However, the use of a -15HU threshold is not adequately justified and may condition the results with most studies using -30HU or lower. Furthermore, Bland-Altman analysis for the -30HU values are not reported, only for -15HU and demonstrate ~60mL 95% CI difference in values with the smallest bias of 0.6% with CT in systole to non-contrast CT at -45HU.

Therefore, areas that remain uncertain are whether differences exist in post-processing software or in the use of contrast or non-contrast CT. Furthermore, several studies continue to publish associations of EAT with disease based on echocardiographic linear thickness measurements despite several opponents to this technique. This may in part be due to a lack of robust data demonstrating a definite inferiority of linear thickness to volumetric assessment.

Figure 7: Different measurement methods for EAT:

A) Depicts echocardiographic measurement B) CT measurement and C) MRI measurement

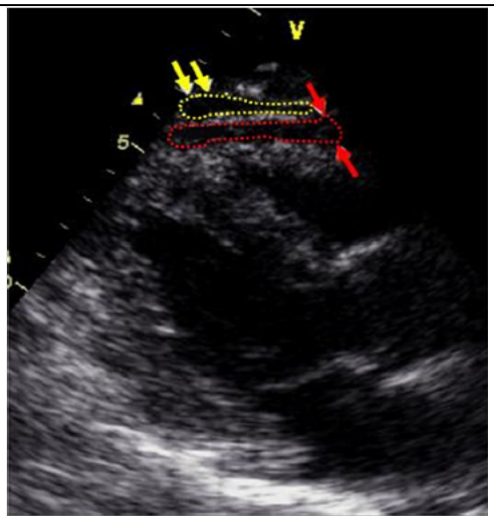

A) Echocardiographic EAT thickness (red shape) identified as the echo-free space between the outer wall of the myocardium and the visceral layer of pericardium in the parasternal long-axis view. Paracardial fat (yellow) is above the fibrous pericardium. EAT thickness is measured during end-systole at the point on the free wall of the right ventricle along the midline of the ultrasound beam, with the best effort to be perpendicular to the aortic annulus, used as an anatomic landmark.

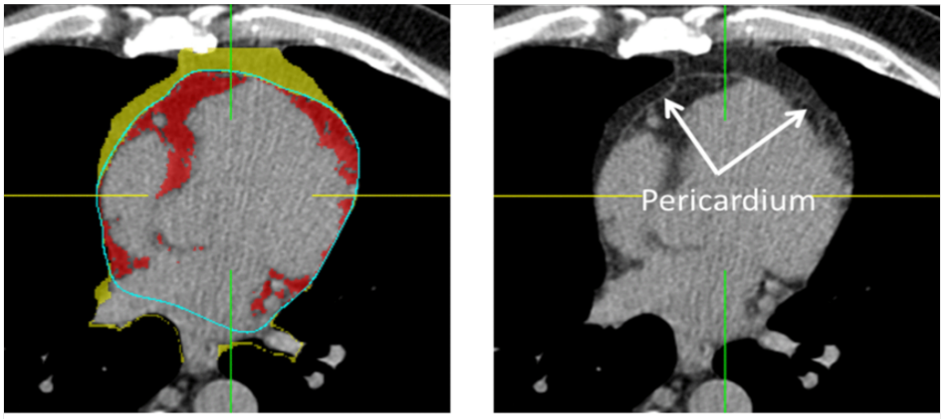

(B) CT measurement of EAT using a semi-automated method with QFAT software.

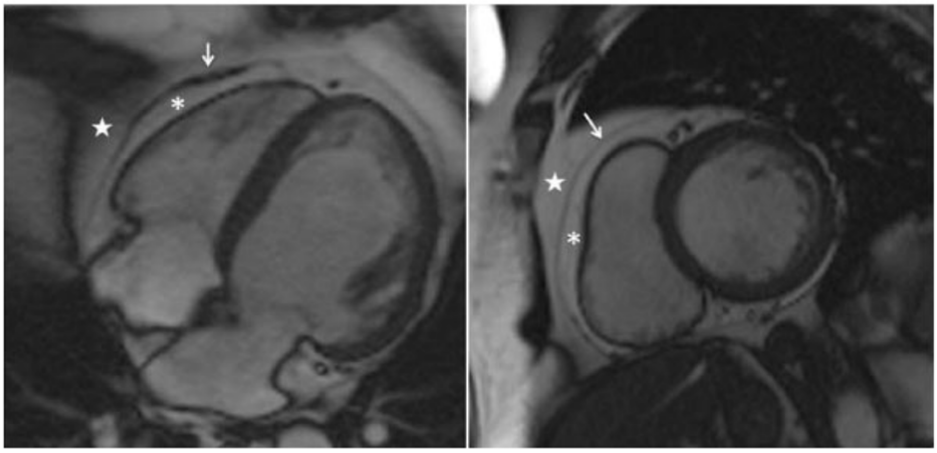

(C): MRI assessment of EAT characterizing pericardium (arrow) and asterisk is EAT, star is PAT.

A) Reproduced with permission from Iacobellis et al (Elsevier) [80]; (C) Reproduced from Bertaso et al[86].

Association with Disease

EAT has been described as a factor for cardiovascular disease including as a mediator through its association with several cardiovascular risk factors and the overall metabolic syndrome, as well as independently with the presence and extent of coronary atherosclerosis, atrial fibrillation and myocardial function and geometry.

As EAT is considered a visceral fat depot, it is unclear whether it represents simply an extension or an independent source of inflammation driving cardiovascular risk. Clear correlation has been demonstrated with EAT and markers of adiposity [87] with the best correlation seen with VAT over and above measures of BMI and WC that are traditional clinical markers of obesity in the general population. Further modest correlation is seen with other markers of the metabolic syndrome including triglycerides, systolic blood pressure and fasting glucose all buttressing the hypothesis of an association of EAT with vascular disease risk. Adjusted models have also demonstrated an independent association of EAT with the metabolic syndrome independent of obesity. *Several of these results are limited by the inclusion of EAT as a linear thickness measurement on echocardiography* (**Table 5**). Studies of CT specific assessment of EAT and coronary artery disease demonstrate a consistent, independent association of EAT with coronary disease adjusted for age, sex, BMI and other potential confounding variables (**Table 6**).

Table 5: Pooled univariable correlation coefficients of EAT with cardiovascular risk factors and markers of adiposity. [87]

Outcome	Pooled correlation coefficient (r)	p-value	Number of studies	Heterogeneity
BMI	0.469	<0.001	26	Q=82.6
Waist circumference	0.567	<0.001	20	Q=75.7
VAT	0.686	<0.001	10	Q=55.9
SBP	0.204	<0.001	11	Q=22.6
Triglycerides	0.292	<0.001	15	Q=89.5
HDL	-0.239	<0.001	13	Q=29.9
Fasting glucose	0.219	<0.001	12	Q=23.2

Table 6: Studies of CT derived EAT and association with CAD

Author	CT	n	Cohort	Exposure	Clinical Variables / outcome	Measure of Association
Ding et al[88]	4-slice	398	Participants of MESA study	1 SD increment in EAT	Calcified coronary plaque	OR:1.92(95%CI 1.27 -2.90) †
Rosito et al[89]	8-slice	1155	Participants of the Framingham Offspring study of free CVD	1 SD increment in EAT	CAC score	OR:1.21(95% 1.005 to 1.46) †
Sarin et al.[90]	64-slice	151	Suspected CAD	EAT volume > 100ml	CAC score	CAC Score - EAT Volume <100mls: 67±155 >100mls: 216±39 (p=0.03)
Ding et al.[91]	4-slice	998	Participants of MESA study	1 SD increment in EAT	Incident CAD	HR:1.26 (95%CI 1.01-1.59) †
Mahabadi et al.[92]	8-slice	1267	Participants of the Framingham Offspring study of free CVD	1 SD increment in EAT	Presence of CVD	OR:1.32(95%CI1.11-1.57) †
Alexopoulos et al.[93]	64-Slice	214	Suspected CAD	EAT volume < 71cm^3	Presence of coronary Plaque	OR:3.9(95%CI:1.1-13.8) †
Cheng et al.[94]	4-slice	232	Suspected CAD	EAT volume >125cm^3	MACE - 4 year follow up.	OR:1.74(95%CI1.03-2.95) †
Konishi et al[95]	64-slice	171	Suspected CAD	1 SD increment in EAT	Any plaque Non Stenotic plaque Non calcified plaque	OR:2.876 (95%CI:1.614–5.125) † OR:3.423 (95%CI:1.764–6.642) † OR:3.316 (95%CI:1.435–7.661) †
Harada et al[96]	64-slice	170	ACS	EAT volume > 100ml	Presence of ACS	OR:2.84(95%CI:1.17-6.87) †
Iwasaki et al[97]	64-slice	197	Suspected CAD	EAT volume > 100 vs < 100 mL	CAC score CAD (>50% stenosis)	384.0±782.0 vs 174.8±395.6; P=0.016 40.2% vs 22.7%; P=0.008
Schlett et al[98]	64-slice	358	Admitted to ED with chest pain	EAT Volume	Presence of high risk lesions vs without high risk lesions and no CAD	151.9 (109-179)cm^3 vs 110.0 (81-137)cm^3 (p=0.04) and 74.8 (58-112)cm^3 (p<0.0001)
Yerramasu et al.[99]	EBCT	333	Type II diabetic patients	Median EAT volume	CAC progression vs no CAC progression	93.1cm^3 vs 68.8cm^3 (p<0.001) † OR 1.12(95%CI1.05-1.19) †
Ito et al[40]	64-slice	1308	Symptomatic patients with a zero calcium score	EAT volume per 10cm^3	Obstructive plaque Vulnerable plaque	OR 1.10(95%CI1.04-1.16) † OR 1.19(95%CI1.12-1.27) †
Mahabadi et al[100]	EBCT	4093	Participants of the Heinz Nixdorf Recall study.	Doubling of EAT volume	Increased risk of coronary events	HR 1.54(95%CI1.09-2.19) †
Rajani et al.[101]	Dual source CT	402	Suspected CAD	EAT Volume	>70% stenosis High risk plaque features	OR 3.0(95%CI 1,3-6.6) † OR 1.7(95%CI 0.9-3.4) †
Iwayama et al[102]	64-slice	69	Non-obese patients with and without severe CAD	1 SD increment in EAT	Incident CAD in non-obese patients	OR 8.27(95%CI1.12-61.60) †
den Dekker et al[103]	Dual source CT	65	Asymptomatic patients with a history of extra-cardiac arterial disease.	10 cm^3 increments of EAT	CAD	OR 1.21(95%CI1.04-1.39) †
Kim et al.[104]	16-slice	209	Suspected CAD	1 SD increment in EAT	Any CAD Significant CAD CAC score	OR 1.67 (95%CI:1.17-2.37) † OR 1.55 (95%CI1.10-2.17) † OR 1.85 (95%CI1.15-3.04) †

CT: computed tomography; MESA: Multi-Ethnic Study of Atherosclerosis; SD: standard deviation; EAT: epicardial adipose tissue; OR: odds ratio; CVD: coronary vascular disease; CAC: coronary artery calcium; EBCT: electron beam computer tomography; CAD: coronary artery disease; HR: hazard ratio;

MACE: major cardiac adverse event; ACS: acute coronary syndrome; ED: emergency department. † Measurements of association are adjusted for age, sex, body mass index and other confounding variables.
Reproduced from Talman et al. with permission [73]

Prognosis

There is also association between EAT and future incident myocardial infarction, with the most robust data from the Heinz-Nixdorf recall study. In this large epidemiologic study of 4,093 patients with a mean follow up of 8 years, higher quartiles of EAT were associated with a 1.5 times increase in the risk of myocardial infarction independent of coronary calcium score and other cardiovascular risk factors[100].

Table 7: Summary of studies of CT derived EAT and prognosis

Author	n	Outcome	Events	EAT aggregation	OR	HR	Covariates in multivariable model
Cheng[94]	232	MACE	58	Log EAT	1.74 (1.03-2.95)		Age, traditional risk factors, CAC and FRS
D'Marco[105]	95	All-cause death	27	10mL increment		1.06 (1.01-1.05)	Age, gender, race, BMI, HDL cholesterol, total CAC
Forouzandeh[106]	760	MACE	45	>125mL		1.59 (0.81-3.09)	FRS, BMI and CAC
Kunita[107]	722	MACE	37	>107.2mL		2.65 (1.23-5.7)	age, sex, BMI, hypertension, diabetes, smoking
Mahabadi[100]	4093	MACE	130	Doubling of volume		1.54 (1.09-2.19	Age, gender and traditional risk factors
Shmilovich[108]	226	MACE	58	>68mL/m2	3.1 (1.4-6.9)		

Reproduced from Spearman et al. with permission [109]

Given the purported pathophysiology of EAT on atherosclerosis genesis, and the links to future cardiovascular prognosis, it is possible that EAT may modify plaque to develop high risk features that have also been associated with future acute coronary syndrome. There has been an influx of new data within this area of EAT research from small studies, however no formal systematic review or analyses has been performed to maximize power to address the association and assess for potential factors of heterogeneity. In addition, the natural history to assess the effect of clinical variables that may modulate EAT is not known as well as the association of EAT with quantifiable plaque measurements. The use of CTCA which is employed in symptomatic patients with low-intermediate probability of coronary artery disease may allow simultaneous assessment of EAT and coronary plaque as well as serial measurement of these with low radiation dose. Importantly, 67% of patients who undergo CTCA will have non-obstructive coronary artery disease[110] and it is in this group of patients that the least knowledge of EAT has been investigated.

CHAPTER 2:

ASSOCIATION OF EPICARDIAL ADIPOSE TISSUE AND HIGH-RISK PLAQUE CHARACTERISTICS: A SYSTEMATIC REVIEW AND META-ANALYSIS

Nitesh Nerlekar, Adam J Brown, Rahul G Muthalaly, Andrew Talman, Thushan Hettige, James D Cameron MD, Dennis TL Wong

Journal of the American Heart Association 2017;6:e006379

ABSTRACT

Background

Epicardial adipose tissue (EAT) is hypothesized to alter atherosclerotic plaque composition, with potential development of high-risk plaques (HRP). EAT may be measured by volumetric assessment (EAT-v) or linear thickness (EAT-t). We performed a systematic review and random effects meta-analysis to assess the association of EAT with HRP, and whether this association is dependent on the measurement method used.

Methods and Results

Electronic databases were systematically searched until October 2016. Studies reporting HRP by computed tomography or intracoronary imaging, and studies measuring EAT-v or EAT-t were included. Odds ratios (OR) were extracted from multivariable models reporting the association of EAT with HRP and are described as pooled estimates with 95% confidence intervals (CI). Analysis was stratified by EAT measurement method. Nine studies (n=3,772 patients) were included with 7 measuring EAT-v and 2 EAT-t. Increasing EAT was significantly associated with the presence of HRP, OR 1.26 (95% CI 1.11-1.43, p<0.001). Patients with HRP had higher EAT-v than those without: weighted mean difference 28.3mL (95% CI 18.8-37.8mL, p<0.001). EAT-v was associated with HRP, OR 1.19 (95% CI 1.06-1.33, p<0.001), however EAT-t was not, OR 3.09 (95% CI 0.56-17, p=0.2). Estimates remained significant when adjusted for small-study effect bias, OR 1.13 (95% CI 1.03-1.28, p=0.04).

Conclusions

Increasing EAT is associated with the presence of HRP and patients with HRP have higher quantified EAT-v. The association of EAT-v with HRP is significant compared to EAT-t however larger scale study is still required and further evaluation needed to assess whether EAT may be a potential therapeutic target for novel pharmaceutical agents.

Clinical trial registration: PROSPERO (Registration number: CRD42017055473). https://www.crd.york.ac.uk/PROSPERO/display_record.asp?ID=CRD42017055473

INTRODUCTION:

Epicardial adipose tissue (EAT) is a metabolically active fat depot, abundant in pro-inflammatory cytokines, and has been correlated with the extent and severity of coronary artery disease[74]. EAT shares the same embryologic origin of omental and mesenteric fat[60, 73] and encases the coronary arteries with no fascial barrier[4]. Therefore, it has been postulated that EAT may display vasocrine or paracrine effects on the adjacent arterial wall to influence atherosclerotic plaque composition, resulting in the development of high-risk plaque (HRP) [89, 91, 111-113]. The presence of HRP has shown association with future adverse prognosis[27, 32], but the management of these patients remains uncertain. HRP may be visualised invasively by several methods including intravascular ultrasound (IVUS) and optical coherence tomography (OCT), and non-invasively by computed tomography coronary angiography (CTCA) with good diagnostic agreement between techniques[28, 114, 115] EAT may be measured either volumetrically by CTCA or non-contrast CT (EAT-v), or by a linear thickness measurement on echocardiography (EAT-t). Both thickness and volume measures have been associated with incident CAD[74], however linear thickness may underrepresent the totality of EAT.

The objective of this systematic review and meta-analysis is to explore the association between EAT and the presence of HRP. The secondary aims are to evaluate whether increasing EAT volume associates with HRP presence as well as the strength of association with presence of HRP by EAT measurement method.

MATERIALS AND METHODS:

Data sources and search strategy:

The search was conducted in Medline, Embase and Pubmed databases with no start date until October 2016. Keywords using Medical Subject Heading included: 'epicardial adipose tissue', 'epicardial fat', 'pericardial adipose tissue', 'pericardial fat', 'vulnerable plaque', 'high risk plaque', 'low attenuation plaque', 'napkin ring', 'positive remodelling', 'spotty calcification', 'coronary artery disease', 'plaque characteristics', 'plaque composition', 'plaque vulnerability', 'thin cap fibroatheroma', 'intravascular ultrasound', 'optical coherence tomography', and 'angioscopy'. The reference lists of eligible articles were hand-searched for additional articles. Searches were restricted to human studies. We conducted this systematic review in accordance with the PRISMA statement and the trial was registered with PROSPERO (Registration number: CRD42017055473). A flow chart describing the study search is presented in **Figure 1**, and example search term strategy in **Supplement Table S1**.

Study selection

The inclusion criteria for the study were: patients undergoing either intracoronary imaging or CTCA evaluation with reported HRP features; non-invasive measurement of epicardial adipose tissue by either CT derived volume (on contrast or non-contrast CT), or linear thickness by CT or echocardiography; fully published in peer-reviewed journals. For intracoronary imaging studies, HRP was defined as the presence of thin-cap fibroatheroma (TCFA). For CT studies, HRP included plaques either with one or more of the following features, including low attenuation plaque (LAP), positive remodelling (PR), spotty calcification and the napkin ring sign (NRS). Study specific definitions of HRP are reported in **Supplementary Table S2.**

Data extraction:

Odds ratios (OR) and their respective 95% confidence intervals (95% CI) for association of EAT with HRP were extracted. Where possible, odds ratios from multivariable models that adjusted for other coronary artery disease risk factors were used, and covariates within the model were recorded. Mean and standard deviation of EAT volume between groups with and without HRP were entered. Studies reporting medians with interquartile ranges were converted to means as previously recommended [116].

Endpoints

The primary endpoint was the pooled association of EAT with the presence of HRP. Secondary endpoints included the pooled quantitative difference of EAT-v in patients with and without HRP, as well as the association of EAT with HRP stratified by EAT measurement method (EAT-v or EAT-t).

Statistical analysis

Statistical analysis was performed using StataMP 14.0 (Stata Corp LP, College Station, TX). OR were examined on the log scale and transformed for graphical presentation with 95% CI reported. In cases where multiple outcomes were reported i.e. by individual plaque feature or by grouped features, the analysed estimate was the association of EAT with any HRP if specified. Random effects modelling was used with the method of DerSimonian and Laird[117]. The weighted mean difference (WMD) for EAT between groups with and without HRP was calculated. Statistical heterogeneity was evaluated by the I^2 statistic and quantified as low (<25%), moderate (25-75%) or high (>75%)[118]. Sensitivity analysis was performed by EAT measurement method (volumetric or thickness based, by pooled estimates of similarly defined EAT covariate parameters i.e. when EAT was included as a continuous variable or assessed in 10mL increments and for individual plaque features where possible). Additional sensitivity analysis using random effects with the Hartung-Knapp-Sidik-Jonkman approach was used to explore effect sizes when 2 studies were grouped [119, 120]. Exploratory meta-regression was performed

to assess the influence of independent variables (mean study ages, mean EAT volume, mean study body mass index, and proportion of HRP). Publication bias was assessed by the Egger and Begg test. The Duval and Tweedie's trim and fill method was also used to investigate publication bias as well as systematic exclusion of individual studies to assess for changes in the pooled estimate. A two-sided p-value of <0.05 was considered significant.

RESULTS:

There were a total of 90 publications reviewed with 9 studies included for final analysis (3,772 subjects) (**Figure 1**). One study was excluded as it presented the association of EAT with plaque lipid percentage rather than specified numbers of patients with HRP[121]. Seven studies reported CT-HRP [40, 98, 101, 122-126] (n=3,573) and 2 studies, invasive-HRP[39, 127] (n=199). Seven studies measured EAT-v [39, 40, 98, 101, 122, 124, 125, 128] (n=3,284), and 2 studies measured EAT-t [126, 127] (n=488). All study designs were cross-sectional. All patients were from suspected coronary artery disease cohorts with 2 studies evaluating patients with suspected acute coronary syndrome[98, 122]. Study characteristics are presented in **Table 1 and 2** and regression modelling outcomes and model covariates presented in **Table 3**. Individual study EAT measurement characteristics and HRP definitions are presented in **Supplement Table S2**.

The prevalence of HRP ranged widely, from 4-59% at a per-patient level (**Table 1**). The primary endpoint demonstrated a significant association of increasing EAT with the presence of HRP: pooled odds ratio (OR) 1.26 (95% CI 1.11-1.43, p<0.001, I^2=81%) (**Figure 2**).

Analysis to assess quantitative differences in EAT between patients with and without HRP demonstrated a weighted mean difference of +28.3mL in those patients with HRP (95% CI 18.8-37.8mL, p<0.001, I^2=58%) based on 4 studies (**Figure 3**).

When stratified by EAT measurement method, in the 7 studies measuring EAT-v, the pooled OR was significantly associated with HRP presence: OR 1.19 (95% CI 1.06-1.33, p<0.001, I^2=78%). However, there was no significant association observed with the two EAT-t studies and presence of HRP: OR 3.09 (95% CI 0.56-17, p=0.20, I^2=90%) (**Figure 4**). This remained statistically non-significant on sensitivity analysis with the HKSJ method (**Table 4**).

Sensitivity analysis was performed to assess pooled estimates of studies using EAT as a similarly measured covariate. Two studies analysed EAT-v in 10mL increments and demonstrated a pooled OR 1.18 (95% CI 1.12-1.24, p<0.001, I^2=0%) which however became non-significant when analysed with the HKSJ method (OR 1.18 (95% CI 0.84-1.64, p=0.10). In the two studies that analysed EAT-v as a continuous variable the pooled OR 1.18 (95% CI 0.77-1.81, p=0.44, I^2=52%) which remained non-significant after analysis with HKSJ (**Table 4**). EAT measured in the remaining studies were modelled as per standard deviation or by a dichotomous threshold level and not formally pooled.

Further sensitivity analysis was performed to assess the association between specific HRP subtypes with information obtainable from 2 studies. There was an association demonstrated between increasing EAT and low attenuation plaque, (OR 2.79, 95% CI 1.71-4.53, p<0.001, I^2=0%), positive remodelling, (OR 1.93, 95% CI 1.25-2.99, p=0.003, I^2=0%) and when both features were present (OR 2.58, 95% CI 1.55-4.28, p=0.001, I^2=0%). However, both the results for LAP and PR became statistically non-significant after application of the HKSJ method, but presence of both features remained significantly associated with increasing EAT (**Table 4**).

Exploratory meta-regression demonstrated no significant influence of varying study-level predictors on the overall effect size: mean BMI (OR 0.95, 95% CI 0.79-1.14, p=0.55); mean age (OR 1.03, 95% CI 0.96-1.10, p=0.38); population proportion of HRP (OR 0.99, 95% CI 0.98-1.00, p=0.42) and mean EAT volume (OR 1.00, 95% CI 0.97-1.03, p=0.99).

There was evidence of publication bias by calculation of the Egger test for small-study effects, p=0.005. Using the trim and fill method, the overall estimate remained significant for the association of EAT and HRP, pooled estimate 1.13 (95% CI 1.03-1.28, p=0.04, I^2=81%) (**Supplementary figure S1**). Analysis to assess the influence of single studies on the effect estimate demonstrated that there was a persistent significant association of increasing EAT with HRP. The lowermost pooled estimate OR 1.16 (95% CI 1.06-1.27, p=0.001, I^2=74%) occurred with the exclusion of Tachibana et al, and the upper most pooled estimate OR 1.27 (95% CI 1.12-1.45, p<0.001, I^2=70%) with the exclusion of Lu et al (**Supplementary Table S3**).

DISCUSSION

The results from this meta-analysis of 9 observational studies demonstrate three important findings. Firstly, increasing EAT is significantly associated with the presence of HRP features. Secondly, patients with HRP have a significantly increased volume of EAT compared to those without HRP. Finally, EAT associates with HRP presence ideally when measured by complete volumetric analysis rather than linear EAT thickness measurements.

EAT is a visceral adipose tissue depot rich in pro-inflammatory and pro-atherogenic cytokines including monocyte chemotactic protein-1, interleukin (IL)-6. IL-1β, IL-6sR and tumour necrosis factor alpha[63]. Due to its anatomic proximity to the adjacent myocardium and lack of fascial barrier with the epicardial coronary arteries, it is postulated that there may be paracrine or vasocrine signalling of cytokines between the surrounding fat and the underlying arterial wall[73]. This suggested pathophysiology is analogous to the visceral intra-abdominal adipose tissue surrounding the portal circulation that is purported to influence the development of hepatic steatosis[129]. It has been demonstrated that increased EAT volume is related to both the extent and lesion severity of coronary stenosis[130] and contains a greater amount of inflammatory cytokines compared to serum circulating

levels and subcutaneous adipose stores[72]. The apposition of EAT with the arterial adventitia lends itself to the "outside-in" hypothesis of atherosclerosis, whereby the inflammatory milieu of EAT leads to vascular inflammation of the adventitia progressing inward to the intima leading to plaque formation. Therefore, it is possible that cellular cross talk may lead to the development of plaque characteristics considered to be of 'high risk' due to their association with major adverse cardiovascular events. It has also been reported that high EAT levels are associated with mortality, although it remains unclear whether these are specifically related to preceding cardiovascular events[75]. Our results indicate a uniform association of increasing EAT with HRP, but further study is needed to establish the influence and interaction of these parameters with prognosis. Importantly, we aimed to use risk estimates from multivariable models, which suggests an incremental effect of EAT with HRP presence beyond traditional cardiovascular risk factors.

As there is no guideline advocated technique for EAT quantification, individual studies are subject to authors' discretion and experience. The inter-observer variability for EAT-t has shown mixed results[131] and a measure of linear thickness by 2-dimensional assessment may under or over-represent total EAT volume due to changes in probe angulation. It has been suggested that a threshold of 7mm confers elevated EAT-t which is significantly higher than our included studies which may also influence interpretation. Only one previous study has evaluated EAT-t vs. EAT-v in 71 patients reporting a modest correlation ($r=0.595$)[81]. However, EAT-v also has limitations, with differing values measurable with the use of contrast media[85], and possible differences related to vendor specific software algorithms. In our analysis of EAT-v vs. EAT-t, we demonstrated that EAT-t had a decidedly wide confidence interval for the association with HRP and failed to reach statistical significance, although this is only based on 2 studies with a total of 488 patients. On the contrary, EAT-v displayed a significant association with HRP with more precise confidence limits. We attempted to explore the association further by analysing the modelling method of EAT which demonstrated uncertainty in

estimates for differing techniques which highlights the need for a standardised and consistent approach when incorporating EAT into models to assess disease outcomes.

In our subgroup analysis of EAT association with HRP subtype, we noted that there was a strong association individually with LAP and positive remodelling as well as with the presence of both features after adjustment for conventional cardiovascular risk factors. However, association with individual plaque features types diminished due to imprecision in 95% confidence intervals, but remained for presence of both high-risk features. The largest study to date of 3,158 patients by Motoyama et al reported that these high-risk plaque characteristics, defined as the presence of either or both these features, is strongly associated with future ACS development (adjusted Hazard Ratio 8.24, 95% CI 5.26-12.96, p<0.001) [27]. EAT was not measured in this study and it remains unclear of its contribution to prognosis.

It is notable that some observational studies have demonstrated a lack of relationship between EAT and significant CAD [132, 133] and similar to our included studies, all of which are observational, are prone to significant bias. These include selection and ascertainment bias and the variable use of predictors in regression modelling that may alter reported estimates and contribute to between study heterogeneity. To assess study quality, we evaluated the GRADE classification [134-136] (**Supplemental Table S4 and S5**), which apportions an overall study quality assessment. As none of the trials are by definition of high quality given they are not randomised controlled trials, the overall information quality is regarded as low and should therefore be interpreted as such without drawing firm conclusions that may alter clinical decision making. Despite the inconsistency of CAD association, given the association of HRP with cardiac prognosis, it remains plausible that EAT may influence plaque composition that may not be diagnosed as functionally or anatomically significant. Rigorous prospective study to assess EAT role in atherogenesis is still warranted.

The management of HRP features is uncertain. EAT is currently only measured for research purposes, however the importance of assessing EAT and its association with HRP relates to a potential target for therapeutic intervention. EAT has demonstrated temporal changes in plaque and cardiovascular risk. In a study of non-obese patients undergoing serial CT over 4 years, an increase in EAT volume was associated with HRP as well as future acute coronary syndrome despite optimal management of cardiovascular risk factors [30]. Calorie restriction and bariatric surgery rather than exercise have shown promise as methods for reduction in EAT as recently explored in a meta-analysis by Rabkin et al. [137] and animal data has demonstrated that selective surgical excision of EAT slows the progression of atherosclerosis[138]. It remains to be seen if targeted EAT reduction may improve dynamic atherosclerosis in human subjects and randomised controlled trial data are lacking.

Study limitations

Our analysis is limited by the observational nature of included studies, as well as a lack of access to patient level data to allow adjustment for other covariates that may influence EAT including sex differences, as well as stratification and assessment by other population features such as traditional cardiovascular risk factors of hypertension, hyperlipidaemia and diabetes. We attempted to account for this by using model estimates that adjusted for several of these variables. The majority of studies were also performed in Japanese centres and may limit the generalizability of our findings to other ethnic populations. A further important limitation is the inclusion of only 2 studies evaluating EAT-thickness and other subgroup parameters. This limits the interpretation of results with this methodology due to potential lack of power and firm conclusions cannot be drawn. Importantly, we note that when more robust statistical methods were applied when few studies were pooled, statistical significance was reversed highlighting the need for more data in these areas. We noted a significant degree of heterogeneity, a limitation that has been demonstrated in other published EAT meta-analyses

that report I^2 values >90% [74, 87]. This is probably in part representative of variable EAT quantification methods, and differing measures of EAT as a covariate in regression analyses. We attempted to adjust for this heterogeneity by systematic exclusion of studies that did not significantly attenuate the summary estimates from statistical significance, as well as sensitivity analysis by sub-group analysis and exploratory meta-regression.

CONCLUSION:

Increasing EAT is associated with the presence of HRP, ideally when measured by complete volumetric analysis. Further investigation is still required to establish the role of EAT-t in evaluating HRP, as well as consistent methods for modelling EAT as a variable for disease outcomes and the effect of EAT on individual high-risk plaque features. Incorporating the measurement of EAT on clinically performed CTCA has potential to improve patient risk stratification and further prospective studies are needed to confirm this finding which holds potential as a novel therapeutic target for atherosclerotic treatment.

Table 1: Demographic, EAT and HRP parameters of included studies

Author	EAT method	Population	Sample size	EAT value	HRP proportions
Lu et al.[122]	EAT-v (CACS)	Suspected ACS	467	**Median EAT:** 108.5 cc (IQR 76.4-140.6cc) **With HRP** 123 cc (IQR 93-156cc) **Without HRP** 98 cc (IQR 68-127cc)	HRP in 167 (36%) patients **NRS** in 15% **PR** in 32.3% **LAP** in 23.4% **SpC**: in 91%
Schlett et al.[98]	EAT-v (CTCA)	Suspected ACS	358	**Median EAT:** 95.2 (IQR 66-130.1) cm^3 **With HRP:** 151.9 (IQR 10.-179.4) cm^3 **Without HRP** 110 (IQR 81.5-137.4) cm^3	Any HRP in 13 (4%) patients
Rajani et al.[101]	EAT-v (CACS)	suspected CAD	402	**Mean EAT:** 103 ± 51 cm^3 **With any HRP** 116 ± 53 cm^3 **Without HRP** 99 ± 57cm^3	Any HRP in 113 (59%) patients **LAP** in 67 (35%) **PR** in 93 (48%)
Oka et al.[124]	EAT-v (CACS)	suspected CAD	357	**Mean EAT:** 125 ± 44 mL	87 (24%) with all three HRP **LAP** EAT<100mL: 52%

				EAT analysis threshold of 100mL	EAT≥100mL: 27% **PR** EAT<100mL: 58% EAT≥100mL: 37% **LAP + PR** EAT<100mL: 46% EAT≥100mL: 25%
Ito et al.[40]	EAT-v (CACS)	Suspected CAD (symptomatic) with zero CACS	1308	**Mean EAT:** 98.1 ± 41.3 cm^3 **With HRP** 133 ± 40.2 cm^3 **Without HRP** 95.1 ± 40.3cm^3	Any HRP in 63 (5%) patients
Nakanishi et al.[125]	EAT-v (CTCA)	suspected CAD in patients with CKD	275	**Mean EAT:** CKD 111 ± 41 mL (n=110) No CKD 81 ± 29 mL (n=165)	Any HRP in 44 (16%) patients
Ito et al.[39]	EAT-v (CTCA)	Scheduled for PCI and underwent CT in addition to OCT	117 (244 plaques)	**EAT-v Tertiles:** **Tertile 1 (T1):** <104.1cm^3 (n=39) **Tertile 2 (T2):** 104.1 – 130.7 cm^3 (n=39) **Tertile 3 (T3):** >130.7 cm^3 (n=39)	Total TCFA: 51 (21%) plaques TCFA: T1: Single TCFA n=6 (15%) Multiple TCFA n=1 (3%) T2: Single TCFA n=7 (18%) Multiple TCFA n=3 (8%) T3: Single TCFA n=12 (31%) Multiple TCFA n=8 (21%) Minimum fibrous cap thickness

					T1: 102.7±69.2µm T2: 102.5±56.5µm T3: 78.2±43.9µm <u>Maximal lipid arc</u> T1: >2 quadrants 13 (33%) T2: >2 quadrants 14 (36%) T3: >2 quadrants 25 (64%) <u>CT characteristics:</u> T1: LAP 4 (10%) PR 8 (21%) T2: LAP 14 (36%) PR 13 (33%) T3: LAP 16 (41%) PR 21 (54%)
Park et al.[127]	EAT-t (Echo)	Angiographically significant CAD undergoing PCI ± IVUS	82	**<u>Mean EAT-t</u>** 3.4 ± 2.2mm EAT-t 3.5mm threshold EAT <3.5mm (n=21) EAT ≥3.5mm (n=39)	<u>TCFA (n)</u>: EAT <3.5mm: 3.3 ± 2.2 EAT ≥3.5mm: 2.1 ± 1.6 <u>Mean volume index necrotic core (mm^3/mm):</u> EAT <3.5mm: 0.3 ± 0.2 EAT ≥3.5mm: 0.6 ± 0.4 Plaque volume (mm^3): EAT <3.5mm: 1360.1 ± 492.1 EAT ≥3.5mm: 1048.5 ± 398.2
Tachibana et al.[126]	EAT-t (Echo)	Suspected CAD	406	EAT-t 5.8mm threshold EAT ≥5.8mm (n=238) EAT <5.8mm (n=168)	HRP in 45 (11%) patients **<u>LAP</u>** EAT <5.8mm: 4% EAT ≥5.8mm: 24% **<u>PR</u>** EAT <5.8mm: 39% EAT ≥5.8mm: 60%

					LAP+PR EAT <5.8mm: 3% EAT ≥5.8mm: 17%

ACS – acute coronary syndrome, CACS – coronary artery calcium score (non-contrast CT), CAD – coronary artery disease, CKD – chronic kidney disease, CTCA – computed tomography coronary angiography, EAT – epicardial adipose tissue, EAT-t – epicardial adipose tissue thickness, EAT-v – epicardial adipose tissue volume, HRP – high risk plaque, IQR – interquartile range, IVUS – intravascular ultrasound, LAP – low attenuation plaque, NRS – napkin ring sign, OCT – optical coherence tomography, PCI – percutaneous coronary intervention, PR – positive remodeling, RI – remodeling index, SAP – stable angina pectoris, SpC – spotty calcification, TCFA – thin-cap fibroatheroma

Table 2: Study demographic data

Author	Diabetes (%)	Hypertension (%)	Hyperlipidaemia (%)	BMI	Ethnicity	Age	Sex (%)
Lu et al.[122]	17	53	45	29 ± 5	Not specified	54 ± 8	53
Schlett et al.[98]	10	39	37	28(25-32)	Not specified	51(45-59)	62
Rajani et al.[101]	14	54	63	27 ± 4	Not specified	66(23-92)	56
Oka et al.[124]	31	68	50	24 ± 5	Japanese institution	66 ± 11	63
Ito et al.[40]	8	33	26	23 ± 4	Japanese institution	59 ± 12	46
Nakanishi et al.[125]	38	65	59	24 ± 4	Japanese institution	65 ± 10	66
Park et al.[127]	29	61	20	25 ± 3	Korean Institution	59 ± 11	54
Ito et al.[39]	24	61	44	24 ± 3	Japanese institution	66 ± 9	82
Tachibana et al.[126]	27	58	31	23 ± 4	Japanese institution	68 ± 13	57

BMI – body mass index. Values represent total study cohort proportions (%), or expressed as mean ± standard deviation or median (IQR).

Table 3: EAT modelling outcomes and model covariates

Author	EAT modelling	Regression outcomes	Covariates in multivariable model	Threshold / ROC AUC values
Lu et al.[122]	Indexed EAT and Absolute EAT	**Any HRP** OR 1.04 (95% CI 1-1.08, p=0.04) with indexed EAT-v **Any HRP** OR 1.02 (95% CI 1-1.03, p=0.046) with absolute EAT-v	Age, sex, number of cardiovascular risk factors, log CACS, >50% stenosis	Optimal threshold 62.3 cc/m^2 with sensitivity 48.5%, specificity 72.7%. No ROC AUC specified
Schlett et al.[98]	EAT per SD (49.8mL)	**Presence of HRP** OR 1.79 (95% CI 1.13-2.76, p=0.008)	Not specified	Not reported
Rajani et al.[101]	Log EAT-v	**Any HRP** OR 1.7 (95% CI 0.9-3.4, p=0.038) **LAP** OR 2.4 (95% CI 1.1-5.1, p=0.02) **PR** OR 1.8 (95% CI 1.0-3.4, p=0.07) **Both HRP features** OR 2.6 (95% CI 1.1-6.2, p=0.03)	Age, BMI, Diabetes, hypercholesterolaemia, smoking, family history, hypertension	ROC AUC 0.756 for any HRP presence with sensitivity 62%, specificity 84% Optimal threshold of EAT <74.07cm^3 excluded any HRP
Oka et al.[124]	High EAT-v vs Low-EAT-v (100mL threshold)	**LAP** OR 3.08 (95% CI 1.66-5.83, p<0.001) **PR** OR 2.08 (95% CI 1.12-3.88, p=0.02) **SpC** OR 1.11 (95% CI 0.61-2.04, p=0.73) **LAP+PR** OR 2.56 (95% CI 0.81-3.44, p=0.003) **All 3 features** OR 1.65 (95% CI 0.17, p=0.17)	Age, sex, hypertension, diabetes, smoking, BMI, VAT area, CACS	Using a threshold of 100mL, sensitivity for LAP + PR 80%, specificity 41%

Ito et al.[40]	EAT-v per 10cm^3	**Any HRP** OR 1.19 (95% CI 1.12-1.27, p<0.01)	Male, Diabetes, hypertension, BMI	ROC AUC 0.75 for any HRP presence at optimal threshold 127.1cm^3 with sensitivity 64%, specificity 81%
Nakanishi et al.[125]	EAT-v per 10mL	**Presence of HRP** OR 1.15 (95% CI 1.05-1.26, p=0.003)	Age per 10y, sex, hypertension, diabetes, hyperlipidaemia, smoking, BMI	
Ito et al.[39]	Highest tertile of EAT	**Presence of TCFA** OR 2.92 (95% CI 1.13-7.55, p=0.027) Correlation of EAT with fibrous cap thickness r= -0.400, p<0.01	ACS, BMI	ROC AUC 0.721 for detection of TCFA with optimal threshold 126.7cm3, sensitivity 69% specificity 71%
Park et al.[127]	High EAT-t vs Low-EAT-t (3.5mm threshold)	**Total TCFAs** in symptom related vessel β-coefficient 0.106 (95% CI 0.004-0.208, p=0.043)	BMI, diabetes, dyslipidaemia, metabolic syndrome	Not specified
Tachibana et al.[126]	High EAT-t vs Low-EAT-t (5.8mm threshold)	**Presence of HRP** OR 7.98 (95% CI 2.77-22.98, p<0.01)	Age, sex, BMI, VAT, hypertension, dyslipidaemia, diabetes, smoker, CACS>100, stenotic vessel number, renal insufficiency, statins	ROC AUC 0.77 for HRP (combination of LAP + PR) at threshold of 5.8mm with sensitivity 83%, specificity 64%

ACS – acute coronary syndrome, BMI – body mass index, CACS – coronary artery calcium score (non-contrast CT), CI – confidence interval, EAT – epicardial adipose tissue, EAT-t – EAT thickness, EAT-v – volumetric EAT, HRP – high risk plaque, LAP – low attenuation plaque, OR – odds ratio, PR – positive remodelling, ROC AUC – receiver operating characteristic area under the curve, SpC – spotty calcification, VAT – visceral adipose tissue

Table 4: Sensitivity analysis of random effects meta-analysis with alternative methods when pooled estimates were from combination of 2 studies.

Variable	Random effects method	Pooled OR	95% CI	p-value
EAT Measurement Method				
EAT thickness [126, 127]	DL	3.09	0.56-17.01	0.20
	HKSJ	3.09	0-19	0.49
Covariate Modelling Method				
EAT continuous [101, 122]	DL	1.18	0.77-1.81	0.44
	HKSJ	1.18	0.08-18.5	0.58
EAT per 10mL [40, 125]	DL	1.18	1.12-1.24	<0.01
	HKSJ	1.18	0.96-1.45	0.06*
HRP subtype				
LAP [101, 124]	DL	2.79	1.71-4.53	<0.01
	HKSJ	2.79	0.59-13.2	0.08*
PR [101, 124]	DL	1.93	1.25-2.99	0.003
	HKSJ	1.93	0.77-4.84	0.07*
Both LAP and PR [101, 124]	DL	2.58	1.55-4.28	<0.01
	HKSJ	2.58	2.34-2.83	0.005

References indicate studies that were pooled. Odds ratios (OR) are presented using DerSimonian and Laird (DL) and Hartung-Knapp-Sidik-Jonkman (HKSJ) methods. *signifies when there was a change in p-value resulting in statistical non-significance (p>0.05) after applying HKSJ method. CI – confidence interval, EAT – Epicardial adipose tissue, HRP – high risk plaque, LAP – low attenuation plaque, PR – positive remodelling

Figure 1: Search strategy

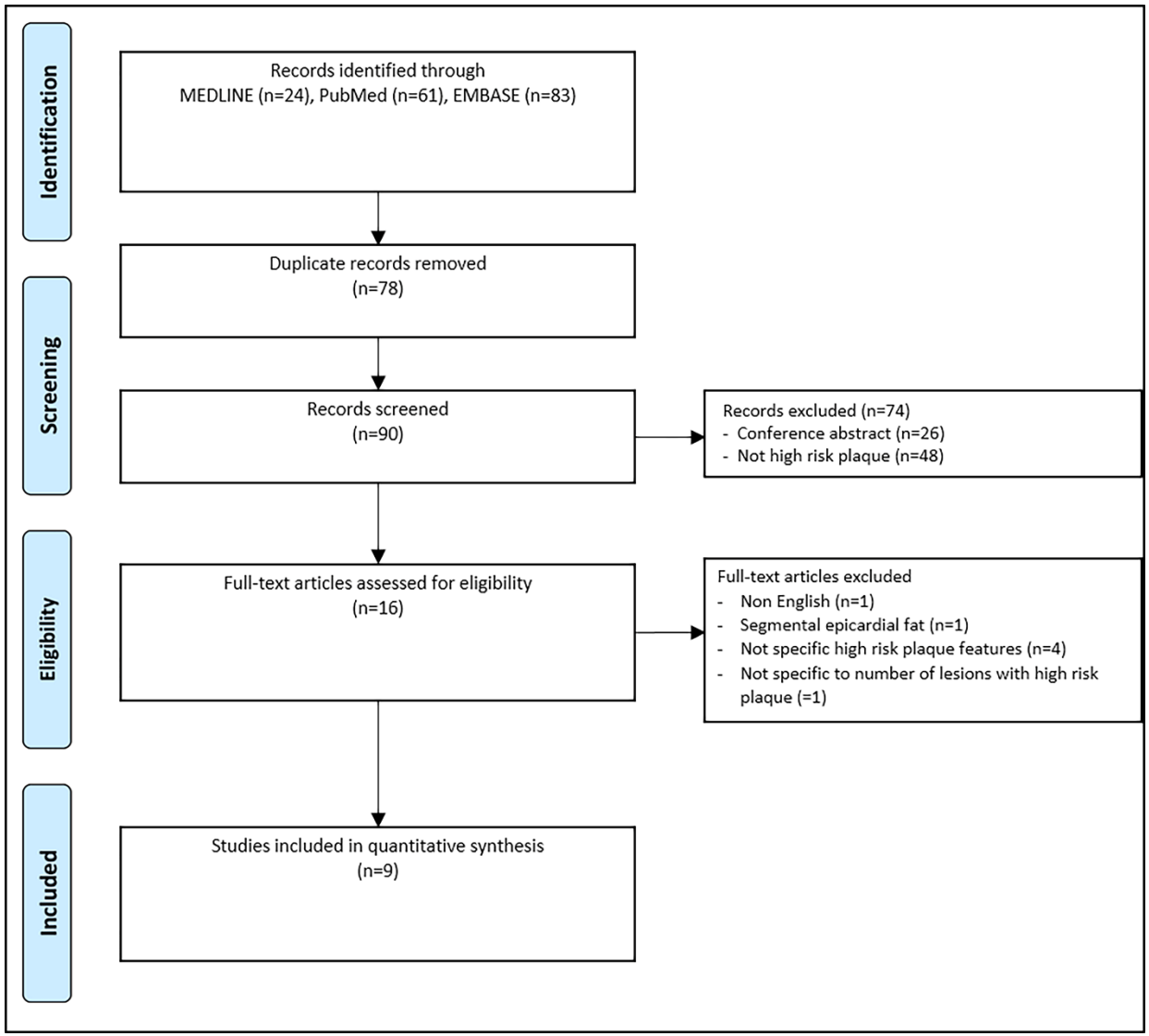

Figure 2: Association of EAT with presence of HRP

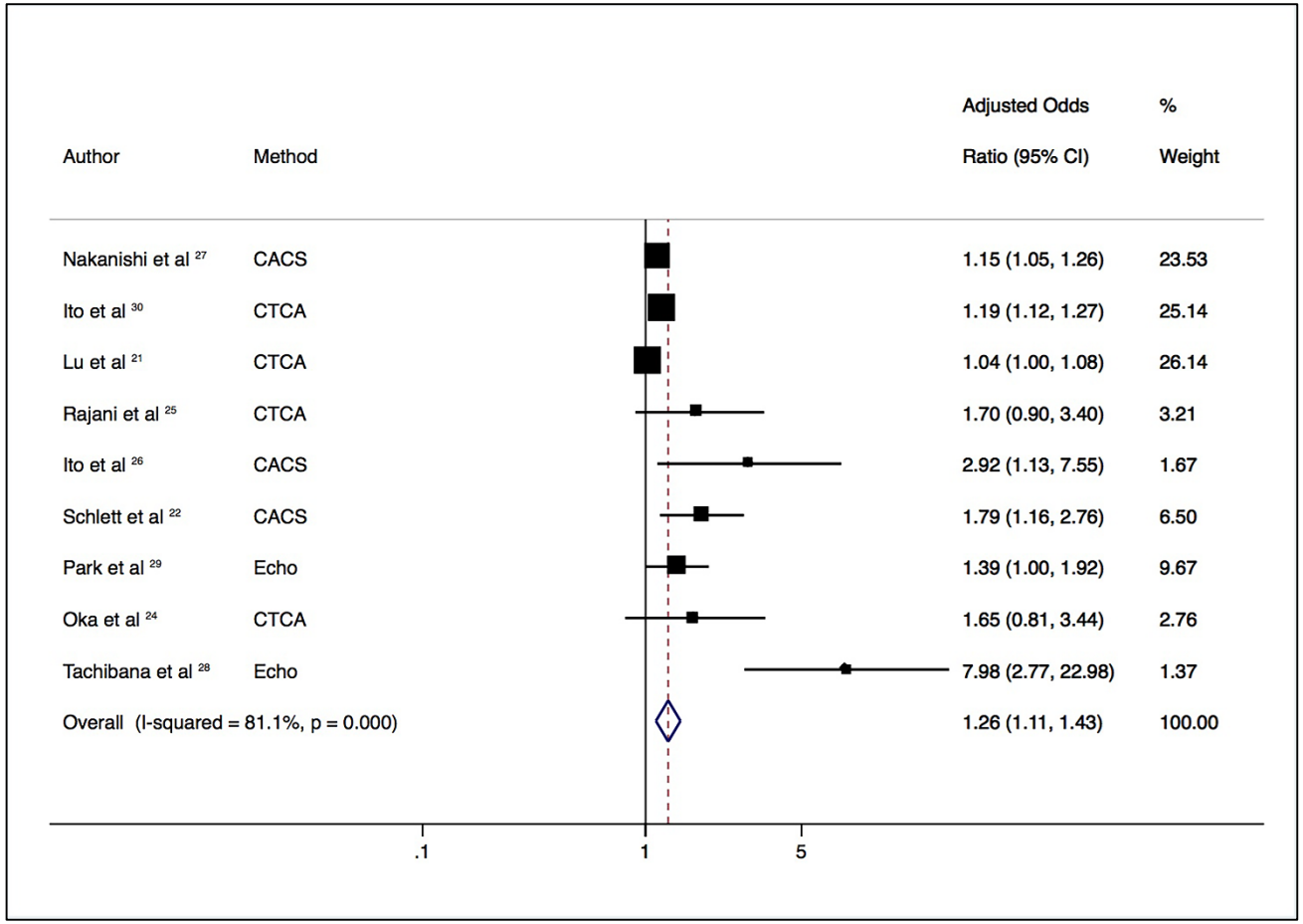

Forest plot displays summary odds ratio and 95% confidence intervals (CI) for the increasing association of EAT with HRP. Method represents radiologic method of calculating EAT. This demonstrates a significant association of increasing EAT with HRP.

CACS – coronary artery calcium score (non-contrast CT); CTCA – computed tomography coronary angiography; EAT – epicardial adipose tissue; Echo – echocardiography; HRP – high risk plaque

Figure 3: Difference in quantitative EAT

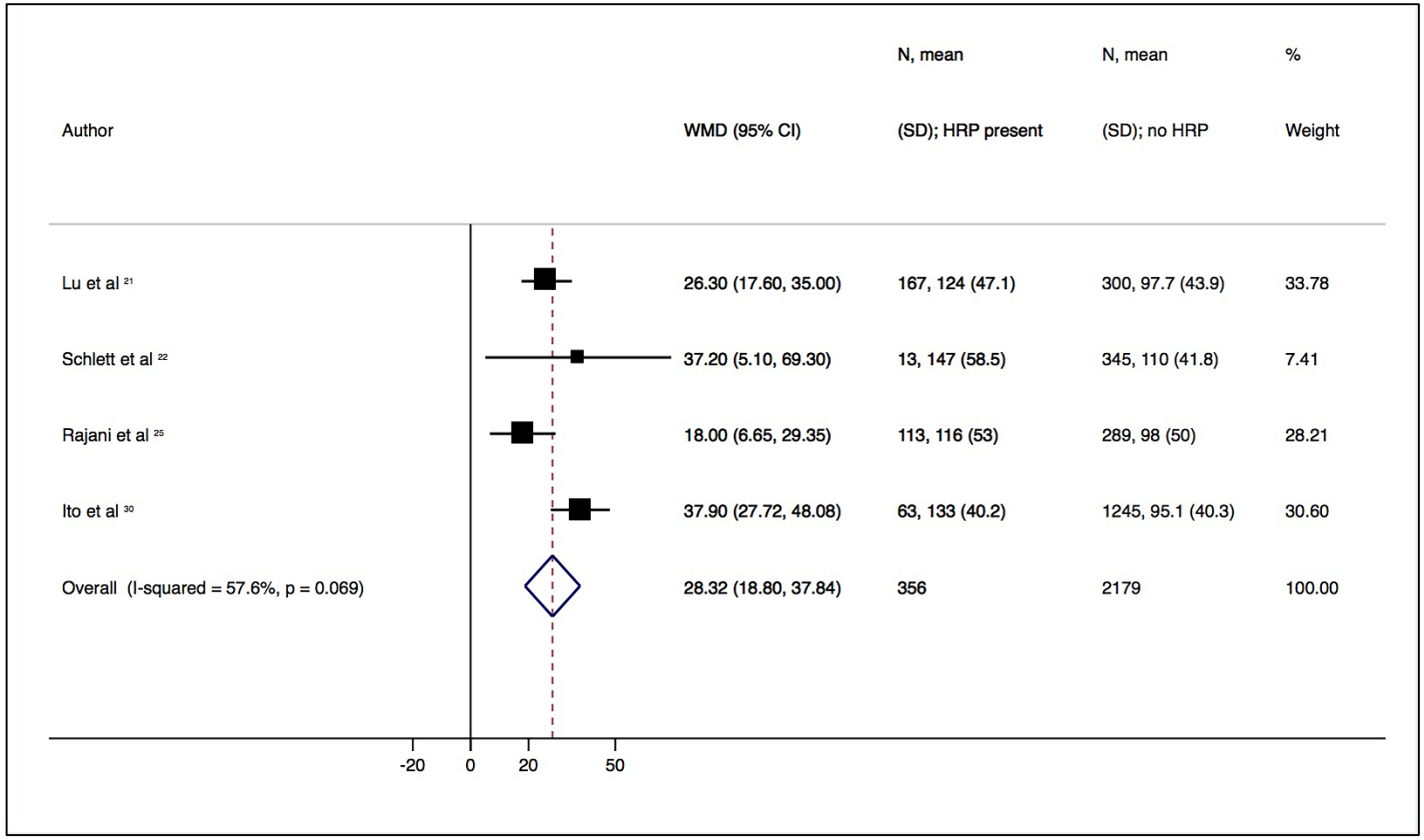

Forest plot displays weighted mean difference (WMD) and 95% confidence intervals (CI) for difference between patients with and without HRP. This indicates that patients with HRP have a significantly higher volume of EAT (28.3mL (18.8-37.8mL) compared to those patients without HRP.

EAT – epicardial adipose tissue; HRP – high risk plaque; mL – milliliters; SD – standard deviation

Figure 4: Pooled estimates by EAT measurement method

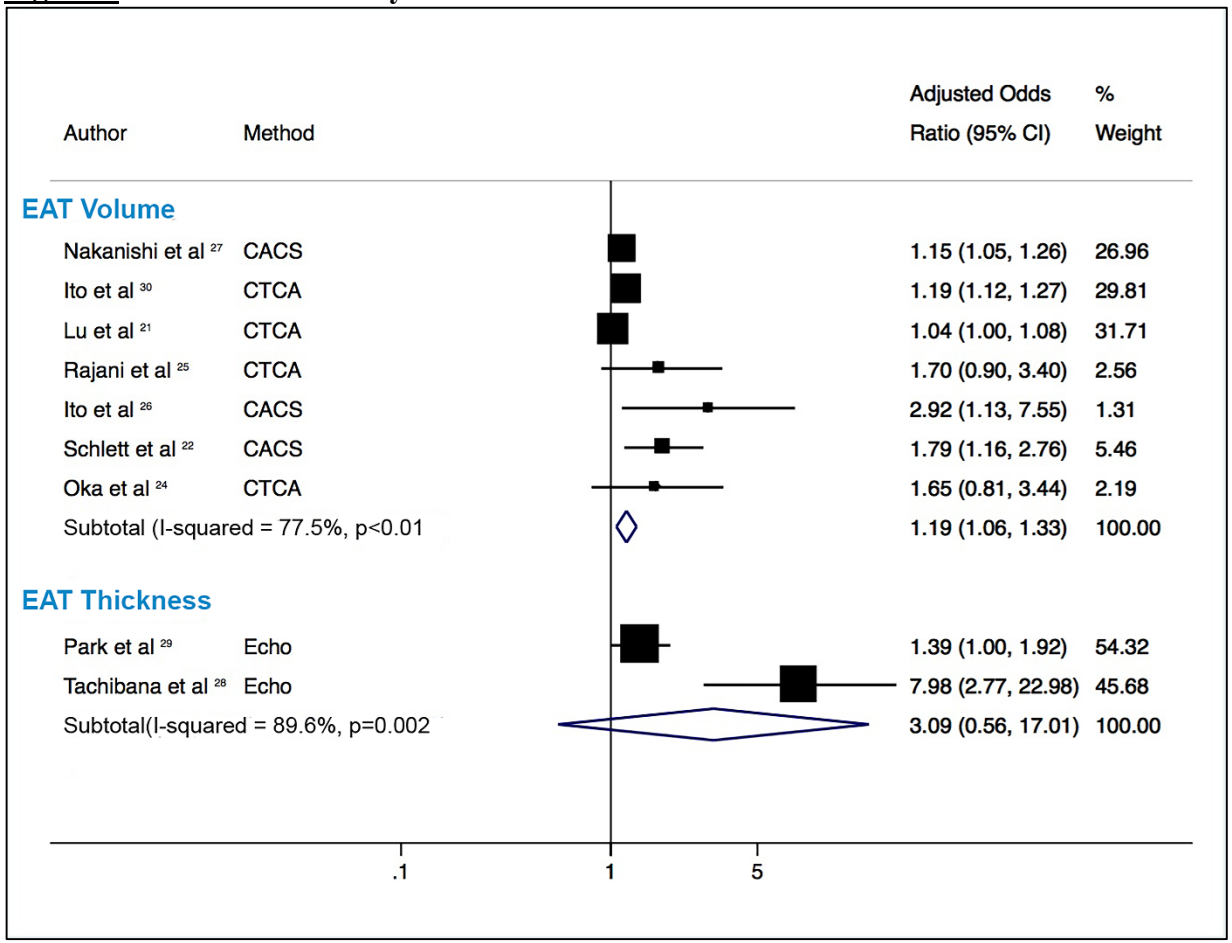

Forest plot displays odds ratio (OR) and 95% confidence intervals (CI) for the association of increasing EAT with HRP stratified by measurement method of EAT measurement, either by volume or thickness. This demonstrates that increasing EAT volume has a significant association with HRP, however increasing EAT thickness is not significantly associated with HRP and has a markedly wide confidence interval crossing the line of unity.

CACS – coronary artery calcium score (non-contrast CT); CTCA – computed tomography coronary angiography; EAT – epicardial adipose tissue; Echo – echocardiography; HRP – high risk plaque

SUPPLEMENTAL MATERIAL

The Association of Epicardial Adipose Tissue and High Risk Plaque Characteristics: a Systematic Review and Meta-Analysis.

Supplemental Table S1. Example search strategy (Embase)

#	***Searches***	***Results***
1	*Epicardial adipose tissue.mp.*	*1249*
2	*Epicardial fat.mp.*	*1481*
3	*Pericardial adipose tissue.mp*	*161*
4	*Pericardial fat.mp*	*550*
5	*Vulnerable plaque.mp*	*2196*
6	*High risk plaque.mp*	*288*
7	*Low attenuation plaque.mp*	*101*
8	*Napkin ring.mp*	*94*
9	*Positive remodelling*	*125*
10	*Spotty calcification*	*170*
11	*Plaque characteristics*	*1228*
12	*Plaque composition*	*1734*
13	*Plaque vulnerability*	*1745*
14	*Thin cap fibroatheroma*	*773*
15	*Necrotic core*	*2091*
16	*Exp intravascular ultrasound/*	*12695*
17	*Exp optical coherence tomography/*	*36156*
18	*Exp computer assisted tomography/*	*778928*
19	*Computed tomography coronary angiography.mp*	*1140*
20	*Cardiac computed tomography.mp*	*2526*
21	*Exp coronary artery calcium score*	*3230*
22	*Exp coronary angiography/*	*2916*
23	*1 or 2 or 3 or 4*	*2877*
24	*5 or 6 or 7 or 8 or 9 or 10 or 11 or 12 or 13 or 14 or 15*	*7800*
25	*16 or 17 or 22*	*51500*
26	*18 or 19 or 20 or 21*	*779979*
27	*23 and 24 and 25*	*26*
28	*23 and 24 and 26*	*57*

Supplemental Table S2: Study EAT measurement parameters and HRP definitions

Author	EAT measure method	Definition of HRP features
Lu et al.[122]	EAT definition: fat within pericardial sac. Method: Semi-automated. Software: Volume Viewer, Siemens Medical Solutions, Germany Interval: 1cm Superior border: mid-level RPA Inferior border: diaphragm HU range: -195 to -45 HU	PR: RI of >1.1 maximal outer vessel diameter at plaque divided by average of the proximal and distal normal vessels LAP: <30 HU SpC: <3mm CP extending <1.5mm long-axis vessel diameter & two-thirds vessel circumference NRS: ring of peripheral high attenuation surrounded by core of low attenuation in a non-calcified plaque
Schlett et al.[98]	EAT definition: fat within pericardial sac. Method: Manual Software: Leonardo, Siemens Medical Solutions Interval: 1cm Superior border: mid-level RPA. Inferior border: not specified. HU range: -190 to -30 HU	PR: >1.05 remodelling index LAP: <30 HU SC: <3mm diameter CP HRP defined as at least 2 characteristics in lesions>50% luminal narrowing
Rajani et al.[101]	EAT definition: fat within pericardial sac. Method: Semi-automated Software: QFAT, Cedars-Sinai Medical Centre Interval: 3mm (total 20-40 slices per pt.) Superior border: RPA take-off Inferior border: First slice where PDA visualised HU range: -190 to -30 HU	LAP: <30 HU PR: >1.05 (maximal outer arterial wall diameter along plaque exceeding proximal reference by 5%
Oka et al.[124]	EAT definition: adipose tissue between epicardial surface of myocardium and pericardium Method: Manual Software: Not specified. VAT measured with Virtual Place, AZE Inc., Japan Interval: 1cm Superior border: 1cm above left main coronary artery (atrial appendage) Inferior border: cardiac apex HU range: -250 to -30 HU	CT-low density plaque: < 39 HU PR: remodelling index >1.05 SpC: calcium burden length <3/2 vessel diameter and width <2/3 vessel diameter
Ito et al.[40]	EAT definition: adipose tissue within the visceral epicardium Method: Manual Software: Not specified Interval: Not specified. 8-12 slices per patient Superior border: Mid left atrium Inferior border: left ventricular apex HU range: -190 to -30 HU	LAP: <30 HU PR: RI >1.1 (ratio of outer vessel area of lesion to outer vessel area of proximal reference site
Nakanishi et al.[125]	EAT definition: adipose tissue within the pericardial sac Method: Semi-automated Software: Synapse Vincent, Japan Interval: not specified. 7-10 planes Superior border: bifurcation pulmonary artery Inferior border: last slice containing any portion of the heart HU range: -250 to -30 HU	LAP: <30 HU PR: RI >1.1
Ito et al.[39]	EAT definition: adipose tissue within the visceral epicardium Method: Manual Software: Not specified. CT with Aquarius NetStation, USA Interval: not specified. Superior border: not specified Inferior border: not specified HU range: -250 to -40 HU	**CT:** LAP: <30 HU PR: RI >1.1 (ratio of outer vessel area of lesion to outer area of proximal reference site) **OCT:** Necrotic lipid pools quantified as number of quadrants Cap thickness measured at thinnest section of distance from lumen to inner border of lipid pool. TCFA = plaque with necrotic lipid pool in ≥2 quadrants within a plaque and fibrous cap <=65µm

Park et al.[127]	Method: 2D parasternal long-axis view; point on the free wall of RV to assess anterior echo-lucent space between linear echo-dense parietal pericardium and RV epicardium Cardiac cycle timing: End-diastole. Thickest point of EAT in each of 3 cycles measured and average value used	Plaque components: Fibrous – areas of dense collagen Fibrofatty – fibrous tissue with interspersed lipid in collagen Dense calcium – calcium with no adjacent necrosis Necrotic core – necrotic regions containing cholesterol clefts, foam cells, microcalcification TCFA: necrotic core ≥10% plaque area without overlying fibrous tissue and having >40% plaque burden in 3 consecutive frames
Tachibana et al.[126]	Method: 2D parasternal long-axis view; point on the free wall of RV along midline of ultrasound beam perpendicular to aortic annulus Cardiac cycle timing: End-systole. Average of three cardiac cycles used	PR: RI >1.05 (cross sectional lesion vessel area divided by proximal reference vessel area) LAP: <30 HU

CT – computed tomography, CP – calcified plaque, EAT – epicardial adipose tissue, HRP – high risk plaque, HU – Hounsfield units, LAP – low attenuation plaque, NRS – napkin ring sign, OCT – optical coherence tomography, PDA – posterior descending artery, PR – positive remodelling, RPA – right pulmonary artery, SpC – spotty calcification, TCFA – thin-cap fibroatheroma. VAT – visceral adipose tissue

Supplemental Table S3: Sensitivity analysis displaying pooled odds ratios and 95% confidence intervals with systematic exclusion of individual studies.

Excluded study	Pooled OR	Lower 95% CI	Upper 95% CI	I^2	p-value
Lu et al[122]	1.27	1.12	1.45	70%	<0.001
Schlett et al.[98]	1.17	1.06	1.30	80%	0.003
Rajani et al.[101]	1.19	1.07	1.33	82%	0.001
Oka et al.[124]	1.20	1.07	1.33	82%	0.001
Ito et al.[40]	1.24	1.08	1.43	78%	0.003
Nakanishi et al.[125]	1.24	1.09	1.42	82%	0.002
Park et al.[127]	1.25	1.09	1.43	83%	0.001
Ito et al.[39]	1.19	1.07	1.32	81%	0.001
Tachibana et al.[126]	1.16	1.06	1.27	74%	0.001

Supplemental Table S4: Newcastle-Ottawa Scale (NOS) Evaluation of Study Quality

STUDY	SELECTION	COMPARABILITY	OUTCOME
Lu et al.[122]	****	**	***
Schlett et al. [98]	****	**	***
Rajani et al. [101]	*****	**	***
Oka et al.[124]	****	**	***
Ito et al.[40]	****	**	***
Nakanishi et al.[125]	***	**	***
Park et al.[127]	****	**	***
Ito et al.[39]	***	**	***
Tachibana et al [126]	****	**	**

The Newcastle-Ottawa Scale (NOS) evaluates the included studies based on selection, comparability and outcome. The maximum score for each criteria is 5, 2 and 3, respectively, with the maximum total score equalling 10

Supplemental Table S5: GRADE quality assessment

STUDY	INITIAL GRADE	BIAS ASSESSMENT	FINAL GRADE
Lu et al.[122]	Low	**Bias**: Low; **Applicability**: Low; **Imprecision**: Low	Low
Schlett et al.[98]	Low	**Bias**: Low; **Applicability**: Low; **Imprecision**: High	Low
Rajani et al.[101]	Low	**Bias**: Low; **Applicability**: Low; **Imprecision**: Low	Low
Oka et al. [124]	Low	**Bias**: Unclear; **Applicability**: Low; **Imprecision**: High	Low
Ito et al. [40]	Low	**Bias**: Unclear; **Applicability**: Low; **Imprecision**: Low	Low
Nakanishi et al[125]	Low	**Bias**: Unclear; **Applicability**: High; **Imprecision**: Low	Low
Park et al.	Low	**Bias**: Unclear; **Applicability**: Unclear; **Imprecision**: Unclear	Low
Ito (2012) et al.	Low	**Bias**: Unclear; **Applicability**: Low; **Imprecision**: Unclear	Low
Tachibana et al	Low	**Bias**: High; **Applicability**: Unclear; **Imprecision**: High	Very Low

GRADE classification adapted from the GRADE Handbook [134-136] to evaluate quality of evidence in observational studies. All studies are observational and therefore considered of low quality. Assessment based on bias (factors including eligibility criteria, control of confounding), applicability (assessment of intervention) and imprecision (assessment of modelling methods and outcomes). Assessment is graded as either a low risk of bias, high risk of bias or unclear risk of bias.

<u>Supplement Figure S1</u>: Funnel plot

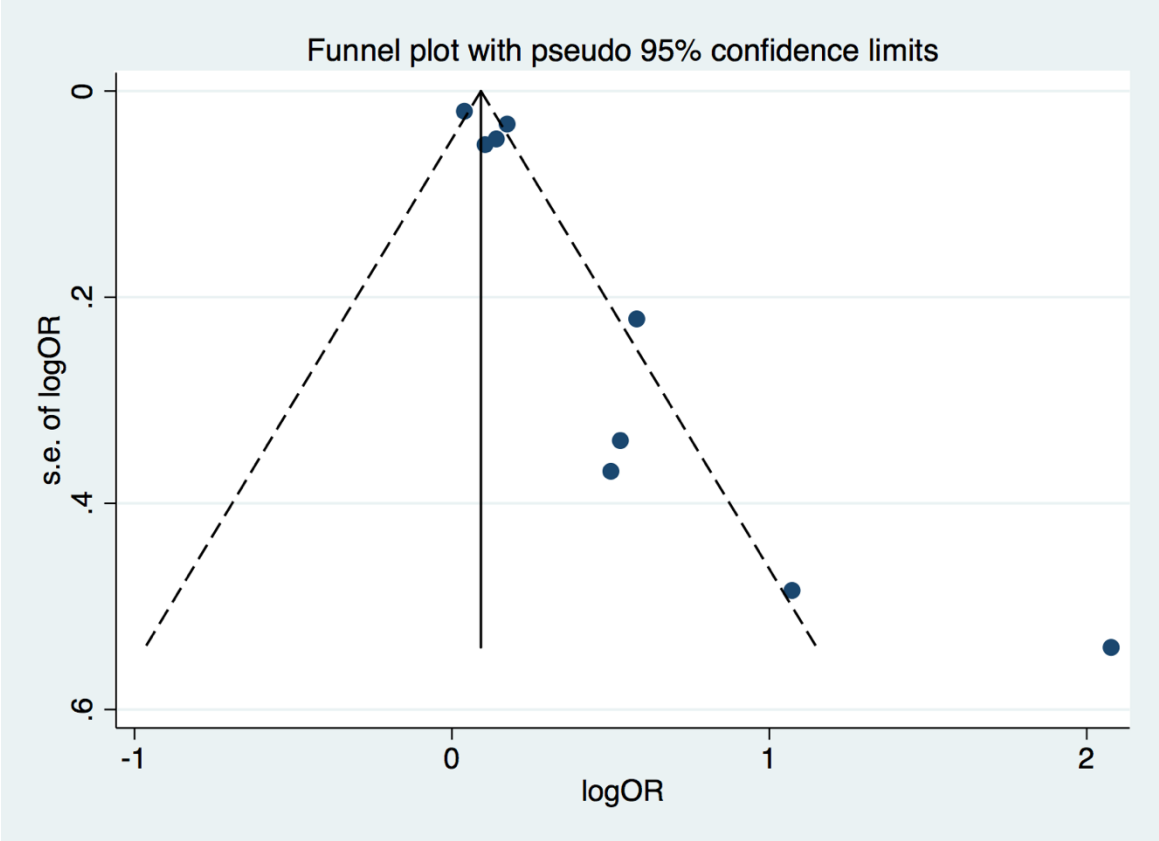

Egger's test for small study effects: p = 0.005
Overall summary estimate using trim and fill method: 1.13 (95% CI 1.03-1.28, p=0.04, I^2=81%)

CHAPTER 3:

ASSOCIATION OF VOLUMETRIC EPICARDIAL ADIPOSE TISSUE QUANTIFICATION AND CARDIAC STRUCTURE AND FUNCTION

Nitesh Nerlekar, Rahul G Muthalaly, Nathan Wong, Udit Thakur, Dennis TL Wong, Adam J Brown, Thomas H Marwick

Journal of the American Heart Association 2018;7:e009975

ABSTRACT

Background: Epicardial adipose tissue (EAT) is in immediate apposition to the underlying myocardium and therefore has the potential to influence myocardial systolic and diastolic function or myocardial geometry, through paracrine or compressive mechanical effects. We aimed to review the association between volumetric epicardial adipose tissue (EAT) and markers of myocardial function and geometry.

Methods and Results: PubMed, Medline and Embase were searched from inception to May 2018. Studies were included only if complete EAT volume or mass was reported and related to a measure of myocardial function and/or geometry. Meta-analysis and meta-regression were used to evaluate the weighted mean difference (WMD) of EAT in patients with and without diastolic dysfunction (DD). Heterogeneity of data reporting precluded meta-analysis for systolic and geometric associations. In the 22 studies included in the analysis, there was a significant correlation with increasing EAT and presence of DD, mean e' and E/e' but not E/A ratio, independent of adiposity measures. There was a greater EAT in patients with DD (WMD 24.43ml [95% CI 18.5-30.4], $p<0.001$) and meta-regression confirmed the association of increasing EAT with DD ($p=0.001$). Reported associations of increasing EAT with increasing LV mass, and the inverse correlation of EAT with LVEF were inconsistent, and not independent from other adiposity measures.

Conclusions: EAT is associated with diastolic function independent of other influential variables. EAT is an effect modifier for chamber size but not systolic function.

Prospero Registration: PROSPERO CRD 42017038400

INTRODUCTION:

Epicardial adipose tissue (EAT) has been widely studied as a potential contributor to cardiovascular pathology. Much of this research has focused on its effect on coronary atherosclerosis[139], but there are unique properties of EAT that may lead to an effect on myocardial function. EAT shares direct anatomic contact with the myocardium without fascial interruption[63] and therefore may exhibit local compressive forces resulting in alteration of myocardial function and geometry. Additionally, the shared blood supply of the coronary circulation to both the myocardium and surrounding EAT may predispose paracrine effects on the neighbouring myocardium with such inflammatory cytokines as MCP-1, interleukin (IL)-beta, IL-6, TNF-alpha and leptin[63]. Persisting inflammation may lead to collagen deposition and subsequent impaired left ventricular (LV) relaxation and further effects on diastolic and systolic function. Furthermore, there is an association between EAT and release of free fatty acids, as well as their myocardial consumption[140]. The relationship between obesity, visceral fat and EAT may also explain effects on myocardial function, chamber size and mass.

A number of methods have been used for measurement of EAT, including echocardiography, computed cardiac tomography (CT) and cardiac magnetic resonance imaging (MRI). Echocardiography may over- or under-estimate total EAT volume, due to single plane assessment and the effects of probe angulation on linear measurement. Single-slice area measurements on CT or MRI are also limited by being only single-plane measures. Recently, we have demonstrated the superiority of volumetric EAT assessment in comparison to 2-dimensional linear echocardiographic EAT thickness[141]. We therefore sought the association of full volume quantification of epicardial adipose tissue (assessed by cardiac CT or cardiac MRI), with myocardial function as assessed by transthoracic echocardiography, full R-R interval cardiac CT or cardiac MRI.

METHODS

Search methodology. We conducted this systematic review in accordance with the PRISMA statement and the trial was registered with PROSPERO (CRD 42017038400). The search was conducted in MEDLINE, EMBASE and PubMed databases, ending in March 2018. References of eligible articles were hand-searched for additional articles. Searches were restricted to human studies and conference abstracts were included. A study search flow-chart is presented in **Figure 1**, and specific search term strategy in Supplementary **Table S1**. The data, analytic methods, and study materials will not be made available to other researchers for purposes of reproducing the results or replicating the procedure.

Our inclusion criteria were: patients undergoing cardiac CT (CT-angiography or calcium score) or MRI with volumetric assessment of EAT (either volume or mass), with cardiac imaging for assessment of myocardial function parameters (full cardiac cycle cardiac CT or MRI or echocardiography), or measurement of myocardial geometry (LV mass, LV volumes, LA size) by validated methods. Assessment of diastolic function was restricted to studies utilizing echocardiography. Exclusion criteria included: any study with linear measurement of EAT thickness, single slice area measures of EAT, measures of myocardial lipid content not differentiated from EAT, measurement of paracardial adipose tissue i.e. fat beyond the parietal pericardium. Two authors (NN and RGM) independently reviewed the abstracts from the search to meet the inclusion criteria and discrepancies were resolved by consensus. Probable overlap of the patient cohort with a similar study led to exclusion of the smaller study[142].

Evaluation of full volume EAT: EAT was regarded as adipose tissue enclosed within the visceral pericardium and mean values (indexed and non-indexed) were recorded.

Evaluation of cardiac function. Included studies measured myocardial performance based on echocardiography or MRI. Measures of diastolic function included: transmitral flow for peak early (E)

and late (A) inflow velocities and their ratio (E/A), deceleration time; septal, lateral and or average myocardial annular velocities on tissue Doppler imaging (e'), early inflow to annular velocity ratio (E/e'); pulmonary vein flow to calculate the time difference between the atrial reversal wave and mitral A-wave duration; and the isovolumic relaxation time. Diastolic class grade was recorded if reported – normal, grade I (impaired relaxation), grade II (pseudonormal), grade III (restrictive). Measures of systolic performance assessed included LV ejection fraction, cardiac output, stroke volume and global longitudinal strain if recorded. Measures of cardiac structure included LV mass, LV end-diastolic and end-systolic volume and left atrial size.

Statistical analysis. Data regarding univariable correlations are presented as this was the most consistent measure seen in included studies. Where multivariable regression was performed, adjusted study estimates and model covariates are reported. Meta-analysis was performed for the weighted mean difference (WMD) in EAT volume between groups with and without diastolic dysfunction. Meta-regression of WMD as an effect size and the combined mean EAT in included studies was performed with the moment based estimate of between-study variance and a permutation test using 1000 Monte Carlo simulations to moderate for potentially spurious results as previously described[143]. Precision of pooled estimates is reported as 95% confidence intervals (CI) and heterogeneity by the I^2 statistic. The Newcastle Ottawa Scale was used to assess risk of bias (**Table S2**) Statistical analysis was performed using StataMP 14.0 (StataCorpLP, College Station, TX).

RESULTS

Study selection. A brief outline summary of the 22 studies (18 published and 4 conference papers) included in this review is presented in **Table 1**[140, 144-165].

Association of EAT with LV diastolic function. There were 11 studies that investigated the relationship between EAT and diastolic parameters, with 5 specifying adherence to an iteration of the

American Society of Echocardiography diastolic guidelines[166]. EAT was associated with diastolic parameters, including peak mitral annular tissue Doppler velocities (e' septal, e' lateral or e' mean) and transmitral flow (early [E] and late (A) diastolic peak flow velocities and their ratio (E/A) (**Table 2**)[146, 150-153, 155, 157-161, 166-169]. Whilst some studies did perform comprehensive Doppler measures such as isovolumic relaxation times, deceleration times and pulmonary vein Doppler, the association with EAT individually with each parameter was not described. The classification of patients with diastolic dysfunction was available in 5 studies. Most patients (26-38% of total cohort) had grade 1 diastolic dysfunction, with fewer qualifying as grade 2 or above (2-28%).

In the 5 studies that measured differences in EAT between groups, EAT was significantly greater in the diastolic dysfunction group compared to normal diastolic function patients: (weighted mean difference 24.4 mL, 95% CI (18.5-30.4 mL), $p<0.001$, $I^2=28\%$)) (**Figure 2**)[152, 153, 157, 158, 160, 163]. Meta-regression performed evaluating the weighted mean difference (effect size) against the mean EAT volume, demonstrated a nominally increasing presence of diastolic dysfunction with increasing EAT values ($\beta=0.17$, standard error=0.09, $p=0.06$). This was statistically significant after Monte Carlo permutation testing, $p=0.001$ (**Figure 3**).

Mean E/e' values were positively correlated with EAT (r-value range 0.21-0.34, $p<0.05$) and mean e' values were inversely correlated (r-value range -0.26 to -0.44, $p<0.05$), and in all but one study but no consistent association was seen with the E/A ratio (r-value range -0.40 to 0.08). Increasing EAT was an independent predictor of diastolic dysfunction, e' and E/e' independent of age, sex and measures of adiposity (**Table 2**). No independent association was identified with the E/A ratio. In 6 studies, hypertension was also an adjusted co-variate in the model and increasing EAT remained a predictor of altered diastolic parameters.

Association of EAT with systolic function.

Of 10 studies describing the association of EAT with systolic parameters, LV function was evaluated with MRI in 5 and echocardiography in 4 (**Table 3**)[140, 147, 148, 153, 155, 156, 159, 164]. One study reported associations between EAT and global longitudinal strain, a subclinical measure of myocardial function[161]. Only one described an independent effect of EAT on LVEF by echocardiography[156]. No univariable correlation with LVEF was reported in the MRI studies[147-149]. Of the 6 studies reporting multivariable regression analysis, an independent association with LVEF was observed in 2 studies – one in patients with established CAD stratified by LVEF and compared to normal controls (hazard ratio [148] 0.48, 95% CI 0.28-0.68, $p<0.01$)[148] and the other in patients undergoing investigation for suspected CAD with reduced LVEF compared to normal LVEF (values not reported)[156].

The only consistent feature across all studies appeared to be a relative decrease in EAT as LVEF decreased. In studies that included control groups (i.e. normal LVEF), no association of EAT with EF was identified in the control group. One study demonstrated a significant inverse correlation with EAT (normalized to LV mass) with cardiac output and stroke volume (but not LVEF) [140] in obese patients (r-value -0.46) but not in corresponding controls.

In studies focusing specifically on patients with reduced LVEF, EAT was reduced compared to those with preserved LVEF. Of note, Doesch et al[148] demonstrated that patients with CAD and preserved LVEF had greater EAT ($36\pm11 g/m^2$) than normal controls without CAD ($31\pm8 g/m^2$), and both had greater EAT than CAD patients with LVEF<50% ($28\pm8 g/m^2$, $p<0.01$). A population of presumed ischaemic cardiomyopathy (CAD with reduced LVEF) also reported a stepwise decrease in EAT volume with reducing grades of LVEF [156]. This stepwise decrease was not found in a different study by Doesch et al[149] in patients with dilated cardiomyopathy against normal controls, although EAT was reduced overall compared to normal controls.

In the study related to strain analysis[161], there was a positive correlation with EAT and impaired 3-dimensional global longitudinal strain ($r=0.601$, $p<0.001$) that remained significant on multivariable regression (standardized $\beta=0.512$, $p<0.001$), independent of markers of obesity and diabetes.

Association of EAT with chamber measures.

There were 14 studies with data relating to a measure of myocardial geometry. All modalities of echocardiography, CT and MRI were represented, with most values indexed to body surface area unless otherwise specified. Some studies avoided indexation as body weight or other adiposity measures were used in regression models and therefore raw measures were used to prevent collinearity. The most often reported univariable correlation coefficient was for EAT and LV mass or indexed mass and was always statistically significantly positively correlated in the diseased patient group (not controls) with ranges from $r=0.19$ to $r=0.42$, $p<0.05$. Only studies by Doesch et al measured LV end diastolic diameter and found a consistent association with EAT (r-value ranges 0.22 to 0.42, $p<0.05$). Similar findings were seen for LV end-diastolic and end-systolic volume. Left atrial size was measured either as volume or diameter and demonstrated significant univariable associations with EAT (**Table 4)**[140, 144-149, 154, 155, 157, 159, 161, 162, 165].

An inconsistent association was seen with measures of adiposity in relation to EAT and cardiac structure. In patients with reduced LVEF, indexed EAT appears to be associated with indexed LV end diastolic mass independent of BMI (**Table 4**)[147-149]. One study assessing patients with suspected CAD and normal LVEF demonstrated that EAT correlated best with LV mass (non-indexed) in the non-obese cohort only ($\beta=0.23$, $p<0.001$)[145]. Finally, in two observational studies, an independent association of EAT with LV mass (non-indexed) adjusted for body weight was only seen in women (**Table 4**)[154, 159].

DISCUSSION

This review of 21 studies has demonstrated the emerging body of work relating EAT to myocardial structure and function. Increasing EAT is associated with: 1) an increasing prevalence of diastolic dysfunction; 2) a concomitant increase in LV mass; 3) no consistent association with markers of systolic function. However, these correlations were no more than moderate - no coefficient exceeded 0.50.

Protective functions of EAT.

EAT has a very high fatty acid content and can both release and scavenge excess free fatty acids to regulate myocardial energy production[63]. Additionally, EAT secretes anti-inflammatory cytokines such as adiponectin, adrenomedullin and omentin which have anti-atherogenic effects, as well as regulating vascular tone and cardiac remodelling[4]. There is a thermogenic role for EAT in providing heat for the myocardium in times of hypoxic or ischemic stress[4]. However, the presence of numerous pro-inflammatory cytokines within EAT may lead to a potential imbalance of harmful vs. protective cytokines and disruption of myocardial function. Higher levels of these molecules (e.g. TNF-alpha, IL-6, IL-1 and MCP-1) are seen in patients with CAD or heart failure. It is uncertain whether the trigger for the imbalance of cytokines is a cause of the pathology or a consequence, and a potential reciprocal or bidirectional role has been proposed[63].

EAT and diastolic dysfunction.

Adipose tissue can modulate the cardiovascular system by mechanisms including sympathetic activation, adipokine secretion and myocardial oxidative stress[65, 66]. EAT is regarded as a visceral fat depot. Visceral fat is metabolically active and is a determinant of diastolic function[67]. The adipokines within EAT can all affect diastolic function through persistent inflammation and subsequent collagen

turnover[68], impaired microvascular relaxation or a direct toxic effect on the myocardium[69, 70]. The loss of protective effects of adiponectin can also modify diastolic function[170].

Mechanical effects may arise from myocardial compression of EAT as it lies within a fixed pericardial sac[154] inducing a similar mechanism as pericardial constriction. Hachiya et al demonstrated an independent correlation of EAT with aortic pulse pressure as another mechanism of diastolic dysfunction which may be mediated by the association of EAT with aortic stiffness, and therefore increased pulse wave velocity and early wave reflection[155]. Increased pressure in late systole may cause slower LV relaxation and subsequent diastolic dysfunction, as well as compromise coronary perfusion, especially if there is underlying CAD leading to impaired LV relaxation[171].

EAT is associated with obesity, which itself is independently associated with diastolic dysfunction[172]. Obese patients often have elevated EAT volumes[154], and indexed EAT has modest incremental value for diastolic dysfunction over traditional covariates such as metabolic syndrome, subclinical CAD and LV mass index[146]. While the results from our analysis demonstrate that EAT had an independent effect on diastolic function parameters over adiposity measures, it should be noted that adiposity measures varied considerably and included BMI, bioimpedence testing and area VAT or SAT, or indexed EAT was used which accounts for body weight. This heterogeneity needs further explanation to adequately isolate the effect of obesity and EAT on diastolic function. The lack of an association of EAT with E/A ratio may be confounded by the effects of age, proportion of CAD patients, measurement in patients with normal LVEF and the U-shaped relationship of E/A ratio with diastolic function that makes it difficult to assess without the addition of other variables[173].

The evaluation of diastolic function is challenging and influenced by a patient's filling status, the presence of CAD, diabetes and obesity as well as 'normal' changes seen in the ageing patient. Whilst most studies aim to account for these in multivariable regression models, no more than association can

be interpreted and causality cannot be proven. Statistically, there may be implications of collinearity of obesity measures and EAT in multivariable models.

EAT and systolic dysfunction.

Our study noted weak and inconsistent associations of EAT and systolic parameters. In the single study that evaluated EAT and longitudinal strain as a marker of subclinical myocardial dysfunction, there was a strong association noted independent of confounders such as obesity and diabetes[161]. This is a notable finding, however causality remains unproven and requires further assessment in larger scale studies as a possible marker of the syndrome of heart failure with preserved ejection fraction. Various hypotheses have developed to relate EAT and systolic function. In studies of patients with ischaemic and dilated cardiomyopathy, there has been a consistent signal of reducing EAT with reducing LVEF with less EAT also seen compared to normal controls, or those with normal LVEF[147-149, 156]. As myocardium becomes progressively dysfunctional, the role of EAT as a source of energy or cytokine homeostasis may become less necessary, contributing to EAT depletion. Conversely, in obese patients, there was no association with EAT (normalised to cardiac mass) and LVEF, and there was a negative correlation with MRI-derived cardiac output as EAT increased[140]. The proposed mechanism is from mechanical restriction of myocardial expansion from EAT in diastole that may lead to less ventricular filling and therefore reduced cardiac output[140]. A further mechanism may involve the effects of a direct cytokine release as seen in patients with decompensated heart failure, but no studies have applied this in the context of EAT volume.

EAT and chamber measures.

Post-mortem and experimental studies[57, 58] have demonstrated a constant ratio of epicardial fat to ventricular myocardium, regardless of underlying pathology of hypertrophy, ischemia or normal muscle. Furthermore, the increase in fat mass parallels LV hypertrophy, although healthy controls have

higher quantities of EAT[147]. Similar findings are seen when evaluating the LV remodelling index (LVRI, ratio of mass to end-diastolic volume) where an inverse correlation is noted with LVEF and the EAT/LVRI ratio. LVEF is inversely correlated with EAT and linearly with LVRI, suggesting that remodelling is not compensated by an adequate increase in EAT[147].

Obesity has shown a positive relationship with increased LV mass and EAT yet the impact of obesity on myocardial geometry may outweigh the local effects of ectopic fat as associations attenuated after adjustment for other adiposity measures including body weight[154]. From a mechanistic perspective, the association of EAT with central obesity and VAT might result in greater LV afterload, subsequent increased LV output and therefore lead to LV remodelling[145]. As LV remodelling progresses, LV diameter, volume and mass increase which may then deplete EAT stores[149] and result in a vicious cycle of reduced protective benefits on the heart and further dysfunction. However, the independent association of EAT with LV mass is limited to non-obese subjects[145]. Associations of EAT with the incidence of CAD has been described in the non-obese[174], and could contribute to the so called obesity paradox[175].

Limitations:

We acknowledge several limitations in our study. EAT measurement by different modalities may lead to differences between studies. Some reported EAT indexed to BSA (therefore accounting for weight) and some report raw values using weight as a covariate in multivariable models. Such normalization, as opposed to normalization to height, may obscure the contribution of obesity to differences in chamber volumes and mass, which is associated with EAT. Not all studies adjusted for hypertension in multivariable models which is also associated with obesity and diastolic function. Variations in the reference literature regarding measures of diastolic function also leads to difficulties with comparing studies. The differences in regional location of EAT was not available in most studies and therefore

the effect of EAT distribution was not assessable. The level of heterogeneity and variable study end-points precluded detailed meta-analysis.

Conclusions: Despite small and heterogeneous studies, there is clear evidence of a consistent effect of volumetric EAT upon myocardial diastolic function and chamber measurements, however robust data is lacking to make causal inferences. These findings are observed despite adjustment for common confounders such as adiposity. No consistent effect is seen with respect to systolic parameters. Further longitudinal studies are necessary in order to generate quantitative summary measures as well as develop potential targets for treatment.

Table 1: Study characteristics

First Author	Year	Country	Study type	Population	Sample size	EAT method	EAT value
Bakkum[145]	2015	Netherlands	Cross-sectional	Suspected CAD	208	PET-CT	113.8 ± 48.1 cm^3
Cavalcante[146]	2012	USA	Cross-sectional	Self referred screening	110	MDCT	Men 101 ± 51cm^3 Women 67 ± 40cm3
Chekakie[144]	2010	USA	Case-control	AF and controls	273	MDCT	Sinus Rhythm 76.1±36.3mL AF 101.6 ± 44.1mL
Doesch[148]	2012	Germany	Case-control	Established CAD	158 cases 40 controls	MRI	control(31 ± 8g/m^2); CAD(29 ± 10g/m^2) CAD-EF<50 (26 ± 8g/m^2) CAD-EF>50 (36 ± 11g/m^2)
Doesch[149]	2013	Germany	Case-control	DCM	112 cases 48 controls	MRI	control (62.1 ± 14.4g) ; DCM (47.2 ± 15.2g) control (66 ± 15.3mL); DCM (50.2 ± 16.2mL) control (31.7 ± 5.6g/m^2); DCM (24 ± 7.5g/m^2) control(33.5 ± 6.4mL/m^2); DCM (25.5 ± 8mL/m^2)
Doesch[147]	2010	Germany	Case-control	CHF (LV<35%) (ICM=36; DCM=30)	66 case 31 controls	MRI	control(71 ± 13mL); CHF (46 ± 11mL) control(36 ± 5mL/m^2); CHF(24 ± 5mL/m^2) control(67 ± 13g); CHF(43 ± 11g) control(34 ± 4g/m^2); CHF(22 ± 5g/m^2)
Ede[150]	2014	Turkey	Cross-sectional	Suspected CAD	106	MDCT	38 ± 31cm^3
Faustino¥[151]	2011	Portugal	Cross-sectional	Not specified	78	MDCT	Threshold of 44.1mL defined by ROC (72% sensitivity, 50% specificity) for diastolic dysfunction
Fernando¥[152]	2015	USA	Cross-sectional	AF prior to ablation	20	MRI	125.7 ± 56.7mL
Fontes-carvalho[153]	2014	Portugal	Cross-sectional	Post myocardial infarction	225	MDCT	113.6 ± 43.2 cm^3
Fox[154]	2009	USA	Cross-sectional	Sub study of Framingham	997	MDCT	Women (108 ± 41cm^3); Men (136.5 ± 54.4cm^3)
Hachiya[155]	2014	Japan	Cross-sectional	Suspected CAD	134	MDCT	77.1 ± 29.6cm^3/m^2

Khawaja[156]	2011	USA	Cross-sectional	Suspected CAD	381	MDCT	Normal LVEF 114.5 ± 98.5cm^3 LVEF <55% 83.5 ± 67.1cm^3
Konishi[157]	2012	Japan	Cross-sectional	Suspected CAD	229	MDCT	Diastolic dysfunction 184 ± 61cm^3 Normal function 154 ± 58cm^3
Lai[158]	2015	Taiwan	Cross-sectional	Self referred screening	318	MDCT	80.6 ± 33mL
Liu[159]	2011	USA	Cross-sectional	African Americans	1402	MDCT	Men (79.8 ± 37.1mL) Women (67.1 ± 29.0)
Longenecker[¥160]	2016		Cross-sectional	HIV patients	46 HIV+ 23 HIV-	MDCT	HIV+ with DD median 120(74-143)mL HIV+ with normal function median 72(54-100)mL HIV- not specified
Ng[161]	2016	Australia	Cross-sectional	Suspected CAD	130	MDCT	Total 97.5 ± 43.7cm^3 Men 103.7 ± 39.5 cm^3 Women 90.9 ± 47.4 cm^3
Ruberg[140]	2010	USA	Cross-sectional	Obese with metabolic syndrome	28 cases 18 controls	MRI	controls (85 ± 66mL); Subjects (161 ± 88mL) controls (1.1 ± 0.7 ml/g); subjects (2.0 ± 1.1 ml/g)
Vanni[¥162]	2015	Italy	Case-control	Not specified	19 NAFLD 9 controls	MRI	NAFLD: 228.1 ± 112.9mL Controls: 66.8 ± 25.2mL
Vural[163]	2014	Turkey	Case-control	Suspected CAD	63	CACS	137 ± 56cm^3
Wu[164]	2015	Taiwan	Cross-sectional	Compensated CHF	50 cases 20 controls	MRI	control (45.8 [39.4-50.3]mL); CHF + VT/VF (51.5 [46.6-59.8]mL); CHF no VT/VF (44.0 [33.9-48.3]mL)
Yamashita[¥165]	2012	Japan	Cross-sectional	Suspected CAD	286	MDCT	EAT: 71.6 ± 37.9 (range 10.5-179.9)mL

[¥] indicates this is a conference abstract

AF – atrial fibrillation, CACS – coronary artery calcium score, CAD – coronary artery disease, CHF – congestive heart failure, DCM – dilated cardiomyopathy, EAT – epicardial adipose tissue, ICM – ischaemic cardiomyopathy, LVEF – left ventricular ejection fraction, MDCT – multi-detector computed tomography, MRI – magnetic resonance imaging, NA – not applicable, NAFLD – non-alcoholic fatty liver disease, VT/VF – ventricular tachycardia/ventricular fibrillation. Values are mean±SD or mean [range]

Table 2: EAT and diastolic function

First Author	Diastolic function reference	Subgroup characteristics		Diastolic parameter correlations			Multivariable regression comments
		Diastolic dysfunction	Normal function	E/A	e'	E/e'	
Cavalcante[146]	ASE [166]	Grade 1 (n=29, 26%) Grade 2 (n=11, 10%)	n=70, 64%		averaged 0.44*	0.34*	Multivariate model outcomes of ≥grade 1 DD, mean e' and mean E/e': EAT was an independent predictor (model included 10 year Framingham Risk Score, Metabolic syndrome, subclinical CAD, LV mass index), β range -0.02 to 0.04, all p<0.05. Indexed EAT was found to increase clinical model for prediction of DD (adjusted R^2 0.16 vs 0.24, p=0.004) and mean e' (adjusted R^2 0.17 vs 0.27, p=0.001) i.e. indexed EAT represents 8-10% of the variation of predictors for DD.
Ede[150]	Lang et al[169]	Grade 1 (n=39, 37%) Grade 2 (n=10, 9%) Grade 3 (n=2, 2%)	n=55, 52%	-0.404			
Faustino[¥151]	Not specified	46 patients with DD and EAT>44.1mL	32 patients with no DD and EAT<44.1mL				EAT not significant on multivariable regression (results and covariates not reported). Relationship of EAT with DD by ROC AUC 0.66, p=0.02
Fernando[¥152]	Not specified	EAT = 164 ± 118 (E/E'>15)	EAT = 114 ± 54 (E/E'<15)		-0.48*	0.22	On multivariable regression adjusted for age, BMI, LA volume, hypertension and CAD, EAT associated with abnormal myocardial relaxation (OR not specified, p=0.04)
Fontes-Carvalho[153]	ASE [166]	EAT =116.7 ± 67.9cm3 Grade 1 (n=57, 28%) Grade 2 (n=58, 28%) Grade 3 (n=10, 5%)	EAT = 93.0±52.3cm3 n=80 (39%)		e' septal (-0.26)* e' lateral (-0.28)*	0.25*	On multivariable regression adjusted for hypertension, age and sex as well as other markers of adiposity (SAT, VAT, Waist-height ratio, Fat mass %) EAT remained significantly predictive of E/e' (β 0.19 (0.06-0.32, p<0.01), as did e' septal and e' lateral.

Hachiya[155]	ASE [166]			-0.05	-0.31*	0.24*	Definition of diastolic dysfunction not specified. On different multivariate models e' inversely correlated with EAT (Standardized β range -0.30 to -0.36, all $p<0.05$) but not E/e' (Standardized β 0.23, $p=0.06$) except when adjusted for age, sex and BMI (model 1) and medication use (model 2) – Standardized β range 0.25 to 0.31, all $p<0.05$.
Konishi[157]	Defined as E/e'>10	EAT = 184 ± 61cm^3 n=141 (62%)	EAT = 154 ± 58cm^3 n=88 (38%)			0.21*	On multivariable regression with age, hypertension, male sex, diabetes and abdominal obesity there was an independent effect of EAT on DD: OR 2.09 (1.15-3.79, $p=0.02$) for EAT per 100cm^3
Lai[158]	Lang et al[169]	EAT = 86.79 ± 31.77 n=100	EAT = 67.32 ± 31.95 n=218		-0.38*	0.284*	On multivariable regression adjusted for age, gender, BMI, systolic blood pressure, LV mass index, hypertension, diabetes, hyperlipidaemia, smoking, EAT was significantly associated with E/A (β -0.002)*, E' (β -0.02)*, E/E' (β 0.02)* and diastolic dyssynchrony (β 0.197)*. ROC derived optimal cut off for DD was 67.3mL (ROC 0.712) (sensitivity 73% specificity 62%)
Liu[159]	Gottdiener et al[168]			Men (-0.12)* Women (-0.12)*			On multivariable linear regression adjusted for age, height, smoking, alcohol, blood pressure, eGFR, haemoglobin, total physical activity score, medications, VAT and weight, E/A no longer became significant (regression co-efficient -0.01±0.02, $p=0.41$ in women and -0.0±0.02 $p=0.64$ in men) – note described as pericardial fat volume.
Longenecker¥[160]	Not specified	Grade 1 (n=29 (HIV+ n=19, HIV- n=10)) Grade 2 (n=2 (HIV+ n=1, HIV- n=2))	n=38 HIV+ n=26 HIV- n=12	-0.392*			On multivariable regression adjusted for age, BMI and gender, EAT remained independently associated with diastolic dysfunction (OR 1.35 95% CI 1.02-1.79) per 10mL increase – note described as pericardial fat volume
Ng[161]	Not specified				e' septal (-0.263)* e' lateral (-0.285)*		

Vural[163]	Alnabhan et al[167]	EAT = 164.4 ± 54cm^3 Grade 1 (n=24, 38%) Grade 2 (n=4, 6%) Grade 3 (n=1, 1.5%)	EAT = 114.1±46.6 cm^3 n=34 (56%)		-0.437*		On multivariable regression adjusted for Age, blood pressure, BMI, waist circumference, cholesterol, EAT was independent predictor of DD (OR 1.03 (1.01-1.06), p=0.006). ROC derived optimal cut-off for DD 129.6cm^3 (ROC 0.758).

* Denotes p-value for univariate correlation is significant at <0.05

¥ Denotes study is a conference abstract

(BMI – body mass index, CAD – coronary artery disease, DD – diastolic dysfunction, eGFR – estimated glomerular filtration rate, HIV – human immunodeficiency virus, OR – odds ratio, ROC – receiver operator characteristic, SAT – subcutaneous adipose tissue, VAT – visceral adipose tissue)

Table 3: EAT and systolic function

First Author	Method	Group	EAT value	Systolic measure	r-value (univariate)	Multivariable regression comment
Doesch[148]	MRI	CAD and EF>50%(n=44) CAD and EF<50% (n=114) Combined CAD (n=158) Controls (n=40)	36 ± 11g/m^2 26 ± 8g/m^2 29 ± 10g/m^2 31 ± 8g/m^2	LVEF	0.171 0.137 0.574* Not specified	On multivariable regression adjusted for BMI, NYHA class I and III, atrial fibrillation, LV-EDVI, LV-ESVI, LV-EDD, LVRI and LGE%, LVEF was an independent predictor of indexed EAT (HR 0.478 (0.28-0.675, p <0.01))#
Doesch[149]	MRI	Control (n=48) DCM (n=112)	31.7 ± 5.6 g/m^2 24 ± 7.5 g/m^2	LVEF LVEF	0.069 0.085	No correlation with LVEF and EAT (p=0.37)
Fontes-Carvalho[153]	Echo			LVEF	-0.07	
Hachiya[155]	Echo			LVEF	0.22*	Significant association on multivariate regression models adjusted for hypertension, diabetes, dyslipidaemia, previous CAD or revascularisation, medication use (standardized β ranges 0.16 to 0.22, all p<0.05) but not adjusted for age, sex, BMI (standardized β 0.13 p>0.05).
Khawaja[156]	Echo	Normal (n=321) EF<55% (n=60) EF 35-55% (n=43) EF<35% (n=17)	114.5 ± 98.5cm^3 83.5 ± 67.1cm^3 96.0 ± 73.9cm^3 52.2 ± 29.7cm^3			Multivariate analysis revealed LVEF and triglyceride levels predicted EAT (values and covariates not reported)
Liu[159]	Echo	Women Men		LVEF LVEF	-0.04 0.03	Not significant on multivariable regression in either sex (adjusted for age, height, smoking, alcohol, blood pressure, eGFR, haemoglobin, total physical activity score, medications, VAT and weight – regression coefficient -0.3±0.4 p=0.51 in women and 0.2±0.6 p=0.72 in men). Note described as pericardial fat volume.

Ruberg[140]	MRI	Obese		CO SV LVEF	 -0.46* inverse* not correlated	Values are normalised to LV mass (mL/g).
		Control		CO SV LVEF	not correlated not correlated not correlated	
Wu[164]	MRI			LVEF	not correlated	

*Denotes $p<0.05$
[¥]Denotes study is a conference abstract
#Directly quoted values from source manuscript.

BMI – body mass index, CAD – coronary artery disease, DCM – dilated cardiomyopathy, eGFR – estimated glomerular filtration rate, HR – hazard ratio, LGE% - percentage of late gadolinium enhancement, LV-EDVI – left ventricular end diastolic volume index, LV-EDD – left ventricular end diastolic diameter, LV-ESVI – left ventricular end systolic volume index, LVEF – left ventricular ejection fraction, NYHA – New York heart association, VAT – visceral adipose tissue

Values are mean ± SD or r-value correlation coefficients unless otherwise stated

Table 4: EAT and chamber geometry

Author	Modality	Subgroup	LVEDD	LA size (diameter / volume)	LVEDMi	LVEDVi	LVESVi	LVRI	Comment
Bukkam[145]	CT				0.42*#				On multivariable regression adjusted for traditional cardiovascular risk factors, CACS and BMI, EAT was not a significant predictor of LV mass in obese patients, but only in non-obese patients (β=0.23, p<0.001).
Cavalcante[146]	Echo				0.41*				Measure not included in multivariate analysis
Chekakie[144]	CT and Echo			0.25 / 0.24					
Doesch[148]	MRI	EF<50 (n=44) EF>50 (n=114) Combined (n=158)	0.076 0.011 0.272*		0.336* 0.305* 0.019	0.201* 0.043 0.16*	0.089 0.056 0.262*	0.137 0.202 0.344*	On multivariable regression including LVEF, BMI, NHYA I and III, atrial fibrillation, LV-EDVI, LV-ESVI, LV-EFF, LVRI, LGE% - best correlates to indexed EAT were LVEF, BMI, LV-ESVI (HR 0.48, p<0.01), LVEDD (HR -0.238, p=0.01). In subgroup analysis by EF <50 or >50%, full model not described however no association with LVEDMI in LVEF>50 but association seen in LVEF>50 (HR 0.105, p-0.01).
Doesch[149]	MRI	Control (n=48) DCM (n=112)	0.01 0.22*		0.346* 0.417*	0.007 0.251*	0.0001 0.239*	0.204 0.116	Increased EAT mass with increasing LVEDMI in DCM, but less values than healthy control group. Greater mass seen in DCM with hypertrophy vs. non-hypertrophy (31.7 ± 5.6 g/m^2 vs. 24.4 ± 7.1g/m^2, p=0.01). On multivariable regression only LVEDMI independently correlated with indexed EAT, as was seen in healthy controls (adjusted for age and BMI – value not reported).

Doesch[147]	MRI	Control CHF	NR 0.42*		0.36* 0.59*				Increased EAT mass in CHF with increasing LVEDM however higher levels of EAT in controls compared to CHF ($34 \pm 4 g/m^2$ vs $22 \pm 5 g/m^2$, $p<0.01$). On multivariate regression adjusted for LVEF, LVEFF, RVEF, LVEDMI, only LVEDMI independently associated with indexed EAT (p=0.0001).
Fox[154]	MRI	Women Men		0.28* 0.37*	ø0.35* ø0.19*	ø0.2* ø0.07			On multivariable regression adjusted for age, height, smoking, alcohol, menopause, hormone replacement therapy, blood pressure, hypertension therapy and weight, only in women LVM (adjusted regression co-efficient 1.66, p=0.01) and in men LA diameter (adjusted regression co-efficient 0.8, p=0.002) were independent predictors of pericardial fat volume.
Hachiya[155]	Echo				0.28*				Measure not included in multivariate analysis
Konishi[157]	Echo			0.32*	0.23*				Measure not included in multivariate analysis
Liu[159]	Echo	Women Men		0.3* 0.11	ø0.24* ø0.21*				On multivariable regression adjusted for age, height, smoking, alcohol, blood pressure, eGFR, haemoglobin, total physical activity score, medications, VAT and weight, only in women LVM (adjusted regression co-efficient 4.1 ± 1.8, p=0.03) and LA diameter (adjusted regression co-efficient 0.4 ± 0.2, p=0.03) were independent predictors of pericardial fat volume.
Ng[161]	Echo					-0.09	0.08		
Ruberg[140]	MRI					Not			

Vanni[¥162]	MRI	Cases					^0.46*		Inversely correlated with EF No other analysis specified
Yamashita[¥165]	CT			0.25*					

[#] value is for LV mass on CT, non-indexed and time in cardiac cycle not specified
[ø] represents a non-indexed measure
^ value is for end systolic LV diameter
[¥]Denotes study is a conference abstract

BMI – body mass index, CAD – coronary artery disease, CHF – congestive heart failure, DCM – dilated cardiomyopathy, eGFR – estimated glomerular filtration rate, HR – hazard ratio, LGE% - percentage of late gadolinium enhancement, LV-EDVI – left ventricular end diastolic volume index, LV-EDD – left ventricular end diastolic diameter, LVEDMI – left ventricular end diastolic mass index, LVEDVI – left ventricular end diastolic volume index, LV-ESVI – left ventricular end systolic volume index, LVEF – left ventricular ejection fraction, NR – not reported, NYHA – New York heart association, VAT – visceral adipose tissue

Values are mean ± SD or r-value correlation coefficients unless otherwise stated

Figure 1: Search strategy

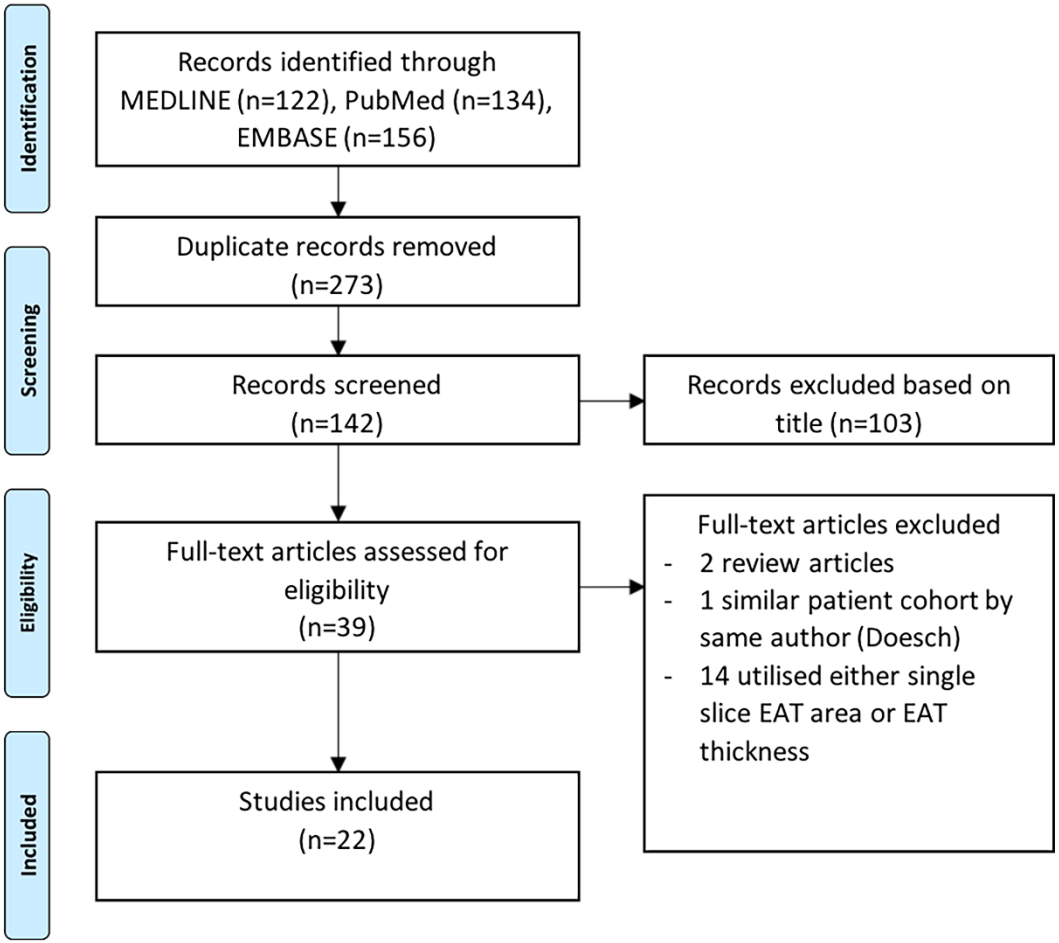

Figure 2: Mean difference of EAT volume in patients with and without Diastolic Dysfunction.

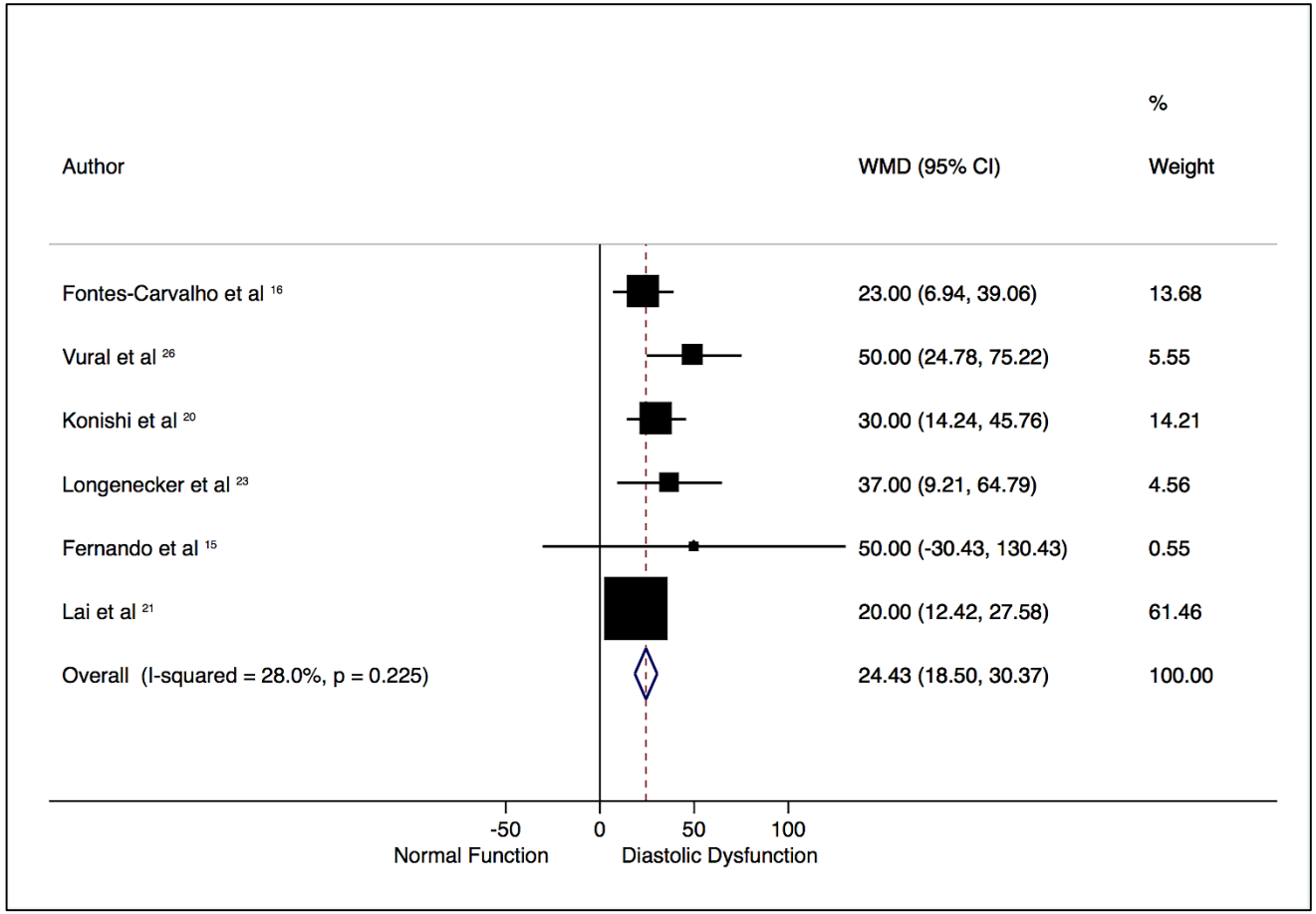

Forest plot demonstrates the weighted mean difference (in mL) of EAT in studies with and without diastolic dysfunction according to a random effect model. Those with diastolic dysfunction have significantly greater EAT volumes. There is mild heterogeneity as seen by the I^2 statistic of 28%. WMD– weighted mean difference, CI– confidence interval

Figure 3: Meta-regression of the effect of increasing EAT volume on the weighted mean difference (effect size) of EAT in patients with and without diastolic dysfunction

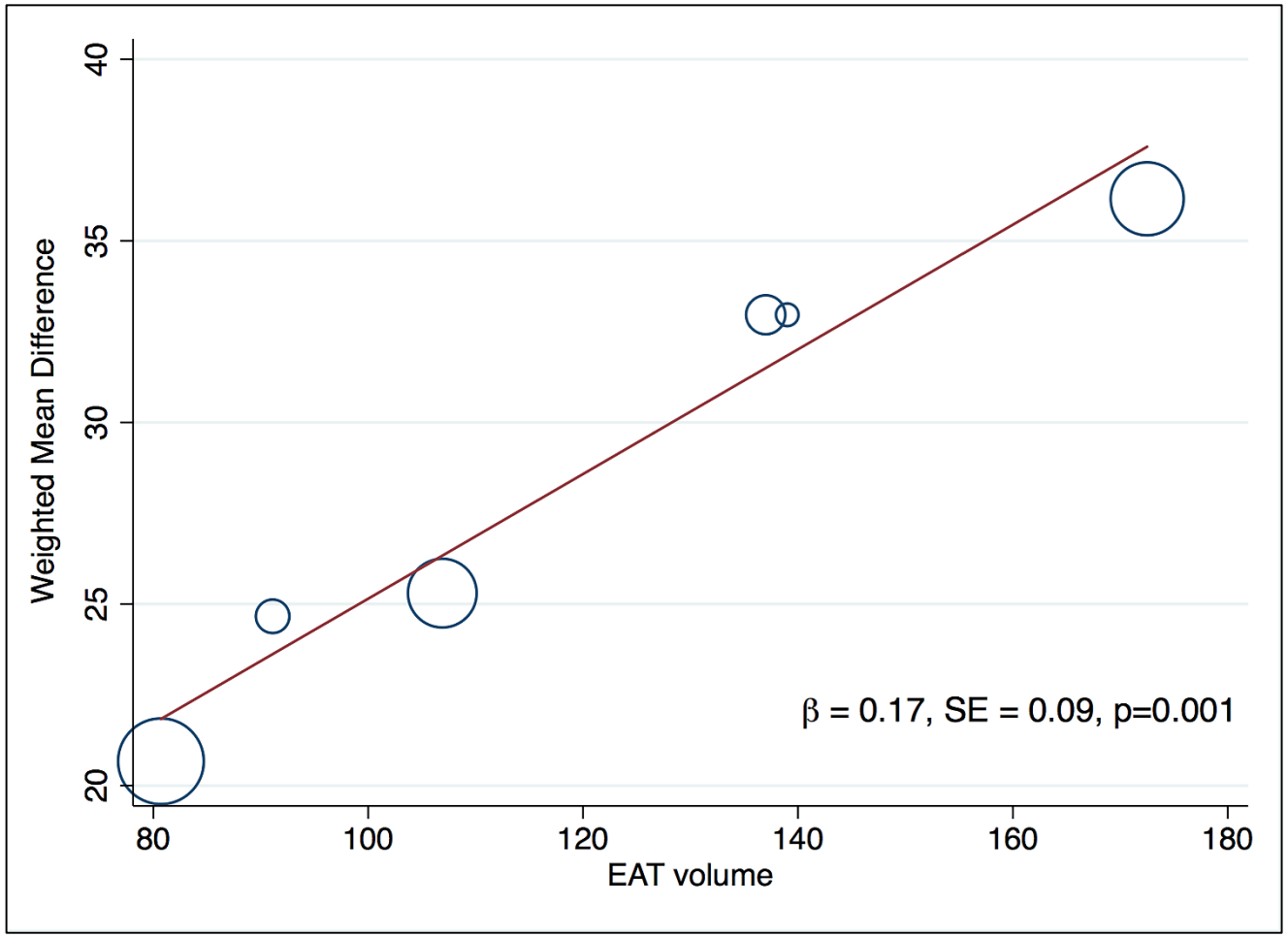

Meta-regression bubble-plot depicts increasing differences in mean EAT volume in patients with diastolic dysfunction as EAT increases. Circles represent the weight of each study. β– beta coefficient from meta-regression with associated standard error (SE) p-value is from Monte-Carlo testing (1000 simulations) and demonstrates a significant association, p=0.001.

SUPPLEMENTAL MATERIAL:

Association of Volumetric Epicardial Adipose Tissue Quantification and Cardiac Structure and Function

Table S1: Example MEDLINE search strategy

#	Searches	Results
1	exp Adipose Tissue/ or epicardial fat.mp.	79789
2	epicardial adipose tissue.mp.	417
3	epicardial fat volume.mp.	56
4	pericardial adipose tissue.mp.	58
5	pericardial fat.mp.	242
6	pericardial fat volume.mp.	31
7	1 or 2 or 3 or 4 or 5 or 6	79916
8	exp Myocardial Contraction/ or exp Heart Failure/ or exp Heart Ventricles/ or exp Echocardiography, Doppler/ or exp Ventricular Dysfunction, Left/ or exp Diastole/ or exp Ventricular Function, Left/ or diastolic function.mp.	260853
9	diastolic dysfunction.mp.	6262
10	systolic function.mp.	9152
11	exp Myocardial Contraction/ or myocardial function.mp.	75943
12	myocardial performance.mp.	2269
13	mitral annular velocities.mp.	154
14	ejection fraction.mp.	44097
15	8 or 9 or 10 or 11 or 12 or 13 or 14	282014
16	exp Tomography, X-Ray Computed/ or cardiac ct.mp.	337987
17	coronary calcium score.mp. or exp Tomography, X-Ray Computed/	337983
18	exp Multidetector Computed Tomography/ or ccta.mp.	4630
19	16 or 17 or 18	338169
20	exp Magnetic Resonance Imaging/	346308
21	cardiac mri.mp.	1739
22	ectopic fat.mp.	396
23	7 or 22	80055
24	20 or 21	346580
25	15 and 19 and 23	53
26	15 and 23 and 24	78
27	25 or 26	122

Table S2a: Newcastle - Ottawa Scale for Assessment of Cross-sectional Studies

First Author	Year	Selection				Comparability	Outcome		Total
		Representativeness of the sample	Sample size	Ascertainment of exposure	Non - respondents	Outcome groups comparable	Assessment of outcome	Correct statistical test	
Bakkum[145]	2015	*	-	**	*	*	*	*	7
Cavalcante[146]	2012	*	-	**	*	**	**	*	9
Ede[150]	2014	*	-	**	*	**	**	*	9
Faustino[¥151]	2011	*	-	**	-	**	*	*	7
Fernando[152]	2015	*	-	**	-	**	*	*	7
Fontes-carvalho[153]	2014	*	-	**	*	**	**	*	9
Fox[154]	2009	*	*	**	*	**	**	*	10
Hachiya[155]	2014	*	-	**	*	*	*	*	7
Khawaja[156]	2011	*	-	**	-	**	**	*	8
Konishi[157]	2012	*	-	**	*	-	*	*	6
Lai[158]	2015	*	-	**	*	**	*	*	8
Liu[159]	2011	*	*	**	*	**	*	*	10
Longenecker[160]	2016	*	-	**	*	**	*	*	8
Ng[161]	2016	*	-	**	*	**	*	*	8
Ruberg[140]	2010	*	-	**	*	*	**	*	8
Wu[164]	2015	*	-	**	*	*	**	*	8
Yamashita[165]	2012	*	-	**	*	**	*	*	8

Table S2b: Newcastle - Ottawa Scale for Assessment of Case Control Studies

First Author	Year	Selection				Comparability	Exposure			Total
		Representativeness of the sample	Adequate case definition?	Selection of controls	Definition of controls	Controls and cases comparable	Ascertainment of exposure	Same method of ascertainment for cases and controls	Non-response rate	
Chekakie[144]	2010	*	*	*	*	**	*	*	*	9
Doesch[148]	2012	*	*	*	*	**	*	*	*	9
Doesch[149]	2013	*	*	*	*	**	**	*	*	10
Doesch[147]	2010	*	*	*	*	**	**	*	*	10
Vanni[162]	2015	*	*	*	*	*	*	*	*	8
Vural[163]	2014	*	*	*	*	**	**	*	*	10

Section/topic	#	Checklist item	Reported on page #
TITLE			
Title	1	Identify the report as a systematic review, meta-analysis, or both.	1
ABSTRACT			
Structured summary	2	Provide a structured summary including, as applicable: background; objectives; data sources; study eligibility criteria, participants, and interventions; study appraisal and synthesis methods; results; limitations; conclusions and implications of key findings; systematic review registration number.	2
INTRODUCTION			
Rationale	3	Describe the rationale for the review in the context of what is already known.	4
Objectives	4	Provide an explicit statement of questions being addressed with reference to participants, interventions, comparisons, outcomes, and study design (PICOS).	4
METHODS			
Protocol and registration	5	Indicate if a review protocol exists, if and where it can be accessed (e.g., Web address), and, if available, provide registration information including registration number.	4
Eligibility criteria	6	Specify study characteristics (e.g., PICOS, length of follow-up) and report characteristics (e.g., years considered, language, publication status) used as criteria for eligibility, giving rationale.	5
Information sources	7	Describe all information sources (e.g., databases with dates of coverage, contact with study authors to identify additional studies) in the search and date last searched.	4
Search	8	Present full electronic search strategy for at least one database, including any limits used, such that it could be repeated.	Supp
Study selection	9	State the process for selecting studies (i.e., screening, eligibility, included in systematic review, and, if applicable, included in the meta-analysis).	5
Data collection process	10	Describe method of data extraction from reports (e.g., piloted forms, independently, in duplicate) and any processes for obtaining and confirming data from investigators.	5
Data items	11	List and define all variables for which data were sought (e.g., PICOS, funding sources) and any assumptions and simplifications made.	5

Risk of bias in individual studies	12	Describe methods used for assessing risk of bias of individual studies (including specification of whether this was done at the study or outcome level), and how this information is to be used in any data synthesis.	6
Summary measures	13	State the principal summary measures (e.g., risk ratio, difference in means).	6
Synthesis of results	14	Describe the methods of handling data and combining results of studies, if done, including measures of consistency (e.g., I^2) for each meta-analysis.	6

Section/topic	#	Checklist item	Reported on page #
Risk of bias across studies	15	Specify any assessment of risk of bias that may affect the cumulative evidence (e.g., publication bias, selective reporting within studies).	6
Additional analyses	16	Describe methods of additional analyses (e.g., sensitivity or subgroup analyses, meta-regression), if done, indicating which were pre-specified.	6
RESULTS			
Study selection	17	Give numbers of studies screened, assessed for eligibility, and included in the review, with reasons for exclusions at each stage, ideally with a flow diagram.	6
Study characteristics	18	For each study, present characteristics for which data were extracted (e.g., study size, PICOS, follow-up period) and provide the citations.	6
Risk of bias within studies	19	Present data on risk of bias of each study and, if available, any outcome level assessment (see item 12).	Supp
Results of individual studies	20	For all outcomes considered (benefits or harms), present, for each study: (a) simple summary data for each intervention group (b) effect estimates and confidence intervals, ideally with a forest plot.	6-8
Synthesis of results	21	Present results of each meta-analysis done, including confidence intervals and measures of consistency.	6-8
Risk of bias across studies	22	Present results of any assessment of risk of bias across studies (see Item 15).	Supp
Additional analysis	23	Give results of additional analyses, if done (e.g., sensitivity or subgroup analyses, meta-regression [see Item 16]).	6-8
DISCUSSION			
Summary of evidence	24	Summarize the main findings including the strength of evidence for each main outcome; consider their relevance to key groups (e.g., healthcare providers, users, and policy makers).	9-11
Limitations	25	Discuss limitations at study and outcome level (e.g., risk of bias), and at review-level (e.g., incomplete retrieval of identified research, reporting bias).	12

Conclusions	26	Provide a general interpretation of the results in the context of other evidence, and implications for future research.	12
FUNDING			
Funding	27	Describe sources of funding for the systematic review and other support (e.g., supply of data); role of funders for the systematic review.	13

From: Moher D, Liberati A, Tetzlaff J, Altman DG, The PRISMA Group (2009). Preferred Reporting Items for Systematic Reviews and Meta-Analyses: The PRISMA Statement. PLoS Med 6(7): e1000097. doi:10.1371/journal.pmed1000097

CHAPTER 4:

COMPUTED TOMOGRAPHY CORONARY ANGIOGRAPHY DERIVED PLAQUE CHARACTERISTICS PREDICT MAJOR ADVERSE CARDIOVASCULAR EVENTS

Nitesh Nerlekar, Francis J. Ha, Caitlin Cheshire, Hashrul Rashid, James D. Cameron, Dennis T. Wong, Sujith Seneviratne, Adam J. Brown

Circulation: Cardiovascular Imaging 2017;10:e006973

ABSTRACT

Background

Computed-tomography coronary angiography (CTCA) is a non-invasive imaging modality that permits identification and characterization of coronary plaques. Despite consensus statements supporting routine reporting of CTCA plaque characteristics, there remains uncertainty whether these data convey prognostic information. We performed a systematic review and meta-analysis assessing the strength of association between CTCA-derived plaque characterization and major adverse cardiovascular events (MACE).

Methods and Results

Electronic databases were searched for studies reporting CTCA plaque characterization and MACE. Data were gathered on plaque morphology (non-calcified, partially-calcified and calcified) and high-risk plaque (HRP) features, including low attenuation plaque, napkin-ring sign, spotty calcification and positive remodelling. Of 5,496 citations, 13 studies met inclusion criteria. 552 (3.9%) MACE occurred in 13,977 patients with mean follow-up ranging between 1.3-8.2yrs. In terms of plaque morphology, the strongest association was observed for non-calcified plaque (Hazard Ratio (HR) 1.45, 95%CI 1.24-1.70, p<0.001), with weaker associations found for partially-calcified (HR 1.37, 95%CI 1.18-1.60, p<0.001) and calcified plaques (HR 1.23, 95%CI 1.16-1.30, p<0.001). All HRP features were strongly associated with MACE, including napkin-ring sign (HR 5.06, 95%CI 3.23-7.94, p<0.001), low-attenuation plaque (HR 2.95, 95%CI 2.03-4.29, p<0.001), positive remodelling (HR 2.58, 95%CI 1.84-3.61, p<0.001) and spotty calcification (HR 2.25, 95%CI 1.26-4.04, p=0.006). The presence of ≥2 HRP features had highest risk of MACE (HR 9.17, 95%CI 4.10-20.50, p<0.001).

Conclusion

These data demonstrate HRP is most likely an independent predictor of MACE, which supports the inclusion of HRP reporting in clinical practice. However, at this point, it remains unclear whether HRP reporting has clinical implications.

INTRODUCTION

Coronary artery disease (CAD) remains a significant healthcare concern despite improvements in preventative strategies and therapeutic possibilities. The majority of sudden ischemic coronary events are precipitated by rupture of a bulky, lipid-rich atheromatous plaque, resulting in the development of intraluminal thrombosis and downstream myocardial injury. Precursor lesions that share similar morphological features to ruptured plaques can be reliably identified using intravascular imaging modalities[176]. Studies using intravascular ultrasound have demonstrated a consistent association between baseline plaque morphology and the occurrence of future major adverse cardiovascular events (MACE) [177-179]. However, the invasive nature of intravascular imaging limits widespread uptake and precludes use in the vast majority of patients with CAD.

Computed tomography coronary angiography (CTCA) is an established, non-invasive imaging modality that can readily identify the presence and distribution of CAD[180]. CTCA allows for qualitative assessment of plaque morphology, classifying lesions either as calcified, non-calcified or partially-calcified type (containing both calcified and non-calcified plaque tissue). Interest in CTCA-derived plaque characteristics has led to identification of specific "high risk" plaque (HRP) features, namely the presence of low attenuation plaque, napkin-ring sign, spotty calcification and positive remodeling[180]. Although prospective observational studies have demonstrated that a number of CTCA-defined plaque features may predict the occurrence of subsequent events[27], the overall strength of the association between individual plaque features and MACE remains unknown. This has led to physician uncertainty as to whether CTCA-defined plaque characteristics should be stated in clinical reports for patients with suspected CAD[181].

We therefore conducted a systematic review and meta-analysis to assess the association between baseline CTCA-defined plaque characteristics and subsequent MACE in patients undergoing imaging for suspected stable CAD.

METHODS

The data, analytic methods, and study materials will be made available to other researchers for purposes of reproducing the results or replicating the procedure. This material can be obtained by contacting the corresponding author.

Data Sources and Search Strategy

A digital literature search was performed through the MEDLINE, EMBASE and PubMed databases for the period up to January 2017. Keywords using Medical Subject Heading (MeSH), where available, included 'coronary artery disease' 'atherosclerosis', 'multidetector computed tomography', 'coronary CT angiography', 'vulnerable plaque', 'high-risk plaque', 'low attenuation plaque', 'spotty calcification', 'napkin ring', 'positive remodelling', 'prognosis' and 'major adverse cardiovascular events'. The search was not limited by language nor date of publication. Reference lists of eligible articles were reviewed for further potential citations. The study protocol was prospectively registered with the PROSPERO international register (CRD42016044003) and adhered to the PRISMA statement (Preferred Reporting Items for Systematic Reviews and Meta-Analyses)[182]. An example search strategy is presented in **Supplemental Table S1**.

Study Selection

Study characteristics for inclusion were as follows: (1) patients with stable cardiovascular disease, (2) assessment of plaque characteristics, including plaque morphology (calcified, non-calcified and partially-calcified) and/or assessment of individual HRP features, including low attenuation plaque, napkin-ring sign, spotty calcification and positive remodelling, (3) evaluation of the association between plaque characteristics and future MACE, (4) clinical follow-up of at least one year after CTCA, and (5) fully published status. We excluded studies that included patients presenting with acute

coronary syndrome (ACS) undergoing CTCA assessment, studies evaluating coronary artery calcium score without specific lesion assessment, studies including asymptomatic patients and studies that included elective revascularization as part of their definition of MACE. Details on the clinical indication for CTCA for each included study are presented in **Supplemental Table S2**. Where multiple studies reported on the same cohort of patients, we only included articles with the longest clinical follow-up and/or largest cohort size.

Data Items and Collection Process

Data items to be collected were specified prior to conducting the literature search. Items for data extraction included study design, clinical rationale for CTCA, patient baseline characteristics and definitions of plaque morphology, HRP features and MACE. We defined plaque morphology and HRP features according to the definitions adopted by each individual study. For HRP features, low attenuation plaque was most commonly defined as plaque with density ≤30 HU, although 1 study used a threshold of ≤38 HU[183]. Napkin ring sign was generally defined as the presence of a plaque core with low CT attenuation surrounded by a rim-like area of higher attenuation. Spotty calcification was either defined as a limit in visualized calcification (<2-3mm) or as a proportion of the vessel dimensions (length of calcium deposit <3/2 of vessel diameter and width of <2/3 of vessel diameter). Full definitions of plaque morphology and HRP features across studies are detailed in **Supplemental Tables S3 and S4,** respectively. Data were also collected on CAD burden at baseline as determined by coronary artery calcium score[184] and proportion of patients with obstructive CAD (≥50% luminal stenosis), follow-up completion and clinical outcomes. Two investigators (N.N. and F.J.H.) independently conducted the literature search and three investigators (F.J.H, C.C. and H.R.) performed the data extraction. Eligible studies and extracted data were verified by the senior author (A.J.B) with any discrepancies resolved by consensus. Risk of bias within individual studies were evaluated according to the Newcastle-Ottawa scale (**Supplemental Table S5**)[185].

Clinical end points

The primary end point of this study was the association between plaque composition (calcified, non-calcified, partially-calcified) and subsequent MACE. Study specific definitions of MACE were used for all analyses. In four studies, MACE was defined as the composite of cardiac death and non-fatal MI[186-189], with nine studies also including unstable angina requiring either hospitalization[183, 190-193] or revascularization[30, 194-196] in their MACE definition. One study did not include death from any cause in their MACE definition[30] (i.e. composite of non-fatal MI and UA), while another study used all-cause death instead of cardiac death[194]. Secondary end points included the associations between specific HRP features on CTCA and subsequent MACE.

Statistical analysis

Data concerning hazard ratio (HR) and 95% confidence intervals (CI) of plaque characteristics and risk of future MACE were extracted and log-transformed, with preference for the HR from the most adjusted model. Full details on the extracted HR and variables used within each model are provided in **Supplemental Table S6**. Data were analysed by random-effects modelling for the primary end point and individual secondary end points to produce overall summary estimates with 95% confidence interval (CI). Statistical heterogeneity was quantified using the I^2 statistic and quantified as low (<25%), moderate (<50%) or high (>75%)[118]. Publication bias was assessed visually by funnel plots and by the Egger test. Sensitivity analyses was performed to explore the effect of systematic exclusion of individual studies to assess for changes in the pooled estimates. Subgroup analysis was performed with studies stratified by clinical endpoints (studies including and excluding revascularization), Asian vs. non-Asian subjects and using a 64-detector row threshold. A 2-sided p-value of <0.05 was considered significant. All statistical analyses were conducted using StataMP 14.0 (Stata Corp LP, College Station, TX).

RESULTS

A total of 5,496 potential citations were screened, with 72 studies identified for potential inclusion and further evaluation. Of these, 59 studies were excluded as they did not specifically evaluate CTCA plaque morphology or HRP features (38 studies), the study patients underwent CTCA for suspected ACS (7 studies), the outcomes reported did not include MACE (7 studies), the definition of MACE included elective coronary revascularization (5 studies), or studies failed to report hazard ratios for individual HRP components or reported on the same patient cohort (2 studies). Full identification and process of study exclusion are detailed in the PRISMA flow diagram (**Figure 1**).

Thirteen studies with a total of 13,977 patients met the pre-specified inclusion criteria and were included in the final quantitative analysis[30, 183, 186-196]. The study period ranged from 2002 to 2011 with 9 prospective studies and 4 studies of retrospective design. The reason for undergoing CTCA was predominantly for suspected CAD (11 studies), although patients with known CAD (e.g., post-coronary intervention excluding bypass grafting) were included in 2 studies[30, 190]. Further details of study design and baseline demographics are presented in **Table 1**.

The slice capability on multi-detector computed tomography (MDCT) varied between studies, with 12 studies using 64-slice MDCT, 2 studies using 16-slice and 1 study using 4-slice (some studies used multiple, different MDCT scanners with different slice capability). The presence of obstructive CAD identified by CTCA ranged from 0-38% in individual study cohorts. Further details of CT characteristics can be found in **Table 2** and **Supplemental Table S7**.

Clinical outcomes

In total, 552 (3.9%) MACE occurred in 13,977 patients with mean study follow-up ranging from 1.3 to 8.2 years. MACE involved cardiac death in 112 patients, non-fatal MI in 330 patients, and unstable

angina requiring hospitalization or revascularization in 110 patients. Full MACE breakdown for each study are presented in **Table 3**.

Plaque morphology and MACE

Nine studies reported outcome data on the association between CTCA plaque morphology and MACE, with 8 studies reporting data on non-calcified plaque, 7 on calcified plaque and 8 on partially-calcified plaque subtypes. The strongest association between CTCA plaque morphology and MACE was observed in non-calcified plaque with an overall HR of 1.45 (95% CI, 1.24-1.70, p<0.001, I^2=63%). Similarly significant, albeit less strong, associations were found both for partially-calcified (HR 1.37, 95% CI, 1.18-1.60, p<0.001 I^2=73%) and calcified plaque (HR 1.23, 95% CI, 1.16-1.30, p<0.001, I^2=13%). Corresponding forest plots illustrating the association between CTCA defined plaque morphology and MACE are presented in **Figure 2**.

In sensitivity analyses, there were no marked differences in the pooled HR for each plaque subtype when the analysis was stratified by those studies including revascularization in their MACE definition, studies using <64 slice multi-detector CT, nor when considering Asian versus non-Asian patient populations (**Supplemental Figures S1-S3, respectively**). Similarly, systematic exclusion of individual studies did not alter the corresponding pooled HR for each plaque subtype (**Tables S8-S10** in Data Supplement). There was no evidence of small-study effects on the Egger test for non-calcified (p=0.07), partially-calcified (p=0.31) or calcified plaque type (p=0.42).

HRP features and MACE

Six studies assessed the secondary end points of the presence of specific HRP features and risk of future MACE, with 6 studies reporting outcomes on low attenuation plaque, 5 on napkin ring sign, 2 on spotty calcification and 6 on positive remodelling. Full details of the included studies are provided

in **Table 2,** with the prevalence of individual HRP features summarized in **Table 4**. Of the four predefined HRP features, napkin-ring sign was associated with the highest risk of future MACE (HR 5.06, 95% CI, 3.23-7.94, p<0.001, I^2=0%). Low attenuation plaque and positive remodelling demonstrated an overall HR of 2.95 (95% CI, 2.03-4.29, p<0.001, I^2=40%) and 2.58 (95% CI, 1.84-3.61, p<0.001, I^2=70%), respectively. Spotty calcification demonstrated the lowest, although still significant, association with risk of future MACE (HR 2.25, 95% CI, 1.26-4.04, p=0.006, I^2=0%). Corresponding forest plots for individual HRP features are presented in **Figure 3**. The significant association between HRP features and MACE remained in sensitivity analyses stratifying studies including Asian versus non-Asian patient populations (**Supplemental Figure S4**). In addition, there remained a significant association between HRP features and MACE when the analysis was limited to studies that included stenosis severity and/or plaque burden in multivariate models (**Supplemental Figure S5**). There was evidence of small-study effects specific to low-attenuation plaque (p=0.003) and positive remodelling (0.01), but not for napkin-ring sign (p=0.13). The presence of ≥2 individual HRP features exhibited the strongest association with MACE (HR 9.17, 95% CI 4.10-20.50, p<0.001, I^2=0%) (**Figure S6** in the Data Supplement).

DISCUSSION

To our knowledge, this is the first meta-analysis to evaluate the association between CTCA-defined plaque characteristics and subsequent MACE. For plaque morphology, we find that the strongest association occurred with non-calcified plaque, with the risk of subsequent clinical events reducing as plaque calcification increases. We also find that all established HRP features are associated with MACE, with the strongest association observed for lesions with the napkin-ring sign. These results demonstrate that the reporting of CTCA-defined plaque characteristics has potential to inform clinicians in the risk stratification of patients.

Pathological studies have established that lipid-rich fibroatheroma are responsible for the majority of ischaemic coronary events through plaque rupture and subsequent intra-luminal thrombosis[197]. Prospective human studies have reaffirmed this observation, demonstrating an independent association between the presence of thin-cap fibroatheromas and future MACE[177]. Our study is consistent with these observations and again highlights that the risk of MACE is highest in non-calcified plaques, which are generally composed of a mixture of lipid-rich and fibrous material. Although detailed analysis of plaque composition is challenging within the spatial resolution of CTCA, lower plaque attenuation values have previously correlated with necrotic core and fibrofatty tissue on virtual-histology intravascular ultrasound imaging[198]. Thus, low attenuation plaques should theoretically have a high proportion of extracellular lipid content. Our data would again be consistent with this, as we find a stronger association between low attenuation plaques and MACE, when compared with non-calcified plaque. Taken together, these data suggest that interpretation of CTCA-defined plaque morphology may impart important prognostic information independent of established calcium scoring algorithms.

Our data again highlights a potentially discrepant relationship between coronary calcification and future cardiovascular risk. On one hand, previous observational studies have consistently demonstrated that the risk of future cardiovascular events is progressively increased with higher coronary artery calcium scores[199]. However, our pooled results suggest that calcified plaques have the weakest association with MACE, while the risk of future events was more than doubled if a lesion displayed evidence of spotty calcification. These data would therefore suggest that the pattern and extent of intimal calcification may be an important determinant of risk. Biomechanical models have suggested that small, microscopic calcific deposits in the fibrous cap and plaque architecture can act to amplify plaque structural stress, acting as a possible driver for plaque rupture[200, 201]. However, as calcification becomes more extensive, the macroscopic plates of calcification can act as a stress shield, protecting the plaque from high mechanical loading[202]. Support for this theory has also emerged from recent data highlighting that statins may promote plaque stabilization through progressive macroscopic intimal calcification[203]. Further studies are now required to ascertain the role of calcification in plaque destabilization and to assess whether the mechanisms that promote intimal calcification can be induced in an effort to improve clinical outcomes.

We find that each pre-specified HRP feature in our analysis was strongly associated with MACE and that there was an incremental risk when ≥2 HRP features were present within the same plaque. While the presence of multiple HRP features in individual lesions was only evaluated in two studies[183, 192], similar results were reported by a large prospective study[27]. In this study, plaques with either low-attenuation, positive remodelling or both features, were a significant predictor of the development of future acute coronary syndrome (adjusted HR 8.24, 95% CI 5.26-12.96). These data imply that future cardiovascular risk could be higher in patients that demonstrate multiple HRP features or even multiple plaques with HRP features. Further prospective studies are now required to assess whether CT-defined

HRP features can be used to guide pharmacological strategies in an effort to improve clinical outcomes in a manner that is economically viable.

Positive predictive value (PPV) was not uniformly reported by the studies in our analysis, and when it was described, estimates were at a segmental-level and the inference at a patient-level remains unclear. In addition, the quoted PPV for individual plaque characteristics were quite discrepant between studies and were likely influenced by the low prevalence of HRP features in patients with stable symptoms, as PPV is influenced by disease prevalence such that, when prevalence is low, so too is PPV. For example, in the study by Otsuka et al.[196], the prevalence of HRP segments was 24% and the associated PPV for MACE was 86%. Conversely, in another analysis by the same group[191], the prevalence of NRS was 0.4% yielding a PPV of 22%. Currently there is no recommendation on the management of individual HRP features, or whether these patients require more aggressive risk factor treatment. Plaque burden and stenosis severity are well-established markers of prognosis and it is hypothesized that HRP may simply be a marker of greater atherosclerotic burden[204]. While no studies have reported HRP significance over plaque extent, in our pooled sensitivity analysis of studies that adjusted for 'obstructive' stenosis, HRP presence was independently associated with MACE. These results should encourage the requirement for a uniform reporting system such as CAD-RADS that incorporates HRP, however should also include plaque morphology and disease extent as well[181]. Application of these parameters both in clinical practice and the research literature will overcome inconsistencies encountered in pooling data and allow future studies to ascertain the true independent effect of HRP on patient prognosis.

Study limitations

There are certain limitations to our analysis that should be considered when interpreting the findings. First, the included studies have used variable definitions for plaque morphology and specific HRP

features that will have introduced a degree of heterogeneity into the analysis. However, the differences in definitions were modest and are unlikely to affect the overall biological association between plaque characteristics and clinical outcomes. Second, CT technology also varied between studies, which may have affected the inter-study reliability for the assessment of plaque morphology and influenced the prevalence of HRP identified. Although the majority of our studies reported outcomes at a patient-level, segment-based risk estimates were utilized for two studies[191, 196] and inclusion of these data may have had subtle effects on the overall pooled estimates. We had no access to patient- or segment-level data and were therefore unable to directly quantify any incremental prognostic information provided by plaque characterization over other known CTCA-derived markers of risk, including stenosis severity and atheroma volume. Unstable angina requiring either revascularization or hospitalization was also part of the MACE definition in nine included studies, which may limit ascertainment of the relative prognostic value of HRP versus stenosis severity. Finally, while some studies suggest that HRP is a predictor of MACE, independent of stenosis, the data do not demonstrate that HRP is a stronger predictor than significant stenosis and most data suggest that it may not be. Given this limitation and the fact that the PPV is low, it remains unclear whether HRP reporting may have management implications.

CONCLUSIONS

Our data demonstrate that HRP is most likely an independent predictor of MACE, which supports the inclusion of HRP reporting in clinical practice. However, at this point it remains unclear whether HRP reporting may have clinical implications.

CLINICAL SUMMARY

Computed-tomography coronary angiography (CTCA) is an established non-invasive imaging modality that permits identification and characterization of atherosclerotic coronary plaques. Despite consensus statements supporting routine reporting of CTCA plaque characteristics, there remains clinical uncertainty on whether such features convey important prognostic information. We therefore performed a systematic review and meta-analysis to assess the strength of association between CTCA-derived plaque characterization and major adverse cardiovascular events (MACE). Of the 5,496 potential citations, 13 studies encompassing 13,977 patients met inclusion criteria. Data were gathered on plaque morphology (non-calcified, partially-calcified and calcified) and high-risk plaque (HRP) features, including low attenuation plaque, napkin-ring sign, spotty calcification and positive remodelling. Overall, 522 (3.9%) of patients sustained MACE with mean follow-up ranging between 1.3-8.2yrs. We find that the strongest association between CTCA-defined plaque morphology and MACE was observed from non-calcified plaque, followed by partially-calcified and then calcified plaque subtypes. All high-risk plaque features were strongly associated with MACE, with the strongest association found for plaques with napkin-ring sign. The presence of ≥2 HRP features within the same plaque conferred the highest risk of MACE. Importantly, sensitivity analysis demonstrated that HRP features had an independent effect on prognosis beyond stenosis severity alone. These data reinforce that routine reporting of CTCA-defined plaque morphology and HRP features have potential to improve patient risk stratification.

Table 1. Baseline characteristics of included studies

Author	Publication year	Study period	Location	Design	Reason for CTCA	No. of patients	Male, %	Age, yrs	HTN, %	Dyslipidaemia, %	DM, %
Matsumoto et al.[190]	2007	2002-2006	Japan	R	Suspected and known CAD	810	59	58±11	37	40	19
van Werkhoven et al. [194]	2009	NR	Europe	P	Suspected CAD	432	59	58±11	57	39	28
Chow et al.[186]	2010	2006-2008	Canada	P	Suspected CAD	2172	76	59±11	51	53	14
Andreini et al.[187]	2012	2005-2008	Italy	P	Suspected CAD	1196	62	62±11	59	45	11
Hou et al.[188]	2012	2007-2008	China	R	Suspected CAD	4425	62	60±11	57	28	15
Miszalski-Jamka et al.[189]	2012	2003-2004	Poland	R	Suspected CAD	494	52	58±10	78	63	11
Petretta et al.[195]	2012	2006-2008	Italy	P	Suspected CAD	326	68	62±12	51	38	12
Otsuka et al.[191]	2013	2007-2010	Japan	P	Suspected CAD	895	66	66±10	66	55	49
Yamamoto et al.[183]	2013	2006-2009	Japan	R	Suspected CAD	453*	63	66±11	61	53	41
Nakanishi et al.[30]	2014	2005-2013	Japan	P	Suspected and known CAD	517	71	66±10	77	58	37
Otsuka et al.[196]	2014	2007-2011	Japan	P	Suspected CAD	543	63	65±10	63	53	44
Conte et al.[192]	2016	2004-2007	Italy	P	Suspected CAD	245	70	63±9	60	48	9
Feutchner et al.[193]	2016	2005-2011	Austria	P	Suspected CAD	1469	56	66	51	51	10

*Data presented on original cohort of 511 patients

CAD, Coronary artery disease; CTCA, Computed tomography coronary angiography; DM, Diabetes mellitus; HTN, Hypertension; P, Prospective; R, Retrospective

Table 2. Plaque characteristics and MACE definitions

Author	Year	MDCT Slice	CACS	Obstructive CAD, %	Analysis	Plaque characteristics analysed							MACE definition	F/U duration, years	F/U completion
						Morphology			Vulnerable features						
						CP	NCP	PCP	LAP	NRS	SC	PR/RI			
Matsumoto et al.[190]	2007	4/16	NS	NS	PP	N	Y	N	N	N	N	N	Cardiac death, MI, UA	2.9±1.5	87%
van Werkhoven et al.[194]	2009	64	290±730	25	PP	Y	Y	Y	N	N	N	N	All-cause death, non-fatal MI, UA requiring revasc.	1.8 (IQR 1.1-2.5)	93%
Chow et al.[186]	2010	64	NS	30	PP	Y	Y	Y	N	N	N	N	Cardiac death, non-fatal MI	1.3±0.7	96%
Andreini et al.[187]	2012	64	151 (range 0-380)	38	PP	Y	Y	Y	N	N	N	N	Cardiac death, non-fatal MI	4.3±1.8	97%
Hou et al.[188]	2012	64	NS	20	PP	N	Y	Y	N	N	N	N	Cardiac death, MI	3.0 (IQR 2.6-3.3)	98%
Miszalski-Jamka et al.[189]	2012	64/16	NS	28	PP	Y	Y	Y	N	N	N	N	Cardiac death, non-fatal MI	3.6±0.9	98%
Petretta et al.[195]	2012	64	87±127	34	PP	Y	N	Y	N	N	N	N	Cardiac death, non-fatal MI, UA requiring revasc.	2.2±1.0	99%
Otsuka et al.[191]	2013	64	NS	NS	PS	N	N	N	Y	Y	N	Y	Cardiac death, MI, UA	2.3±0.8	100%
Yamamoto et al.[183]	2013	64	NS	27	UK	Y	Y	Y	Y	N	Y	Y	Cardiac death, non-fatal MI, UA requiring urgent hosp.	3.3±1.2	89%
Nakanishi et al.[30]	2014	64	NS	NS	PP	N	N	N	Y	Y	N	Y	MI, UA requiring immediate revasc.	4.1±1.8	NS
Otsuka et al.[196]	2014	64	NS	30	PS	Y	Y	Y	Y	Y	N	Y	Cardiac death, non-fatal MI, UA requiring revasc.	3.4 (range, 1-5.4)	96%
Conte et al.[192]	2016	64	NS	0	PP	N	N	N	Y	Y	N	Y	Cardiac death, MI, UA	8.2±1.7	94%
Feutchner et al.[193]	2016	64	143±359	NS	PP	N	N	N	Y	Y	Y	Y	Cardiac death, MI, UA	7.8 (range, 4.8-9.8)	49%

CACS, Coronary artery calcium score; CAD, Coronary artery disease; CP, Calcified plaque; F/U, Follow-up; Hosp., Hospitalization; IQR, Interquartile range; LAP, Low-attenuation plaque; MACE, Major adverse cardiovascular events; MDCT, Multi-detector computed tomography; MI, Myocardial infarction; N. No; NCP, Non-calcified plaque; NRS, Napkin-ring sign; NS, Not specified; PCP, Partially-calcified plaque; PP, Per patient; PR, Positive remodelling; PS, Per segment; Revasc., Revascularization; RI, Remodelling index; SC, Spotty calcification; UA, Unstable angina; UK, Unknown

Table 3. Individual study breakdown of MACE

Author	Year	MACE			
		Total	Cardiac death	Non-fatal MI	UA requiring hosp./revasc.
Matsumoto et al.[190]	2007	28	6	7	15
van Werkhoven et al.[194]	2009	21	6	8	7
Chow et al.[186]	2010	34	11	23	N/A
Andreini et al.[187]	2012	136	18	118	N/A
Hou et al.[188]	2012	127	40	87	N/A
Miszalski-Jamka et al.[189]	2012	17	9	8	N/A
Petretta et al.[195]	2012	34	13	9	12
Otsuka et al.[191]	2013	24	1	4	19
Yamamoto et al.[183]	2013	15	2	7	6
Nakanishi et al.[30]	2014	43	0	13	30
Otsuka et al.[196]	2014	24	1	4	19
Conte et al.[192]	2016	8	2	6	N/A
Feutchner et al.[193]	2016	41	3	36	2

Hosp, Hospitalization; MACE, Major adverse cardiovascular events; MI, Myocardial Infarction; N/A, Not applicable; NR, Not recorded; Revasc., Revascularization; UA, Unstable angina;

Table 4. Prevalence of high-risk plaque features

Author	LAP	PR	NRS	SC
Plaque level				
Otsuka et al.*[191]	107/1174 (9.1%)	130/1174 (11%)	45/1174 (3.8%)	N/A
Yamamoto et al.[183]	NS	NS	NS	NS
Nakanishi et al.*[30]	113/864 (13%)	108/864 (13%)	26/864 (3%)	N/A
Otsuka et al.*[196]	133/1107 (12%)	183/1107 (16%)	30/1107 (2.7%)	N/A
Patient level				
Conte et al.†[192]	8/245 (3.3%)	196/245 (80%)	3/245 (1.2%)	51/245 (21%)
Feutchner et al.†[193]	55/1469 (3.7%)	NS	66/1469 (4.4%)	231/1469 (16%)

*Proportion of total coronary plaques

†Proportion of total patients

HRP, High-risk plaque; LAP, Low-attenuation plaque; N/A, Not applicable; NRS, Napkin-ring sign; NS, Not specified; PR, Positive remodelling; SC, Spotty calcification

Figure 1. Study flow chart

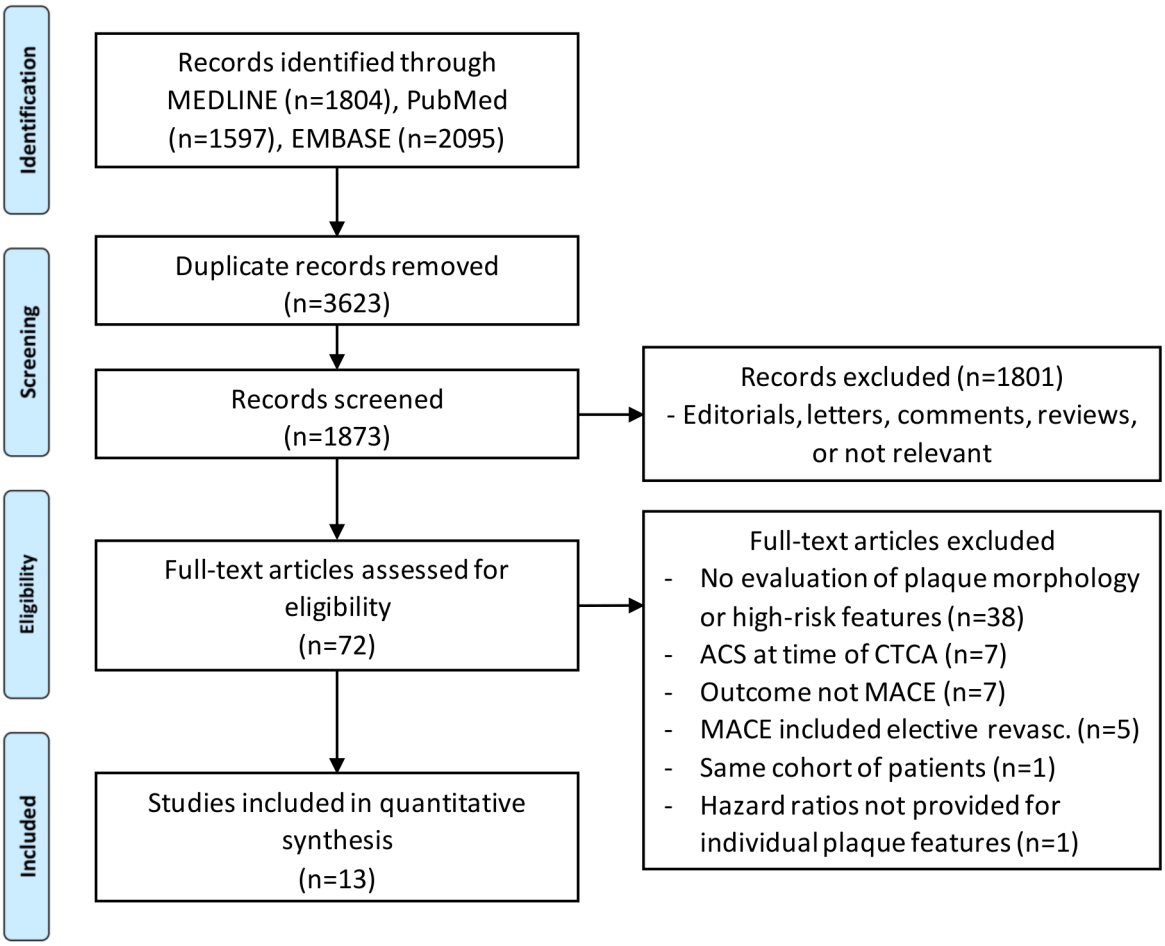

PRISMA flow diagram illustrating the study selection process for the systematic review and meta-analysis.

Figure 2. Plaque morphology and risk of major adverse cardiovascular events

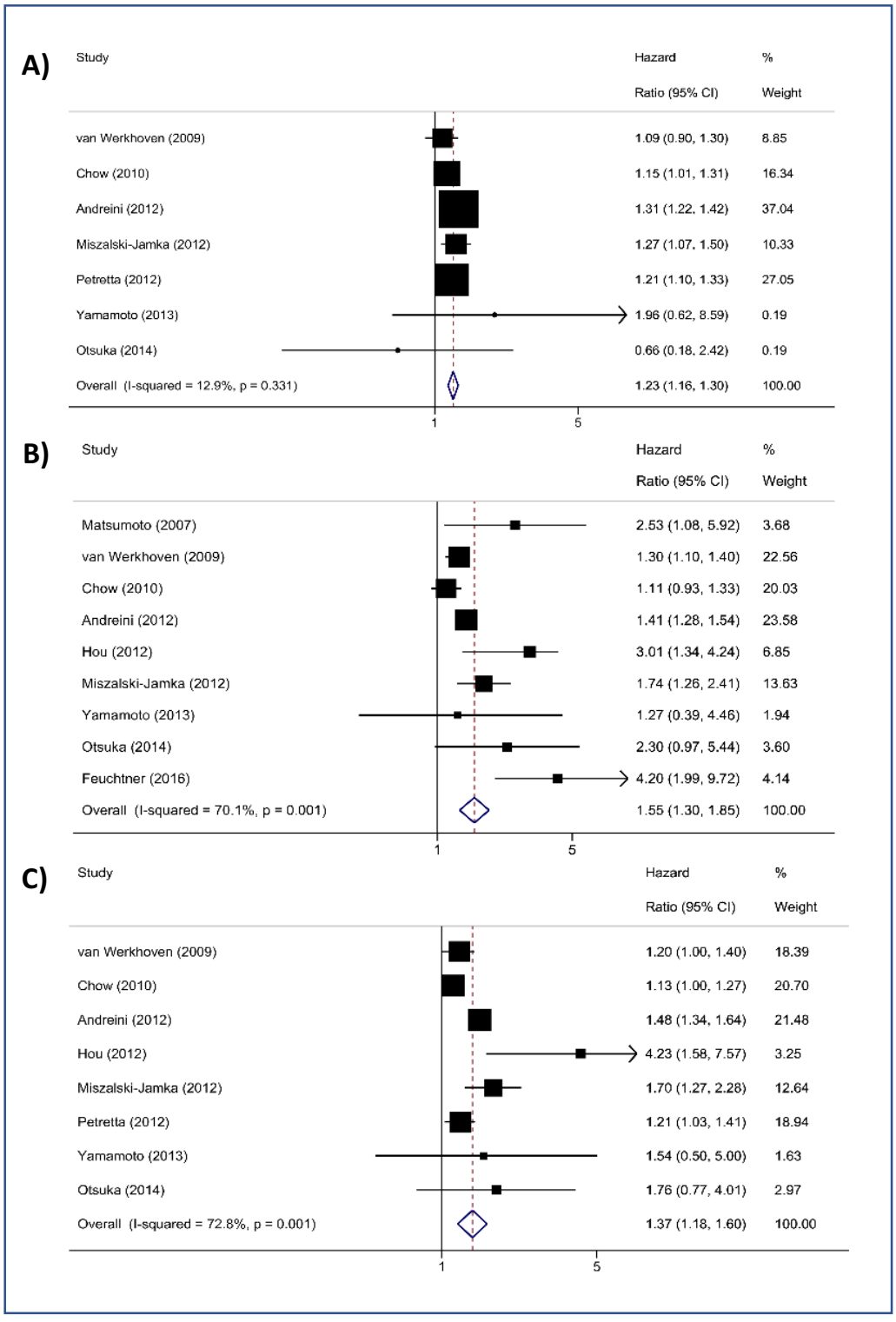

Forest plot displays summary hazard ratio (HR) and 95% confidence intervals (CI) for future MACE stratified by (**A**) calcified plaque, (**B**) non-calcified plaque, and (**C**) partially-calcified plaque subtypes.

Figure 3. High-risk plaque features and risk of major adverse cardiovascular events

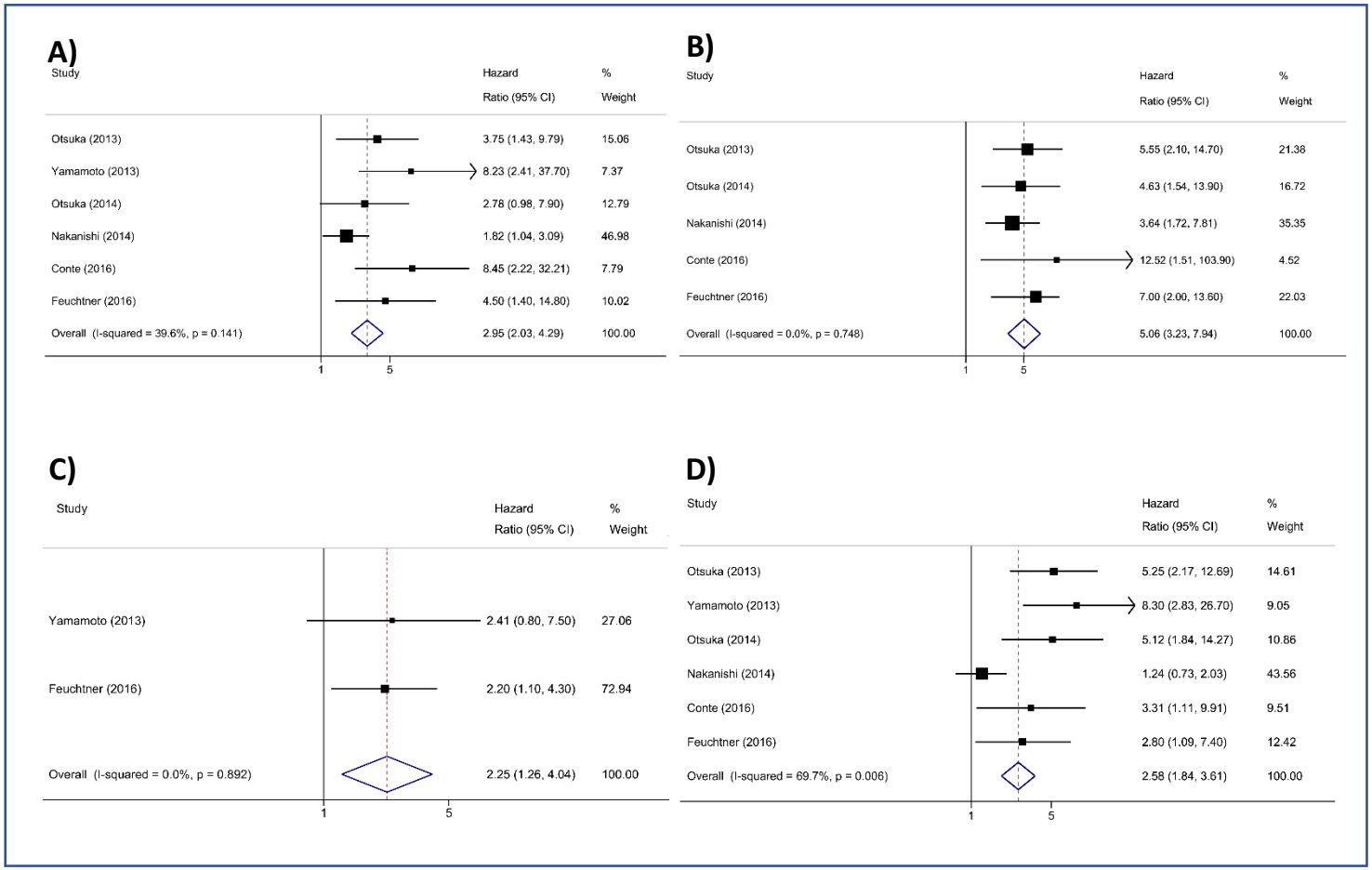

Forest plot displays summary hazard ratio (HR) and 95% confidence intervals (CI) for future MACE stratified by (**A**) low-attenuation plaque, (**B**) napkin-ring sign, (**C**) spotty calcification, and (**D**) positive remodelling.

SUPPLEMENTAL MATERIAL:

Computed tomography coronary angiography derived plaque characteristics predict major adverse cardiovascular events

Table S1. Example search strategy for Medline

#	Searches	Results
1	Coronary Artery Disease/	54096
2	Coronary Stenosis/	10503
3	Atherosclerosis/	33413
4	Acute Coronary Syndrome/	11741
5	Non-obstructive coronary artery disease.mp	57
6	Coronary Vessels/	57645
7	Multidetector Computed Tomography/	5403
8	Tomography, X-Ray Computed/	389198
9	Tomography, Spiral Computed/	7435
10	Coronary CT angiography.mp	1249
11	Vulnerable plaque.mp	1057
12	High-risk plaque.mp	145
13	Plaque, Atherosclerotic/	6422
14	Low-attenuation plaque.mp	44
15	Napkin ring.mp	47
16	Spotty calcification.mp	82
17	Positive remodeling.mp	370
18	Prognosis/	457689
19	Myocardial Infarction/	168210
20	Myocardial Revascularization/	10933
21	Kaplan-Meier Estimate/	51833
22	Major adverse cardiovascular events.mp	1561
23	1 or 2 or 3 or 4 or 5 or 6	153520
24	7 or 8 or 9 or 10 or 11 or 12 or 13 or 14 or 15 or 16 or 17	407784
25	18 or 19 or 20 or 21 or 22	655305
26	23 and 24 and 25	1804

Table S2. Indications for CTCA for each included study

Author	Year	Indications for CTCA
Matsumoto et al.	2007	– Evaluation of chest pain (61%) – Post-coronary intervention status (9%) – Evaluation of CAD in asymptomatic patients with multiple CVD risk factors (15%) – Not specified (15%)
van Werkhoven et al.	2009	– Suspected CAD referred for further assessment because of chest pain, positive exercise ECG test, or high-risk profile for CVD (100%)
Chow et al.	2010	– Evaluation of chest pain (58%) o Typical angina (16%) o Atypical angina (15%) o Non-anginal chest pain (28%) – Evaluation of dyspnoea (16%) – Evaluation of palpitations (1%) – Evaluation of syncope (1%) – Asymptomatic o Rule out CAD/CVD risk factors (11%) o Equivocal/abnormal stress test (6%) o Pre-cardiac surgery (4%) o LV dysfunction (0.6%) o Other, not specified (2%)
Andreini et al.	2012	– Evaluation of chest pain (43%) – Evaluation of CAD in asymptomatic patients with multiple CVD risk factors (28%) – Equivocal/abnormal stress test (29%)
Hou et al.	2012	– Evaluation of chest pain (69%) o Typical angina (6%) o Atypical angina (16%) o Non-anginal chest pain (47%) – Evaluation of CAD in asymptomatic patients with ≥1 CVD risk factors (NS %) – Evaluation of ECG abnormalities (NS %) – Evaluation of prior revascularization (NS %)
Miszalski-Jamka et al.	2012	– Evaluation of chest pain (100%) o Typical angina (40%) o Atypical angina (30%) o Non-anginal chest pain (30%)
Petretta et al.	2012	– Evaluation of chest pain o Typical angina (32%) o Atypical angina (63%) o Non-anginal chest pain (5%)
Otsuka et al.	2013	– Evaluation of chest pain (60%) – Evaluation of CAD in asymptomatic patients with multiple CVD risk factors and abnormal findings on exercise-stress echocardiography or single-photon emission computed tomography (40%)

Yamamoto et al.	2013	– Evaluation of chest pain (54%) – Asymptomatic with ischemic findings (25%) – Evaluation of CAD in asymptomatic patients with multiple CVD risk factors (22%)
Nakanishi et al.	2014	– Evaluation of chest pain (77%) o Typical angina (27%) o Atypical angina (34%) o Non-anginal chest pain (16%) – Evaluation of CAD in asymptomatic patients with multiple CVD risk factors, PAD, cerebrovascular disease, abnormal findings ECG or echocardiography (23%)
Otsuka et al.	2014	– Evaluation of chest pain (62%) – Evaluation of CAD in asymptomatic patients with multiple CVD risk factors (38%)
Conte et al.	2017	– Evaluation of chest pain (50%) o Typical angina (6%) o Atypical angina (44%) – Evaluation of dyspnoea (10%) – Evaluation of CAD in asymptomatic patients with multiple CVD risk factors (40%)
Feuchtner et al.	2017	– Evaluation of chest pain (NS %) – Evaluation of CAD in asymptomatic patients with multiple CVD risk factors (NS %)

Table S3. Definitions of plaque morphology

Author	Year	Plaque Morphology Definition		
		Calcified plaque	Non-Calcified plaque	Partially-calcified
Matsumoto et al.[190]	2007	N/A	Low-density plaque defined as <68 HU	N/A
van Werkhoven et al.[194]	2009	High-density plaques	Lower density than contrast-enhanced lumen	Both calcified and non-calcified components
Chow et al.[186]	2010	NS	NS	NS
Andreini et al.[187]	2012	High-density plaques	Density less than contrast-enhanced vessel lumen	Both calcified and non-calcified components
Hou et al.[188]	2012	Exclusively high-density material >130 HU	Exclusively material of density ≤130 HU	Both calcified and non-calcified components
Miszalski-Jamka et al.[189]	2012	Density greater than contrast-enhanced lumen	Lower density than contrast-enhanced lumen	Both calcified and non-calcified components
Petretta et al.[195]	2012	Exclusively high-density material >130 HU	Exclusively material of density ≤130 HU	Both calcified and non-calcified components
Yamamoto et al.[183]	2013	CT density >130 HU or greater than that of the contrast-enhanced coronary lumen	Low-density area <1 mm^2 in size with CT density ≤130 HU	N/A
Otsuka et al.[196]	2014	Predominantly calcification	Density less than contrast-enhanced vessel lumen without any calcification	Small amount of calcification elements within a single plaque

CT, Computed tomography; HU, Hounsfield unit; N/A, Not applicable; NS, Not specified; PR, Positive remodelling; RI, Remodelling index

Table S4. Definitions of specific high-risk plaque features

Author	Year	HRP Features Definition			
		LAP	NRS	SC	PR
Otsuka et al.[191]	2013	<30 HU	Presence of a plaque core with low CT attenuation surrounded by a rim-like area of higher attenuation	N/A	RI>1.1
Yamamoto et al.[183]	2013	≤38 HU	N/A	Length of calcium deposit <3/2 of vessel diameter and width <2/3 of vessel diameter	RI ≥1.05
Nakanishi et al.[30]	2014	<30 HU	Presence of a plaque core with low CT attenuation surrounded by a rim-like area of higher CT attenuation	N/A	RI >1.1
Otsuka et al.[196]	2014	<30 HU	Plaque core with low attenuation surrounded by rim-like area of higher attenuation. CTCA attenuation of the ring presenting higher than those of adjacent plaque and no >150 HU	N/A	RI >1.1
Conte et al.[192]	2017	<30 HU	Presence of semicircular thin enhancement around the plaque along the outer contour of the vessel	Calcification <2mm	RI >1.1
Feutchner et al.[193]	2017	<130 HU, although specify <30 HU, <60 HU and <90 HU	Outer high-density rim (<200 HU) with inner hypodense area (<130 HU) not adjacent to calcification and present in ≥2 adjacent axial 1mm slices	Calcification <3 mm	No specific limit set – analysed as continuous variable)

HRP, high-risk plaque; HU, Hounsfield Units; LAP, Low-attenuation plaque; N/A, Not applicable; NRS, Napkin-ring sign; PR, Positive remodelling; RI, Remodelling index; SC, Spotty calcification

Table S5. Assessment of study quality using the Newcastle-Ottawa scale

Author	Year	Study quality			
		Selection	Comparability	Outcome/exposure	Total score
Matsumoto et al.[190]	2007	***	-	**	5
van Werkhoven et al.[194]	2009	****	-	**	5
Chow et al.[186]	2010	****	-	***	7
Andreini et al.[187]	2012	****	-	***	7
Hou et al.[188]	2012	****	*	**	7
Miszalski-Jamka et al.[189]	2012	****	-	***	7
Petretta et al.[195]	2012	****	-	**	6
Otsuka et al.[191]	2013	****	-	***	7
Yamamoto et al.[183]	2013	****	-	***	7
Nakanishi et al.[30]	2014	****	-	***	7
Otsuka et al.[196]	2014	***	-	***	6
Conte et al.[192]	2017	****	-	**	6
Feutchner et al.[193]	2017	****	-	**	6

Table S6. Individual hazard ratios for plaque characteristics and variables included in multivariable modelling

Author	Year	Plaque	Hazard Ratio (95% CI)	Variables included in adjusted model
Matsumoto et al.	2007	NCP	2.53 (1.08-5.92)	Diabetes, previous MI*
van Werkhoven et al.	2009	CP	1.09 (0.9-1.3)	Age, sex, calcium score ≥1000
		NCP	1.3 (1.1-1.4)	
		Mixed	1.2 (1-1.4)	
Chow et al.	2010	CP	1.15 (1.01-1.31)	Patient baseline characteristics (not further specified), CAD severity, LVEF
		NCP	1.11 (0.93-1.33)	
		Mixed	1.13 (1-1.27)	
Andreini et al.	2012	CP	1.31 (1.22-1.42)	Unadjusted
		NCP	1.41 (1.28-1.54)	
		Mixed	1.48 (1.34-1.64)	
Hou et al.	2012	NCP	3.01 (1.34-4.24)	Unadjusted
		Mixed	4.23 (1.58-7.57)	
Miszalski-Jamka et al.	2012	CP	1.7 (1.27-2.28)	Plaque morphology (non-calcified, partially calcified, calcified)*
		NCP	1.74 (1.26-2.41)	
		Mixed	1.27 (1.07-1.5)	
Petretta et al.	2012	CP	1.21 (1.1-1.33)	Calcium score, significant CAD, plaque morphology (non-calcified, partially calcified, calcified), segment involvement score, segments-at-risk score*
		Mixed	1.21 (1.03-1.41)	
Otsuka et al.	2013	LAP	3.75 (1.43-9.79)	Patient baseline characteristics (not further specified), obstructive plaque
		NR	5.55 (2.1-14.7)	
		PR	5.25 (2.17-12.69)	
Yamamoto et al.	2013	CP	1.96 (0.62-8.59)	Age, sex, diameter stenosis >50%
		NCP	1.27 (0.39-4.46)	
		Mixed	1.54 (0.5-5.0)	
		LAP	8.23 (2.41-37.7)	
		PR	8.3 (2.83-26.7)	
		SC	2.41 (0.8-7.5)	
		HRP	11.2 (3.71-36.7)	
Nakanishi et al.	2014	LAP	1.82 (1.04-3.09)	Previous revascularization, Δ LDL-C
		NRS	3.64 (1.72-7.81)	
		PR	1.24 (0.73-2.03)	
Otsuka et al.	2014	CP	0.66 (0.18-2.42)	Hypertension, CT luminal stenosis, 2 or 3 vessel disease, calcified plaque, obstructive plaque, PR, LAP, NRS*
		NCP	2.3 (0.97-5.44)	
		Mixed	1.76 (0.77-4.01)	
		LAP	2.78 (0.98-7.9)	
		NRS	4.63 (1.54-13.9)	
		PR	5.12 (1.84-14.27)	
Conte et al.	2017	LAP	8.45 (2.22-32.21)	Beta-blocker use
		NRS	12.5 (1.51-103.9)	
		PR	3.31 (1.11-9.91)	
		HRP	7.54 (2.43-23.34)	

Feutchner et al.	2017	LAP	4.5 (1.4-14.8)	Age, gender, arterial hypertension, nicotine, positive family history, BMI, dyslipidaemia, diabetes, CT stenosis severity, CT plaque type
		NRS	7 (2-13.6)	
		SC	2.2 (1.1-4.3)	
		PR	2.8 (1.09-7.4)	

*Only variables which reached significance ($p<0.05$) in the univariable model where included in the multivariable, adjusted model

CAD, Coronary artery disease; CP, Calcified plaque; CT, Computed tomography; HRP, High risk plaque (≥2 features) LAP, Low attenuation plaque; LDL-C, Low density lipoprotein – cholesterol; LVEF, Left ventricular ejection fraction; MI, Myocardial Infarction; NCP, Non calcified plaque; NRS, Napkin ring sign; PR, Positive remodelling; SC, Spotty calcification

Table S7. Characteristics of computed tomography coronary angiography

Author	Year	CT scanner	mA	kV	Software
Matsumoto et al.[190]	2007	SOMATOM Volume Zoom (4 slice)	320	140	3D Virtuoso
		Aquilion 16	400	140	M900 Quadra
van Werkhoven et al.[194]	2009	Aquilion 64	200-250	120	Vitrea2
		GE Lightspeed VCT (64-slice)			Advantage
Chow et al.[186]	2010	GE Volume CT (64-slice)	400-800	120	GE Advantage Volume Share Workstation
Andreini et al.[187]	2012	GE Volume CT (64-slice)	NS	NS	CardioQ3 package
Hou et al.[188]	2012	Light Speed VCT (64-slice)	200-550	120	Deep Blu, ADW 4.3
Miszalski-Jamka et al.[189]	2012	Somatom Sensation 64	350-400	120	3D Leonardo
		Somatom Sensation 16	400-500	120	3D Leonardo
Petretta et al.[195]	2012	Lightspeed VCT (64-slice)	600	100-120	Advantage Workstation
Otsuka et al.[191]	2013	Somatom 64	770-850	120	NS
Yamamoto et al.[183]	2013	Lightspeed VCT (64-slice)	300	120	NS
Nakanishi et al.[30]	2014	Somatom Sensation 64	770-850	120	Synapse Vincent
Otsuka et al.[196]	2014	SOMATOM 64	770-850	120	NS
Conte et al.[192]	2017	GE Volume CT (64-slice)	NS	NS	NS
Feutchner et al.[193]	2017	Sensation 64	NS	NS	SyngoVia
		Definition FLASH 128			

CT; Computed Tomography; NS, Not specified

Table S8. Calcified plaque and risk of MACE: Sensitivity Analyses with systematic exclusion of individual studies

Excluded study	Year	Pooled Hazard Ratio	Lower 95% CI	Upper 95% CI
Van Werkhoven et al.[194]	2009	1.25	1.19	1.32
Chow et al.[186]	2010	1.25	1.18	1.33
Andreini et al.[187]	2012	1.19	1.11	1.27
Miszalski-Jamka et al.[189]	2012	1.22	1.14	1.31
Petretta et al.[195]	2012	1.23	1.13	1.33
Yamamoto et al.[183]	2013	1.23	1.15	1.30
Otsuka et al.[196]	2014	1.23	1.16	1.30
All studies included		**1.23**	**1.16**	**1.30**

Table S9. Non-calcified plaque and risk of MACE: Sensitivity Analyses with systematic exclusion of individual studies

Excluded study	Year	Pooled Hazard Ratio	Lower 95% CI	Upper 95% CI
Matsumoto et al.[190]	2007	1.42	1.22	1.66
Van Werkhoven et al.[194]	2009	1.58	1.26	1.98
Chow et al.[186]	2010	1.54	1.31	1.82
Andreini et al.[187]	2012	1.56	1.23	1.98
Hou et al.[188]	2012	1.36	1.20	1.55
Miszalski-Jamka et al.[189]	2012	1.41	1.20	1.67
Yamamoto et al.[183]	2013	1.46	1.25	1.72
Otsuka et al.[196]	2014	1.43	1.22	1.67
All studies included		**1.45**	**1.24**	**1.70**

Table S10. Partially-calcified plaque and risk of MACE: Sensitivity Analyses with systematic exclusion of individual studies

Excluded study	Year	Pooled Hazard Ratio	Lower 95% CI	Upper 95% CI
Van Werkhoven et al.[194]	2009	1.43	1.19	1.72
Chow et al.[186]	2010	1.44	1.22	1.70
Andreini et al.[187]	2012	1.34	1.13	1.60
Hou et al.[188]	2012	1.31	1.15	1.49
Miszalski-Jamka et al.[189]	2012	1.33	1.13	1.56
Petretta et al.[195]	2012	1.43	1.19	1.72
Yamamoto et al.[183]	2013	1.37	1.17	1.61
Otsuka et al.[196]	2014	1.36	1.17	1.60
All studies included		**1.37**	**1.18**	**1.60**

Figure S1. Forest plots of pooled hazard ratio estimates in studies grouped by the inclusion or exclusion of unstable angina requiring revascularization.

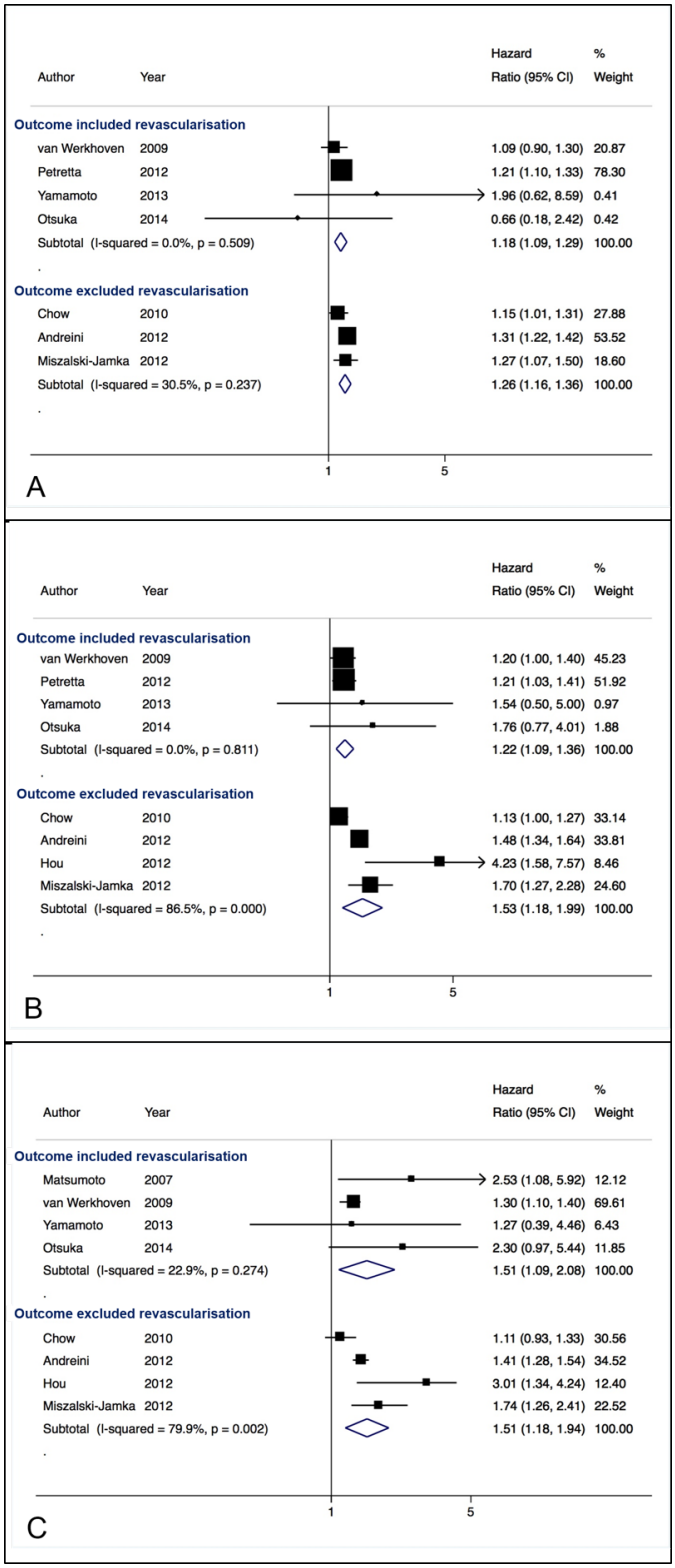

(**A**) calcified plaque, (**B**) partially-calcified plaque and (**C**) non-calcified plaque

Figure S2. Forest plots of pooled hazard ratio estimates grouped in studies using either <64 versus ≥64 detector row scanners

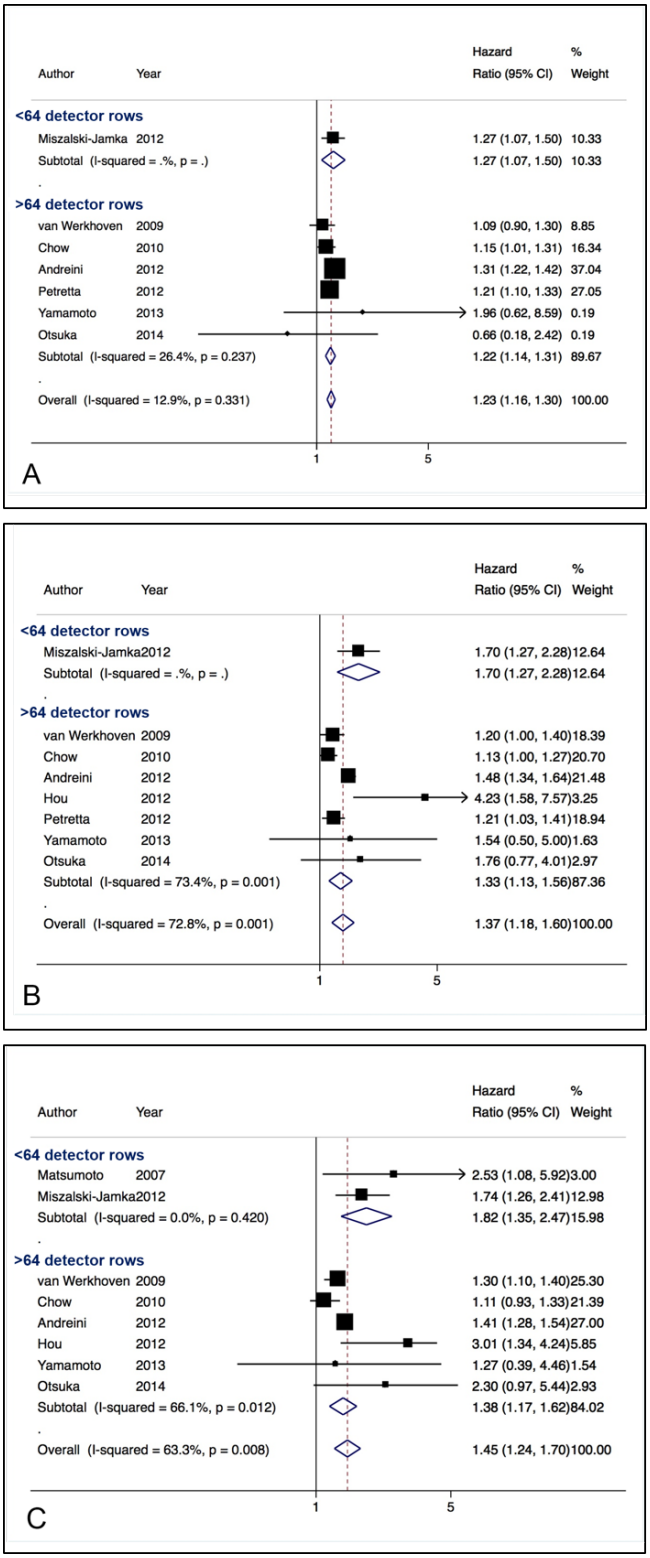

(**A**) calcified plaque, (**B**) partially calcified plaque and (**C**) non-calcified plaque

Figure S3. Forest plots of pooled hazard ratio estimates stratified by Asian vs. non-Asian subjects for plaque morphology.

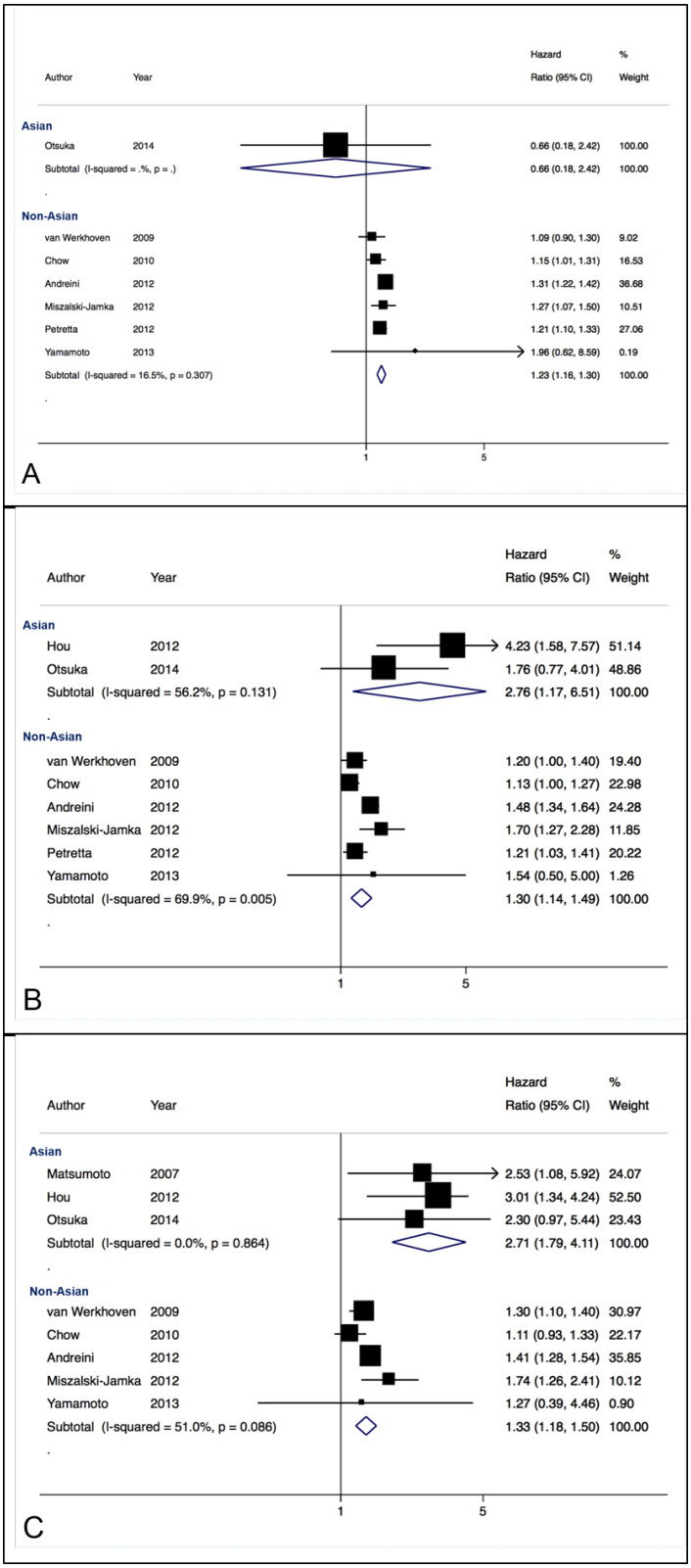

(**A**) calcified plaque, (**B**) partially calcified plaque and (**C**) non-calcified plaque.

Figure S4. Forest plots of pooled hazard ratio estimates stratified by Asian vs. non-Asian subjects for HRP features

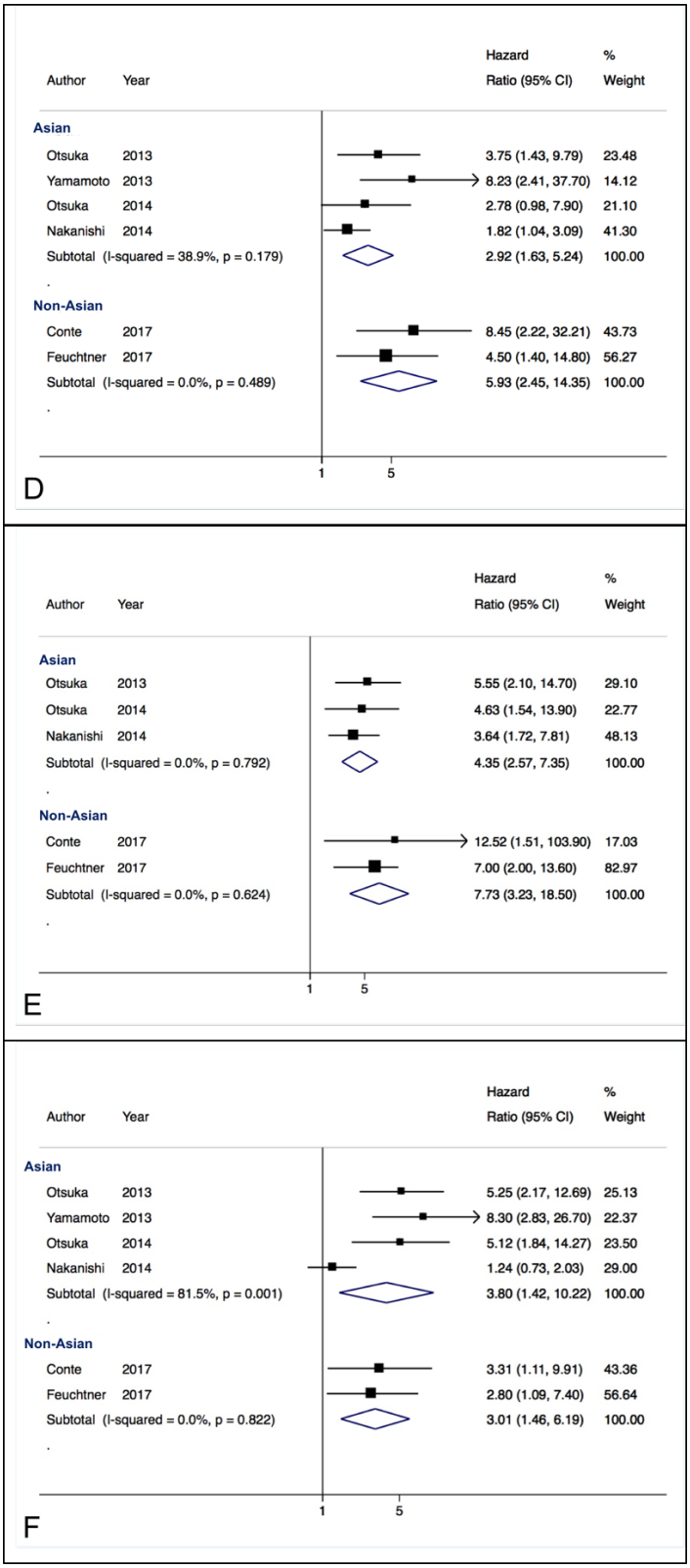

(**D**) low attenuation plaque, (**E**) napkin ring sign and, (**F**) positive remodelling.

Figure S5. Forest plots of pooled hazard ratio estimates limited to studies that included stenosis severity and/or plaque burden in multivariable modelling.

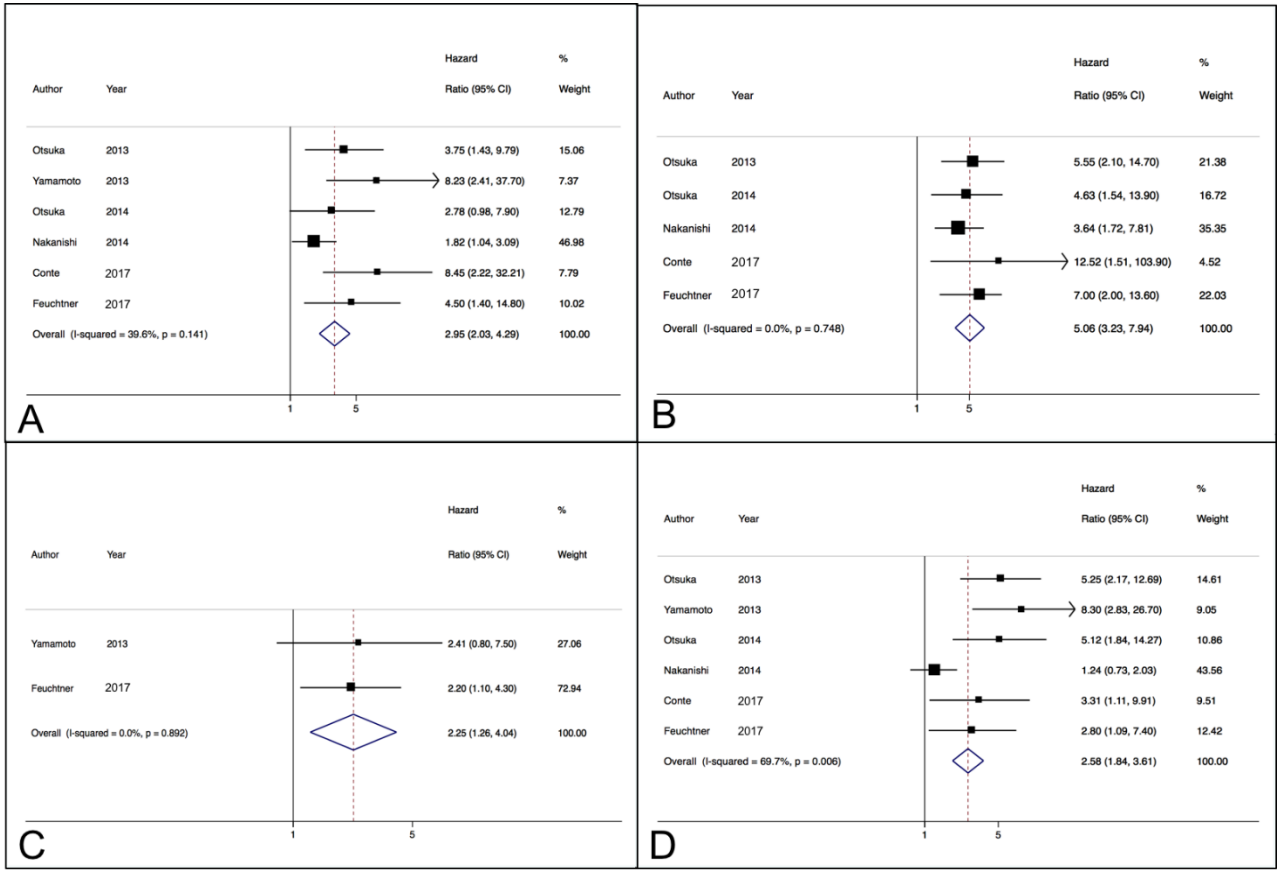

(**A**) low attenuation plaque, (**B**) napkin ring sign, (**C**) positive remodelling and, (**D**) spotty calcification.

Figure S6. Forest plot of overall hazard ratio for the presence of 2 or more high-risk plaque features

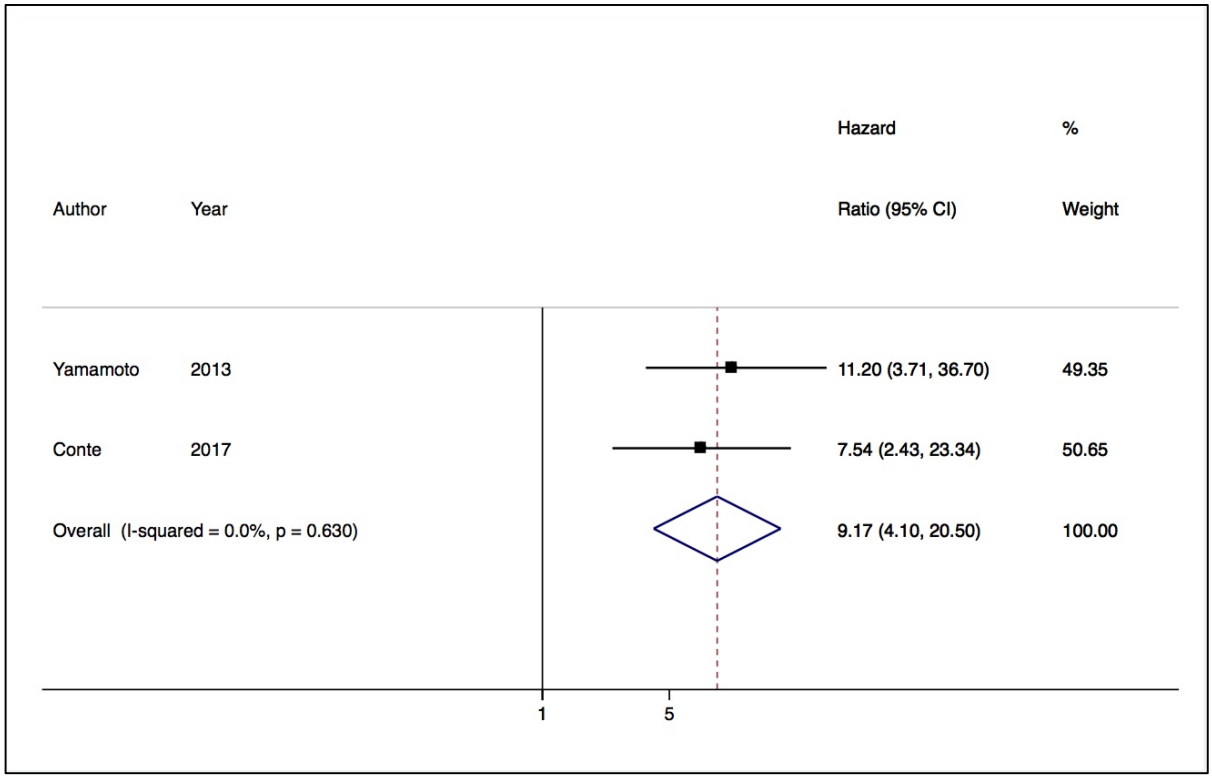

CHAPTER 5:

POOR CORRELATION, REPRODUCIBILITY AND AGREEMENT BETWEEN VOLUMETRIC VS. LINEAR EPICARDIAL ADIPOSE TISSUE MEASUREMENT: A 3D COMPUTED TOMOGRAPHY VS. 2D ECHOCARDIOGRAPHY COMPARISON.

Nitesh Nerlekar, Yi-Wei Baey, Adam J Brown, Rahul G Muthalaly, Damini Dey, Balaji Tamarappoo, James D Cameron, Thomas H Marwick, Dennis T Wong

Adapted from**: Journal of the American College of Cardiology: Cardiovascular Imaging 2018** Jul; 11(7):1035-1036

INTRODUCTION

Epicardial adipose tissue (EAT) is the natural visceral adipose tissue depot layer that lies within the pericardial cavity and is in direct continuity with the myocardium as well as encasing the epicardial coronary vessels. It is considered an ectopic visceral fat depot and as such has been widely investigated as a potential marker of cardiovascular risk due to its potential inflammatory nature. It has been associated with coronary artery disease and myocardial dysfunction[139, 205], and remains a burgeoning subject of research due to its potential as a therapeutic target. No endorsed guidelines exist on the measurement of EAT with studies predominantly reporting linear thickness by transthoracic echocardiography (EAT-TTE) or area/volume measures by cardiac computed tomography (EAT-CT) or cardiac MRI. TTE is advantageous in its rapid performance at the bedside and low cost, but its reproducibility and accuracy may be limited by the effects of probe angulation on 2D imaging, as well as an inability to quantify periatrial fat or total EAT volume. Both CT and MRI allow 3-dimensional assessment of the heart and to quantify the complete EAT volume. CT holds the drawback of ionizing radiation exposure but is regularly performed for assessment of anatomic and functional coronary artery stenosis in patients at low to intermediate cardiovascular risk. MRI is far less accessible, requires a greater amount of time to perform including prolonged breath-holding and is not yet acceptable for coronary luminal stenosis assessment. As EAT is not uniformly distributed around the heart, volumetric quantification is arguably preferred [139]. Scarce data compares agreement between these modalities, therefore we aimed to compare EAT-TTE against volumetric EAT-CT using commonly described methods.

METHODS:

We studied 106 consecutive patients who underwent clinically indicated CT for suspected CAD who also had TTE performed within 30 days. CT was performed on a 320-row scanner using previously described protocol [206] and EAT-CT was measured using a research specific tool (QFAT 2.0, Cedar-Sinai Medical Centre) [207]. Briefly, CT was performed on a second generation 320-detector row system (AquilionOne Vison, Toshiba Medical Systems, Tokyo, Japan). Oral or intravenous rate control therapy was administered to aim for an optimal heart rate <60 beats per minute. Nitro-glycerine 400 μg sublingually was administered 1 minute before contrast injection. A bolus of 75mL of 100% Iohexal (Omnipaque 350) was administered at 6mL/s followed by a 50mL normal saline chaser. Scanning was manually triggered when peak contrast enhancement in the left

ventricle was observed with no enhancement in the right ventricle. Scans were performed via an axial technique with detector collimation of 320mm x 0.5mm. No table motion was required due to complete cardiac axis coverage. Automatic tube current was determined by automatic exposure control systems based on attenuation of scout imaging. Tube potential was manually set by the radiographer. All scans were performed with prospective electrocardiographic triggering using 70-85% of the phase window.

EAT was measured using QFAT 2.0 and considered to be fat within the pericardial cavity. The superior boundary was the bifurcation of the pulmonary trunk, and in inferior boundary was the cardiac apex. Manual pericardial contours were drawn at 5-10 interval slices. Catmull-Rom spline functions were automatically generated to form a smooth contour and scans were assessed for slice-interpolation and corrected as required. Contiguous voxels between -190 and -30 Hounsfield units were used to define and quantify EAT.

EAT-TTE was performed by the commonly described technique of Iacobellis et al [208]; All studies were resting bedside TTE using either Vivid E9 (GE Healthcare, Milwaukee, WI) or iE33 (Philips Healthcare, Best, The Netherlands). EAT was considered to be the echo free space between the outer wall of the myocardium and the visceral layer of the pericardium. The thickness was measured from the parasternal long-axis view as a linear measure at end-systole at the free wall of the right ventricle along the midline of the ultrasound beam perpendicular to the aortic annulus. The average value of three cardiac cycles at end-systole was used. Observers were asked to note cases when there was uncertainty about EAT measurement which was thought to be a fluid space or a pericardial space.

Pearson correlation coefficients, and linear regression with 95% prediction intervals between methods are reported. Thirty random studies were assessed for inter and intra-observer agreement statistically analysed by the intraclass correlation coefficient (ICC). Bland Altman plots with 95% limits of agreement were performed to assess the agreement between EAT volume and thickness measurement. Analysis was performed in Stata 14/MP (StataCorp)

RESULTS

Demographics of the patient cohort are displayed in **Table 1**. EAT-CT vs. EAT-TTE demonstrated poor correlation (r=0.29, p=0.002). Poor precision was also demonstrated by the broad prediction limits of TTE compared to CT (**Figure 1**). In 28 (26%) cases, observers reported uncertainty as to placement of the linear marker for EAT-TTE suggesting reduced confidence. When these cases were excluded correlation did not significantly alter (r=0.25, p=0.01), nor did estimated prediction limits (data not shown).

Poor inter and intra-observer agreement was seen with EAT-TTE (ICC 0.39, 95% CI 0.04-0.65, p=0.02 and ICC 0.56, 95% CI 0.07-0.79, p=0.001 respectively). Bland-Altman analysis for inter-observer agreement demonstrated a mean bias of -0.35mm with 95% limits of agreement (LoA) from -4.5mm to 3.8mm (**Figure 2**). Dispersion was particularly evident at higher EAT thickness measurements. Excellent ICC was noted for EAT-CT (ICC 0.99 95% CI 0.98-1, p<0.001 for both inter and intra-observer agreement). Inter-observer agreement on Bland-Altman plots demonstrated mean bias 0.9mL and 95% LoA -11.6mL to 13.4mL. No visual evidence of dispersion was noted between observers.

DISCUSSION

In this study we have compared the most commonly used method of echocardiographic and CT EAT measurements in a consecutive series of patients. We demonstrate that EAT-TTE has poor reproducibility and agreement at both inter and intra-observer levels compared to EAT-CT. We also demonstrate that the agreement between EAT-TTE and CT is poor with wide prediction limits for corresponding CT volumes based on linear thickness measures. This imprecision in modalities may have vast clinical implications on patient classification and disease association when EAT is considered as an independent variable.

There is significant research interest in EAT-TTE, with its proponents advocating the benefits of easy bedside assessment. However, the poor reproducibility and uncertainty of measurement requires caution in drawing associative or causative relationships with EAT. The difference of ~8mm in inter-rater EAT-TTE, and corresponding wide prediction limits for EAT-CT may have significant effects on patient misclassification. Additionally, TTE studies are further confounded by a lack of standardisation in cardiac-cycle measurement. It

is suggested that EAT is compressible and therefore should be measured at end-systole where it would theoretically be largest[80]. However, the differential anatomical distribution of EAT would still confound this 2D measurement. There is also recommendation to evaluate EAT in parasternal or subcostal views, although we did not perform these measurements and chose the most commonly described technique of parasternal imaging.

There are no well conducted studies comparing imaging-measured EAT to human autopsy specimens, likely due to the extreme adherence of EAT to the underlying myocardium. There are also inconsistencies in the measurement methods for EAT which include varying inferior and superior boundaries, the use of only single slice measurements or areas rather than volumes, and differing vendor software and adipose tissue voxel thresholds. However, CT allows adipose tissue thresh-holding, optimal spatial resolution for pericardium identification and high reproducibility regardless of the use of iodinated contrast [209]. Intuitively, a complete volume would seem to have a better overall assessment of EAT than a single slice or linear thickness measurement alone. We specifically chose the most commonly described techniques to reflect current approaches to EAT measurement and cannot be certain that alternative evaluation may result in different results. We have also not compared MRI measurements, however this requires a further conversion factor for mass[149], and is also visually based with no ability to threshold for different tissue attenuation and in effect gives a pericardial cavity volume rather than a true epicardial fat volume. As MRI is also not widely performed in clinical practice, but rather reserved for specific indications, it has less role in current research strategies of EAT but a comparison with CT is an important area for further research.

In conclusion, EAT-CT is highly reproducible compared to EAT-TTE and should be considered as the optimal reference standard for EAT based research.

Table 1: Patient demographics

Demographic	**n=106**
Age (years)	56 ± 8
Sex (male)	69 (65%)
Hypertension (n, %)	32 (30%)
Hyperlipidaemia (n, %)	41 (39%)
Diabetes (n, %)	22 (21%)
Smoking (n, %)	12 (11%)
Body Mass Index (kg/m^2)	27.5 ± 5
No coronary artery disease (n, %)	28 (26%)
Non-obstructive disease (n, %)	64 (60%)
Obstructive coronary disease (n, %)	14 (13%)
Mean EAT thickness (mm)	2.9 ± 1.4
Mean EAT volume (mL)	74 ± 22

Figure 1: Prediction modelling of EAT-CT from EAT-TTE

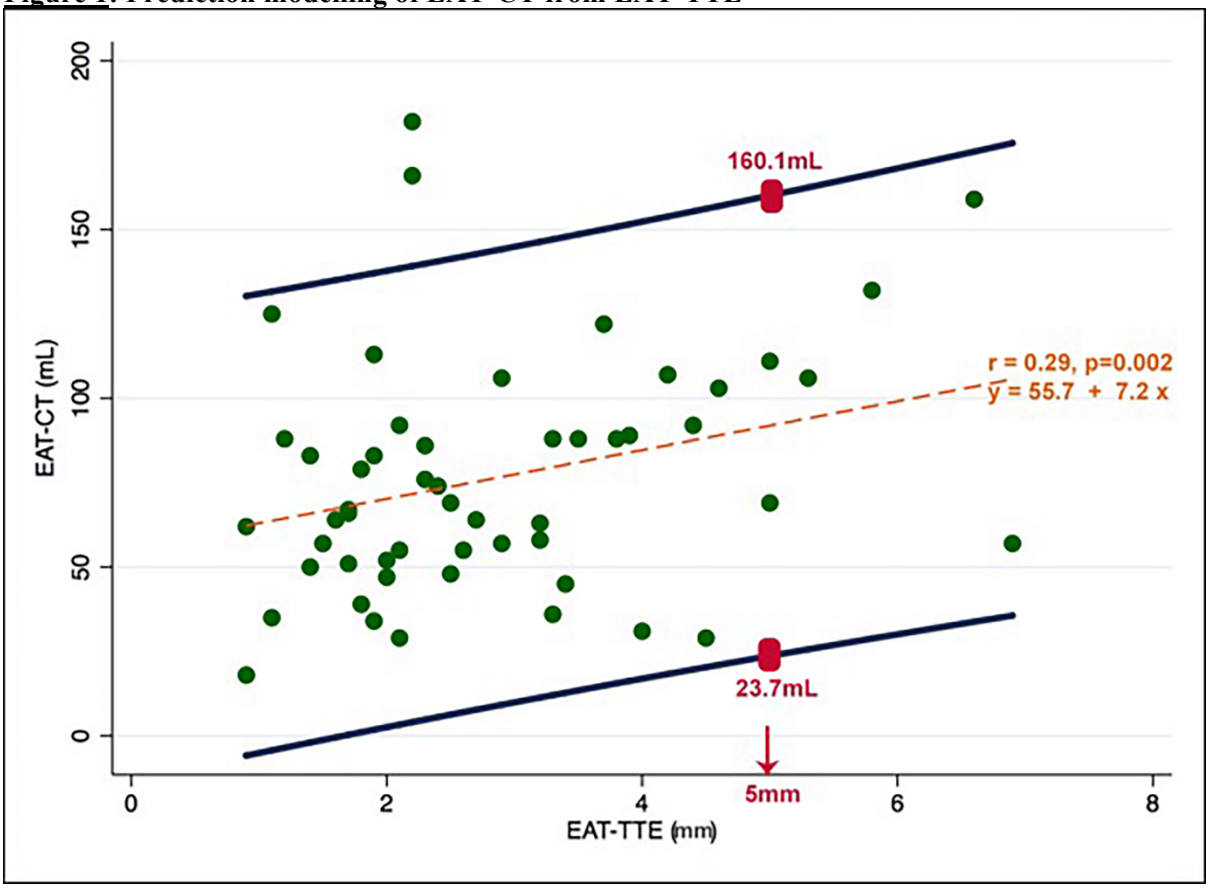

Figure 1: Scatter plot between EAT-CT and EAT-TTE. Orange dashed line represents the regression line of best fit. R-value is the correlation coefficient and the regression equation with EAT-CT as the outcome variable (y) and EAT-TTE as the independent (x). Dark blue lines represent 95% prediction intervals. An example is demonstrated by the red boxes: When EAT-TTE is 5mm the predicted EAT-CT is between 23.7mL and 160.1mL representing wide variability suggesting poor precision.

Figure 2: Inter-observer correlation and agreement

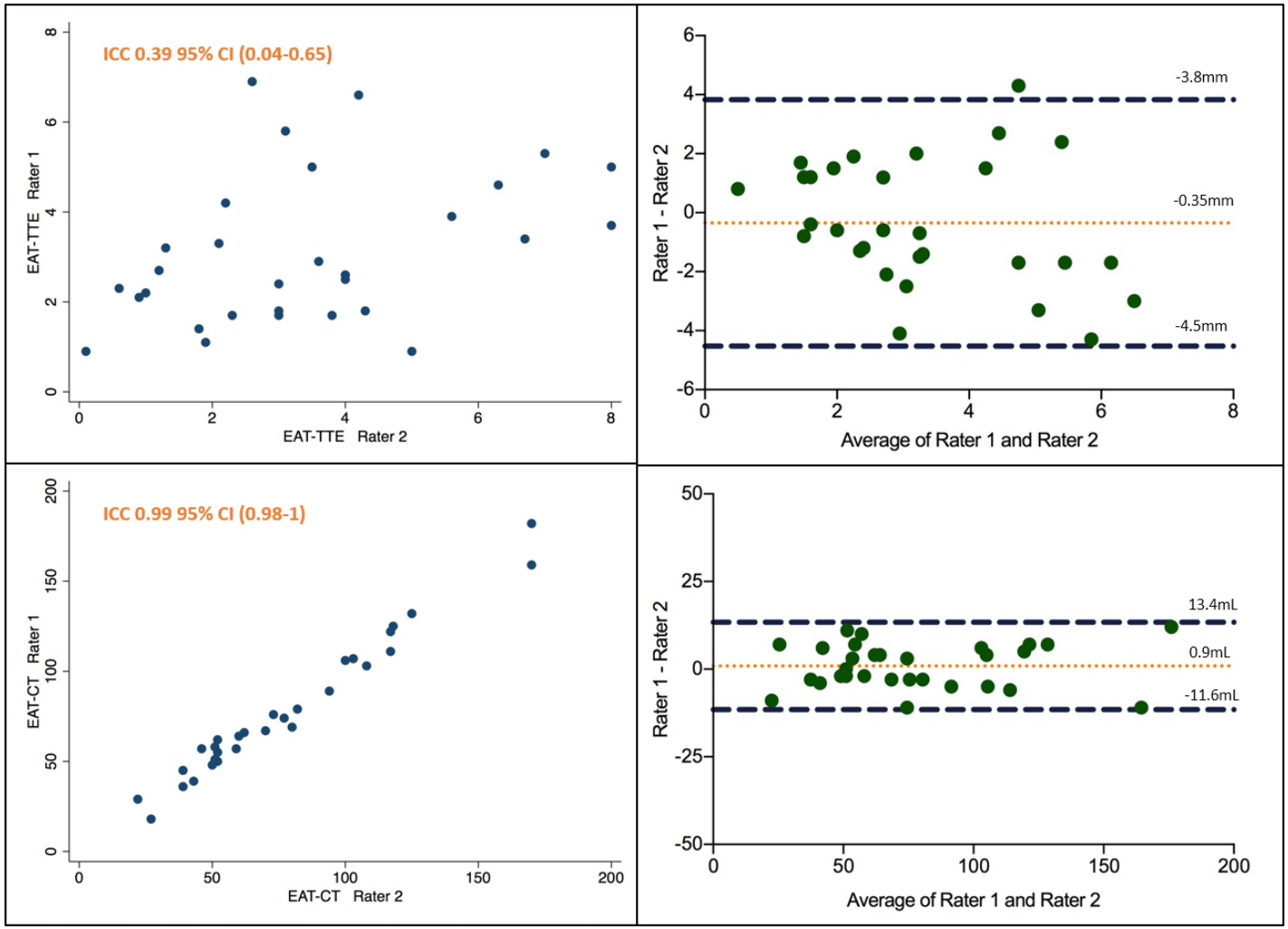

Figure 2: Inter-rater agreement is depicted by scatter plots and Bland-Altman plots with reported intraclass correlation (ICC) and 95% confidence intervals (CI) and mean bias and 95% limits of agreement respectively. Top left panel is EAT-TTE by two raters demonstrating poor correlation and Bland-Altman top right demonstrates wide limits of agreement particularly at higher EAT measures. Lower left panel depicts EAT-CT showing near linear correlation between raters and Bland-Altman plot bottom right shows minimal bias with narrow limits of agreement.

CHAPTER 6:

INTER-SOFTWARE AND INTER-SCAN VARIABILITY IN MEASUREMENT OF EPICARDIAL ADIPOSE TISSUE: A THREE-WAY COMPARISON OF A RESEARCH SPECIFIC, A FREEWARE AND A CORONARY APPLICATION SOFTWARE PLATFORM.

Nitesh Nerlekar, Udit Thakur, Rahul G Muthalaly, Andrew Talman, Damini Dey, Adam J Brown, Angel IY Wu, Sujith K Seneviratne, Cameron JD, Wong DT

Under Review in**: Radiology**

ABSTRACT

Purpose:

Epicardial adipose tissue (EAT) is a proposed marker of cardiovascular risk, however clinical application may be limited by variability in post-processing software platforms. We assessed inter-vendor agreement of EAT volume (EATv) and attenuation on both contrast-enhanced (CE) and non-contrast CT (NCT) using a standard coronary CT reporting software (Vitrea), an EAT research-specific software (QFAT) and a freeware imaging software (OsiriX).

Methods:

76 consecutive patients undergoing simultaneous CE and NCT had complete volumetric EAT measurement. Between-software, within-software NCT vs. CE, and inter and intra-observer agreement were evaluated with analysis by ANOVA (with post-hoc adjustment), Bland-Altman with 95% levels of agreement (LoA) and intraclass correlation coefficient (ICC).

Results:

Mean EATv (freeware 53±31mL vs. research 93±43mL vs coronary 157±64mL) and attenuation (freeware -72±25HU vs. research -75±3HU vs. coronary -61±10HU) was significantly different between all vendors (ANOVA $p<0.001$). EATv was consistently higher in NCT vs. CE for research software (bias 26mL, 95% LoA: 2 to 56mL) with marked over and underestimation by freeware (bias 11mL 95% LoA: -46mL to 69mL) and coronary software (bias 10mL 95% LoA: -127 to 147mL). Research software had similar NCT vs CE attenuation (-75 vs -72HU) compared to freeware (-72 vs -57HU) and coronary (-61 vs -39HU). Excellent inter-observer agreement was seen with research (ICC 0.98) compared to freeware (ICC 0.73) and coronary software (ICC 0.75) with very narrow LoA on Bland-Altman analysis.

Conclusion:

There are significant inter-vendor differences in EAT assessment. Research-specific software has the highest level of agreement, reliability and precision compared to freeware or coronary software platforms.

Implications for patient care:

- Epicardial adipose tissue is often investigated as a cause of disease and as a potential target for therapy. Therefore, it is vital that measurement software be robust and reproducible to allow accurate evaluation of treatment response.
- Research-specific epicardial fat measurement software demonstrates the high levels of agreement and reproducibility and may be the preferred tool for assessment in future studies.

Summary statement

There are significant differences between post-processing software packages for epicardial adipose tissue volume at attenuation measurement for both contrast-enhanced and non-contrast CT. Research-specific software has the highest level of agreement, reliability and precision compared to freeware or coronary software platforms.

INTRODUCTION

Epicardial adipose tissue has been widely studied as a proposed marker of cardiovascular risk across multiple domains including coronary artery disease[139], myocardial function[154] and cardiac dysrhythmia[144]. It has also been investigated in systemic disorders, particularly those pertaining to inflammation including chronic rheumatic, pulmonary and renal diseases[125, 210]. While several studies have utilised echocardiographic linear thickness measures for EAT assessment, this has demonstrated suboptimal reproducibility and agreement with full volumetric assessment as assessed by computed tomography[211].

Volumetric EAT has been derived from both non-contrast (NCT) and contrast enhanced (CE) studies that most often employ a lower threshold of -190 Hounsfield units (HU) and upper threshold of -30HU to define adipose tissue within a contoured region. However, discrepancies are seen in absolute volumes with smaller values in CE, possibly due to the effects of contrast blooming and adjacent calcification that can cause partial volume artefact in contrast enhanced scans[212]. An additional cause for discrepancy between scan modalities that has not been investigated is the influence of post-processing software packages.

As EAT is not routinely reported in clinical studies, different software has been employed from bespoke research programs, to extending the use of coronary artery reporting platforms, or manipulating plugins on DICOM image viewing software. This lack of standardisation may significantly influence interpretation and robustness of EAT as a cardiovascular risk marker. There is no gold standard for EAT measurement, likely due to difficulty in obtaining exact autopsy volumes of EAT due to its extreme adherence to the underlying myocardium[213]. However, provided software is readily reproducible with high precision (as determined from clustering around the sample mean) and has high inter and intra-observer agreement, this at least allows for relative confidence that results can be generalizable. As EAT volume as well as attenuation can be measured which in effect represents the quantity and quality of adipose tissue, it is important to identify a high fidelity post-processing software package that appropriately encompasses both these parameters.

We therefore sought to assess inter-vendor differences and agreement in EAT measurement volumes and attenuation in patients who had simultaneous contrast and non-contrast CT using a traditional coronary CT reporting software, an EAT research specific software and a free post-processing DICOM imaging software.

METHODS

We retrospectively studied 76 consecutive patients who had simultaneous non-contrast and contrast enhanced CT for suspected coronary artery disease (July 2018). Patients with previous known coronary artery disease or intervention or cardiac prostheses were excluded. All CTs were performed using a Siemens Definition AS+ (128 slice, Siemens Medical Solutions, Erlangen, Germany). The scan of the thorax was acquired during injection of non-ionic iodinated contrast agent, iopromide (Ultravist 370 mg/mL, Bayer Healthcare, Tarrytown, New York) in an antecubital vein by a dual injector (Medrad Stellant, USA). Individualized weight-based contrast volumes were injected at 6 mL/s in a triple phase pattern of pure contrast / 50:50 saline mix / saline. Nitro-glycerine 400 micrograms was administered sublingually 1 minute before contrast injection.

A contrast bolus monitoring technique evaluating time to peak enhancement in the descending aorta was used to determine the scan delay (tube voltage 100 kVp and 20 mAs). The entire thorax was scanned using prospective EKG-gating with tube modulation technique (120 kV; 280-350 mAs; pitch of 0.18 and 300ms gantry rotation time). Images were acquired at 0.6mm slice thickness at 0.3mm increments and reconstructed using a medium smooth kernel (B26, Siemens Medical Solutions, Erlangen, Germany) throughout the cardiac cycle at 10% increments of the RR interval

We used three previously published software packages for EAT assessment. A high-quality software specifically designed for coronary CT assessment, Vitrea 6.7 (Vital Images, Minnetonka, USA), an EAT-specific software designed for research use, QFAT 2.0 (Cedars Sinai, USA), and a free widely used DICOM software, OsiriX MD 9.0.2 (Pixmeo SARL, Switzerland). Images were anonymized prior to measurement.

For all EAT assessment the upper and lower boundaries were considered to be the bifurcation of the pulmonary trunk and the lower most portion of the apex of the heart where the posterior descending artery could be seen. Individual software examples on the same patient are demonstrated in **Figure 1**.

Results are presented as mean ± standard deviations. Data distribution was assessed for normality with the Shapiro Wilk test. Statistical tests of inference performed with t-tests or ANOVA as appropriate and Scheffe's method for post-hoc analysis. Bland Altman graphs of the difference vs. the average of measurements with 95% limits of agreement were plotted to assess agreement between methods. Additional statistical assessment of observer agreement was performed with the intraclass correlation coefficient. Analysis was performed with Stata MP14 (StataCorp, College Station, TX, USA) and Graphpad Prism (La Jolla, CA, USA).

RESULTS

All patients had satisfactory image quality for assessment of EAT volume. The demographics of included patients are summarised in **Table 1**.

EAT volume by software type

There were significantly different measures of mean EAT volume between each software platform for both NCT and CE scans. Mean NCT EAT volume by Freeware software was 53 ± 31 mL, 93 ± 43 mL for Research software and 157 ± 64 mL for Coronary software; ANOVA $p<0.001$. Similarly, significant differences were noted for CE datasets: Freeware 41 ± 23 mL vs. Research 71 ± 38 mL vs. 147 ± 50 mL, $p<0.001$ (**Figure 2, Table 2**). Significant differences were seen between individual comparisons of volumes between each software type on post-hoc testing.

EAT attenuation by software type

There were significant differences noted with EAT attenuation values between platforms for NCT. Research software demonstrated the narrowest range and standard deviation of HU attenuation with mean -75±3 HU compared to freeware software which had the widest dispersion of data (mean -72 ± 25HU) and coronary software (mean -61 ± 10HU), ANOVA $p<0.001$. There were significant differences between groups on post-hoc testing as well (**Figure 2, Table 2**).

Inter-scan and within software variability

There were notable differences of NCT compared to CE scan EAT volumes and attenuation. Consistently, non-contrast scans had higher overall EAT volume as well as attenuation compared to CE (**Figure 3**). Bland-Altman plot analysis demonstrated a very high level of agreement with research software for both EAT volume as well as attenuation (**Figure 4**) with no specific visual systematic differences. Research software consistently demonstrated a higher volume on NCT scans (bias 26mL) with 95% lower bound limit of agreement 2mL. Comparatively, freeware and coronary software also consistently demonstrate average higher EAT volume on NCT with smaller bias values than research, but markedly variable lower bound limits of agreement (Freeware bias 11mL, 95% lower LOA -46mL; Coronary bias 10mL, 95% lower LOA -127mL). The absolute differences in attenuation were significantly lower with research specific software, (mean difference 3 ± 3HU) compared to freeware (14 ± 29HU) and coronary software (22 ± 13HU).

Inter-observer agreement

There was an excellent level of agreement of EAT volume with research software with an intra-class correlation co-efficient of 0.98 (95% CI 0.96-0.99, $p<0.001$). Moderate agreement was noted with coronary and freeware software, although not as high as research specific software: coronary ICC 0.75, 95% CI 0.55-0.87, $p<0.001$); freeware ICC 0.73, 95% CI 0.38-0.88, $p<0.001$). Bland-Altman plots similarly demonstrated a high level of agreement for research software with narrow limits of agreement (bias 0.9mL, 95% LoA -12 to 12mL) compared to freeware (bias -3mL, 95% LoA -56 to 50mL) and coronary software (bias 30mL, 95% LoA -42 to 100mL). Similarly, high levels of agreement were seen for attenuation with research software with excellent agreement, ICC 0.95 (95% CI 0.92-0.99) and poor agreement for freeware (ICC 0.52 (95% CI 0.03-0.76)) and coronary software (ICC 0.54 (0.06-0.78)) (**Table 3, Figure 4**).

DISCUSSION

This is the first study of an inter-software and inter-scan comparison of EAT volume and attenuation measurements utilising a research specific, freeware DICOM processing and coronary specific software. Our main findings can be summarized as follows: (1) Calculated EAT volumes differ significantly between software programs regardless of scan type; (2) NCT scans have higher mean EAT volume and attenuation compared to

contrast-enhanced scans, although only research specific software maintains this consistently compared to other vendors; (3) Research specific software has the highest reproducibility, agreement and precision for both inter-scan and observer agreement compared to a freeware and a coronary-specific software program. In the absence of an anatomical gold standard, this suggests that a robust research specific software is the ideal platform for analysis of EAT.

Epicardial Fat Measurement

Epicardial fat is the natural visceral adipose tissue of the heart lying beneath the visceral pericardial layer and the myocardium. Paracardial fat is situated above the fibrous pericardial layer. Together, paracardial and epicardial fat are often regarded as pericardial adipose tissue[214]. However, both are highly unique with different embryologic origins, blood supply and relationships with disease. EAT is immediately apposed to the underlying myocardium without any fascial separation and often extends into the adjacent muscle [26]. EAT is also differentially distributed around the heart with the greatest volumes seen around the right ventricle [57]. Therefore, the ability to adequately excise and measure complete EAT at autopsy is technically challenging and time consuming, with potential contamination from adjacent paracardial fat as an additional confounder. As such, no large systematic studies have been performed to compare post-mortem and radiographic EAT volume. It is for this reason that there remains no consensus on population thresholds for EAT measurements and reliance is placed on radiographic imaging techniques to delineate and measure EAT.

This lack of a gold standard for EAT assessment has resulted in variably reported volumes from several imaging studies which has the effect of decreasing generalisability and diminishing the clinical utility of this parameter. Furthermore, much of the literature has adopted linear EAT thickness measurements which has shown poor reproducibility and disease association compared to volumetric measures [211]. Despite this, multiple studies are still routinely performed with EAT volume or thickness measures to assess associations with cardiac and non-cardiac disease. The rationale for EAT assessment is due to its idiosyncratic location and potential as an endocrine organ. Adipose tissue is abundant in pro-inflammatory mediators which may infiltrate, by vasocrine and paracrine effects, into the neighbouring coronary arteries and myocardium resulting in pathologic dysfunction[73]. EAT is also proposed to have protective benefits, by providing a cushioning support for the

coronary arteries and as an energy store in times of cardiac stress [215]. As all patients have some degree of EAT, it may in fact not be the quantity but rather, the quality of EAT that leads to disease. Recent evidence suggests that EAT attenuation may be a marker of adipose dysfunction over volume alone and has shown promise in refining the role of EAT in cardiovascular disease [216-220]. CT assessment of adipose tissue is reliant upon radiologic attenuation. Higher, or more 'negative' HU values suggest greater lipid content and more 'positive' values suggest higher water content, or alternatively, smaller and less mature lipids[221]. It has been suggested that inflammation is a driving force for arrest of lipid maturation[222] and therefore EAT may serve as a marker of adjacent vascular inflammation[223]. Conversely, larger lipid content may result in a greater proportion of dysfunctional adipokines that can cause vascular and metabolic damage[224]. This bidirectional communication of cytokines is a principal hypothesis for the pathologic relationship between EAT and cardiac disease[225]. This may suggest a dynamic relationship between inflammation and adipose tissue and EAT may be influential to atherogenesis and alteration in plaque morphology which is strongly related to poor outcome[226].

Inter-software volume and attenuation

In our study, we demonstrated marked differences in EAT volume assessed between software programs. This important finding reflects the uncertainty of a generalizable threshold for EAT volume that associates with disease with several suggested cut-off values within the literature[139]. Similarly, significant differences were seen with mean HU attenuation. However, it is notable that the standard deviation of attenuation with research software was very low (±3 HU) compared to other software (±25 HU for freeware and ±10 HU for coronary), suggesting significantly better precision (standard error 0.6HU). This finding held true for both NCT and CE scans. Contrast enhancement significantly lowered the mean attenuation in all software programs, although the absolute difference with research software was very low, at 3HU which overlaps the standard deviation of NCT.

Inter-scan volume and attenuation

We noted a significant difference in EAT volume between scan types. This has been previously reported in similar small studies that report higher values of EAT volume with NCT [212, 227]. This is not a surprising finding and can be explained by partial voluming artefact from luminal contrast enhancement, image interpolation and differing spatial resolution, as well as potential vascularity of adipose tissue[72]. Research software consistently

demonstrated higher NCT volumes (mean difference 26mL) with a lower 95% limit of agreement of 2mL with no cases of discordance. While freeware and coronary software also had positive mean differences indicating a general disposition of higher NCT vs CE EAT volumes, the comparative lower 95% limits of agreement with freeware and coronary software were -46mL and -127mL respectively suggesting potentially marked underestimation of EAT. Previous studies have suggested changing the upper attenuation threshold to better approximate volumes between scans[212], however this alteration will dramatically alter mean attenuation values which may then be uninterpretable.

Marked differences were noted between NCT and CT mean attenuation values for freeware and coronary software, with nominally very small absolute difference for research software, despite a significant difference between scan type reflective of the narrow data spread. The marked differences in non-research software accompanied by their imprecision demonstrated by their wide dispersion of data reduces confidence with these post-processing methods. Given emergent data of the importance of HU attenuation thresholds associated with disease, a more resolute software is preferable. Higher attenuation values may mislead researchers given the association with vascular inflammation and dysfunctional adipose tissue.

Observer Agreement

While most EAT studies do report inter and intraobserver agreement for volume measures, no study has compared differences in post-processing software. We show that inter-observer agreement was near perfect with research software with very narrow limits of agreement on the Bland Altman plot. While good agreement was still demonstrated with coronary and freeware software based on the intraclass correlation coefficient, a wider dispersion of data points was visually noted on Bland Altman plot with broad limits of agreement suggesting less satisfactory agreement.

There is inherent appeal to extend the use of a standard coronary reporting platform, or use a freely available and modifiable image processing software rather than a dedicated software tool which requires additional time for measurement. However, similar to any diagnostic software tool, rigorous assessment is required before any software can be considered satisfactory for clinical application. Our findings suggest that software variability

may explain some of the contrasting results seen in epicardial fat research. The research software employed (QFAT) has been rigorously tested for its application of adipose tissue measurement. In its inception, individual voxel limits pertaining to adipose tissue were determined from training datasets and then applied to epicardial adipose tissue boundaries by segmentation of connected voxels within a defined CT attenuation range (-190 to -30HU) [207]. This technique has been further refined with serial improvements and image filtering to a point of complete automation with deep learning techniques[228]. The technique and calculation algorithms of other software is not readily available, and does not have as substantial a publication background.

Limitations

We acknowledge several limitations with our study. Firstly, we have tested only three of the multiple software packages available for EAT research and our results may not be germane to other platforms. Additional analysis with other software is required to assess if our results hold true. Secondly, as mentioned, given the lack of a reference standard for EAT volume we instead focused on agreement and precision of sample estimates to guide a more robust radiographic tool which arguably may be superior to autopsy sampling given the challenge of EAT dissection. Thirdly, our sample size is small and heterogeneous. Finally, we did not have access to underlying algorithms for fat segmentation and therefore cannot mechanistically or mathematically explain our results or provide a correction factor. The inference of narrow standard deviation in research software however, infers a higher degree of fidelity.

CONCLUSION:

We found significant differences in inter-platform EAT assessment for both volume and attenuation measures. Research-specific software appears to have the highest level of agreement, reliability and precision compared to the tested freeware and coronary software platform and may be the preferable tool for EAT assessment in future studies.

Table 1: Patient demographics

Age (years)	**58 ± 15**
Male gender (%)	**56%**
Hypertension (%)	**48%**
Hyperlipidaemia (%)	**45%**
Diabetes (%)	**24%**
Smoking (%)	**36%**
BMI kg/m^2	**28 ± 4**
No coronary atheroma (%)	**15%**
Non-obstructive <50% stenosis (%)	**59%**
Obstructive ≥50% stenosis (%)	**26%**

Data presented as percentage of the whole population or mean ± standard deviation
Stenosis is at a patient level
BMI – body mass index

Table 2: Summary of CT EAT volume and attenuation

	Freeware	Research	Coronary	p-value
	NCT			
Volume (Mean ± SD) (mL)	53 ± 31	93 ± 43	157 ± 63	<0.001
Attenuation (Mean ± SD) (HU)	-72 ± 25	-75 ± 3	-61 ± 8	0.001
	CE			
Volume (Mean ± SD) (mL)	41 ± 23	71 ± 38	147 ± 50	<0.001
Attenuation (Mean ± SD) (HU)	-57 ± 26	-72 ± 4	-39 ± 14	<0.001

p-value for trend by ANOVA. CE – contrast enhanced. NCT – non-contrast CT

Table 3: Observer variability for inter- and intra-observer differences

	Freeware			Research			Coronary		
	Bias	**95% LoA**	**ICC (95% CI)**	**Bias**	**95% LoA**	**ICC (95% CI)**	**Bias**	**95% LoA**	**ICC (95% CI)**
Volume	11	-46 to 69	0.73 (0.38-0.88)	26	2 to 53	0.98 (0.96-0.99)	10	-127 to 147	0.75 (0.55-0.87)
Attenuation	-14	-71 to 43	0.52 (0.03-0.76)	-3	-9 to 3	0.95 (0.92-0.99)	-22	-48 to 4	0.54 (0.06-0.78)

Data from non-contrast CT

Figure 1: Inter-vendor EATv and EATa comparison

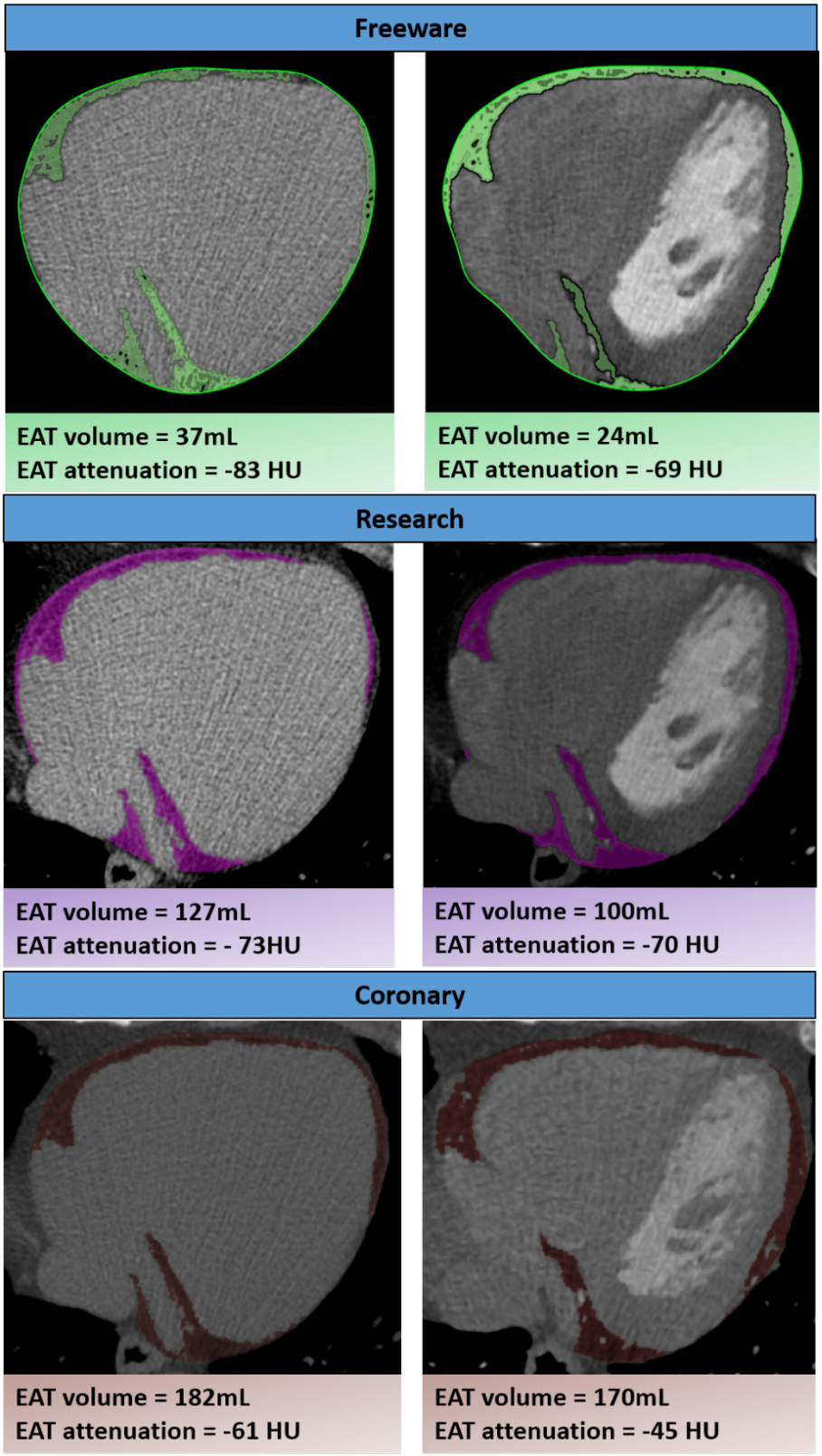

Inter-vendor comparison of EAT volume and attenuation in non-contrast (left) and contrast enhanced (right) images by freeware, research and coronary software platforms. This demonstrates marked differences in calculated volumes despite similar visual appearance.

EAT – epicardial adipose tissue, mL – millilitres, HU – Hounsfield units

Figure 2: Differences in EAT parameters by contrast and non-contrast CT

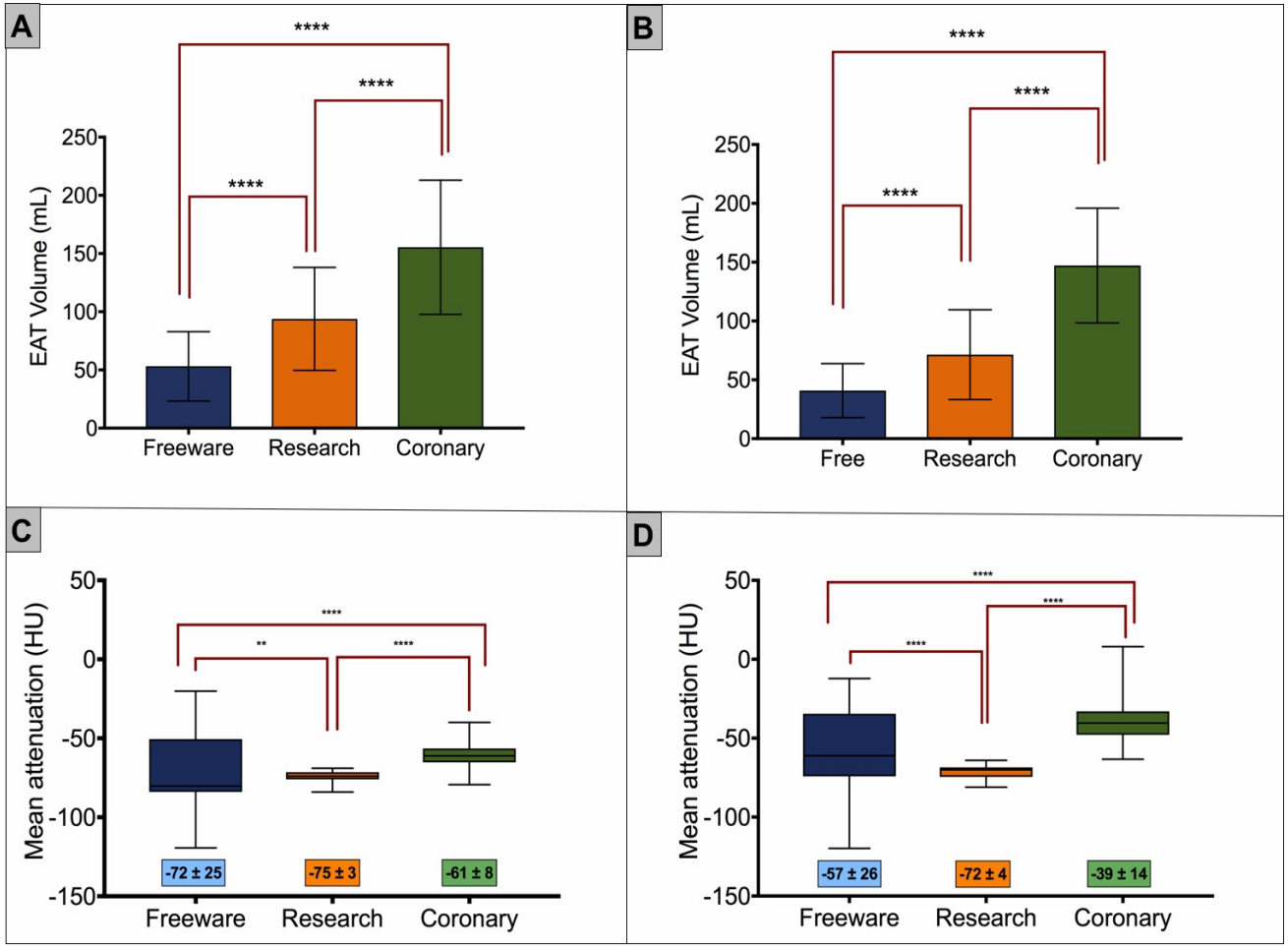

Differences in EAT volumes and attenuation for non-contrast (A, C) and contrast enhanced (B, D). There are significant volumetric and attenuation differences seen between each software platform overall and with pairwise comparison. Notably, the standard deviation for EAT attenuation with research software is narrower compared to other software.

Figure 3: Inter-scan differences by software type

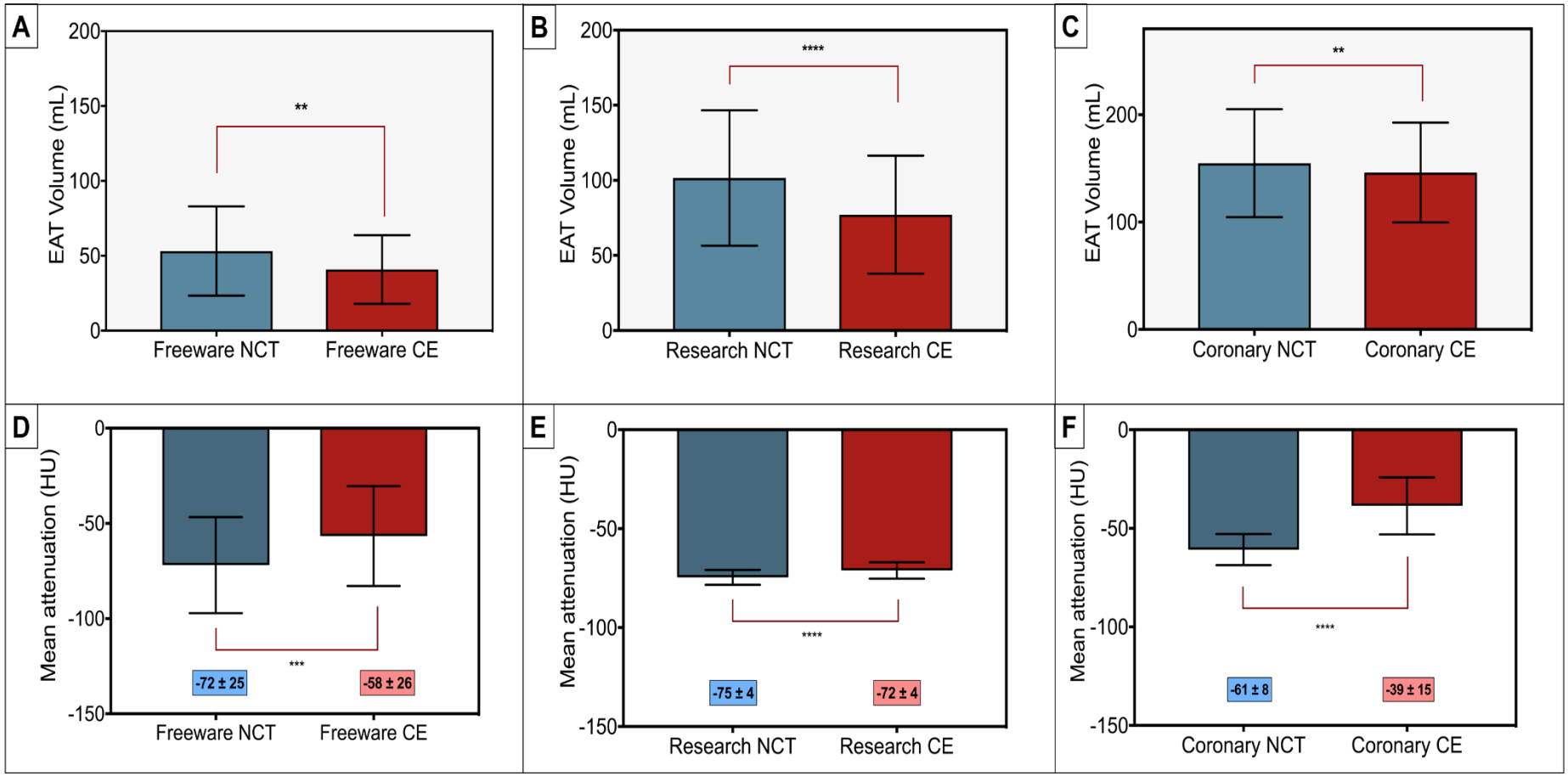

Inter-scan differences by software type. EAT volume by non-contrast vs. contrast (A-C) and attenuation (D-F) are depicted. This demonstrates that there are significant differences between NCT and CE regardless of software with a smaller volume and higher attenuation on contrast scans. However, absolute differences with research software attenuation is low (-3 HU) compared to -14HU for freeware and -21HU for coronary software.

CE – contrast enhanced, EAT – epicardial adipose tissue, HU – Hounsfield units, mL – milliliters, NCT – non-contrast CT

Figure 4: Bland-Altman comparison for inter-scan differences and inter-observer variability

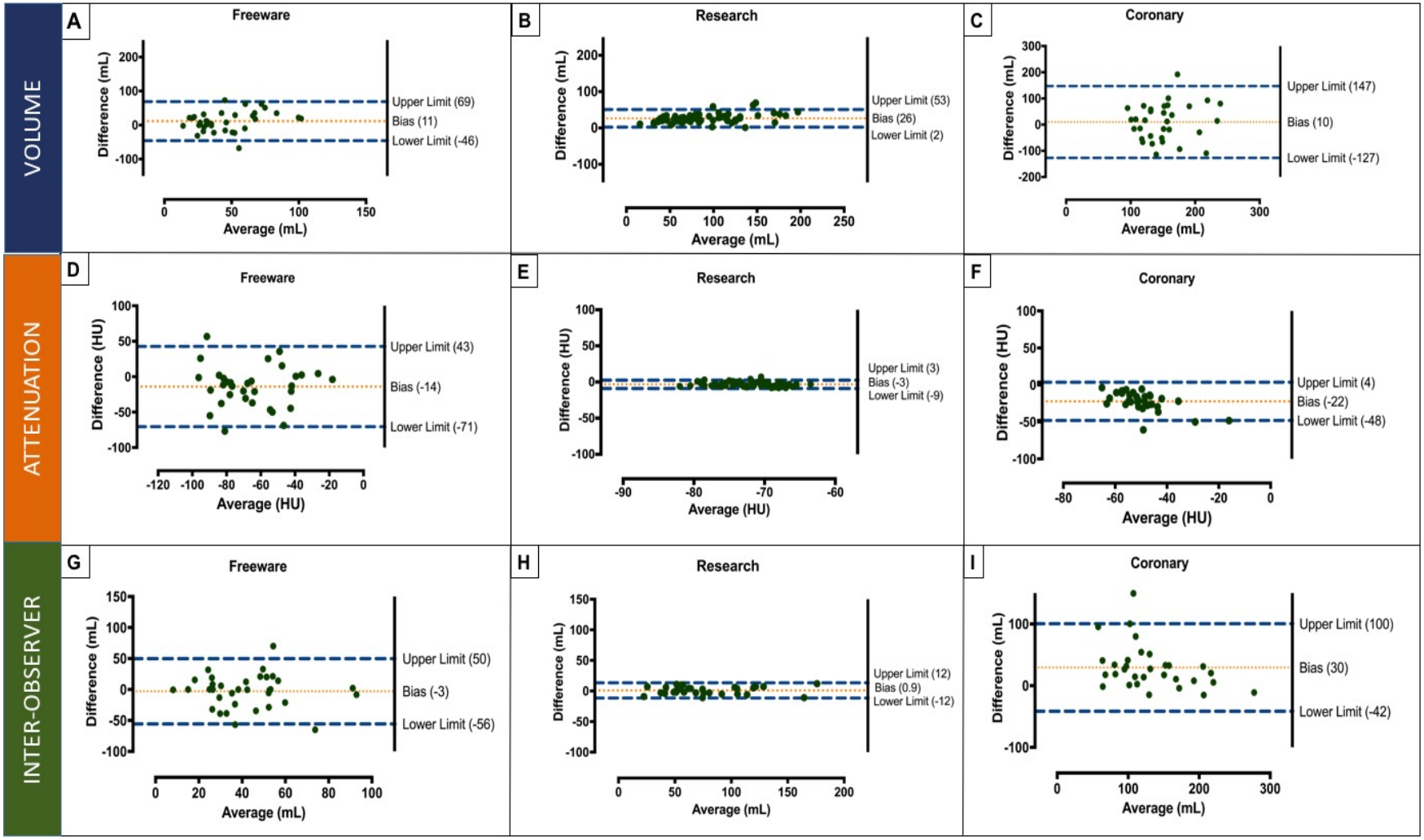

Bland-Altman plots for inter-scan differences by volume, attenuation and inter-observer variability by software type (freeware-left panel; research- middle panel; coronary- right panel) This visually demonstrates high levels of agreement for research software (all y-axis scales are consistent). Importantly, NCT consistently had a higher volume than contrast only with research software (mean difference 26mL) with over and underestimation on freeware and research software

CHAPTER 7:

The Natural history of Epicardial Adipose Tissue Volume and Attenuation: A long-term prospective cohort follow-up study

Nitesh Nerlekar, Udit Thakur, Samuel Koh, Elizabeth Potter, Rahul G Muthalaly, Hashrul Rashid, James D Cameron, Damini Dey, Dennis TL Wong

Under Review: **Nature Scientific Reports**

ABSTRACT

Background

Epicardial adipose tissue (EAT) is cross-sectionally associated with cardiovascular risk. However, the longitudinal change in EAT volume (EATv) and density (EATd), and potential modulators of these parameters, has not been described.

Methods

We prospectively recruited patients with non-obstructive coronary atherosclerosis on baseline computed tomography coronary angiography (CTCA) performed for suspected coronary artery disease to undergo a repeat research CTCA. EATv in millilitres (mL) and EATd in Hounsfield units (HU) were measured by observers blinded to clinical and scan data. Multivariable regression analysis controlling for traditional cardiovascular risk factors (CVRF) was performed to assess for any predictors of change. Secondary analysis was performed based on statin therapy.

Results

There were 90 patients included for analysis with median duration between CTCA of 4.3 years. Mean EATv increased at follow-up (72±33mL to 89±43mL, $p<0.001$) and mean EATd decreased (baseline -76±6 HU vs. -86±5 HU, $p<0.001$). There were no associations between baseline variables of body mass index, age, sex, hypertension, hyperlipidaemia, diabetes or smoking on change in EATv or EATd. No difference in baseline, follow-up or delta EATv or EATd was seen in patients with (60%) or without statin therapy.

Conclusions

In this select group of patients, EATv consistently increased and EATd consistently decreased at long-term follow-up and these changes were independent of CVRF, age and statin use. Together with the knowledge of strong associations between EAT and cardiac disease, these findings may suggest that EAT is an independent parameter rather than a surrogate for cardiovascular risk.

Keywords: Epicardial adipose tissue, Epicardial fat, Natural History, Longitudinal

INTRODUCTION

Epicardial adipose tissue (EAT) has been described to associate with coronary artery disease[139] as well as influence myocardial function and geometry[205]. It has been suggested that vasocrine or paracrine effects may be the intermediary for transmission of pro-inflammatory adipokines from dysfunctional adipose tissue to the adjacent myocardium or coronary vasculature[73]. Additionally, local compressive forces of excess EAT may result in reduced myocardial compliance and subsequent diastolic dysfunction. However, most studies are cross-sectional in nature and the natural history of EAT is not well described. The few published studies are limited to small cohorts of either asymptomatic patients undergoing cardiac screening[30, 229], or elevated-risk patients either after an acute coronary syndrome, or with the presence of high risk coronary plaque characteristics[230] . EAT is best evaluated by volumetric measurement on computed tomography (EAT)[141], a non-invasive radiography modality designed for use in low-intermediate risk symptomatic patients. As EAT is universal to human anatomy, it is important to evaluate its natural evolution in this cohort to better understand what cardiovascular risk factors may influence its change as it thus far remains simply an associative marker of cardiac risk that is thought to be modulated by other metabolic markers or obesity measures. Furthermore, the notion of EAT function as assessed by the attenuation of fat, has emerged as an alternative marker of risk beyond simply the total volume of EAT alone[217]. The long-term natural history of EAT has not been assessed in general cohorts of suspected coronary artery disease that comprise the vast majority of patients undergoing coronary assessment on CT coronary angiography, most of whom will have non-obstructive CAD[110].

Therefore, we sought to prospectively examine the long-term changes in EAT volume and density in a cohort of patients with mild, non-obstructive coronary artery disease only. We also sought to evaluate the potential effect of statin therapy on these markers.

METHODS

Patients were retrospectively identified from a registry of patients who underwent CT coronary angiography at Monash Heart, Monash Health, Melbourne, Australia between 2010-2012. The primary inclusion criteria for all patients was the presence of coronary atherosclerosis in at least 1 coronary segment and no visual diameter stenosis of ≥50% of the lumen. Patients were excluded if they had any previous coronary intervention. Patients were randomly selected from the registry in a consecutive fashion using a random number generator to avoid selection bias. Once the primary inclusion and exclusion criteria was met, they were contacted and invited to return for a research specific coronary CT. In the event of pregnancy or a reduction in glomerular filtration rate (GFR) <30mL/min or withdrawal of consent, research CTCA would not be performed. Baseline cardiovascular risk factors, and statin use were obtained from the medical record and patient interview and prospectively recorded at follow-up scan. All follow-up scans were performed between 2015-2018. Written informed consent was obtained in all patients and the study was approved by the local ethics committee

All efforts were made to match scan parameters, particularly for kV between baseline and follow-up CT and all CT were performed using a 320-row multi-detector CT using previous institutional protocol[206]. Briefly, all studies were performed on a 320-detector row system (AquilionOne, Toshiba Medical Systems, Tokyo, Japan). Nitro-glycerine 400 μg sublingually was administered prior to contrast injection. A bolus of 75mL of 100% Iohexal (Omnipaque 350) was administered at 6mL/s followed by a 50mL normal saline chaser. Scanning was manually triggered when peak contrast enhancement in the left ventricle was observed with no enhancement in the right ventricle. Scans were performed via an axial technique with detector collimation of 320mmx0.5mm and no requirement for table movement due to 16cm cranio-caudal coverage. Prospective electrocardiographic triggering at 70-85% phase window was performed in all patients. Images were reconstructed with a 512x512 matrix, 0.5mm thick sections and 0.25mm increments with adaptive iterative dose reduction and

standard and asymmetric cone beam reconstruction. Rate control therapy was used to aim for acquisition heart rate <65bpm.

Measurement of EAT was performed according to previously described methods[141]. Briefly, the upper EAT boundary was considered to be the bifurcation of the pulmonary trunk and the lower most portion of the cardiac apex were the last slice of the posterior descending artery was seen. Pericardial contours were manually traced at 5-10 slice intervals with observation for interpolation and adjustment performed if required. Adipose tissue was quantified using threshold of -190 Hounsfield units (HU) and -30 HU. The mean density of EAT was recorded. Inter and intra-observer variability demonstrated excellent correlation with both intra-class correlation coefficients of 0.98 respectively.

Outcomes:

There were two co-primary outcomes

1. The first co-primary outcome was the difference in follow-up compared to baseline EAT volume
2. The second co-primary outcome was the difference in follow-up compared to baseline EAT density.
3. Secondary analysis was performed to assess differences in the primary outcomes based on statin use

Statistical analysis

Analysis was performed using STATA 14/MP (StataCorp Ltd, TX). Categorical variables are presented as number and percentage, and continuous variables as mean with standard deviation, or median inter-quartile range. Normality was assessed visually using histogram plots. Categorical variables were compared using McNemar test for paired observations, and chi-squared test for

unpaired observations. Continuous data was compared using the paired t-test. Spearman rank correlation coefficients (rho) were reported for baseline comparison of EAT with independent variables. Ordinary least squares simple and multiple linear regression was used with change in EAT volume and change in EAT density (follow up – baseline) as the outcome variable of interest. Beta-coefficients with standard errors are reported for linear regression. We performed a binary logistic regression for analysis with a change of 10% EAT from baseline as the outcome variable and report results as odds ratios with 95% confidence intervals on univariable and multivariable regression. For body mass index, the delta value (BMI at second scan – BMI at first scan) as well as percentage change in BMI [(BMI at second scan – BMI at first scan) / BMI at first scan × 100] was used. Inter- and intra-observer agreement was evaluated by the intra-class correlation coefficient. A two-tailed $p<0.05$ was considered statistically significant.

RESULTS:

There were 100 patients initially identified with 90 patients included in the final analysis. Of the 10 excluded patients, 3 withdrew consent, 3 had GFR<30mL/min, and 4 had image quality that was suboptimal for adequate evaluation of EAT on the baseline CT scan. None of the identified patients had a significant coronary or cardiac event in the antecedent time period.

Baseline demographics are presented in **Table 1**. The mean age was 59 ± 11 and 58 (64%) were male patients. There was no difference in traditional risk factors of hypertension, diabetes, dyslipidaemia, smoking or family history of premature coronary disease. There were 54 (60%) of patients on statin therapy which was not different at follow-up. The mean segment involvement score was 2 ± 1.5. The median follow-up duration was 4.3years (IQR 4.1 to 5.5y, range 3 to 7.8y).

Baseline EATv correlated with baseline BMI (rho = 0.39, p=0.009) but no other clinical cardiovascular risk factors (**Table 2**). This relationship remained consistent when all variables were forced into a multivariable regression model (BMI β=1.935, p=0.03) (**Table 2**).

Primary outcome:

Mean EAT volume significantly increased at follow-up (baseline 72 ± 33mL vs follow-up 89 ± 43mL, p<0.001 (**Figure 1A**). Mean EAT density significantly decreased (more negative) over time (baseline -76 ± 6 HU vs. -86 ± 5 HU, p<0.001) (**Figure 1B**).

The mean change in EAT was 16mL ± 15mL (range -20mL to 71mL). Only two patients demonstrated an absolute reduction in EATv. We further analysed EAT change by an increase in 10% of the baseline EAT value which demonstrated that 72 (80%) of patients had an increase of 10% of the baseline EAT. On assessment restricted to subjects who had an absolute increase in EAT there were no significant associations between clinical variables and increase in EAT at follow-up (**Table 3).** Increasing age was associated with a reduction in the odds of a greater than 10% change in EAT at a univariable level (OR 0.91 95% CI (0.83-0.99), p=0.03), however this association was attenuated, and no longer statistically significant in the multivariable logistic regression model (**Table 3**).

There was no significant association either at univariable or multivariable analysis for EAT density (**Table 4**). The mean change in EATd was -10 ± 6 HU with 3 patients demonstrating an increase of density over time. Only absolute change in BMI was associated with a change in EATd at a univariable level with increasing change in BMI associated with decreasing (more negative) EATd (beta -0.39, p=0.008), but this was no longer significant at multivariable analysis (beta -0.16, p=0.22). No other variables were associated with a change in EATd (**Table 4**).

Effect of statin therapy:

There was no difference in baseline EATv by statin use although numerically, statin-taking patients had a higher EATv (statin EATv 76 ± 31mL vs 66 ± 35mL, p=0.29). No significant difference was noted with follow-up EATv by statin group (statin EATv 94 ± 41mL vs. 81 ± 44mL, p=0.15). There was no difference in delta EATv by statin group (statin 17 ± 14mL vs. 15 ± 17mL, p=0.48).

No difference was demonstrated for EATd at baseline or follow-up by statin stratification: baseline statin -76 ± 6 HU vs -77 ± 5 HU, p=0.34; follow-up -87 ± 5 HU vs. -85 ± 5 HU, p=0.18) and no predictors of change in density on simple and multivariable regression modelling (data not shown). Inclusion of statin therapy in the multivariable models of EATd or EATv did not result in statistical significance.

DISCUSSION

In this select cohort of symptomatic low-risk suspected CAD patients with long-term follow-up and serial CTCA, we demonstrate a consistent increase in absolute EATv and decrease in EATd over time. We also show that there were no significant clinical risk factors that independently associated with longitudinal changes in EATv or EATd. Furthermore, the use of statin therapy did not influence baseline or follow-up values. Coupled with the knowledge that EAT has demonstrated significant associations with cardiac disease, these findings may suggest that EAT is an independent parameter rather than a surrogate for cardiovascular risk.

EAT volume, and more recently attenuation have been increasingly investigated in the literature for associations with cardiac disease[133, 217, 220, 231-233]. Several studies have demonstrated significant cross-sectional relationships between EAT and cardiac disease, however a lack of longitudinal data prevents understanding of what therapies or targets may be a modulating factor for EAT.

We noted a significant relationship between EAT and baseline BMI which confirms the findings of other studies that suggest EAT is related to markers of clinical obesity[87]. However, this association was no longer significant after inclusion of other clinical risk factors. This is likely due to confounding from other variables such as hypertension, diabetes and dyslipidaemia that are also strongly related to BMI and mirrors the attenuated relationship of obesity and future coronary disease risk when traditional risk factors are included in multivariable modelling[25]. While several studies have suggested weight loss may result in EAT reduction[137], these reports are significantly limited by the use of linear thickness measurements of EAT which has been shown to be substandard compared to volumetric measures[141]. In a study evaluating the effect of bariatric surgery in severely obese patients, there was a significant reduction in EATv as assessed on cardiac magnetic resonance imaging, however this was not correlated with body fat percentage loss or non-epicardial visceral fat loss[234]. Another study that evaluated serial non-contrast CT change in EAT in an asymptomatic observational cohort, a greater percentage change in BMI on follow-up was associated with a greater percentage change in EAT[230]. However, this study is significantly different to ours in that only a third of the patients had established atheroma, follow-up CT was incidentally performed rather than mandated by research protocol which may result in selection bias, and there was no change in mean BMI between scans with an absolute difference of only 0.2kg/m^2.

In a community cohort of 623 asymptomatic Japanese men aged 40-79 years, serial cardiac CT at 4.7 year mean follow up demonstrated a significant increase in EAT volume[229]. The only clinical risk factor associated with change in EATv was current smoking. In our study, smoking did not associate with change in EATv however this may be driven by a very low prevalence (<20%) of smokers in our cohort that combined both ex- and current smokers compared to a 30% prevalence of current and 52% ex-smoker cohort in the aforementioned study. No other studies have described potential predictors

of change in EATv on serial prospective CT, and there are no studies that review serial changes in EATd.

EATd is hypothesised to be a marker of adipose tissue activity, or may even represent a marker of vascular inflammation[217]. As EAT is present in all human anatomy and differentially distributed around the myocardium, it is possible that the activity of EAT may have a greater effect on cardiac and coronary dysfunction. Statins are well described pleiotropic agents that have anti-inflammatory properties[235]. Interestingly, we did not demonstrate any difference in mean EATd by statin stratification and this may be due to EATd representing a mean attenuation of the totality of EATv. There may be influence on regional EAT differences or on pericoronary adipose tissue attenuation, a novel proposed imaging biomarker of vascular inflammation[216]. We did note a nominally higher EATv in statin taking patients. The association between statin use and accumulation of organ and body fat has been described[236], however it remains a subject for further study to evaluate whether statin use may increase EAT volume but alter EATd, as well as other potential anti-inflammatory agents that have effects on cardiovascular disease[237].

While higher volumes of EATv are considered to be pathologic in the associations with cardiac disease, it is not certain whether changes in EATv associate with disease. It is possible that EAT increased as a function of age. EATv has been described to increase in parallel to changes in LV mass on necropsy assessment[57]. LV mass significantly increases with age[238] and it is possible that changes in LV mass may account for the increase in EATv. Further analysis of this factor as well as association with any progression of coronary disease or cardiac dysfunction are required. In addition, there are no endorsed populations thresholds for EATv or EATd that associate with disease with numerous cut-points described in the literature. As the purpose of this study was purely an observational assessment of the

natural history of EAT parameters, it is not clear whether these changes may result in disease or whether change in coronary atheroma was evident. This remains a subject for further assessment.

We acknowledge several limitations in our study. Firstly, this is a small cohort of highly selected patients with only minimal or mild coronary artery disease and therefore our results may only apply to similar patient populations. Secondly, we did not evaluate continuous markers of cardiovascular risk factors such as bloods pressure levels, cholesterol profile indices or HbA1c levels and instead used binary variables of presence or absence of pathology. There may be specific thresholds which may associate with changes in EATv or EATd and this needs to be further investigated. Thirdly, we only evaluated clinical risk factors that were forced into a multivariable model and cannot account for other potential mediators such as ethnicity, coronary artery disease extent and severity or other medical therapies. However this is reflective of the current literature in examining relevant associations of EAT. Finally, there is potential for error in using delta EAT values with potential overlap from test-retest variability. Our previous work has demonstrated limits of agreement up to 10mL higher or lower between observers with a mean bias however of only 1mL, however our inter-observer correlation was excellent at 0.98 with assessors blinded to scan timing and patient details.

CONCLUSION

Epicardial adipose tissue volume and density significantly change longitudinally in patients with non-obstructive coronary artery disease with a consistent increase in EAT volume and consistent decrease in EAT density. There are no clinical risk factors that appear to associate with the change in EAT parameters and this effect is also independent of statin therapy. This finding may suggest that EAT is an independent marker, rather than surrogate of cardiovascular risk.

Table 1: Baseline and follow-up demographics in the 90 included patients

Variable	Baseline	Follow-Up	p-value
Age (years)	59 ± 11	64 ± 9	P<0.001
Sex (male)	58 (64%)	-	-
BMI (kg/m^2)	28.8 ± 6	29.0 ± 6	0.79
Hypertension	50 (56%)	52 (58%)	0.83
Hyperlipidaemia	56 (62%)	64 (71%)	0.37
Family History	56 (62%)	-	-
Smoking	26 (29%)	30 (33%)	0.65
Diabetes	14 (16%)	20 (22%)	0.42

Results are mean ± standard deviation or frequency (%).
BMI – body mass index

Table 2: Univariable correlation and multivariable linear regression between clinical variables and baseline EATv

	Correlation		Multivariable		
Variable	**Spearman rho**	**p-value**	**β-coefficient**	**Standard Error**	**p-value**
Hypertension	0.21	0.16	11.461	9.622	0.241
Smoking	0.07	0.65	2.389	10.779	0.826
Hyperlipidaemia	0.16	0.27	-0.644	10.033	0.949
Family History	0.03	0.86	-3.663	9.858	0.712
Diabetes	0.17	0.26	2.420	13.494	0.859
BMI	0.39	0.009*	1.935	0.857	0.03*
Age	0.29	0.054	0.755	0.436	0.092
Sex	-0.17	0.24	-13.716	9.989	0.178

BMI – body mass index; EATv – epicardial adipose tissue volume; IHD – ischaemic heart disease,
** Denotes p<0.05*

Table 3: Multivariable baseline associations of cardiovascular risk factors with delta EATv (absolute difference in EAT at follow-up and baseline), and when EAT modelled as >10% change compared to baseline

	Multivariable linear regression (delta EAT volume)			Multivariable logistic regression (EAT >10% baseline)		
Variable	**β-coefficient**	**Standard Error**	**p-value**	**OR**	**95% CI**	**p-value**
Hypertension	-0.128	4.583	0.978	0.67	0.09-5.01	0.69
Smoking	7.176	4.764	0.141	3.77	0.29 – 49.54	0.31
Hyperlipidaemia	-6.296	4.920	0.209	0.24	0.03 – 2.36	0.22
Family History	-0.678	4.487	0.881	3.31	0.49 – 22.38	0.22
Diabetes	8.751	6.106	0.161	3.71	0.21 – 66.89	0.37
Δ BMI	0.582	0.363	0.118	1.01	0.90-1.14	0.83
Age	0.185	0.193	0.343	0.91	0.81 – 1.007	0.07
Sex	-6.951	4.396	0.123	1.29	0.17 – 9.66	0.80

Table 4: Univariable correlation and multivariable linear regression between clinical variables and baseline EAT density; and delta density.

	Correlation		Multivariable baseline			Multivariable delta EAT density		
Variable	**Spearman rho**	**p-value**	**β-coefficient**	**Standard Error**	**p-value**	**β-coefficient**	**Standard Error**	**p-value**
Hypertension	-0.14	0.37	-1.834	2.020	0.370	1.162	1.985	0.562
Smoking	-0.004	0.98	-0.097	2.263	0.966	-0.457	2.149	0.833
Hyperlipidaemia	0.11	0.49	0.798	2.106	0.707	-1.630	2.148	0.453
Family History	0.06	0.68	0.392	2.070	0.851	-0.140	1.936	0.943
Diabetes	0.12	0.45	0.400	2.833	0.889	-2.360	2.746	0.396
BMI^	0.06	0.68	0.148	0.180	0.416	-0.335	0.163	0.074
Age	-0.11	0.49	-0.082	0.092	0.377	-0.028	0.085	0.742
Sex	-0.22	0.16	-3.581	2.097	0.096	1.986	1.940	0.313

^ for change in density, the Δ BMI was used as the independent variable

Figure 1: Longitudinal changes in mean EAT volume (A) and EAT radiodensity (B).

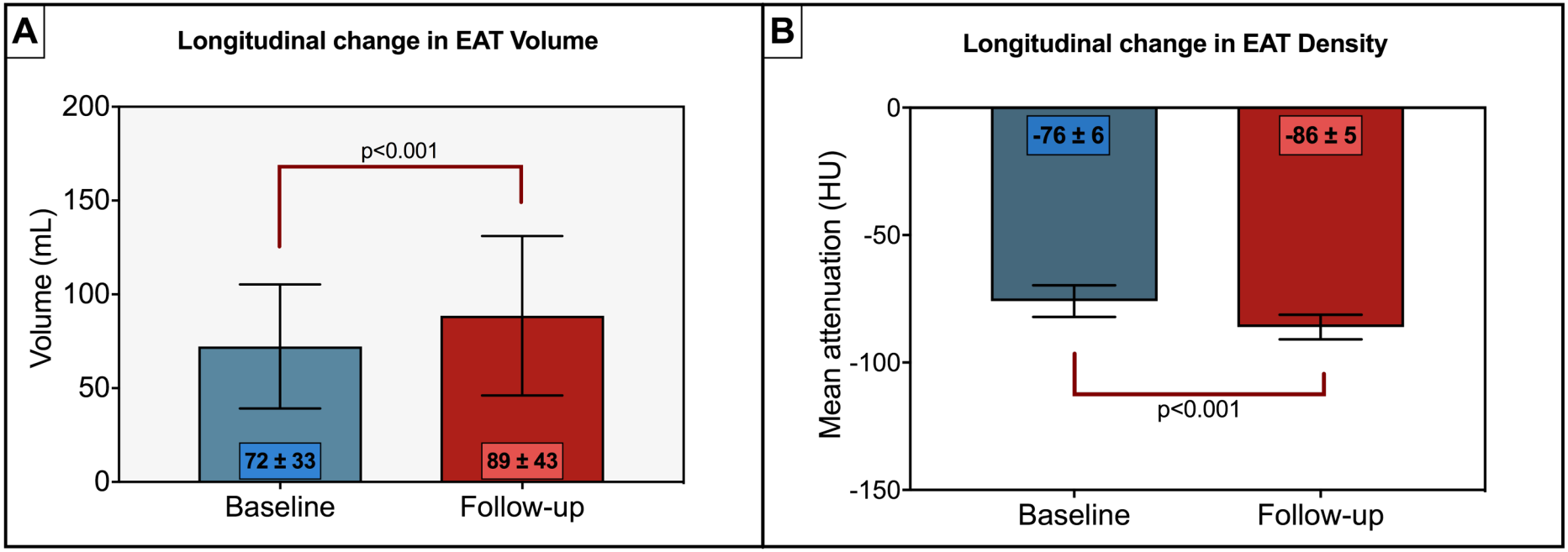

Bar graphs with standard deviations demonstrate change in EAT volume and density from baseline to follow-up

EAT – Epicardial Adipose Tissue, HU – Hounsfield Units, mL – millilitres

CHAPTER 8:

Epicardial Adipose Tissue Volume but not Density is associated with High Risk Plaque Composition on Coronary Computed Tomography Angiography in patients with Non-Obstructive Coronary Artery Disease

Nitesh Nerlekar, Udit Thakur, Samuel Koh, Elizabeth Potter, Rahul G Muthalaly, Abdul-Rahman Ihdayhid, James D Cameron, Damini Dey, Dennis TL Wong

Under Review: **Cardiovascular Diabetology**

ABSTRACT

Epicardial adipose tissue (EAT) is associated with invasively-derived coronary plaque composition in high-risk patients undergoing coronary intervention. EAT is optimally measured on computed tomography (CT) and quantified coronary plaque composition is feasibly evaluated on CT coronary angiography (CTCA) with good correlation to invasive methods. Therefore, CTCA allows simultaneous EAT and plaque evaluation in a single non-invasive test. The relationship between EAT volume (EATv) or density (EATd) and CTCA-quantified coronary plaque is not known. Two-thirds of patients undergoing CTCA will have non-obstructive (<50% diameter stenosis) coronary artery disease (CAD). We evaluated 100 consecutive patients with non-obstructive CAD to assess the cross-sectional relationship between EAT and plaque composition in a typical CTCA population. EAT and plaque quantification was performed on semi-automated software for total plaque and high-risk plaque (HRP) features of fibro-fatty and necrotic core volume, and more stable phenotypes of fibrous and calcified plaque volumes. We evaluated qualitative HRP features, and qualitative plaque burden by the CT-Leamen and segment involvement score (SIS). Mean EATv was 66±30 millilitres and mean EATd -75±7 Hounsfield Units. On multivariable linear regression adjusted for cardiovascular risk factors, body mass index, age and gender, EATv was significantly and independently associated with total and quantified HRP volumes (all $p<0.001$), but not fibrous or calcified plaque ($p>0.05$). There was no association with plaque parameters and EATd. EATv independently associated with qualitative HRP (adjusted OR 1.04, 95% CI 1.01-1.08, $p=0.01$) but not with SIS or CT-Leamen score. CTCA feasibly evaluates quantified coronary plaque and EAT and there is a strong independent association with EATv and total and HRP composition.

INTRODUCTION

Epicardial adipose tissue is a dynamic, biologically active fat repository that surrounds the myocardium. It encases the coronary arteries sharing a similar blood supply, as well as immediately apposing the epicardial coronary arteries with no fascial separation[4]. As such, it has been widely studied as a potential factor for atherogenesis with several studies demonstrating association with coronary artery disease presence and vulnerability[139]. Qualitative high-risk coronary artery plaque characteristics have been strongly associated with future major adverse cardiovascular events and are feasibly assessed using computed tomography coronary angiography[226]. More recently, quantitative methods of high risk plaque measurement using CTCA have demonstrated that components such as fibro-fatty plaque and necrotic core volume are of prognostic potential and correlate well with invasive markers of high risk plaque[52]. Published studies to assess an association of EAT with quantitative HRP have only been performed using invasive studies in patients planned for future coronary intervention or after acute coronary syndromes[39, 128]. These patients are already at elevated future cardiac risk and it remains uncertain whether EAT associates with quantifiable plaque characteristics in stable cohorts with non-obstructive CAD that comprise the majority of patients who undergo CTCA. Furthermore, EAT volume has been the only parameter evaluated in these studies, yet there is increasing investigation into whether EAT density as a marker of the functional activity of adipose tissue may effect dynamic coronary plaque modification through enhanced inflammation.

We sought to evaluate the association of EAT volume (EATv) and EAT density (EATd) to the presence of quantitative high-risk plaque characteristics in a cohort of stable chest pain patients with non-obstructive coronary artery disease.

METHODS

We retrospectively identified patients with previous CT coronary angiography performed for suspected coronary artery disease, who were randomly selected from the Monash Heart CT coronary angiography database. Patients were consecutively selected through a random number generator. Patients included in the study had the presence of at least one segment of coronary plaque with no stenosis >50%. Patients with previously known CAD or previous intervention were excluded. Once patients were identified, baseline cardiovascular risk factors, lipid profile analysis and use of statin therapy was obtained from the medical record. We aimed to analyse 100 successive patients due to the significant time required for plaque level analysis in all coronary vessels.

The protocol for CTCA examinations was performed according to departmental guidelines[206]. Briefly, all scans were performed on a 320-detector row CT (AquilionONE, Toshiba Medical Systems). Rate control therapy was prescribed at physician discretion to aim for an acquisition heart rate <65bpm. All patients received sublingual nitro-glycerine 1 minute prior to contrast injection. A bolus of 50mL of 100% Iohexal (Omnipaque 350) was administered at 6mL/s followed by a 50mL normal saline chaser. Scanning was manually triggered when peak contrast enhancement in the left ventricle was observed with no enhancement in the right ventricle. Scans were performed via an axial technique with detector collimation of 320mmx0.5mm and no requirement for table movement due to 16cm cranio-caudal coverage. Prospective electrocardiographic triggering at 70-85% phase window was performed in all patients. Images were reconstructed with a 512x512 matrix, 0.5mm thick sections and 0.25mm increments with adaptive iterative dose reduction and standard and asymmetric cone beam reconstruction.

Measurement of EAT was performed according to previously described methods[141] using the QFAT software (Cedar Sinai, USA). The upper EAT boundary was considered to be the bifurcation of the

pulmonary trunk and the lower boundary as the last slice of the heart where the posterior descending artery was seen. Pericardial contours were manually traced at 5-10 slice intervals with observation for adequate slice interpolation and manual adjustment performed if required. Adipose tissue was quantified using a lower threshold of -190 Hounsfield units (HU) and upper threshold of -30 HU.

All CTCA were anonymised and blinded to observer assessment. Plaque quantification was performed using the semi-automated AutoPlaq Software v9.7 (Cedar Sinai, USA) [239]. CT images were examined in reformatted multiplanar views and a regional of interest placed in the aorta for each patient to define the reference blood pool attenuation. The three major epicardial coronary vessels (left anterior descending artery, right coronary artery and left circumflex artery) were examined from the ostium to the distal most portion of the vessel where the diameter <2mm. Contours for lumen and outer-wall were automatically generated after proximal and distal vessel points were selected, and these were then manually modified in longitudinal and cross-sectional planes as required. Pre-defined HU thresholds were utilised to define plaque characteristics: Necrotic core (-30 to 30HU), Fibro-Fatty (30 to 130HU), Fibrous (131 to 350HU) and Calcified plaque (CP) (>350HU) [51]. High-risk quantified plaque was the summation of necrotic core and fibro-fatty volume. Non-calcified plaque (NCP) was the summation of necrotic core, fibro-fatty and fibrous plaque volume. Plaque burden was defined as the plaque volume normalized to the vessel volume (plaque volume/vessel volume x 100%). Plaque composition was determined as a proportion (%) of each plaque component in reference to measurements of total plaque volume. We also quantified low-attenuation plaque (LAP) volume as any lesions with plaque <30HU[27]. Qualitative plaque characterisation was also performed. Plaque burden was qualitatively assessed by the segment involvement score[240] as well as the CT-Leamen score[241]. High risk plaque features were also evaluated for presence of low attenuation plaque, positive remodelling, spotty calcification and napkin ring sign[242]. Representative example of EAT, quantitative and qualitative plaque measurement is displayed in **Figure 1**.

Statistical Analysis:

Categorical variables are expressed as frequency and percentage, and continuous variables as mean with standard deviation. Univariable and multivariable linear regression analysis was performed with individual plaque parameters as outcomes and independent variables of EATv or EATd which were forced into respective models with cardiovascular risk factors of body mass index, age, sex, hypertension, hyperlipidaemia, smoking and diabetes presence. To avoid model overfit, we also performed sensitivity analysis with forward and backward stepwise regression analysis which did not alter statistical significance in the forced entry model which is the final model reported. Results are presented as beta-coefficients with standard errors and a two-sided p-value of <0.05 was considered statistically significant. We also performed binary logistic regression analysis based on the presence of qualitative HRP and EATv and EATd adjusted for risk factors, and linear regression analysis as above for segment involvement score and CT-Leamen score as qualitative measures of plaque burden. We report the associations of only EATv and EATd in the body of the manuscript with the remaining independent variable parameters in regression models in the supplement. All analysis was performed in Stata 14/MP (StataCorp Ltd, TX, USA).

RESULTS:

There were initially 112 patients identified with 100 patients finally included for analysis. The 12 excluded patients had corrupted images or imaging that was performed out of the required protocol. Baseline demographics are reported in **Table 1**. There were 12 patients on lipid lowering therapy (12%). The mean EATv was 66 ± 30mL and mean EATd was -75 ± 7 HU. Plaque composition and burden are reported in **Table 1**. The mean SIS score was 3 ± 2 segments, and the mean CT-Leamen score was 5 ± 4. There were 19 patients with at least one qualitative high risk plaque feature. EATd was moderately negatively correlated to EATv (-0.43, $p<0.001$).

Significant univariable associations were demonstrated between EATv and total plaque volume, total NCP volume, total LAP volume, total necrotic core volume, total fibro-fatty volume and total quantitative HRP volume (all $p<0.001$) with no association on total fibrous volume and calcified plaque volume (**Table 2**). On multivariable analysis adjusting for BMI, cardiovascular risk factors, age and gender, the associations attenuated but remained statistically significant (all $p<0.01$) (**Table 3, Figure 2**). There were no significant associations for EATv with fibrous or calcified volume.

There were no significant associations between the mean EATd and any absolute quantitative measure of plaque on univariable or multivariable regression analysis (**Table 4, Figure 3**). We demonstrated similar results between EATv and plaque burden with independent associations of increasing EATv and total plaque burden, total non-calcified, low attenuation, necrotic core and fibro-fatty burden. No association was demonstrated with fibrous and calcified burden. There was an independent association of increasing EATd with total plaque burden (beta 0.55, $p=0.04$) and fibro-fatty burden (beta 0.39, $p=0.02$), but no other plaque characteristics.

There was no association between EATv or EATd and CT-Leamen score or SIS. There was a significant independent association of EATv with the presence of any qualitative HRP feature (OR 1.04, 95% CI 1.01-1.08, $p=0.01$) (**Supplement Table 1**).

DISCUSSION:

In this consecutive cohort of patients with non-obstructive coronary artery disease undergoing CTCA, we report that EATv is associated with total coronary plaque volume and burden and quantifiable high-risk plaque features of necrotic core and fibro-fatty plaque, but no association with more favourable characteristics of fibrous plaque and calcified plaque. This relationship is independent of traditional cardiovascular risk factors. We also demonstrate the EATd appears to associate with fibro-fatty plaque

burden, but no other measure of coronary plaque composition or burden. We believe this is the first such report of a study performed with CTCA which allows both EAT and plaque to be evaluated in a single test.

EAT has been widely studied as a potential mediator of coronary artery disease. EAT is a visceral adipose tissue store[4]. Given its unique relationship with direct contact with the underlying myocardium and coronary arteries, it has been hypothesised to influence the development of atherogenesis due to the dynamic nature of dysfunctional adipose tissue which is abundant in cytokines known to associate with coronary plaque[243]. Through vasocrine and paracrine mechanisms, these cytokines might accelerate the atherosclerotic process and possibly result in plaque rupture[73].

Coronary atherosclerotic plaque is readily assessed on CTCA and now emerged as the first line recommendation for chest pain assessment in some guidelines[244]. The non-invasive nature of CTCA allows for rapid quantification of coronary plaque with limited adverse effects. The emergence of high-fidelity software to assess both adipose tissue composition, as well as coronary plaque composition renders CTCA an ideal tool to evaluate the relationship between fat and plaque. Previous studies examining high risk plaque features on CT and association with EAT have been limited to qualitative characteristics only[30, 122]. While these demonstrate a significant association with prognosis, the prevalence of qualitative HRP is highly variable and dependent on the study population which greatly affects the positive predictive value[226]. The prevalence of qualitative HRP in large cohorts of stable chest pain populations is approximately 9%[27] with greater proportions in patients with acute coronary syndrome[242]. The importance of compositional assessment of high risk coronary plaque was recently highlighted in the ICONIC trial. In this propensity-matched study, only 50% of patients with an ACS demonstrated qualitative HRP, however quantitative assessment of necrotic core and fibrofatty volumes were significantly higher in the plaques of patients who progressed to an acute coronary

syndrome[52]. The ability to quantify high risk plaque volumes rather than dichotomise according to the presence of qualitative HRP may better inform and risk stratify patients.

Previous studies of EAT and quantified HRP features are restricted to invasive studies of patients undergoing coronary intervention. Our results confirm the findings of these intracoronary imaging studies in that higher EAT volume is associated with higher risk plaque features of necrotic core and fibro-fatty plaques, however represents a lower risk cohort of patients with non-obstructive disease. It is not feasible to routinely perform invasive assessment of stable coronary disease patients and the ability of CTCA to allow simultaneous assessment of EAT and plaque analysis in a single non-invasive test may allow refinement of this association across the full spectrum of patient risk.

The radiodensity of adipose tissue has been considered a measure of the 'quality' of fat however there are significantly conflicting associations with heterogeneous study populations. Some studies have suggested a higher (less negative) attenuation represents underlying inflammation or fibrosis[218, 220, 245], however lower attenuation is also associated with an adverse risk profile, coronary plaque presence, and thought to constitute lipid dense tissue[122, 217, 219, 231, 246]. Most recently, perivascular adipose tissue attenuation (the immediate layer of fat around the coronary arteries), has demonstrated a linear relationship between higher attenuation and cardiac mortality. These findings suggest a complex and dynamic interplay between cardiac adipose tissue, coronary plaque and systemic inflammatory status. We demonstrate that increasing EAT density was associated with greater fibro-fatty and total plaque burden. The significance of this association remains unclear given the lack of association with other plaque parameters. The ongoing study of inflammation and cellular cross-talk between fat and plaque features remains a subject for investigation

Limitations:

We acknowledge several limitations in our study. Firstly this is a cross-sectional study of patients with non-obstructive coronary disease and the results cannot be immediately applied to other cohorts, particularly those with obstructive stenosis. However, we believe this is informative as our population is representative of the majority of patients undergoing CTCA. Secondly, we did not evaluate data pertaining to absolute lipid levels which have associations with coronary plaque characteristics as this data was not reliably available in all patients. We also did not analyse patients based on lipid-lowering and other cardiovascular therapies. There were very few patients on established statin therapy and therefore we chose not to perform subgroup analysis on this small cohort. However, given the low-intermediate risk nature of these patients and the lack of definitive evidence that statin therapy is mandated in this population, we feel this is also reflective of the majority of patients who undergo CTCA. We also do not have outcome data to establish the prognostic relationship between fat and plaque.

CONCLUSION:

CTCA allows measurement of both EAT and quantification of coronary artery plaque. We demonstrate an association between EAT volume and increasing markers of high risk coronary artery plaque volume and burden that is independent of traditional cardiovascular risk factors. There is no association between EAT volume and fibrous or calcified plaque. The association between EAT density and coronary plaque composition is uncertain and requires further investigation.

Table 1: Demographics, Plaque Volumes and Plaque Burden

Characteristic	n=100
Age	59 ± 9
Sex (male)	69 (69%)
Hypertension	38 (38%)
Hyperlipidaemia	31 (31%)
Diabetes	19 (19%)
Smoking	18 (18%)
Body Mass Index	28.5 ± 4
Family History of CAD	14 (14%)
Total plaque volume (mm^3)	1347.9 ± 6231
Total non-calcified plaque volume (mm^3)	1309.8 ± 601.7
Total low-attenuation plaque volume (mm^3)	249.9 ± 179.9
Total calcified plaque volume (mm^3)	38.1 ± 52
Total vessel volume (mm^3)	3984.8 ± 1315.7
Total necrotic plaque volume (mm^3)	248.6 ± 179.9
Total fibro-fatty volume (mm^3)	833.5 ± 383.4
Total fibrous volume (mm^3)	211.4 ± 124.9
Total necrotic + fibrous (mm^3)	1082.1 ± 545
Total plaque burden (%)	33.7 ± 10.1
Total non-calcified plaque burden (%)	32.7 ± 9.7
Total low-attenuation plaque burden (%)	6.1 ± 3.2
Total necrotic plaque burden (%)	6.1 ± 3.3
Total fibro-fatty plaque burden (%)	20.8 ± 6.2
Total necrotic + fibro-fatty burden (%)	26.8 ± 8.9
Total fibrous plaque burden (%)	5.4 ± 2.4
Total calcified plaque burden (%)	0.99 ± 1.4
Segment Involvement Score	3 ± 2
CT-Leamen	5 ± 4
HRP prevalence	19 (19%)
EAT volume (mL)	66 ± 30
EAT density (HU)	-75 ± 7

CAD – coronary artery disease, CT- computed tomography, HRP – high risk plaque, HU – Hounsfield Units, mL (millilitres)

Table 2: Univariable associations of EAT volume and EAT density with plaque volumes

	EAT Volume			EAT Density		
Plaque volumes (mm^3)	**β-coefficient**	**Standard Error**	**p-value**	**β-coefficient**	**Standard Error**	**p-value**
Total plaque volume	**10.84**	**2.59**	**<0.001**	23.92	15.49	0.13
Total non-calcified volume	**10.58**	**2.49**	**<0.001**	22.53	14.99	0.14
Total low attenuation volume	**3.06**	**0.76**	**<0.001**	1.06	4.61	0.82
Total necrotic core volume	**3.09**	**0.75**	**<0.001**	0.93	4.60	0.84
Total fibro-fatty volume	**6.45**	**1.62**	**<0.001**	18.12	9.39	0.06
Total high risk plaque	**9.55**	**2.26**	**<0.001**	19.05	13.62	0.17
Total fibrous volume	0.98	0.60	0.11	3.31	3.16	0.30
Total calcified volume	0.26	0.26	0.32	1.39	1.34	0.30

High-risk plaque represents necrotic core + fibro-fatty volumes.
EAT- Epicardial adipose tissue

Table 3: Multivariable associations of EAT volume and EAT density with plaque volumes

	EAT Volume			EAT Density		
Plaque volumes (mm^3)	**β-coefficient**	**Standard Error**	**p-value**	**β-coefficient**	**Standard Error**	**p-value**
Total plaque volume	**10.39**	**3.19**	**0.003**	20.33	17.19	0.25
Total non-calcified volume	**10.26**	**3.08**	**0.002**	18.87	16.69	0.27
Total low attenuation volume	**3.01**	**0.94**	**0.003**	0.21	5.14	0.97
Total necrotic core volume	**3.05**	**0.94**	**0.003**	0.03	5.14	0.99
Total fibro-fatty volume	**6.41**	**1.99**	**0.003**	15.78	10.53	0.14
Total high risk plaque	**9.55**	**2.26**	**<0.001**	19.05	13.62	0.17
Total fibrous volume	0.85	0.75	0.26	2.89	3.59	0.43
Total calcified volume	0.14	0.32	0.67	1.46	1.49	0.33

Models adjusted for body mass index, age, sex, hypertension, hyperlipidaemia, diabetes, smoking

Table 4: Multivariable associations of EAT volume and EAT density with plaque burden

	EAT Volume			EAT Density		
Plaque burden (%)	**β-coefficient**	**Standard Error**	**p-value**	**β-coefficient**	**Standard Error**	**p-value**
Total plaque burden	**0.11**	**0.06**	**0.05**	**0.55**	**0.25**	**0.04**
Total non-calcified burden	**0.12**	**0.06**	**0.04**	0.49	0.25	0.06
Total low attenuation burden	**0.05**	**0.02**	**0.02**	-0.02	0.09	0.84
Total necrotic core burden	**0.05**	**0.02**	**0.02**	-0.02	0.09	0.79
Total fibro-fatty burden	**0.07**	**0.04**	**0.05**	**0.39**	**0.16**	**0.02**
Total high risk burden	**0.12**	**0.05**	**0.02**	0.35	0.23	0.15
Total fibrous burden	0.001	0.01	0.94	0.12	0.06	0.08
Total calcified burden	-0.004	0.008	0.96	0.07	0.04	0.09

Models adjusted for body mass index, age, sex, hypertension, hyperlipidaemia, diabetes, smoking

<u>Figure 1</u>: Case example of Epicardial fat, Qualitative and Quantitative plaque analysis from semi-automated software. Epicardial fat performed in QFAT and plaque performed using AutoPlaq.

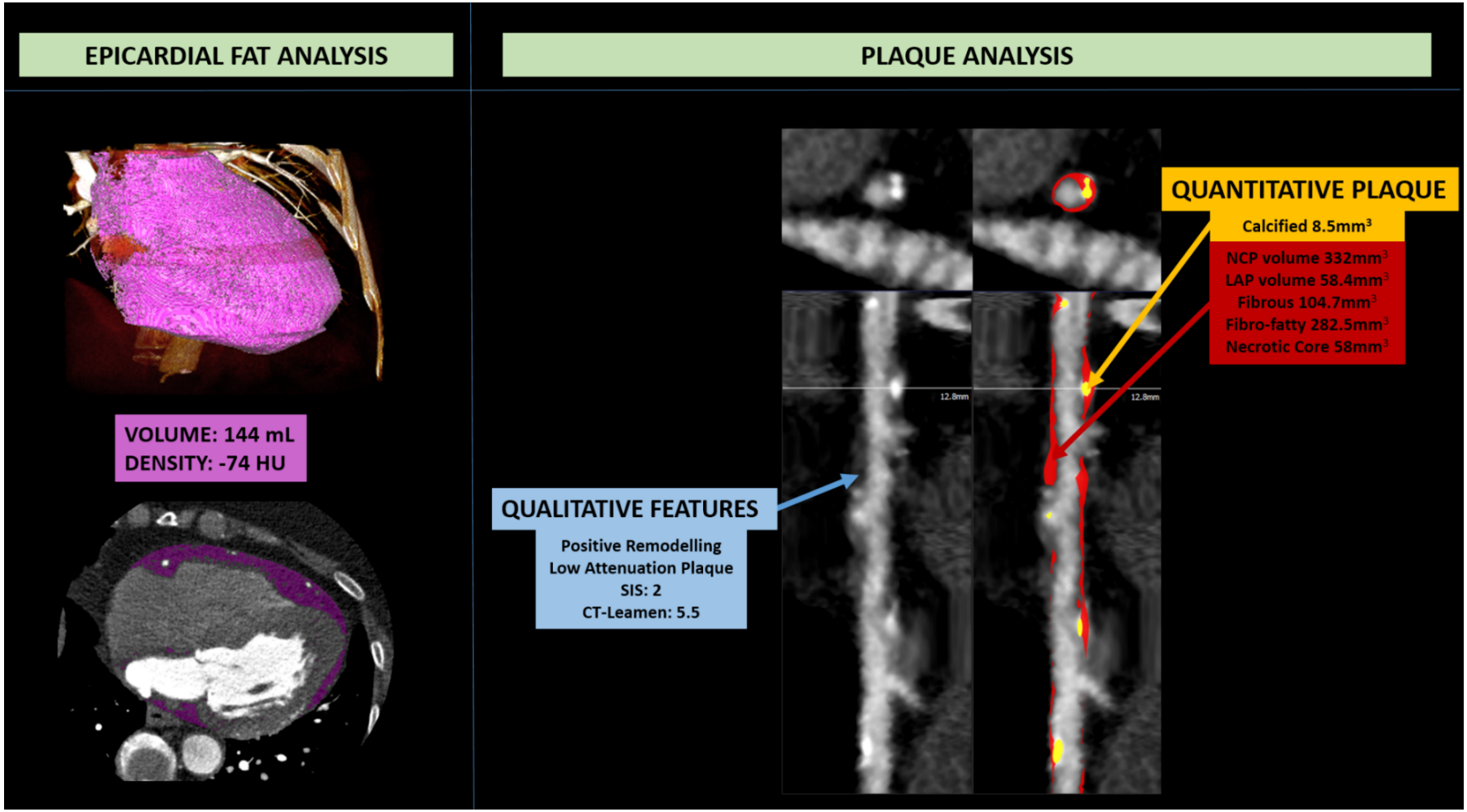

EAT volume and mean density in Hounsfield units (HU) is reported. Qualitative features based on visual assessment – there is positive remodelling and low-attenuation plaque which are qualitative high-risk plaque features. The segment involvement score (SIS) is 2 and CT-Leamen score is 5.5 to demonstrate plaque burden. Quantified plaque after manual vessel contouring with calcified plaque (yellow) and non-calcified plaque (red). Plaque volumes are automatically derived based on published thresholds

Figure 2: Scatter plots of EAT volume and plaque parameters of (A) Total Plaque Volume, (B) High-risk plaque (necrotic core + fibrofatty plaque), (C) Fibrous plaque and (D) Calcified plaque volume. Adjusted beta-coefficients and p-values from multivariable linear regression are displayed.

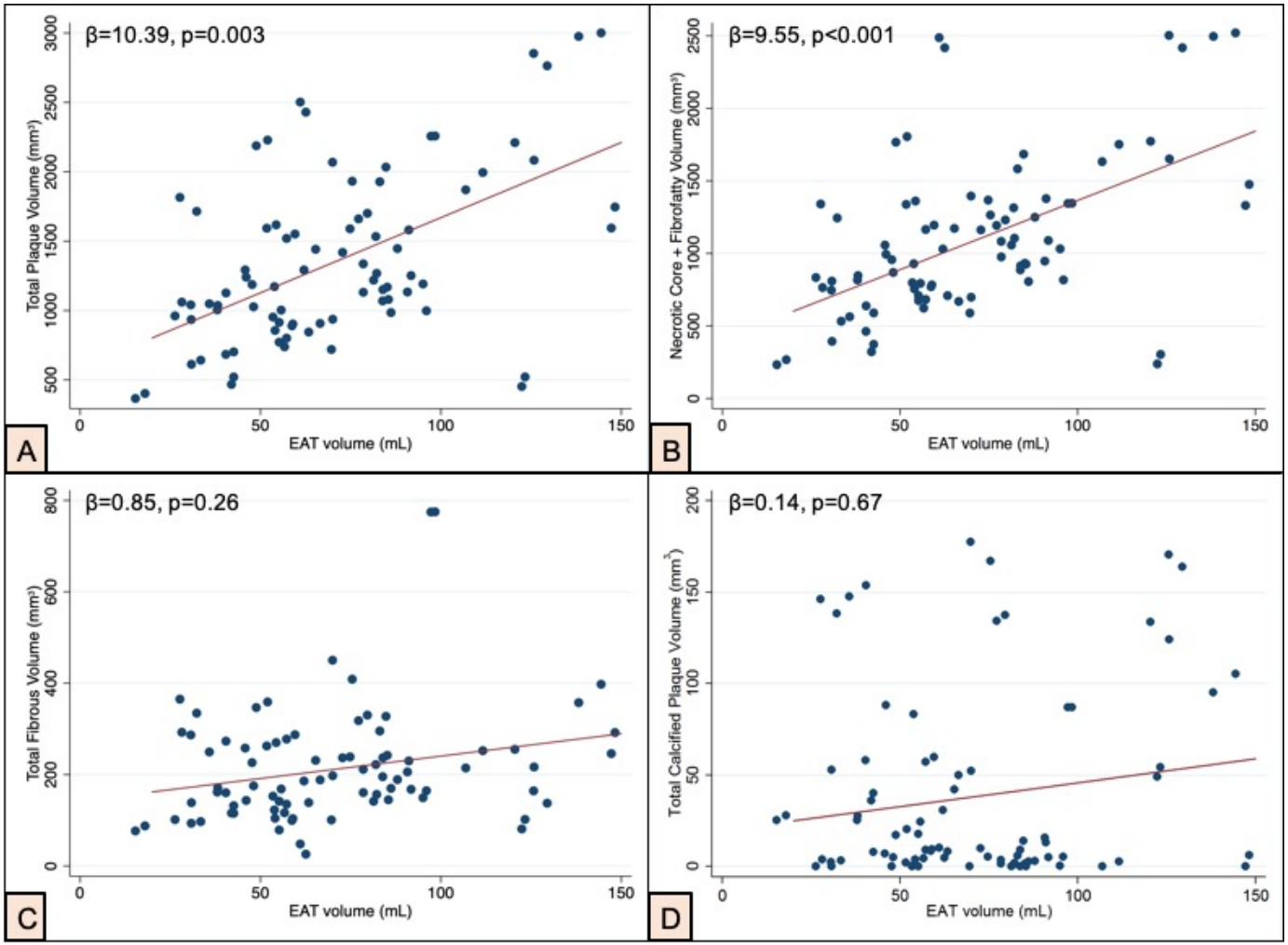

<u>Figure 3</u>: Scatter plots of EAT density and plaque parameters of (A) Total Plaque Volume, (B) High-risk plaque (necrotic core + fibrofatty plaque), (C) Fibrous plaque and (D) Calcified plaque volume. Adjusted beta-coefficients and p-values from multivariable linear regression are displayed.

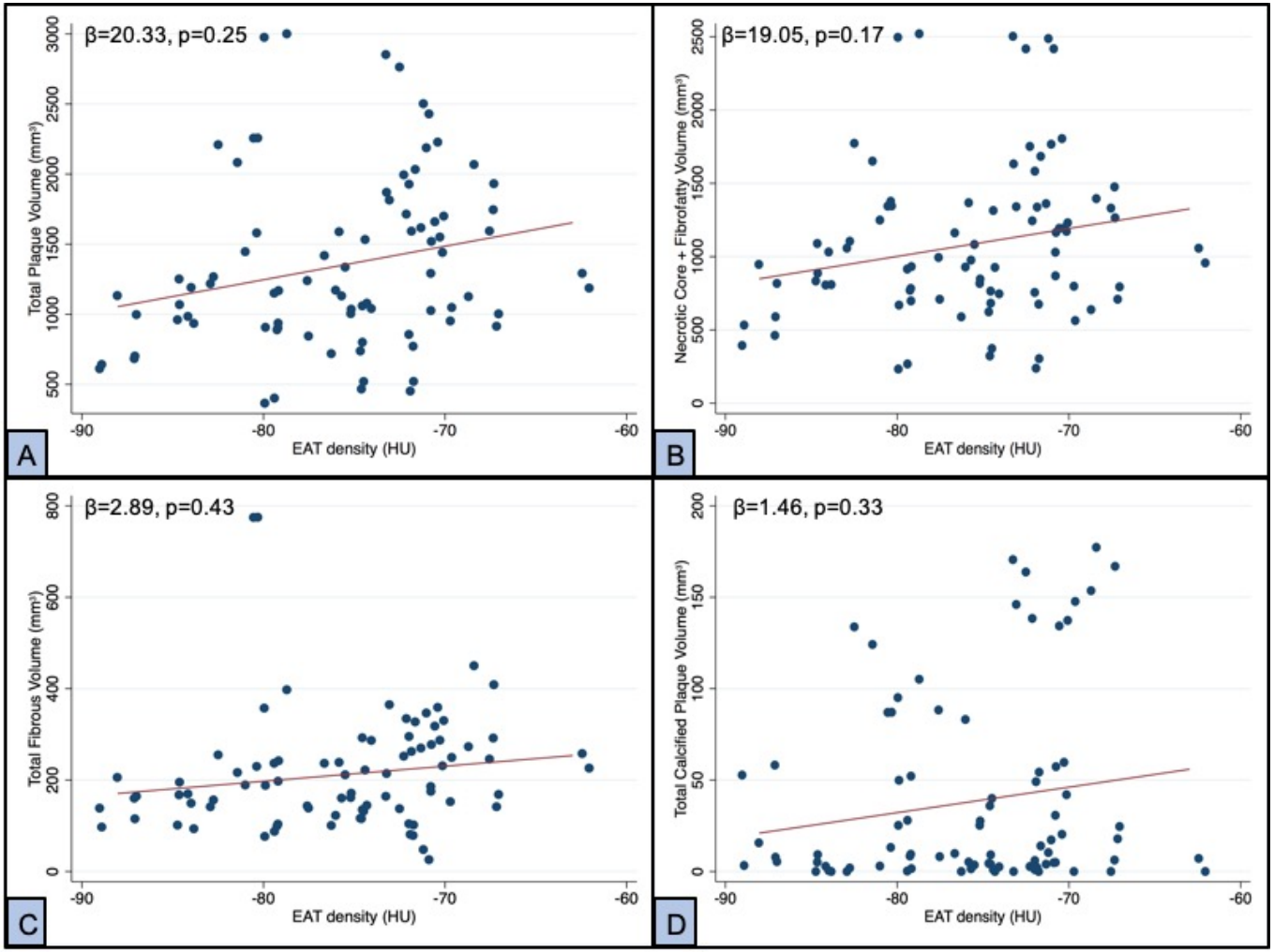

Supplemental Tables: Full linear regression models for association of plaque and cardiovascular risk factors

Total Plaque Volume	Beta coefficient	Std Error	p-value
EAT volume	13.092	3.280	0.000
Age	2.137	8.463	0.802
Sex (male)	-44.027	196.759	0.824
Body Mass Index	-35.174	16.260	0.038
Smoking	92.969	201.400	0.647
Hypertension	34.647	192.038	0.858
Hyperlipidaemia	-95.994	210.606	0.652
Family History	53.434	184.167	0.774
Diabetes	144.546	253.875	0.573

Total Plaque Volume	Beta coefficient	Std Error	p-value
EAT density	22.379	17.503	0.210
Age	12.331	9.759	0.215
Sex (male)	-208.322	232.781	0.378
Body Mass Index	-14.008	18.161	0.446
Smoking	114.520	240.560	0.637
Hypertension	152.791	229.121	0.510
Hyperlipidaemia	-141.732	251.197	0.577
Family History	56.231	220.037	0.800
Diabetes	222.207	302.186	0.467

Total NCP Volume	Beta coefficient	Std Error	p-value
EAT volume	12.943	3.142	0.000
Age	1.659	8.108	0.839
Sex (male)	-36.274	188.503	0.849
Body Mass Index	-35.012	15.577	0.032
Smoking	85.174	192.949	0.662
Hypertension	16.412	183.980	0.929
Hyperlipidaemia	-82.648	201.768	0.685
Family History	63.110	176.439	0.723
Diabetes	132.581	243.222	0.589

Total NCP Volume	Beta coefficient	Std Error	p-value
EAT density	20.902	16.978	0.227
Age	11.680	9.466	0.226
Sex (male)	-203.479	225.803	0.374
Body Mass Index	-13.895	17.617	0.436
Smoking	107.483	233.349	0.648
Hypertension	131.483	222.253	0.558
Hyperlipidaemia	-127.504	243.667	0.604
Family History	66.581	213.441	0.757
Diabetes	209.343	293.127	0.480

Total LAP Volume	Beta coefficient	Std Error	p-value
EAT volume	3.708	0.981	0.001
Age	0.408	2.531	0.873
Sex (male)	20.536	58.834	0.729
Body Mass Index	-9.089	4.862	0.071
Smoking	12.320	60.222	0.839
Hypertension	19.760	57.422	0.733
Hyperlipidaemia	3.726	62.974	0.953
Family History	9.385	55.069	0.866
Diabetes	30.811	75.913	0.688

Total LAP Volume	Beta coefficient	Std Error	p-value
EAT density	0.525	5.272	0.921
Age	3.026	2.940	0.311
Sex (male)	-48.737	70.119	0.492
Body Mass Index	-2.180	5.471	0.693
Smoking	23.198	72.463	0.751
Hypertension	45.015	69.017	0.519
Hyperlipidaemia	-7.514	75.667	0.922
Family History	13.536	66.281	0.839
Diabetes	52.737	91.026	0.566

Total Necrotic Core Volume	Beta coefficient	Std Error	p-value
EAT volume	3.747	0.976	0.001
Age	0.391	2.518	0.878
Sex (male)	20.572	58.547	0.728
Body Mass Index	-9.075	4.838	0.070
Smoking	14.169	59.928	0.815
Hypertension	17.250	57.142	0.765
Hyperlipidaemia	1.753	62.667	0.978
Family History	9.225	54.800	0.867
Diabetes	32.958	75.542	0.666

Total Necrotic Core Volume	Beta coefficient	Std Error	p-value
EAT density	0.328	5.272	0.951
Age	3.027	2.939	0.311
Sex (male)	-50.212	70.116	0.479
Body Mass Index	-2.063	5.470	0.709
Smoking	25.326	72.459	0.729
Hypertension	42.481	69.013	0.543
Hyperlipidaemia	-9.544	75.663	0.900
Family History	13.535	66.277	0.839
Diabetes	55.110	91.021	0.549

Total Fibrofatty Volume	Beta coefficient	Std Error	p-value
EAT density	17.086	10.712	0.121
Age	7.057	5.972	0.246
Sex (male)	-126.809	142.463	0.380
Body Mass Index	-8.918	11.115	0.428
Smoking	79.450	147.224	0.593
Hypertension	60.797	140.223	0.668
Hyperlipidaemia	-103.727	153.734	0.505
Family History	61.232	134.664	0.652
Diabetes	103.542	184.939	0.579

Total Fibrofatty Volume	Beta coefficient	Std Error	p-value
EAT volume	8.055	2.042	0.000
Age	0.632	5.270	0.905
Sex (male)	-38.701	122.519	0.754
Body Mass Index	-21.419	10.125	0.042
Smoking	68.915	125.409	0.586
Hypertension	-16.573	119.579	0.891
Hyperlipidaemia	-74.609	131.141	0.573
Family History	61.427	114.678	0.596
Diabetes	55.721	158.084	0.727

Total Fibrous Volume	Beta coefficient	Std Error	p-value
EAT volume	1.229	0.800	0.135
Age	0.339	2.065	0.871
Sex (male)	-13.686	48.004	0.777
Body Mass Index	-4.919	3.967	0.224
Smoking	0.871	49.136	0.986
Hypertension	9.741	46.852	0.837
Hyperlipidaemia	-17.529	51.382	0.735
Family History	2.364	44.932	0.958
Diabetes	36.890	61.939	0.556

Total Fibrous Volume	Beta coefficient	Std Error	p-value
EAT density	3.351	3.659	0.367
Age	1.354	2.040	0.512
Sex (male)	-24.210	48.661	0.622
Body Mass Index	-3.129	3.796	0.416
Smoking	1.866	50.287	0.971
Hypertension	22.594	47.896	0.640
Hyperlipidaemia	-22.190	52.511	0.675
Family History	1.903	45.997	0.967
Diabetes	44.192	63.169	0.489

Total HRP volume	Beta coefficient	Std Error	p-value
EAT volume	11.802	2.874	0.000
Age	1.023	7.416	0.891
Sex (male)	-18.129	172.414	0.917
Body Mass Index	-30.494	14.248	0.040
Smoking	83.084	176.481	0.641
Hypertension	0.677	168.278	0.997
Hyperlipidaemia	-72.856	184.548	0.696
Family History	70.653	161.381	0.664
Diabetes	88.679	222.464	0.693

Total HRP volume	Beta coefficient	Std Error	p-value
EAT density	17.414	15.574	0.272
Age	10.084	8.683	0.254
Sex (male)	-177.021	207.131	0.399
Body Mass Index	-10.981	16.160	0.502
Smoking	104.776	214.053	0.628
Hypertension	103.278	203.874	0.616
Hyperlipidaemia	-113.271	223.518	0.616
Family History	74.767	195.791	0.705
Diabetes	158.652	268.888	0.559

Total Calcified Volume	Beta coefficient	Std Error	p-value
EAT volume	0.149	0.346	0.669
Age	0.479	0.893	0.596
Sex (male)	-7.755	20.771	0.711
Body Mass Index	-0.162	1.716	0.925
Smoking	7.796	21.261	0.716
Hypertension	18.232	20.273	0.375
Hyperlipidaemia	-13.345	22.233	0.553
Family History	-9.676	19.442	0.622
Diabetes	11.964	26.801	0.658

Total Calcified Volume	Beta coefficient	Std Error	p-value
EAT density	1.478	1.530	0.341
Age	0.652	0.853	0.451
Sex (male)	-4.846	20.350	0.813
Body Mass Index	-0.113	1.588	0.944
Smoking	7.037	21.030	0.740
Hypertension	21.305	20.030	0.295
Hyperlipidaemia	-14.227	21.960	0.522
Family History	-10.350	19.236	0.594
Diabetes	12.864	26.418	0.630

Supplemental Tables: Full logistic regression models for association of any qualitative HRP presence and cardiovascular risk factors

Qualitative HRP	Odds Ratio	Std Error	p-value
EAT volume	1.042	0.017	0.014
Body Mass Index	0.910	0.081	0.284
Hypertension	0.553	0.476	0.491
Smoking	3.326	3.521	0.256
Diabetes	0.207	0.262	0.214
Family History	0.216	0.197	0.092
Hyperlipidaemia	3.358	3.449	0.238
Age	0.996	0.038	0.913
Sex (male)	0.183	0.166	0.061

Qualitative HRP	Odds Ratio	Std Error	p-value
EAT density	0.951	0.059	0.416
Body Mass Index	1.026	0.080	0.742
Hypertension	0.819	0.623	0.793
Smoking	3.145	2.913	0.216
Diabetes	0.258	0.287	0.224
Family History	0.234	0.195	0.082
Hyperlipidaemia	2.720	2.459	0.268
Age	1.016	0.034	0.632
Sex (male)	0.112	0.100	0.014

CONCLUSION
AND
FUTURE DIRECTIONS

CONCLUSIONS:

In this thesis we have identified several important findings that have clinical implications. Firstly, there is a significant association between epicardial adipose tissue volume and high-risk coronary artery plaque both at a qualitative and quantitative level. The latter is of significant importance as we have demonstrated feasibility of measuring these high-risk plaque features in patients who do not have any obstructive coronary stenosis which allows applications to lower risk patient cohorts. We also report the potential dynamic nature of coronary plaque with a risk continuum for cardiac events based on the composition of plaque whereby calcified plaques may represent a more stable phenotype compared to non-calcified and partially calcified plaques.

Secondly, we believe we have identified the optimal method of measuring epicardial adipose tissue which is by complete volumetric assessment, far superior to linear measurements on echocardiography. We have also identified differences in volumes and density of EAT dependent upon the software platform as well as the use of contrast. The implications of this are that researchers will need to perform in-house reproducibility studies to be confident in the utilisation of these measurements for clinical research. In particular, it appears that linear thickness is inferior and this notion needs to be highlighted beyond the cardiovascular community where echocardiographic EAT thickness is often employed.

We have also demonstrated that EAT not only affects coronary artery disease, but also cardiac structure and diastolic function, similarly when volumetric measurements are used. Although not the main focus of this thesis, this indicates that this adipose tissue depot is an important marker of cardiac pathophysiology, with several studies also describing an association with cardiac dysrhythmia. Finally, this leads to the important description of the natural history of EAT in a non-obstructive coronary artery disease population, a cohort reflective of two-thirds of patients who would undergo cardiac CT.

We have shown that EAT appears to be an independent variable that is not modulated by other cardiovascular risk factors, particularly weight change.

We hope that our analyses have further refined the understanding of EAT measurement and disease association to better inform researchers who may build upon this work for future, and necessary research.

FUTURE DIRECTIONS:

The notion of quantity vs. quality is the underpinning conviction where I believe the future of adipose tissue and cardiac disease lies. In our thesis, the majority of studies focussed on amount of EAT, mainly because it has been thought that the greater the volume of adipose tissue, possibly the more abundant the pro-inflammatory adipokines. However, given EAT is a universal anatomical depot, it may not be the quantity but rather the activity, or the 'quality' of fat that leads to disease. Furthermore, it may be a more dynamic process that ebbs and flows between disease and stability, much the same way that coronary artery disease behaves.

Important work that emerged during my candidature was a refined idea of pericoronary adipose tissue (the fat immediately surrounding the coronary arteries) as a potential sensor of vascular inflammation. Antonopoulos et al. elegantly demonstrated this pathophysiologic imaging biomarker in a journey of in-vitro and in-vivo experiments to highlight that inflammatory activity from the adjacent coronaries may affect the fat quality and hence fat density or attenuation[247]. This was also further shown to associate with long-term prognosis in a large collaborative retrospective study[248] as well as associated with high-risk plaques at a lesion level in patients with an acute coronary syndrome[216].

I believe that these findings are simply the tip of the iceberg, or the first flame in a paradigm shift in the investigation of inflammation and cardiac disease. These studies hypothesise that pericoronary adipose tissue attenuation (PCAT) is a surrogate for vascular inflammation. The overarching idea is inflammation in the coronaries with resulting atherosclerosis will work inside-out (from vessel to fat) to induce an anatomical change in the lipid cells. Inflammation arrests lipid maturation and therefore smaller, less dense lipids will have a higher attenuation on CT imaging which is an ideal test for adipose tissue quantification. Conversely, less inflammation leads to greater lipid volumes and more

negative densities based on Hounsfield Unit thresholding. There is however a larger body of evidence supporting an outside-in theory (from fat to vessel) with associations of coronary and cardiac disease. This bidirectional communication may suggest that PCAT is actually a sensor for both the surrounding epicardial fat and the vascular inflammatory activity (**Figure**). How to define which is playing a greater part and how this varies temporally is the next chapter for investigation. The final destination is the ability to predict which patients will develop plaque-rupture precursor lesions non-invasively using this radiographic tool.

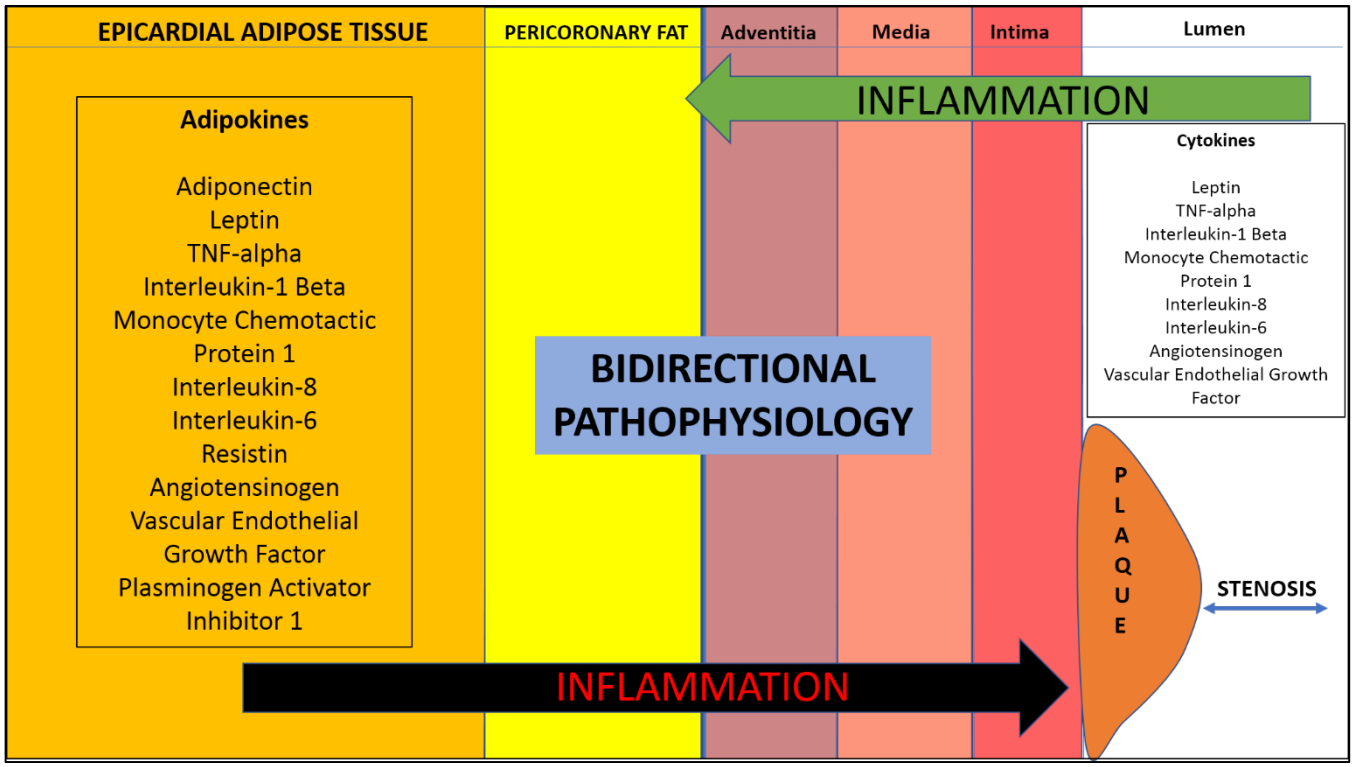

Figure demonstrates bidirectional inflammatory physiology of cellular cross-talk between adipokines from epicardial fat and from systemic circulation in the coronary lumen. The pericoronary fat is an ideal location for interrogation of the effects of inflammation.

Ultimately, while it is desirable to predict who is at risk, the other tale to be told is what therapies may be effective in this arena. There has been a recent eruption of research into pharmacologic therapies aimed at reducing vascular inflammation, but most have required the use of systemic biomarkers such as high sensitivity C-reactive protein which may not be reflective of the local coronary inflammatory

processes. The use of PCAT may therefore be an additional tool to detect lesion level inflammation to better evaluate the effectiveness of anti-inflammatory therapies.

REFERENCES

1. Cornier MA, Despres JP, Davis N, Grossniklaus DA, Klein S, Lamarche B, Lopez-Jimenez F, Rao G, St-Onge MP, Towfighi A and Poirier P. Assessing adiposity: a scientific statement from the American Heart Association. *Circulation*. 2011;124:1996-2019.

2. Gustafson B, Hammarstedt A, Andersson CX and Smith U. Inflamed adipose tissue: a culprit underlying the metabolic syndrome and atherosclerosis. *Arterioscler Thromb Vasc Biol*. 2007;27:2276-83.

3. Sun K, Kusminski CM and Scherer PE. Adipose tissue remodeling and obesity. *J Clin Invest*. 2011;121:2094-101.

4. Fitzgibbons TP and Czech MP. Epicardial and perivascular adipose tissues and their influence on cardiovascular disease: basic mechanisms and clinical associations. *J Am Heart Assoc*. 2014;3:e000582.

5. Kataoka Y and Nicholls SJ. Imaging of atherosclerotic plaques in obesity: excessive fat accumulation, plaque progression and vulnerability. *Expert review of cardiovascular therapy*. 2014;12:1471-89.

6. Statistics ABS. 2012.

7. Colagiuri S, Lee CM, Colagiuri R, Magliano D, Shaw JE, Zimmet PZ and Caterson ID. The cost of overweight and obesity in Australia. *The Medical journal of Australia*. 2010;192:260-4.

8. Nichols M PK, Alston S, Allender S. Australian Heart Disease Statistics 2014. 2014.

9. Ford ES, Ajani UA, Croft JB, Critchley JA, Labarthe DR, Kottke TE, Giles WH and Capewell S. Explaining the decrease in U.S. deaths from coronary disease, 1980-2000. *The New England journal of medicine*. 2007;356:2388-98.

10. Allan GM, Nouri F, Korownyk C, Kolber MR, Vandermeer B and McCormack J. Agreement among cardiovascular disease risk calculators. *Circulation*. 2013;127:1948-56.

11. Smith SC, Jr., Benjamin EJ, Bonow RO, Braun LT, Creager MA, Franklin BA, Gibbons RJ, Grundy SM, Hiratzka LF, Jones DW, Lloyd-Jones DM, Minissian M, Mosca L, Peterson ED, Sacco RL, Spertus J, Stein JH, Taubert KA, World Heart F and the Preventive Cardiovascular Nurses A. AHA/ACCF Secondary Prevention and Risk Reduction Therapy for Patients with Coronary and other Atherosclerotic Vascular Disease: 2011 update: a guideline from the American Heart Association and American College of Cardiology Foundation. *Circulation*. 2011;124:2458-73.

12. Prospective Studies C, Whitlock G, Lewington S, Sherliker P, Clarke R, Emberson J, Halsey J, Qizilbash N, Collins R and Peto R. Body-mass index and cause-specific mortality in 900 000 adults: collaborative analyses of 57 prospective studies. *Lancet*. 2009;373:1083-96.

13. Eckel RH. Obesity and heart disease: a statement for healthcare professionals from the Nutrition Committee, American Heart Association. *Circulation*. 1997;96:3248-50.

14. Pack QR, Rodriguez-Escudero JP, Thomas RJ, Ades PA, West CP, Somers VK and Lopez-Jimenez F. The prognostic importance of weight loss in coronary artery disease: a systematic review and meta-analysis. *Mayo Clinic proceedings*. 2014;89:1368-77.

15. Ornish D, Brown SE, Scherwitz LW, Billings JH, Armstrong WT, Ports TA, McLanahan SM, Kirkeeide RL, Brand RJ and Gould KL. Can lifestyle changes reverse coronary heart disease? The Lifestyle Heart Trial. *Lancet*. 1990;336:129-33.

16. Jahangir E, De Schutter A and Lavie CJ. The relationship between obesity and coronary artery disease. *Translational research : the journal of laboratory and clinical medicine*. 2014;164:336-44.

17. Romero-Corral A, Montori VM, Somers VK, Korinek J, Thomas RJ, Allison TG, Mookadam F and Lopez-Jimenez F. Association of bodyweight with total mortality and with cardiovascular events in coronary artery disease: a systematic review of cohort studies. *Lancet*. 2006;368:666-78.

18. Shah NR and Braverman ER. Measuring adiposity in patients: the utility of body mass index (BMI), percent body fat, and leptin. *PLoS One*. 2012;7:e33308.

19. Bluher M. The distinction of metabolically 'healthy' from 'unhealthy' obese individuals. *Current opinion in lipidology*. 2010;21:38-43.

20. Drapeau V, Lemieux I, Richard D, Bergeron J, Tremblay A, Biron S, Marceau P and Mauriege P. Metabolic profile in severely obese women is less deteriorated than expected when compared to moderately obese women. *Obesity surgery*. 2006;16:501-9.

21. Karelis AD, Faraj M, Bastard JP, St-Pierre DH, Brochu M, Prud'homme D and Rabasa-Lhoret R. The metabolically healthy but obese individual presents a favorable inflammation profile. *The Journal of clinical endocrinology and metabolism*. 2005;90:4145-50.

22. Lemieux I, Drapeau V, Richard D, Bergeron J, Marceau P, Biron S and Mauriege P. Waist girth does not predict metabolic complications in severely obese men. *Diabetes care*. 2006;29:1417-9.

23. Ruderman N, Chisholm D, Pi-Sunyer X and Schneider S. The metabolically obese, normal-weight individual revisited. *Diabetes*. 1998;47:699-713.

24. Wildman RP, Muntner P, Reynolds K, McGinn AP, Rajpathak S, Wylie-Rosett J and Sowers MR. The obese without cardiometabolic risk factor clustering and the normal weight with cardiometabolic risk factor clustering: prevalence and correlates of 2 phenotypes among the US population (NHANES 1999-2004). *Archives of internal medicine*. 2008;168:1617-24.

25. Yusuf S, Hawken S, Ounpuu S, Bautista L, Franzosi MG, Commerford P, Lang CC, Rumboldt Z, Onen CL, Lisheng L, Tanomsup S, Wangai P, Jr., Razak F, Sharma AM and Anand SS. Obesity

and the risk of myocardial infarction in 27,000 participants from 52 countries: a case-control study. *Lancet*. 2005;366:1640-9.

26. Tansey DK, Aly Z and Sheppard MN. Fat in the right ventricle of the normal heart. *Histopathology*. 2005;46:98-104.

27. Motoyama S, Ito H, Sarai M, Kondo T, Kawai H, Nagahara Y, Harigaya H, Kan S, Anno H, Takahashi H, Naruse H, Ishii J, Hecht H, Shaw LJ, Ozaki Y and Narula J. Plaque Characterization by Coronary Computed Tomography Angiography and the Likelihood of Acute Coronary Events in Mid-Term Follow-Up. *J Am Coll Cardiol*. 2015;66:337-46.

28. Nakazato R, Otake H, Konishi A, Iwasaki M, Koo BK, Fukuya H, Shinke T, Hirata K, Leipsic J, Berman DS and Min JK. Atherosclerotic plaque characterization by CT angiography for identification of high-risk coronary artery lesions: a comparison to optical coherence tomography. *Eur Heart J Cardiovasc Imaging*. 2015;16:373-9.

29. Virmani R, Burke AP, Farb A and Kolodgie FD. Pathology of the vulnerable plaque. *J Am Coll Cardiol*. 2006;47:C13-8.

30. Nakanishi K, Fukuda S, Tanaka A, Otsuka K, Jissho S, Taguchi H, Yoshikawa J and Shimada K. Persistent epicardial adipose tissue accumulation is associated with coronary plaque vulnerability and future acute coronary syndrome in non-obese subjects with coronary artery disease. *Atherosclerosis*. 2014;237:353-60.

31. Burke AP, Farb A, Malcom GT, Liang YH, Smialek J and Virmani R. Coronary risk factors and plaque morphology in men with coronary disease who died suddenly. *The New England journal of medicine*. 1997;336:1276-82.

32. Stone GW, Maehara A, Lansky AJ, de Bruyne B, Cristea E, Mintz GS, Mehran R, McPherson J, Farhat N, Marso SP, Parise H, Templin B, White R, Zhang Z, Serruys PW and Investigators P. A prospective natural-history study of coronary atherosclerosis. *The New England journal of medicine*. 2011;364:226-35.

33. Kato K, Yonetsu T, Kim SJ, Xing L, Lee H, McNulty I, Yeh RW, Sakhuja R, Zhang S, Uemura S, Yu B, Mizuno K and Jang IK. Nonculprit plaques in patients with acute coronary syndromes have more vulnerable features compared with those with non-acute coronary syndromes: a 3-vessel optical coherence tomography study. *Circulation Cardiovascular imaging*. 2012;5:433-40.

34. Virmani R, Kolodgie FD, Burke AP, Farb A and Schwartz SM. Lessons from sudden coronary death: a comprehensive morphological classification scheme for atherosclerotic lesions. *Arterioscler Thromb Vasc Biol*. 2000;20:1262-75.

35. Asakura M, Ueda Y, Yamaguchi O, Adachi T, Hirayama A, Hori M and Kodama K. Extensive development of vulnerable plaques as a pan-coronary process in patients with myocardial infarction: an angioscopic study. *J Am Coll Cardiol*. 2001;37:1284-8.

36. Hong MK, Mintz GS, Lee CW, Lee BK, Yang TH, Kim YH, Song JM, Han KH, Kang DH, Cheong SS, Song JK, Kim JJ, Park SW and Park SJ. The site of plaque rupture in native coronary arteries: a three-vessel intravascular ultrasound analysis. *J Am Coll Cardiol*. 2005;46:261-5.

37. Kunimasa T, Sato Y, Sugi K and Moroi M. Evaluation by multislice computed tomography of atherosclerotic coronary artery plaques in non-culprit, remote coronary arteries of patients with acute coronary syndrome. *Circulation journal : official journal of the Japanese Circulation Society*. 2005;69:1346-51.

38. Kang SJ, Mintz GS, Witzenbichler B, Metzger DC, Rinaldi MJ, Duffy PL, Weisz G, Stuckey TD, Brodie BR, Shimizu T, Xu K, Kirtane AJ, Stone GW and Maehara A. Effect of obesity on coronary atherosclerosis and outcomes of percutaneous coronary intervention: grayscale and virtual histology intravascular ultrasound substudy of assessment of dual antiplatelet therapy with drug-eluting stents. *Circulation Cardiovascular interventions*. 2015;8.

39. Ito T, Nasu K, Terashima M, Ehara M, Kinoshita Y, Ito T, Kimura M, Tanaka N, Habara M, Tsuchikane E and Suzuki T. The impact of epicardial fat volume on coronary plaque vulnerability: insight from optical coherence tomography analysis. *Eur Heart J Cardiovasc Imaging*. 2012;13:408-15.

40. Ito T, Suzuki Y, Ehara M, Matsuo H, Teramoto T, Terashima M, Nasu K, Kinoshita Y, Tsuchikane E, Suzuki T and Kimura G. Impact of epicardial fat volume on coronary artery disease in symptomatic patients with a zero calcium score. *Int J Cardiol*. 2013;167:2852-8.

41. Kubo T, Maehara A, Mintz GS, Doi H, Tsujita K, Choi SY, Katoh O, Nasu K, Koenig A, Pieper M, Rogers JH, Wijns W, Bose D, Margolis MP, Moses JW, Stone GW and Leon MB. The dynamic nature of coronary artery lesion morphology assessed by serial virtual histology intravascular ultrasound tissue characterization. *J Am Coll Cardiol*. 2010;55:1590-7.

42. Ringqvist I, Fisher LD, Mock M, Davis KB, Wedel H, Chaitman BR, Passamani E, Russell RO, Jr., Alderman EL, Kouchoukas NT, Kaiser GC, Ryan TJ, Killip T and Fray D. Prognostic value of angiographic indices of coronary artery disease from the Coronary Artery Surgery Study (CASS). *J Clin Invest*. 1983;71:1854-66.

43. Arbab-Zadeh A, Nakano M, Virmani R and Fuster V. Acute coronary events. *Circulation*. 2012;125:1147-56.

44. Bittencourt MS, Hulten E, Ghoshhajra B, O'Leary D, Christman MP, Montana P, Truong QA, Steigner M, Murthy VL, Rybicki FJ, Nasir K, Gowdak LH, Hainer J, Brady TJ, Di Carli MF, Hoffmann

U, Abbara S and Blankstein R. Prognostic value of nonobstructive and obstructive coronary artery disease detected by coronary computed tomography angiography to identify cardiovascular events. *Circulation Cardiovascular imaging*. 2014;7:282-91.

45. Nicholls SJ, Hsu A, Wolski K, Hu B, Bayturan O, Lavoie A, Uno K, Tuzcu EM and Nissen SE. Intravascular ultrasound-derived measures of coronary atherosclerotic plaque burden and clinical outcome. *J Am Coll Cardiol*. 2010;55:2399-407.

46. Voros S, Rinehart S, Qian Z, Joshi P, Vazquez G, Fischer C, Belur P, Hulten E and Villines TC. Coronary atherosclerosis imaging by coronary CT angiography: current status, correlation with intravascular interrogation and meta-analysis. *JACC Cardiovascular imaging*. 2011;4:537-48.

47. Inoue K, Motoyama S, Sarai M, Sato T, Harigaya H, Hara T, Sanda Y, Anno H, Kondo T, Wong ND, Narula J and Ozaki Y. Serial coronary CT angiography-verified changes in plaque characteristics as an end point: evaluation of effect of statin intervention. *JACC Cardiovascular imaging*. 2010;3:691-8.

48. Min JK, Dunning A, Lin FY, Achenbach S, Al-Mallah M, Budoff MJ, Cademartiri F, Callister TQ, Chang HJ, Cheng V, Chinnaiyan K, Chow BJ, Delago A, Hadamitzky M, Hausleiter J, Kaufmann P, Maffei E, Raff G, Shaw LJ, Villines T, Berman DS and Investigators C. Age- and sex-related differences in all-cause mortality risk based on coronary computed tomography angiography findings results from the International Multicenter CONFIRM (Coronary CT Angiography Evaluation for Clinical Outcomes: An International Multicenter Registry) of 23,854 patients without known coronary artery disease. *J Am Coll Cardiol*. 2011;58:849-60.

49. Wong DT, Soh SY, Ko BS, Cameron JD, Crossett M, Nasis A, Troupis J, Meredith IT and Seneviratne SK. Superior CT coronary angiography image quality at lower radiation exposure with second generation 320-detector row CT in patients with elevated heart rate: a comparison with first generation 320-detector row CT. *Cardiovascular diagnosis and therapy*. 2014;4:299-306.

50. Pundziute G, Schuijf JD, Jukema JW, Decramer I, Sarno G, Vanhoenacker PK, Boersma E, Reiber JH, Schalij MJ, Wijns W and Bax JJ. Evaluation of plaque characteristics in acute coronary syndromes: non-invasive assessment with multi-slice computed tomography and invasive evaluation with intravascular ultrasound radiofrequency data analysis. *European heart journal*. 2008;29:2373-81.

51. de Graaf MA, Broersen A, Kitslaar PH, Roos CJ, Dijkstra J, Lelieveldt BP, Jukema JW, Schalij MJ, Delgado V, Bax JJ, Reiber JH and Scholte AJ. Automatic quantification and characterization of coronary atherosclerosis with computed tomography coronary angiography: cross-correlation with intravascular ultrasound virtual histology. *Int J Cardiovasc Imaging*. 2013;29:1177-90.

52. Chang HJ, Lin FY, Lee SE, Andreini D, Bax J, Cademartiri F, Chinnaiyan K, Chow BJW, Conte E, Cury RC, Feuchtner G, Hadamitzky M, Kim YJ, Leipsic J, Maffei E, Marques H, Plank F,

Pontone G, Raff GL, van Rosendael AR, Villines TC, Weirich HG, Al'Aref SJ, Baskaran L, Cho I, Danad I, Han D, Heo R, Lee JH, Rivzi A, Stuijfzand WJ, Gransar H, Lu Y, Sung JM, Park HB, Berman DS, Budoff MJ, Samady H, Shaw LJ, Stone PH, Virmani R, Narula J and Min JK. Coronary Atherosclerotic Precursors of Acute Coronary Syndromes. *J Am Coll Cardiol*. 2018;71:2511-2522.

53. Kissebah AH, Vydelingum N, Murray R, Evans DJ, Hartz AJ, Kalkhoff RK and Adams PW. Relation of body fat distribution to metabolic complications of obesity. *The Journal of clinical endocrinology and metabolism*. 1982;54:254-60.

54. Despres JP, Moorjani S, Lupien PJ, Tremblay A, Nadeau A and Bouchard C. Regional distribution of body fat, plasma lipoproteins, and cardiovascular disease. *Arteriosclerosis (Dallas, Tex)*. 1990;10:497-511.

55. Nicklas BJ, Penninx BW, Cesari M, Kritchevsky SB, Newman AB, Kanaya AM, Pahor M, Jingzhong D and Harris TB. Association of visceral adipose tissue with incident myocardial infarction in older men and women: the Health, Aging and Body Composition Study. *American journal of epidemiology*. 2004;160:741-9.

56. Shirani J, Berezowski K and Roberts WC. Quantitative measurement of normal and excessive (cor adiposum) subepicardial adipose tissue, its clinical significance, and its effect on electrocardiographic QRS voltage. *The American journal of cardiology*. 1995;76:414-8.

57. Corradi D, Maestri R, Callegari S, Pastori P, Goldoni M, Luong TV and Bordi C. The ventricular epicardial fat is related to the myocardial mass in normal, ischemic and hypertrophic hearts. *Cardiovasc Pathol*. 2004;13:313-6.

58. Company JM, Booth FW, Laughlin MH, Arce-Esquivel AA, Sacks HS, Bahouth SW and Fain JN. Epicardial fat gene expression after aerobic exercise training in pigs with coronary atherosclerosis: relationship to visceral and subcutaneous fat. *Journal of applied physiology (Bethesda, Md : 1985)*. 2010;109:1904-12.

59. Yamaguchi Y, Cavallero S, Patterson M, Shen H, Xu J, Kumar SR and Sucov HM. Adipogenesis and epicardial adipose tissue: a novel fate of the epicardium induced by mesenchymal transformation and PPARgamma activation. *Proceedings of the National Academy of Sciences of the United States of America*. 2015;112:2070-5.

60. Sacks HS and Fain JN. Human epicardial adipose tissue: a review. *Am Heart J*. 2007;153:907-17.

61. Iacobellis G, Malavazos AE and Corsi MM. Epicardial fat: from the biomolecular aspects to the clinical practice. *The international journal of biochemistry & cell biology*. 2011;43:1651-4.

62. Wong CX, Ganesan AN and Selvanayagam JB. Epicardial fat and atrial fibrillation: current evidence, potential mechanisms, clinical implications, and future directions. *European heart journal*. 2017;38:1294-1302.

63. Iacobellis G. Local and systemic effects of the multifaceted epicardial adipose tissue depot. *Nat Rev Endocrinol*. 2015;11:363-71.

64. Szasz T and Webb RC. Perivascular adipose tissue: more than just structural support. *Clinical science (London, England : 1979)*. 2012;122:1-12.

65. Vincent HK, Powers SK, Stewart DJ, Shanely RA, Demirel H and Naito H. Obesity is associated with increased myocardial oxidative stress. *International journal of obesity and related metabolic disorders : journal of the International Association for the Study of Obesity*. 1999;23:67-74.

66. Falcao-Pires I, Castro-Chaves P, Miranda-Silva D, Lourenco AP and Leite-Moreira AF. Physiological, pathological and potential therapeutic roles of adipokines. *Drug discovery today*. 2012;17:880-9.

67. Canepa M, Strait JB, Milaneschi Y, AlGhatrif M, Ramachandran R, Makrogiannis S, Moni M, David M, Brunelli C, Lakatta EG and Ferrucci L. The relationship between visceral adiposity and left ventricular diastolic function: results from the Baltimore Longitudinal Study of Aging. *Nutrition, metabolism, and cardiovascular diseases : NMCD*. 2013;23:1263-70.

68. Mak GJ, Ledwidge MT, Watson CJ, Phelan DM, Dawkins IR, Murphy NF, Patle AK, Baugh JA and McDonald KM. Natural history of markers of collagen turnover in patients with early diastolic dysfunction and impact of eplerenone. *J Am Coll Cardiol*. 2009;54:1674-82.

69. Silberman GA, Fan TH, Liu H, Jiao Z, Xiao HD, Lovelock JD, Boulden BM, Widder J, Fredd S, Bernstein KE, Wolska BM, Dikalov S, Harrison DG and Dudley SC, Jr. Uncoupled cardiac nitric oxide synthase mediates diastolic dysfunction. *Circulation*. 2010;121:519-28.

70. Kankaanpaa M, Lehto HR, Parkka JP, Komu M, Viljanen A, Ferrannini E, Knuuti J, Nuutila P, Parkkola R and Iozzo P. Myocardial triglyceride content and epicardial fat mass in human obesity: relationship to left ventricular function and serum free fatty acid levels. *The Journal of clinical endocrinology and metabolism*. 2006;91:4689-95.

71. Iacobellis G, Lonn E, Lamy A, Singh N and Sharma AM. Epicardial fat thickness and coronary artery disease correlate independently of obesity. *Int J Cardiol*. 2011;146:452-4.

72. Mazurek T, Zhang L, Zalewski A, Mannion JD, Diehl JT, Arafat H, Sarov-Blat L, O'Brien S, Keiper EA, Johnson AG, Martin J, Goldstein BJ and Shi Y. Human epicardial adipose tissue is a source of inflammatory mediators. *Circulation*. 2003;108:2460-6.

73. Talman AH, Psaltis PJ, Cameron JD, Meredith IT, Seneviratne SK and Wong DT. Epicardial adipose tissue: far more than a fat depot. *Cardiovascular diagnosis and therapy*. 2014;4:416-29.

74. Xu Y, Cheng X, Hong K, Huang C and Wan L. How to interpret epicardial adipose tissue as a cause of coronary artery disease: a meta-analysis. *Coron Artery Dis*. 2012;23:227-33.

75. Larsen BA, Laughlin GA, Saad SD, Barrett-Connor E, Allison MA and Wassel CL. Pericardial fat is associated with all-cause mortality but not incident CVD: the Rancho Bernardo Study. *Atherosclerosis*. 2015;239:470-5.

76. Iacobellis G, Zaki MC, Garcia D and Willens HJ. Epicardial fat in atrial fibrillation and heart failure. *Horm Metab Res*. 2014;46:587-90.

77. Mazurek T, Kiliszek M, Kobylecka M, Skubisz-Gluchowska J, Kochman J, Filipiak K, Krolicki L and Opolski G. Relation of proinflammatory activity of epicardial adipose tissue to the occurrence of atrial fibrillation. *The American journal of cardiology*. 2014;113:1505-8.

78. Kremen J, Dolinkova M, Krajickova J, Blaha J, Anderlova K, Lacinova Z, Haluzikova D, Bosanska L, Vokurka M, Svacina S and Haluzik M. Increased subcutaneous and epicardial adipose tissue production of proinflammatory cytokines in cardiac surgery patients: possible role in postoperative insulin resistance. *The Journal of clinical endocrinology and metabolism*. 2006;91:4620-7.

79. Cheng KH, Chu CS, Lee KT, Lin TH, Hsieh CC, Chiu CC, Voon WC, Sheu SH and Lai WT. Adipocytokines and proinflammatory mediators from abdominal and epicardial adipose tissue in patients with coronary artery disease. *Int J Obes (Lond)*. 2008;32:268-74.

80. Iacobellis G and Willens HJ. Echocardiographic epicardial fat: a review of research and clinical applications. *J Am Soc Echocardiogr*. 2009;22:1311-9; quiz 1417-8.

81. Hirata Y, Yamada H, Kusunose K, Iwase T, Nishio S, Hayashi S, Bando M, Amano R, Yamaguchi K, Soeki T, Wakatsuki T and Sata M. Clinical Utility of Measuring Epicardial Adipose Tissue Thickness with Echocardiography Using a High-Frequency Linear Probe in Patients with Coronary Artery Disease. *J Am Soc Echocardiogr*. 2015;28:1240-1246 e1.

82. Fluchter S, Haghi D, Dinter D, Heberlein W, Kuhl HP, Neff W, Sueselbeck T, Borggrefe M and Papavassiliu T. Volumetric assessment of epicardial adipose tissue with cardiovascular magnetic resonance imaging. *Obesity (Silver Spring)*. 2007;15:870-8.

83. Rossner S, Bo WJ, Hiltbrandt E, Hinson W, Karstaedt N, Santago P, Sobol WT and Crouse JR. Adipose tissue determinations in cadavers--a comparison between cross-sectional planimetry and computed tomography. *Int J Obes*. 1990;14:893-902.

84. Kvist H, Sjostrom L and Tylen U. Adipose tissue volume determinations in women by computed tomography: technical considerations. *Int J Obes*. 1986;10:53-67.

85. Bucher AM, Joseph Schoepf U, Krazinski AW, Silverman J, Spearman JV, De Cecco CN, Meinel FG, Vogl TJ and Geyer LL. Influence of technical parameters on epicardial fat volume quantification at cardiac CT. *Eur J Radiol*. 2015;84:1062-7.

86. Bertaso AG, Bertol D, Duncan BB and Foppa M. Epicardial fat: definition, measurements and systematic review of main outcomes. *Arq Bras Cardiol*. 2013;101:e18-28.

87. Rabkin SW. The relationship between epicardial fat and indices of obesity and the metabolic syndrome: a systematic review and meta-analysis. *Metab Syndr Relat Disord*. 2014;12:31-42.

88. Ding J, Kritchevsky SB, Harris TB, Burke GL, Detrano RC, Szklo M and Jeffrey Carr J. The association of pericardial fat with calcified coronary plaque. *Obesity (Silver Spring)*. 2008;16:1914-9.

89. Rosito GA, Massaro JM, Hoffmann U, Ruberg FL, Mahabadi AA, Vasan RS, O'Donnell CJ and Fox CS. Pericardial fat, visceral abdominal fat, cardiovascular disease risk factors, and vascular calcification in a community-based sample: the Framingham Heart Study. *Circulation*. 2008;117:605-13.

90. Sarin S, Wenger C, Marwaha A, Qureshi A, Go BD, Woomert CA, Clark K, Nassef LA and Shirani J. Clinical significance of epicardial fat measured using cardiac multislice computed tomography. *The American journal of cardiology*. 2008;102:767-71.

91. Ding J, Hsu FC, Harris TB, Liu Y, Kritchevsky SB, Szklo M, Ouyang P, Espeland MA, Lohman KK, Criqui MH, Allison M, Bluemke DA and Carr JJ. The association of pericardial fat with incident coronary heart disease: the Multi-Ethnic Study of Atherosclerosis (MESA). *Am J Clin Nutr*. 2009;90:499-504.

92. Mahabadi AA, Massaro JM, Rosito GA, Levy D, Murabito JM, Wolf PA, O'Donnell CJ, Fox CS and Hoffmann U. Association of pericardial fat, intrathoracic fat, and visceral abdominal fat with cardiovascular disease burden: the Framingham Heart Study. *European heart journal*. 2009;30:850-6.

93. Alexopoulos N, McLean DS, Janik M, Arepalli CD, Stillman AE and Raggi P. Epicardial adipose tissue and coronary artery plaque characteristics. *Atherosclerosis*. 2010;210:150-4.

94. Cheng VY, Dey D, Tamarappoo B, Nakazato R, Gransar H, Miranda-Peats R, Ramesh A, Wong ND, Shaw LJ, Slomka PJ and Berman DS. Pericardial fat burden on ECG-gated noncontrast CT in asymptomatic patients who subsequently experience adverse cardiovascular events. *JACC Cardiovascular imaging*. 2010;3:352-60.

95. Konishi M, Sugiyama S, Sugamura K, Nozaki T, Ohba K, Matsubara J, Matsuzawa Y, Sumida H, Nagayoshi Y, Nakaura T, Awai K, Yamashita Y, Jinnouchi H, Matsui K, Kimura K, Umemura S and Ogawa H. Association of pericardial fat accumulation rather than abdominal obesity with coronary atherosclerotic plaque formation in patients with suspected coronary artery disease. *Atherosclerosis*. 2010;209:573-8.

96. Harada K, Amano T, Uetani T, Tokuda Y, Kitagawa K, Shimbo Y, Kunimura A, Kumagai S, Yoshida T, Kato B, Kato M, Marui N, Ishii H, Matsubara T and Murohara T. Cardiac 64-multislice computed tomography reveals increased epicardial fat volume in patients with acute coronary syndrome. *The American journal of cardiology*. 2011;108:1119-23.

97. Iwasaki K, Matsumoto T, Aono H, Furukawa H and Samukawa M. Relationship between epicardial fat measured by 64-multidetector computed tomography and coronary artery disease. *Clinical cardiology*. 2011;34:166-71.

98. Schlett CL, Ferencik M, Kriegel MF, Bamberg F, Ghoshhajra BB, Joshi SB, Nagurney JT, Fox CS, Truong QA and Hoffmann U. Association of pericardial fat and coronary high-risk lesions as determined by cardiac CT. *Atherosclerosis*. 2012;222:129-34.

99. Yerramasu A, Dey D, Venuraju S, Anand DV, Atwal S, Corder R, Berman DS and Lahiri A. Increased volume of epicardial fat is an independent risk factor for accelerated progression of sub-clinical coronary atherosclerosis. *Atherosclerosis*. 2012;220:223-30.

100. Mahabadi AA, Berg MH, Lehmann N, Kalsch H, Bauer M, Kara K, Dragano N, Moebus S, Jockel KH, Erbel R and Mohlenkamp S. Association of epicardial fat with cardiovascular risk factors and incident myocardial infarction in the general population: the Heinz Nixdorf Recall Study. *J Am Coll Cardiol*. 2013;61:1388-95.

101. Rajani R, Shmilovich H, Nakazato R, Nakanishi R, Otaki Y, Cheng VY, Hayes SW, Thomson LE, Friedman JD, Slomka PJ, Min JK, Berman DS and Dey D. Relationship of epicardial fat volume to coronary plaque, severe coronary stenosis, and high-risk coronary plaque features assessed by coronary CT angiography. *J Cardiovasc Comput Tomogr*. 2013;7:125-32.

102. Iwayama T, Nitobe J, Watanabe T, Ishino M, Tamura H, Nishiyama S, Takahashi H, Arimoto T, Shishido T, Miyashita T, Miyamoto T, Toyama S, Sadahiro M and Kubota I. The role of epicardial adipose tissue in coronary artery disease in non-obese patients. *Journal of cardiology*. 2014;63:344-9.

103. den Dekker MA, Takashima R, van den Heuvel ER, van den Dungen JJ, Tio RA, Oudkerk M and Vliegenthart R. Relationship between epicardial adipose tissue and subclinical coronary artery disease in patients with extra-cardiac arterial disease. *Obesity (Silver Spring)*. 2014;22:72-8.

104. Kim SH, Chung JH, Kwon BJ, Song SW and Choi WS. The associations of epicardial adipose tissue with coronary artery disease and coronary atherosclerosis. *International heart journal*. 2014;55:197-203.

105. D'Marco LG, Bellasi A, Kim S, Chen Z, Block GA and Raggi P. Epicardial adipose tissue predicts mortality in incident hemodialysis patients: a substudy of the Renagel in New Dialysis trial. *Nephrol Dial Transplant*. 2013;28:2586-95.

106. Forouzandeh F, Chang SM, Muhyieddeen K, Zaid RR, Trevino AR, Xu J, Nabi F and Mahmarian JJ. Does quantifying epicardial and intrathoracic fat with noncontrast computed tomography improve risk stratification beyond calcium scoring alone? *Circulation Cardiovascular imaging*. 2013;6:58-66.

107. Kunita E, Yamamoto H, Kitagawa T, Ohashi N, Oka T, Utsunomiya H, Urabe Y, Tsushima H, Awai K, Budoff MJ and Kihara Y. Prognostic value of coronary artery calcium and epicardial adipose tissue assessed by non-contrast cardiac computed tomography. *Atherosclerosis*. 2014;233:447-53.

108. Shmilovich H, Dey D, Cheng VY, Rajani R, Nakazato R, Otaki Y, Nakanishi R, Slomka PJ, Thomson LE, Hayes SW, Friedman JD, Gransar H, Wong ND, Shaw LJ, Budoff M, Rozanski A and Berman DS. Threshold for the upper normal limit of indexed epicardial fat volume: derivation in a healthy population and validation in an outcome-based study. *The American journal of cardiology*. 2011;108:1680-5.

109. Spearman JV, Renker M, Schoepf UJ, Krazinski AW, Herbert TL, De Cecco CN, Nietert PJ and Meinel FG. Prognostic value of epicardial fat volume measurements by computed tomography: a systematic review of the literature. *Eur Radiol*. 2015;25:3372-81.

110. Wang ZJ, Zhang LL, Elmariah S, Han HY and Zhou YJ. Prevalence and Prognosis of Nonobstructive Coronary Artery Disease in Patients Undergoing Coronary Angiography or Coronary Computed Tomography Angiography: A Meta-Analysis. *Mayo Clinic proceedings*. 2017;92:329-346.

111. Psaltis PJ, Talman AH, Munnur K, Cameron JD, Ko BS, Meredith IT, Seneviratne SK and Wong DT. Relationship between epicardial fat and quantitative coronary artery plaque progression: insights from computer tomography coronary angiography. *Int J Cardiovasc Imaging*. 2016;32:317-28.

112. Shimabukuro M, Hirata Y, Tabata M, Dagvasumberel M, Sato H, Kurobe H, Fukuda D, Soeki T, Kitagawa T, Takanashi S and Sata M. Epicardial adipose tissue volume and adipocytokine imbalance are strongly linked to human coronary atherosclerosis. *Arterioscler Thromb Vasc Biol*. 2013;33:1077-84.

113. Prati F. Eccentric atherosclerotic plaques with positive remodelling have a pericardial distribution: a permissive role of epicardial fat? A three-dimensional intravascular ultrasound study of left anterior descending artery lesions. *European heart journal*. 2003;24:329-336.

114. Marwan M, Taher MA, El Meniawy K, Awadallah H, Pflederer T, Schuhback A, Ropers D, Daniel WG and Achenbach S. In vivo CT detection of lipid-rich coronary artery atherosclerotic plaques using quantitative histogram analysis: a head to head comparison with IVUS. *Atherosclerosis*. 2011;215:110-5.

115. Gauss S, Achenbach S, Pflederer T, Schuhback A, Daniel WG and Marwan M. Assessment of coronary artery remodelling by dual-source CT: a head-to-head comparison with intravascular ultrasound. *Heart*. 2011;97:991-7.

116. Wan X, Wang W, Liu J and Tong T. Estimating the sample mean and standard deviation from the sample size, median, range and/or interquartile range. *BMC Med Res Methodol*. 2014;14:135.

117. DerSimonian R and Laird N. Meta-analysis in clinical trials. *Control Clin Trials*. 1986;7:177-88.

118. Higgins JP, Thompson SG, Deeks JJ and Altman DG. Measuring inconsistency in meta-analyses. *BMJ*. 2003;327:557-60.

119. IntHout J, Ioannidis JP and Borm GF. The Hartung-Knapp-Sidik-Jonkman method for random effects meta-analysis is straightforward and considerably outperforms the standard DerSimonian-Laird method. *BMC Med Res Methodol*. 2014;14:25.

120. Rover C, Knapp G and Friede T. Hartung-Knapp-Sidik-Jonkman approach and its modification for random-effects meta-analysis with few studies. *BMC Med Res Methodol*. 2015;15:99.

121. Harada K, Harada K, Uetani T, Kataoka T, Takeshita M, Kunimura A, Takayama Y, Shinoda N, Kato B, Kato M, Marui N, Ishii H, Matsubara T, Amano T and Murohara T. The different association of epicardial fat with coronary plaque in patients with acute coronary syndrome and patients with stable angina pectoris: analysis using integrated backscatter intravascular ultrasound. *Atherosclerosis*. 2014;236:301-6.

122. Lu MT, Park J, Ghemigian K, Mayrhofer T, Puchner SB, Liu T, Fleg JL, Udelson JE, Truong QA, Ferencik M and Hoffmann U. Epicardial and paracardial adipose tissue volume and attenuation - Association with high-risk coronary plaque on computed tomographic angiography in the ROMICAT II trial. *Atherosclerosis*. 2016;251:47-54.

123. Poster Session 5. *European Journal of Heart Failure Supplements*. 2011;10:S218-S263.

124. Oka T, Yamamoto H, Ohashi N, Kitagawa T, Kunita E, Utsunomiya H, Yamazato R, Urabe Y, Horiguchi J, Awai K and Kihara Y. Association between epicardial adipose tissue volume and characteristics of non-calcified plaques assessed by coronary computed tomographic angiography. *Int J Cardiol*. 2012;161:45-9.

125. Nakanishi K, Fukuda S, Tanaka A, Otsuka K, Taguchi H, Yoshikawa J and Shimada K. Epicardial Adipose Tissue Accumulation Is Associated With Renal Dysfunction and Coronary Plaque Morphology on Multidetector Computed Tomography. *Circulation journal : official journal of the Japanese Circulation Society*. 2016;80:196-201.

126. Tachibana M, Miyoshi T, Osawa K, Toh N, Oe H, Nakamura K, Naito T, Sato S, Kanazawa S and Ito H. Measurement of epicardial fat thickness by transthoracic echocardiography for predicting high-risk coronary artery plaques. *Heart Vessels*. 2016;31:1758-1766.

127. Park JS, Choi SY, Zheng M, Yang HM, Lim HS, Choi BJ, Yoon MH, Hwang GS, Tahk SJ and Shin JH. Epicardial adipose tissue thickness is a predictor for plaque vulnerability in patients with significant coronary artery disease. *Atherosclerosis*. 2013;226:134-9.

128. Yamashita K, Yamamoto MH, Ebara S, Okabe T, Saito S, Hoshimoto K, Yakushiji T, Isomura N, Araki H, Obara C and Ochiai M. Association between increased epicardial adipose tissue volume and coronary plaque composition. *Heart Vessels*. 2014;29:569-77.

129. Nov O, Shapiro H, Ovadia H, Tarnovscki T, Dvir I, Shemesh E, Kovsan J, Shelef I, Carmi Y, Voronov E, Apte RN, Lewis E, Haim Y, Konrad D, Bashan N and Rudich A. Interleukin-1beta regulates fat-liver crosstalk in obesity by auto-paracrine modulation of adipose tissue inflammation and expandability. *PLoS One*. 2013;8:e53626.

130. Bo X, Ma L, Fan J, Jiang Z, Zhou Y, Zhang L and Li W. Epicardial fat volume is correlated with coronary lesion and its severity. *Int J Clin Exp Med*. 2015;8:4328-34.

131. Saura DO, MJ; Rodriguez, D; Pascual-Figal, DA; Hurtado, JA; Pinar, E; de la Morena, G; Valdes, M. Reproducibility of echocardiographic measurements of epicardial fat thickness. *Int J Cardiol*. 2010;141:311-312.

132. Tanami Y, Jinzaki M, Kishi S, Matheson M, Vavere AL, Rochitte CE, Dewey M, Chen MY, Clouse ME, Cox C, Kuribayashi S, Lima JA and Arbab-Zadeh A. Lack of association between epicardial fat volume and extent of coronary artery calcification, severity of coronary artery disease, or presence of myocardial perfusion abnormalities in a diverse, symptomatic patient population: results from the CORE320 multicenter study. *Circulation Cardiovascular imaging*. 2015;8:e002676.

133. Muthalaly RG, Nerlekar N, Wong DT, Cameron JD, Seneviratne SK and Ko BS. Epicardial adipose tissue and myocardial ischemia assessed by computed tomography perfusion imaging and invasive fractional flow reserve. *J Cardiovasc Comput Tomogr*. 2017;11:46-53.

134. Guyatt GH, Oxman AD, Kunz R, Brozek J, Alonso-Coello P, Rind D, Devereaux PJ, Montori VM, Freyschuss B, Vist G, Jaeschke R, Williams JW, Jr., Murad MH, Sinclair D, Falck-Ytter Y, Meerpohl J, Whittington C, Thorlund K, Andrews J and Schunemann HJ. GRADE guidelines 6. Rating the quality of evidence--imprecision. *Journal of clinical epidemiology*. 2011;64:1283-93.

135. Guyatt GH, Oxman AD, Kunz R, Woodcock J, Brozek J, Helfand M, Alonso-Coello P, Glasziou P, Jaeschke R, Akl EA, Norris S, Vist G, Dahm P, Shukla VK, Higgins J, Falck-Ytter Y and Schunemann HJ. GRADE guidelines: 7. Rating the quality of evidence--inconsistency. *Journal of clinical epidemiology*. 2011;64:1294-302.

136. Guyatt GH, Oxman AD, Vist G, Kunz R, Brozek J, Alonso-Coello P, Montori V, Akl EA, Djulbegovic B, Falck-Ytter Y, Norris SL, Williams JW, Jr., Atkins D, Meerpohl J and Schunemann HJ. GRADE guidelines: 4. Rating the quality of evidence--study limitations (risk of bias). *Journal of clinical epidemiology*. 2011;64:407-15.

137. Rabkin SW and Campbell H. Comparison of reducing epicardial fat by exercise, diet or bariatric surgery weight loss strategies: a systematic review and meta-analysis. *Obes Rev*. 2015;16:406-15.

138. McKenney ML, Schultz KA, Boyd JH, Byrd JP, Alloosh M, Teague SD, Arce-Esquivel AA, Fain JN, Laughlin MH, Sacks HS and Sturek M. Epicardial adipose excision slows the progression of porcine coronary atherosclerosis. *J Cardiothorac Surg*. 2014;9:2.

139. Nerlekar N, Brown AJ, Muthalaly RG, Talman A, Hettige T, Cameron JD and Wong DTL. Association of Epicardial Adipose Tissue and High-Risk Plaque Characteristics: A Systematic Review and Meta-Analysis. *J Am Heart Assoc*. 2017;6.

140. Ruberg FL, Chen Z, Hua N, Bigornia S, Guo Z, Hallock K, Jara H, LaValley M, Phinikaridou A, Qiao Y, Viereck J, Apovian CM and Hamilton JA. The relationship of ectopic lipid accumulation to cardiac and vascular function in obesity and metabolic syndrome. *Obesity (Silver Spring)*. 2010;18:1116-21.

141. Nerlekar N, Baey YW, Brown AJ, Muthalaly RG, Dey D, Tamarappoo B, Cameron JD, Marwick TH and Wong DT. Poor Correlation, Reproducibility, and Agreement Between Volumetric Versus Linear Epicardial Adipose Tissue Measurement: A 3D Computed Tomography Versus 2D Echocardiography Comparison. *JACC Cardiovascular imaging*. 2018;11:1035-1036.

142. Doesch C, Suselbeck T, Leweling H, Fluechter S, Haghi D, Schoenberg SO, Borggrefe M and Papavassiliu T. Bioimpedance analysis parameters and epicardial adipose tissue assessed by cardiac magnetic resonance imaging in patients with heart failure. *Obesity (Silver Spring)*. 2010;18:2326-32.

143. Harbord RM and Higgins JPT. Meta-regression in Stata. *Stata Journal*. 2008;8:493-519.

144. Al Chekakie MO, Welles CC, Metoyer R, Ibrahim A, Shapira AR, Cytron J, Santucci P, Wilber DJ and Akar JG. Pericardial fat is independently associated with human atrial fibrillation. *J Am Coll Cardiol*. 2010;56:784-8.

145. Bakkum MJ, Danad I, Romijn MA, Stuijfzand WJ, Leonora RM, Tulevski, II, Somsen GA, Lammertsma AA, van Kuijk C, van Rossum AC, Raijmakers PG and Knaapen P. The impact of obesity on the relationship between epicardial adipose tissue, left ventricular mass and coronary microvascular function. *Eur J Nucl Med Mol Imaging*. 2015;42:1562-73.

146. Cavalcante JL, Tamarappoo BK, Hachamovitch R, Kwon DH, Alraies MC, Halliburton S, Schoenhagen P, Dey D, Berman DS and Marwick TH. Association of epicardial fat, hypertension,

subclinical coronary artery disease, and metabolic syndrome with left ventricular diastolic dysfunction. *The American journal of cardiology*. 2012;110:1793-8.

147. Doesch C, Haghi D, Fluchter S, Suselbeck T, Schoenberg SO, Michaely H, Borggrefe M and Papavassiliu T. Epicardial adipose tissue in patients with heart failure. *J Cardiovasc Magn Reson*. 2010;12:40.

148. Doesch C, Haghi D, Suselbeck T, Schoenberg SO, Borggrefe M and Papavassiliu T. Impact of Functional, Morphological and Clinical Parameters on Epicardial Adipose Tissue in Patients With Coronary Artery Disease. *Circulation Journal*. 2012;76:2426-2434.

149. Doesch C, Streitner F, Bellm S, Suselbeck T, Haghi D, Heggemann F, Schoenberg SO, Michaely H, Borggrefe M and Papavassiliu T. Epicardial adipose tissue assessed by cardiac magnetic resonance imaging in patients with heart failure due to dilated cardiomyopathy. *Obesity (Silver Spring)*. 2013;21:E253-61.

150. Ede H, Erkoc MF, Okur A and Erbay AR. Impaired aortic elasticity and diastolic functions are associated with findings of coronary computed tomographic angiography. *Med Sci Monit*. 2014;20:2061-8.

151. Faustino AP, R; Paiva, L; Mota, P; Costa, M; Leito-Marques, A. Pericardial fat, a new marker of impaired left ventricle diastolic dysfunction. *European Journal of Heart Failure Supplements* 2011;10:S248.

152. Fernando RS, B; Syed, MA; Wilber, D; Singh, S; Teme, T; Rabbat, M. Epicardial adipose tissue volume by cardiac magnetic resonance imaging predicts abnormal myocardial relaxation in patients with atrial fibrillation. *Journal of Cardiovascular Magnetic Resonance*. 2015;17:P352.

153. Fontes-Carvalho R, Fontes-Oliveira M, Sampaio F, Mancio J, Bettencourt N, Teixeira M, Rocha Goncalves F, Gama V and Leite-Moreira A. Influence of epicardial and visceral fat on left ventricular diastolic and systolic functions in patients after myocardial infarction. *The American journal of cardiology*. 2014;114:1663-9.

154. Fox CS, Gona P, Hoffmann U, Porter SA, Salton CJ, Massaro JM, Levy D, Larson MG, D'Agostino RB, Sr., O'Donnell CJ and Manning WJ. Pericardial fat, intrathoracic fat, and measures of left ventricular structure and function: the Framingham Heart Study. *Circulation*. 2009;119:1586-91.

155. Hachiya K, Fukuta H, Wakami K, Goto T, Tani T and Ohte N. Relation of epicardial fat to central aortic pressure and left ventricular diastolic function in patients with known or suspected coronary artery disease. *Int J Cardiovasc Imaging*. 2014;30:1393-8.

156. Khawaja T, Greer C, Chokshi A, Chavarria N, Thadani S, Jones M, Schaefle K, Bhatia K, Collado JE, Shimbo D, Einstein AJ and Schulze PC. Epicardial fat volume in patients with left ventricular systolic dysfunction. *The American journal of cardiology*. 2011;108:397-401.

157. Konishi M, Sugiyama S, Sugamura K, Nozaki T, Matsubara J, Akiyama E, Utsunomiya D, Matsuzawa Y, Yamashita Y, Kimura K, Umemura S and Ogawa H. Accumulation of pericardial fat correlates with left ventricular diastolic dysfunction in patients with normal ejection fraction. *Journal of cardiology*. 2012;59:344-51.

158. Lai YH, Hou CJ, Yun CH, Sung KT, Su CH, Wu TH, Yang FS, Hung TC, Hung CL, Bezerra HG and Yeh HI. The association among MDCT-derived three-dimensional visceral adiposities on cardiac diastology and dyssynchrony in asymptomatic population. *BMC Cardiovasc Disord*. 2015;15:142.

159. Liu J, Fox CS, Hickson DA, May WL, Ding J, Carr JJ and Taylor HA. Pericardial fat and echocardiographic measures of cardiac abnormalities: the Jackson Heart Study. *Diabetes care*. 2011;34:341-6.

160. Longenecker CAK, S; Serhal, M; Kinley, B; Labbato, D; McComsey, GA. Diastolic Function Correlates With Pericardial Fat [fat around the heart] and Vascular Remodeling in HIV. *Conference on Retroviruses and Opportunistic Infections (CROI)*. 2016.

161. Ng AC, Goo SY, Roche N, van der Geest RJ and Wang WY. Epicardial Adipose Tissue Volume and Left Ventricular Myocardial Function Using 3-Dimensional Speckle Tracking Echocardiography. *Can J Cardiol*. 2016;32:1485-1492.

162. Vanni EM, A; Faletti, R; Morello, M; Mezzabotta, L; Battisti, G; Frea, S; Cannillo, M; Mosso, E; Rosso, C; Bergamasco, L; Rizzetto, M; Bugianesi, E. Incerased Epicardial Fat and Early Signs of Impaired Diastolic and Systolic Left Ventricular Function in Non-diabetic, normotensive patients with nonalcoholic fatty liver disease. *Journal of Hepatology*. 2015;62:S745.

163. Vural M, Talu A, Sahin D, Elalmis OU, Durmaz HA, Uyanik S and Dolek BA. Evaluation of the relationship between epicardial fat volume and left ventricular diastolic dysfunction. *Jpn J Radiol*. 2014;32:331-9.

164. Wu CK, Tsai HY, Su MY, Wu YF, Hwang JJ, Tseng WY, Lin JL and Lin LY. Pericardial fat is associated with ventricular tachyarrhythmia and mortality in patients with systolic heart failure. *Atherosclerosis*. 2015;241:607-14.

165. Yamashita KO, M; Ebara, S; Yamamoto, MH; Obara, C. Increased epicardial adipose tissue are associated with left ventricular diastolic dysfunction. *Journal of the American College of Cardiology*. 2012;59:E1349.

166. Nagueh SF, Appleton CP, Gillebert TC, Marino PN, Oh JK, Smiseth OA, Waggoner AD, Flachskampf FA, Pellikka PA and Evangelista A. Recommendations for the evaluation of left ventricular diastolic function by echocardiography. *J Am Soc Echocardiogr*. 2009;22:107-33.

167. Alnabhan N, Kerut EK, Geraci SA, McMullan MR and Fox E. An approach to analysis of left ventricular diastolic function and loading conditions in the echocardiography laboratory. *Echocardiography (Mount Kisco, NY)*. 2008;25:105-16.

168. Gottdiener JS, Bednarz J, Devereux R, Gardin J, Klein A, Manning WJ, Morehead A, Kitzman D, Oh J, Quinones M, Schiller NB, Stein JH and Weissman NJ. American Society of Echocardiography recommendations for use of echocardiography in clinical trials. *J Am Soc Echocardiogr*. 2004;17:1086-119.

169. Lang RM, Bierig M, Devereux RB, Flachskampf FA, Foster E, Pellikka PA, Picard MH, Roman MJ, Seward J, Shanewise JS, Solomon SD, Spencer KT, Sutton MS and Stewart WJ. Recommendations for chamber quantification: a report from the American Society of Echocardiography's Guidelines and Standards Committee and the Chamber Quantification Writing Group, developed in conjunction with the European Association of Echocardiography, a branch of the European Society of Cardiology. *J Am Soc Echocardiogr*. 2005;18:1440-63.

170. Greenstein AS, Khavandi K, Withers SB, Sonoyama K, Clancy O, Jeziorska M, Laing I, Yates AP, Pemberton PW, Malik RA and Heagerty AM. Local inflammation and hypoxia abolish the protective anticontractile properties of perivascular fat in obese patients. *Circulation*. 2009;119:1661-70.

171. Buckberg GD, Fixler DE, Archie JP and Hoffman JI. Experimental subendocardial ischemia in dogs with normal coronary arteries. *Circulation research*. 1972;30:67-81.

172. Wong C and Marwick TH. Obesity cardiomyopathy: pathogenesis and pathophysiology. *Nat Clin Pract Cardiovasc Med*. 2007;4:436-43.

173. Nagueh SF, Smiseth OA, Appleton CP, Byrd BF, 3rd, Dokainish H, Edvardsen T, Flachskampf FA, Gillebert TC, Klein AL, Lancellotti P, Marino P, Oh JK, Popescu BA and Waggoner AD. Recommendations for the Evaluation of Left Ventricular Diastolic Function by Echocardiography: An Update from the American Society of Echocardiography and the European Association of Cardiovascular Imaging. *J Am Soc Echocardiogr*. 2016;29:277-314.

174. Iwayama T, Nitobe J, Watanabe T, Ishino M, Tamura H, Nishiyama S, Takahashi H, Arimoto T, Shishido T, Miyashita T, Miyamoto T, Toyama S, Sadahiro M and Kubota I. Role of epicardial adipose tissue in coronary artery disease in non-obese patients. *J Cardiol*. 2014;63:344-9.

175. Lavie CJ, De Schutter A, Parto P, Jahangir E, Kokkinos P, Ortega FB, Arena R and Milani RV. Obesity and Prevalence of Cardiovascular Diseases and Prognosis-The Obesity Paradox Updated. *Prog Cardiovasc Dis*. 2016;58:537-47.

176. Brown AJ, Obaid DR, Costopoulos C, Parker RA, Calvert PA, Teng Z, Hoole SP, West NEJ, Goddard M and Bennett MR. Direct Comparison of Virtual-Histology Intravascular Ultrasound and

Optical Coherence Tomography Imaging for Identification of Thin-Cap Fibroatheroma. *Circulation: Cardiovascular Imaging*. 2015;8:e003487.

177. Stone GW, Maehara A, Lansky AJ, de Bruyne B, Cristea E, Mintz GS, Mehran R, McPherson J, Farhat N, Marso SP, Parise H, Templin B, White R, Zhang Z and Serruys PW. A prospective natural-history study of coronary atherosclerosis. *New England Journal of Medicine*. 2011;364:226-35.

178. Brown AJ, Teng Z, Calvert PA, Rajani NK, Hennessy O, Nerlekar N, Obaid DR, Costopoulos C, Huang Y, Hoole SP, Goddard M, West NE, Gillard JH and Bennett MR. Plaque Structural Stress Estimations Improve Prediction of Future Major Adverse Cardiovascular Events After Intracoronary Imaging. *Circulation Cardiovascular imaging*. 2016;9:e004172.

179. Cheng JM, Garcia-Garcia HM, de Boer SPM, Kardys I, Heo JH, Akkerhuis KM, Oemrawsingh RM, van Domburg RT, Ligthart J, Witberg KT, Regar E, Serruys PW, van Geuns R-J and Boersma E. In vivo detection of high-risk coronary plaques by radiofrequency intravascular ultrasound and cardiovascular outcome: results of the ATHEROREMO-IVUS study. *European heart journal*. 2014;35:639-647.

180. Maurovich-Horvat P, Ferencik M, Voros S, Merkely B and Hoffmann U. Comprehensive plaque assessment by coronary CT angiography. *Nat Rev Cardiol*. 2014;11:390-402.

181. Cury RC, Abbara S, Achenbach S, Agatston A, Berman DS, Budoff MJ, Dill KE, Jacobs JE, Maroules CD, Rubin GD, Rybicki FJ, Schoepf UJ, Shaw LJ, Stillman AE, White CS, Woodard PK and Leipsic JA. Coronary Artery Disease - Reporting and Data System (CAD-RADS): An Expert Consensus Document of SCCT, ACR and NASCI: Endorsed by the ACC. *JACC Cardiovascular imaging*. 2016;9:1099-1113.

182. Liberati A, Altman DG, Tetzlaff J, Mulrow C, Gotzsche PC, Ioannidis JP, Clarke M, Devereaux PJ, Kleijnen J and Moher D. The PRISMA statement for reporting systematic reviews and meta-analyses of studies that evaluate health care interventions: explanation and elaboration. *Annals of internal medicine*. 2009;151:W65-94.

183. Yamamoto H, Kitagawa T, Ohashi N, Utsunomiya H, Kunita E, Oka T, Urabe Y, Tsushima H, Awai K and Kihara Y. Noncalcified atherosclerotic lesions with vulnerable characteristics detected by coronary CT angiography and future coronary events. *J Cardiovasc Comput Tomogr*. 2013;7:192-9.

184. Agatston AS, Janowitz WR, Hildner FJ, Zusmer NR, Viamonte M, Jr. and Detrano R. Quantification of coronary artery calcium using ultrafast computed tomography. *J Am Coll Cardiol*. 1990;15:827-32.

185. Stang A. Critical evaluation of the Newcastle-Ottawa scale for the assessment of the quality of nonrandomized studies in meta-analyses. *European Journal of Epidemiology*. 2010;25:603-605.

186. Chow BJ, Wells GA, Chen L, Yam Y, Galiwango P, Abraham A, Sheth T, Dennie C, Beanlands RS and Ruddy TD. Prognostic value of 64-slice cardiac computed tomography severity of coronary artery disease, coronary atherosclerosis, and left ventricular ejection fraction. *J Am Coll Cardiol*. 2010;55:1017-28.

187. Andreini D, Pontone G, Mushtaq S, Bartorelli AL, Bertella E, Antonioli L, Formenti A, Cortinovis S, Veglia F, Annoni A, Agostoni P, Montorsi P, Ballerini G, Fiorentini C and Pepi M. A long-term prognostic value of coronary CT angiography in suspected coronary artery disease. *JACC Cardiovascular imaging*. 2012;5:690-701.

188. Hou ZH, Lu B, Gao Y, Jiang SL, Wang Y, Li W and Budoff MJ. Prognostic value of coronary CT angiography and calcium score for major adverse cardiac events in outpatients. *JACC Cardiovascular imaging*. 2012;5:990-9.

189. Miszalski-Jamka T, Klimeczek P, Banys R, Krupinski M, Nycz K, Bury K, Lada M, Pelberg R, Kereiakes D and Mazur W. The composition and extent of coronary artery plaque detected by multislice computed tomographic angiography provides incremental prognostic value in patients with suspected coronary artery disease. *Int J Cardiovasc Imaging*. 2012;28:621-31.

190. Matsumoto N, Sato Y, Yoda S, Nakano Y, Kunimasa T, Matsuo S, Komatsu S, Saito S and Hirayama A. Prognostic value of non-obstructive CT low-dense coronary artery plaques detected by multislice computed tomography. *Circulation journal : official journal of the Japanese Circulation Society*. 2007;71:1898-903.

191. Otsuka K, Fukuda S, Tanaka A, Nakanishi K, Taguchi H, Yoshikawa J, Shimada K and Yoshiyama M. Napkin-ring sign on coronary CT angiography for the prediction of acute coronary syndrome. *JACC Cardiovascular imaging*. 2013;6:448-57.

192. Conte E, Annoni A, Pontone G, Mushtaq S, Guglielmo M, Baggiano A, Volpato V, Agalbato C, Bonomi A, Veglia F, Formenti A, Fiorentini C, Bartorelli AL, Pepi M and Andreini D. Evaluation of coronary plaque characteristics with coronary computed tomography angiography in patients with non-obstructive coronary artery disease: a long-term follow-up study. *Eur Heart J Cardiovasc Imaging*. 2017;18:1170-1178.

193. Feuchtner G, Kerber J, Burghard P, Dichtl W, Friedrich G, Bonaros N and Plank F. The high-risk criteria low-attenuation plaque <60 HU and the napkin-ring sign are the most powerful predictors of MACE: a long-term follow-up study. *Eur Heart J Cardiovasc Imaging*. 2017;18:772-779.

194. van Werkhoven JM, Schuijf JD, Gaemperli O, Jukema JW, Kroft LJ, Boersma E, Pazhenkottil A, Valenta I, Pundziute G, de Roos A, van der Wall EE, Kaufmann PA and Bax JJ. Incremental prognostic value of multi-slice computed tomography coronary angiography over coronary artery

calcium scoring in patients with suspected coronary artery disease. *European heart journal*. 2009;30:2622-9.

195. Petretta M, Daniele S, Acampa W, Imbriaco M, Pellegrino T, Messalli G, Xhoxhi E, Del Prete G, Nappi C, Accardo D, Angeloni F, Bonaduce D and Cuocolo A. Prognostic value of coronary artery calcium score and coronary CT angiography in patients with intermediate risk of coronary artery disease. *Int J Cardiovasc Imaging*. 2012;28:1547-56.

196. Otsuka K, Fukuda S, Tanaka A, Nakanishi K, Taguchi H, Yoshiyama M, Shimada K and Yoshikawa J. Prognosis of vulnerable plaque on computed tomographic coronary angiography with normal myocardial perfusion image. *Eur Heart J Cardiovasc Imaging*. 2014;15:332-40.

197. Virmani R, Kolodgie FD, Burke AP, Farb A and Schwartz SM. Lessons from sudden coronary death: a comprehensive morphological classification scheme for atherosclerotic lesions. *Arteriosclerosis, Thrombosis and Vascular Biology*. 2000;20:1262-75.

198. Voros S, Rinehart S, Qian Z, Vazquez G, Anderson H, Murrieta L, Wilmer C, Carlson H, Taylor K, Ballard W, Karmpaliotis D, Kalynych A and Brown C, 3rd. Prospective validation of standardized, 3-dimensional, quantitative coronary computed tomographic plaque measurements using radiofrequency backscatter intravascular ultrasound as reference standard in intermediate coronary arterial lesions: results from the ATLANTA (assessment of tissue characteristics, lesion morphology, and hemodynamics by angiography with fractional flow reserve, intravascular ultrasound and virtual histology, and noninvasive computed tomography in atherosclerotic plaques) I study. *JACC Cardiovasc Interv*. 2011;4:198-208.

199. Detrano R, Guerci AD, Carr JJ, Bild DE, Burke G, Folsom AR, Liu K, Shea S, Szklo M, Bluemke DA, O'Leary DH, Tracy R, Watson K, Wong ND and Kronmal RA. Coronary calcium as a predictor of coronary events in four racial or ethnic groups. *The New England journal of medicine*. 2008;358:1336-45.

200. Kelly-Arnold A, Maldonado N, Laudier D, Aikawa E, Cardoso L and Weinbaum S. Revised microcalcification hypothesis for fibrous cap rupture in human coronary arteries. *Proceedings of the National Academy of Sciences*. 2013;110:10741-10746.

201. Teng Z, Brown AJ, Calvert PA, Parker RA, Obaid DR, Huang Y, Hoole SP, West NE, Gillard JH and Bennett MR. Coronary plaque structural stress is associated with plaque composition and subtype and higher in acute coronary syndrome: the BEACON I (Biomechanical Evaluation of Atheromatous Coronary Arteries) study. *Circulation Cardiovascular Imaging*. 2014;7:461-70.

202. Brown AJ, Teng Z, Evans PC, Gillard JH, Samady H and Bennett MR. Role of biomechanical forces in the natural history of coronary atherosclerosis. *Nature reviews Cardiology*. 2016.

203. Puri R, Nicholls SJ, Shao M, Kataoka Y, Uno K, Kapadia SR, Tuzcu EM and Nissen SE. Impact of Statins on Serial Coronary Calcification During Atheroma Progression and Regression. *Journal of the American College of Cardiology*. 2015;65:1273-1282.

204. Arbab-Zadeh A and Fuster V. The myth of the "vulnerable plaque": transitioning from a focus on individual lesions to atherosclerotic disease burden for coronary artery disease risk assessment. *J Am Coll Cardiol*. 2015;65:846-55.

205. Nerlekar N, Muthalaly RG, Wong N, Thakur U, Wong DTL, Brown AJ and Marwick TH. Association of Volumetric Epicardial Adipose Tissue Quantification and Cardiac Structure and Function. *Journal of the American Heart Association*. 2018;7:e009975.

206. Nerlekar N, Ko BS, Nasis A, Cameron JD, Leung M, Brown AJ, Wong DTL, Ngu PJ, Troupis JM and Seneviratne SK. Impact of heart rate on diagnostic accuracy of second generation 320-detector computed tomography coronary angiography. *Cardiovascular diagnosis and therapy*. 2017;7:296-304.

207. Dey D, Suzuki Y, Suzuki S, Ohba M, Slomka PJ, Polk D, Shaw LJ and Berman DS. Automated quantitation of pericardiac fat from noncontrast CT. *Invest Radiol*. 2008;43:145-53.

208. Iacobellis G, Assael F, Ribaudo MC, Zappaterreno A, Alessi G, Di Mario U and Leonetti F. Epicardial fat from echocardiography: a new method for visceral adipose tissue prediction. *Obes Res*. 2003;11:304-10.

209. Marwan M and Achenbach S. Quantification of epicardial fat by computed tomography: why, when and how? *J Cardiovasc Comput Tomogr*. 2013;7:3-10.

210. Ormseth MJ, Lipson A, Alexopoulos N, Hartlage GR, Oeser AM, Bian A, Gebretsadik T, Shintani A, Raggi P and Stein CM. Association of epicardial adipose tissue with cardiometabolic risk and metabolic syndrome in patients with rheumatoid arthritis. *Arthritis Care Res (Hoboken)*. 2013;65:1410-5.

211. Nerlekar N, Baey YW, Brown AJ, Muthalaly RG, Dey D, Tamarappoo B, Cameron JD, Marwick TH and Wong DT. Poor Correlation, Reproducibility, and Agreement Between Volumetric vs. Linear Epicardial Adipose Tissue Measurement: A 3D Computed Tomography vs. 2D Echocardiography Comparison. *JACC Cardiovascular imaging*. 2018.

212. Xu L, Xu Y, Coulden R, Sonnex E, Hrybouski S, Paterson I and Butler C. Comparison of epicardial adipose tissue radiodensity threshold between contrast and non-contrast enhanced computed tomography scans: A cohort study of derivation and validation. *Atherosclerosis*. 2018;275:74-79.

213. Nelson AJ, Worthley MI, Psaltis PJ, Carbone A, Dundon BK, Duncan RF, Piantadosi C, Lau DH, Sanders P, Wittert GA and Worthley SG. Validation of cardiovascular magnetic resonance assessment of pericardial adipose tissue volume. *J Cardiovasc Magn Reson*. 2009;11:15.

214. Aldiss P, Davies G, Woods R, Budge H, Sacks HS and Symonds ME. 'Browning' the cardiac and peri-vascular adipose tissues to modulate cardiovascular risk. *Int J Cardiol*. 2017;228:265-274.

215. Marchington JM, Mattacks CA and Pond CM. Adipose tissue in the mammalian heart and pericardium: structure, foetal development and biochemical properties. *Comp Biochem Physiol B*. 1989;94:225-32.

216. Goeller M, Achenbach S, Cadet S, Kwan AC, Commandeur F, Slomka PJ, Gransar H, Albrecht MH, Tamarappoo BK, Berman DS, Marwan M and Dey D. Pericoronary Adipose Tissue Computed Tomography Attenuation and High-Risk Plaque Characteristics in Acute Coronary Syndrome Compared With Stable Coronary Artery Disease. *JAMA Cardiol*. 2018.

217. Goeller M, Achenbach S, Marwan M, Doris MK, Cadet S, Commandeur F, Chen X, Slomka PJ, Gransar H, Cao JJ, Wong ND, Albrecht MH, Rozanski A, Tamarappoo BK, Berman DS and Dey D. Epicardial adipose tissue density and volume are related to subclinical atherosclerosis, inflammation and major adverse cardiac events in asymptomatic subjects. *Journal of Cardiovascular Computed Tomography*. 2018;12:67-73.

218. Pracon R, Kruk M, Kepka C, Pregowski J, Opolski MP, Dzielinska Z, Michalowska I, Chmielak Z, Demkow M and Ruzyllo W. Epicardial Adipose Tissue Radiodensity Is Independently Related to Coronary Atherosclerosis. *Circulation Journal*. 2011;75:391-397.

219. Alvey NJ, Pedley A, Rosenquist KJ, Massaro JM, O'Donnell CJ, Hoffmann U and Fox CS. Association of fat density with subclinical atherosclerosis. *J Am Heart Assoc*. 2014;3.

220. Mahabadi AA, Balcer B, Dykun I, Forsting M, Schlosser T, Heusch G and Rassaf T. Cardiac computed tomography-derived epicardial fat volume and attenuation independently distinguish patients with and without myocardial infarction. *PLoS One*. 2017;12:e0183514.

221. Baba S, Jacene HA, Engles JM, Honda H and Wahl RL. CT Hounsfield units of brown adipose tissue increase with activation: preclinical and clinical studies. *J Nucl Med*. 2010;51:246-50.

222. Bassols J, Ortega FJ, Moreno-Navarrete JM, Peral B, Ricart W and Fernandez-Real JM. Study of the proinflammatory role of human differentiated omental adipocytes. *J Cell Biochem*. 2009;107:1107-17.

223. Omar A, Chatterjee TK, Tang Y, Hui DY and Weintraub NL. Proinflammatory phenotype of perivascular adipocytes. *Arterioscler Thromb Vasc Biol*. 2014;34:1631-6.

224. Rosenquist KJ, Pedley A, Massaro JM, Therkelsen KE, Murabito JM, Hoffmann U and Fox CS. Visceral and subcutaneous fat quality and cardiometabolic risk. *JACC Cardiovascular imaging*. 2013;6:762-71.

225. Cherian S, Lopaschuk GD and Carvalho E. Cellular cross-talk between epicardial adipose tissue and myocardium in relation to the pathogenesis of cardiovascular disease. *Am J Physiol Endocrinol Metab*. 2012;303:E937-49.

226. Nerlekar N, Ha FJ, Cheshire C, Rashid H, Cameron JD, Wong DT, Seneviratne S and Brown AJ. Computed Tomographic Coronary Angiography-Derived Plaque Characteristics Predict Major Adverse Cardiovascular Events: A Systematic Review and Meta-Analysis. *Circulation Cardiovascular imaging*. 2018;11:e006973.

227. La Grutta L, Toia P, Farruggia A, Albano D, Grassedonio E, Palmeri A, Maffei E, Galia M, Vitabile S, Cademartiri F and Midiri M. Quantification of epicardial adipose tissue in coronary calcium score and CT coronary angiography image data sets: comparison of attenuation values, thickness and volumes. *Br J Radiol*. 2016;89:20150773.

228. Commandeur F, Goeller M, Betancur J, Cadet S, Doris M, Chen X, Berman DS, Slomka PJ, Tamarappoo BK and Dey D. Deep Learning for Quantification of Epicardial and Thoracic Adipose Tissue From Non-Contrast CT. *IEEE Trans Med Imaging*. 2018;37:1835-1846.

229. Miyazawa I, Ohkubo T, Kadowaki S, Fujiyoshi A, Hisamatsu T, Kadota A, Arima H, Budoff M, Murata K, Miura K, Maegawa H, Ueshima H and Group SR. Change in Pericardial Fat Volume and Cardiovascular Risk Factors in a General Population of Japanese Men. *Circulation journal : official journal of the Japanese Circulation Society*. 2018;82:2542-2548.

230. Nakazato R, Rajani R, Cheng VY, Shmilovich H, Nakanishi R, Otaki Y, Gransar H, Slomka PJ, Hayes SW, Thomson LE, Friedman JD, Wong ND, Shaw LJ, Budoff M, Rozanski A, Berman DS and Dey D. Weight change modulates epicardial fat burden: a 4-year serial study with non-contrast computed tomography. *Atherosclerosis*. 2012;220:139-44.

231. Franssens BT, Nathoe HM, Visseren FL, van der Graaf Y, Leiner T and Group SS. Relation of Epicardial Adipose Tissue Radiodensity to Coronary Artery Calcium on Cardiac Computed Tomography in Patients at High Risk for Cardiovascular Disease. *The American journal of cardiology*. 2017;119:1359-1365.

232. Ahmadi N, Nabavi V, Yang E, Hajsadeghi F, Lakis M, Flores F, Zeb I, Bevinal M, Ebrahimi R and Budoff M. Increased epicardial, pericardial, and subcutaneous adipose tissue is associated with the presence and severity of coronary artery calcium. *Acad Radiol*. 2010;17:1518-24.

233. Dey D, Nakazato R, Li D and Berman DS. Epicardial and thoracic fat - Noninvasive measurement and clinical implications. *Cardiovascular diagnosis and therapy*. 2012;2:85-93.

234. Gaborit B, Jacquier A, Kober F, Abdesselam I, Cuisset T, Boullu-Ciocca S, Emungania O, Alessi MC, Clement K, Bernard M and Dutour A. Effects of bariatric surgery on cardiac ectopic fat:

lesser decrease in epicardial fat compared to visceral fat loss and no change in myocardial triglyceride content. *J Am Coll Cardiol*. 2012;60:1381-9.

235. Lefer David J. Statins as Potent Antiinflammatory Drugs. *Circulation*. 2002;106:2041-2042.

236. Aguirre L, Hijona E, Macarulla MT, Gracia A, Larrechi I, Bujanda L, Hijona L and Portillo MP. Several statins increase body and liver fat accumulation in a model of metabolic syndrome. *Journal of physiology and pharmacology : an official journal of the Polish Physiological Society*. 2013;64:281-8.

237. Nerlekar N, Beale A and Harper RW. Colchicine--a short history of an ancient drug. *The Medical journal of Australia*. 2014;201:687-8.

238. Akasheva DU, Plokhova EV, Tkacheva ON, Strazhesko ID, Dudinskaya EN, Kruglikova AS, Pykhtina VS, Brailova NV, Pokshubina IA, Sharashkina NV, Agaltsov MV, Skvortsov D and Boytsov SA. Age-Related Left Ventricular Changes and Their Association with Leukocyte Telomere Length in Healthy People. *PLoS One*. 2015;10:e0135883.

239. Dey D, Schepis T, Marwan M, Slomka PJ, Berman DS and Achenbach S. Automated three-dimensional quantification of noncalcified coronary plaque from coronary CT angiography: comparison with intravascular US. *Radiology*. 2010;257:516-22.

240. Min JK, Shaw LJ, Devereux RB, Okin PM, Weinsaft JW, Russo DJ, Lippolis NJ, Berman DS and Callister TQ. Prognostic value of multidetector coronary computed tomographic angiography for prediction of all-cause mortality. *J Am Coll Cardiol*. 2007;50:1161-70.

241. de Araujo Goncalves P, Garcia-Garcia HM, Dores H, Carvalho MS, Jeronimo Sousa P, Marques H, Ferreira A, Cardim N, Campante Teles R, Raposo L, Mesquita Gabriel H, Sousa Almeida M, Aleixo A, Mota Carmo M, Pereira Machado F and Mendes M. Coronary computed tomography angiography-adapted Leaman score as a tool to noninvasively quantify total coronary atherosclerotic burden. *Int J Cardiovasc Imaging*. 2013;29:1575-84.

242. Puchner SB, Liu T, Mayrhofer T, Truong QA, Lee H, Fleg JL, Nagurney JT, Udelson JE, Hoffmann U and Ferencik M. High-risk plaque detected on coronary CT angiography predicts acute coronary syndromes independent of significant stenosis in acute chest pain: results from the ROMICAT-II trial. *J Am Coll Cardiol*. 2014;64:684-92.

243. Iacobellis G, Corradi D and Sharma AM. Epicardial adipose tissue: anatomic, biomolecular and clinical relationships with the heart. *Nat Clin Pract Cardiovasc Med*. 2005;2:536-43.

244. Moss AJ, Williams MC, Newby DE and Nicol ED. The Updated NICE Guidelines: Cardiac CT as the First-Line Test for Coronary Artery Disease. *Curr Cardiovasc Imaging Rep*. 2017;10:15.

245. Konishi M, Sugiyama S, Sato Y, Oshima S, Sugamura K, Nozaki T, Ohba K, Matsubara J, Sumida H, Nagayoshi Y, Sakamoto K, Utsunomiya D, Awai K, Jinnouchi H, Matsuzawa Y, Yamashita

Y, Asada Y, Kimura K, Umemura S and Ogawa H. Pericardial fat inflammation correlates with coronary artery disease. *Atherosclerosis*. 2010;213:649-55.

246. Abazid RM, Smettei OA, Kattea MO, Sayed S, Saqqah H, Widyan AM and Opolski MP. Relation Between Epicardial Fat and Subclinical Atherosclerosis in Asymptomatic Individuals. *J Thorac Imaging*. 2017;32:378-382.

247. Antonopoulos AS, Sanna F, Sabharwal N, Thomas S, Oikonomou EK, Herdman L, Margaritis M, Shirodaria C, Kampoli A-M, Akoumianakis I, Petrou M, Sayeed R, Krasopoulos G, Psarros C, Ciccone P, Brophy CM, Digby J, Kelion A, Uberoi R, Anthony S, Alexopoulos N, Tousoulis D, Achenbach S, Neubauer S, Channon KM and Antoniades C. Detecting human coronary inflammation by imaging perivascular fat. *Science Translational Medicine*. 2017;9.

248. Oikonomou EK, Marwan M, Desai MY, Mancio J, Alashi A, Hutt Centeno E, Thomas S, Herdman L, Kotanidis CP, Thomas KE, Griffin BP, Flamm SD, Antonopoulos AS, Shirodaria C, Sabharwal N, Deanfield J, Neubauer S, Hopewell JC, Channon KM, Achenbach S and Antoniades C. Non-invasive detection of coronary inflammation using computed tomography and prediction of residual cardiovascular risk (the CRISP CT study): a post-hoc analysis of prospective outcome data. *The Lancet*. 2018;392:929-939.

APPENDIX:
PDF of PUBLISHED MANUSCRIPTS DURING CANDIDATURE

The following is a list of PDF publications of the published manuscripts included in this thesis, as well as selected manuscripts not specific to the PhD topic where I was first author or co-primary / second author.

SYSTEMATIC REVIEW AND META-ANALYSIS

Association of Epicardial Adipose Tissue and High-Risk Plaque Characteristics: A Systematic Review and Meta-Analysis

Nitesh Nerlekar, MBBS, MPH; Adam J. Brown, MD, PhD; Rahul G. Muthalaly, MBBS; Andrew Talman, BBiomedSc, MD; Thushan Hettige, MBBS; James D. Cameron, MD, MEngSc; Dennis T. L. Wong, MBBS, PhD

***Background*—**Epicardial adipose tissue (EAT) is hypothesized to alter atherosclerotic plaque composition, with potential development of high-risk plaque (HRP). EAT can be measured by volumetric assessment (EAT-v) or linear thickness (EAT-t). We performed a systematic review and random-effects meta-analysis to assess the association of EAT with HRP and whether this association is dependent on the measurement method used.

***Methods and Results*—**Electronic databases were systematically searched up to October 2016. Studies reporting HRP by computed tomography or intracoronary imaging and studies measuring EAT-v or EAT-t were included. Odds ratios were extracted from multivariable models reporting the association of EAT with HRP and described as pooled estimates with 95% confidence intervals (CIs). Analysis was stratified by EAT measurement method. Nine studies (n=3772 patients) were included with 7 measuring EAT-v and 2 measuring EAT-t. Increasing EAT was significantly associated with the presence of HRP (odds ratio: 1.26 [95% CI, 1.11–1.43]; $P<0.001$). Patients with HRP had higher EAT-v than those without (weighted mean difference: 28.3 mL [95% CI, 18.8–37.8 mL]; $P<0.001$). EAT-v was associated with HRP (odds ratio: 1.19 [95% CI, 1.06–1.33]; $P<0.001$); however, EAT-t was not (odds ratio: 3.09 [95% CI, 0.56–17]; $P=0.2$). Estimates remained significant when adjusted for small-study effect bias (odds ratio: 1.13 [95% CI, 1.03–1.28]; $P=0.04$).

***Conclusions*—**Increasing EAT is associated with the presence of HRP, and patients with HRP have higher quantified EAT-v. The association of EAT-v with HRP is significant compared with EAT-t; however, a larger scale study is still required, and further evaluation is needed to assess whether EAT may be a potential therapeutic target for novel pharmaceutical agents.

***Clinical Trial Registration*—**URL: https://www.crd.york.ac.uk/. Unique identifier: CRD42017055473. **(*J Am Heart Assoc.* 2017;6:e006379. DOI: 10.1161/JAHA.117.006379.)**

Key Words: epicardial fat • high-risk plaque • meta-analysis • vulnerable plaque

Epicardial adipose tissue (EAT) is a metabolically active fat depot, abundant in proinflammatory cytokines, and has been correlated with the extent and severity of coronary artery disease (CAD).[1] EAT shares the same embryologic origin of omental and mesenteric fat[2,3] and encases the coronary arteries with no fascial barrier.[4] Consequently, it has been postulated that EAT may display vasocrine or paracrine effects on the adjacent arterial wall to influence atherosclerotic plaque composition, resulting in the development of high-risk plaque (HRP).[5–9] The presence of HRP has shown association with future adverse prognosis,[10,11] but the management of these patients remains uncertain. HRP may be visualized invasively by several methods including intravascular ultrasound and optical coherence tomography and noninvasively by computed tomography (CT) coronary angiography with good diagnostic agreement between techniques.[12–14] EAT may be measured either volumetrically by CT coronary angiography or noncontrast CT (EAT-v) or by a linear thickness measurement on echocardiography (EAT-t). Both thickness and volume measures have been associated with incident CAD[1]; however, linear thickness may underrepresent the totality of EAT.

The objective of this systematic review and meta-analysis was to explore the association between EAT and the presence of HRP. The secondary aims were to evaluate whether increasing EAT volume is associated with HRP presence and

From the Monash Cardiovascular Research Centre, Monash University and MonashHeart, Monash Health, Clayton, Victoria, Australia.

Accompanying Tables S1 through S5 and Figure S1 are available at http://jaha.ahajournals.org/content/6/8/e006379/DC1/embed/inline-supplementary-material-1.pdf

Correspondence to: Nitesh Nerlekar, MBBS, MPH, Monash Cardiovascular Research Centre and MonashHeart, Monash Health, Clayton, Victoria, Australia. E-mail: [redacted]

Received April 17, 2017; accepted July 18, 2017.

Clinical Perspective

What Is New?

- Increasing epicardial adipose tissue (EAT) volume is associated with the presence of high-risk coronary artery plaque characteristics.
- Patients with high-risk coronary plaque features have quantitatively higher EAT volumes.
- EAT should ideally be measured by complete volumetric analysis rather than by linear thickness measurements.

What Are the Clinical Implications?

- Incorporation of EAT measurement with routinely performed cardiac computed tomography may assist in improved risk stratification for patients.
- EAT may represent an important cardiovascular therapeutic target.

the strength of association with presence of HRP by EAT measurement method.

Materials and Methods

Data Sources and Search Strategy

The search was conducted using the Medline, Embase, and PubMed databases with no start date up to October 2016. Keywords using Medical Subject Headings included *epicardial adipose tissue, epicardial fat, pericardial adipose tissue, pericardial fat, vulnerable plaque, high-risk plaque, low-attenuation plaque, napkin ring, positive remodeling, spotty calcification, coronary artery disease, plaque characteristics, plaque composition, plaque vulnerability, thin-cap fibroatheroma, intravascular ultrasound, optical coherence tomography*, and *angioscopy*. The reference lists of eligible articles were hand-searched for additional articles. Searches were restricted to human studies. We conducted this systematic review in accordance with the PRISMA (Preferred Reporting Items for Systematic Reviews and Meta-Analyses) statement, and the trial was registered with PROSPERO (registration no. CRD42017055473). A flow chart describing the study search is presented in Figure 1, and an example of the search term strategy is shown in Table S1.

Study Selection

The following inclusion criteria were used for the study: patients undergoing either intracoronary imaging or CT coronary angiography evaluation with reported HRP features, noninvasive measurement of EAT by either CT-derived volume (on contrast or noncontrast CT) or linear thickness (by CT or echocardiography), and reports fully published in peer-reviewed journals. For intracoronary imaging studies, HRP was defined as the presence of thin-cap fibroatheroma. For CT studies, HRP included plaques with ≥1 of the following features: low-attenuation plaque, positive remodeling, spotty calcification, and the napkin ring sign. Study specific definitions of HRP are reported in Table S2.

Data Extraction

Odds ratios (ORs) and their respective 95% confidence intervals (95% CIs) for association of EAT with HRP were extracted. If possible, ORs from multivariable models that adjusted for other CAD risk factors were used, and covariates within the model were recorded. Mean and standard deviation of EAT volume between groups with and without HRP were entered. Studies reporting medians with interquartile ranges were converted to means, as recommended previously.[15]

End Points

The primary end point was the pooled association of EAT with the presence of HRP. Secondary end points included the pooled quantitative difference of EAT-v in patients with and without HRP and the association of EAT with HRP stratified by EAT measurement method (EAT-v or EAT-t).

Statistical Analysis

Statistical analysis was performed using StataMP 14.0 (StataCorp). ORs were examined on the log scale and transformed for graphical presentation with 95% CI reported. If multiple outcomes were reported (ie, by individual plaque feature or by grouped features), the analyzed estimate was the association of EAT with any HRP if specified. Random-effects modeling was used with the method of DerSimonian and Laird.[16] The weighted mean difference for EAT between groups with and without HRP was calculated. Statistical heterogeneity was evaluated by the I^2 statistic and quantified as low (<25%), moderate (25–75%), or high (>75%).[17] Sensitivity analysis was performed by EAT measurement method (EAT-v or EAT-t, by pooled estimates of similarly defined EAT covariate parameters; ie, when EAT was included as a continuous variable or assessed in 10-mL increments and for individual plaque features, if possible). Additional sensitivity analysis using random effects with the Hartung–Knapp–Sidik–Jonkman (HKSJ) approach was used to explore effect sizes when 2 studies were grouped.[18,19] Exploratory metaregression was performed to assess the influence of independent variables (mean study ages, mean EAT volume, mean study body mass index, and proportion of HRP). Publication bias was assessed by the Egger and Begg test. In addition, the Duval and Tweedie trim-and-fill method was used to investigate publication bias,

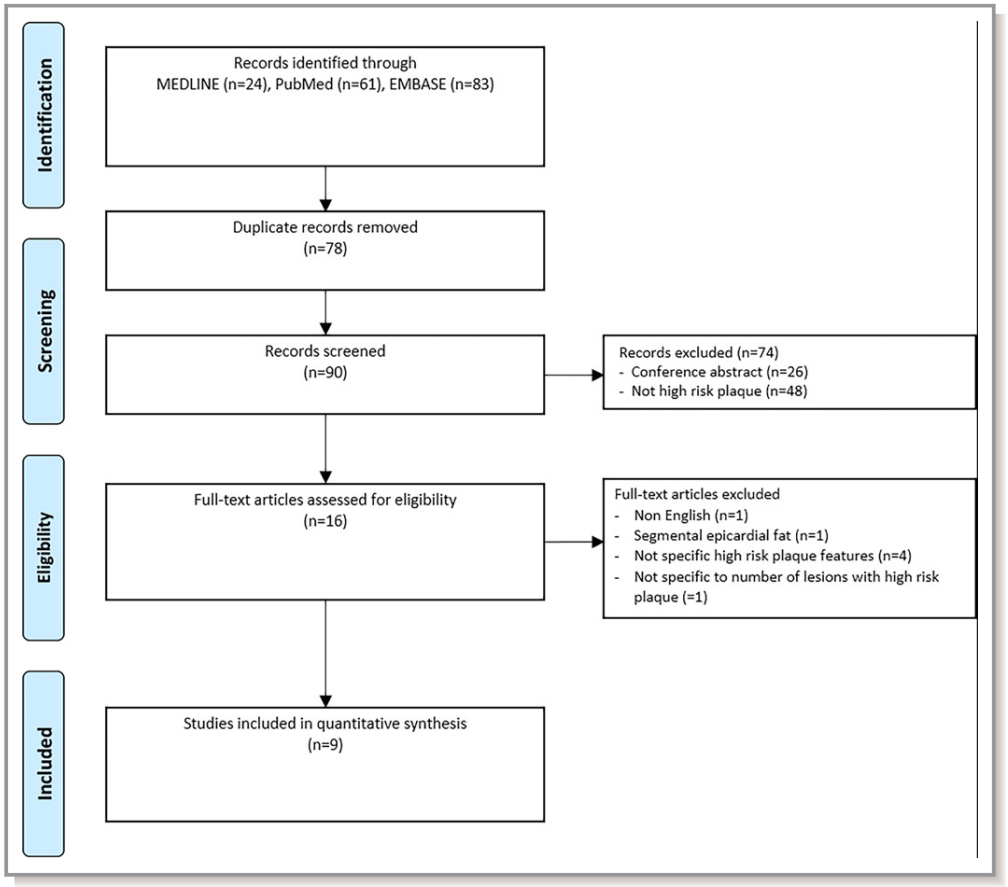

Figure 1. Search strategy.

and systematic exclusion of individual studies was used to assess changes in the pooled estimate. A 2-sided *P* value of <0.05 was considered significant.

Results

A total of 90 publications were reviewed with 9 studies included for final analysis (3772 participants; Figure 1). One study was excluded because it presented the association of EAT with plaque lipid percentage rather than specified numbers of patients with HRP.[20] Seven studies reported CT assessment of HRP[21–27] (n=3573) and 2 studies reported invasive assessment of HRP[29,30] (n=199). Seven studies measured EAT-v[21–26,29,30] (n=3284), and 2 studies measured EAT-t[27,28] (n=488). All study designs were cross-sectional. All patients were from cohorts with suspected CAD, with 2 studies evaluating patients with suspected acute coronary syndrome.[21,22] Study characteristics are presented in Tables 1 and 2, and regression modeling outcomes and model covariates are presented in Table 3. Individual-study EAT measurement characteristics and HRP definitions are presented in Table S2.

The prevalence of HRP ranged widely, from 4% to 59% at a per-patient level (Table 1). The primary end point demonstrated a significant association of increasing EAT with the presence of HRP (pooled OR: 1.26 [95% CI, 1.11–1.43]; $P<0.001$, $I^2=81\%$; Figure 2).

Analysis to assess quantitative differences in EAT between patients with and without HRP demonstrated a weighted mean difference of +28.3 mL in those patients with HRP (95% CI, 18.8–37.8 mL]; $P<0.001$; I^2: 58%) based on 4 studies (Figure 3).

When stratified by EAT measurement method, in the 7 studies measuring EAT-v, the pooled OR was significantly associated with HRP presence (OR: 1.19 [95% CI, 1.06–1.33]; $P<0.001$, I^2: 78%). However, no significant association was observed with the 2 EAT-t studies and presence of HRP (OR: 3.09 [95% CI, 0.56–17]; $P=0.20$; I^2: 90%; Figure 4). This remained statistically nonsignificant on sensitivity analysis with the HKSJ method (Table 4).

Sensitivity analysis was performed to assess pooled estimates of studies using EAT as a similarly measured covariate. Two studies analyzed EAT-v in 10-mL increments and demonstrated a pooled OR of 1.18 (95% CI, 1.12–1.24;

Table 1. Demographic, EAT, and HRP Parameters of Included Studies

Study	EAT Method	Population	N	EAT Value	HRP Proportions
Lu et al[21]	EAT-v (CACS)	Suspected ACS	467	Median EAT: 108.5 cm^3 (IQR: 76.4–140.6 cm^3) With HRP: 123 cm^3 (IQR: 93–156 cm^3) Without HRP: 98 cm^3 (IQR: 68–127 cm^3)	HRP in 167 (36%) patients; NRS in 15%; PR in 32.3%; LAP in 23.4%; SpC: in 91%
Schlett et al[22]	EAT-v (CTCA)	Suspected ACS	358	Median EAT: 95.2 cm^3 (IQR: 66–130.1) With HRP: 151.9 cm^3 (IQR: 109.0–179.4) Without HRP: 110 cm^3 (IQR: 81.5–137.4)	Any HRP in 13 (4%) patients
Rajani et al[24]	EAT-v (CACS)	Suspected CAD	402	Mean EAT: 103±51 cm^3 With any HRP: 116±53 cm^3 Without HRP: 99±57 cm^3	Any HRP in 113 (59%) patients; LAP in 67 (35%); PR in 93 (48%)
Oka et al[23]	EAT-v (CACS)	Suspected CAD	357	Mean EAT: 125±44 mL; EAT analysis threshold of 100 mL	87 (24%) with all 3 HRPs LAP: EAT <100 mL: 52%; EAT ≥100 mL: 27% PR: EAT <100 mL: 58%; EAT ≥100 mL: 37% LAP with or without PR: EAT <100 mL: 46%; EAT ≥100 mL: 25%
Ito et al[25]	EAT-v (CACS)	Suspected CAD (symptomatic) with CACS 0	1308	Mean EAT: 98.1±41.3 cm^3 With HRP: 133±40.2 cm^3 Without HRP: 95.1±40.3 cm^3	Any HRP in 63 (5%) patients
Nakanishi et al[26]	EAT-v (CTCA)	Suspected CAD in patients with CKD	275	Mean EAT: CKD: 111±41 mL (n=110) No CKD: 81±29 mL (n=165)	Any HRP in 44 (16%) patients
Ito et al[29]	EAT-v (CTCA)	Scheduled for PCI and underwent CT in addition to OCT	117 (244 plaques)	EAT-v Tertiles: T1: <104.1 cm^3 (n=39) T2: 104.1 to 130.7 cm^3 (n=39) T3: >130.7 cm^3 (n=39)	Total TCFA: 51 (21%) plaques T1: Single TCFA n=6 (15%); Multiple TCFA n=1 (3%) T2: Single TCFA n=7 (18%); Multiple TCFA n=3 (8%) T3: Single TCFA n=12 (31%); Multiple TCFA n=8 (21%) Minimum fibrous cap thickness: T1: 102.7±69.2 μm; T2: 102.5±56.5 μm; T3: 78.2±43.9 μm Maximal lipid arc: T1: >2 quadrants, 13 (33%); T2: >2 quadrants, 14 (36%); T3: >2 quadrants, 25 (64%) CT characteristics: T1: LAP, 4 (10%); PR, 8 (21%) T2: LAP, 14 (36%); PR, 13 (33%) T3: LAP, 16 (41%); PR, 21 (54%)
Park et al[28]	EAT-t (Echo)	Angiographically significant CAD undergoing PCI with or without IVUS	82	Mean EAT-t: 3.4±2.2 mm EAT-t 3.5 mm threshold: EAT <3.5 mm (n=21); EAT ≥3.5 mm (n=39)	TCFA (n): EAT <3.5 mm: 3.3±2.2; EAT ≥3.5 mm: 2.1±1.6 Mean volume index necrotic core (mm^3/mm): EAT <3.5 mm: 0.3±0.2; EAT ≥3.5 mm: 0.6±0.4 Plaque volume (mm^3): EAT <3.5 mm: 1360.1±492.1; EAT ≥3.5 mm: 1048.5±398.2

Continued

Table 1. Continued

Study	EAT Method	Population	N	EAT Value	HRP Proportions
Tachibana et al[27]	EAT-t (Echo)	Suspected CAD	406	EAT-t 5.8 mm threshold: EAT ≥5.8 mm (n=238); EAT <5.8 mm (n=168)	HRP in 45 (11%) patients LAP: EAT <5.8 mm: 4%; EAT ≥5.8 mm: 24% PR: EAT <5.8 mm: 39%; EAT ≥5.8 mm: 60% LAP+PR: EAT <5.8 mm: 3%; EAT ≥5.8 mm: 17%

ACS indicates acute coronary syndrome; CACS, coronary artery calcium score (noncontrast computed tomography); CAD, coronary artery disease; CKD, chronic kidney disease; CT, computed tomography; CTCA, computed tomography coronary angiography; EAT, epicardial adipose tissue; EAT-t, epicardial adipose tissue thickness; EAT-v, epicardial adipose tissue volume; HRP, high-risk plaque; IQR, interquartile range; IVUS, intravascular ultrasound; LAP, low-attenuation plaque; NRS, napkin ring sign; OCT, optical coherence tomography; PCI, percutaneous coronary intervention; PR, positive remodeling; SpC, spotty calcification; T, tertile; TCFA, thin-cap fibroatheroma.

P<0.001; I^2: 0%) that became nonsignificant when analyzed with the HKSJ method (OR: 1.18 [95% CI, 0.84–1.64]; P=0.10). In the 2 studies that analyzed EAT-v as a continuous variable, the pooled OR was 1.18 (95% CI, 0.77–1.81; P=0.44; I^2: 52%), which remained nonsignificant after analysis with HKSJ (Table 4). EAT measured in the remaining studies were modeled as per standard deviation or by a dichotomous threshold level and not formally pooled.

Further sensitivity analysis was performed to assess the association between specific HRP subtypes with information obtainable from 2 studies. An association was demonstrated between increasing EAT and low-attenuation plaque (OR: 2.79 [95% CI, 1.71–4.53]; P<0.001; I^2: 0%), positive remodeling, (OR: 1.93 [95% CI, 1.25–2.99]; P=0.003; I^2: 0%), and the presence of both features (OR: 2.58 [95% CI, 1.55–4.28]; P=0.001; I^2: 0%). The results for both low-attenuation plaque and positive remodeling became statistically nonsignificant after application of the HKSJ method, but the presence of both features remained significantly associated with increasing EAT (Table 4).

Exploratory metaregression demonstrated no significant influence of varying study-level predictors on the overall effect size; these included mean BMI (OR: 0.95 [95% CI, 0.79–1.14]; P=0.55), mean age (OR: 1.03 [95% CI, 0.96–1.10]; P=0.38), population proportion of HRP (OR: 0.99 [95% CI, 0.98–1.00]; P=0.42), and mean EAT volume (OR: 1.00 [95% CI, 0.97–1.03]; P=0.99).

There was evidence of publication bias by calculation of the Egger test for small-study effects (P=0.005). Using the trim-and-fill method, the overall estimate remained significant for the association of EAT and HRP (pooled estimate OR: 1.13 [95% CI, 1.03–1.28]; P=0.04; I^2: 81%; Figure S1). Analysis to assess the influence of single studies on the effect estimate demonstrated a persistent significant association of increasing EAT with HRP. The lowest pooled estimate OR of 1.16 (95% CI, 1.06–1.27; P=0.001; I^2: 74%) occurred with the exclusion of Tachibana et al, and the highest pooled estimate OR of 1.27 (95% CI, 1.12–1.45; P<0.001; I^2: 70%) occurred with the exclusion of Lu et al (Table S3).

Discussion

The results from this meta-analysis of 9 observational studies demonstrate 3 important findings. First, increasing EAT is

Table 2. Study Demographic Data

Study	Diabetes Mellitus(%)	Hypertension (%)	Hyperlipidemia (%)	BMI	Ethnicity	Age, y	Sex (%)
Lu et al[21]	17	53	45	29±5	Not specified	54±8	53
Schlett et al[22]	10	39	37	28 (25–32)	Not specified	51 (45–59)	62
Rajani et al[24]	14	54	63	27±4	Not specified	66 (23–92)	56
Oka et al[23]	31	68	50	24±5	Japanese institution	66±11	63
Ito et al[25]	8	33	26	23±4	Japanese institution	59±12	46
Nakanishi et al[26]	38	65	59	24±4	Japanese institution	65±10	66
Park et al[28]	29	61	20	25±3	Korean Institution	59±11	54
Ito et al[29]	24	61	44	24±3	Japanese institution	66±9	82
Tachibana et al[27]	27	58	31	23±4	Japanese institution	68±13	57

Values are expressed as total study cohort proportions (%), mean±SD, or median (interquartile range). BMI indicates body mass index.

Table 3. EAT Modeling Outcomes and Model Covariates

Study	EAT Modeling	Regression Outcomes	Covariates in Multivariable Model	Threshold/ROC AUC Values
Lu et al[21]	Indexed and absolute EAT	Any HRP with indexed EAT-v: OR: 1.04 (95% CI, 1–1.08; *P*=0.04) Any HRP with absolute EAT-v: OR: 1.02 (95% CI, 1–1.03; *P*=0.046)	Age, sex, number of cardiovascular risk factors, log CACS, >50% stenosis	Optimal threshold 62.3 cm^3/m^2 with sensitivity 48.5%, specificity 72.7%; no ROC AUC specified
Schlett et al[22]	EAT per SD (49.8 mL)	Presence of HRP: OR: 1.79 (95% CI, 1.13–2.76; *P*=0.008)	Not specified	Not reported
Rajani et al[24]	Log EAT-v	Any HRP: OR: 1.7 (95% CI, 0.9–3.4; P=0.038) LAP: OR: 2.4 (95% CI, 1.1–5.1; *P*=0.02) PR: OR: 1.8 (95% CI, 1.0–3.4; *P*=0.07) Both HRP features: OR: 2.6 (95% CI, 1.1–6.2; *P*=0.03)	Age, BMI, diabetes mellitus, hypercholesterolemia, smoking, family history, hypertension	ROC AUC of 0.756 for any HRP presence with sensitivity 62%, specificity 84%; optimal threshold of EAT <74.07 cm^3 excluded any HRP
Oka et al[23]	High vs low-EAT-v (100 mL threshold)	LAP: OR: 3.08 (95% CI, 1.66–5.83; *P*<0.001) PR: OR: 2.08 (95% CI, 1.12–3.88; *P*=0.02) SpC: OR: 1.11 (95% CI, 0.61–2.04; *P*=0.73) LAP+PR: OR: 2.56 (95% CI, 1.38–4.85; *P*=0.003) All 3 features: OR: 1.65 (95% CI 0.81–3.44; *P*=0.17)	Age, sex, hypertension, diabetes mellitus, smoking, BMI, VAT area, CACS	Using a threshold of 100 mL, sensitivity for LAP+PR was 80%, specificity was 41%
Ito et al[25]	EAT-v per 10 cm^3	Any HRP: OR: 1.19 (95% CI, 1.12–1.27; *P*<0.01)	Male, diabetes mellitus, hypertension, BMI	ROC AUC of 0.75 for any HRP presence at optimal threshold 127.1 cm^3 with sensitivity 64%, specificity 81%
Nakanishi et al[26]	EAT-v per 10 mL	Presence of HRP: OR: 1.15 (95% CI, 1.05–1.26; *P*=0.003)	Age per 10 y, sex, hypertension, diabetes mellitus, hyperlipidemia, smoking, BMI	. . .
Ito et al[29]	Highest tertile of EAT	Presence of TCFA: OR: 2.92 (95% CI, 1.13–7.55; *P*=0.027) Correlation of EAT with fibrous cap thickness: *r*=−0.400, *P*<0.01	ACS, BMI	ROC AUC of 0.721 for detection of TCFA with optimal threshold 126.7 cm3, sensitivity 69% specificity 71%
Park et al[28]	High vs low-EAT-t (3.5 mm threshold)	Total TCFAs in symptom-related vessel: β=0.106 (95% CI, 0.004–0.208; *P*=0.043)	BMI, diabetes mellitus, dyslipidemia, metabolic syndrome	Not specified
Tachibana et al[27]	High vs low-EAT-t (5.8 mm threshold)	Presence of HRP: OR: 7.98 (95% CI, 2.77–22.98; *P*<0.01)	Age, sex, BMI, VAT, hypertension, dyslipidemia, diabetes mellitus, smoker, CACS >100, stenotic vessel number, renal insufficiency, statins	ROC AUC of 0.77 for HRP (combination of LAP+PR) at threshold of 5.8 mm with sensitivity 83%, specificity 64%

ACS indicates acute coronary syndrome; BMI, body mass index; CACS, coronary artery calcium score (noncontrast computed tomography); CI, confidence interval; EAT, epicardial adipose tissue; EAT-t, EAT thickness; EAT-v, volumetric EAT; HRP, high-risk plaque; LAP, low-attenuation plaque; OR, odds ratio; PR, positive remodeling; ROC AUC, receiver operating characteristic area under the curve; SpC, spotty calcification; TCFA, thin-cap fibroatheroma; VAT, visceral adipose tissue.

significantly associated with the presence of HRP features. Second, patients with HRP have a significantly increased volume of EAT compared with those without HRP. Third, EAT is associated with HRP presence ideally when measured by complete volumetric analysis rather than EAT linear thickness measurements.

EAT is a visceral adipose tissue depot rich in proinflammatory and proatherogenic cytokines including monocyte

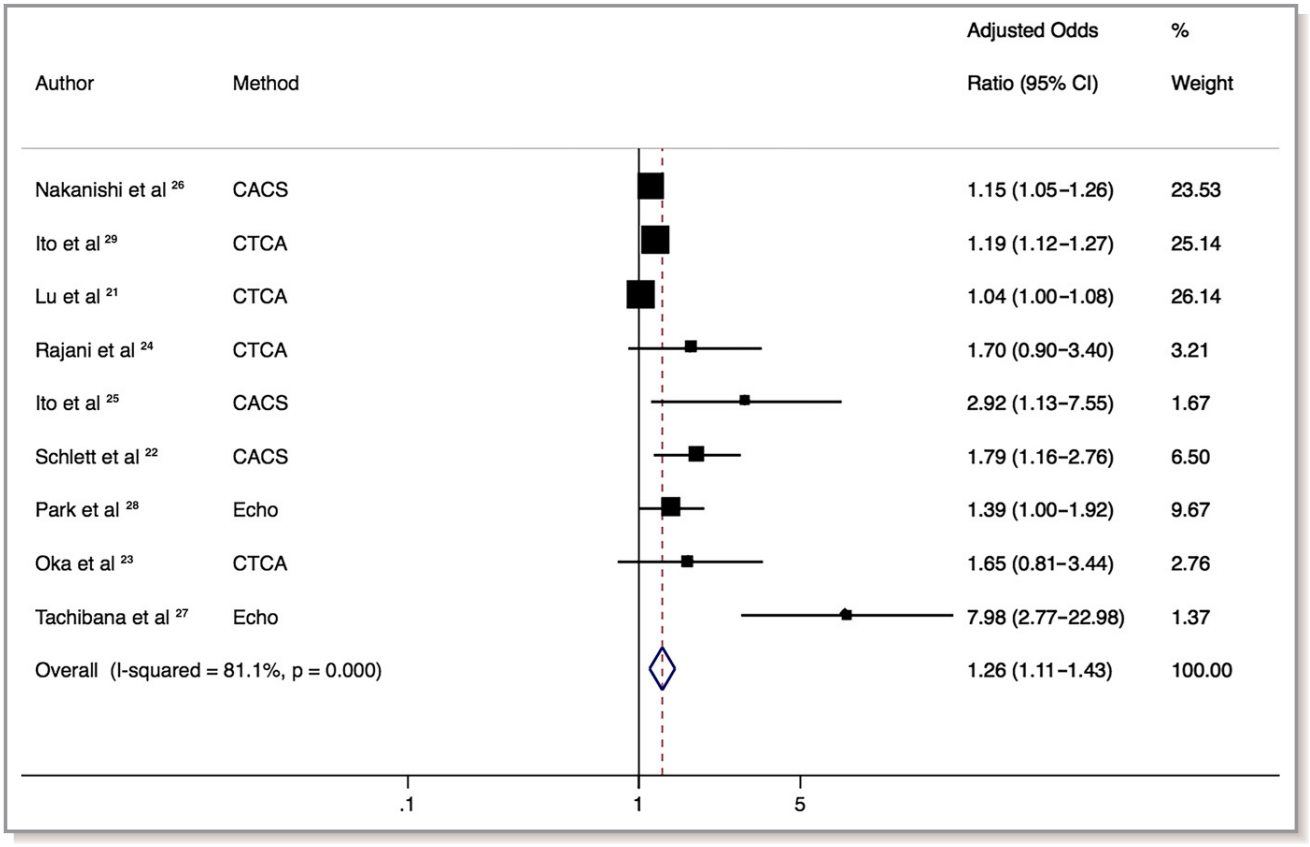

Figure 2. Association of epicardial adipose tissue (EAT) with presence of high-risk plaque (HRP). Forest plot displays summary odds ratios and 95% confidence intervals (CIs) for the increasing association of EAT with HRP. Method represents the radiologic method of calculating EAT. This demonstrates a significant association of increasing EAT with HRP. CACS indicates coronary artery calcium score (noncontrast computed tomography); CTCA, computed tomography coronary angiography; Echo, echocardiography.

chemoattractant protein 1, IL-6 (interleukin 6). IL-1β, IL-6sR, and tumor necrosis factor α.[31] Because of EAT's anatomic proximity to the adjacent myocardium and lack of fascial barrier with the epicardial coronary arteries, there may be paracrine or vasocrine signaling of cytokines between the surrounding fat and the underlying arterial wall.[2] This suggested pathophysiology is analogous to the visceral intra-abdominal adipose tissue surrounding the portal circulation that is purported to influence the development of hepatic steatosis.[32] It has been demonstrated that increased EAT volume is related to both the extent and the lesion severity of coronary stenosis[33] and that EAT contains a greater amount of inflammatory cytokines than serum circulating levels and subcutaneous adipose stores.[34] The apposition of EAT with the arterial adventitia suggests the "outside-in" hypothesis of atherosclerosis, whereby the inflammatory milieu of EAT leads to vascular inflammation of the adventitia progressing inward to the intima, leading to plaque formation. Consequently, it is possible that cellular cross-talk may lead to the development of plaque characteristics considered to be "high risk" given their association with major adverse cardiovascular events. It has also been reported that high EAT levels are associated with mortality, although it remains unclear whether these levels are specifically related to preceding cardiovascular events.[35] Our results indicate a uniform association of increasing EAT with HRP, but further study is needed to establish the influence and interaction of these parameters with prognosis. Importantly, we aimed to use risk estimates from multivariable models, which suggests an incremental effect of EAT with HRP presence beyond traditional cardiovascular risk factors.

Because there is no guideline-advocated technique for EAT quantification, individual studies are subject to authors' discretion and experience. The interobserver variability for EAT-t has shown mixed results,[36] and a measure of linear thickness by 2-dimensional assessment may under- or overrepresent total EAT volume due to changes in probe angulation. It has been suggested that a threshold of 7 mm confers elevated EAT-t; this is a significantly higher threshold than our included studies and may also influence interpretation. Only 1 previous study evaluated EAT-t versus EAT-v, in 71 patients, and reported a modest correlation (r=0.595).[37]

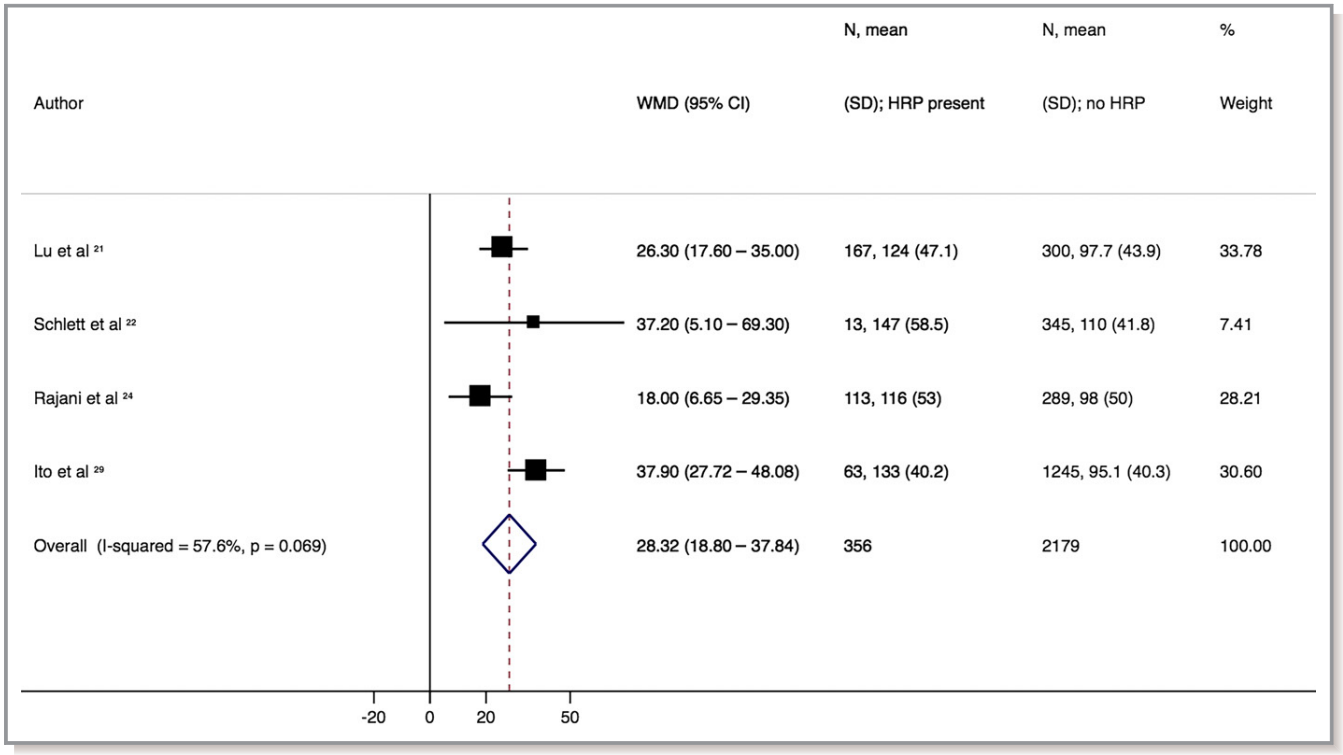

Figure 3. Difference in quantitative epicardial adipose tissue (EAT). Forest plot displays weighted mean differences (WMDs) and 95% confidence intervals (CIs) for differences between patients with and without high-risk plaque (HRP). This indicates that patients with HRP have a significantly higher volume of EAT (WMD: 28.3 mL [95% CI, 18.8–37.8 mL]) compared with those patients without HRP.

EAT-v, however, also has limitations, with differing values measurable with the use of contrast media[38] and possible differences related to vendor-specific software algorithms. In our analysis of EAT-v versus EAT-t, we demonstrated that EAT-t had a decidedly wide CI for the association with HRP and failed to reach statistical significance, although this is based on only 2 studies with a total of 488 patients. On the contrary, EAT-v displayed a significant association with HRP with more precise confidence limits. We attempted to explore the association further by analyzing the modeling method of EAT, which demonstrated uncertainty in estimates for differing techniques and highlighted the need for a standardized and consistent approach when incorporating EAT into models to assess disease outcomes.

In our subgroup analysis of EAT association with HRP subtype, we noted a strong association individually with low-attenuation plaque and positive remodeling as well as with the presence of both features after adjustment for conventional cardiovascular risk factors. Association with individual plaque feature types diminished due to imprecision in 95% CIs but remained for the presence of both high-risk features. The largest study to date, of 3158 patients by Motoyama et al, reported that these HRP characteristics, defined as the presence of either feature or both, are strongly associated with future acute coronary syndrome development (adjusted hazard ratio: 8.24 [95% CI, 5.26–12.96]; $P<0.001$).[10] EAT was not measured in this study, and its contribution to prognosis remains unclear.

It is notable that some observational studies have demonstrated a lack of relationship between EAT and significant CAD[39,40]—similar to our included studies, all of which are observational and prone to significant bias. Biases include selection and ascertainment bias and variable use of predictors in regression modeling that may alter reported estimates and contribute to between-study heterogeneity. To assess study quality, we evaluated the Grading of Recommendations Assessment, Development and Evaluation (GRADE) classification[41–43] (Tables S4 and S5), which apportions an overall study-quality assessment. Because none of the trials are, by definition, of high quality, given that they are not randomized controlled trials, the overall information quality is regarded as low and should be interpreted as such without drawing firm conclusions that may alter clinical decision making. Despite the inconsistency of CAD association, given the association of HRP with cardiac prognosis, it remains plausible that EAT may influence plaque composition that may not be diagnosed as functionally or anatomically significant. Rigorous prospective study to assess the role of EAT in atherogenesis is still warranted.

The management of HRP features is uncertain. EAT is currently measured only for research purposes; however, the

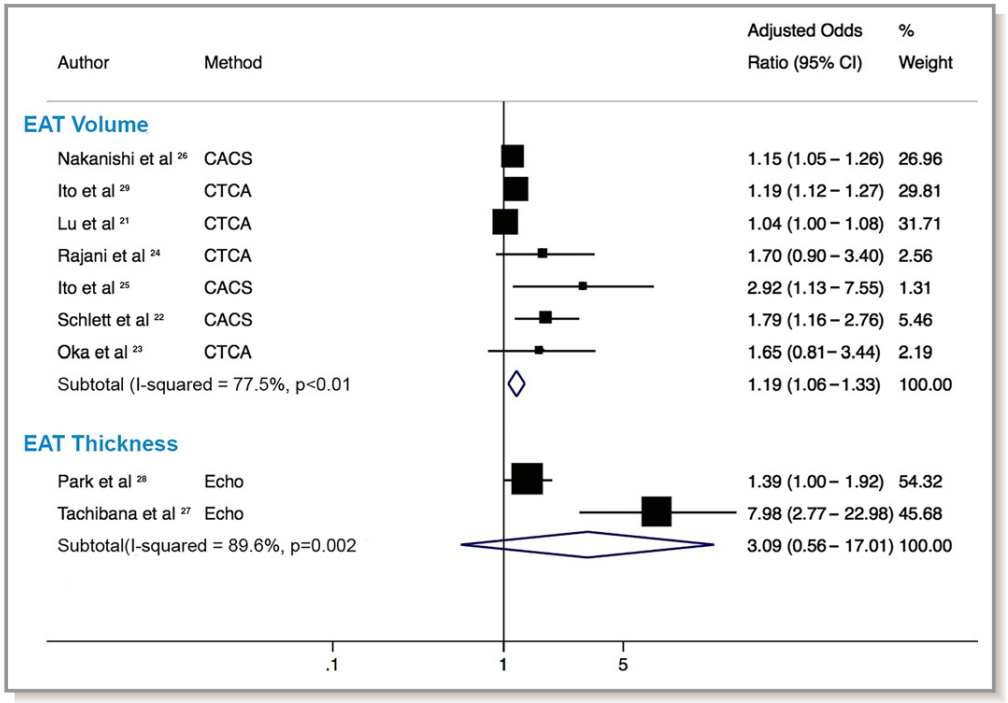

Figure 4. Pooled estimates by epicardial adipose tissue (EAT) measurement method. Forest plot displays odds ratios and 95% confidence intervals (CIs) for the association of increasing EAT with high-risk plaque (HRP) stratified by measurement method of EAT measurement, either by volume or thickness. This demonstrates that increasing EAT volume has a significant association with HRP; however, increasing EAT thickness is not significantly associated with HRP and has a markedly wide CI crossing the line of unity. CACS indicates coronary artery calcium score (noncontrast computed tomography); CTCA, computed tomography coronary angiography; Echo, echocardiography.

importance of assessing EAT and its association with HRP relates to a potential target for therapeutic intervention. EAT has demonstrated temporal changes in plaque and cardiovascular risk. In a study of nonobese patients undergoing serial CT over 4 years, an increase in EAT volume was associated with HRP as well as future acute coronary syndrome despite optimal management of cardiovascular risk factors.[44] Calorie restriction and bariatric surgery rather than exercise have shown promise as methods for EAT reduction, as explored recently in a meta-analysis by Rabkin and Campbell,[45] and animal data have demonstrated that selective surgical excision of EAT slows the progression of atherosclerosis.[46] It remains to be seen whether targeted EAT reduction may improve dynamic atherosclerosis in human participants, and randomized controlled trial data are lacking.

Study Limitations

Our analysis is limited by the observational nature of included studies and by a lack of access to patient-level data to allow adjustment for other covariates that may influence EAT including sex differences and stratification and assessment by other population features such as traditional cardiovascular risk factors of hypertension, hyperlipidemia and diabetes mellitus. We attempted to account for this by using model estimates that adjusted for several of these variables. The majority of studies were also performed in Japanese centers, which may limit the generalizability of our findings to other ethnic populations. Another important limitation is the inclusion of only 2 studies evaluating EAT thickness and other subgroup parameters. The interpretation of results is limited by this methodology because of the potential lack of power and the inability to draw firm conclusions. Importantly, we noted that when more robust statistical methods were applied when few studies were pooled, statistical significance was reversed, highlighting the need for more data in these areas. We noted a significant degree of heterogeneity, a limitation that has been demonstrated in other published EAT meta-analyses that report I^2 values >90%.[1,47] This is probably in part representative of variable EAT quantification methods and differing measures of EAT as a covariate in regression analyses. We attempted to adjust for this heterogeneity by systematic exclusion of studies that did not significantly attenuate the summary estimates from statistical significance and by sensitivity analysis by subgroup analysis and exploratory metaregression.

Table 4. Sensitivity Analysis of Random-Effects Meta-Analysis With Alternative Methods When Pooled Estimates Were From Combination of 2 Studies

Variable	Random-Effects Method	Pooled OR	95% CI	*P* Value
EAT measurement method				
EAT thickness[27,28]	DL	3.09	0.56–17.01	0.20
	HKSJ	3.09	0–19	0.49
Covariate modeling method				
EAT continuous[21,24]	DL	1.18	0.77–1.81	0.44
	HKSJ	1.18	0.08–18.5	0.58
EAT per 10 mL[25,26]	DL	1.18	1.12–1.24	<0.01
	HKSJ	1.18	0.96–1.45	0.06*
HRP subtype				
LAP[23,24]	DL	2.79	1.71–4.53	<0.01
	HKSJ	2.79	0.59–13.2	0.08*
PR[23,24]	DL	1.93	1.25–2.99	0.003
	HKSJ	1.93	0.77–4.84	0.07*
Both LAP and PR[23,24]	DL	2.58	1.55–4.28	<0.01
	HKSJ	2.58	2.34–2.83	0.005

References indicate studies that were pooled. ORs are presented using DL and HKSJ methods. CI indicates confidence interval; DL, DerSimonian and Laird; EAT, epicardial adipose tissue; HKSJ, Hartung–Knapp–Sidik–Jonkman; HRP, high-risk plaque; LAP, low attenuation plaque; OR, odds ratio; PR, positive remodeling.
*Signifies when there was a change in *P* value resulting in statistical nonsignificance (*P*>0.05) after applying the HKSJ method.

Conclusion

Increasing EAT is associated with the presence of HRP, ideally, when measured by complete volumetric analysis. Further investigation is still required to establish the role of EAT-t in evaluating HRP and consistent methods for modeling EAT as a variable for disease outcomes and the effect of EAT on individual HRP features. Incorporating the measurement of EAT into clinically performed CT coronary angiography has the potential to improve patient risk stratification. Further prospective studies are needed to confirm this finding, which holds potential as a novel therapeutic target for atherosclerotic treatment.

Disclosures

None.

Funding

Dr. Nerlekar is supported by the National Health and Medical Research Council of Australia and National Heart Foundation Scholarship. Dr Brown is supported through a Monash University Early Career Practitioner Fellowship.

References

1. Xu Y, Cheng X, Hong K, Huang C, Wan L. How to interpret epicardial adipose tissue as a cause of coronary artery disease: a meta-analysis. *Coron Artery Dis*. 2012;23:227–233.
2. Talman AH, Psaltis PJ, Cameron JD, Meredith IT, Seneviratne SK, Wong DT. Epicardial adipose tissue: far more than a fat depot. *Cardiovasc Diagn Ther*. 2014;4:416–429.
3. Sacks HS, Fain JN. Human epicardial adipose tissue: a review. *Am Heart J*. 2007;153:907–917.
4. Fitzgibbons TP, Czech MP. Epicardial and perivascular adipose tissues and their influence on cardiovascular disease: basic mechanisms and clinical associations. *J Am Heart Assoc*. 2014;3:e000582. DOI: 10.1161/JAHA.113.000582.
5. Psaltis PJ, Talman AH, Munnur K, Cameron JD, Ko BS, Meredith IT, Seneviratne SK, Wong DT. Relationship between epicardial fat and quantitative coronary artery plaque progression: insights from computer tomography coronary angiography. *Int J Cardiovasc Imaging*. 2016;32:317–328.
6. Rosito GA, Massaro JM, Hoffmann U, Ruberg FL, Mahabadi AA, Vasan RS, O'Donnell CJ, Fox CS. Pericardial fat, visceral abdominal fat, cardiovascular disease risk factors, and vascular calcification in a community-based sample: the Framingham Heart Study. *Circulation*. 2008;117:605–613.
7. Shimabukuro M, Hirata Y, Tabata M, Dagvasumberel M, Sato H, Kurobe H, Fukuda D, Soeki T, Kitagawa T, Takanashi S, Sata M. Epicardial adipose tissue volume and adipocytokine imbalance are strongly linked to human coronary atherosclerosis. *Arterioscler Thromb Vasc Biol*. 2013;33:1077–1084.
8. Ding J, Hsu FC, Harris TB, Liu Y, Kritchevsky SB, Szklo M, Ouyang P, Espeland MA, Lohman KK, Criqui MH, Allison M, Bluemke DA, Carr JJ. The association of pericardial fat with incident coronary heart disease: the Multi-Ethnic Study of Atherosclerosis (MESA). *Am J Clin Nutr*. 2009;90:499–504.
9. Prati F. Eccentric atherosclerotic plaques with positive remodelling have a pericardial distribution: a permissive role of epicardial fat? A three-dimensional intravascular ultrasound study of left anterior descending artery lesions. *Eur Heart J*. 2003;24:329–336.
10. Motoyama S, Ito H, Sarai M, Kondo T, Kawai H, Nagahara Y, Harigaya H, Kan S, Anno H, Takahashi H, Naruse H, Ishii J, Hecht H, Shaw LJ, Ozaki Y, Narula J. Plaque characterization by coronary computed tomography angiography and the likelihood of acute coronary events in mid-term follow-up. *J Am Coll Cardiol*. 2015;66:337–346.
11. Stone GW, Maehara A, Lansky AJ, de Bruyne B, Cristea E, Mintz GS, Mehran R, McPherson J, Farhat N, Marso SP, Parise H, Templin B, White R, Zhang Z, Serruys PW; Investigators P. A prospective natural-history study of coronary atherosclerosis. *N Engl J Med*. 2011;364:226–235.
12. Nakazato R, Otake H, Konishi A, Iwasaki M, Koo BK, Fukuya H, Shinke T, Hirata K, Leipsic J, Berman DS, Min JK. Atherosclerotic plaque characterization by ct angiography for identification of high-risk coronary artery lesions: a comparison to optical coherence tomography. *Eur Heart J Cardiovasc Imaging*. 2015;16:373–379.
13. Marwan M, Taher MA, El Meniawy K, Awadallah H, Pflederer T, Schuhback A, Ropers D, Daniel WG, Achenbach S. In vivo CT detection of lipid-rich coronary artery atherosclerotic plaques using quantitative histogram analysis: a head to head comparison with IVUS. *Atherosclerosis*. 2011;215:110–115.
14. Gauss S, Achenbach S, Pflederer T, Schuhback A, Daniel WG, Marwan M. Assessment of coronary artery remodelling by dual-source CT: a head-to-head comparison with intravascular ultrasound. *Heart*. 2011;97:991–997.
15. Wan X, Wang W, Liu J, Tong T. Estimating the sample mean and standard deviation from the sample size, median, range and/or interquartile range. *BMC Med Res Methodol*. 2014;14:135.
16. DerSimonian R, Laird N. Meta-analysis in clinical trials. *Control Clin Trials*. 1986;7:177–188.
17. Higgins JP, Thompson SG, Deeks JJ, Altman DG. Measuring inconsistency in meta-analyses. *BMJ*. 2003;327:557–560.
18. IntHout J, Ioannidis JP, Borm GF. The Hartung-Knapp-Sidik-Jonkman method for random effects meta-analysis is straightforward and considerably outperforms the standard DerSimonian-Laird method. *BMC Med Res Methodol*. 2014;14:25.
19. Rover C, Knapp G, Friede T. Hartung-Knapp-Sidik-Jonkman approach and its modification for random-effects meta-analysis with few studies. *BMC Med Res Methodol*. 2015;15:99.
20. Harada K, Harada K, Uetani T, Kataoka T, Takeshita M, Kunimura A, Takayama Y, Shinoda N, Kato B, Kato M, Marui N, Ishii H, Matsubara T, Amano T, Murohara T. The different association of epicardial fat with coronary plaque in patients with acute coronary syndrome and patients with stable angina pectoris: analysis using integrated backscatter intravascular ultrasound. *Atherosclerosis*. 2014;236:301–306.

21. Lu MT, Park J, Ghemigian K, Mayrhofer T, Puchner SB, Liu T, Fleg JL, Udelson JE, Truong QA, Ferencik M, Hoffmann U. Epicardial and paracardial adipose tissue volume and attenuation—association with high-risk coronary plaque on computed tomographic angiography in the ROMICAT II trial. *Atherosclerosis*. 2016;251:47–54.
22. Schlett CL, Ferencik M, Kriegel MF, Bamberg F, Ghoshhajra BB, Joshi SB, Nagurney JT, Fox CS, Truong QA, Hoffmann U. Association of pericardial fat and coronary high-risk lesions as determined by cardiac CT. *Atherosclerosis*. 2012;222:129–134.
23. Oka T, Yamamoto H, Ohashi N, Kitagawa T, Kunita E, Utsunomiya H, Yamazato R, Urabe Y, Horiguchi J, Awai K, Kihara Y. Association between epicardial adipose tissue volume and characteristics of non-calcified plaques assessed by coronary computed tomographic angiography. *Int J Cardiol*. 2012;161:45–49.
24. Rajani R, Shmilovich H, Nakazato R, Nakanishi R, Otaki Y, Cheng VY, Hayes SW, Thomson LE, Friedman JD, Slomka PJ, Min JK, Berman DS, Dey D. Relationship of epicardial fat volume to coronary plaque, severe coronary stenosis, and high-risk coronary plaque features assessed by coronary CT angiography. *J Cardiovasc Comput Tomogr*. 2013;7:125–132.
25. Ito T, Suzuki Y, Ehara M, Matsuo H, Teramoto T, Terashima M, Nasu K, Kinoshita Y, Tsuchikane E, Suzuki T, Kimura G. Impact of epicardial fat volume on coronary artery disease in symptomatic patients with a zero calcium score. *Int J Cardiol*. 2013;167:2852–2858.
26. Nakanishi K, Fukuda S, Tanaka A, Otsuka K, Taguchi H, Yoshikawa J, Shimada K. Epicardial adipose tissue accumulation is associated with renal dysfunction and coronary plaque morphology on multidetector computed tomography. *Circ J*. 2016;80:196–201.
27. Tachibana M, Miyoshi T, Osawa K, Toh N, Oe H, Nakamura K, Naito T, Sato S, Kanazawa S, Ito H. Measurement of epicardial fat thickness by transthoracic echocardiography for predicting high-risk coronary artery plaques. *Heart Vessels*. 2016;31:1758–1766.
28. Park JS, Choi SY, Zheng M, Yang HM, Lim HS, Choi BJ, Yoon MH, Hwang GS, Tahk SJ, Shin JH. Epicardial adipose tissue thickness is a predictor for plaque vulnerability in patients with significant coronary artery disease. *Atherosclerosis*. 2013;226:134–139.
29. Ito T, Nasu K, Terashima M, Ehara M, Kinoshita Y, Ito T, Kimura M, Tanaka N, Habara M, Tsuchikane E, Suzuki T. The impact of epicardial fat volume on coronary plaque vulnerability: insight from optical coherence tomography analysis. *Eur Heart J Cardiovasc Imaging*. 2012;13:408–415.
30. Yamashita K, Yamamoto MH, Ebara S, Okabe T, Saito S, Hoshimoto K, Yakushiji T, Isomura N, Araki H, Obara C, Ochiai M. Association between increased epicardial adipose tissue volume and coronary plaque composition. *Heart Vessels*. 2014;29:569–577.
31. Iacobellis G. Local and systemic effects of the multifaceted epicardial adipose tissue depot. *Nat Rev Endocrinol*. 2015;11:363–371.
32. Nov O, Shapiro H, Ovadia H, Tarnovscki T, Dvir I, Shemesh E, Kovsan J, Shelef I, Carmi Y, Voronov E, Apte RN, Lewis E, Haim Y, Konrad D, Bashan N, Rudich A. Interleukin-1beta regulates fat-liver crosstalk in obesity by auto-paracrine modulation of adipose tissue inflammation and expandability. *PLoS One*. 2013;8:e53626.
33. Bo X, Ma L, Fan J, Jiang Z, Zhou Y, Zhang L, Li W. Epicardial fat volume is correlated with coronary lesion and its severity. *Int J Clin Exp Med*. 2015;8:4328–4334.
34. Mazurek T, Zhang L, Zalewski A, Mannion JD, Diehl JT, Arafat H, Sarov-Blat L, O'Brien S, Keiper EA, Johnson AG, Martin J, Goldstein BJ, Shi Y. Human epicardial adipose tissue is a source of inflammatory mediators. *Circulation*. 2003;108:2460–2466.
35. Larsen BA, Laughlin GA, Saad SD, Barrett-Connor E, Allison MA, Wassel CL. Pericardial fat is associated with all-cause mortality but not incident CVD: the Rancho Bernardo Study. *Atherosclerosis*. 2015;239:470–475.
36. Saura DO, Oliva MJ, Rodriguez D, Pascual-Figal DA, Hurtado JA, Pinar E, de la Morena G, Valdes M. Reproducibility of echocardiographic measurements of epicardial fat thickness. *Int J Cardiol*. 2010;141:311–312.
37. Hirata Y, Yamada H, Kusunose K, Iwase T, Nishio S, Hayashi S, Bando M, Amano R, Yamaguchi K, Soeki T, Wakatsuki T, Sata M. Clinical utility of measuring epicardial adipose tissue thickness with echocardiography using a high-frequency linear probe in patients with coronary artery disease. *J Am Soc Echocardiogr*. 2015;28:1240–1246.e1241.
38. Bucher AM, Joseph Schoepf U, Krazinski AW, Silverman J, Spearman JV, De Cecco CN, Meinel FG, Vogl TJ, Geyer LL. Influence of technical parameters on epicardial fat volume quantification at cardiac CT. *Eur J Radiol*. 2015;84:1062–1067.
39. Tanami Y, Jinzaki M, Kishi S, Matheson M, Vavere AL, Rochitte CE, Dewey M, Chen MY, Clouse ME, Cox C, Kuribayashi S, Lima JA, Arbab-Zadeh A. Lack of association between epicardial fat volume and extent of coronary artery calcification, severity of coronary artery disease, or presence of myocardial perfusion abnormalities in a diverse, symptomatic patient population: results from the CORE320 multicenter study. *Circ Cardiovasc Imaging*. 2015;8:e002676.
40. Muthalaly RG, Nerlekar N, Wong DT, Cameron JD, Seneviratne SK, Ko BS. Epicardial adipose tissue and myocardial ischemia assessed by computed tomography perfusion imaging and invasive fractional flow reserve. *J Cardiovasc Comput Tomogr*. 2017;11:46–53.
41. Guyatt GH, Oxman AD, Kunz R, Brozek J, Alonso-Coello P, Rind D, Devereaux PJ, Montori VM, Freyschuss B, Vist G, Jaeschke R, Williams JW Jr, Murad MH, Sinclair D, Falck-Ytter Y, Meerpohl J, Whittington C, Thorlund K, Andrews J, Schunemann HJ. Grade guidelines 6. Rating the quality of evidence—imprecision. *J Clin Epidemiol*. 2011;64:1283–1293.
42. Guyatt GH, Oxman AD, Kunz R, Woodcock J, Brozek J, Helfand M, Alonso-Coello P, Glasziou P, Jaeschke R, Akl EA, Norris S, Vist G, Dahm P, Shukla VK, Higgins J, Falck-Ytter Y, Schunemann HJ. Grade guidelines: 7. Rating the quality of evidence—inconsistency. *J Clin Epidemiol*. 2011;64:1294–1302.
43. Guyatt GH, Oxman AD, Vist G, Kunz R, Brozek J, Alonso-Coello P, Montori V, Akl EA, Djulbegovic B, Falck-Ytter Y, Norris SL, Williams JW Jr, Atkins D, Meerpohl J, Schunemann HJ. Grade guidelines: 4. Rating the quality of evidence—study limitations (risk of bias). *J Clin Epidemiol*. 2011;64:407–415.
44. Nakanishi K, Fukuda S, Tanaka A, Otsuka K, Jissho S, Taguchi H, Yoshikawa J, Shimada K. Persistent epicardial adipose tissue accumulation is associated with coronary plaque vulnerability and future acute coronary syndrome in non-obese subjects with coronary artery disease. *Atherosclerosis*. 2014;237:353–360.
45. Rabkin SW, Campbell H. Comparison of reducing epicardial fat by exercise, diet or bariatric surgery weight loss strategies: a systematic review and meta-analysis. *Obes Rev*. 2015;16:406–415.
46. McKenney ML, Schultz KA, Boyd JH, Byrd JP, Alloosh M, Teague SD, Arce-Esquivel AA, Fain JN, Laughlin MH, Sacks HS, Sturek M. Epicardial adipose excision slows the progression of porcine coronary atherosclerosis. *J Cardiothorac Surg*. 2014;9:2.
47. Rabkin SW. The relationship between epicardial fat and indices of obesity and the metabolic syndrome: a systematic review and meta-analysis. *Metab Syndr Relat Disord*. 2014;12:31–42.

SUPPLEMENTAL MATERIAL

Table S1. Example search strategy (Embase)

#	Searches	Results
1	Epicardial adipose tissue.mp.	1249
2	Epicardial fat.mp.	1481
3	Pericardial adipose tissue.mp	161
4	Pericardial fat.mp	550
5	Vulnerable plaque.mp	2196
6	High risk plaque.mp	288
7	Low attenuation plaque.mp	101
8	Napkin ring.mp	94
9	Positive remodelling	125
10	Spotty calcification	170
11	Plaque characteristics	1228
12	Plaque composition	1734
13	Plaque vulnerability	1745
14	Thin cap fibroatheroma	773
15	Necrotic core	2091
16	Exp intravascular ultrasound/	12695
17	Exp optical coherence tomography/	36156
18	Exp computer assisted tomography/	778928
19	Computed tomography coronary angiography.mp	1140
20	Cardiac computed tomography.mp	2526
21	Exp coronary artery calcium score	3230
22	Exp coronary angiography/	2916
23	1 or 2 or 3 or 4	2877
24	5 or 6 or 7 or 8 or 9 or 10 or 11 or 12 or 13 or 14 or 15	7800
25	16 or 17 or 22	51500
26	18 or 19 or 20 or 21	779979
27	23 and 24 and 25	26
28	23 and 24 and 26	57

Table S2. Study EAT measurement parameters and HRP definitions

Author	EAT measure method	Definition of HRP features
Lu et al.[1]	EAT definition: fat within pericardial sac. Method: Semi-automated. Software: Volume Viewer, Siemens Medical Solutions, Germany Interval: 1cm Superior border: mid-level RPA Inferior border: diaphragm HU range: -195 to -45 HU	PR: RI of >1.1 maximal outer vessel diameter at plaque divided by average of the proximal and distal normal vessels LAP: <30 HU SpC: <3mm CP extending <1.5mm long-axis vessel diameter & two-thirds vessel circumference NRS: ring of peripheral high attenuation surrounded by core of low attenuation in a non-calcified plaque
Schlett et al.[2]	EAT definition: fat within pericardial sac. Method: Manual Software: Leonardo, Siemens Medical Solutions Interval: 1cm Superior border: mid-level RPA. Inferior border: not specified. HU range: -190 to -30 HU	PR: >1.05 remodelling index LAP: <30 HU SC: <3mm diameter CP HRP defined as at least 2 characteristics in lesions>50% luminal narrowing
Rajani et al.[3]	EAT definition: fat within pericardial sac. Method: Semi-automated Software: QFAT, Cedars-Sinai Medical Centre Interval: 3mm (total 20-40 slices per pt) Superior border: RPA take-off Inferior border: First slice where PDA visualised HU range: -190 to -30 HU	LAP: <30 HU PR: >1.05 (maximal outer arterial wall diameter along plaque exceeding proximal reference by 5%
Oka et al.[4]	EAT definition: adipose tissue between epicardial surface of myocardium and pericardium Method: Manual Software: Not specified. VAT measured with Virtual Place, AZE Inc., Japan Interval: 1cm Superior border: 1cm above left main coronary artery (atrial appendage) Inferior border: cardiac apex HU range: -250 to -30 HU	CT-low density plaque: < 39 HU PR: remodelling index >1.05 SpC: calcium burden length <3/2 vessel diameter and width <2/3 vessel diameter
Ito et al.[5]	EAT definition: adipose tissue within the visceral epicardium Method: Manual Software: Not specified Interval: Not specified. 8-12 slices per patient Superior border: Mid left atrium Inferior border: left ventricular apex HU range: -190 to -30 HU	LAP: <30 HU PR: RI >1.1 (ratio of outer vessel area of lesion to outer vessel area of proximal reference site
Nakanishi et al.[6]	EAT definition: adipose tissue within the pericardial sac Method: Semi-automated Software: Synapse Vincent, Japan Interval: not specified. 7-10 planes Superior border: bifurcation pulmonary artery Inferior border: last slice containing any portion of the heart HU range: -250 to -30 HU	LAP: <30 HU PR: RI >1.1
Ito et al.[7]	EAT definition: adipose tissue within the visceral epicardium Method: Manual Software: Not specified. CT with Aquarius NetStation, USA Interval: not specified. Superior border: not specified Inferior border: not specified HU range: -250 to -40 HU	**CT:** LAP: <30 HU PR: RI >1.1 (ratio of outer vessel area of lesion to outer area of proximal reference site) **OCT:** Necrotic lipid pools quantified as number of quadrants Cap thickness measured at thinnest section of distance from lumen to inner border of lipid pool. TCFA = plaque with necrotic lipid pool in ≥2 quadrants within a plaque and fibrous cap <=65μm

Park et al.[8]	Method: 2D parasternal long-axis view; point on the free wall of RV to assess anterior echo-lucent space between linear echo-dense parietal pericardium and RV epicardium Cardiac cycle timing: End-diastole. Thickest point of EAT in each of 3 cycles measured and average value used	Plaque components: Fibrous – areas of dense collagen Fibrofatty – fibrous tissue with interspersed lipid in collagen Dense calcium – calcium with no adjacent necrosis Necrotic core – necrotic regions containing cholesterol clefts, foam cells, microcalcification TCFA: necrotic core ≥10% plaque area without overlying fibrous tissue and having >40% plaque burden in 3 consecutive frames
Tachibana et al.[9]	Method: 2D parasternal long-axis view; point on the free wall of RV along midline of ultrasound beam perpendicular to aortic annulus Cardiac cycle timing: End-systole. Average of three cardiac cycles used	PR: RI >1.05 (cross sectional lesion vessel area divided by proximal reference vessel area) LAP: <30 HU

CT – computed tomography, CP – calcified plaque, EAT – epicardial adipose tissue, HRP – high risk plaque, HU – Hounsfield units, LAP – low attenuation plaque, NRS – napkin ring sign, OCT – optical coherence tomogprahy, PDA – posterior descending artery, PR – positive remodelling, RPA – right pulmonary artery, SpC – spotty calcification, TCFA – thin-cap fibroatheroma. VAT – visceral adipose tissue

Table S3. Sensitivity analysis displaying pooled odds ratios and 95% confidence intervals with systematic exclusion of individual studies.

Excluded study	Pooled OR	Lower 95% CI	Upper 95% CI	I^2	p-value
Lu et al[1]	1.27	1.12	1.45	70%	<0.001
Schlett et al.[2]	1.17	1.06	1.30	80%	0.003
Rajani et al.[3]	1.19	1.07	1.33	82%	0.001
Oka et al.[4]	1.20	1.07	1.33	82%	0.001
Ito et al.[5]	1.24	1.08	1.43	78%	0.003
Nakanishi et al.[6]	1.24	1.09	1.42	82%	0.002
Park et al.[8]	1.25	1.09	1.43	83%	0.001
Ito et al.[7]	1.19	1.07	1.32	81%	0.001
Tachibana et al.[9]	1.16	1.06	1.27	74%	0.001

Table S4. Newcastle-Ottawa Scale (NOS) Evaluation of Study Quality

STUDY	SELECTION	COMPARABILITY	OUTCOME
Lu et al.[1]	****	**	***
Schlett et al. [2]	****	**	***
Rajani et al. [3]	*****	**	***
Oka et al.[4]	****	**	***
Ito et al.[5]	****	**	***
Nakanishi et al.[6]	***	**	***
Park et al.[8]	****	**	***
Ito et al.[7]	***	**	***
Tachibana et al [9]	****	**	**

The Newcastle-Ottawa Scale (NOS) evaluates the included studies based on selection, comparability and outcome. The maximum score for each criteria is 5, 2 and 3, respectively, with the maximum total score equalling 10

Table S5. GRADE quality assessment

STUDY	INITIAL GRADE	BIAS ASSESSMENT	FINAL GRADE
Lu et al.[1]	Low	**Bias**: Low; **Applicability**: Low; **Imprecision**: Low	Low
Schlett et al.[2]	Low	**Bias**: Low; **Applicability**: Low; **Imprecision**: High	Low
Rajani et al.[3]	Low	**Bias**: Low; **Applicability**: Low; **Imprecision**: Low	Low
Oka et al. [4]	Low	**Bias**: Unclear; **Applicability**: Low; **Imprecision**: High	Low
Ito et al. [5]	Low	**Bias**: Unclear; **Applicability**: Low; **Imprecision**: Low	Low
Nakanishi et al[6]	Low	**Bias**: Unclear; **Applicability**: High; **Imprecision**: Low	Low
Park et al.	Low	**Bias**: Unclear; **Applicability**: Unclear; **Imprecision**: Unclear	Low
Ito (2012) et al.	Low	**Bias**: Unclear; **Applicability**: Low; **Imprecision**: Unclear	Low
Tachibana et al	Low	**Bias**: High; **Applicability**: Unclear; **Imprecision**: High	Very Low

GRADE classification adapted from the GRADE Handbook [10-12] to evaluate quality of evidence in observational studies. All studies are observational and therefore considered of low quality. Assessment based on bias (factors including eligibility criteria, control of confounding), applicability (assessment of intervention) and imprecision (assessment of modelling methods and outcomes). Assessment is graded as either a low risk of bias, high risk of bias or unclear risk of bias.

Figure S1. Funnel plot

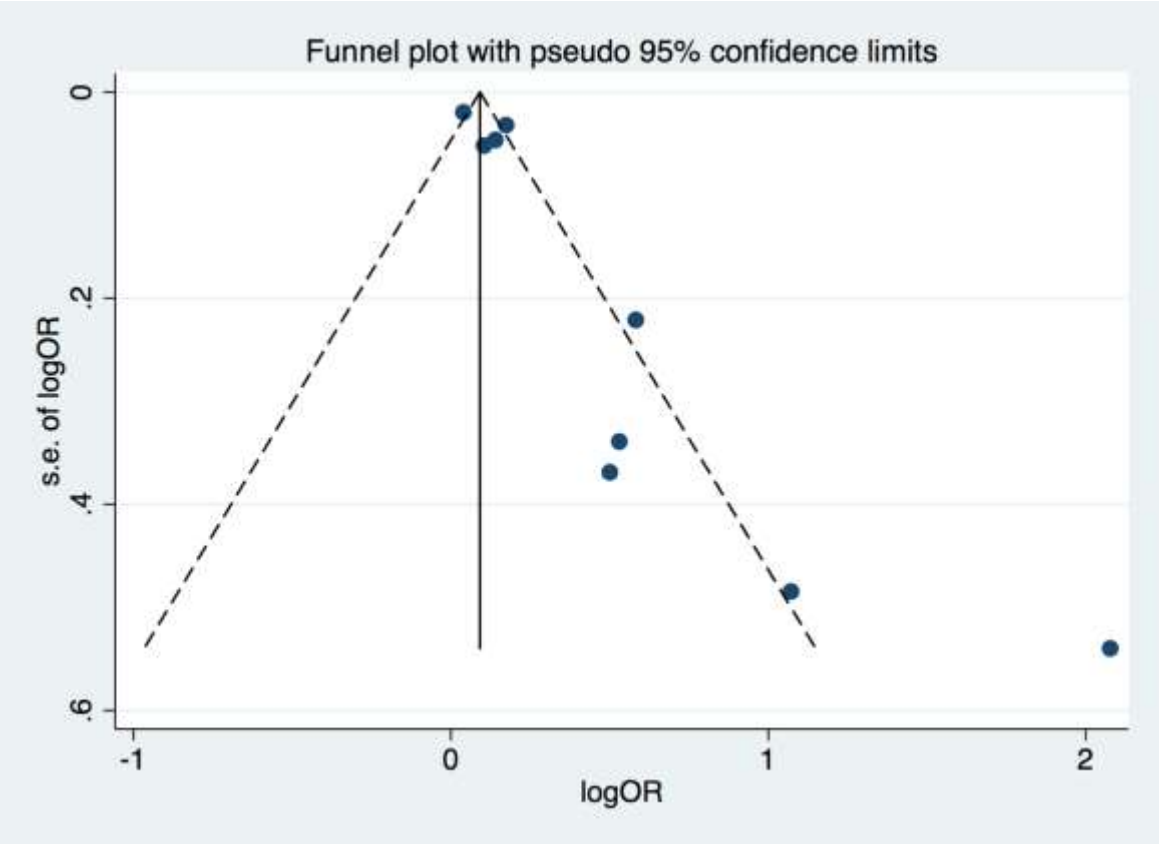

Egger's test for small study effects: p = 0.005

Overall summary estimate using trim and fill method: 1.13 (95% CI 1.03-1.28, p=0.04, I^2=81%)

Supplemental References:

1. Lu MT, Park J, Ghemigian K, Mayrhofer T, Puchner SB, Liu T, Fleg JL, Udelson JE, Truong QA, Ferencik M, Hoffmann U. Epicardial and paracardial adipose tissue volume and attenuation - association with high-risk coronary plaque on computed tomographic angiography in the romicat ii trial. *Atherosclerosis*. 2016;251:47-54.

2. Schlett CL, Ferencik M, Kriegel MF, Bamberg F, Ghoshhajra BB, Joshi SB, Nagurney JT, Fox CS, Truong QA, Hoffmann U. Association of pericardial fat and coronary high-risk lesions as determined by cardiac ct. *Atherosclerosis*. 2012;222:129-134.

3. Rajani R, Shmilovich H, Nakazato R, Nakanishi R, Otaki Y, Cheng VY, Hayes SW, Thomson LE, Friedman JD, Slomka PJ, Min JK, Berman DS, Dey D. Relationship of epicardial fat volume to coronary plaque, severe coronary stenosis, and high-risk coronary plaque features assessed by coronary ct angiography. *J Cardiovasc Comput Tomogr*. 2013;7:125-132.

4. Oka T, Yamamoto H, Ohashi N, Kitagawa T, Kunita E, Utsunomiya H, Yamazato R, Urabe Y, Horiguchi J, Awai K, Kihara Y. Association between epicardial adipose tissue volume and characteristics of non-calcified plaques assessed by coronary computed tomographic angiography. *Int J Cardiol*. 2012;161:45-49.

5. Ito T, Suzuki Y, Ehara M, Matsuo H, Teramoto T, Terashima M, Nasu K, Kinoshita Y, Tsuchikane E, Suzuki T, Kimura G. Impact of epicardial fat volume on coronary artery disease in symptomatic patients with a zero calcium score. *Int J Cardiol*. 2013;167:2852-2858.

6. Nakanishi K, Fukuda S, Tanaka A, Otsuka K, Taguchi H, Yoshikawa J, Shimada K. Epicardial adipose tissue accumulation is associated with renal dysfunction and coronary plaque morphology on multidetector computed tomography. *Circ J*. 2016;80:196-201.

7. Ito T, Nasu K, Terashima M, Ehara M, Kinoshita Y, Ito T, Kimura M, Tanaka N, Habara M, Tsuchikane E, Suzuki T. The impact of epicardial fat volume on coronary plaque vulnerability: Insight from optical coherence tomography analysis. *Eur Heart J Cardiovasc Imaging*. 2012;13:408-415.

8. Park JS, Choi SY, Zheng M, Yang HM, Lim HS, Choi BJ, Yoon MH, Hwang GS, Tahk SJ, Shin JH. Epicardial adipose tissue thickness is a predictor for plaque vulnerability in patients with significant coronary artery disease. *Atherosclerosis*. 2013;226:134-139

9. Tachibana M, Miyoshi T, Osawa K, Toh N, Oe H, Nakamura K, Naito T, Sato S, Kanazawa S, Ito H. Measurement of epicardial fat thickness by transthoracic echocardiography for predicting high-risk coronary artery plaques. *Heart Vessels*. 2016;31:1758-1766.

10. Guyatt GH, Oxman AD, Kunz R, Brozek J, Alonso-Coello P, Rind D, Devereaux PJ, Montori VM, Freyschuss B, Vist G, Jaeschke R, Williams JW, Jr., Murad MH, Sinclair D, Falck-Ytter Y, Meerpohl J, Whittington C, Thorlund K, Andrews J, Schunemann HJ. Grade guidelines 6. Rating the quality of evidence--imprecision. *J. Clin. Epidemiol.* 2011;64:1283-1293.

11. Guyatt GH, Oxman AD, Kunz R, Woodcock J, Brozek J, Helfand M, Alonso-Coello P, Glasziou P, Jaeschke R, Akl EA, Norris S, Vist G, Dahm P, Shukla VK, Higgins J, Falck-Ytter Y, Schunemann HJ. Grade guidelines: 7. Rating the quality of evidence--inconsistency. *J Clin Epidemiol.* 2011;64:1294-1302.

12. Guyatt GH, Oxman AD, Vist G, Kunz R, Brozek J, Alonso-Coello P, Montori V, Akl EA, Djulbegovic B, Falck-Ytter Y, Norris SL, Williams JW, Jr., Atkins D, Meerpohl J, Schunemann HJ. Grade guidelines: 4. Rating the quality of evidence--study limitations (risk of bias). *J. Clin. Epidemiol.* 2011;64:407-415.

SYSTEMATIC REVIEW AND META-ANALYSIS

Association of Volumetric Epicardial Adipose Tissue Quantification and Cardiac Structure and Function

Nitesh Nerlekar, MBBS, MPH; Rahul G. Muthalaly, MBBS; Nathan Wong, MBBS; Udit Thakur, MBBS; Dennis T. L. Wong, MD, PhD; Adam J. Brown, MD, PhD; Thomas H. Marwick, MBBS, MPH, PhD

***Background*—**Epicardial adipose tissue (EAT) is in immediate apposition to the underlying myocardium and, therefore, has the potential to influence myocardial systolic and diastolic function or myocardial geometry, through paracrine or compressive mechanical effects. We aimed to review the association between volumetric EAT and markers of myocardial function and geometry.

***Methods and Results*—**PubMed, Medline, and Embase were searched from inception to May 2018. Studies were included only if complete EAT volume or mass was reported and related to a measure of myocardial function and/or geometry. Meta-analysis and meta-regression were used to evaluate the weighted mean difference of EAT in patients with and without diastolic dysfunction. Heterogeneity of data reporting precluded meta-analysis for systolic and geometric associations. In the 22 studies included in the analysis, there was a significant correlation with increasing EAT and presence of diastolic dysfunction and mean e′ (average mitral annular tissue Doppler velocity) and E/e′ (early inflow / annular velocity ratio) but not E/A (ratio of peak early (E) and late (A) transmitral inflow velocities), independent of adiposity measures. There was a greater EAT in patients with diastolic dysfunction (weighted mean difference, 24.43 mL; 95% confidence interval, 18.5–30.4 mL; $P<0.001$), and meta-regression confirmed the association of increasing EAT with diastolic dysfunction ($P=0.001$). Reported associations of increasing EAT with increasing left ventricular mass and the inverse correlation of EAT with left ventricular ejection fraction were inconsistent, and not independent from other adiposity measures.

***Conclusions*—**EAT is associated with diastolic function, independent of other influential variables. EAT is an effect modifier for chamber size but not systolic function. **(*J Am Heart Assoc*. 2018;7:e009975. DOI: 10.1161/JAHA.118.009975.)**

Key Words: diastolic function • epicardial fat • systolic dysfunction

Epicardial adipose tissue (EAT) has been widely studied as a potential contributor to cardiovascular pathological characteristics. Much of this research has focused on its effect on coronary atherosclerosis,[1] but there are unique properties of EAT that may lead to an effect on myocardial function. EAT shares direct anatomic contact with the myocardium without fascial interruption[2] and, therefore, may exhibit local compressive forces, resulting in alteration of myocardial function and geometry. In addition, the shared blood supply of the coronary circulation to both the myocardium and surrounding EAT may predispose paracrine effects on the neighboring myocardium with such inflammatory cytokines as MCP-1 (monocyte chemoattractant), interleukin-β, interleukin-6, tumor necrosis factor-α, and leptin.[2] Persisting inflammation may lead to collagen deposition and subsequent impaired left ventricular (LV) relaxation and further effects on diastolic and systolic function. Furthermore, there is an association between EAT and release of free fatty acids, as well as their myocardial consumption.[3] The relationship between obesity, visceral fat, and EAT may also explain effects on myocardial function, chamber size, and mass.

Several methods have been used for measurement of EAT, including echocardiography, cardiac computed tomography (CT), and cardiac magnetic resonance imaging (MRI). Echocardiography may overestimate or underestimate total EAT volume because of single-plane assessment and the effects of probe angulation on linear measurement. Single-slice area measurements on CT or MRI are also limited by being only single-plane measures. Recently, we have demonstrated the

From the Monash Cardiovascular Research Centre, Department of Medicine (Monash Medical Centre), Monash University and Monash Heart, Monash Health, Clayton, Australia (N.N., R.G.M., N.W., U.T., D.T.L.W., A.J.B.); Baker Heart and Diabetes Institute, Melbourne, Australia (N.N., T.H.M.); and South Australian Health and Medical Research Institute, Adelaide, Australia (D.T.L.W.).

Accompanying Tables S1 through S3 are available at https://www.ahajournals.org/doi/suppl/10.1161/JAHA.118.009975

Correspondence to: Thomas H. Marwick, MBBS, MPH, PhD, Baker Heart and Diabetes Institute, 75 Commercial Rd, Melbourne, Victoria 3004, Australia. E-mail: [redacted]

Received May 31, 2018; accepted October 3, 2018.

Clinical Perspective

What Is New?

- Increasing epicardial adipose tissue volume is associated with diastolic dysfunction, independent of other markers of adiposity.
- Epicardial adipose tissue is an effect modifier for left ventricle chamber geometry.
- Epicardial adipose tissue is not associated with systolic function.

What Are the Clinical Implications?

- Epicardial adipose tissue may represent an important target for therapy associated with diastolic dysfunction.

superiority of volumetric EAT assessment in comparison to 2-dimensional linear echocardiographic EAT thickness.[4] We, therefore, sought the association of full-volume quantification of EAT (assessed by cardiac CT or cardiac MRI) with myocardial function, as assessed by transthoracic echocardiography, full R-R interval cardiac CT, or cardiac MRI.

Methods

Search Method

We conducted this systematic review in accordance with the Preferred Reporting Items for Systematic Reviews and Meta-Analyses (PRISMA) statement, and the trial was registered with PROSPERO (CRD 42017038400). The search was conducted in MEDLINE, EMBASE, and PubMed databases, ending in March 2018. References of eligible articles were hand searched for additional articles. Searches were restricted to human studies, and conference abstracts were included. A study search flowchart is presented in Figure 1, and the specific search term strategy is given in Table S1. The data, analytic methods, and study materials will not be made available to other researchers for purposes of reproducing the results or replicating the procedure.

Our inclusion criteria were as follows: patients undergoing cardiac CT (CT angiography or calcium score) or MRI with volumetric assessment of EAT (either volume or mass), with cardiac imaging for assessment of myocardial function parameters (full cardiac cycle cardiac CT or MRI or echocardiography), or measurement of myocardial geometry (LV mass, LV volumes, and left atrium size) by validated methods.

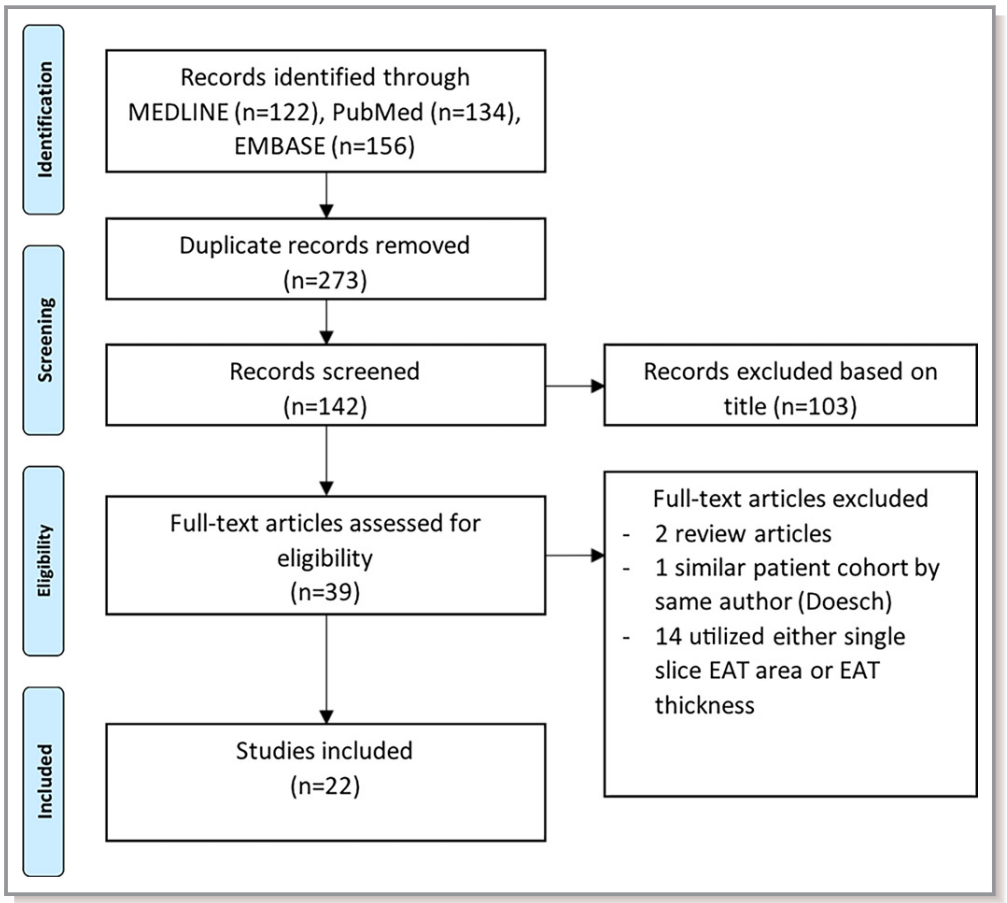

Figure 1. Search strategy. EAT indicates epicardial adipose tissue.

Assessment of diastolic function was restricted to studies using echocardiography. Exclusion criteria included the following: any study with linear measurement of EAT thickness, single-slice area measures of EAT, measures of myocardial lipid content not differentiated from EAT, and measurement of paracardial adipose tissue (ie, fat beyond the parietal pericardium). Two authors (N.N. and R.G.M.) independently reviewed the abstracts from the search to meet the inclusion criteria, and discrepancies were resolved by consensus. Probable overlap of the patient cohort with a similar study led to exclusion of the smaller study.[5]

Evaluation of Full-Volume EAT

EAT was regarded as adipose tissue enclosed within the visceral pericardium, and mean values (indexed and nonindexed) were recorded.

Evaluation of Cardiac Function

Included studies measured myocardial performance based on echocardiography or MRI. Measures of diastolic function included the following: transmitral flow for peak early (E) and late (A) inflow velocities and their ratio (E/A); deceleration time; septal, lateral, and/or average myocardial annular velocities on tissue Doppler imaging (e′); early inflow/annular velocity ratio (E/e′); pulmonary vein flow to calculate the time difference between the atrial reversal wave and mitral A-wave duration; and the isovolumic relaxation time. Diastolic class grade was recorded if reported: normal, grade 1 (impaired relaxation), grade 2 (pseudonormal), and grade 3 (restrictive). Measures of systolic performance assessed included LV ejection fraction, cardiac output, stroke volume, and global longitudinal strain, if recorded. Measures of cardiac structure included LV mass, LV end-diastolic and end-systolic volumes, and left atrial size.

Statistical Analysis

Data on univariable correlations are presented because this was the most consistent measure seen in included studies. Where multivariable regression was performed, adjusted study estimates and model covariates are reported. Meta-analysis was performed for the weighted mean difference in EAT volume between groups with and without diastolic dysfunction. Meta-regression of weighted mean difference as an effect size and the combined mean EAT in included studies were performed with the moment-based estimate of between-study variance and a permutation test using 1000 Monte Carlo simulations to moderate for potentially spurious results, as previously described.[6] Precision of pooled estimates is reported as 95% confidence intervals, and heterogeneity is reported by the I^2 statistic. The Newcastle Ottawa Scale was used to assess risk of bias (Tables S2 and S3). Statistical analysis was performed using StataMP 14.0 (StataCorpLP, College Station, TX).

Results

Study Selection

A brief outline summary of the 22 studies (18 published and 4 conference papers) included in this review is presented in Table 1.[3,7–28]

Association of EAT With LV Diastolic Function

There were 11 studies that investigated the relationship between EAT and diastolic parameters, with 5 specifying adherence to an iteration of the American Society of Echocardiography diastolic guidelines.[29] EAT was associated with diastolic parameters, including peak mitral annular tissue Doppler velocities (e′ septal, e′ lateral, or e′ mean) and transmitral flow (early [E] and late [A] diastolic peak flow velocities and their ratio [E/A]) (Table 2).[9,13–16,18,20–24,29–32] Although some studies did perform comprehensive Doppler measures, such as isovolumic relaxation times, deceleration times, and pulmonary vein Doppler, the association with EAT individually with each parameter was not described. The classification of patients with diastolic dysfunction was available in 5 studies. Most patients (26%–38% of total cohort) had grade 1 diastolic dysfunction, with fewer qualifying as grade ≥2 (2%–28%).

In the 5 studies that measured differences in EAT between groups, EAT was significantly greater in the diastolic dysfunction group compared with patients with normal diastolic function (weighted mean difference, 24.4 mL; 95% confidence interval, 18.5–30.4 mL; $P<0.001$; $I^2=28\%$) (Figure 2).[15,16,20,21,23,26] Meta-regression, performed evaluating the weighted mean difference (effect size) against the mean EAT volume, demonstrated a nominally increasing presence of diastolic dysfunction with increasing EAT values ($\beta=0.17$, SEE=0.09, $P=0.06$). This was statistically significant after Monte Carlo permutation testing, $P=0.001$ (Figure 3).

Mean E/e′ values were positively correlated with EAT (r value range, 0.21–0.34; $P<0.05$), and mean e′ values were inversely correlated (r value range, −0.26 to −0.44; $P<0.05$); in all but one study, no consistent association was seen with the E/A ratio (r value range, −0.40 to 0.08). Increasing EAT was an independent predictor of diastolic dysfunction, e′ and E/e′ independent of age, sex, and measures of adiposity (Table 2). No independent association was identified with the E/A ratio. In 6 studies, hypertension was also an adjusted covariate in the model, and increasing EAT remained a predictor of altered diastolic parameters.

Association of EAT With Systolic Function

Of 10 studies describing the association of EAT with systolic parameters, LV function was evaluated with MRI in 5 and echocardiography in 4 (Table 3).[3,10,11,16,18,19,22,27] One study

DOI: 10.1161/JAHA.118.009975

Table 1. Study Characteristics

First Author	Year	Country	Study Type	Population	Sample Size	EAT Method	EAT Value
Bakkum[8]	2015	the Netherlands	Cross-sectional	Suspected CAD	208	PET-CT	113.8±48.1 cm^3
Cavalcante[9]	2012	United States	Cross-sectional	Self-referred screening	110	MDCT	Men, 101±51 cm^3 Women, 67±40 cm^3
Al Chekakie[7]	2010	United States	Case-control	AF and controls	273	MDCT	Sinus rhythm, 76.1±36.3 mL; AF, 101.6±44.1 mL
Doesch[11]	2012	Germany	Case-control	Established CAD	158 Cases and 40 controls	MRI	Control, 31±8 g/m^2; CAD, 29±10 g/m^2; CAD and EF <50%, 26±8 g/m^2; CAD and EF >50%, 36±11 g/m^2
Doesch[12]	2013	Germany	Case-control	DCM	112 Cases and 48 controls	MRI	Control, 62.1±14.4 g; DCM, 47.2±15.2 g; control, 66±15.3 mL; DCM, 50.2±16.2 mL; control, 31.7±5.6 g/m^2; DCM, 24±7.5 g/m^2; control, 33.5±6.4 mL/m^2; DCM, 25.5±8 mL/m^2
Doesch[10]	2010	Germany	Case-control	CHF (LVEF <35%) (ICM=36; DCM=30)	66 Cases and 31 controls	MRI	Control, 71±13 mL; CHF, 46±11 mL; control, 36±5 mL/m^2; CHF, 24±5 mL/m^2; control, 67±13 g; CHF, 43±11 g; control, 34±4 g/m^2; CHF, 22±5 g/m^2
Ede[13]	2014	Turkey	Cross-sectional	Suspected CAD	106	MDCT	38±31 cm^3
Faustino[14]*	2011	Portugal	Cross-sectional	Not specified	78	MDCT	Threshold of 44.1 mL defined by ROC curve (72% sensitivity and 50% specificity) for diastolic dysfunction
Fernando[15]*	2015	United States	Cross-sectional	AF before ablation	20	MRI	125.7±56.7 mL
Fontes-Carvalho[16]	2014	Portugal	Cross-sectional	Postmyocardial infarction	225	MDCT	113.6±43.2 cm^3
Fox[17]	2009	United States	Cross-sectional	Substudy of Framingham	997	MDCT	Women, 108±41 cm^3; men, 136.5±54.4 cm^3
Hachiya[18]	2014	Japan	Cross-sectional	Suspected CAD	134	MDCT	77.1±29.6 cm^3/m^2
Khawaja[19]	2011	Unites States	Cross-sectional	Suspected CAD	381	MDCT	Normal LVEF, 114.5±98.5 cm^3; LVEF <55%, 83.5±67.1 cm^3
Konishi[20]	2012	Japan	Cross-sectional	Suspected CAD	229	MDCT	Diastolic dysfunction, 184±61 cm^3; normal function, 154±58 cm^3
Lai[21]	2015	Taiwan	Cross-sectional	Self-referred screening	318	MDCT	80.6±33 mL
Liu[22]	2011	United States	Cross-sectional	Blacks	1402	MDCT	Men, 79.8±37.1 mL; women, 67.1±29.0 mL
Longenecker[23]*	2016		Cross-sectional	Patients with HIV	46 HIV+ and 23 HIV−	MDCT	HIV+ with DD, median of 120 (74–143) mL; HIV+ with normal function, median of 72 (54–100) mL; HIV−, not specified

Continued

Table 1. Continued

First Author	Year	Country	Study Type	Population	Sample Size	EAT Method	EAT Value
Ng[24]	2016	Australia	Cross-sectional	Suspected CAD	130	MDCT	Total, 97.5±43.7 cm^3; men, 103.7±39.5 cm^3; women, 90.9±47.4 cm^3
Ruberg[3]	2010	United States	Cross-sectional	Obese with metabolic syndrome	28 Cases and 18 controls	MRI	Controls, 85±66 mL; subjects, 161±88 mL; controls, 1.1±0.7 mL/g; subjects, 2.0±1.1 mL/g
Vanni[25]*	2015	Italy	Case-control	Not specified	19 NAFLD and 9 controls	MRI	NAFLD, 228.1±112.9 mL; controls, 66.8±25.2 mL
Vural[26]	2014	Turkey	Case-control	Suspected CAD	63	CACS	137±56 cm^3
Wu[27]	2015	Taiwan	Cross-sectional	Compensated CHF	50 Cases and 20 controls	MRI	Control, 45.8 (39.4–50.3) mL; CHF+VT/VF, 51.5 (46.6–59.8) mL); CHF and no VT/VF, 44.0 (33.9–48.3) mL
Yamashita[28]*	2012	Japan	Cross-sectional	Suspected CAD	286	MDCT	EAT, 71.6±37.9 (10.5–179.9) mL

Values are mean±SD or mean (range). AF indicates atrial fibrillation; CACS, coronary artery calcium score; CAD, coronary artery disease; CHF, congestive heart failure; DCM, dilated cardiomyopathy; DD, diastolic dysfunction; EAT, epicardial adipose tissue; ICM, ischemic cardiomyopathy; LVEF, left ventricular ejection fraction; MDCT, multidetector computed tomography; MRI, magnetic resonance imaging; NAFLD, nonalcoholic fatty liver disease; PET-CT, positron emission tomography–computed tomography; ROC, receiver operating characteristic; VT/VF, ventricular tachycardia/ventricular fibrillation.
*This is a conference abstract.

reported associations between EAT and global longitudinal strain, a subclinical measure of myocardial function.[24] Only one described an independent effect of EAT on LV ejection fraction (LVEF) by echocardiography.[19] No univariable correlation with LVEF was reported in the MRI studies.[10–12] Of the 6 studies reporting multivariable regression analysis, an independent association with LVEF was observed in 2 studies: one study was performed in patients with established coronary artery disease (CAD) stratified by LVEF and compared with normal controls (hazard ratio, 0.48; 95% confidence interval, 0.28–0.68; $P<0.01$),[11] and the other study was performed in patients undergoing investigation for suspected CAD with reduced LVEF compared with normal LVEF (values not reported).[19]

The only consistent feature across all studies appeared to be a relative decrease in EAT as LVEF decreased. In studies that included control groups (ie, normal LVEF), no association of EAT with EF was identified in the control group. One study demonstrated a significant inverse correlation with EAT (normalized to LV mass) with cardiac output and stroke volume (but not LVEF)[3] in obese patients (r value, −0.46) but not in corresponding controls.

In studies focusing specifically on patients with reduced LVEF, EAT was reduced compared with those with preserved LVEF. Doesch et al[11] demonstrated that patients with CAD and preserved LVEF had greater EAT (36±11 g/m^2) than normal controls without CAD (31±8 g/m^2), and both had greater EAT than patients with CAD with LVEF <50% (28±8 g/m^2; $P<0.01$). A population with presumed ischemic cardiomyopathy (CAD with reduced LVEF) also reported a stepwise decrease in EAT volume with reducing grades of LVEF.[19] This stepwise decrease was not found in a different study by Doesch et al[12] in patients with dilated cardiomyopathy against normal controls, although EAT was reduced overall compared with normal controls.

In the study related to strain analysis,[24] there was a positive correlation with EAT and impaired 3-dimensional global longitudinal strain ($r=0.601$, $P<0.001$) that remained significant on multivariable regression (standardized $\beta=0.512$, $P<0.001$), independent of markers of obesity and diabetes mellitus.

Association of EAT With Chamber Measures

There were 14 studies with data relating to a measure of myocardial geometry. All modalities of echocardiography, CT, and MRI were represented, with most values indexed to body surface area, unless otherwise specified. Some studies avoided indexation because body weight or other adiposity measures were used in regression models and, therefore, raw measures were used to prevent collinearity.

The most often reported univariable correlation coefficient was for EAT and LV mass or indexed mass and was always

Table 2. EAT and Diastolic Function

First Author	Diastolic Function Reference	Subgroup Characteristics		Diastolic Parameter Correlations			Multivariable Regression Comments
		DD	Normal Function	E/A	e′	E/e′	
Cavalcante[9]	ASE[29]	Grade 1 (n=29, 26%) Grade 2 (n=11, 10%)	n=70, 64%		Averaged 0.44*	0.34*	Multivariate model outcomes of grade 1 or higher DD, mean e′, and mean E/e′: EAT was an independent predictor (model included 10-y Framingham Risk Score, metabolic syndrome, subclinical CAD, and LV mass index), β range, −0.02 to 0.04 (all P<0.05). Indexed EAT was found to increase clinical model for prediction of DD (adjusted R^2=0.16 vs 0.24; P=0.004) and mean e′ (adjusted R^2=0.17 vs 0.27; P=0.001) (ie, indexed EAT represents 8%–10% of the variation of predictors for DD
Ede[13]	Lang et al[32]	Grade 1 (n=39, 37%) Grade 2 (n=10, 9%) Grade 3 (n=2, 2%)	n=55, 52%	−0.404			
Faustino[14†]	Not specified	46 Patients with DD and EAT >44.1 mL	32 Patients with no DD and EAT <44.1 mL				EAT not significant on multivariable regression (results and covariates not reported). Relationship of EAT with DD by ROC AUC of 0.66 (P=0.02)
Fernando[15†]	Not specified	EAT=164±118 mL (E/E′ >15)	EAT=114±54 mL (E/E′ <15)		−0.48*	0.22	On multivariable regression adjusted for age, BMI, LA volume, hypertension, and CAD, EAT associated with abnormal myocardial relaxation (OR, not specified; P=0.04)
Fontes-Carvalho[16]	ASE[29]	EAT=116.7±67.9 cm^3 Grade 1 (n=57, 28%) Grade 2 (n=58, 28%) Grade 3 (n=10, 5%)	EAT=93.0±52.3 cm^3 n=80 (39%)		e′ Septal, −0.26* e′ lateral, −0.28*	0.25*	On multivariable regression adjusted for hypertension, age, sex, and other markers of adiposity (SAT, VAT, waist/height ratio, and fat mass %), EAT remained significantly predictive of E/e′ (β, 0.19 [0.06–0.32]; P<0.01), as did e′ septal and e′ lateral
Hachiya[18]	ASE[29]			−0.05	−0.31*	0.24*	Definition of diastolic dysfunction not specified. On different multivariate models, e′ inversely correlated with EAT (standardized β range, −0.30 to −0.36; all P<0.05) but not E/e′ (standardized β, 0.23; P=0.06), except when adjusted for age, sex, and BMI (model 1) and medication use (model 2) (standardized β range, 0.25–0.31; all P<0.05)
Konishi[20]	Defined as E/e′ >10	EAT=184±61 cm^3 n=141 (62%)	EAT=154±58 cm^3 n=88 (38%)			0.21*	On multivariable regression with age, hypertension, male sex, diabetes mellitus, and abdominal obesity, there was an independent effect of EAT on DD: OR, 2.09 (1.15–3.79; P=0.02) for EAT per 100 cm^3

Continued

DOI: 10.1161/JAHA.118.009975

Table 2. Continued

First Author	Diastolic Function Reference	Subgroup Characteristics		Diastolic Parameter Correlations			Multivariable Regression Comments
		DD	Normal Function	E/A	e′	E/e′	
Lai[21]	Lang et al[32]	EAT=86.79±31.77 n=100	EAT=67.32±31.95 n=218		−0.38*	0.284*	On multivariable regression adjusted for age, sex, BMI, systolic blood pressure, LV mass index, hypertension, diabetes mellitus, hyperlipidemia, and smoking, EAT was significantly associated with E/A (β, −0.002),* E′ (β, −0.02),* E/E′ (β, 0.02),* and diastolic dyssynchrony (β, 0.197).* ROC-derived optimal cutoff for DD was 67.3 mL (ROC, 0.712; sensitivity, 73%; specificity, 62%)
Liu[22]	Gottdiener et al[31]			Men, −0.12)* women, −0.12*			On multivariable linear regression adjusted for age, height, smoking, alcohol, blood pressure, eGFR, hemoglobin, total physical activity score, medications, VAT, and weight, E/A no longer became significant (regression co-efficient, −0.01±0.02 [*P*=0.41] in women and −0.0±0.02 [*P*=0.64] in men) (described as pericardial fat volume)
Longenecker[23†]	Not specified	Grade 1 (n=29 [HIV+, n=19; HIV−, n=10]) Grade 2 (n=2 [HIV+, n=1; HIV−, n=2])	n=38 (HIV+) n=26 and n=12 (HIV−)	−0.392*			On multivariable regression adjusted for age, BMI, and sex, EAT remained independently associated with diastolic dysfunction (OR, 1.35; 95% CI, 1.02–1.79) per 10-mL increase (described as pericardial fat volume)
Ng[24]	Not specified				e′ Septal, −0.263)*; e′ lateral, −0.285*		
Vural[26]	Alnabhan et al[30]	EAT=164.4±54 cm^3 Grade 1 (n=24, 38%) Grade 2 (n=4, 6%) Grade 3 (n=1, 1.5%)	EAT=114.1±46.6 cm^3 n=34 (56%)		−0.437*		On multivariable regression adjusted for age, blood pressure, BMI, waist circumference, and cholesterol, EAT was an independent predictor of DD (OR, 1.03 [1.01–1.06]; *P*=0.006). ROC-derived optimal cutoff for DD, 129.6 cm^3 (ROC curve, 0.758)

Correlations represent the correlation co-efficient.

Values are mean±SD or mean (range). ASE indicates American Society of Echocardiography; AUC, area under the curve; BMI, body mass index; CAD, coronary artery disease; CI, confidence interval; DD, diastolic dysfunction; e′, average mitral annular tissue Doppler velocity; E/e′, early inflow / annular velocity ratio; E/A, ratio of peak early (E) and late (A) transmitral inflow velocities; EAT, epicardial adipose tissue; eGFR, estimated glomerular filtration rate; LA, left atrial; LV, left ventricular; OR, odds ratio; ROC, receiver operating characteristic; SAT, subcutaneous adipose tissue; VAT, visceral adipose tissue.

**P* value for univariate correlation is significant at <0.05.

†Study is a conference abstract.

DOI: 10.1161/JAHA.118.009975

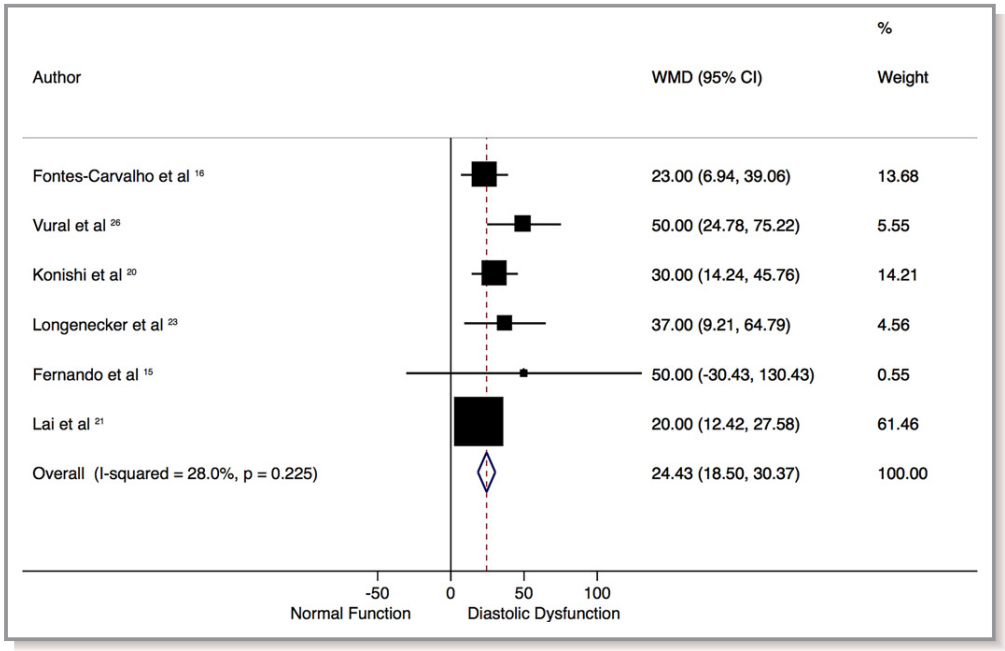

Figure 2. Mean difference of epicardial adipose tissue (EAT) volume in patients with and without diastolic dysfunction. Forest plot demonstrates the weighted mean difference (WMD; in mL) of EAT in studies with and without diastolic dysfunction, according to a random-effect model. Those with diastolic dysfunction have significantly greater EAT volumes. There is mild heterogeneity, as seen by the I^2 statistic of 28%. CI indicates confidence interval.

statistically significantly positively correlated in the diseased patient group (not controls), with ranges from r=0.19 to r=0.42 (P<0.05). Only studies by Doesch et al[11,12] measured LV end-diastolic diameter and found a consistent association with EAT (r value range, 0.22–0.42; P<0.05). Similar findings were seen for LV end-diastolic and end-systolic volume. Left atrial size was measured either as volume or diameter and demonstrated significant univariable associations with EAT (Table 4).*

An inconsistent association was seen with measures of adiposity in relation to EAT and cardiac structure. In patients with reduced LVEF, indexed EAT appears to be associated with indexed LV end-diastolic mass independent of BMI (Table 4).[10–12] One study assessing patients with suspected CAD and normal LVEF demonstrated that EAT correlated best with LV mass (nonindexed) in the nonobese cohort only (β=0.23, P<0.001).[8] Finally, in 2 observational studies, an independent association of EAT with LV mass (nonindexed), adjusted for body weight, was only seen in women (Table 4).[17,22]

Discussion

This review of 21 studies has demonstrated the emerging body of work relating EAT to myocardial structure and function. Increasing EAT is associated with the following: (1) an increasing prevalence of diastolic dysfunction; (2) a concomitant increase in LV mass; and (3) no consistent association with markers of systolic function. However, these

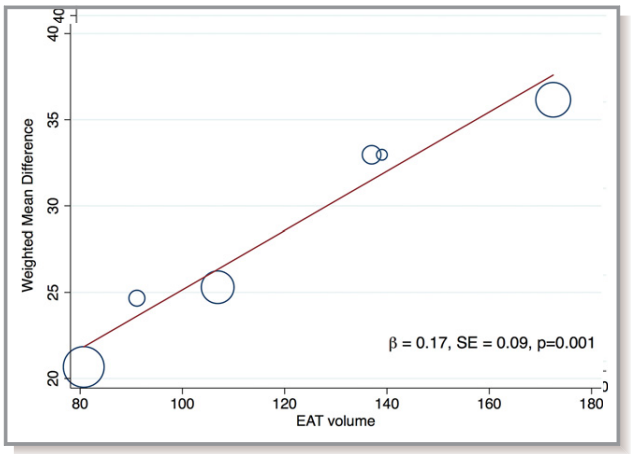

Figure 3. Meta-regression of the effect of increasing epicardial adipose tissue (EAT) volume on the weighted mean difference (effect size) of EAT in patients with and without diastolic dysfunction. Meta-regression bubble plot depicts increasing differences in mean EAT volume in patients with diastolic dysfunction as EAT increases. Circles represent the weight of each study. β coefficient is from meta-regression with associated SEE; P value is from Monte-Carlo testing (1000 simulations) and demonstrates a significant association (P=0.001).

*References 3, 7–12, 17, 18, 20, 22, 24, 25, 28.

Table 3. EAT and Systolic Function

First Author	Method	Group	EAT Value	Systolic Measure	*r* Value (Univariate)	Multivariable Regression Comment
Doesch[11]	MRI	CAD and EF >50% (n=44) CAD and EF <50% (n=114) Combined CAD (n=158) Controls (n=40)	36±11 g/m^2 26±8 g/m^2 29±10 g/m^2 31±8 g/m^2	LVEF	0.171 0.137 0.574* Not specified	On multivariable regression adjusted for BMI, NYHA classes I and III, atrial fibrillation, LV-EDVI, LV-ESVI, LV-EDD, LVRI, and LGE%, LVEF was an independent predictor of indexed EAT (HR, 0.478 [0.28–0.675]; *P*<0.01)†
Doesch[12]	MRI	Control (n=48) DCM (n=112)	31.7±5.6 g/m^2 24±7.5 g/m^2	LVEF LVEF	0.069 0.085	No correlation with LVEF and EAT (*P*=0.37)
Fontes-Carvalho[16]	Echocardiography			LVEF	−0.07	
Hachiya[18]	Echocardiography			LVEF	0.22*	Significant association on multivariate regression models adjusted for hypertension, diabetes mellitus, dyslipidemia, previous CAD or revascularization, and medication use (standardized β range, 0.16–0.22; all *P*<0.05) but not adjusted for age, sex, or BMI (standardized β, 0.13; *P*>0.05)
Khawaja[19]	Echocardiography	Normal (n=321) EF <55% (n=60) EF 35%–55% (n=43) EF <35% (n=17)	114.5±98.5 cm^3 83.5±67.1 cm^3 96.0±73.9 cm^3 52.2±29.7 cm^3			Multivariate analysis revealed LVEF and triglyceride levels predicted EAT (values and covariates not reported)
Liu[22]	Echocardiography	Women Men		LVEF LVEF	−0.04 0.03	Not significant on multivariable regression in either sex (adjusted for age, height, smoking, alcohol, blood pressure, eGFR, hemoglobin, total physical activity score, medications, VAT, and weight: regression coefficient, −0.3±0.4 [*P*=0.51] in women and 0.2±0.6 [*P*=0.72] in men). Note: described as pericardial fat volume.
Ruberg[3]	MRI	Obese		CO SV LVEF	−0.46* Inverse* Not correlated	Values are normalized to LV mass (mL/g)
		Control		CO SV LVEF	Not correlated Not correlated Not correlated	
Wu[27]	MRI			LVEF	Not correlated	

Values are mean±SD or *r* value correlation coefficients, unless otherwise stated. BMI indicates body mass index; CAD, coronary artery disease; CO, cardiac output; DCM, dilated cardiomyopathy; EAT, epicardial adipose tissue; EF, ejection fraction; eGFR, estimated glomerular filtration rate; HR, hazard ratio; LGE%, percentage of late gadolinium enhancement; LV, left ventricular; LV-EDD, LV end-diastolic diameter; LV-EDVI, LV end-diastolic volume index; LV-ESVI, left ventricular end-systolic volume index; LVRI, LV remodeling index; MRI, magnetic resonance imaging; NYHA, New York Heart Association; SV, stroke volume; VAT, visceral adipose tissue.

*P<0.05.

†Directly quoted values from source article.

correlations were no more than moderate; no coefficient exceeded 0.50.

Protective Functions of EAT

EAT has a high fatty acid content and can both release and scavenge excess free fatty acids to regulate myocardial energy production.[2] In addition, EAT secretes anti-inflammatory cytokines, such as adiponectin, adrenomedullin, and omentin, which have antiatherogenic effects; EAT also regulates vascular tone and cardiac remodelling.[33] There is a thermogenic role for EAT in providing heat for the myocardium in times of hypoxic or ischemic stress.[33] However, the presence of numerous proinflammatory

Table 4. EAT and Chamber Geometry

Author	Modality	Subgroup	LV-EDD	LA Size (Diameter/ Volume)	LVEDMI	LV-EDVI	LV-ESVI	LVRI	Comment
Bukkam[8]	CT				0.42*,†				On multivariable regression adjusted for traditional cardiovascular risk factors, CACS and BMI, EAT was not a significant predictor of LV mass in obese patients, but only in nonobese patients (β=0.23, P<0.001)
Cavalcante[9]	Echocardiography				0.41*				Measure not included in multivariate analysis
Al Chekakie[7]	CT and echocardiography			0.25/0.24					
Doesch[11]	MRI	EF <50% (n=44) EF >50% (n=114) Combined (n=158)	0.076 0.011 0.272*		0.336* 0.305* 0.019	0.201* 0.043 0.16*	0.089 0.056 0.262*	0.137 0.202 0.344*	On multivariable regression including LVEF, BMI, NYHA classes I and III, atrial fibrillation, LV-EDVI, LV-ESVI, LV-EFF, LVRI, and LGE%, best correlates to indexed EAT were LVEF, BMI, LV-ESVI (HR, 0.48; P<0.01), and LV-EDD (HR, −0.238; P=0.01). In subgroup analysis by EF <50% or >50%, full model not described; however, no association with LVEDMI in LVEF >50% but association seen in LVEF >50% (HR, 0.105; P=0.01)
Doesch[12]	MRI	Control (n=48) DCM (n=112)	0.01 0.22*		0.346* 0.417*	0.007 0.251*	0.0001 0.239*	0.204 0.116	Increased EAT mass with increasing LVEDMI in DCM, but less values than healthy control group. Greater mass seen in DCM with hypertrophy vs nonhypertrophy (31.7±5.6 vs 24.4±7.1 g/m^2; P=0.01). On multivariable regression only, LVEDMI independently correlated with indexed EAT, as was seen in healthy controls (adjusted for age and BMI [value not reported]).
Doesch[10]	MRI	Control CHF	NR 0.42*		0.36* 0.59*				Increased EAT mass in CHF with increasing LVEDMI; however, higher levels of EAT in controls compared with CHF (34±4 vs 22±5 g/m^2; P<0.01). On multivariate regression adjusted for LVEF, LV-EDD, RVEF, and LVEDMI, only LVEDMI independently associated with indexed EAT (P=0.0001)
Fox[17]	MRI	Women Men		0.28* 0.37*	0.35*,‡ 0.19*,‡	0.2*,‡ 0.07‡			On multivariable regression adjusted for age, height, smoking, alcohol, menopause, hormone replacement therapy, blood pressure, hypertension therapy, and weight, only in women, LVM (adjusted regression coefficient, 1.66; P=0.01), and in men, LA diameter (adjusted regression coefficient, 0.8; P=0.002) were independent predictors of pericardial fat volume
Hachiya[18]	Echocardiography				0.28*				Measure not included in multivariate analysis

Continued

DOI: 10.1161/JAHA.118.009975

Table 4. Continued

Author	Modality	Subgroup	LV-EDD	LA Size (Diameter/ Volume)	LVEDMI	LV-EDVI	LV-ESVI	LVRI	Comment
Konishi[20]	Echocardiography			0.32*	0.23*				Measure not included in multivariate analysis
Liu[22]	Echocardiography	Women Men		0.3* 0.11	0.24*,‡ 0.21*,‡				On multivariable regression adjusted for age, height, smoking, alcohol, blood pressure, eGFR, hemoglobin, total physical activity score, medications, VAT, and weight, only in women, LVM (adjusted regression coefficient, 4.1±1.8; P=0.03) and LA diameter (adjusted regression coefficient, 0.4±0.2; P=0.03) were independent predictors of pericardial fat volume
Ng[24]	Echocardiography					−0.09	0.08		
Ruberg[3]	MRI					Not			
Vanni[25§]	MRI	Cases					0.46*,‖		Inversely correlated with EF No other analysis specified
Yamashita[28§]	CT			0.25*					

Values are mean±SD or r value correlation coefficients, unless otherwise stated. BMI indicates body mass index; CACS, coronary artery calcium score; CHF, congestive heart failure; CT, computed tomography; DCM, dilated cardiomyopathy; EAT, epicardial adipose tissue; EF, ejection fraction; eGFR, estimated glomerular filtration rate; HR, hazard ratio; LA, left atrial; LGE%, percentage of late gadolinium enhancement; LV, left ventricular; LV-EDVI, LV end-diastolic volume index; LV-EDD, LV end-diastolic diameter; LVEF, LV ejection fraction; LVEDMI, LV end-diastolic mass index; LV-EDVI, LV end-diastolic volume index; LV-ESVI, LV end-systolic volume index; LVRI, LV remodeling index; MRI, magnetic resonance imaging; NR, not reported; NYHA, New York Heart Association; RVEF, right ventricular EF; VAT, visceral adipose tissue.

*P < 0.05.

†Value is for LV mass on CT, nonindexed and time in cardiac cycle not specified.

‡Represents a nonindexed measure.

§Study is a conference abstract.

‖Value is for end-systolic LV diameter.

DOI: 10.1161/JAHA.118.009975

cytokines within EAT may lead to a potential imbalance of harmful versus protective cytokines and disruption of myocardial function. Higher levels of these molecules (eg, tumor necrosis factor-α, interleukin-6, interleukin-1, and MCP-1) are seen in patients with CAD or heart failure. It is uncertain whether the trigger for the imbalance of cytokines is a cause of the pathological characteristics or a consequence, and a potential reciprocal or bidirectional role has been proposed.[2]

EAT and Diastolic Dysfunction

Adipose tissue can modulate the cardiovascular system by mechanisms including sympathetic activation, adipokine secretion, and myocardial oxidative stress.[34,35] EAT is regarded as a visceral fat depot. Visceral fat is metabolically active and is a determinant of diastolic function.[36] The adipokines within EAT can all affect diastolic function through persistent inflammation and subsequent collagen turnover,[37] impaired microvascular relaxation, or a direct toxic effect on the myocardium.[38,39] The loss of protective effects of adiponectin can also modify diastolic function.[40]

Mechanical effects may arise from myocardial compression of EAT because it lies within a fixed pericardial sac,[17] inducing a similar mechanism as pericardial constriction. Hachiya et al demonstrated an independent correlation of EAT with aortic pulse pressure as another mechanism of diastolic dysfunction that may be mediated by the association of EAT with aortic stiffness and, therefore, increased pulse wave velocity and early wave reflection.[18] Increased pressure in late systole may cause slower LV relaxation and subsequent diastolic dysfunction, as well as compromise coronary perfusion, especially if there is underlying CAD leading to impaired LV relaxation.[41]

EAT is associated with obesity, which itself is independently associated with diastolic dysfunction.[42] Obese patients often have elevated EAT volumes,[17] and indexed EAT has modest incremental value for diastolic dysfunction over traditional covariates, such as metabolic syndrome, subclinical CAD, and LV mass index.[9] Although the results from our analysis demonstrate that EAT had an independent effect on diastolic function parameters over adiposity measures, adiposity measures varied considerably and included BMI, bioimpedence testing, area of visceral adipose tissue or subcutaneous adipose tissue, or indexed EAT, which accounts for body weight. This heterogeneity needs further explanation to adequately isolate the effect of obesity and EAT on diastolic function. The lack of an association of EAT with E/A ratio may be confounded by the effects of age, proportion of patients with CAD, measurement in patients with normal LVEF, and the U-shaped relationship of E/A ratio with diastolic function that makes it difficult to assess without the addition of other variables.[43]

The evaluation of diastolic function is challenging and influenced by a patient's filling status, the presence of CAD, diabetes mellitus, obesity, as well as "normal" changes seen in the ageing patient. Although most studies aim to account for these factors in multivariable regression models, no more than association can be interpreted, and causality cannot be proved. Statistically, there may be implications of collinearity of obesity measures and EAT in multivariable models.

EAT and Systolic Dysfunction

Our study noted weak and inconsistent associations of EAT and systolic parameters. In the single study that evaluated EAT and longitudinal strain as a marker of subclinical myocardial dysfunction, there was a strong association noted independent of confounders, such as obesity and diabetes mellitus.[24] This is a notable finding; however, causality remains unproved and requires further assessment in larger-scale studies as a possible marker of the syndrome of heart failure with preserved ejection fraction. Various hypotheses have been developed to relate EAT and systolic function. In studies of patients with ischemic and dilated cardiomyopathy, there has been a consistent signal of reducing EAT with reducing LVEF, with less EAT also seen compared with normal controls or those with normal LVEF.[10–12,19] As myocardium becomes progressively dysfunctional, the role of EAT as a source of energy or cytokine homeostasis may become less necessary, contributing to EAT depletion. Conversely, in obese patients, there was no association with EAT (normalized to cardiac mass) and LVEF, and there was a negative correlation with MRI-derived cardiac output as EAT increased.[3] The proposed mechanism is from mechanical restriction of myocardial expansion from EAT in diastole that may lead to less ventricular filling and, therefore, reduced cardiac output.[3] A further mechanism may involve the effects of a direct cytokine release, as seen in patients with decompensated heart failure, but no studies have applied this in the context of EAT volume.

EAT and Chamber Measures

Postmortem and experimental studies[44,45] have demonstrated a constant ratio of epicardial fat/ventricular myocardium, regardless of underlying pathological characteristics of hypertrophy, ischemia, or normal muscle. Furthermore, the increase in fat mass parallels LV hypertrophy, although healthy controls have higher quantities of EAT.[10] Similar findings are seen when evaluating the LV remodeling index (ratio of mass/end-diastolic volume), where an inverse correlation is noted with LVEF and the EAT/LV remodeling index ratio. LVEF is inversely correlated with EAT and linearly correlated with LV remodeling index, suggesting that remodeling is not compensated by an adequate increase in EAT.[10]

Obesity has shown a positive relationship with increased LV mass and EAT, yet the impact of obesity on myocardial

geometry may outweigh the local effects of ectopic fat because associations attenuated after adjustment for other adiposity measures, including body weight.[17] From a mechanistic perspective, the association of EAT with central obesity and visceral adipose tissue might result in greater LV afterload and subsequent increased LV output, therefore leading to LV remodeling.[8] As LV remodeling progresses, LV diameter, volume, and mass increase, which may then deplete EAT stores[12] and result in a vicious cycle of reduced protective benefits on the heart and further dysfunction. However, the independent association of EAT with LV mass is limited to nonobese subjects.[8] Associations of EAT with the incidence of CAD have been described in nonobese people[46] and could contribute to the so-called obesity paradox.[47]

Limitations

We acknowledge several limitations in our study. EAT measurement by different modalities may lead to differences between studies. Some reported EAT indexed to Body Surface Area (BSA) (therefore accounting for weight), and some reported raw values using weight as a covariate in multivariable models. Such normalization, as opposed to normalization to height, may obscure the contribution of obesity to differences in chamber volumes and mass, which are associated with EAT. Not all studies adjusted for hypertension in multivariable models, which is also associated with obesity and diastolic function. Variations in the reference literature on measures of diastolic function also lead to difficulties with comparing studies. The differences in regional location of EAT were not available in most studies and, therefore, the effect of EAT distribution was not assessable. The level of heterogeneity and variable study end points precluded detailed meta-analysis.

Conclusions

Despite small and heterogeneous studies, there is clear evidence of a consistent effect of volumetric EAT on myocardial diastolic function and chamber measurements; however, robust data are lacking to make causal inferences. These findings are observed despite adjustment for common confounders, such as adiposity. No consistent effect is seen with respect to systolic parameters. Further longitudinal studies are necessary to generate quantitative summary measures as well as develop potential targets for treatment.

Sources of Funding

Nerlekar is supported by a scholarship from the National Medical Health and Research Council and the National Heart Foundation. Brown is supported by an Early Career Fellowship from Monash University.

Disclosures

None.

References

1. Nerlekar N, Brown AJ, Muthalaly RG, Talman A, Hettige T, Cameron JD, Wong DTL. Association of epicardial adipose tissue and high-risk plaque characteristics: a systematic review and meta-analysis. *J Am Heart Assoc*. 2017;6:e006379. DOI: 10.1161/JAHA.117.006379.
2. Iacobellis G. Local and systemic effects of the multifaceted epicardial adipose tissue depot. *Nat Rev Endocrinol*. 2015;11:363–371.
3. Ruberg FL, Chen Z, Hua N, Bigornia S, Guo Z, Hallock K, Jara H, LaValley M, Phinikaridou A, Qiao Y, Viereck J, Apovian CM, Hamilton JA. The relationship of ectopic lipid accumulation to cardiac and vascular function in obesity and metabolic syndrome. *Obesity (Silver Spring)*. 2010;18:1116–1121.
4. Nerlekar N, Baey YW, Brown AJ, Muthalaly RG, Dey D, Tamarappoo B, Cameron JD, Marwick TH, Wong DT. Poor correlation, reproducibility, and agreement between volumetric versus linear epicardial adipose tissue measurement: a 3D computed tomography versus 2D echocardiography comparison. *JACC Cardiovasc Imaging*. 2018;11:1035–1036.
5. Doesch C, Suselbeck T, Leweling H, Fluechter S, Haghi D, Schoenberg SO, Borggrefe M, Papavassiliu T. Bioimpedance analysis parameters and epicardial adipose tissue assessed by cardiac magnetic resonance imaging in patients with heart failure. *Obesity (Silver Spring)*. 2010;18:2326–2332.
6. Harbord RM, Higgins JPT. Meta-regression in Stata. *Stata J*. 2008;8:493–519.
7. Al Chekakie MO, Welles CC, Metoyer R, Ibrahim A, Shapira AR, Cytron J, Santucci P, Wilber DJ, Akar JG. Pericardial fat is independently associated with human atrial fibrillation. *J Am Coll Cardiol*. 2010;56:784–788.
8. Bakkum MJ, Danad I, Romijn MA, Stuijfzand WJ, Leonora RM, Tulevski II, Somsen GA, Lammertsma AA, van Kuijk C, van Rossum AC, Raijmakers PG, Knaapen P. The impact of obesity on the relationship between epicardial adipose tissue, left ventricular mass and coronary microvascular function. *Eur J Nucl Med Mol Imaging*. 2015;42:1562–1573.
9. Cavalcante JL, Tamarappoo BK, Hachamovitch R, Kwon DH, Alraies MC, Halliburton S, Schoenhagen P, Dey D, Berman DS, Marwick TH. Association of epicardial fat, hypertension, subclinical coronary artery disease, and metabolic syndrome with left ventricular diastolic dysfunction. *Am J Cardiol*. 2012;110:1793–1798.
10. Doesch C, Haghi D, Fluchter S, Suselbeck T, Schoenberg SO, Michaely H, Borggrefe M, Papavassiliu T. Epicardial adipose tissue in patients with heart failure. *J Cardiovasc Magn Reson*. 2010;12:40.
11. Doesch C, Haghi D, Suselbeck T, Schoenberg SO, Borggrefe M, Papavassiliu T. Impact of functional, morphological and clinical parameters on epicardial adipose tissue in patients with coronary artery disease. *Circ J*. 2012;76:2426–2434.
12. Doesch C, Streitner F, Bellm S, Suselbeck T, Haghi D, Heggemann F, Schoenberg SO, Michaely H, Borggrefe M, Papavassiliu T. Epicardial adipose tissue assessed by cardiac magnetic resonance imaging in patients with heart failure due to dilated cardiomyopathy. *Obesity (Silver Spring)*. 2013;21:E253–E261.
13. Ede H, Erkoc MF, Okur A, Erbay AR. Impaired aortic elasticity and diastolic functions are associated with findings of coronary computed tomographic angiography. *Med Sci Monit*. 2014;20:2061–2068.
14. Faustino AP, Paiva L, Mota P, Costa M, Leito-Marques A. Pericardial fat, a new marker of impaired left ventricle diastolic dysfunction. *Eur J Heart Fail Suppl*. 2011;10:S248.
15. Fernando RS, Syed MA, Wilber D, Singh S, Teme T, Rabbat M. Epicardial adipose tissue volume by cardiac magnetic resonance imaging predicts abnormal myocardial relaxation in patients with atrial fibrillation. *J Cardiovasc Magn Reson*. 2015;17:P352.
16. Fontes-Carvalho R, Fontes-Oliveira M, Sampaio F, Mancio J, Bettencourt N, Teixeira M, Rocha Goncalves F, Gama V, Leite-Moreira A. Influence of epicardial and visceral fat on left ventricular diastolic and systolic functions in patients after myocardial infarction. *Am J Cardiol*. 2014;114:1663–1669.
17. Fox CS, Gona P, Hoffmann U, Porter SA, Salton CJ, Massaro JM, Levy D, Larson MG, D'Agostino RB Sr, O'Donnell CJ, Manning WJ. Pericardial fat, intrathoracic fat, and measures of left ventricular structure and function: the Framingham Heart Study. *Circulation*. 2009;119:1586–1591.

18. Hachiya K, Fukuta H, Wakami K, Goto T, Tani T, Ohte N. Relation of epicardial fat to central aortic pressure and left ventricular diastolic function in patients with known or suspected coronary artery disease. *Int J Cardiovasc Imaging*. 2014;30:1393–1398.
19. Khawaja T, Greer C, Chokshi A, Chavarria N, Thadani S, Jones M, Schaefle K, Bhatia K, Collado JE, Shimbo D, Einstein AJ, Schulze PC. Epicardial fat volume in patients with left ventricular systolic dysfunction. *Am J Cardiol*. 2011;108:397–401.
20. Konishi M, Sugiyama S, Sugamura K, Nozaki T, Matsubara J, Akiyama E, Utsunomiya D, Matsuzawa Y, Yamashita Y, Kimura K, Umemura S, Ogawa H. Accumulation of pericardial fat correlates with left ventricular diastolic dysfunction in patients with normal ejection fraction. *J Cardiol*. 2012;59:344–351.
21. Lai YH, Hou CJ, Yun CH, Sung KT, Su CH, Wu TH, Yang FS, Hung TC, Hung CL, Bezerra HG, Yeh HI. The association among MDCT-derived three-dimensional visceral adiposities on cardiac diastology and dyssynchrony in asymptomatic population. *BMC Cardiovasc Disord*. 2015;15:142.
22. Liu J, Fox CS, Hickson DA, May WL, Ding J, Carr JJ, Taylor HA. Pericardial fat and echocardiographic measures of cardiac abnormalities: the Jackson Heart Study. *Diabetes Care*. 2011;34:341–346.
23. Longenecker CAK, Serhal M, Kinley B, Labbato D, McComsey GA. Diastolic function correlates with pericardial fat [fat around the heart] and vascular remodeling in HIV. *Conference on Retroviruses and Opportunistic Infections (CROI) February 22-25*. Boston, MA; 2016.
24. Ng AC, Goo SY, Roche N, van der Geest RJ, Wang WY. Epicardial adipose tissue volume and left ventricular myocardial function using 3-dimensional speckle tracking echocardiography. *Can J Cardiol*. 2016;32:1485–1492.
25. Vanni EM, Faletti R, Morello M, Mezzabotta L, Battisti G, Frea S, Cannillo M, Mosso E, Rosso C, Bergamasco L, Rizzetto M, Bugianesi E. Incerased epicardial fat and early signs of impaired diastolic and systolic left ventricular function in non-diabetic, normotensive patients with nonalcoholic fatty liver disease. *J Hepatol*. 2015;62:S745.
26. Vural M, Talu A, Sahin D, Elalmis OU, Durmaz HA, Uyanik S, Dolek BA. Evaluation of the relationship between epicardial fat volume and left ventricular diastolic dysfunction. *Jpn J Radiol*. 2014;32:331–339.
27. Wu CK, Tsai HY, Su MY, Wu YF, Hwang JJ, Tseng WY, Lin JL, Lin LY. Pericardial fat is associated with ventricular tachyarrhythmia and mortality in patients with systolic heart failure. *Atherosclerosis*. 2015;241:607–614.
28. Yamashita KO, Ebara S, Yamamoto MH, Obara C. Increased epicardial adipose tissue are associated with left ventricular diastolic dysfunction. *J Am Coll Cardiol*. 2012;59:E1349.
29. Nagueh SF, Appleton CP, Gillebert TC, Marino PN, Oh JK, Smiseth OA, Waggoner AD, Flachskampf FA, Pellikka PA, Evangelista A. Recommendations for the evaluation of left ventricular diastolic function by echocardiography. *J Am Soc Echocardiogr*. 2009;22:107–133.
30. Alnabhan N, Kerut EK, Geraci SA, McMullan MR, Fox E. An approach to analysis of left ventricular diastolic function and loading conditions in the echocardiography laboratory. *Echocardiography*. 2008;25:105–116.
31. Gottdiener JS, Bednarz J, Devereux R, Gardin J, Klein A, Manning WJ, Morehead A, Kitzman D, Oh J, Quinones M, Schiller NB, Stein JH, Weissman NJ. American Society of Echocardiography recommendations for use of echocardiography in clinical trials. *J Am Soc Echocardiogr*. 2004;17:1086–1119.
32. Lang RM, Bierig M, Devereux RB, Flachskampf FA, Foster E, Pellikka PA, Picard MH, Roman MJ, Seward J, Shanewise JS, Solomon SD, Spencer KT, Sutton MS, Stewart WJ. Recommendations for chamber quantification: a report from the American Society of Echocardiography's Guidelines and Standards Committee and the Chamber Quantification Writing Group, developed in conjunction with the European Association of Echocardiography, a branch of the European Society of Cardiology. *J Am Soc Echocardiogr*. 2005;18:1440–1463.
33. Fitzgibbons TP, Czech MP. Epicardial and perivascular adipose tissues and their influence on cardiovascular disease: basic mechanisms and clinical associations. *J Am Heart Assoc*. 2014;3:e000582. DOI: 10.1161/JAHA.113.000582.
34. Vincent HK, Powers SK, Stewart DJ, Shanely RA, Demirel H, Naito H. Obesity is associated with increased myocardial oxidative stress. *Int J Obes Relat Metab Disord*. 1999;23:67–74.
35. Falcao-Pires I, Castro-Chaves P, Miranda-Silva D, Lourenco AP, Leite-Moreira AF. Physiological, pathological and potential therapeutic roles of adipokines. *Drug Discov Today*. 2012;17:880–889.
36. Canepa M, Strait JB, Milaneschi Y, AlGhatrif M, Ramachandran R, Makrogiannis S, Moni M, David M, Brunelli C, Lakatta EG, Ferrucci L. The relationship between visceral adiposity and left ventricular diastolic function: results from the Baltimore Longitudinal Study of Aging. *Nutr Metab Cardiovasc Dis*. 2013;23:1263–1270.
37. Mak GJ, Ledwidge MT, Watson CJ, Phelan DM, Dawkins IR, Murphy NF, Patle AK, Baugh JA, McDonald KM. Natural history of markers of collagen turnover in patients with early diastolic dysfunction and impact of eplerenone. *J Am Coll Cardiol*. 2009;54:1674–1682.
38. Silberman GA, Fan TH, Liu H, Jiao Z, Xiao HD, Lovelock JD, Boulden BM, Widder J, Fredd S, Bernstein KE, Wolska BM, Dikalov S, Harrison DG, Dudley SC Jr. Uncoupled cardiac nitric oxide synthase mediates diastolic dysfunction. *Circulation*. 2010;121:519–528.
39. Kankaanpaa M, Lehto HR, Parkka JP, Komu M, Viljanen A, Ferrannini E, Knuuti J, Nuutila P, Parkkola R, Iozzo P. Myocardial triglyceride content and epicardial fat mass in human obesity: relationship to left ventricular function and serum free fatty acid levels. *J Clin Endocrinol Metab*. 2006;91:4689–4695.
40. Greenstein AS, Khavandi K, Withers SB, Sonoyama K, Clancy O, Jeziorska M, Laing I, Yates AP, Pemberton PW, Malik RA, Heagerty AM. Local inflammation and hypoxia abolish the protective anticontractile properties of perivascular fat in obese patients. *Circulation*. 2009;119:1661–1670.
41. Buckberg GD, Fixler DE, Archie JP, Hoffman JI. Experimental subendocardial ischemia in dogs with normal coronary arteries. *Circ Res*. 1972;30:67–81.
42. Wong C, Marwick TH. Obesity cardiomyopathy: pathogenesis and pathophysiology. *Nat Clin Pract Cardiovasc Med*. 2007;4:436–443.
43. Nagueh SF, Smiseth OA, Appleton CP, Byrd BF III, Dokainish H, Edvardsen T, Flachskampf FA, Gillebert TC, Klein AL, Lancellotti P, Marino P, Oh JK, Popescu BA, Waggoner AD. Recommendations for the evaluation of left ventricular diastolic function by echocardiography: an update from the American Society of Echocardiography and the European Association of Cardiovascular Imaging. *J Am Soc Echocardiogr*. 2016;29:277–314.
44. Corradi D, Maestri R, Callegari S, Pastori P, Goldoni M, Luong TV, Bordi C. The ventricular epicardial fat is related to the myocardial mass in normal, ischemic and hypertrophic hearts. *Cardiovasc Pathol*. 2004;13:313–316.
45. Company JM, Booth FW, Laughlin MH, Arce-Esquivel AA, Sacks HS, Bahouth SW, Fain JN. Epicardial fat gene expression after aerobic exercise training in pigs with coronary atherosclerosis: relationship to visceral and subcutaneous fat. *J Appl Physiol (1985)*. 2010;109:1904–1912.
46. Iwayama T, Nitobe J, Watanabe T, Ishino M, Tamura H, Nishiyama S, Takahashi H, Arimoto T, Shishido T, Miyashita T, Miyamoto T, Toyama S, Sadahiro M, Kubota I. Role of epicardial adipose tissue in coronary artery disease in non-obese patients. *J Cardiol*. 2014;63:344–349.
47. Lavie CJ, De Schutter A, Parto P, Jahangir E, Kokkinos P, Ortega FB, Arena R, Milani RV. Obesity and prevalence of cardiovascular diseases and prognosis—the obesity paradox updated. *Prog Cardiovasc Dis*. 2016;58:537–547.

Supplemental Material

Table S1. Example MEDLINE search strategy.

#	Searches	Results
1	exp Adipose Tissue/ or epicardial fat.mp.	79789
2	epicardial adipose tissue.mp.	417
3	epicardial fat volume.mp.	56
4	pericardial adipose tissue.mp.	58
5	pericardial fat.mp.	242
6	pericardial fat volume.mp.	31
7	1 or 2 or 3 or 4 or 5 or 6	79916
8	exp Myocardial Contraction/ or exp Heart Failure/ or exp Heart Ventricles/ or exp Echocardiography, Doppler/ or exp Ventricular Dysfunction, Left/ or exp Diastole/ or exp Ventricular Function, Left/ or diastolic function.mp.	260853
9	diastolic dysfunction.mp.	6262
10	systolic function.mp.	9152
11	exp Myocardial Contraction/ or myocardial function.mp.	75943
12	myocardial performance.mp.	2269
13	mitral annular velocities.mp.	154
14	ejection fraction.mp.	44097
15	8 or 9 or 10 or 11 or 12 or 13 or 14	282014
16	exp Tomography, X-Ray Computed/ or cardiac ct.mp.	337987
17	coronary calcium score.mp. or exp Tomography, X-Ray Computed/	337983
18	exp Multidetector Computed Tomography/ or ccta.mp.	4630
19	16 or 17 or 18	338169
20	exp Magnetic Resonance Imaging/	346308
21	cardiac mri.mp.	1739
22	ectopic fat.mp.	396
23	7 or 22	80055
24	20 or 21	346580
25	15 and 19 and 23	53
26	15 and 23 and 24	78
27	25 or 26	122

Table S2. Newcastle - Ottawa Scale for Assessment of Cross-sectional Studies.

First Author	Year	Selection				Comparability	Outcome		Total
		Representativeness of the sample	Sample size	Ascertainment of exposure	Non - respondents	Outcome groups comparable	Assessment of outcome	Correct statistical test	
Bakkum[1]	2015	*	-	**	*	*	*	*	7
Cavalcante[2]	2012	*	-	**	*	**	**	*	9
Ede[3]	2014	*	-	**	*	**	**	*	9
Faustino[¥4]	2011	*	-	**	-	**	*	*	7
Fernando[5]	2015	*	-	**	-	**	*	*	7
Fontes-carvalho[6]	2014	*	-	**	*	**	**	*	9
Fox[7]	2009	*	*	**	*	**	**	*	10
Hachiya[8]	2014	*	-	**	*	*	*	*	7
Khawaja[9]	2011	*	-	**	-	**	**	*	8
Konishi[10]	2012	*	-	**	*	-	*	*	6
Lai[11]	2015	*	-	**	*	**	*	*	8
Liu[12]	2011	*	*	**	*	**	*	*	10
Longenecker[13]	2016	*	-	**	*	**	*	*	8
Ng[14]	2016	*	-	**	*	**	*	*	8
Ruberg[15]	2010	*	-	**	*	*	**	*	8
Wu[16]	2015	*	-	**	*	*	**	*	8
Yamashita[17]	2012	*	-	**	*	**	*	*	8

Table S3. Newcastle - Ottawa Scale for Assessment of Case Control Studies.

First Author	Year	Selection			Comparability		Exposure			Total
		Representativeness of the sample	Adequate case definition?	Selection of controls	Definition of controls	Controls and cases comparable	Ascertainment of exposure	Same method of ascertainment for cases and controls	Non-response rate	
Chekakie[18]	2010	*	*	*	*	**	*	*	*	9
Doesch[19]	2012	*	*	*	*	**	*	*	*	9
Doesch[20]	2013	*	*	*	*	**	**	*	*	10
Doesch[21]	2010	*	*	*	*	**	**	*	*	10
Vanni[22]	2015	*	*	*	*	*	*	*	*	8
Vural[23]	2014	*	*	*	*	**	**	*	*	10

Supplemental References:

1. Bakkum MJ, Danad I, Romijn MA, Stuijfzand WJ, Leonora RM, Tulevski, II, Somsen GA, Lammertsma AA, van Kuijk C, van Rossum AC, Raijmakers PG, Knaapen P. The impact of obesity on the relationship between epicardial adipose tissue, left ventricular mass and coronary microvascular function. *Eur J Nucl Med Mol Imaging*. 2015;42:1562-73.
2. Cavalcante JL, Tamarappoo BK, Hachamovitch R, Kwon DH, Alraies MC, Halliburton S, Schoenhagen P, Dey D, Berman DS, Marwick TH. Association of epicardial fat, hypertension, subclinical coronary artery disease, and metabolic syndrome with left ventricular diastolic dysfunction. *Am J Cardiol*. 2012;110:1793-8.
3. Ede H, Erkoc MF, Okur A, Erbay AR. Impaired aortic elasticity and diastolic functions are associated with findings of coronary computed tomographic angiography. *Med Sci Monit*. 2014;20:2061-8.
4. Faustino AP, Paiva L, Mota P, Costa M, Leito-Marques A. Pericardial fat, a new marker of impaired left ventricle diastolic dysfunction. *European Journal of Heart Failure Supplements* 2011;10:S248.
5. Fernando RS, Syed MA, Wilber D, Singh S, Teme T, Rabbat M. Epicardial adipose tissue volume by cardiac magnetic resonance imaging predicts abnormal myocardial relaxation in patients with atrial fibrillation. *Journal of Cardiovascular Magnetic Resonance*. 2015;17:P352.
6. Fontes-Carvalho R, Fontes-Oliveira M, Sampaio F, Mancio J, Bettencourt N, Teixeira M, Rocha Goncalves F, Gama V, Leite-Moreira A. Influence of epicardial and visceral fat on left ventricular diastolic and systolic functions in patients after myocardial infarction. *Am J Cardiol*. 2014;114:1663-9.
7. Fox CS, Gona P, Hoffmann U, Porter SA, Salton CJ, Massaro JM, Levy D, Larson MG, D'Agostino RB, Sr., O'Donnell CJ, Manning WJ. Pericardial fat, intrathoracic fat, and measures of left ventricular structure and function: the Framingham Heart Study. *Circulation*. 2009;119:1586-91.
8. Hachiya K, Fukuta H, Wakami K, Goto T, Tani T, Ohte N. Relation of epicardial fat to central aortic pressure and left ventricular diastolic function in patients with known or suspected coronary artery disease. *Int J Cardiovasc Imaging*. 2014;30:1393-8.
9. Khawaja T, Greer C, Chokshi A, Chavarria N, Thadani S, Jones M, Schaefle K, Bhatia K, Collado JE, Shimbo D, Einstein AJ, Schulze PC. Epicardial fat volume in patients with left ventricular systolic dysfunction. *Am J Cardiol*. 2011;108:397-401.
10. Konishi M, Sugiyama S, Sugamura K, Nozaki T, Matsubara J, Akiyama E, Utsunomiya D, Matsuzawa Y, Yamashita Y, Kimura K, Umemura S and Ogawa H. Accumulation of pericardial fat correlates with left ventricular diastolic dysfunction in patients with normal ejection fraction. *J Cardiol*. 2012;59:344-51.
11. Lai YH, Hou CJ, Yun CH, Sung KT, Su CH, Wu TH, Yang FS, Hung TC, Hung CL, Bezerra HG, Yeh HI. The association among MDCT-derived three-dimensional visceral adiposities on cardiac diastology and dyssynchrony in asymptomatic population. *BMC Cardiovasc Disord*. 2015;15:142.
12. Liu J, Fox CS, Hickson DA, May WL, Ding J, Carr JJ, Taylor HA. Pericardial fat and echocardiographic measures of cardiac abnormalities: the Jackson Heart Study. *Diabetes Care*. 2011;34:341-6.
13. Longenecker CAK, S; Serhal, M; Kinley, B; Labbato, D; McComsey, GA. Diastolic Function Correlates With Pericardial Fat [fat around the heart] and Vascular Remodeling in HIV. *Conference on Retroviruses and Opportunistic Infections (CROI)*. 2016.
14. Ng AC, Goo SY, Roche N, van der Geest RJ, Wang WY. Epicardial Adipose Tissue Volume and Left Ventricular Myocardial Function Using 3-Dimensional Speckle Tracking Echocardiography. *Can J Cardiol*. 2016;32:1485-1492.
15. Ruberg FL, Chen Z, Hua N, Bigornia S, Guo Z, Hallock K, Jara H, LaValley M, Phinikaridou A, Qiao Y, Viereck J, Apovian CM, Hamilton JA. The relationship of ectopic lipid accumulation to cardiac and vascular function in obesity and metabolic syndrome. *Obesity (Silver Spring)*. 2010;18:1116-21.
16. Wu CK, Tsai HY, Su MY, Wu YF, Hwang JJ, Tseng WY, Lin JL, Lin LY. Pericardial fat is associated with ventricular tachyarrhythmia and mortality in patients with systolic heart failure. *Atherosclerosis*. 2015;241:607-14.
17. Yamashita KO, Ebara S, Yamamoto MH, Obara C. Increased epicardial adipose tissue are associated with left ventricular diastolic dysfunction. *Journal of the American College of Cardiology*. 2012;59:E1349.
18. Al Chekakie MO, Welles CC, Metoyer R, Ibrahim A, Shapira AR, Cytron J, Santucci P, Wilber DJ, Akar JG. Pericardial fat is independently associated with human atrial fibrillation. *J Am Coll Cardiol*. 2010;56:784-8.
19. Doesch C, Haghi D, Suselbeck T, Schoenberg SO, Borggrefe M, Papavassiliu T. Impact of Functional, Morphological and Clinical Parameters on Epicardial Adipose Tissue in Patients With Coronary Artery Disease. *Circulation Journal*. 2012;76:2426-2434.

20. Doesch C, Streitner F, Bellm S, Suselbeck T, Haghi D, Heggemann F, Schoenberg SO, Michaely H, Borggrefe M, Papavassiliu T. Epicardial adipose tissue assessed by cardiac magnetic resonance imaging in patients with heart failure due to dilated cardiomyopathy. *Obesity (Silver Spring)*. 2013;21:E253-61.
21. Doesch C, Haghi D, Fluchter S, Suselbeck T, Schoenberg SO, Michaely H, Borggrefe M, Papavassiliu T. Epicardial adipose tissue in patients with heart failure. *J Cardiovasc Magn Reson*. 2010;12:40.
22. Vanni EM, Faletti R, Morello M, Mezzabotta L, Battisti G, Frea S, Cannillo M, Mosso E, Rosso C, Bergamasco L, Rizzetto M, Bugianesi E. Incerased Epicardial Fat and Early Signs of Impaired Diastolic and Systolic Left Ventricular Function in Non-diabetic, normotensive patients with nonalcoholic fatty liver disease. *Journal of Hepatology*. 2015;62:S745.
23. Vural M, Talu A, Sahin D, Elalmis OU, Durmaz HA, Uyanik S, Dolek BA. Evaluation of the relationship between epicardial fat volume and left ventricular diastolic dysfunction. *Jpn J Radiol*. 2014;32:331-9.

SYSTEMATIC REVIEW AND META-ANALYSIS

Association of Volumetric Epicardial Adipose Tissue Quantification and Cardiac Structure and Function

Nitesh Nerlekar, MBBS, MPH; Rahul G. Muthalaly, MBBS; Nathan Wong, MBBS; Udit Thakur, MBBS; Dennis T. L. Wong, MD, PhD; Adam J. Brown, MD, PhD; Thomas H. Marwick, MBBS, MPH, PhD

***Background*—**Epicardial adipose tissue (EAT) is in immediate apposition to the underlying myocardium and, therefore, has the potential to influence myocardial systolic and diastolic function or myocardial geometry, through paracrine or compressive mechanical effects. We aimed to review the association between volumetric EAT and markers of myocardial function and geometry.

***Methods and Results*—**PubMed, Medline, and Embase were searched from inception to May 2018. Studies were included only if complete EAT volume or mass was reported and related to a measure of myocardial function and/or geometry. Meta-analysis and meta-regression were used to evaluate the weighted mean difference of EAT in patients with and without diastolic dysfunction. Heterogeneity of data reporting precluded meta-analysis for systolic and geometric associations. In the 22 studies included in the analysis, there was a significant correlation with increasing EAT and presence of diastolic dysfunction and mean e′ (average mitral annular tissue Doppler velocity) and E/e′ (early inflow / annular velocity ratio) but not E/A (ratio of peak early (E) and late (A) transmitral inflow velocities), independent of adiposity measures. There was a greater EAT in patients with diastolic dysfunction (weighted mean difference, 24.43 mL; 95% confidence interval, 18.5–30.4 mL; $P<0.001$), and meta-regression confirmed the association of increasing EAT with diastolic dysfunction ($P=0.001$). Reported associations of increasing EAT with increasing left ventricular mass and the inverse correlation of EAT with left ventricular ejection fraction were inconsistent, and not independent from other adiposity measures.

***Conclusions*—**EAT is associated with diastolic function, independent of other influential variables. EAT is an effect modifier for chamber size but not systolic function. **(*J Am Heart Assoc*. 2018;7:e009975. DOI: 10.1161/JAHA.118.009975.)**

Key Words: diastolic function • epicardial fat • systolic dysfunction

Epicardial adipose tissue (EAT) has been widely studied as a potential contributor to cardiovascular pathological characteristics. Much of this research has focused on its effect on coronary atherosclerosis,[1] but there are unique properties of EAT that may lead to an effect on myocardial function. EAT shares direct anatomic contact with the myocardium without fascial interruption[2] and, therefore, may exhibit local compressive forces, resulting in alteration of myocardial function and geometry. In addition, the shared blood supply of the coronary circulation to both the myocardium and surrounding EAT may predispose paracrine effects on the neighboring myocardium with such inflammatory cytokines as MCP-1 (monocyte chemoattractant), interleukin-β, interleukin-6, tumor necrosis factor-α, and leptin.[2] Persisting inflammation may lead to collagen deposition and subsequent impaired left ventricular (LV) relaxation and further effects on diastolic and systolic function. Furthermore, there is an association between EAT and release of free fatty acids, as well as their myocardial consumption.[3] The relationship between obesity, visceral fat, and EAT may also explain effects on myocardial function, chamber size, and mass.

Several methods have been used for measurement of EAT, including echocardiography, cardiac computed tomography (CT), and cardiac magnetic resonance imaging (MRI). Echocardiography may overestimate or underestimate total EAT volume because of single-plane assessment and the effects of probe angulation on linear measurement. Single-slice area measurements on CT or MRI are also limited by being only single-plane measures. Recently, we have demonstrated the

From the Monash Cardiovascular Research Centre, Department of Medicine (Monash Medical Centre), Monash University and Monash Heart, Monash Health, Clayton, Australia (N.N., R.G.M., N.W., U.T., D.T.L.W., A.J.B.); Baker Heart and Diabetes Institute, Melbourne, Australia (N.N., T.H.M.); and South Australian Health and Medical Research Institute, Adelaide, Australia (D.T.L.W.).

Accompanying Tables S1 through S3 are available at https://www.ahajournals.org/doi/suppl/10.1161/JAHA.118.009975

Correspondence to: Thomas H. Marwick, MBBS, MPH, PhD, Baker Heart and Diabetes Institute, 75 Commercial Rd, Melbourne, Victoria 3004, Australia. [redacted]

Received May 31, 2018; accepted October 3, 2018.

Clinical Perspective

What Is New?

- Increasing epicardial adipose tissue volume is associated with diastolic dysfunction, independent of other markers of adiposity.
- Epicardial adipose tissue is an effect modifier for left ventricle chamber geometry.
- Epicardial adipose tissue is not associated with systolic function.

What Are the Clinical Implications?

- Epicardial adipose tissue may represent an important target for therapy associated with diastolic dysfunction.

superiority of volumetric EAT assessment in comparison to 2-dimensional linear echocardiographic EAT thickness.[4] We, therefore, sought the association of full-volume quantification of EAT (assessed by cardiac CT or cardiac MRI) with myocardial function, as assessed by transthoracic echocardiography, full R-R interval cardiac CT, or cardiac MRI.

Methods

Search Method

We conducted this systematic review in accordance with the Preferred Reporting Items for Systematic Reviews and Meta-Analyses (PRISMA) statement, and the trial was registered with PROSPERO (CRD 42017038400). The search was conducted in MEDLINE, EMBASE, and PubMed databases, ending in March 2018. References of eligible articles were hand searched for additional articles. Searches were restricted to human studies, and conference abstracts were included. A study search flowchart is presented in Figure 1, and the specific search term strategy is given in Table S1. The data, analytic methods, and study materials will not be made available to other researchers for purposes of reproducing the results or replicating the procedure.

Our inclusion criteria were as follows: patients undergoing cardiac CT (CT angiography or calcium score) or MRI with volumetric assessment of EAT (either volume or mass), with cardiac imaging for assessment of myocardial function parameters (full cardiac cycle cardiac CT or MRI or echocardiography), or measurement of myocardial geometry (LV mass, LV volumes, and left atrium size) by validated methods.

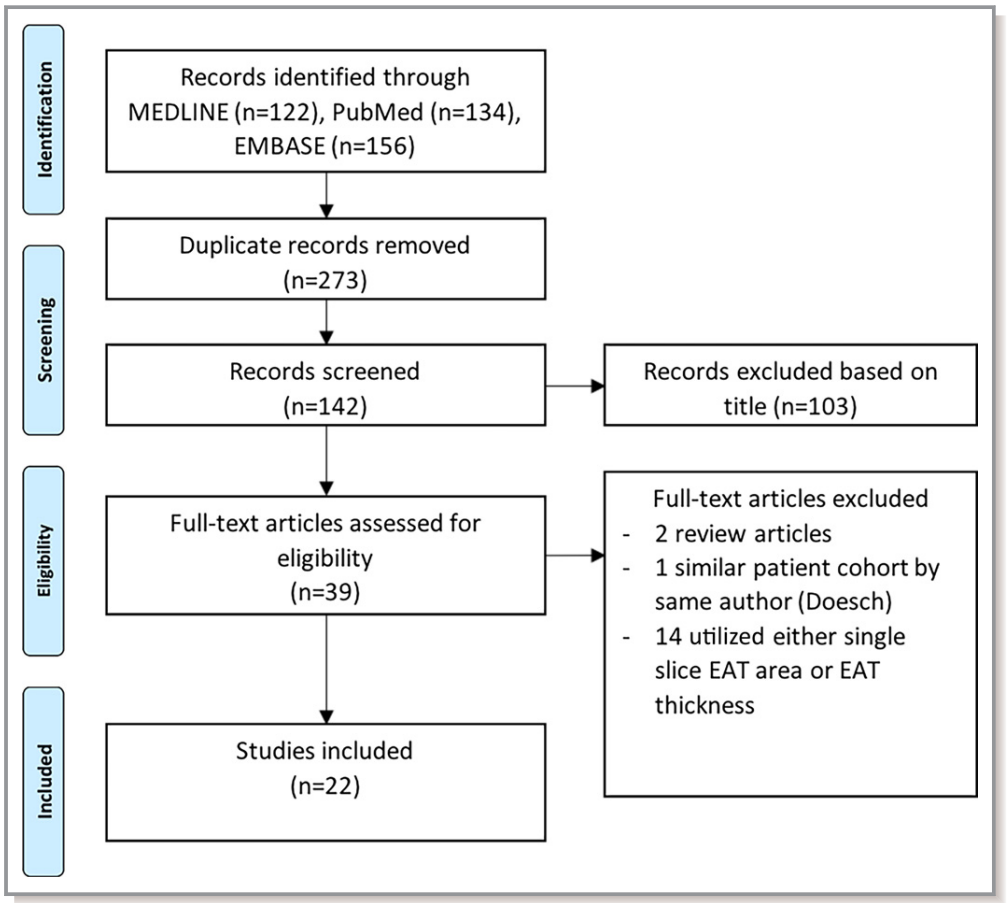

Figure 1. Search strategy. EAT indicates epicardial adipose tissue.

Assessment of diastolic function was restricted to studies using echocardiography. Exclusion criteria included the following: any study with linear measurement of EAT thickness, single-slice area measures of EAT, measures of myocardial lipid content not differentiated from EAT, and measurement of paracardial adipose tissue (ie, fat beyond the parietal pericardium). Two authors (N.N. and R.G.M.) independently reviewed the abstracts from the search to meet the inclusion criteria, and discrepancies were resolved by consensus. Probable overlap of the patient cohort with a similar study led to exclusion of the smaller study.[5]

Evaluation of Full-Volume EAT

EAT was regarded as adipose tissue enclosed within the visceral pericardium, and mean values (indexed and nonindexed) were recorded.

Evaluation of Cardiac Function

Included studies measured myocardial performance based on echocardiography or MRI. Measures of diastolic function included the following: transmitral flow for peak early (E) and late (A) inflow velocities and their ratio (E/A); deceleration time; septal, lateral, and/or average myocardial annular velocities on tissue Doppler imaging (e′); early inflow/annular velocity ratio (E/e′); pulmonary vein flow to calculate the time difference between the atrial reversal wave and mitral A-wave duration; and the isovolumic relaxation time. Diastolic class grade was recorded if reported: normal, grade 1 (impaired relaxation), grade 2 (pseudonormal), and grade 3 (restrictive). Measures of systolic performance assessed included LV ejection fraction, cardiac output, stroke volume, and global longitudinal strain, if recorded. Measures of cardiac structure included LV mass, LV end-diastolic and end-systolic volumes, and left atrial size.

Statistical Analysis

Data on univariable correlations are presented because this was the most consistent measure seen in included studies. Where multivariable regression was performed, adjusted study estimates and model covariates are reported. Meta-analysis was performed for the weighted mean difference in EAT volume between groups with and without diastolic dysfunction. Meta-regression of weighted mean difference as an effect size and the combined mean EAT in included studies were performed with the moment-based estimate of between-study variance and a permutation test using 1000 Monte Carlo simulations to moderate for potentially spurious results, as previously described.[6] Precision of pooled estimates is reported as 95% confidence intervals, and heterogeneity is reported by the I^2 statistic. The Newcastle Ottawa Scale was used to assess risk of bias (Tables S2 and S3). Statistical analysis was performed using StataMP 14.0 (StataCorpLP, College Station, TX).

Results

Study Selection

A brief outline summary of the 22 studies (18 published and 4 conference papers) included in this review is presented in Table 1.[3,7–28]

Association of EAT With LV Diastolic Function

There were 11 studies that investigated the relationship between EAT and diastolic parameters, with 5 specifying adherence to an iteration of the American Society of Echocardiography diastolic guidelines.[29] EAT was associated with diastolic parameters, including peak mitral annular tissue Doppler velocities (e′ septal, e′ lateral, or e′ mean) and transmitral flow (early [E] and late [A] diastolic peak flow velocities and their ratio [E/A]) (Table 2).[9,13–16,18,20–24,29–32] Although some studies did perform comprehensive Doppler measures, such as isovolumic relaxation times, deceleration times, and pulmonary vein Doppler, the association with EAT individually with each parameter was not described. The classification of patients with diastolic dysfunction was available in 5 studies. Most patients (26%–38% of total cohort) had grade 1 diastolic dysfunction, with fewer qualifying as grade ≥2 (2%–28%).

In the 5 studies that measured differences in EAT between groups, EAT was significantly greater in the diastolic dysfunction group compared with patients with normal diastolic function (weighted mean difference, 24.4 mL; 95% confidence interval, 18.5–30.4 mL; $P<0.001$; $I^2=28\%$) (Figure 2).[15,16,20,21,23,26] Meta-regression, performed evaluating the weighted mean difference (effect size) against the mean EAT volume, demonstrated a nominally increasing presence of diastolic dysfunction with increasing EAT values ($\beta=0.17$, SEE=0.09, $P=0.06$). This was statistically significant after Monte Carlo permutation testing, $P=0.001$ (Figure 3).

Mean E/e′ values were positively correlated with EAT (r value range, 0.21–0.34; $P<0.05$), and mean e′ values were inversely correlated (r value range, −0.26 to −0.44; $P<0.05$); in all but one study, no consistent association was seen with the E/A ratio (r value range, −0.40 to 0.08). Increasing EAT was an independent predictor of diastolic dysfunction, e′ and E/e′ independent of age, sex, and measures of adiposity (Table 2). No independent association was identified with the E/A ratio. In 6 studies, hypertension was also an adjusted covariate in the model, and increasing EAT remained a predictor of altered diastolic parameters.

Association of EAT With Systolic Function

Of 10 studies describing the association of EAT with systolic parameters, LV function was evaluated with MRI in 5 and echocardiography in 4 (Table 3).[3,10,11,16,18,19,22,27] One study

DOI: 10.1161/JAHA.118.009975

Table 1. Study Characteristics

First Author	Year	Country	Study Type	Population	Sample Size	EAT Method	EAT Value
Bakkum[8]	2015	the Netherlands	Cross-sectional	Suspected CAD	208	PET-CT	113.8±48.1 cm^3
Cavalcante[9]	2012	United States	Cross-sectional	Self-referred screening	110	MDCT	Men, 101±51 cm^3 Women, 67±40 cm^3
Al Chekakie[7]	2010	United States	Case-control	AF and controls	273	MDCT	Sinus rhythm, 76.1±36.3 mL; AF, 101.6±44.1 mL
Doesch[11]	2012	Germany	Case-control	Established CAD	158 Cases and 40 controls	MRI	Control, 31±8 g/m^2; CAD, 29±10 g/m^2; CAD and EF <50%, 26±8 g/m^2; CAD and EF >50%, 36±11 g/m^2
Doesch[12]	2013	Germany	Case-control	DCM	112 Cases and 48 controls	MRI	Control, 62.1±14.4 g; DCM, 47.2±15.2 g; control, 66±15.3 mL; DCM, 50.2±16.2 mL; control, 31.7±5.6 g/m^2; DCM, 24±7.5 g/m^2; control, 33.5±6.4 mL/m^2; DCM, 25.5±8 mL/m^2
Doesch[10]	2010	Germany	Case-control	CHF (LVEF <35%) (ICM=36; DCM=30)	66 Cases and 31 controls	MRI	Control, 71±13 mL; CHF, 46±11 mL; control, 36±5 mL/m^2; CHF, 24±5 mL/m^2; control, 67±13 g; CHF, 43±11 g; control, 34±4 g/m^2; CHF, 22±5 g/m^2
Ede[13]	2014	Turkey	Cross-sectional	Suspected CAD	106	MDCT	38±31 cm^3
Faustino[14]*	2011	Portugal	Cross-sectional	Not specified	78	MDCT	Threshold of 44.1 mL defined by ROC curve (72% sensitivity and 50% specificity) for diastolic dysfunction
Fernando[15]*	2015	United States	Cross-sectional	AF before ablation	20	MRI	125.7±56.7 mL
Fontes-Carvalho[16]	2014	Portugal	Cross-sectional	Postmyocardial infarction	225	MDCT	113.6±43.2 cm^3
Fox[17]	2009	United States	Cross-sectional	Substudy of Framingham	997	MDCT	Women, 108±41 cm^3; men, 136.5±54.4 cm^3
Hachiya[18]	2014	Japan	Cross-sectional	Suspected CAD	134	MDCT	77.1±29.6 cm^3/m^2
Khawaja[19]	2011	Unites States	Cross-sectional	Suspected CAD	381	MDCT	Normal LVEF, 114.5±98.5 cm^3; LVEF <55%, 83.5±67.1 cm^3
Konishi[20]	2012	Japan	Cross-sectional	Suspected CAD	229	MDCT	Diastolic dysfunction, 184±61 cm^3; normal function, 154±58 cm^3
Lai[21]	2015	Taiwan	Cross-sectional	Self-referred screening	318	MDCT	80.6±33 mL
Liu[22]	2011	United States	Cross-sectional	Blacks	1402	MDCT	Men, 79.8±37.1 mL; women, 67.1±29.0 mL
Longenecker[23]*	2016		Cross-sectional	Patients with HIV	46 HIV+ and 23 HIV−	MDCT	HIV+ with DD, median of 120 (74–143) mL; HIV+ with normal function, median of 72 (54–100) mL; HIV−, not specified

Continued

Table 1. Continued

First Author	Year	Country	Study Type	Population	Sample Size	EAT Method	EAT Value
Ng[24]	2016	Australia	Cross-sectional	Suspected CAD	130	MDCT	Total, 97.5±43.7 cm^3; men, 103.7±39.5 cm^3; women, 90.9±47.4 cm^3
Ruberg[3]	2010	United States	Cross-sectional	Obese with metabolic syndrome	28 Cases and 18 controls	MRI	Controls, 85±66 mL; subjects, 161±88 mL; controls, 1.1±0.7 mL/g; subjects, 2.0±1.1 mL/g
Vanni[25]*	2015	Italy	Case-control	Not specified	19 NAFLD and 9 controls	MRI	NAFLD, 228.1±112.9 mL; controls, 66.8±25.2 mL
Vural[26]	2014	Turkey	Case-control	Suspected CAD	63	CACS	137±56 cm^3
Wu[27]	2015	Taiwan	Cross-sectional	Compensated CHF	50 Cases and 20 controls	MRI	Control, 45.8 (39.4–50.3) mL; CHF+VT/VF, 51.5 (46.6–59.8) mL); CHF and no VT/VF, 44.0 (33.9–48.3) mL
Yamashita[28]*	2012	Japan	Cross-sectional	Suspected CAD	286	MDCT	EAT, 71.6±37.9 (10.5–179.9) mL

Values are mean±SD or mean (range). AF indicates atrial fibrillation; CACS, coronary artery calcium score; CAD, coronary artery disease; CHF, congestive heart failure; DCM, dilated cardiomyopathy; DD, diastolic dysfunction; EAT, epicardial adipose tissue; ICM, ischemic cardiomyopathy; LVEF, left ventricular ejection fraction; MDCT, multidetector computed tomography; MRI, magnetic resonance imaging; NAFLD, nonalcoholic fatty liver disease; PET-CT, positron emission tomography–computed tomography; ROC, receiver operating characteristic; VT/VF, ventricular tachycardia/ventricular fibrillation.
*This is a conference abstract.

reported associations between EAT and global longitudinal strain, a subclinical measure of myocardial function.[24] Only one described an independent effect of EAT on LV ejection fraction (LVEF) by echocardiography.[19] No univariable correlation with LVEF was reported in the MRI studies.[10–12] Of the 6 studies reporting multivariable regression analysis, an independent association with LVEF was observed in 2 studies: one study was performed in patients with established coronary artery disease (CAD) stratified by LVEF and compared with normal controls (hazard ratio, 0.48; 95% confidence interval, 0.28–0.68; $P<0.01$),[11] and the other study was performed in patients undergoing investigation for suspected CAD with reduced LVEF compared with normal LVEF (values not reported).[19]

The only consistent feature across all studies appeared to be a relative decrease in EAT as LVEF decreased. In studies that included control groups (ie, normal LVEF), no association of EAT with EF was identified in the control group. One study demonstrated a significant inverse correlation with EAT (normalized to LV mass) with cardiac output and stroke volume (but not LVEF)[3] in obese patients (r value, −0.46) but not in corresponding controls.

In studies focusing specifically on patients with reduced LVEF, EAT was reduced compared with those with preserved LVEF. Doesch et al[11] demonstrated that patients with CAD and preserved LVEF had greater EAT (36±11 g/m^2) than normal controls without CAD (31±8 g/m^2), and both had greater EAT than patients with CAD with LVEF <50% (28±8 g/m^2; $P<0.01$). A population with presumed ischemic cardiomyopathy (CAD with reduced LVEF) also reported a stepwise decrease in EAT volume with reducing grades of LVEF.[19] This stepwise decrease was not found in a different study by Doesch et al[12] in patients with dilated cardiomyopathy against normal controls, although EAT was reduced overall compared with normal controls.

In the study related to strain analysis,[24] there was a positive correlation with EAT and impaired 3-dimensional global longitudinal strain ($r=0.601$, $P<0.001$) that remained significant on multivariable regression (standardized $\beta=0.512$, $P<0.001$), independent of markers of obesity and diabetes mellitus.

Association of EAT With Chamber Measures

There were 14 studies with data relating to a measure of myocardial geometry. All modalities of echocardiography, CT, and MRI were represented, with most values indexed to body surface area, unless otherwise specified. Some studies avoided indexation because body weight or other adiposity measures were used in regression models and, therefore, raw measures were used to prevent collinearity.

The most often reported univariable correlation coefficient was for EAT and LV mass or indexed mass and was always

Table 2. EAT and Diastolic Function

First Author	Diastolic Function Reference	Subgroup Characteristics		Diastolic Parameter Correlations			Multivariable Regression Comments
		DD	Normal Function	E/A	e′	E/e′	
Cavalcante[9]	ASE[29]	Grade 1 (n=29, 26%) Grade 2 (n=11, 10%)	n=70, 64%		Averaged 0.44*	0.34*	Multivariate model outcomes of grade 1 or higher DD, mean e′, and mean E/e′: EAT was an independent predictor (model included 10-y Framingham Risk Score, metabolic syndrome, subclinical CAD, and LV mass index), β range, −0.02 to 0.04 (all P<0.05). Indexed EAT was found to increase clinical model for prediction of DD (adjusted R^2=0.16 vs 0.24; P=0.004) and mean e′ (adjusted R^2=0.17 vs 0.27; P=0.001) (ie, indexed EAT represents 8%–10% of the variation of predictors for DD
Ede[13]	Lang et al[32]	Grade 1 (n=39, 37%) Grade 2 (n=10, 9%) Grade 3 (n=2, 2%)	n=55, 52%	−0.404			
Faustino[14†]	Not specified	46 Patients with DD and EAT >44.1 mL	32 Patients with no DD and EAT <44.1 mL				EAT not significant on multivariable regression (results and covariates not reported). Relationship of EAT with DD by ROC AUC of 0.66 (P=0.02)
Fernando[15†]	Not specified	EAT=164±118 mL (E/E′ >15)	EAT=114±54 mL (E/E′ <15)		−0.48*	0.22	On multivariable regression adjusted for age, BMI, LA volume, hypertension, and CAD, EAT associated with abnormal myocardial relaxation (OR, not specified; P=0.04)
Fontes-Carvalho[16]	ASE[29]	EAT=116.7±67.9 cm^3 Grade 1 (n=57, 28%) Grade 2 (n=58, 28%) Grade 3 (n=10, 5%)	EAT=93.0±52.3 cm^3 n=80 (39%)		e′ Septal, −0.26* e′ lateral, −0.28*	0.25*	On multivariable regression adjusted for hypertension, age, sex, and other markers of adiposity (SAT, VAT, waist/height ratio, and fat mass %), EAT remained significantly predictive of E/e′ (β, 0.19 [0.06–0.32]; P<0.01), as did e′ septal and e′ lateral
Hachiya[18]	ASE[29]			−0.05	−0.31*	0.24*	Definition of diastolic dysfunction not specified. On different multivariate models, e′ inversely correlated with EAT (standardized β range, −0.30 to −0.36; all P<0.05) but not E/e′ (standardized β, 0.23; P=0.06), except when adjusted for age, sex, and BMI (model 1) and medication use (model 2) (standardized β range, 0.25–0.31; all P<0.05)
Konishi[20]	Defined as E/e′ >10	EAT=184±61 cm^3 n=141 (62%)	EAT=154±58 cm^3 n=88 (38%)			0.21*	On multivariable regression with age, hypertension, male sex, diabetes mellitus, and abdominal obesity, there was an independent effect of EAT on DD: OR, 2.09 (1.15–3.79; P=0.02) for EAT per 100 cm^3

Continued

DOI: 10.1161/JAHA.118.009975

Table 2. Continued

First Author	Diastolic Function Reference	Subgroup Characteristics		Diastolic Parameter Correlations			Multivariable Regression Comments
		DD	Normal Function	E/A	e′	E/e′	
Lai[21]	Lang et al[32]	EAT=86.79±31.77 n=100	EAT=67.32±31.95 n=218		−0.38*	0.284*	On multivariable regression adjusted for age, sex, BMI, systolic blood pressure, LV mass index, hypertension, diabetes mellitus, hyperlipidemia, and smoking, EAT was significantly associated with E/A (β, −0.002),* E′ (β, −0.02),* E/E′ (β, 0.02),* and diastolic dyssynchrony (β, 0.197).* ROC-derived optimal cutoff for DD was 67.3 mL (ROC, 0.712; sensitivity, 73%; specificity, 62%)
Liu[22]	Gottdiener et al[31]			Men, −0.12)* women, −0.12*			On multivariable linear regression adjusted for age, height, smoking, alcohol, blood pressure, eGFR, hemoglobin, total physical activity score, medications, VAT, and weight, E/A no longer became significant (regression co-efficient, −0.01±0.02 [*P*=0.41] in women and −0.0±0.02 [*P*=0.64] in men) (described as pericardial fat volume)
Longenecker[23†]	Not specified	Grade 1 (n=29 [HIV+, n=19; HIV−, n=10]) Grade 2 (n=2 [HIV+, n=1; HIV−, n=2])	n=38 (HIV+) n=26 and n=12 (HIV−)	−0.392*			On multivariable regression adjusted for age, BMI, and sex, EAT remained independently associated with diastolic dysfunction (OR, 1.35; 95% CI, 1.02–1.79) per 10-mL increase (described as pericardial fat volume)
Ng[24]	Not specified				e′ Septal, −0.263)*; e′ lateral, −0.285*		
Vural[26]	Alnabhan et al[30]	EAT=164.4±54 cm^3 Grade 1 (n=24, 38%) Grade 2 (n=4, 6%) Grade 3 (n=1, 1.5%)	EAT=114.1±46.6 cm^3 n=34 (56%)		−0.437*		On multivariable regression adjusted for age, blood pressure, BMI, waist circumference, and cholesterol, EAT was an independent predictor of DD (OR, 1.03 [1.01–1.06]; *P*=0.006). ROC-derived optimal cutoff for DD, 129.6 cm^3 (ROC curve, 0.758)

Correlations represent the correlation co-efficient.

Values are mean±SD or mean (range). ASE indicates American Society of Echocardiography; AUC, area under the curve; BMI, body mass index; CAD, coronary artery disease; CI, confidence interval; DD, diastolic dysfunction; e′, average mitral annular tissue Doppler velocity; E/e′, early inflow / annular velocity ratio; E/A, ratio of peak early (E) and late (A) transmitral inflow velocities; EAT, epicardial adipose tissue; eGFR, estimated glomerular filtration rate; LA, left atrial; LV, left ventricular; OR, odds ratio; ROC, receiver operating characteristic; SAT, subcutaneous adipose tissue; VAT, visceral adipose tissue.

**P* value for univariate correlation is significant at <0.05.

†Study is a conference abstract.

DOI: 10.1161/JAHA.118.009975

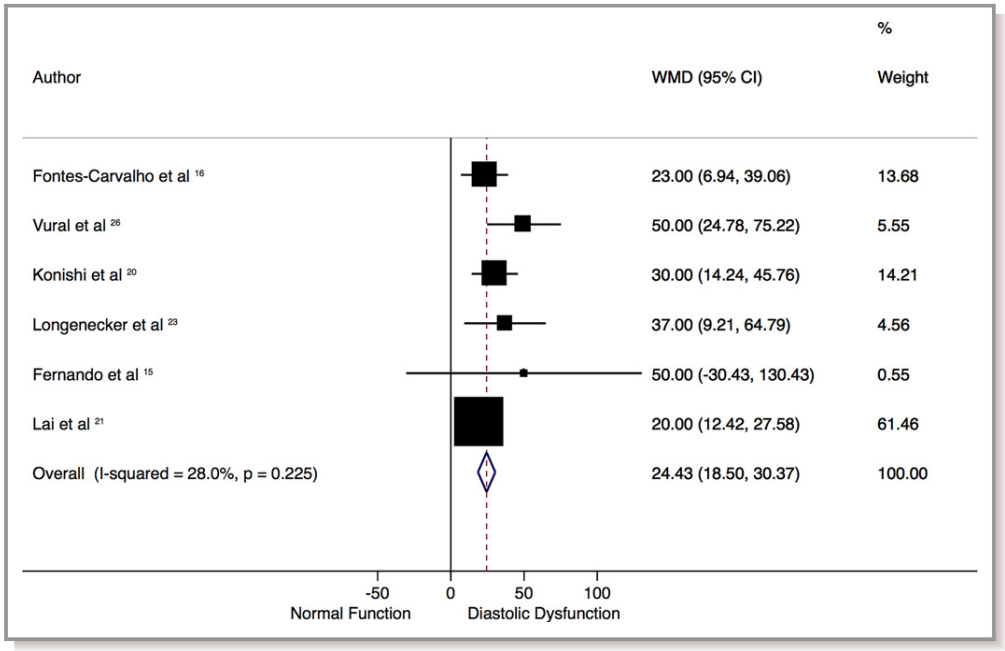

Figure 2. Mean difference of epicardial adipose tissue (EAT) volume in patients with and without diastolic dysfunction. Forest plot demonstrates the weighted mean difference (WMD; in mL) of EAT in studies with and without diastolic dysfunction, according to a random-effect model. Those with diastolic dysfunction have significantly greater EAT volumes. There is mild heterogeneity, as seen by the I^2 statistic of 28%. CI indicates confidence interval.

statistically significantly positively correlated in the diseased patient group (not controls), with ranges from r=0.19 to r=0.42 (P<0.05). Only studies by Doesch et al[11,12] measured LV end-diastolic diameter and found a consistent association with EAT (r value range, 0.22–0.42; P<0.05). Similar findings were seen for LV end-diastolic and end-systolic volume. Left atrial size was measured either as volume or diameter and demonstrated significant univariable associations with EAT (Table 4).*

An inconsistent association was seen with measures of adiposity in relation to EAT and cardiac structure. In patients with reduced LVEF, indexed EAT appears to be associated with indexed LV end-diastolic mass independent of BMI (Table 4).[10–12] One study assessing patients with suspected CAD and normal LVEF demonstrated that EAT correlated best with LV mass (nonindexed) in the nonobese cohort only (β=0.23, P<0.001).[8] Finally, in 2 observational studies, an independent association of EAT with LV mass (nonindexed), adjusted for body weight, was only seen in women (Table 4).[17,22]

Discussion

This review of 21 studies has demonstrated the emerging body of work relating EAT to myocardial structure and function. Increasing EAT is associated with the following: (1) an increasing prevalence of diastolic dysfunction; (2) a concomitant increase in LV mass; and (3) no consistent association with markers of systolic function. However, these

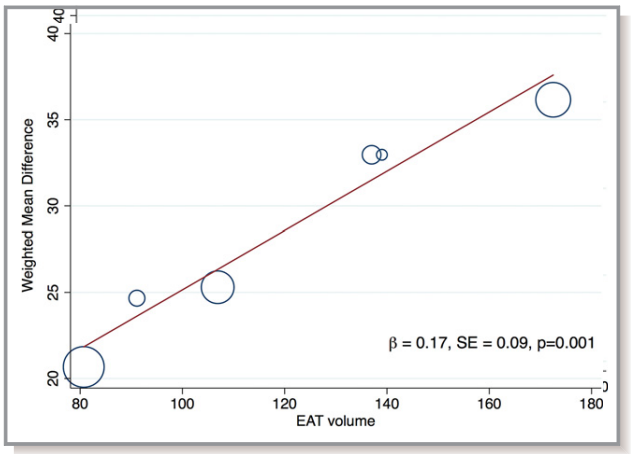

Figure 3. Meta-regression of the effect of increasing epicardial adipose tissue (EAT) volume on the weighted mean difference (effect size) of EAT in patients with and without diastolic dysfunction. Meta-regression bubble plot depicts increasing differences in mean EAT volume in patients with diastolic dysfunction as EAT increases. Circles represent the weight of each study. β coefficient is from meta-regression with associated SEE; P value is from Monte-Carlo testing (1000 simulations) and demonstrates a significant association (P=0.001).

*References 3, 7–12, 17, 18, 20, 22, 24, 25, 28.

Table 3. EAT and Systolic Function

First Author	Method	Group	EAT Value	Systolic Measure	*r* Value (Univariate)	Multivariable Regression Comment
Doesch[11]	MRI	CAD and EF >50% (n=44) CAD and EF <50% (n=114) Combined CAD (n=158) Controls (n=40)	36±11 g/m^2 26±8 g/m^2 29±10 g/m^2 31±8 g/m^2	LVEF	0.171 0.137 0.574* Not specified	On multivariable regression adjusted for BMI, NYHA classes I and III, atrial fibrillation, LV-EDVI, LV-ESVI, LV-EDD, LVRI, and LGE%, LVEF was an independent predictor of indexed EAT (HR, 0.478 [0.28–0.675]; *P*<0.01)†
Doesch[12]	MRI	Control (n=48) DCM (n=112)	31.7±5.6 g/m^2 24±7.5 g/m^2	LVEF LVEF	0.069 0.085	No correlation with LVEF and EAT (*P*=0.37)
Fontes-Carvalho[16]	Echocardiography			LVEF	−0.07	
Hachiya[18]	Echocardiography			LVEF	0.22*	Significant association on multivariate regression models adjusted for hypertension, diabetes mellitus, dyslipidemia, previous CAD or revascularization, and medication use (standardized β range, 0.16–0.22; all *P*<0.05) but not adjusted for age, sex, or BMI (standardized β, 0.13; *P*>0.05)
Khawaja[19]	Echocardiography	Normal (n=321) EF <55% (n=60) EF 35%–55% (n=43) EF <35% (n=17)	114.5±98.5 cm^3 83.5±67.1 cm^3 96.0±73.9 cm^3 52.2±29.7 cm^3			Multivariate analysis revealed LVEF and triglyceride levels predicted EAT (values and covariates not reported)
Liu[22]	Echocardiography	Women Men		LVEF LVEF	−0.04 0.03	Not significant on multivariable regression in either sex (adjusted for age, height, smoking, alcohol, blood pressure, eGFR, hemoglobin, total physical activity score, medications, VAT, and weight: regression coefficient, −0.3±0.4 [*P*=0.51] in women and 0.2±0.6 [*P*=0.72] in men). Note: described as pericardial fat volume.
Ruberg[3]	MRI	Obese		CO SV LVEF	−0.46* Inverse* Not correlated	Values are normalized to LV mass (mL/g)
		Control		CO SV LVEF	Not correlated Not correlated Not correlated	
Wu[27]	MRI			LVEF	Not correlated	

Values are mean±SD or *r* value correlation coefficients, unless otherwise stated. BMI indicates body mass index; CAD, coronary artery disease; CO, cardiac output; DCM, dilated cardiomyopathy; EAT, epicardial adipose tissue; EF, ejection fraction; eGFR, estimated glomerular filtration rate; HR, hazard ratio; LGE%, percentage of late gadolinium enhancement; LV, left ventricular; LV-EDD, LV end-diastolic diameter; LV-EDVI, LV end-diastolic volume index; LV-ESVI, left ventricular end-systolic volume index; LVRI, LV remodeling index; MRI, magnetic resonance imaging; NYHA, New York Heart Association; SV, stroke volume; VAT, visceral adipose tissue.

*P<0.05.

†Directly quoted values from source article.

correlations were no more than moderate; no coefficient exceeded 0.50.

Protective Functions of EAT

EAT has a high fatty acid content and can both release and scavenge excess free fatty acids to regulate myocardial energy production.[2] In addition, EAT secretes anti-inflammatory cytokines, such as adiponectin, adrenomedullin, and omentin, which have antiatherogenic effects; EAT also regulates vascular tone and cardiac remodelling.[33] There is a thermogenic role for EAT in providing heat for the myocardium in times of hypoxic or ischemic stress.[33] However, the presence of numerous proinflammatory

Table 4. EAT and Chamber Geometry

Author	Modality	Subgroup	LV-EDD	LA Size (Diameter/ Volume)	LVEDMI	LV-EDVI	LV-ESVI	LVRI	Comment
Bukkam[8]	CT				0.42*,†				On multivariable regression adjusted for traditional cardiovascular risk factors, CACS and BMI, EAT was not a significant predictor of LV mass in obese patients, but only in nonobese patients (β=0.23, P<0.001)
Cavalcante[9]	Echocardiography				0.41*				Measure not included in multivariate analysis
Al Chekakie[7]	CT and echocardiography			0.25/0.24					
Doesch[11]	MRI	EF <50% (n=44) EF >50% (n=114) Combined (n=158)	0.076 0.011 0.272*		0.336* 0.305* 0.019	0.201* 0.043 0.16*	0.089 0.056 0.262*	0.137 0.202 0.344*	On multivariable regression including LVEF, BMI, NYHA classes I and III, atrial fibrillation, LV-EDVI, LV-ESVI, LV-EFF, LVRI, and LGE%, best correlates to indexed EAT were LVEF, BMI, LV-ESVI (HR, 0.48; P<0.01), and LV-EDD (HR, −0.238; P=0.01). In subgroup analysis by EF <50% or >50%, full model not described; however, no association with LVEDMI in LVEF >50% but association seen in LVEF >50% (HR, 0.105; P=0.01)
Doesch[12]	MRI	Control (n=48) DCM (n=112)	0.01 0.22*		0.346* 0.417*	0.007 0.251*	0.0001 0.239*	0.204 0.116	Increased EAT mass with increasing LVEDMI in DCM, but less values than healthy control group. Greater mass seen in DCM with hypertrophy vs nonhypertrophy (31.7±5.6 vs 24.4±7.1 g/m^2; P=0.01). On multivariable regression only, LVEDMI independently correlated with indexed EAT, as was seen in healthy controls (adjusted for age and BMI [value not reported]).
Doesch[10]	MRI	Control CHF	NR 0.42*		0.36* 0.59*				Increased EAT mass in CHF with increasing LVEDMI; however, higher levels of EAT in controls compared with CHF (34±4 vs 22±5 g/m^2; P<0.01). On multivariate regression adjusted for LVEF, LV-EDD, RVEF, and LVEDMI, only LVEDMI independently associated with indexed EAT (P=0.0001)
Fox[17]	MRI	Women Men		0.28* 0.37*	0.35*,‡ 0.19*,‡	0.2*,‡ 0.07‡			On multivariable regression adjusted for age, height, smoking, alcohol, menopause, hormone replacement therapy, blood pressure, hypertension therapy, and weight, only in women, LVM (adjusted regression coefficient, 1.66; P=0.01), and in men, LA diameter (adjusted regression coefficient, 0.8; P=0.002) were independent predictors of pericardial fat volume
Hachiya[18]	Echocardiography				0.28*				Measure not included in multivariate analysis

Continued

DOI: 10.1161/JAHA.118.009975

Table 4. Continued

Author	Modality	Subgroup	LV-EDD	LA Size (Diameter/ Volume)	LVEDMI	LV-EDVI	LV-ESVI	LVRI	Comment
Konishi[20]	Echocardiography			0.32*	0.23*				Measure not included in multivariate analysis
Liu[22]	Echocardiography	Women Men		0.3* 0.11	0.24*,‡ 0.21*,‡				On multivariable regression adjusted for age, height, smoking, alcohol, blood pressure, eGFR, hemoglobin, total physical activity score, medications, VAT, and weight, only in women, LVM (adjusted regression coefficient, 4.1±1.8; P=0.03) and LA diameter (adjusted regression coefficient, 0.4±0.2; P=0.03) were independent predictors of pericardial fat volume
Ng[24]	Echocardiography					−0.09	0.08		
Ruberg[3]	MRI					Not			
Vanni[25§]	MRI	Cases					0.46*,‖		Inversely correlated with EF No other analysis specified
Yamashita[28§]	CT			0.25*					

Values are mean±SD or r value correlation coefficients, unless otherwise stated. BMI indicates body mass index; CACS, coronary artery calcium score; CHF, congestive heart failure; CT, computed tomography; DCM, dilated cardiomyopathy; EAT, epicardial adipose tissue; EF, ejection fraction; eGFR, estimated glomerular filtration rate; HR, hazard ratio; LA, left atrial; LGE%, percentage of late gadolinium enhancement; LV, left ventricular; LV-EDVI, LV end-diastolic volume index; LV-EDD, LV end-diastolic diameter; LVEF, LV ejection fraction; LVEDMI, LV end-diastolic mass index; LV-EDVI, LV end-diastolic volume index; LV-ESVI, LV end-systolic volume index; LVRI, LV remodeling index; MRI, magnetic resonance imaging; NR, not reported; NYHA, New York Heart Association; RVEF, right ventricular EF; VAT, visceral adipose tissue.

*P < 0.05.

†Value is for LV mass on CT, nonindexed and time in cardiac cycle not specified.

‡Represents a nonindexed measure.

§Study is a conference abstract.

‖Value is for end-systolic LV diameter.

DOI: 10.1161/JAHA.118.009975

cytokines within EAT may lead to a potential imbalance of harmful versus protective cytokines and disruption of myocardial function. Higher levels of these molecules (eg, tumor necrosis factor-α, interleukin-6, interleukin-1, and MCP-1) are seen in patients with CAD or heart failure. It is uncertain whether the trigger for the imbalance of cytokines is a cause of the pathological characteristics or a consequence, and a potential reciprocal or bidirectional role has been proposed.[2]

EAT and Diastolic Dysfunction

Adipose tissue can modulate the cardiovascular system by mechanisms including sympathetic activation, adipokine secretion, and myocardial oxidative stress.[34,35] EAT is regarded as a visceral fat depot. Visceral fat is metabolically active and is a determinant of diastolic function.[36] The adipokines within EAT can all affect diastolic function through persistent inflammation and subsequent collagen turnover,[37] impaired microvascular relaxation, or a direct toxic effect on the myocardium.[38,39] The loss of protective effects of adiponectin can also modify diastolic function.[40]

Mechanical effects may arise from myocardial compression of EAT because it lies within a fixed pericardial sac,[17] inducing a similar mechanism as pericardial constriction. Hachiya et al demonstrated an independent correlation of EAT with aortic pulse pressure as another mechanism of diastolic dysfunction that may be mediated by the association of EAT with aortic stiffness and, therefore, increased pulse wave velocity and early wave reflection.[18] Increased pressure in late systole may cause slower LV relaxation and subsequent diastolic dysfunction, as well as compromise coronary perfusion, especially if there is underlying CAD leading to impaired LV relaxation.[41]

EAT is associated with obesity, which itself is independently associated with diastolic dysfunction.[42] Obese patients often have elevated EAT volumes,[17] and indexed EAT has modest incremental value for diastolic dysfunction over traditional covariates, such as metabolic syndrome, subclinical CAD, and LV mass index.[9] Although the results from our analysis demonstrate that EAT had an independent effect on diastolic function parameters over adiposity measures, adiposity measures varied considerably and included BMI, bioimpedence testing, area of visceral adipose tissue or subcutaneous adipose tissue, or indexed EAT, which accounts for body weight. This heterogeneity needs further explanation to adequately isolate the effect of obesity and EAT on diastolic function. The lack of an association of EAT with E/A ratio may be confounded by the effects of age, proportion of patients with CAD, measurement in patients with normal LVEF, and the U-shaped relationship of E/A ratio with diastolic function that makes it difficult to assess without the addition of other variables.[43]

The evaluation of diastolic function is challenging and influenced by a patient's filling status, the presence of CAD, diabetes mellitus, obesity, as well as "normal" changes seen in the ageing patient. Although most studies aim to account for these factors in multivariable regression models, no more than association can be interpreted, and causality cannot be proved. Statistically, there may be implications of collinearity of obesity measures and EAT in multivariable models.

EAT and Systolic Dysfunction

Our study noted weak and inconsistent associations of EAT and systolic parameters. In the single study that evaluated EAT and longitudinal strain as a marker of subclinical myocardial dysfunction, there was a strong association noted independent of confounders, such as obesity and diabetes mellitus.[24] This is a notable finding; however, causality remains unproved and requires further assessment in larger-scale studies as a possible marker of the syndrome of heart failure with preserved ejection fraction. Various hypotheses have been developed to relate EAT and systolic function. In studies of patients with ischemic and dilated cardiomyopathy, there has been a consistent signal of reducing EAT with reducing LVEF, with less EAT also seen compared with normal controls or those with normal LVEF.[10–12,19] As myocardium becomes progressively dysfunctional, the role of EAT as a source of energy or cytokine homeostasis may become less necessary, contributing to EAT depletion. Conversely, in obese patients, there was no association with EAT (normalized to cardiac mass) and LVEF, and there was a negative correlation with MRI-derived cardiac output as EAT increased.[3] The proposed mechanism is from mechanical restriction of myocardial expansion from EAT in diastole that may lead to less ventricular filling and, therefore, reduced cardiac output.[3] A further mechanism may involve the effects of a direct cytokine release, as seen in patients with decompensated heart failure, but no studies have applied this in the context of EAT volume.

EAT and Chamber Measures

Postmortem and experimental studies[44,45] have demonstrated a constant ratio of epicardial fat/ventricular myocardium, regardless of underlying pathological characteristics of hypertrophy, ischemia, or normal muscle. Furthermore, the increase in fat mass parallels LV hypertrophy, although healthy controls have higher quantities of EAT.[10] Similar findings are seen when evaluating the LV remodeling index (ratio of mass/end-diastolic volume), where an inverse correlation is noted with LVEF and the EAT/LV remodeling index ratio. LVEF is inversely correlated with EAT and linearly correlated with LV remodeling index, suggesting that remodeling is not compensated by an adequate increase in EAT.[10]

Obesity has shown a positive relationship with increased LV mass and EAT, yet the impact of obesity on myocardial

geometry may outweigh the local effects of ectopic fat because associations attenuated after adjustment for other adiposity measures, including body weight.[17] From a mechanistic perspective, the association of EAT with central obesity and visceral adipose tissue might result in greater LV afterload and subsequent increased LV output, therefore leading to LV remodeling.[8] As LV remodeling progresses, LV diameter, volume, and mass increase, which may then deplete EAT stores[12] and result in a vicious cycle of reduced protective benefits on the heart and further dysfunction. However, the independent association of EAT with LV mass is limited to nonobese subjects.[8] Associations of EAT with the incidence of CAD have been described in nonobese people[46] and could contribute to the so-called obesity paradox.[47]

Limitations

We acknowledge several limitations in our study. EAT measurement by different modalities may lead to differences between studies. Some reported EAT indexed to Body Surface Area (BSA) (therefore accounting for weight), and some reported raw values using weight as a covariate in multivariable models. Such normalization, as opposed to normalization to height, may obscure the contribution of obesity to differences in chamber volumes and mass, which are associated with EAT. Not all studies adjusted for hypertension in multivariable models, which is also associated with obesity and diastolic function. Variations in the reference literature on measures of diastolic function also lead to difficulties with comparing studies. The differences in regional location of EAT were not available in most studies and, therefore, the effect of EAT distribution was not assessable. The level of heterogeneity and variable study end points precluded detailed meta-analysis.

Conclusions

Despite small and heterogeneous studies, there is clear evidence of a consistent effect of volumetric EAT on myocardial diastolic function and chamber measurements; however, robust data are lacking to make causal inferences. These findings are observed despite adjustment for common confounders, such as adiposity. No consistent effect is seen with respect to systolic parameters. Further longitudinal studies are necessary to generate quantitative summary measures as well as develop potential targets for treatment.

Sources of Funding

Nerlekar is supported by a scholarship from the National Medical Health and Research Council and the National Heart Foundation. Brown is supported by an Early Career Fellowship from Monash University.

Disclosures

None.

References

1. Nerlekar N, Brown AJ, Muthalaly RG, Talman A, Hettige T, Cameron JD, Wong DTL. Association of epicardial adipose tissue and high-risk plaque characteristics: a systematic review and meta-analysis. *J Am Heart Assoc*. 2017;6:e006379. DOI: 10.1161/JAHA.117.006379.
2. Iacobellis G. Local and systemic effects of the multifaceted epicardial adipose tissue depot. *Nat Rev Endocrinol*. 2015;11:363–371.
3. Ruberg FL, Chen Z, Hua N, Bigornia S, Guo Z, Hallock K, Jara H, LaValley M, Phinikaridou A, Qiao Y, Viereck J, Apovian CM, Hamilton JA. The relationship of ectopic lipid accumulation to cardiac and vascular function in obesity and metabolic syndrome. *Obesity (Silver Spring)*. 2010;18:1116–1121.
4. Nerlekar N, Baey YW, Brown AJ, Muthalaly RG, Dey D, Tamarappoo B, Cameron JD, Marwick TH, Wong DT. Poor correlation, reproducibility, and agreement between volumetric versus linear epicardial adipose tissue measurement: a 3D computed tomography versus 2D echocardiography comparison. *JACC Cardiovasc Imaging*. 2018;11:1035–1036.
5. Doesch C, Suselbeck T, Leweling H, Fluechter S, Haghi D, Schoenberg SO, Borggrefe M, Papavassiliu T. Bioimpedance analysis parameters and epicardial adipose tissue assessed by cardiac magnetic resonance imaging in patients with heart failure. *Obesity (Silver Spring)*. 2010;18:2326–2332.
6. Harbord RM, Higgins JPT. Meta-regression in Stata. *Stata J*. 2008;8:493–519.
7. Al Chekakie MO, Welles CC, Metoyer R, Ibrahim A, Shapira AR, Cytron J, Santucci P, Wilber DJ, Akar JG. Pericardial fat is independently associated with human atrial fibrillation. *J Am Coll Cardiol*. 2010;56:784–788.
8. Bakkum MJ, Danad I, Romijn MA, Stuijfzand WJ, Leonora RM, Tulevski II, Somsen GA, Lammertsma AA, van Kuijk C, van Rossum AC, Raijmakers PG, Knaapen P. The impact of obesity on the relationship between epicardial adipose tissue, left ventricular mass and coronary microvascular function. *Eur J Nucl Med Mol Imaging*. 2015;42:1562–1573.
9. Cavalcante JL, Tamarappoo BK, Hachamovitch R, Kwon DH, Alraies MC, Halliburton S, Schoenhagen P, Dey D, Berman DS, Marwick TH. Association of epicardial fat, hypertension, subclinical coronary artery disease, and metabolic syndrome with left ventricular diastolic dysfunction. *Am J Cardiol*. 2012;110:1793–1798.
10. Doesch C, Haghi D, Fluchter S, Suselbeck T, Schoenberg SO, Michaely H, Borggrefe M, Papavassiliu T. Epicardial adipose tissue in patients with heart failure. *J Cardiovasc Magn Reson*. 2010;12:40.
11. Doesch C, Haghi D, Suselbeck T, Schoenberg SO, Borggrefe M, Papavassiliu T. Impact of functional, morphological and clinical parameters on epicardial adipose tissue in patients with coronary artery disease. *Circ J*. 2012;76:2426–2434.
12. Doesch C, Streitner F, Bellm S, Suselbeck T, Haghi D, Heggemann F, Schoenberg SO, Michaely H, Borggrefe M, Papavassiliu T. Epicardial adipose tissue assessed by cardiac magnetic resonance imaging in patients with heart failure due to dilated cardiomyopathy. *Obesity (Silver Spring)*. 2013;21:E253–E261.
13. Ede H, Erkoc MF, Okur A, Erbay AR. Impaired aortic elasticity and diastolic functions are associated with findings of coronary computed tomographic angiography. *Med Sci Monit*. 2014;20:2061–2068.
14. Faustino AP, Paiva L, Mota P, Costa M, Leito-Marques A. Pericardial fat, a new marker of impaired left ventricle diastolic dysfunction. *Eur J Heart Fail Suppl*. 2011;10:S248.
15. Fernando RS, Syed MA, Wilber D, Singh S, Teme T, Rabbat M. Epicardial adipose tissue volume by cardiac magnetic resonance imaging predicts abnormal myocardial relaxation in patients with atrial fibrillation. *J Cardiovasc Magn Reson*. 2015;17:P352.
16. Fontes-Carvalho R, Fontes-Oliveira M, Sampaio F, Mancio J, Bettencourt N, Teixeira M, Rocha Goncalves F, Gama V, Leite-Moreira A. Influence of epicardial and visceral fat on left ventricular diastolic and systolic functions in patients after myocardial infarction. *Am J Cardiol*. 2014;114:1663–1669.
17. Fox CS, Gona P, Hoffmann U, Porter SA, Salton CJ, Massaro JM, Levy D, Larson MG, D'Agostino RB Sr, O'Donnell CJ, Manning WJ. Pericardial fat, intrathoracic fat, and measures of left ventricular structure and function: the Framingham Heart Study. *Circulation*. 2009;119:1586–1591.

18. Hachiya K, Fukuta H, Wakami K, Goto T, Tani T, Ohte N. Relation of epicardial fat to central aortic pressure and left ventricular diastolic function in patients with known or suspected coronary artery disease. *Int J Cardiovasc Imaging*. 2014;30:1393–1398.
19. Khawaja T, Greer C, Chokshi A, Chavarria N, Thadani S, Jones M, Schaefle K, Bhatia K, Collado JE, Shimbo D, Einstein AJ, Schulze PC. Epicardial fat volume in patients with left ventricular systolic dysfunction. *Am J Cardiol*. 2011;108:397–401.
20. Konishi M, Sugiyama S, Sugamura K, Nozaki T, Matsubara J, Akiyama E, Utsunomiya D, Matsuzawa Y, Yamashita Y, Kimura K, Umemura S, Ogawa H. Accumulation of pericardial fat correlates with left ventricular diastolic dysfunction in patients with normal ejection fraction. *J Cardiol*. 2012;59:344–351.
21. Lai YH, Hou CJ, Yun CH, Sung KT, Su CH, Wu TH, Yang FS, Hung TC, Hung CL, Bezerra HG, Yeh HI. The association among MDCT-derived three-dimensional visceral adiposities on cardiac diastology and dyssynchrony in asymptomatic population. *BMC Cardiovasc Disord*. 2015;15:142.
22. Liu J, Fox CS, Hickson DA, May WL, Ding J, Carr JJ, Taylor HA. Pericardial fat and echocardiographic measures of cardiac abnormalities: the Jackson Heart Study. *Diabetes Care*. 2011;34:341–346.
23. Longenecker CAK, Serhal M, Kinley B, Labbato D, McComsey GA. Diastolic function correlates with pericardial fat [fat around the heart] and vascular remodeling in HIV. *Conference on Retroviruses and Opportunistic Infections (CROI) February 22-25*. Boston, MA; 2016.
24. Ng AC, Goo SY, Roche N, van der Geest RJ, Wang WY. Epicardial adipose tissue volume and left ventricular myocardial function using 3-dimensional speckle tracking echocardiography. *Can J Cardiol*. 2016;32:1485–1492.
25. Vanni EM, Faletti R, Morello M, Mezzabotta L, Battisti G, Frea S, Cannillo M, Mosso E, Rosso C, Bergamasco L, Rizzetto M, Bugianesi E. Incerased epicardial fat and early signs of impaired diastolic and systolic left ventricular function in non-diabetic, normotensive patients with nonalcoholic fatty liver disease. *J Hepatol*. 2015;62:S745.
26. Vural M, Talu A, Sahin D, Elalmis OU, Durmaz HA, Uyanik S, Dolek BA. Evaluation of the relationship between epicardial fat volume and left ventricular diastolic dysfunction. *Jpn J Radiol*. 2014;32:331–339.
27. Wu CK, Tsai HY, Su MY, Wu YF, Hwang JJ, Tseng WY, Lin JL, Lin LY. Pericardial fat is associated with ventricular tachyarrhythmia and mortality in patients with systolic heart failure. *Atherosclerosis*. 2015;241:607–614.
28. Yamashita KO, Ebara S, Yamamoto MH, Obara C. Increased epicardial adipose tissue are associated with left ventricular diastolic dysfunction. *J Am Coll Cardiol*. 2012;59:E1349.
29. Nagueh SF, Appleton CP, Gillebert TC, Marino PN, Oh JK, Smiseth OA, Waggoner AD, Flachskampf FA, Pellikka PA, Evangelista A. Recommendations for the evaluation of left ventricular diastolic function by echocardiography. *J Am Soc Echocardiogr*. 2009;22:107–133.
30. Alnabhan N, Kerut EK, Geraci SA, McMullan MR, Fox E. An approach to analysis of left ventricular diastolic function and loading conditions in the echocardiography laboratory. *Echocardiography*. 2008;25:105–116.
31. Gottdiener JS, Bednarz J, Devereux R, Gardin J, Klein A, Manning WJ, Morehead A, Kitzman D, Oh J, Quinones M, Schiller NB, Stein JH, Weissman NJ. American Society of Echocardiography recommendations for use of echocardiography in clinical trials. *J Am Soc Echocardiogr*. 2004;17:1086–1119.
32. Lang RM, Bierig M, Devereux RB, Flachskampf FA, Foster E, Pellikka PA, Picard MH, Roman MJ, Seward J, Shanewise JS, Solomon SD, Spencer KT, Sutton MS, Stewart WJ. Recommendations for chamber quantification: a report from the American Society of Echocardiography's Guidelines and Standards Committee and the Chamber Quantification Writing Group, developed in conjunction with the European Association of Echocardiography, a branch of the European Society of Cardiology. *J Am Soc Echocardiogr*. 2005;18:1440–1463.
33. Fitzgibbons TP, Czech MP. Epicardial and perivascular adipose tissues and their influence on cardiovascular disease: basic mechanisms and clinical associations. *J Am Heart Assoc*. 2014;3:e000582. DOI: 10.1161/JAHA.113.000582.
34. Vincent HK, Powers SK, Stewart DJ, Shanely RA, Demirel H, Naito H. Obesity is associated with increased myocardial oxidative stress. *Int J Obes Relat Metab Disord*. 1999;23:67–74.
35. Falcao-Pires I, Castro-Chaves P, Miranda-Silva D, Lourenco AP, Leite-Moreira AF. Physiological, pathological and potential therapeutic roles of adipokines. *Drug Discov Today*. 2012;17:880–889.
36. Canepa M, Strait JB, Milaneschi Y, AlGhatrif M, Ramachandran R, Makrogiannis S, Moni M, David M, Brunelli C, Lakatta EG, Ferrucci L. The relationship between visceral adiposity and left ventricular diastolic function: results from the Baltimore Longitudinal Study of Aging. *Nutr Metab Cardiovasc Dis*. 2013;23:1263–1270.
37. Mak GJ, Ledwidge MT, Watson CJ, Phelan DM, Dawkins IR, Murphy NF, Patle AK, Baugh JA, McDonald KM. Natural history of markers of collagen turnover in patients with early diastolic dysfunction and impact of eplerenone. *J Am Coll Cardiol*. 2009;54:1674–1682.
38. Silberman GA, Fan TH, Liu H, Jiao Z, Xiao HD, Lovelock JD, Boulden BM, Widder J, Fredd S, Bernstein KE, Wolska BM, Dikalov S, Harrison DG, Dudley SC Jr. Uncoupled cardiac nitric oxide synthase mediates diastolic dysfunction. *Circulation*. 2010;121:519–528.
39. Kankaanpaa M, Lehto HR, Parkka JP, Komu M, Viljanen A, Ferrannini E, Knuuti J, Nuutila P, Parkkola R, Iozzo P. Myocardial triglyceride content and epicardial fat mass in human obesity: relationship to left ventricular function and serum free fatty acid levels. *J Clin Endocrinol Metab*. 2006;91:4689–4695.
40. Greenstein AS, Khavandi K, Withers SB, Sonoyama K, Clancy O, Jeziorska M, Laing I, Yates AP, Pemberton PW, Malik RA, Heagerty AM. Local inflammation and hypoxia abolish the protective anticontractile properties of perivascular fat in obese patients. *Circulation*. 2009;119:1661–1670.
41. Buckberg GD, Fixler DE, Archie JP, Hoffman JI. Experimental subendocardial ischemia in dogs with normal coronary arteries. *Circ Res*. 1972;30:67–81.
42. Wong C, Marwick TH. Obesity cardiomyopathy: pathogenesis and pathophysiology. *Nat Clin Pract Cardiovasc Med*. 2007;4:436–443.
43. Nagueh SF, Smiseth OA, Appleton CP, Byrd BF III, Dokainish H, Edvardsen T, Flachskampf FA, Gillebert TC, Klein AL, Lancellotti P, Marino P, Oh JK, Popescu BA, Waggoner AD. Recommendations for the evaluation of left ventricular diastolic function by echocardiography: an update from the American Society of Echocardiography and the European Association of Cardiovascular Imaging. *J Am Soc Echocardiogr*. 2016;29:277–314.
44. Corradi D, Maestri R, Callegari S, Pastori P, Goldoni M, Luong TV, Bordi C. The ventricular epicardial fat is related to the myocardial mass in normal, ischemic and hypertrophic hearts. *Cardiovasc Pathol*. 2004;13:313–316.
45. Company JM, Booth FW, Laughlin MH, Arce-Esquivel AA, Sacks HS, Bahouth SW, Fain JN. Epicardial fat gene expression after aerobic exercise training in pigs with coronary atherosclerosis: relationship to visceral and subcutaneous fat. *J Appl Physiol (1985)*. 2010;109:1904–1912.
46. Iwayama T, Nitobe J, Watanabe T, Ishino M, Tamura H, Nishiyama S, Takahashi H, Arimoto T, Shishido T, Miyashita T, Miyamoto T, Toyama S, Sadahiro M, Kubota I. Role of epicardial adipose tissue in coronary artery disease in non-obese patients. *J Cardiol*. 2014;63:344–349.
47. Lavie CJ, De Schutter A, Parto P, Jahangir E, Kokkinos P, Ortega FB, Arena R, Milani RV. Obesity and prevalence of cardiovascular diseases and prognosis—the obesity paradox updated. *Prog Cardiovasc Dis*. 2016;58:537–547.

Supplemental Material

Table S1. Example MEDLINE search strategy.

#	Searches	Results
1	exp Adipose Tissue/ or epicardial fat.mp.	79789
2	epicardial adipose tissue.mp.	417
3	epicardial fat volume.mp.	56
4	pericardial adipose tissue.mp.	58
5	pericardial fat.mp.	242
6	pericardial fat volume.mp.	31
7	1 or 2 or 3 or 4 or 5 or 6	79916
8	exp Myocardial Contraction/ or exp Heart Failure/ or exp Heart Ventricles/ or exp Echocardiography, Doppler/ or exp Ventricular Dysfunction, Left/ or exp Diastole/ or exp Ventricular Function, Left/ or diastolic function.mp.	260853
9	diastolic dysfunction.mp.	6262
10	systolic function.mp.	9152
11	exp Myocardial Contraction/ or myocardial function.mp.	75943
12	myocardial performance.mp.	2269
13	mitral annular velocities.mp.	154
14	ejection fraction.mp.	44097
15	8 or 9 or 10 or 11 or 12 or 13 or 14	282014
16	exp Tomography, X-Ray Computed/ or cardiac ct.mp.	337987
17	coronary calcium score.mp. or exp Tomography, X-Ray Computed/	337983
18	exp Multidetector Computed Tomography/ or ccta.mp.	4630
19	16 or 17 or 18	338169
20	exp Magnetic Resonance Imaging/	346308
21	cardiac mri.mp.	1739
22	ectopic fat.mp.	396
23	7 or 22	80055
24	20 or 21	346580
25	15 and 19 and 23	53
26	15 and 23 and 24	78
27	25 or 26	122

Table S2. Newcastle - Ottawa Scale for Assessment of Cross-sectional Studies.

First Author	Year	Selection				Comparability	Outcome		Total
		Representativeness of the sample	Sample size	Ascertainment of exposure	Non - respondents	Outcome groups comparable	Assessment of outcome	Correct statistical test	
Bakkum[1]	2015	*	-	**	*	*	*	*	7
Cavalcante[2]	2012	*	-	**	*	**	**	*	9
Ede[3]	2014	*	-	**	*	**	**	*	9
Faustino[¥4]	2011	*	-	**	-	**	*	*	7
Fernando[5]	2015	*	-	**	-	**	*	*	7
Fontes-carvalho[6]	2014	*	-	**	*	**	**	*	9
Fox[7]	2009	*	*	**	*	**	**	*	10
Hachiya[8]	2014	*	-	**	*	*	*	*	7
Khawaja[9]	2011	*	-	**	-	**	**	*	8
Konishi[10]	2012	*	-	**	*	-	*	*	6
Lai[11]	2015	*	-	**	*	**	*	*	8
Liu[12]	2011	*	*	**	*	**	*	*	10
Longenecker[13]	2016	*	-	**	*	**	*	*	8
Ng[14]	2016	*	-	**	*	**	*	*	8
Ruberg[15]	2010	*	-	**	*	*	**	*	8
Wu[16]	2015	*	-	**	*	*	**	*	8
Yamashita[17]	2012	*	-	**	*	**	*	*	8

Table S3. Newcastle - Ottawa Scale for Assessment of Case Control Studies.

First Author	Year	Selection			Comparability		Exposure			Total
		Representativeness of the sample	Adequate case definition?	Selection of controls	Definition of controls	Controls and cases comparable	Ascertainment of exposure	Same method of ascertainment for cases and controls	Non-response rate	
Chekakie[18]	2010	*	*	*	*	**	*	*	*	9
Doesch[19]	2012	*	*	*	*	**	*	*	*	9
Doesch[20]	2013	*	*	*	*	**	**	*	*	10
Doesch[21]	2010	*	*	*	*	**	**	*	*	10
Vanni[22]	2015	*	*	*	*	*	*	*	*	8
Vural[23]	2014	*	*	*	*	**	**	*	*	10

Supplemental References:

1. Bakkum MJ, Danad I, Romijn MA, Stuijfzand WJ, Leonora RM, Tulevski, II, Somsen GA, Lammertsma AA, van Kuijk C, van Rossum AC, Raijmakers PG, Knaapen P. The impact of obesity on the relationship between epicardial adipose tissue, left ventricular mass and coronary microvascular function. *Eur J Nucl Med Mol Imaging*. 2015;42:1562-73.
2. Cavalcante JL, Tamarappoo BK, Hachamovitch R, Kwon DH, Alraies MC, Halliburton S, Schoenhagen P, Dey D, Berman DS, Marwick TH. Association of epicardial fat, hypertension, subclinical coronary artery disease, and metabolic syndrome with left ventricular diastolic dysfunction. *Am J Cardiol*. 2012;110:1793-8.
3. Ede H, Erkoc MF, Okur A, Erbay AR. Impaired aortic elasticity and diastolic functions are associated with findings of coronary computed tomographic angiography. *Med Sci Monit*. 2014;20:2061-8.
4. Faustino AP, Paiva L, Mota P, Costa M, Leito-Marques A. Pericardial fat, a new marker of impaired left ventricle diastolic dysfunction. *European Journal of Heart Failure Supplements* 2011;10:S248.
5. Fernando RS, Syed MA, Wilber D, Singh S, Teme T, Rabbat M. Epicardial adipose tissue volume by cardiac magnetic resonance imaging predicts abnormal myocardial relaxation in patients with atrial fibrillation. *Journal of Cardiovascular Magnetic Resonance*. 2015;17:P352.
6. Fontes-Carvalho R, Fontes-Oliveira M, Sampaio F, Mancio J, Bettencourt N, Teixeira M, Rocha Goncalves F, Gama V, Leite-Moreira A. Influence of epicardial and visceral fat on left ventricular diastolic and systolic functions in patients after myocardial infarction. *Am J Cardiol*. 2014;114:1663-9.
7. Fox CS, Gona P, Hoffmann U, Porter SA, Salton CJ, Massaro JM, Levy D, Larson MG, D'Agostino RB, Sr., O'Donnell CJ, Manning WJ. Pericardial fat, intrathoracic fat, and measures of left ventricular structure and function: the Framingham Heart Study. *Circulation*. 2009;119:1586-91.
8. Hachiya K, Fukuta H, Wakami K, Goto T, Tani T, Ohte N. Relation of epicardial fat to central aortic pressure and left ventricular diastolic function in patients with known or suspected coronary artery disease. *Int J Cardiovasc Imaging*. 2014;30:1393-8.
9. Khawaja T, Greer C, Chokshi A, Chavarria N, Thadani S, Jones M, Schaefle K, Bhatia K, Collado JE, Shimbo D, Einstein AJ, Schulze PC. Epicardial fat volume in patients with left ventricular systolic dysfunction. *Am J Cardiol*. 2011;108:397-401.
10. Konishi M, Sugiyama S, Sugamura K, Nozaki T, Matsubara J, Akiyama E, Utsunomiya D, Matsuzawa Y, Yamashita Y, Kimura K, Umemura S and Ogawa H. Accumulation of pericardial fat correlates with left ventricular diastolic dysfunction in patients with normal ejection fraction. *J Cardiol*. 2012;59:344-51.
11. Lai YH, Hou CJ, Yun CH, Sung KT, Su CH, Wu TH, Yang FS, Hung TC, Hung CL, Bezerra HG, Yeh HI. The association among MDCT-derived three-dimensional visceral adiposities on cardiac diastology and dyssynchrony in asymptomatic population. *BMC Cardiovasc Disord*. 2015;15:142.
12. Liu J, Fox CS, Hickson DA, May WL, Ding J, Carr JJ, Taylor HA. Pericardial fat and echocardiographic measures of cardiac abnormalities: the Jackson Heart Study. *Diabetes Care*. 2011;34:341-6.
13. Longenecker CAK, S; Serhal, M; Kinley, B; Labbato, D; McComsey, GA. Diastolic Function Correlates With Pericardial Fat [fat around the heart] and Vascular Remodeling in HIV. *Conference on Retroviruses and Opportunistic Infections (CROI)*. 2016.
14. Ng AC, Goo SY, Roche N, van der Geest RJ, Wang WY. Epicardial Adipose Tissue Volume and Left Ventricular Myocardial Function Using 3-Dimensional Speckle Tracking Echocardiography. *Can J Cardiol*. 2016;32:1485-1492.
15. Ruberg FL, Chen Z, Hua N, Bigornia S, Guo Z, Hallock K, Jara H, LaValley M, Phinikaridou A, Qiao Y, Viereck J, Apovian CM, Hamilton JA. The relationship of ectopic lipid accumulation to cardiac and vascular function in obesity and metabolic syndrome. *Obesity (Silver Spring)*. 2010;18:1116-21.
16. Wu CK, Tsai HY, Su MY, Wu YF, Hwang JJ, Tseng WY, Lin JL, Lin LY. Pericardial fat is associated with ventricular tachyarrhythmia and mortality in patients with systolic heart failure. *Atherosclerosis*. 2015;241:607-14.
17. Yamashita KO, Ebara S, Yamamoto MH, Obara C. Increased epicardial adipose tissue are associated with left ventricular diastolic dysfunction. *Journal of the American College of Cardiology*. 2012;59:E1349.
18. Al Chekakie MO, Welles CC, Metoyer R, Ibrahim A, Shapira AR, Cytron J, Santucci P, Wilber DJ, Akar JG. Pericardial fat is independently associated with human atrial fibrillation. *J Am Coll Cardiol*. 2010;56:784-8.
19. Doesch C, Haghi D, Suselbeck T, Schoenberg SO, Borggrefe M, Papavassiliu T. Impact of Functional, Morphological and Clinical Parameters on Epicardial Adipose Tissue in Patients With Coronary Artery Disease. *Circulation Journal*. 2012;76:2426-2434.

20. Doesch C, Streitner F, Bellm S, Suselbeck T, Haghi D, Heggemann F, Schoenberg SO, Michaely H, Borggrefe M, Papavassiliu T. Epicardial adipose tissue assessed by cardiac magnetic resonance imaging in patients with heart failure due to dilated cardiomyopathy. *Obesity (Silver Spring)*. 2013;21:E253-61.
21. Doesch C, Haghi D, Fluchter S, Suselbeck T, Schoenberg SO, Michaely H, Borggrefe M, Papavassiliu T. Epicardial adipose tissue in patients with heart failure. *J Cardiovasc Magn Reson*. 2010;12:40.
22. Vanni EM, Faletti R, Morello M, Mezzabotta L, Battisti G, Frea S, Cannillo M, Mosso E, Rosso C, Bergamasco L, Rizzetto M, Bugianesi E. Incerased Epicardial Fat and Early Signs of Impaired Diastolic and Systolic Left Ventricular Function in Non-diabetic, normotensive patients with nonalcoholic fatty liver disease. *Journal of Hepatology*. 2015;62:S745.
23. Vural M, Talu A, Sahin D, Elalmis OU, Durmaz HA, Uyanik S, Dolek BA. Evaluation of the relationship between epicardial fat volume and left ventricular diastolic dysfunction. *Jpn J Radiol*. 2014;32:331-9.

Computed Tomographic Coronary Angiography–Derived Plaque Characteristics Predict Major Adverse Cardiovascular Events

A Systematic Review and Meta-Analysis

Nitesh Nerlekar, MBBS, MPH; Francis J. Ha, BMedSci; Caitlin Cheshire, MBBS; Hashrul Rashid, MBBS; James D. Cameron, MBBS, MD, MEngSc; Dennis T. Wong, MBBS, MD, PhD; Sujith Seneviratne, MBBS; Adam J. Brown, MBBChir, PhD

Background—Computed tomographic coronary angiography is a noninvasive imaging modality that permits identification and characterization of coronary plaques. Despite consensus statements supporting routine reporting of computed tomographic coronary angiography plaque characteristics, there remains uncertainty whether these data convey prognostic information. We performed a systematic review and meta-analysis assessing the strength of association between computed tomographic coronary angiography–derived plaque characterization and major adverse cardiovascular events (MACE).

Methods and Results—Electronic databases were searched for studies reporting computed tomographic coronary angiography plaque characterization and MACE. Data were gathered on plaque morphology (noncalcified, partially calcified, and calcified) and high-risk plaque (HRP) features, including low-attenuation plaque, napkin-ring sign, spotty calcification, and positive remodeling. Of 5496 citations, 13 studies met inclusion criteria. Five hundred fifty-two (3.9%) MACE occurred in 13 977 patients with mean follow-up ranging between 1.3 and 8.2 years. In terms of plaque morphology, the strongest association was observed for noncalcified plaque (hazard ratio [HR], 1.45; 95% confidence interval [CI], 1.24–1.70; $P<0.001$), with weaker associations found for partially calcified (HR, 1.37; 95% CI, 1.18–1.60; $P<0.001$) and calcified plaques (HR, 1.23; 95% CI, 1.16–1.30; $P<0.001$). All HRP features were strongly associated with MACE, including napkin-ring sign (HR, 5.06; 95% CI, 3.23–7.94; $P<0.001$), low-attenuation plaque (HR, 2.95; 95% CI, 2.03–4.29; $P<0.001$), positive remodeling (HR, 2.58; 95% CI, 1.84–3.61; $P<0.001$), and spotty calcification (HR, 2.25; 95% CI, 1.26–4.04; $P=0.006$). The presence of ≥2 HRP features had highest risk of MACE (HR, 9.17; 95% CI, 4.10–20.50; $P<0.001$).

Conclusions—These data demonstrate that HRP is most likely an independent predictor of MACE, which supports the inclusion of HRP reporting in clinical practice. However, at this point, it remains unclear whether HRP reporting has clinical implications. (***Circ Cardiovasc Imaging*. 2017;10:e006973. DOI: 10.1161/CIRCIMAGING.117.006973.**)

Key Words: atherosclerosis ■ coronary angiography ■ coronary artery disease ■ meta-analysis ■ tomography

Coronary artery disease (CAD) remains a significant healthcare concern despite improvements in preventative strategies and therapeutic possibilities. The majority of sudden ischemic coronary events are precipitated by rupture of a bulky, lipid-rich atheromatous plaque, resulting in the development of intraluminal thrombosis and downstream myocardial injury. Precursor lesions that share similar morphological features to ruptured plaques can be reliably identified using intravascular imaging modalities.[1] Studies using intravascular ultrasound have demonstrated a consistent association between baseline plaque morphology and the occurrence of future major adverse cardiovascular events (MACE).[2–4] However, the invasive nature of intravascular imaging limits widespread uptake and precludes use in the vast majority of patients with CAD.

See Editorial by Ferencik and Hoffmann
See Clinical Perspective

Computed tomographic coronary angiography (CTCA) is an established, noninvasive imaging modality that can readily identify the presence and distribution of CAD.[5] CTCA allows for qualitative assessment of plaque morphology, classifying lesions as calcified, noncalcified, or partially calcified type (containing both calcified and noncalcified plaque tissue). Interest in CTCA-derived plaque characteristics has led to identification of specific high-risk plaque (HRP) features,

Received July 26, 2017; accepted November 1, 2017.
From the Monash Cardiovascular Research Centre, Monash University and MonashHeart, Monash Health, Clayton, Victoria, Australia.
The Data Supplement is available at http://circimaging.ahajournals.org/lookup/suppl/doi:10.1161/CIRCIMAGING.117.006973/-/DC1.
Correspondence to Adam J. Brown, MBBChir, PhD, Monash Cardiovascular Research Centre, Monash University and MonashHeart, Monash Health, Clayton, Victoria, Australia. E-mail [redacted]

namely, the presence of low-attenuation plaque, napkin-ring sign, spotty calcification, and positive remodeling.[5] Although prospective observational studies have demonstrated that many CTCA-defined plaque features may predict the occurrence of subsequent events,[6] the overall strength of the association between individual plaque features and MACE remains unknown. This has led to physician uncertainty as to whether CTCA-defined plaque characteristics should be stated in clinical reports for patients with suspected CAD.[7]

We, therefore, conducted a systematic review and meta-analysis to assess the association between baseline CTCA-defined plaque characteristics and subsequent MACE in patients undergoing imaging for suspected stable CAD.

Methods

The data, analytic methods, and study materials will be made available to other researchers for purposes of reproducing the results or replicating the procedure. This material can be obtained by contacting the corresponding author.

Data Sources and Search Strategy

A digital literature search was performed through the MEDLINE, EMBASE, and PubMed databases for the period up to January 2017. Keywords using Medical Subject Heading (MeSH), where available, included coronary artery disease atherosclerosis, multidetector computed tomography, coronary CT angiography, vulnerable plaque, high-risk plaque, low attenuation plaque, spotty calcification, napkin ring, positive remodeling, prognosis, and major adverse cardiovascular events. The search was not limited by language nor date of publication. Reference lists of eligible articles were reviewed for further potential citations. The study protocol was prospectively registered with the PROSPERO international register (CRD42016044003) and adhered to the PRISMA statement (Preferred Reporting Items for Systematic Reviews and Meta-Analyses).[8] An example search strategy is presented in Table I in the Data Supplement.

Study Selection

Study characteristics for inclusion were as follows: (1) patients with stable cardiovascular disease; (2) assessment of plaque characteristics, including plaque morphology (calcified, noncalcified, and partially calcified) and assessment of individual HRP features, including low-attenuation plaque, napkin-ring sign, spotty calcification, and positive remodeling; (3) evaluation of the association between plaque characteristics and future MACE; (4) clinical follow-up of at least 1 year after CTCA; and (5) fully published status. We excluded studies that included patients presenting with acute coronary syndrome undergoing CTCA assessment, studies evaluating coronary artery calcium score without specific lesion assessment, studies including asymptomatic patients, and studies that included elective revascularization as part of their definition of MACE. Details on the clinical indication for CTCA for each included study are presented in Table II in the Data Supplement. Where multiple studies reported on the same cohort of patients, we only included articles with the longest clinical follow-up and largest cohort size.

Data Items and Collection Process

Data items to be collected were specified before conducting the literature search. Items for data extraction included study design; clinical rationale for CTCA; patient baseline characteristics; and definitions of plaque morphology, HRP features, and MACE. We defined plaque morphology and HRP features according to the definitions adopted by each individual study. For HRP features, low-attenuation plaque was most commonly defined as plaque with density ≤30 HU, although 1 study used a threshold of ≤38 HU.[9] Napkin-ring sign was generally defined as the presence of a plaque core with low computerized tomographic (CT) attenuation surrounded by a rim-like area of higher attenuation. Spotty calcification was either defined as a limit in visualized calcification (<2–3 mm) or as a proportion of the vessel dimensions (length of calcium deposit <3/2 of vessel diameter and width of <2/3 of vessel diameter). Full definitions of plaque morphology and HRP features across studies are detailed in Tables III and IV in the Data Supplement, respectively. Data were also collected on CAD burden at baseline as determined by coronary artery calcium score[10] and proportion of patients with obstructive CAD (≥50% luminal stenosis), follow-up completion, and clinical outcomes. Two investigators (N.N. and F.J.H.) independently conducted the literature search, and 3 investigators (F.J.H, C.C., and H.R.) performed the data extraction. Eligible studies and extracted data were verified by the senior author (A.J.B) with any discrepancies resolved by consensus. Risk of bias within individual studies were evaluated according to the Newcastle-Ottawa scale (Table V in the Data Supplement).[11]

Clinical End Points

The primary end point of this study was the association between plaque composition (calcified, noncalcified, and partially calcified) and subsequent MACE. Study-specific definitions of MACE were used for all analyses. In 4 studies, MACE was defined as the composite of cardiac death and nonfatal MI,[12–15] with 9 studies also including unstable angina requiring either hospitalization[9,16–19] or revascularization[20–23] in their MACE definition. One study did not include death from any cause in their MACE definition[22] (ie, composite of nonfatal myocardial infarction and unstable angina), whereas another study used all-cause death instead of cardiac death.[20] Secondary end points included the associations between specific HRP features on CTCA and subsequent MACE.

Statistical Analysis

Data concerning hazard ratio (HR) and 95% confidence intervals (CI) of plaque characteristics and risk of future MACE were extracted and log-transformed, with preference for the HR from the most adjusted model. Full details on the extracted HR and variables used within each model are provided in Table VI in the Data Supplement. Data were analyzed by random-effects modeling for the primary end point and individual secondary end points to produce overall summary estimates with 95% CI. Statistical heterogeneity was quantified using the I^2 statistic and quantified as low (<25%), moderate (<50%), or high (>75%).[24] Publication bias was assessed visually by funnel plots and by the Egger test. Sensitivity analyses were performed to explore the effect of systematic exclusion of individual studies to assess for changes in the pooled estimates. Subgroup analysis was performed with studies stratified by clinical end points (studies including and excluding revascularization), Asian versus non-Asian subjects, and using a 64-detector row threshold. A 2-sided P value <0.05 was considered significant. All statistical analyses were conducted using StataMP 14.0 (Stata Corp LP, College Station, TX).

Results

A total of 5496 potential citations were screened, with 72 studies identified for potential inclusion and further evaluation. Of these, 59 studies were excluded because they did not specifically evaluate CTCA plaque morphology or HRP features (38 studies), the study patients underwent CTCA for suspected acute coronary syndrome (7 studies), the outcomes reported did not include MACE (7 studies), the definition of MACE included elective coronary revascularization (5 studies), or studies failed to report HRs for individual HRP components or reported on the same patient cohort (2 studies). Full identification and process of study exclusion are detailed in the PRISMA flow diagram (Figure 1).

Thirteen studies with a total of 13 977 patients met the prespecified inclusion criteria and were included in the final

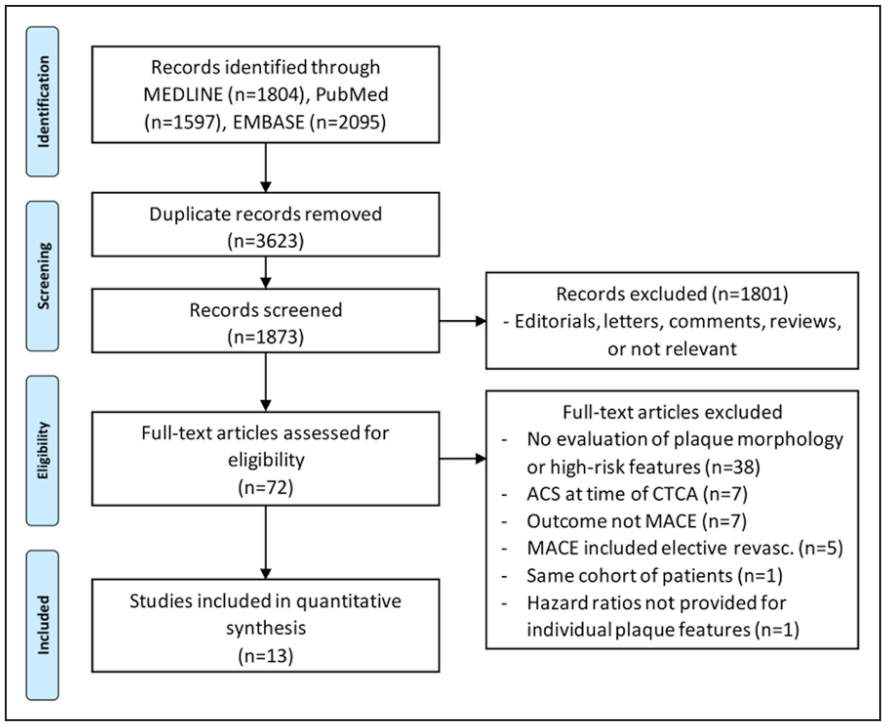

Figure 1. Study flow chart. PRISMA (Preferred Reporting Items for Systematic Reviews and Meta-Analyses) flow diagram illustrating the study selection process for the systematic review and meta-analysis. ACS indicates acute coronary syndrome; CTCA, computed tomographic coronary angiography; and MACE, major adverse cardiovascular events.

quantitative analysis.[9,12–23] The study period ranged from 2002 to 2011 with 9 prospective studies and 4 studies of retrospective design. The reason for undergoing CTCA was predominantly for suspected CAD (11 studies), although patients with known CAD (eg, postcoronary intervention excluding bypass grafting) were included in 2 studies.[16,22] Further details of study design and baseline demographics are presented in Table 1.

The slice capability on multidetector computed tomography (MDCT) varied between studies, with 12 studies using 64-slice MDCT, 2 studies using 16-slice MDCT, and 1 study using 4-slice MDCT (some studies used multiple, different MDCT scanners with different slice capability). The presence of obstructive CAD identified by CTCA ranged from 0% to 38% in individual study cohorts. Further details of CT characteristics can be found in Table 2 and Table VII in the Data Supplement.

Clinical Outcomes

In total, 552 (3.9%) MACE occurred in 13 977 patients with mean study follow-up ranging from 1.3 to 8.2 years. MACE

Table 1. Baseline Characteristics of Included Studies

Author	Publication Year	Study Period	Location	Design	Reason for CTCA	No. of Patients	Male, %	Age, y	HTN, %	Dyslipidemia, %	DM, %
Matsumoto et al[16]	2007	2002–2006	Japan	R	Suspected and known CAD	810	59	58±11	37	40	19
van Werkhoven et al[20]	2009	NR	Europe	P	Suspected CAD	432	59	58±11	57	39	28
Chow et al[12]	2010	2006–2008	Canada	P	Suspected CAD	2172	76	59±11	51	53	14
Andreini et al[13]	2012	2005–2008	Italy	P	Suspected CAD	1196	62	62±11	59	45	11
Hou et al[14]	2012	2007–2008	China	R	Suspected CAD	4425	62	60±11	57	28	15
Miszalski-Jamka et al[15]	2012	2003–2004	Poland	R	Suspected CAD	494	52	58±10	78	63	11
Petretta et al[21]	2012	2006–2008	Italy	P	Suspected CAD	326	68	62±12	51	38	12
Otsuka et al[17]	2013	2007–2010	Japan	P	Suspected CAD	895	66	66±10	66	55	49
Yamamoto et al[9]	2013	2006–2009	Japan	R	Suspected CAD	453*	63	66±11	61	53	41
Nakanishi et al[22]	2014	2005–2013	Japan	P	Suspected and known CAD	517	71	66±10	77	58	37
Otsuka et al[23]	2014	2007–2011	Japan	P	Suspected CAD	543	63	65±10	63	53	44
Conte et al[18]	2016	2004–2007	Italy	P	Suspected CAD	245	70	63±9	60	48	9
Feuchtner et al[19]	2016	2005–2011	Austria	P	Suspected CAD	1469	56	66	51	51	10

*Data presented on original cohort of 511 patients. CAD indicates coronary artery disease; CTCA, computed tomographic coronary angiography; DM, diabetes mellitus; HTN, hypertension; P, prospective; and R, retrospective.

Table 2. Plaque Characteristics and MACE Definitions

Author	Year	MDCT Slice	CACS	Obstructive CAD, %	Plaque Characteristics Analyzed								MACE Definition	F/U Duration, y	F/U Completion, %
					Analysis	Morphology			Vulnerable features						
						CP	NCP	PCP	LAP	NRS	SC	PR/RI			
Matsumoto et al[16]	2007	4/16	NS	NS	PP	N	Y	N	N	N	N	N	Cardiac death, MI, UA	2.9±1.5	87
van Werkhoven et al[20]	2009	64	290±730	25	PP	Y	Y	Y	N	N	N	N	All-cause death, nonfatal MI, UA requiring revascularization	1.8 (IQR, 1.1–2.5)	93
Chow et al[12]	2010	64	NS	30	PP	Y	Y	Y	N	N	N	N	Cardiac death, nonfatal MI	1.3±0.7	96
Andreini et al[13]	2012	64	151 (range, 0–380)	38	PP	Y	Y	Y	N	N	N	N	Cardiac death, nonfatal MI	4.3±1.8	97
Hou et al[14]	2012	64	NS	20	PP	N	Y	Y	N	N	N	N	Cardiac death, MI	3.0 (IQR, 2.6–3.3)	98
Miszalski-Jamka et al[15]	2012	64/16	NS	28	PP	Y	Y	Y	N	N	N	N	Cardiac death, nonfatal MI	3.6±0.9	98
Petretta et al[21]	2012	64	87±127	34	PP	Y	N	Y	N	N	N	N	Cardiac death, nonfatal MI, UA requiring revasc.	2.2±1.0	99
Otsuka et al[17]	2013	64	NS	NS	PS	N	N	N	Y	Y	N	Y	Cardiac death, MI, UA	2.3±0.8	100
Yamamoto et al[9]	2013	64	NS	27	UK	Y	Y	Y	Y	N	Y	Y	Cardiac death, nonfatal MI, UA requiring urgent hospitalization	3.3±1.2	89
Nakanishi et al[22]	2014	64	NS	NS	PP	N	N	N	Y	Y	N	Y	MI, UA requiring immediate revascularization	4.1±1.8	NS
Otsuka et al[23]	2014	64	NS	30	PS	Y	Y	Y	Y	Y	N	Y	Cardiac death, nonfatal MI, UA requiring revascularization	3.4 (range, 1–5.4)	96
Conte et al[18]	2016	64	NS	0	PP	N	N	N	Y	Y	N	Y	Cardiac death, MI, UA	8.2±1.7	94
Feuchtner et al[19]	2016	64	143±359	NS	PP	N	N	N	Y	Y	Y	Y	Cardiac death, MI, UA	7.8 (range, 4.8–9.8)	49

CACS indicates coronary artery calcium score; CAD, coronary artery disease; CP, calcified plaque; F/U, follow-up; IQR, interquartile range; LAP, low-attenuation plaque; MACE, major adverse cardiovascular events; MDCT, multidetector computed tomography; MI, myocardial infarction; N, No; NCP, noncalcified plaque; NRS, napkin-ring sign; NS, not specified; PCP, partially calcified plaque; PP, per patient; PR, positive remodeling; PS, per segment; RI, remodeling index; SC, spotty calcification; UA, unstable angina; UK, unknown; and Y, yes.

involved cardiac death in 112 patients, nonfatal myocardial infarction in 330 patients, and unstable angina requiring hospitalization or revascularization in 110 patients. Full MACE breakdown for each study are presented in Table 3.

Plaque Morphology and MACE

Nine studies reported outcome data on the association between CTCA plaque morphology and MACE, with 8 studies reporting data on noncalcified plaque, 7 on calcified plaque, and 8 on partially calcified plaque subtypes. The strongest association between CTCA plaque morphology and MACE was observed in noncalcified plaque with an overall HR of 1.45 (95% CI, 1.24–1.70; $P<0.001$; $I^2=63\%$). Similarly significant, albeit less strong, associations were found both for partially calcified (HR, 1.37; 95% CI, 1.18–1.60; $P<0.001$; $I^2=73\%$) and calcified plaques (HR, 1.23; 95% CI; 1.16–1.30; $P<0.001$; $I^2=13\%$). Corresponding forest plots illustrating the association between CTCA-defined plaque morphology and MACE are presented in Figure 2.

In sensitivity analyses, there were no marked differences in the pooled HR for each plaque subtype when the analysis was stratified by those studies including revascularization in their MACE definition, studies using <64-slice MDCT, nor when considering Asian versus non-Asian patient populations (Figures I through III in the Data Supplement, respectively). Similarly, systematic exclusion of individual studies did not

Table 3. Individual Study Breakdown of MACE

Author	Year	MACE			
		Total	Cardiac Death	Nonfatal MI	UA Requiring Hospitalization/Revascularization
Matsumoto et al[16]	2007	28	6	7	15
van Werkhoven et al[20]	2009	21	6	8	7
Chow et al[12]	2010	34	11	23	N/A
Andreini et al[13]	2012	136	18	118	N/A
Hou et al[14]	2012	127	40	87	N/A
Miszalski-Jamka et al[15]	2012	17	9	8	N/A
Petretta et al[21]	2012	34	13	9	12
Otsuka et al[17]	2013	24	1	4	19
Yamamoto et al[9]	2013	15	2	7	6
Nakanishi et al[22]	2014	43	0	13	30
Otsuka et al[23]	2014	24	1	4	19
Conte et al[18]	2016	8	2	6	N/A
Feuchtner et al[19]	2016	41	3	36	2

MACE indicates major adverse cardiovascular events; MI, myocardial infarction; N/A, not applicable; NR, not recorded; and UA, unstable angina.

alter the corresponding pooled HR for each plaque subtype (Tables VIII through X in the Data Supplement). There was no evidence of small-study effects on the Egger test for noncalcified (P=0.07), partially calcified (P=0.31), or calcified plaque type (P=0.42).

HRP Features and MACE

Six studies assessed the secondary end points of the presence of specific HRP features and risk of future MACE, with 6 studies reporting outcomes on low-attenuation plaque, 5 on napkin-ring sign, 2 on spotty calcification, and 6 on positive remodeling. Full details of the included studies are provided in Table 2, with the prevalence of individual HRP features summarized in Table 4. Of the 4 predefined HRP features, napkin-ring sign was associated with the highest risk of future MACE (HR, 5.06; 95% CI, 3.23–7.94; P<0.001; I^2=0%). Low-attenuation plaque and positive remodeling demonstrated an overall HR of 2.95 (95% CI, 2.03–4.29; P<0.001; I^2=40%) and 2.58 (95% CI, 1.84–3.61; P<0.001; I^2=70%), respectively. Spotty calcification demonstrated the lowest, although still significant, association with risk of future MACE (HR 2.25; 95% CI, 1.26–4.04; P=0.006; I^2=0%). Corresponding forest plots for individual HRP features are presented in Figure 3. The significant association between HRP features and MACE remained in sensitivity analyses stratifying studies including Asian versus non-Asian patient populations (Figure IV in the Data Supplement). In addition, there remained a significant association between HRP features and MACE when the analysis was limited to studies that included stenosis severity and plaque burden in multivariate models (Figure V in the Data Supplement). There was evidence of small-study effects specific to low-attenuation plaque (P=0.003) and positive remodeling (0.01) but not for napkin-ring sign (P=0.13). The presence of ≥2 individual HRP features exhibited the strongest association with MACE (HR, 9.17; 95% CI, 4.10–20.50; P<0.001; I^2=0%; Figure VI in the Data Supplement).

Discussion

To our knowledge, this is the first meta-analysis to evaluate the association between CTCA-defined plaque characteristics and subsequent MACE. For plaque morphology, we find that the strongest association occurred with noncalcified plaque, with the risk of subsequent clinical events reducing as plaque calcification increases. We also find that all established HRP features are associated with MACE, with the strongest association observed for lesions with the napkin-ring sign. These results demonstrate that the reporting of CTCA-defined plaque characteristics has potential to inform clinicians in the risk stratification of patients.

Pathological studies have established that lipid-rich fibroatheroma are responsible for the majority of ischemic coronary events through plaque rupture and subsequent intraluminal thrombosis.[25] Prospective human studies have reaffirmed this observation, demonstrating an independent association between the presence of thin-cap fibroatheromata and future MACE.[2] Our study is consistent with these observations and again highlights that the risk of MACE is highest in noncalcified plaques, which are generally composed of a mixture of lipid-rich and fibrous material. Although detailed analysis of plaque composition is challenging within the spatial resolution of CTCA, lower plaque attenuation values have previously correlated with necrotic core and fibrofatty tissue on virtual histology intravascular ultrasound imaging.[26] Thus, low-attenuation plaques should theoretically have a high proportion of extracellular lipid content. Our data would again be consistent with this because we find a stronger association between low-attenuation plaques and MACE, when compared with noncalcified plaque. Taken together, these data suggest that interpretation of CTCA-defined plaque morphology may impart important prognostic information independent of established calcium-scoring algorithms.

Our data again highlights a potentially discrepant relationship between coronary calcification and future cardiovascular risk. On one hand, previous observational studies have consistently demonstrated that the risk of future cardiovascular events is progressively increased with higher coronary artery calcium scores.[27] However, our pooled results suggest that calcified plaques have the weakest association with MACE, whereas the risk of future events was more than doubled if a lesion displayed evidence of spotty calcification. These data would, therefore, suggest that the pattern and extent of intimal calcification may be an important determinant of risk. Biomechanical models have suggested that small, microscopic calcific deposits in the fibrous cap and plaque architecture can act to amplify plaque structural stress, acting as a possible driver for plaque rupture.[28,29] However, as calcification becomes more extensive, the macroscopic plates of calcification can act as a stress shield, protecting the plaque from high mechanical loading.[30] Support for this theory has also emerged from recent data highlighting that statins may promote plaque stabilization through progressive macroscopic intimal calcification.[31] Further studies are now required

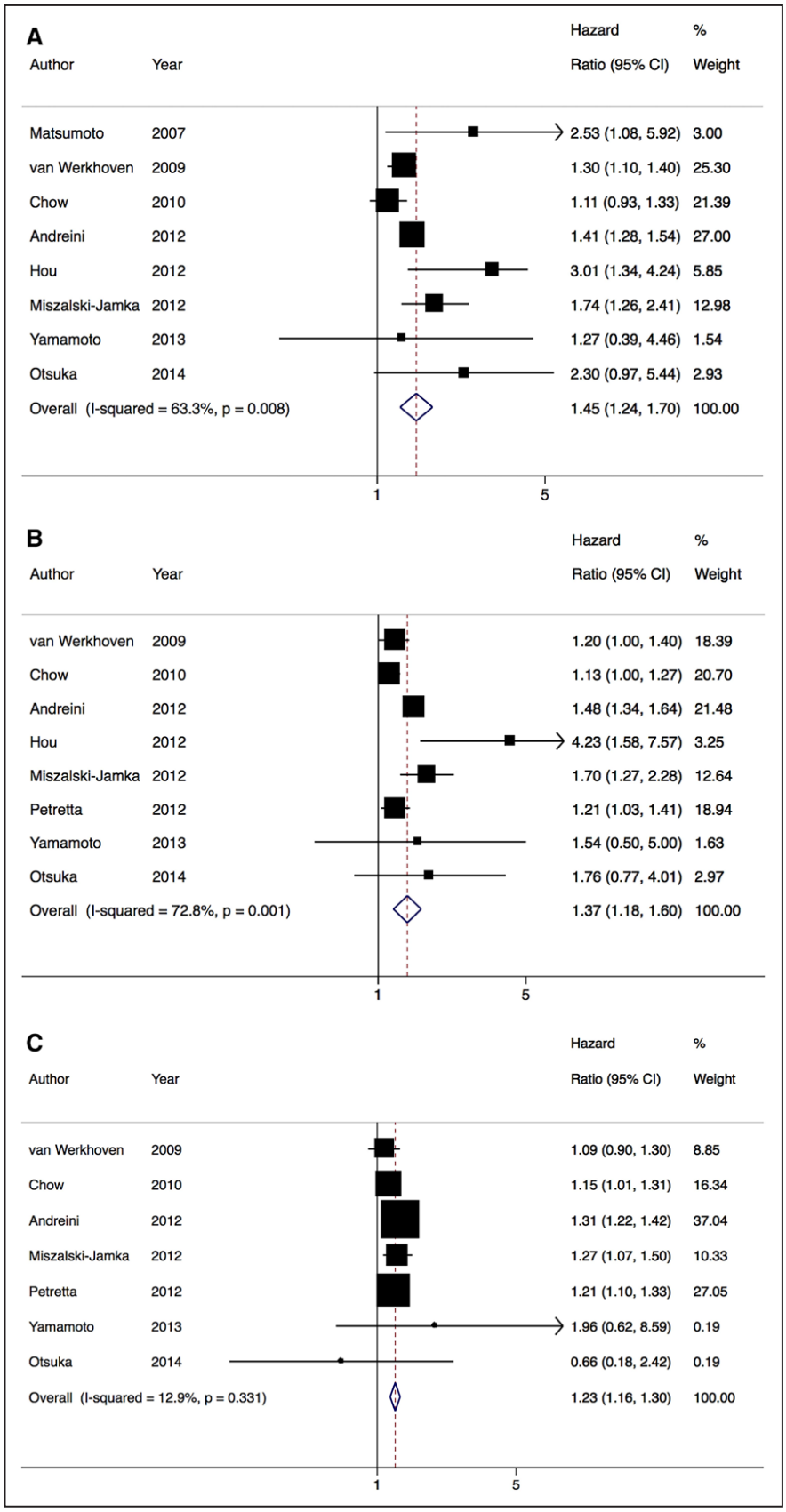

Figure 2. Plaque morphology and risk of major adverse cardiovascular events (MACE). Forest plot displays summary hazard ratio (HR) and 95% confidence intervals (CI) for future MACE stratified by (**A**) calcified plaque, (**B**) noncalcified plaque, and (**C**) partially calcified plaque subtypes.[9,12–16, 20, 21, 23]

to ascertain the role of calcification in plaque destabilization and to assess whether the mechanisms that promote intimal calcification can be induced in an effort to improve clinical outcomes.

We find that each prespecified HRP feature in our analysis was strongly associated with MACE and that there was an incremental risk when ≥2 HRP features were present within the same plaque. Although the presence of multiple

Table 4. Prevalence of HRP Features

Author	LAP	PR	NRS	SC
Plaque level				
Otsuka et al*[17]	107/1174 (9.1%)	130/1174 (11%)	45/1174 (3.8%)	N/A
Yamamoto et al[9]	NS	NS	NS	NS
Nakanishi et al*[22]	113/864 (13%)	108/864 (13%)	26/864 (3%)	N/A
Otsuka et al*[23]	133/1107 (12%)	183/1107 (16%)	30/1107 (2.7%)	N/A
Patient level				
Conte et al†[18]	8/245 (3.3%)	196/245 (80%)	3/245 (1.2%)	51/245 (21%)
Feuchtner et al†[19]	55/1469 (3.7%)	NS	66/1469 (4.4%)	231/1469 (16%)

HRP indicates high-risk plaque; LAP, low-attenuation plaque; N/A, not applicable; NRS, napkin-ring sign; NS, not specified; PR, positive remodeling; and SC, spotty calcification.

*Proportion of total coronary plaques.

†Proportion of total patients.

HRP features in individual lesions was only evaluated in 2 studies,[9,18] similar results were reported by a large prospective study.[6] In this study, plaques with low-attenuation, positive remodeling, or both features were a significant predictor of the development of future acute coronary syndrome (adjusted HR, 8.24; 95% CI, 5.26–12.96). These data imply that future cardiovascular risk could be higher in patients who demonstrate multiple HRP features or even multiple plaques with HRP features. Further prospective studies are now required to assess whether CT-defined HRP features can be used to guide pharmacological strategies in an effort to improve clinical outcomes in a manner that is economically viable.

Positive predictive value (PPV) was not uniformly reported by the studies in our analysis, and when it was described, estimates were at a segmental level, and the inference at a patient-level remains unclear. In addition, the quoted PPV for individual plaque characteristics were discrepant between studies and were likely influenced by the low prevalence of HRP features in patients with stable symptoms because PPV is influenced by disease prevalence such that, when prevalence is low, so too is PPV. For example, in the study by Otsuka

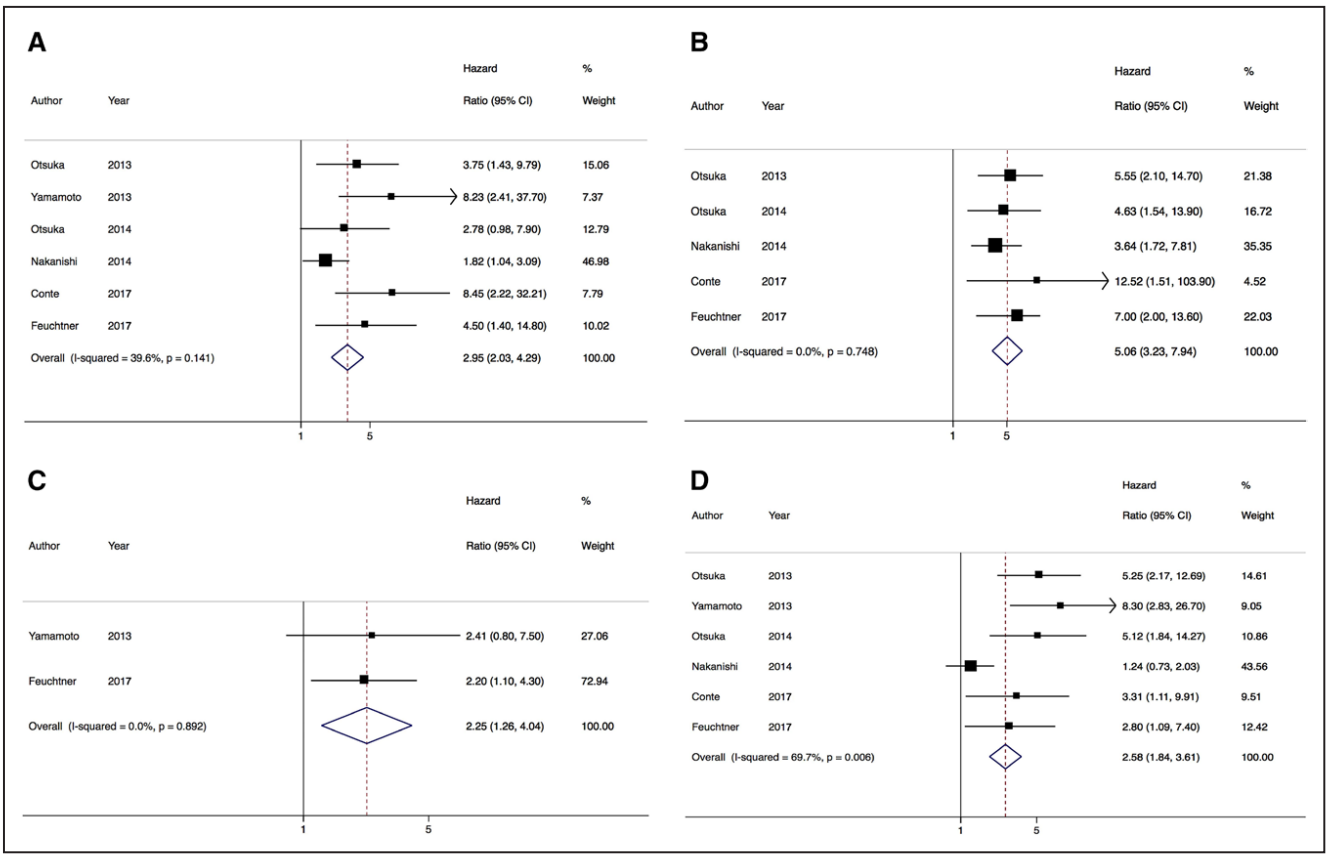

Figure 3. High-risk plaque features and risk of major adverse cardiovascular events (MACE). Forest plot displays summary hazard ratio (HR) and 95% confidence intervals (CI) for future MACE stratified by (**A**) low-attenuation plaque, (**B**) napkin-ring sign, (**C**) spotty calcification, and (**D**) positive remodeling.[9,17–19,22,23]

et al,[23] the prevalence of HRP segments was 24%, and the associated PPV for MACE was 86%. Conversely, in another analysis by the same group,[17] the prevalence of napkin-ring sign was 0.4%, yielding a PPV of 22%. Currently, there is no recommendation on the management of individual HRP features or whether these patients require more aggressive risk factor treatment. Plaque burden and stenosis severity are well-established markers of prognosis, and it is hypothesized that HRP may simply be a marker of greater atherosclerotic burden.[32] Although no studies have reported HRP significance over plaque extent, in our pooled sensitivity analysis of studies that adjusted for obstructive stenosis, HRP presence was independently associated with MACE. These results should encourage the requirement for a uniform reporting system such as CAD-Reporting and Data System that incorporates HRP; however, it should also include plaque morphology and disease extent as well.[7] Application of these parameters both in clinical practice and the research literature will overcome inconsistencies encountered in pooling data and allow future studies to ascertain the true independent effect of HRP on patient prognosis.

Study Limitations

There are certain limitations to our analysis that should be considered when interpreting the findings. First, the included studies have used variable definitions for plaque morphology and specific HRP features that will have introduced a degree of heterogeneity into the analysis. However, the differences in definitions were modest and are unlikely to affect the overall biological association between plaque characteristics and clinical outcomes. Second, CT technology also varied between studies, which may have affected the interstudy reliability for the assessment of plaque morphology and influenced the prevalence of HRP identified. Although the majority of our studies reported outcomes at a patient-level, segment-based risk estimates were used for 2 studies,[17,23] and inclusion of these data may have had subtle effects on the overall pooled estimates. We had no access to patient- or segment-level data and were, therefore, unable to directly quantify any incremental prognostic information provided by plaque characterization over other known CTCA-derived markers of risk, including stenosis severity and atheroma volume. Unstable angina requiring either revascularization or hospitalization was also part of the MACE definition in 9 included studies, which may limit ascertainment of the relative prognostic value of HRP versus stenosis severity. Finally, although some studies suggest that HRP is a predictor of MACE, independent of stenosis, the data do not demonstrate that HRP is a stronger predictor than significant stenosis, and most data suggest that it may not be. Given this limitation and the fact that the PPV is low, it remains unclear whether HRP reporting may have management implications.

Conclusions

Our data demonstrate that HRP is most likely an independent predictor of MACE, which supports the inclusion of HRP reporting in clinical practice. However, at this point, it remains unclear whether HRP reporting may have clinical implications.

Sources of Funding

N. Nerlekar is supported by a postgraduate scholarship from the National Health and Medical Research Council and National Heart Foundation. Dr Brown is supported by a School of Clinical Sciences at Monash Health, Monash University Early Career Practitioner Fellowship award.

Disclosures

None.

References

1. Brown AJ, Obaid DR, Costopoulos C, Parker RA, Calvert PA, Teng Z, Hoole SP, West NE, Goddard M, Bennett MR. Direct comparison of virtual-histology intravascular ultrasound and optical coherence tomography imaging for identification of thin-cap fibroatheroma. *Circ Cardiovasc Imaging*. 2015;8:e003487. doi: 10.1161/CIRCIMAGING.115.003487.
2. Stone GW, Maehara A, Lansky AJ, de Bruyne B, Cristea E, Mintz GS, Mehran R, McPherson J, Farhat N, Marso SP, Parise H, Templin B, White R, Zhang Z, Serruys PW; PROSPECT Investigators. A prospective natural-history study of coronary atherosclerosis. *N Engl J Med*. 2011;364:226–235. doi: 10.1056/NEJMoa1002358.
3. Brown AJ, Teng Z, Calvert PA, Rajani NK, Hennessy O, Nerlekar N, Obaid DR, Costopoulos C, Huang Y, Hoole SP, Goddard M, West NE, Gillard JH, Bennett MR. Plaque structural stress estimations improve prediction of future major adverse cardiovascular events after intracoronary imaging. *Circ Cardiovasc Imaging*. 2016;9:e004172.
4. Cheng JM, Garcia-Garcia HM, de Boer SP, Kardys I, Heo JH, Akkerhuis KM, Oemrawsingh RM, van Domburg RT, Ligthart J, Witberg KT, Regar E, Serruys PW, van Geuns RJ, Boersma E. *In vivo* detection of high-risk coronary plaques by radiofrequency intravascular ultrasound and cardiovascular outcome: results of the ATHEROREMO-IVUS study. *Eur Heart J*. 2014;35:639–647. doi: 10.1093/eurheartj/eht484.
5. Maurovich-Horvat P, Ferencik M, Voros S, Merkely B, Hoffmann U. Comprehensive plaque assessment by coronary CT angiography. *Nat Rev Cardiol*. 2014;11:390–402. doi: 10.1038/nrcardio.2014.60.
6. Motoyama S, Ito H, Sarai M, Kondo T, Kawai H, Nagahara Y, Harigaya H, Kan S, Anno H, Takahashi H, Naruse H, Ishii J, Hecht H, Shaw LJ, Ozaki Y, Narula J. Plaque characterization by coronary computed tomography angiography and the likelihood of acute coronary events in mid-term follow-up. *J Am Coll Cardiol*. 2015;66:337–346. doi: 10.1016/j.jacc.2015.05.069.
7. Cury RC, Abbara S, Achenbach S, Agatston A, Berman DS, Budoff MJ, Dill KE, Jacobs JE, Maroules CD, Rubin GD, Rybicki FJ, Schoepf UJ, Shaw LJ, Stillman AE, White CS, Woodard PK, Leipsic JA. Coronary Artery Disease - Reporting and Data System (CAD-RADS): an expert consensus document of SCCT, ACR and NASCI: endorsed by the ACC. *JACC Cardiovasc Imaging*. 2016;9:1099–1113. doi: 10.1016/j.jcmg.2016.05.005.
8. Liberati A, Altman DG, Tetzlaff J, Mulrow C, Gøtzsche PC, Ioannidis JP, Clarke M, Devereaux PJ, Kleijnen J, Moher D. The PRISMA statement for reporting systematic reviews and meta-analyses of studies that evaluate health care interventions: explanation and elaboration. *Ann Intern Med*. 2009;151:W65–W94.
9. Yamamoto H, Kitagawa T, Ohashi N, Utsunomiya H, Kunita E, Oka T, Urabe Y, Tsushima H, Awai K, Kihara Y. Noncalcified atherosclerotic lesions with vulnerable characteristics detected by coronary CT angiography and future coronary events. *J Cardiovasc Comput Tomogr*. 2013;7:192–199. doi: 10.1016/j.jcct.2013.05.008.
10. Agatston AS, Janowitz WR, Hildner FJ, Zusmer NR, Viamonte M Jr, Detrano R. Quantification of coronary artery calcium using ultrafast computed tomography. *J Am Coll Cardiol*. 1990;15:827–832.
11. Stang A. Critical evaluation of the Newcastle-Ottawa scale for the assessment of the quality of nonrandomized studies in meta-analyses. *Eur J Epidemiol*. 2010;25:603–605. doi: 10.1007/s10654-010-9491-z.
12. Chow BJ, Wells GA, Chen L, Yam Y, Galiwango P, Abraham A, Sheth T, Dennie C, Beanlands RS, Ruddy TD. Prognostic value of 64-slice cardiac computed tomography severity of coronary artery disease, coronary atherosclerosis, and left ventricular ejection fraction. *J Am Coll Cardiol*. 2010;55:1017–1028. doi: 10.1016/j.jacc.2009.10.039.
13. Andreini D, Pontone G, Mushtaq S, Bartorelli AL, Bertella E, Antonioli L, Formenti A, Cortinovis S, Veglia F, Annoni A, Agostoni P, Montorsi P, Ballerini G, Fiorentini C, Pepi M. A long-term prognostic value of

coronary CT angiography in suspected coronary artery disease. *JACC Cardiovasc Imaging*. 2012;5:690–701. doi: 10.1016/j.jcmg.2012.03.009.
14. Hou ZH, Lu B, Gao Y, Jiang SL, Wang Y, Li W, Budoff MJ. Prognostic value of coronary CT angiography and calcium score for major adverse cardiac events in outpatients. *JACC Cardiovasc Imaging*. 2012;5:990–999. doi: 10.1016/j.jcmg.2012.06.006.
15. Miszalski-Jamka T, Klimeczek P, Banyś R, Krupiński M, Nycz K, Bury K, Lada M, Pelberg R, Kereiakes D, Mazur W. The composition and extent of coronary artery plaque detected by multislice computed tomographic angiography provides incremental prognostic value in patients with suspected coronary artery disease. *Int J Cardiovasc Imaging*. 2012;28:621–631. doi: 10.1007/s10554-011-9799-0.
16. Matsumoto N, Sato Y, Yoda S, Nakano Y, Kunimasa T, Matsuo S, Komatsu S, Saito S, Hirayama A. Prognostic value of non-obstructive CT low-dense coronary artery plaques detected by multislice computed tomography. *Circ J*. 2007;71:1898–1903.
17. Otsuka K, Fukuda S, Tanaka A, Nakanishi K, Taguchi H, Yoshikawa J, Shimada K, Yoshiyama M. Napkin-ring sign on coronary CT angiography for the prediction of acute coronary syndrome. *JACC Cardiovasc Imaging*. 2013;6:448–457. doi: 10.1016/j.jcmg.2012.09.016.
18. Conte E, Annoni A, Pontone G, Mushtaq S, Guglielmo M, Baggiano A, Volpato V, Agalbato C, Bonomi A, Veglia F, Formenti A, Fiorentini C, Bartorelli AL, Pepi M, Andreini D. Evaluation of coronary plaque characteristics with coronary computed tomography angiography in patients with non-obstructive coronary artery disease: a long-term follow-up study. *Eur Heart J Cardiovasc Imaging*. 2017;18:1170–1178. doi: 10.1093/ehjci/jew200.
19. Feuchtner G, Kerber J, Burghard P, Dichtl W, Friedrich G, Bonaros N, Plank F. The high-risk criteria low-attenuation plaque <60 HU and the napkin-ring sign are the most powerful predictors of MACE: a long-term follow-up study. *Eur Heart J Cardiovasc Imaging*. 2017;18:772–779. doi: 10.1093/ehjci/jew167.
20. van Werkhoven JM, Schuijf JD, Gaemperli O, Jukema JW, Kroft LJ, Boersma E, Pazhenkottil A, Valenta I, Pundziute G, de Roos A, van der Wall EE, Kaufmann PA, Bax JJ. Incremental prognostic value of multislice computed tomography coronary angiography over coronary artery calcium scoring in patients with suspected coronary artery disease. *Eur Heart J*. 2009;30:2622–2629. doi: 10.1093/eurheartj/ehp272.
21. Petretta M, Daniele S, Acampa W, Imbriaco M, Pellegrino T, Messalli G, Xhoxhi E, Del Prete G, Nappi C, Accardo D, Angeloni F, Bonaduce D, Cuocolo A. Prognostic value of coronary artery calcium score and coronary CT angiography in patients with intermediate risk of coronary artery disease. *Int J Cardiovasc Imaging*. 2012;28:1547–1556. doi: 10.1007/s10554-011-9948-5.
22. Nakanishi K, Fukuda S, Tanaka A, Otsuka K, Jissho S, Taguchi H, Yoshikawa J, Shimada K. Persistent epicardial adipose tissue accumulation is associated with coronary plaque vulnerability and future acute coronary syndrome in non-obese subjects with coronary artery disease. *Atherosclerosis*. 2014;237:353–360. doi: 10.1016/j.atherosclerosis.2014.09.015.
23. Otsuka K, Fukuda S, Tanaka A, Nakanishi K, Taguchi H, Yoshiyama M, Shimada K, Yoshikawa J. Prognosis of vulnerable plaque on computed tomographic coronary angiography with normal myocardial perfusion image. *Eur Heart J Cardiovasc Imaging*. 2014;15:332–340. doi: 10.1093/ehjci/jet232.
24. Higgins JP, Thompson SG, Deeks JJ, Altman DG. Measuring inconsistency in meta-analyses. *BMJ*. 2003;327:557–560. doi: 10.1136/bmj.327.7414.557.
25. Virmani R, Kolodgie FD, Burke AP, Farb A, Schwartz SM. Lessons from sudden coronary death: a comprehensive morphological classification scheme for atherosclerotic lesions. *Arterioscler Thromb Vasc Biol*. 2000;20:1262–1275.
26. Voros S, Rinehart S, Qian Z, Vazquez G, Anderson H, Murrieta L, Wilmer C, Carlson H, Taylor K, Ballard W, Karmpaliotis D, Kalynych A, Brown C III. Prospective validation of standardized, 3-dimensional, quantitative coronary computed tomographic plaque measurements using radiofrequency backscatter intravascular ultrasound as reference standard in intermediate coronary arterial lesions: results from the ATLANTA (assessment of tissue characteristics, lesion morphology, and hemodynamics by angiography with fractional flow reserve, intravascular ultrasound and virtual histology, and noninvasive computed tomography in atherosclerotic plaques) I study. *JACC Cardiovasc Interv*. 2011;4:198–208. doi: 10.1016/j.jcin.2010.10.008.
27. Detrano R, Guerci AD, Carr JJ, Bild DE, Burke G, Folsom AR, Liu K, Shea S, Szklo M, Bluemke DA, O'Leary DH, Tracy R, Watson K, Wong ND, Kronmal RA. Coronary calcium as a predictor of coronary events in four racial or ethnic groups. *N Engl J Med*. 2008;358:1336–1345. doi: 10.1056/NEJMoa072100.
28. Kelly-Arnold A, Maldonado N, Laudier D, Aikawa E, Cardoso L, Weinbaum S. Revised microcalcification hypothesis for fibrous cap rupture in human coronary arteries. *Proc Natl Acad Sci USA*. 2013;110:10741–10746. doi: 10.1073/pnas.1308814110.
29. Teng Z, Brown AJ, Calvert PA, Parker RA, Obaid DR, Huang Y, Hoole SP, West NE, Gillard JH, Bennett MR. Coronary plaque structural stress is associated with plaque composition and subtype and higher in acute coronary syndrome: the BEACON I (Biomechanical Evaluation of Atheromatous Coronary Arteries) study. *Circ Cardiovasc Imaging*. 2014;7:461–470. doi: 10.1161/CIRCIMAGING.113.001526.
30. Brown AJ, Teng Z, Evans PC, Gillard JH, Samady H, Bennett MR. Role of biomechanical forces in the natural history of coronary atherosclerosis. *Nat Rev Cardiol*. 2016;13:201–220. doi: 10.1038/nrcardio.2015.203.
31. Puri R, Nicholls SJ, Shao M, Kataoka Y, Uno K, Kapadia SR, Tuzcu EM, Nissen SE. Impact of statins on serial coronary calcification during atheroma progression and regression. *J Am Coll Cardiol*. 2015;65:1273–1282. doi: 10.1016/j.jacc.2015.01.036.
32. Arbab-Zadeh A, Fuster V. The myth of the "vulnerable plaque": transitioning from a focus on individual lesions to atherosclerotic disease burden for coronary artery disease risk assessment. *J Am Coll Cardiol*. 2015;65:846–855. doi: 10.1016/j.jacc.2014.11.041.

CLINICAL PERSPECTIVE

Computed tomographic coronary angiography (CTCA) is an established noninvasive imaging modality that permits identification and characterization of atherosclerotic coronary plaques. Despite consensus statements supporting routine reporting of CTCA plaque characteristics, there remains clinical uncertainty on whether such features convey important prognostic information. We, therefore, performed a systematic review and meta-analysis to assess the strength of association between CTCA-derived plaque characterization and major adverse cardiovascular events (MACE). Of the 5496 potential citations, 13 studies encompassing 13 977 patients met inclusion criteria. Data were gathered on plaque morphology (noncalcified, partially calcified, and calcified) and high-risk plaque (HRP) features, including low-attenuation plaque, napkin-ring sign, spotty calcification, and positive remodeling. Overall, 522 (3.9%) patients sustained MACE with mean follow-up ranging between 1.3 and 8.2 years. We found that the strongest association between CTCA-defined plaque morphology and MACE was observed from noncalcified plaque, followed by partially calcified and then calcified plaque subtypes. All HRP features were strongly associated with MACE, with the strongest association found for plaques with napkin-ring sign. The presence of ≥2 HRP features within the same plaque conferred the highest risk of MACE. Importantly, sensitivity analysis demonstrated that HRP features had an independent effect on prognosis beyond stenosis severity alone. These data reinforce that routine reporting of CTCA-defined plaque morphology and HRP features have potential to improve patient risk stratification.

Circulation
Cardiovascular Imaging

Computed Tomographic Coronary Angiography–Derived Plaque Characteristics Predict Major Adverse Cardiovascular Events: A Systematic Review and Meta-Analysis

Nitesh Nerlekar, Francis J. Ha, Caitlin Cheshire, Hashrul Rashid, James D. Cameron, Dennis T. Wong, Sujith Seneviratne and Adam J. Brown

Circ Cardiovasc Imaging. 2018;11:
doi: 10.1161/CIRCIMAGING.117.006973
Circulation: Cardiovascular Imaging is published by the American Heart Association, 7272 Greenville Avenue, Dallas, TX 75231

Print ISSN: 1941-9651. Online ISSN: 1942-0080

SUPPLEMENTAL MATERIAL

Computed tomography coronary angiography derived plaque characteristics predict major adverse cardiovascular events: a systematic review and meta-analysis

Nitesh Nerlekar, Francis J. Ha, Caitlin Cheshire, Hashrul Rashid,

James D. Cameron, Dennis T. Wong, Sujith Seneviratne and Adam J. Brown

Table of Contents

Table S1. Example search strategy for Medline

#	Searches	Results
1	Coronary Artery Disease/	54096
2	Coronary Stenosis/	10503
3	Atherosclerosis/	33413
4	Acute Coronary Syndrome/	11741
5	Non-obstructive coronary artery disease.mp	57
6	Coronary Vessels/	57645
7	Multidetector Computed Tomography/	5403
8	Tomography, X-Ray Computed/	389198
9	Tomography, Spiral Computed/	7435
10	Coronary CT angiography.mp	1249
11	Vulnerable plaque.mp	1057
12	High-risk plaque.mp	145
13	Plaque, Atherosclerotic/	6422
14	Low-attenuation plaque.mp	44
15	Napkin ring.mp	47
16	Spotty calcification.mp	82
17	Positive remodeling.mp	370
18	Prognosis/	457689
19	Myocardial Infarction/	168210
20	Myocardial Revascularization/	10933
21	Kaplan-Meier Estimate/	51833
22	Major adverse cardiovascular events.mp	1561
23	1 or 2 or 3 or 4 or 5 or 6	153520
24	7 or 8 or 9 or 10 or 11 or 12 or 13 or 14 or 15 or 16 or 17	407784
25	18 or 19 or 20 or 21 or 22	655305
26	23 and 24 and 25	1804

Table S2. Indications for CTCA for each included study

Author	Year	Indications for CTCA
Matsumoto et al.	2007	– Evaluation of chest pain (61%) – Post-coronary intervention status (9%) – Evaluation of CAD in asymptomatic patients with multiple CVD risk factors (15%) – Not specified (15%)
van Werkhoven et al.	2009	– Suspected CAD referred for further assessment because of chest pain, positive exercise ECG test, or high-risk profile for CVD (100%)
Chow et al.	2010	– Evaluation of chest pain (58%) o Typical angina (16%) o Atypical angina (15%) o Non-anginal chest pain (28%) – Evaluation of dyspnea (16%) – Evaluation of palpitations (1%) – Evaluation of syncope (1%) – Asymptomatic o Rule out CAD/CVD risk factors (11%) o Equivocal/abnormal stress test (6%) o Pre-cardiac surgery (4%) o LV dysfunction (0.6%) o Other, not specified (2%)
Andreini et al.	2012	– Evaluation of chest pain (43%) – Evaluation of CAD in asymptomatic patients with multiple CVD risk factors (28%) – Equivocal/abnormal stress test (29%)
Hou et al.	2012	– Evaluation of chest pain (69%) o Typical angina (6%) o Atypical angina (16%) o Non-anginal chest pain (47%) – Evaluation of CAD in asymptomatic patients with ≥1 CVD risk factors (NS %) – Evaluation of ECG abnormalities (NS %) – Evaluation of prior revascularization (NS %)
Miszalski-Jamka et al.	2012	– Evaluation of chest pain (100%) o Typical angina (40%) o Atypical angina (30%) o Non-anginal chest pain (30%)
Petretta et al.	2012	– Evaluation of chest pain o Typical angina (32%) o Atypical angina (63%) o Non-anginal chest pain (5%)
Otsuka et al.	2013	– Evaluation of chest pain (60%) – Evaluation of CAD in asymptomatic patients with multiple CVD risk factors and abnormal findings on exercise-stress echocardiography or single-photon emission computed tomography (40%)

Yamamoto et al.	2013	– Evaluation of chest pain (54%) – Asymptomatic with ischemic findings (25%) – Evaluation of CAD in asymptomatic patients with multiple CVD risk factors (22%)
Nakanishi et al.	2014	– Evaluation of chest pain (77%) o Typical angina (27%) o Atypical angina (34%) o Non-anginal chest pain (16%) – Evaluation of CAD in asymptomatic patients with multiple CVD risk factors, PAD, cerebrovascular disease, abnormal findings ECG or echocardiography (23%)
Otsuka et al.	2014	– Evaluation of chest pain (62%) – Evaluation of CAD in asymptomatic patients with multiple CVD risk factors (38%)
Conte et al.	2017	– Evaluation of chest pain (50%) o Typical angina (6%) o Atypical angina (44%) – Evaluation of dyspnea (10%) – Evaluation of CAD in asymptomatic patients with multiple CVD risk factors (40%)
Feuchtner et al.	2017	– Evaluation of chest pain (NS %) – Evaluation of CAD in asymptomatic patients with multiple CVD risk factors (NS %)

Table S3. Definitions of plaque morphology

Author	Year	Plaque Morphology Definition		
		Calcified plaque	**Non-Calcified plaque**	**Partially-calcified**
Matsumoto et al.[1]	2007	N/A	Low-density plaque defined as <68 HU	N/A
van Werkhoven et al.[2]	2009	High-density plaques	Lower density than contrast-enhanced lumen	Both calcified and non-calcified components
Chow et al.[3]	2010	NS	NS	NS
Andreini et al.[4]	2012	High-density plaques	Density less than contrast-enhanced vessel lumen	Both calcified and non-calcified components
Hou et al.[5]	2012	Exclusively high-density material >130 HU	Exclusively material of density ≤130 HU	Both calcified and non-calcified components
Miszalski-Jamka et al.[6]	2012	Density greater than contrast-enhanced lumen	Lower density than contrast-enhanced lumen	Both calcified and non-calcified components
Petretta et al.[7]	2012	Exclusively high-density material >130 HU	Exclusively material of density ≤130 HU	Both calcified and non-calcified components
Yamamoto et al.[8]	2013	CT density >130 HU or greater than that of the contrast-enhanced coronary lumen	Low-density area <1 mm^2 in size with CT density ≤130 HU	N/A
Otsuka et al.[9]	2014	Predominantly calcification	Density less than contrast-enhanced vessel lumen without any calcification	Small amount of calcification elements within a single plaque

CT, Computed tomography; HU, Hounsfield unit; N/A, Not applicable; NS, Not specified; PR, Positive remodelling; RI, Remodelling index

Table S4. Definitions of specific high-risk plaque features

Author	Year	HRP Features Definition			
		LAP	NRS	SC	PR
Otsuka et al.[10]	2013	<30 HU	Presence of a plaque core with low CT attenuation surrounded by a rim-like area of higher attenuation	N/A	RI>1.1
Yamamoto et al.[8]	2013	≤38 HU	N/A	Length of calcium deposit <3/2 of vessel diameter and width <2/3 of vessel diameter	RI ≥1.05
Nakanishi et al.[11]	2014	<30 HU	Presence of a plaque core with low CT attenuation surrounded by a rim-like area of higher CT attenuation	N/A	RI >1.1
Otsuka et al.[9]	2014	<30 HU	Plaque core with low attenuation surrounded by rim-like area of higher attenuation. CTCA attenuation of the ring presenting higher than those of adjacent plaque and no >150 HU	N/A	RI >1.1
Conte et al.[12]	2017	<30 HU	Presence of semicircular thin enhancement around the plaque along the outer contour of the vessel	Calcification <2mm	RI >1.1
Feutchner et al.[13]	2017	<130 HU, although specify <30 HU, <60 HU and <90 HU	Outer high-density rim (<200 HU) with inner hypodense area (<130 HU) not adjacent to calcification and present in ≥2 adjacent axial 1mm slices	Calcification <3 mm	No specific limit set – analyzed as continuous variable)

HRP, high-risk plaque; HU, Hounsfield Units; LAP, Low-attenuation plaque; N/A, Not applicable; NRS, Napkin-ring sign; PR, Positive remodeling; RI, Remodeling index; SC, Spotty calcification

Table S5. Assessment of study quality using the Newcastle-Ottawa scale

Author	Year	Study quality			
		Selection	Comparability	Outcome/exposure	Total score
Matsumoto et al.[1]	2007	***	-	**	5
van Werkhoven et al.[2]	2009	****	-	**	5
Chow et al.[3]	2010	****	-	***	7
Andreini et al.[4]	2012	****	-	***	7
Hou et al.[5]	2012	****	*	**	7
Miszalski-Jamka et al.[6]	2012	****	-	***	7
Petretta et al.[7]	2012	****	-	**	6
Otsuka et al.[10]	2013	****	-	***	7
Yamamoto et al.[8]	2013	****	-	***	7
Nakanishi et al.[11]	2014	****	-	***	7
Otsuka et al.[9]	2014	***	-	***	6
Conte et al.[12]	2016	****	-	**	6
Feutchner et al.[13]	2016	****	-	**	6

Table S6. Individual hazard ratios for plaque characteristics and variables included in multivariable modelling

Author	Year	Plaque	Hazard Ratio (95% CI)	Variables included in adjusted model
Matsumoto et al.	2007	NCP	2.53 (1.08-5.92)	Diabetes, previous MI*
van Werkhoven et al.	2009	CP	1.09 (0.9-1.3)	Age, sex, calcium score ≥1000
		NCP	1.3 (1.1-1.4)	
		Mixed	1.2 (1-1.4)	
Chow et al.	2010	CP	1.15 (1.01-1.31)	Patient baseline characteristics (not further specified), CAD severity, LVEF
		NCP	1.11 (0.93-1.33)	
		Mixed	1.13 (1-1.27)	
Andreini et al.	2012	CP	1.31 (1.22-1.42)	Unadjusted
		NCP	1.41 (1.28-1.54)	
		Mixed	1.48 (1.34-1.64)	
Hou et al.	2012	NCP	3.01 (1.34-4.24)	Unadjusted
		Mixed	4.23 (1.58-7.57)	
Miszalski-Jamka et al.	2012	CP	1.7 (1.27-2.28)	Plaque morphology (non-calcified, partially calcified, calcified)*
		NCP	1.74 (1.26-2.41)	
		Mixed	1.27 (1.07-1.5)	
Petretta et al.	2012	CP	1.21 (1.1-1.33)	Calcium score, significant CAD, plaque morphology (non-calcified, partially calcified, calcified), segment involvement score, segments-at-risk score*
		Mixed	1.21 (1.03-1.41)	
Otsuka et al.	2013	LAP	3.75 (1.43-9.79)	Patient baseline characteristics (not further specified), obstructive plaque
		NR	5.55 (2.1-14.7)	
		PR	5.25 (2.17-12.69)	
Yamamoto et al.	2013	CP	1.96 (0.62-8.59)	Age, sex, diameter stenosis >50%
		NCP	1.27 (0.39-4.46)	
		Mixed	1.54 (0.5-5.0)	
		LAP	8.23 (2.41-37.7)	
		PR	8.3 (2.83-26.7)	
		SC	2.41 (0.8-7.5)	
		HRP	11.2 (3.71-36.7)	
Nakanishi et al.	2014	LAP	1.82 (1.04-3.09)	Previous revascularization, Δ LDL-C
		NRS	3.64 (1.72-7.81)	
		PR	1.24 (0.73-2.03)	
Otsuka et al.	2014	CP	0.66 (0.18-2.42)	Hypertension, CT luminal stenosis, 2 or 3 vessel disease, calcified plaque, obstructive plaque, PR, LAP, NRS*
		NCP	2.3 (0.97-5.44)	
		Mixed	1.76 (0.77-4.01)	
		LAP	2.78 (0.98-7.9)	
		NRS	4.63 (1.54-13.9)	
		PR	5.12 (1.84-14.27)	
Conte et al.	2017	LAP	8.45 (2.22-32.21)	Beta-blocker use
		NRS	12.5 (1.51-103.9)	
		PR	3.31 (1.11-9.91)	
		HRP	7.54 (2.43-23.34)	

Feutchner et al.	2017	LAP	4.5 (1.4-14.8)	Age, gender, arterial hypertension, nicotine, positive family history, BMI, dyslipidaemia, diabetes, CT stenosis severity, CT plaque type
		NRS	7 (2-13.6)	
		SC	2.2 (1.1-4.3)	
		PR	2.8 (1.09-7.4)	

*Only variables which reached significance ($p<0.05$) in the univariable model where included in the multivariable, adjusted model

CAD, Coronary artery disease; CP, Calcified plaque; CT, Computed tomography; HRP, High risk plaque (≥2 features) LAP, Low attenuation plaque; LDL-C, Low density lipoprotein – cholesterol; LVEF, Left ventricular ejection fraction; MI, Myocardial Infarction; NCP, Non calcified plaque; NRS, Napkin ring sign; PR, Positive remodelling; SC, Spotty calcification

Table S7. Characteristics of computed tomography coronary angiography

Author	Year	CT scanner	mA	kV	Software
Matsumoto et al.[1]	2007	SOMATOM Volume Zoom (4 slice)	320	140	3D Virtuoso
		Aquilion 16	400	140	M900 Quadra
van Werkhoven et al.[2]	2009	Aquilion 64	200-250	120	Vitrea2
		GE Lightspeed VCT (64-slice)			Advantage
Chow et al.[3]	2010	GE Volume CT (64-slice)	400-800	120	GE Advantage Volume Share Workstation
Andreini et al.[4]	2012	GE Volume CT (64-slice)	NS	NS	CardioQ3 package
Hou et al.[5]	2012	Light Speed VCT (64-slice)	200-550	120	Deep Blu, ADW 4.3
Miszalski-Jamka et al.[6]	2012	Somatom Sensation 64	350-400	120	3D Leonardo
		Somatom Sensation 16	400-500	120	3D Leonardo
Petretta et al.[7]	2012	Lightspeed VCT (64-slice)	600	100-120	Advantage Workstation
Otsuka et al.[10]	2013	Somatom 64	770-850	120	NS
Yamamoto et al.[8]	2013	Lightspeed VCT (64-slice)	300	120	NS
Nakanishi et al.[11]	2014	Somatom Sensation 64	770-850	120	Synapse Vincent
Otsuka et al.[9]	2014	SOMATOM 64	770-850	120	NS
Conte et al.[12]	2016	GE Volume CT (64-slice)	NS	NS	NS
Feutchner et al.[13]	2016	Sensation 64	NS	NS	SyngoVia
		Definition FLASH 128			

CT; Computed Tomography; NS, Not specified

Table S8. Calcified plaque and risk of MACE: Sensitivity Analyses with systematic exclusion of individual studies

Excluded study	**Year**	**Pooled Hazard Ratio**	**Lower 95% CI**	**Upper 95% CI**
Van Werkhoven et al.[2]	2009	1.25	1.19	1.32
Chow et al.[3]	2010	1.25	1.18	1.33
Andreini et al.[4]	2012	1.19	1.11	1.27
Miszalski-Jamka et al.[6]	2012	1.22	1.14	1.31
Petretta et al.[7]	2012	1.23	1.13	1.33
Yamamoto et al.[8]	2013	1.23	1.15	1.30
Otsuka et al.[9]	2014	1.23	1.16	1.30
All studies included		**1.23**	**1.16**	**1.30**

Table S9. Non-calcified plaque and risk of MACE: Sensitivity Analyses with systematic exclusion of individual studies

Excluded study	Year	Pooled Hazard Ratio	Lower 95% CI	Upper 95% CI
Matsumoto et al.[1]	2007	1.42	1.22	1.66
Van Werkhoven et al.[2]	2009	1.58	1.26	1.98
Chow et al.[3]	2010	1.54	1.31	1.82
Andreini et al.[4]	2012	1.56	1.23	1.98
Hou et al.[5]	2012	1.36	1.20	1.55
Miszalski-Jamka et al.[6]	2012	1.41	1.20	1.67
Yamamoto et al.[8]	2013	1.46	1.25	1.72
Otsuka et al.[9]	2014	1.43	1.22	1.67
All studies included		**1.45**	**1.24**	**1.70**

Table S10. Partially-calcified plaque and risk of MACE: Sensitivity Analyses with systematic exclusion of individual studies

Excluded study	Year	Pooled Hazard Ratio	Lower 95% CI	Upper 95% CI
Van Werkhoven et al.[2]	2009	1.43	1.19	1.72
Chow et al.[3]	2010	1.44	1.22	1.70
Andreini et al.[4]	2012	1.34	1.13	1.60
Hou et al.[5]	2012	1.31	1.15	1.49
Miszalski-Jamka et al.[6]	2012	1.33	1.13	1.56
Petretta et al.[7]	2012	1.43	1.19	1.72
Yamamoto et al.[8]	2013	1.37	1.17	1.61
Otsuka et al.[9]	2014	1.36	1.17	1.60
All studies included		**1.37**	**1.18**	**1.60**

Figure S1. Forest plots of pooled hazard ratio estimates in studies grouped by the inclusion or exclusion of unstable angina requiring revascularization.

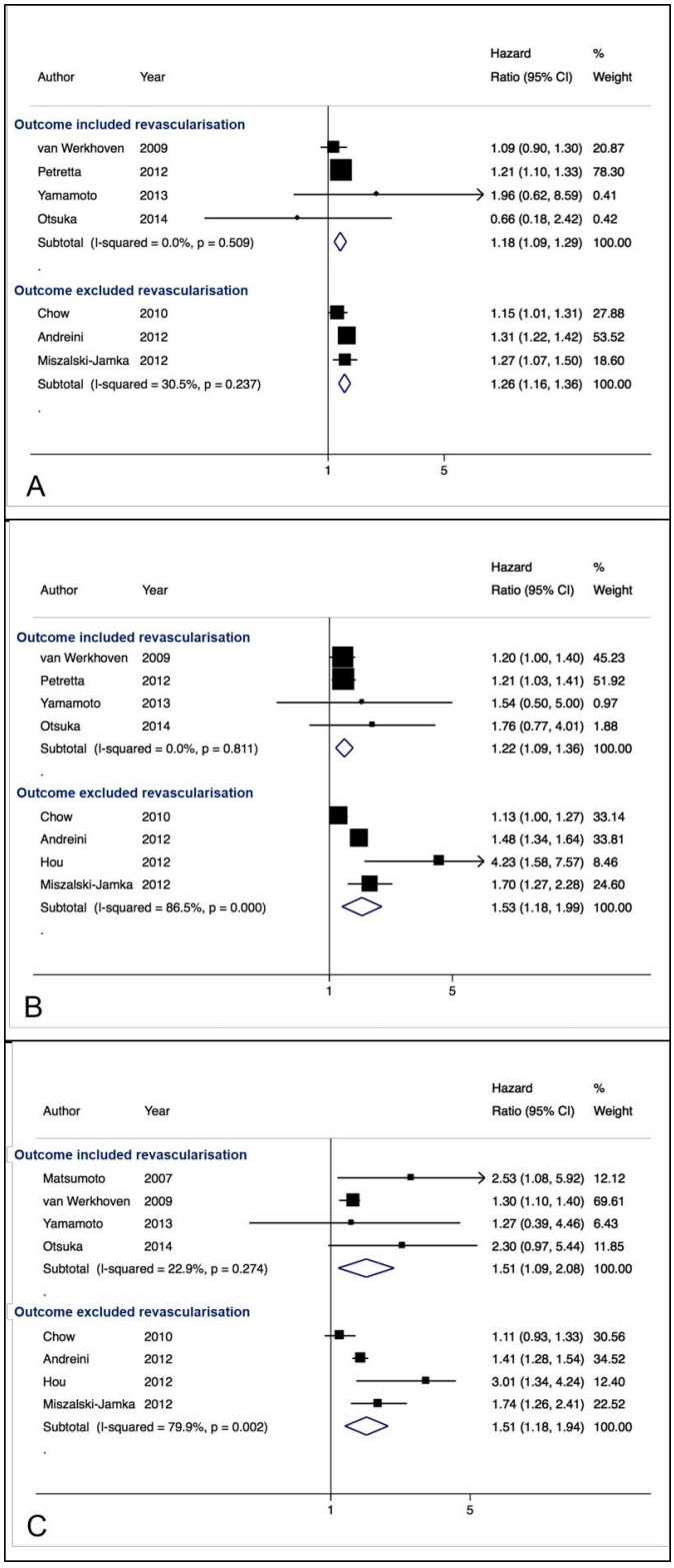

(**A**) calcified plaque, (**B**) partially-calcified plaque and (**C**) non-calcified plaque

Figure S2. Forest plots of pooled hazard ratio estimates grouped in studies using either <64 versus ≥64 detector row scanners

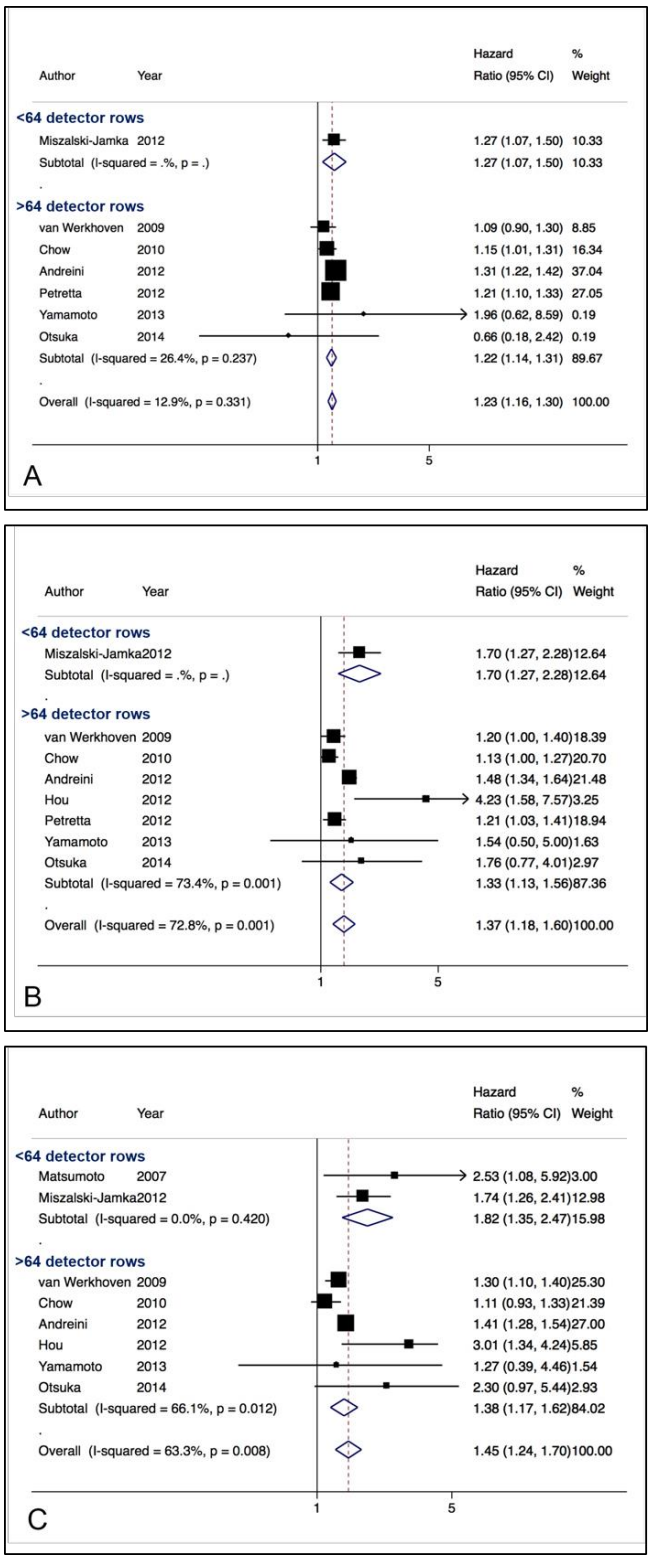

(**A**) calcified plaque, (**B**) partially calcified plaque and (**C**) non-calcified plaque

Figure S3. Forest plots of pooled hazard ratio estimates stratified by Asian vs. non-Asian subjects for plaque morphology.

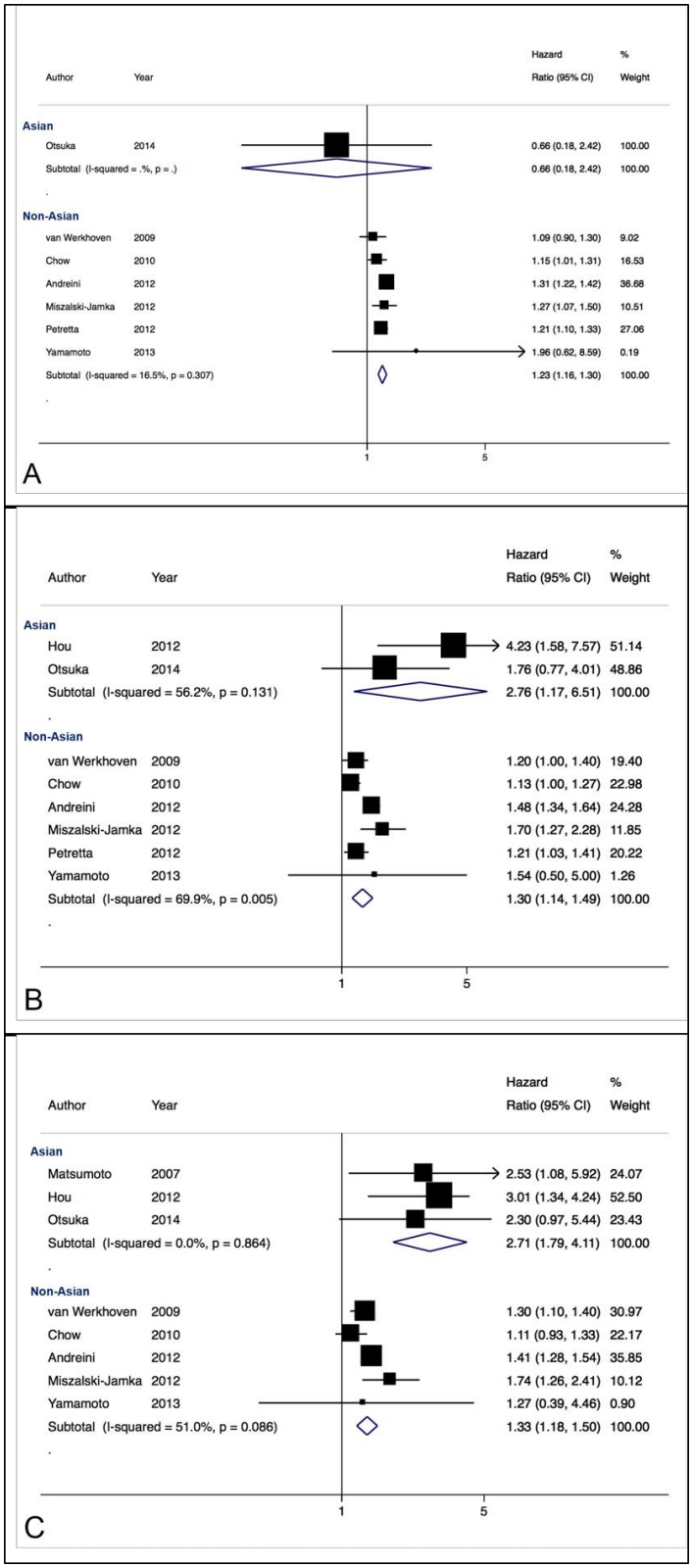

(**A**) calcified plaque, (**B**) partially calcified plaque and (**C**) non-calcified plaque.

Figure S4. Forest plots of pooled hazard ratio estimates stratified by Asian vs. non-Asian subjects for HRP features

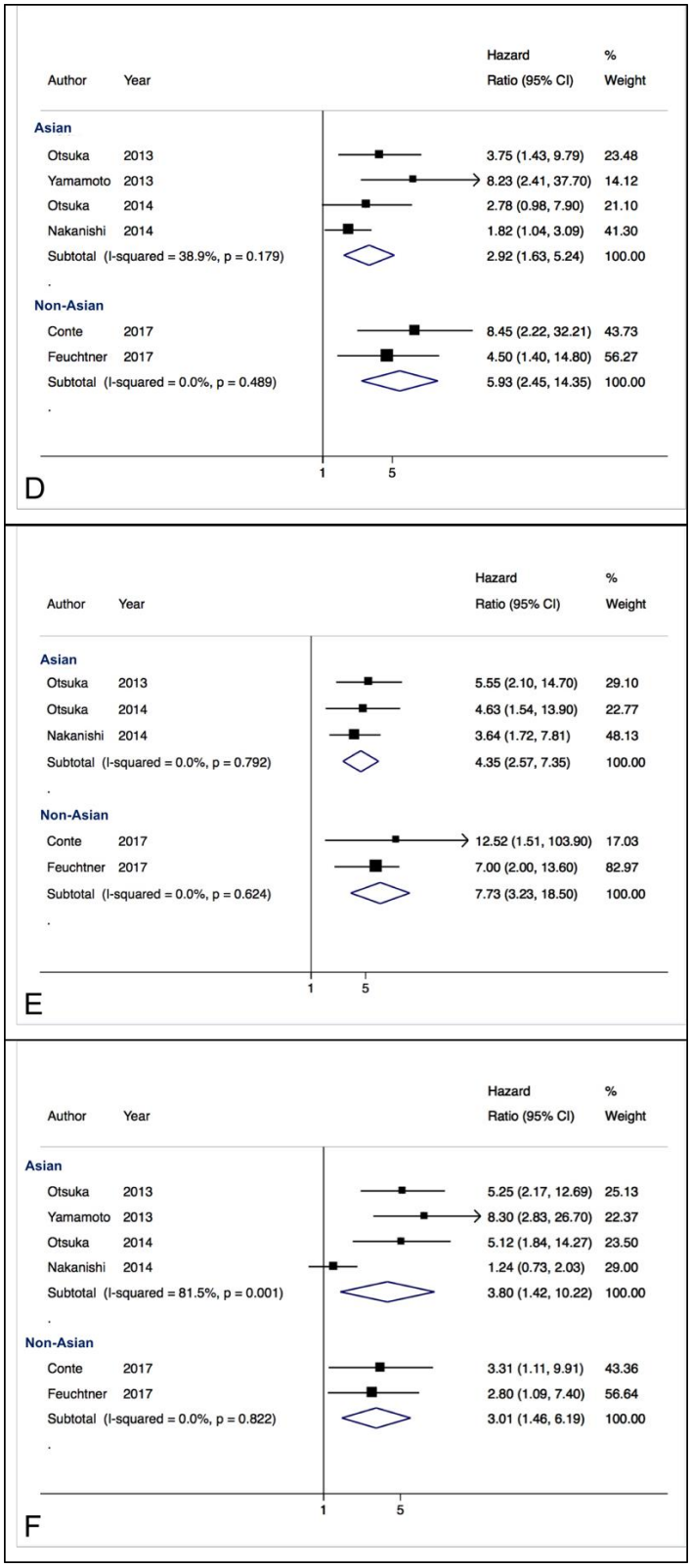

(**D**) low attenuation plaque, (**E**) napkin ring sign and, (**F**) positive remodeling.

Figure S5. Forest plots of pooled hazard ratio estimates limited to studies that included stenosis severity and/or plaque burden in multivariable modelling.

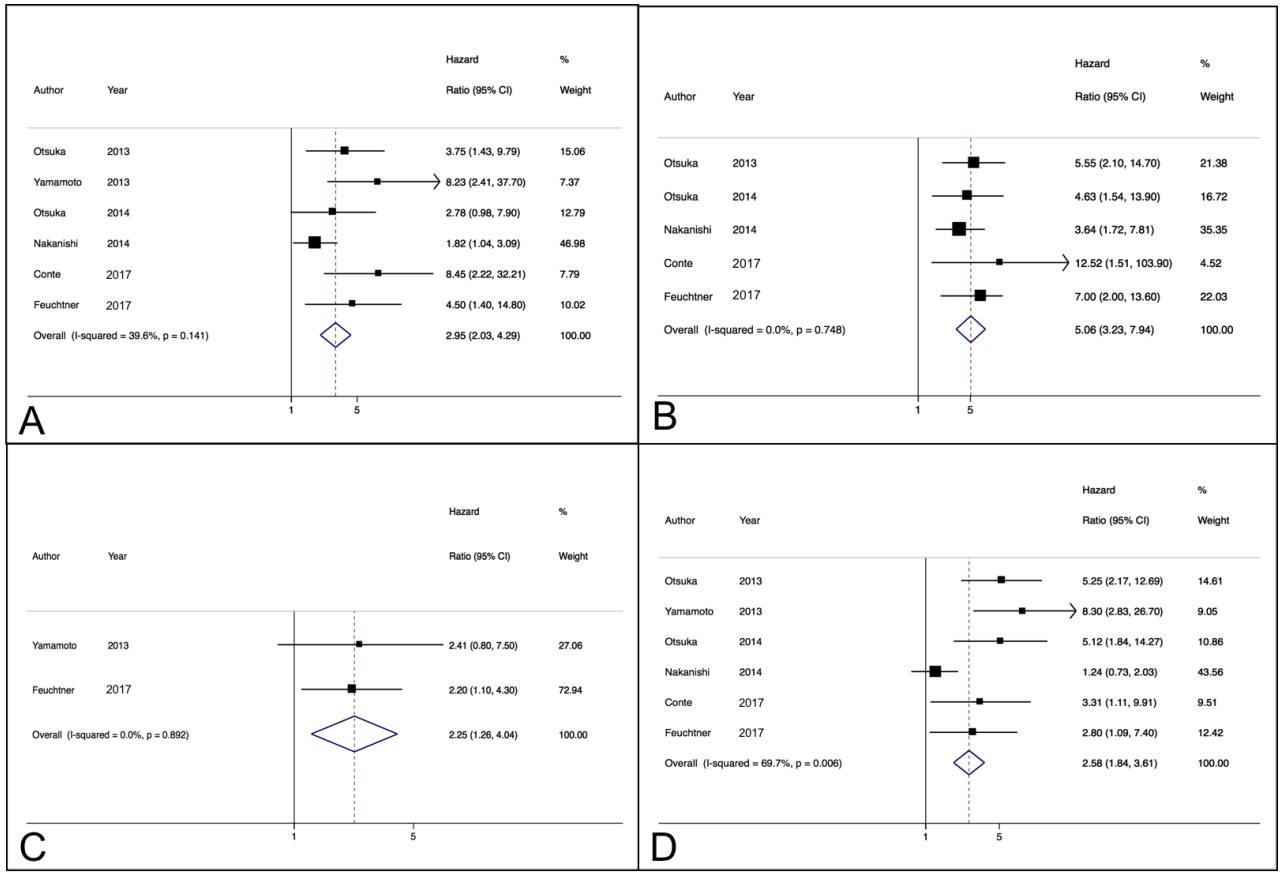

(**A**) low attenuation plaque, (**B**) napkin ring sign, (**C**) positive remodeling and, (**D**) spotty calcification.

Figure S6. Forest plot of overall hazard ratio for the presence of 2 or more high-risk plaque features

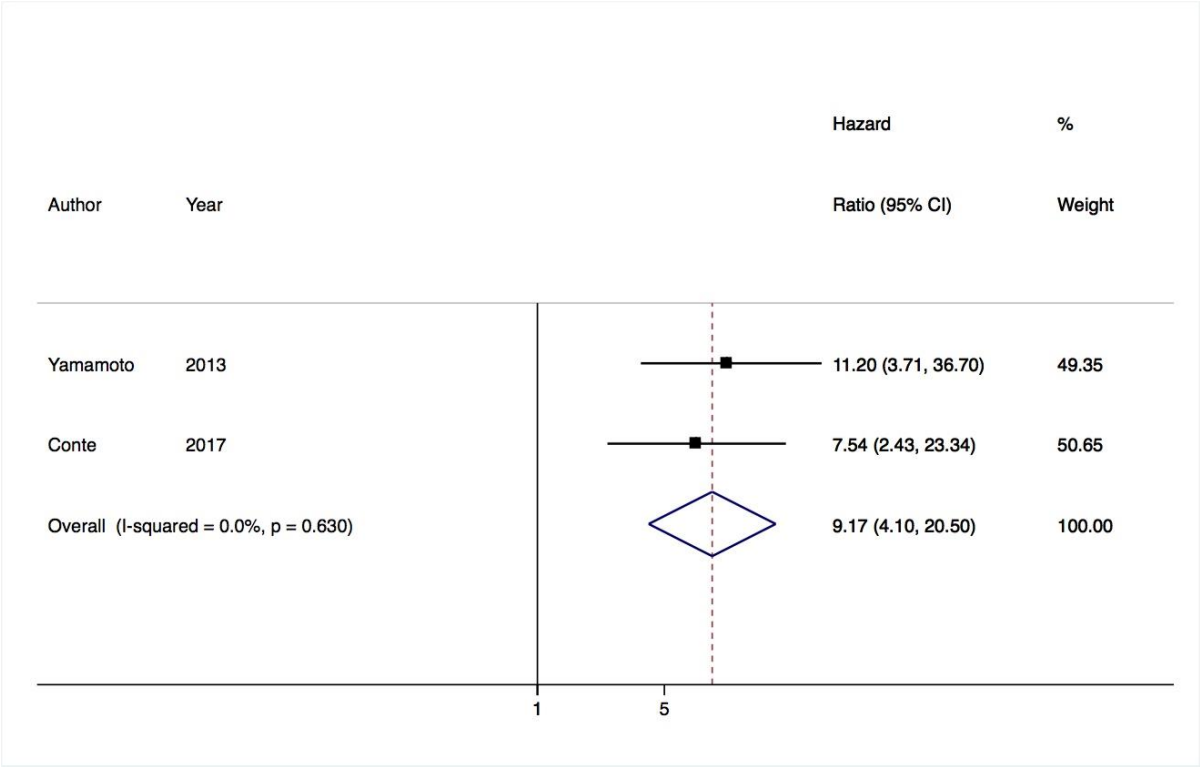

References

1. Matsumoto N, Sato Y, Yoda S, Nakano Y, Kunimasa T, Matsuo S, Komatsu S, Saito S and Hirayama A. Prognostic value of non-obstructive CT low-dense coronary artery plaques detected by multislice computed tomography. *Circulation journal : official journal of the Japanese Circulation Society*. 2007;71:1898-903.

2. van Werkhoven JM, Schuijf JD, Gaemperli O, Jukema JW, Kroft LJ, Boersma E, Pazhenkottil A, Valenta I, Pundziute G, de Roos A, van der Wall EE, Kaufmann PA and Bax JJ. Incremental prognostic value of multi-slice computed tomography coronary angiography over coronary artery calcium scoring in patients with suspected coronary artery disease. *European heart journal*. 2009;30:2622-9.

3. Chow BJ, Wells GA, Chen L, Yam Y, Galiwango P, Abraham A, Sheth T, Dennie C, Beanlands RS and Ruddy TD. Prognostic value of 64-slice cardiac computed tomography severity of coronary artery disease, coronary atherosclerosis, and left ventricular ejection fraction. *Journal of the American College of Cardiology*. 2010;55:1017-28.

4. Andreini D, Pontone G, Mushtaq S, Bartorelli AL, Bertella E, Antonioli L, Formenti A, Cortinovis S, Veglia F, Annoni A, Agostoni P, Montorsi P, Ballerini G, Fiorentini C and Pepi M. A long-term prognostic value of coronary CT angiography in suspected coronary artery disease. *JACC Cardiovascular imaging*. 2012;5:690-701.

5. Hou ZH, Lu B, Gao Y, Jiang SL, Wang Y, Li W and Budoff MJ. Prognostic value of coronary CT angiography and calcium score for major adverse cardiac events in outpatients. *JACC Cardiovascular imaging*. 2012;5:990-9.

6. Miszalski-Jamka T, Klimeczek P, Banys R, Krupinski M, Nycz K, Bury K, Lada M, Pelberg R, Kereiakes D and Mazur W. The composition and extent of coronary artery plaque detected by multislice computed tomographic angiography provides incremental prognostic

value in patients with suspected coronary artery disease. *The international journal of cardiovascular imaging*. 2012;28:621-31.

7. Petretta M, Daniele S, Acampa W, Imbriaco M, Pellegrino T, Messalli G, Xhoxhi E, Del Prete G, Nappi C, Accardo D, Angeloni F, Bonaduce D and Cuocolo A. Prognostic value of coronary artery calcium score and coronary CT angiography in patients with intermediate risk of coronary artery disease. *The international journal of cardiovascular imaging*. 2012;28:1547-56.

8. Yamamoto H, Kitagawa T, Ohashi N, Utsunomiya H, Kunita E, Oka T, Urabe Y, Tsushima H, Awai K and Kihara Y. Noncalcified atherosclerotic lesions with vulnerable characteristics detected by coronary CT angiography and future coronary events. *Journal of cardiovascular computed tomography*. 2013;7:192-9.

9. Otsuka K, Fukuda S, Tanaka A, Nakanishi K, Taguchi H, Yoshiyama M, Shimada K and Yoshikawa J. Prognosis of vulnerable plaque on computed tomographic coronary angiography with normal myocardial perfusion image. *European heart journal cardiovascular Imaging*. 2014;15:332-40.

10. Otsuka K, Fukuda S, Tanaka A, Nakanishi K, Taguchi H, Yoshikawa J, Shimada K and Yoshiyama M. Napkin-ring sign on coronary CT angiography for the prediction of acute coronary syndrome. *JACC Cardiovascular imaging*. 2013;6:448-57.

11. Nakanishi K, Fukuda S, Tanaka A, Otsuka K, Jissho S, Taguchi H, Yoshikawa J and Shimada K. Persistent epicardial adipose tissue accumulation is associated with coronary plaque vulnerability and future acute coronary syndrome in non-obese subjects with coronary artery disease. *Atherosclerosis*. 2014;237:353-60.

12. Conte E, Annoni A, Pontone G, Mushtaq S, Guglielmo M, Baggiano A, Volpato V, Agalbato C, Bonomi A, Veglia F, Formenti A, Fiorentini C, Bartorelli AL, Pepi M and Andreini D. Evaluation of coronary plaque characteristics with coronary computed

tomography angiography in patients with non-obstructive coronary artery disease: a long-term follow-up study. *European heart journal cardiovascular Imaging*. 2017;18:1170-1178.

13. Feuchtner G, Kerber J, Burghard P, Dichtl W, Friedrich G, Bonaros N and Plank F. The high-risk criteria low-attenuation plaque <60 HU and the napkin-ring sign are the most powerful predictors of MACE: a long-term follow-up study. *European heart journal cardiovascular Imaging*. 2017;18:772-779.

JACC: CARDIOVASCULAR IMAGING
VOL. ■, NO. ■, 2018

ISSN 1936-878X/$36.00
PUBLISHED BY ELSEVIER

iMAIL

LETTER TO THE EDITOR

Poor Correlation, Reproducibility, and Agreement Between Volumetric vs. Linear Epicardial Adipose Tissue Measurement

A 3D Computed Tomography vs. 2D Echocardiography Comparison

Epicardial adipose tissue (EAT) is a visceral adipose tissue depot and, as such, has been investigated in several metabolic and inflammatory disorders. EAT has been associated with coronary artery disease and myocardial dysfunction, and it remains a burgeoning subject of research due to its potential as a therapeutic target. No endorsed guidelines exist on the measurement of EAT, with studies predominantly reporting linear thickness according to transthoracic echocardiography (EAT-TTE) or area/volume measured by using cardiac computed tomography (EAT-CT). TTE is advantageous because of its rapid performance at the bedside and low cost, but its reproducibility and accuracy may be limited by the effects of probe angulation on 2-dimensional imaging, as well as an inability to quantify periatrial fat or total EAT volume. CT imaging has the drawback of radiation exposure but allows 3-dimensional volumetric quantification. Because EAT is not uniformly distributed around the heart, volumetric quantification is arguably preferred (1). Few data compare agreement between these modalities, and we aimed to compare EAT-TTE versus volumetric EAT-CT by using commonly described methods.

We studied 106 consecutive patients who underwent clinically indicated CT scanning for suspected coronary artery disease who also had TTE performed within 30 days. CT imaging was performed on a 320-row scanner by using a previously described protocol (2), and EAT-CT images were measured by using a research-specific tool (QFAT 2.0, Cedars-Sinai Medical Center, Los Angeles, California) (3). Briefly, EAT was measured from the bifurcation of the pulmonary trunk to the cardiac apex. Manual pericardial contours were drawn at 5- to 10-interval slices with assessment for slice interpolation and corrected as required. Contiguous voxels between −190 and −30 Hounsfield units were used to define and quantify EAT. EAT-TTE was performed by using the technique of Iacobellis et al. (4); EAT was considered the echo-free space in the parasternal long-axis view between the free wall of the right ventricle and the pericardium. The average value of 3 cycles at end-systole was used with linear measurement along the midline of the ultrasound beam perpendicular to the aortic annulus. Pearson correlation coefficients and linear regression with 95% prediction intervals between methods are reported. Thirty random studies were assessed for interobserver and intraobserver agreement.

EAT-CT compared with EAT-TTE revealed poor correlation (r = 0.29; p = 0.002), and poor precision was demonstrated by the broad prediction limits (**Figure 1**). In 28 (26%) cases, observers reported uncertainty as to placement of the linear marker for EAT-TTE, suggesting reduced confidence. When these cases were excluded, correlation was not significantly altered (r = 0.25; p = 0.01); estimated prediction limits were also not significantly altered (data not shown). Poor interobserver and intraobserver agreement was seen with EAT-TTE (intraclass correlation coefficient [ICC]: 0.39; 95% confidence interval [CI]: 0.04 to 0.65; p = 0.02; ICC: 0.56; 95% CI: 0.07 to 0.79; p = 0.001, respectively);

FIGURE 1 Scatter Plot Between EAT-CT and EAT-TTE

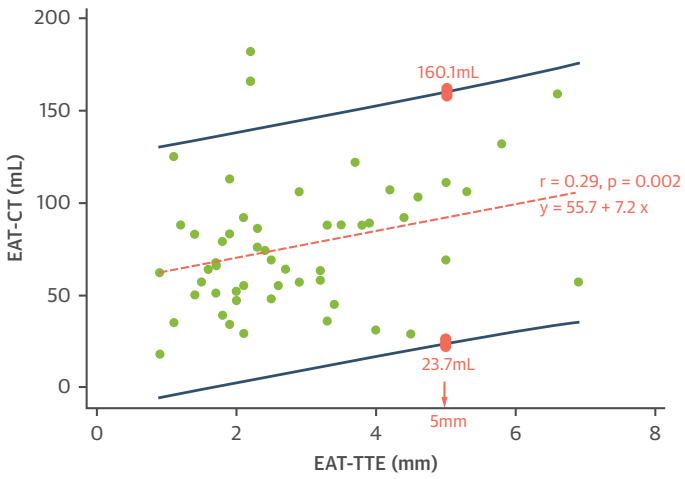

The **orange dashed line** represents the regression line of best fit. R value is the correlation coefficient, and the regression equation is the epicardial adipose tissue area/volume measured by using cardiac computed tomography (EAT-CT) as the outcome variable (y) and epicardial adipose tissue linear thickness according to transthoracic echocardiography (EAT-TTE) as the independent variable (x). The **dark blue lines** represent 95% prediction intervals. An example is illustrated by the **pink boxes**: when EAT-TTE is 5 mm, the predicted EAT-CT is between 23.7 and 160.1 ml, representing wide variability and suggesting poor precision.

Bland-Altman analysis demonstrated a mean bias of −0.35 mm with 95% limits of agreement from −4.5 to 3.8 mm. Dispersion was particularly evident at higher EAT thickness measurements. Conversely, excellent ICC was noted for EAT-CT (ICC: 0.99; 95% CI: 0.98 to 1; $p < 0.001$ for both interobserver and intraobserver) with a mean bias of 0.9 ml and 95% limits of agreement of −11.6 to 13.4 ml.

There is significant research interest in EAT-TTE, with its proponents advocating the benefits of easy bedside assessment. However, the poor reproducibility and uncertainty of measurement require caution in drawing associative or causative relationships with EAT. The difference of approximately 8 mm in interrater EAT-TTE, and corresponding wide prediction limits for EAT-CT, may have significant implications in patient misclassification. There are no well-conducted studies comparing imaging-measured EAT versus human autopsy specimens, likely due to the extreme adherence of EAT to the underlying myocardium. However, CT scanning allows adipose tissue thresholding, optimal spatial resolution for pericardium identification, and high reproducibility regardless of the use of iodinated contrast (5).

In conclusion, EAT-CT is highly reproducible compared with EAT-TTE and could be considered as the optimal reference standard for EAT-based research.

Nitesh Nerlekar, MBBS, MPH*
Yi-Wei Baey, MBBS
Adam J. Brown, MD, PhD
Rahul G. Muthalaly, MBBS, MPH
Damini Dey, PhD
Balaji Tamarappoo, MD, PhD
James D. Cameron, MD, MEngSc
Thomas H. Marwick, MBBS, MPH, PhD
Dennis T. Wong, MBBS, MD, PhD

*Monash Cardiovascular Research Centre and MonashHeart
Monash Health
246 Clayton Road
Clayton, Victoria 3168, Australia
E-mail: [redacted]

https://doi.org/10.1016/j.jcmg.2017.10.019

Please note: Dr. Nerlekar is supported by a scholarship from the National Medical Health and Research Council and the National Heart Foundation. Dr. Brown is supported by an early career investigator scholarship from Monash University. Dr. Dey is supported by a National Heart, Lung, and Blood Institute grant (1R01HL133616). Dr. Wong is supported by Early Career Fellowship by National Health and Medical Research Council (Australia). All other authors have reported that they have no relationships relevant to the contents of this paper to disclose. Jonathon Leipsic, MD, served as the Guest Editor for this paper.

REFERENCES

1. Nerlekar N, Brown AJ, Muthalaly RG, et al. Association of epicardial adipose tissue and high-risk plaque characteristics: a systematic review and meta-analysis. J Am Heart Assoc 2017;6:e006379.

2. Nerlekar N, Ko BS, Nasis A, et al. Impact of heart rate on diagnostic accuracy of second generation 320-detector computed tomography coronary angiography. Cardiovasc Diagn Ther 2017;7:296–304.

3. Dey D, Suzuki Y, Suzuki S, et al. Automated quantitation of pericardiac fat from noncontrast CT. Invest Radiol 2008;43:145–53.

4. Iacobellis G, Assael F, Ribaudo MC, et al. Epicardial fat from echocardiography: a new method for visceral adipose tissue prediction. Obes Res 2003;11:304–10.

5. Marwan M, Achenbach S. Quantification of epicardial fat by computed tomography: why, when and how? J Cardiovasc Comput Tomogr 2013;7:3–10.

Expedited Publication

Percutaneous Coronary Intervention Using Drug-Eluting Stents Versus Coronary Artery Bypass Grafting for Unprotected Left Main Coronary Artery Stenosis

A Meta-Analysis of Randomized Trials

Nitesh Nerlekar, MBBS, MPH; Francis J. Ha, BMedSci; Kunal P. Verma, MBBS; Martin R. Bennett, MD, PhD; James D. Cameron, MBBS, MD, MEngSc; Ian T. Meredith, MBBS, PhD; Adam J. Brown, MD, PhD

Background—Current guidelines suggest that coronary artery bypass grafting (CABG) should be the preferred revascularization method for unprotected left main coronary artery stenosis. In light of evidence from recent randomized trials, we assessed whether percutaneous coronary intervention (PCI) using drug-eluting stents is as safe and effective as CABG for the treatment of unprotected left main coronary artery disease.

Methods and Results—Digital databases and manual searches were performed for randomized trials comparing PCI and CABG for unprotected left main coronary artery stenosis. Among 3887 potentially relevant studies, 5 met inclusion criteria. The primary safety end point was defined as the composite of all-cause death, myocardial infarction, or stroke. Secondary end points included a clinical effectiveness composite, which was defined as all-cause death, myocardial infarction, stroke, or repeat revascularization. Summary estimates were obtained using random-effects modeling. In total, 4594 patients were included in the analysis. There was no significant difference in the primary safety end point between the revascularization strategies (odds ratio [OR], 0.97; 95% confidence interval [CI], 0.79–1.17; P=0.73). However, when compared with CABG, PCI was less effective (OR, 1.36; 95% CI, 1.18–1.58; P<0.001) because of significantly higher rates of repeat revascularization (OR, 1.85; 95% CI, 1.53–2.23; P<0.001). The incidence of all-cause death (OR, 1.03; 95% CI, 0.78–1.35; P=0.61), myocardial infarction (OR, 1.46; 95% CI, 0.88–2.45; P=0.08), and stroke (OR, 0.88; 95% CI, 0.39–1.97; P=0.53) did not differ between PCI and CABG.

Conclusions—PCI using drug-eluting stents and CABG are equally safe methods of revascularization for patients at low surgical risk with significant unprotected left main coronary artery stenosis. However, CABG is associated with significantly lower rates of repeat revascularization. (***Circ Cardiovasc Interv*. 2016;9:e004729. DOI: 10.1161/CIRCINTERVENTIONS.116.004729.)**

Key Words: coronary angiography ■ coronary artery bypass ■ drug-eluting stent ■ meta-analysis ■ percutaneous coronary intervention

Around 5% of patients undergoing coronary angiography are found to have significant unprotected left main coronary artery (ULMCA) stenosis.[1] Patients with ULMCA stenosis are typically advised to undergo revascularization because this has been shown to improve prognosis when compared with optimal medical therapy.[2] Historically, coronary artery bypass grafting (CABG) has been considered the preferred method for revascularization based on a wealth of data demonstrating the safety and durability of surgery.[3] This has been reflected in current international guidelines, where CABG carries a class I recommendation for ULMCA disease.[4,5]

Percutaneous coronary intervention (PCI) is becoming increasingly used as an alternative method of ULMCA revascularization. The development of drug-eluting stents (DES) has significantly reduced repeat revascularization rates after PCI, whereas advances in technique permit treatment of more complex coronary anatomies including the distal ULMCA bifurcation. Clinical trials comparing PCI and CABG for ULMCA stenosis have shown that subsequent major adverse cardiovascular event rates between treatment strategies were similar. However, these trials were limited in their ability to definitely answer whether individual clinical end points were

Received November 9, 2016; accepted November 17, 2016.

From the Monash Cardiovascular Research Centre, Monash University, Clayton, Victoria, Australia (N.N., F.J.H., K.P.V., J.D.C., I.T.M., A.J.B.); MonashHeart, Clayton, Victoria, Australia (N.N., F.J.H., K.P.V., J.D.C., I.T.M., A.J.B.); Monash Health, Clayton, Victoria, Australia (N.N., F.J.H., K.P.V., J.D.C., I.T.M., A.J.B.); and Division of Cardiovascular Medicine, University of Cambridge, United Kingdom (M.R.B., A.J.B.).

The Data Supplement is available at http://circinterventions.ahajournals.org/lookup/suppl/doi:10.1161/CIRCINTERVENTIONS.116.004729/-/DC1.

Correspondence to Adam J. Brown, MD, PhD, Monash Cardiovascular Research Centre, Monash University, Clayton, Victoria, Australia. E-mail ajdbrown@me.com

WHAT IS KNOWN

- There is continued debate on the optimal revascularization strategy for patients with significant left main coronary artery stenosis.
- Previous meta-analyses comparing percutaneous coronary intervention and coronary artery bypass grafting have demonstrated equivalence between revascularization strategies but are influenced by inclusion of observational data.

WHAT THE STUDY ADDS

- This meta-analysis is limited to randomized trials at the longest reported follow-up duration and demonstrates no difference in clinical safety outcomes between percutaneous coronary intervention using drug-eluting stents and coronary artery bypass grafting in patients at low surgical risk.
- However, coronary artery bypass grafting may be a more clinically effective revascularization strategy because percutaneous coronary intervention is associated with significantly higher rates of repeat revascularization at long-term follow-up.

significantly different between revascularization strategies. Previous meta-analyses have been influenced by the inclusion of observational studies,[6,7] whereas results of additional multicenter randomized trials are now available.[8,9] We, therefore, performed an updated systematic review and meta-analysis of randomized trials to evaluate clinical outcomes with PCI using DES compared with CABG in patients with significant ULMCA stenosis.

Methods

Data Sources and Search Strategy

A digital literature search was performed through the MEDLINE, EMBASE, and PubMed databases for the period January 1, 2000, to October 31, 2016. Keywords using Medical Subject Heading (MeSH), where available, included percutaneous coronary intervention, drug-eluting stent, coronary artery bypass, coronary artery disease, and left main. The search was not limited by language. Reference lists of eligible articles and previous meta-analyses were reviewed for further potential citations, along with a manual search through presentations and abstracts of major international conferences. The study protocol was prospectively registered with the PROSPERO international register (CRD42016050141) and fully adhered to the PRISMA statement (Preferred Reporting Items for Systematic Reviews and Meta-Analyses).[10] An example search strategy is presented in Table I in the Data Supplement.

Study Selection

Study characteristics for inclusion were as follows: (1) randomized controlled clinical trial, (2) involvement of left main coronary artery, (3) comparison of clinical outcomes between CABG and PCI using DES, and (4) fully published status. Only studies that specified outcomes in treatment of left main coronary artery disease and evaluated PCI involving DES platforms were included. Studies that did not specify clinical outcomes in the treatment of ULMCA specifically or used bare-metal stents or a combination of bare-metal stents and DES were excluded. Studies arising from observational registry data or that evaluated only angiographic outcomes without assessment of clinical outcomes at follow-up were also excluded. We evaluated clinical outcomes for each trial, with preference for the longest reported follow-up. The study characteristics are presented in Table II in the Data Supplement.

Data Items and Collection Process

Data items to be collected were specified before the literature search. Two investigators (N.N. and F.J.H.) independently conducted the literature search and performed data extraction for study design, baseline demographics, angiographic characteristics, and clinical outcomes. Extracted data were verified by the senior author (A.J.B.), with any discrepancies resolved by consensus. Risk of bias within individual articles was assessed according to the Cochrane Collaboration Assessment for risk of bias in included studies (Table III in the Data Supplement).

Clinical End Points

The primary end point of this study was clinical safety, defined as a composite of all-cause death, myocardial infarction (MI), or stroke. Secondary end points included an effectiveness/safety composite (henceforth called effectiveness end point), which was defined as all-cause death, MI, stroke, or repeat revascularization. Other secondary end points included all individual components of the effectiveness composite. Although the definition of MI varied slightly between trials, all required an elevation in cardiac biomarkers (either creatine kinase MB or troponin). However, the thresholds used for MI diagnosis and timing of definitions varied between trials. Periprocedural MI was included in 4 trials,[9,11–13] whereas 1 trial only assessed nonprocedural MI.[8] Stroke was generally defined as the rapid or sudden onset of new neurological deficit persisting for >24 hours with no apparent nonvascular cause. Repeat revascularization was preferentially defined as ischemia-driven revascularization by either PCI or CABG. If these data were not reported, then data on any repeat revascularization were taken. Comprehensive details of individual trial end points and trial definitions are presented in Tables IV and V in the Data Supplement.

Statistical Analysis

Data were analyzed by random-effects modeling for the primary end point and for analysis of individual secondary end points. We also performed additional analyses for both the primary and secondary effectiveness composites in studies reporting 1-year outcomes. Sensitivity analyses were performed to assess differences between early- and newer-generation DES, by duration of clinical follow-up (≤36 versus >36 months), by patients with and without diabetes mellitus, and by complexity of coronary artery disease as defined by the SYNTAX (Synergy Between Percutaneous Coronary Intervention With TAXUS and Cardiac Surgery) score (<22 versus ≥22). Summary statistics are reported as pooled odds ratios (ORs) with 95% confidence intervals (CIs). Statistical heterogeneity was quantified with the I^2 statistic. Heterogeneity was quantified as low, moderate, or high based on I^2 values of 25%, 50%, and 75%, respectively.[14] Publication bias was visually assessed by funnel plots. A 2-sided P value of <0.05 was considered significant. Statistical analyses were performed using Stata MP 14.0 (Stata Corp LP, College Station, TX) and the metan suite of commands.

Results

A total of 3887 citations were reviewed and screened, with 27 studies identified for potential inclusion and further evaluation. Of these articles, 22 studies were excluded because they either did not specifically report clinical outcomes in ULMCA disease (13 studies) or reported clinical outcomes at an earlier time point (3 studies). Other reasons for study exclusion are provided in the PRISMA study flow chart (Figure 1).

Five randomized trials met the predefined inclusion criteria and were included in the final quantitative analysis. The multicenter randomized controlled trials included were PRECOMBAT (Premier of Randomized Comparison of Bypass Surgery versus Angioplasty Using Sirolimus-Eluting Stent in Patients with Left Main Coronary Artery Disease)[12] (60-month follow-up), SYNTAX[13] (60-month follow up), NOBLE (Coronary Artery Bypass Grafting Vs Drug Eluting Stent Percutaneous Coronary Angioplasty in the Treatment of Unprotected Left Main Stenosis)[8] (60-month follow-up), EXCEL[9] (36-month follow-up), and 1 trial with 12-month clinical follow-up.[11] Overall, 4594 patients were included in the analysis with 2297 patients (50.0%) undergoing PCI using DES. The prevalence of isolated ULMCA stenosis ranged from 10% to 29%, with between 55% and 80% of patients having a distal bifurcation ULMCA lesion. Three trials compared PCI using early-generation DES with CABG,[11–13] with 2 trials using newer-generation DES.[8,9] The baseline clinical, angiographic, and procedural characteristics for the included studies are presented in Table 1.

Primary Safety End Point

Four studies reported the incidence of the primary safety end point, the composite of all-cause death, MI, and stroke. The summary OR for these studies was 0.97 (95% CI, 0.79–1.17; P=0.73), demonstrating no significant difference in safety outcomes between PCI and CABG for the treatment of ULMCA stenosis (Figure 2). Clinical event rates for each trial in the analysis are presented in Table 2. There was no evidence of statistical heterogeneity between studies (I^2=0%). The equipoise between revascularization strategies was also present in those studies reporting 1-year outcomes (OR, 0.73; 95% CI, 0.48–1.12; P=0.16; I^2=0%; Figure I in the Data Supplement). In sensitivity analyses, again there remained no difference between PCI and CABG in terms of safety when the analysis was stratified by DES type ($P_{interaction}$=0.45; Figure II in the Data Supplement), nor by clinical follow-up duration ($P_{interaction}$=0.69; Figure III in the Data Supplement). Further sensitivity analysis was performed for the 2 studies reporting data of patients with diabetes mellitus,[9,13] again demonstrating no difference in outcomes ($P_{interaction}$=0.84; Table VI in the Data Supplement). Two studies reported SYNTAX score–specific outcomes. This demonstrated that in patients with anatomically more complex disease (SYNTAX ≥22), the safety composite rates were significantly higher in patients undergoing PCI using DES (OR, 1.64; 95% CI, 1.22–2.20; $P_{interaction}$=0.006; Table VI in the Data Supplement).

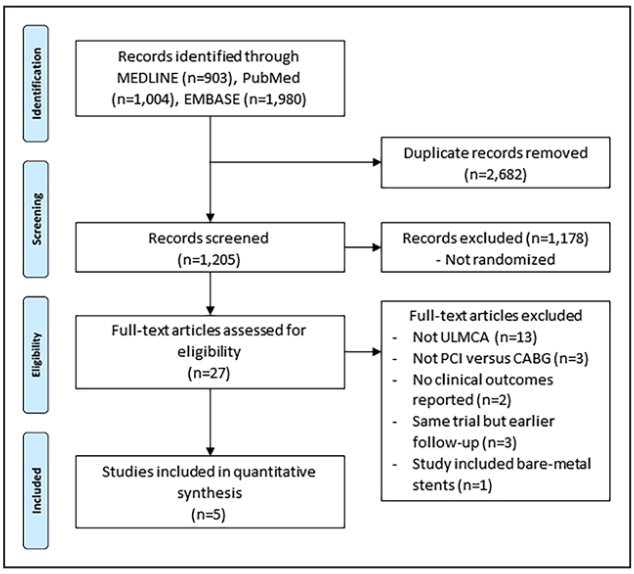

Figure 1. Study flow chart. Flow diagram illustrating the study selection process for the systematic review and meta-analysis. CABG indicates coronary artery bypass grafting; PCI, percutaneous coronary intervention; and ULMCA, unprotected left main coronary artery.

Secondary Effectiveness End Point

Four trials reported the incidence of the secondary effectiveness composite end point, which included all-cause death, MI, stroke, or repeat revascularization. The summary OR was 1.36 (95% CI, 1.18–1.58; P<0.001) in favor of CABG (Figure 3), with again no evidence of statistical heterogeneity (I^2=0%). However, in the 3 trials reporting 1-year data, there was no significant difference between PCI and CABG in terms of effectiveness (OR, 1.14; 95% CI, 0.86–1.49; P=0.33; I^2=0%). In sensitivity analyses performed at longest clinical follow-up, PCI continued to have a significantly higher risk of events, regardless of DES generation used ($P_{interaction\ between\ early-\ and\ newer-generation\ DES}$=0.85; Figure II in the Data Supplement). Analysis by trial duration confirmed the benefit of CABG, with no demonstrable differences between studies that reported outcomes at ≤36- and >36-month follow-up ($P_{interaction}$=0.38; Figure III in the Data Supplement), and no difference observed in patients with diabetes mellitus ($P_{interaction}$=0.51; Table VI in the Data Supplement).

Individual Clinical End Points

All five trials individually reported the incidence of all-cause death, MI, and repeat revascularization (Figure 4). The incidence of all-cause death was not significantly different between revascularization strategies (OR, 1.03; 95% CI, 0.78–1.35; P=0.61; I^2=23.7%). Similar outcomes between PCI and CABG were also observed for the incidence of MI (OR, 1.46; 95% CI, 0.88–2.45; P=0.08; I^2=58.1%). However, CABG was associated with a significant reduction in the risk of repeat revascularization (OR, 1.85; 95% CI, 1.53–2.23; P<0.001; I^2=0%). Four studies reported the incidence of stroke, with again no difference observed in this outcome between revascularization strategies (OR, 0.88; 95% CI, 0.39–1.97; P=0.53; I^2=62.5%).

Publication Bias

There was no visually observed publication bias either in the trials included in the primary safety outcome, nor the secondary effectiveness outcome (Figure IV in the Data Supplement). However, the small number of trials included in the analysis does limit the interpretation of funnel plots.

Discussion

To our knowledge, this is the largest meta-analysis of randomized trials investigating whether PCI using DES is as effective as CABG for the treatment of ULMCA stenosis. Our major

Table 1. Study Patient Demographics, Angiographic Characteristics, and Procedural Characteristics

	Boudriot et al[11]	PRECOMBAT[12]	SYNTAX[13]	NOBLE[8]	EXCEL[9]
Sample, n	100/100	300/300	357/348	592/592	948/957
Age, y	66/69	62/63	65/66	66/66	66/66
Male sex, %	72/77	76/77	72/76	80/76	76/78
Diabetes mellitus, %	40/33	34/30	24/26	15/15	30/28
Hypertension, %	82/82	54/51	67/62	65/66	75/74
Hyperlipidemia, %	68/64	42/40	81/75	82/78	72/69
CRF, %	NR	1/0	½	NR	18/15
Current smoker, %	35/28	30/28	18/24	19/22	24/21
Previous CVA, %	3/6	NR	5/4	NR	6/7
Previous MI, %	19/14	4/7	29/25	NR	18/17
ACS, %	NR	47/54	31/29	18/17	39/39
LVEF, %	65/65	62/61	NR	60/60	57/57
BMI, kg/m^2	27/27	25/25	28/28	28/28	29/29
EuroSCORE	2.4/2.6	2.6/2.8	3.9/3.9	2/2	NR
LMCA only, %	28/29	9/11	12/14	NR	17/18
LMCA+SVD, %	35/27	17/18	19/20	NR	31/31
LMCA+DVD, %	26/28	34/30	31/31	NR	35/32
LMCA+TVD, %	11/17	41/41	38/35	NR	17/19
SYNTAX score, mean	24/23	24/26	30/30	23/22	21/21
Distal LMCA involvement, %	74/69	67/62	56/52	81/81	NR
DES type	SES	SES	PES	BES*	EES
No. of stents†	NR	2.7±1.4	NR	1 (IQR, 1–2)	2.4±1.5
Stent length†, mm	NR	60±42	NR	NR	49±36
Bifurcation: FKB, %	100	70	NR	55	NR
IVUS guided, %	NR	91	NR	75‡	77
No. of grafts†	NR	2.7±0.9	NR	2.5	2.6±0.8
IMA, %	99	94	NR	NR	99
Off-pump surgery, %	46	64	NR	16	29

Data are presented as percentage treated with PCI/percentage treated with CABG unless otherwise stated.

ACS indicates acute coronary syndrome; BES, biolimus-eluting stent; BMI, body mass index; CABG, coronary artery bypass grafting; CRF, chronic renal failure; CVA, cerebrovascular accident; DES, drug-eluting stent; DVD, double-vessel disease; EES, everolimus-eluting stent; EXCEL, Evaluation of the Xience Everolimus-Eluting Stent Versus Coronary Artery Bypass Surgery for Effectiveness of Left Main Revascularization; FKB, final kissing balloon; IMA, internal mammary artery; IQR, interquartile range; IVUS, intravascular ultrasound; LMCA, left main coronary artery; LVEF, left ventricular ejection fraction (presented as median or mean); MI, myocardial infarction; NOBLE, Coronary Artery Bypass Grafting Vs Drug Eluting Stent Percutaneous Coronary Angioplasty in the Treatment of Unprotected Left Main Stenosis; NR, not recorded; PCI, percutaneous coronary intervention; PES, paclitaxel-eluting stent; PRECOMBAT, Premier of Randomized Comparison of Bypass Surgery versus Angioplasty Using Sirolimus-Eluting Stent in Patients with Left Main Coronary Artery Disease; SES, sirolimus-eluting stent; SVD, single-vessel disease; SYNTAX, Synergy Between Percutaneous Coronary Intervention With TAXUS and Cardiac Surgery; and TVD, triple-vessel disease.

*BES was the recommended study stent but other Conformité Européene-marked DES could be used at the operators' discretion.

†Per-patient level analysis.

‡Postimplantation IVUS evaluation only.

finding is to demonstrate that rates of the safety composite were similar between PCI using DES and CABG for revascularization of significant ULMCA stenosis in patients at low surgical risk. In addition, we find that CABG is associated with a reduction in rates of the effectiveness composite, although this benefit was not apparent within the first year. In terms of individual clinical end points, there was no difference in the rates of all-cause death, MI, or stroke between PCI using DES and CABG. However, CABG was associated with significantly lower rates of repeat revascularization. These results are important for informing treatment decisions made by multidisciplinary teams worldwide.

Revascularization of ULMCA stenosis is frequently performed for prognostic gain because CABG has been shown

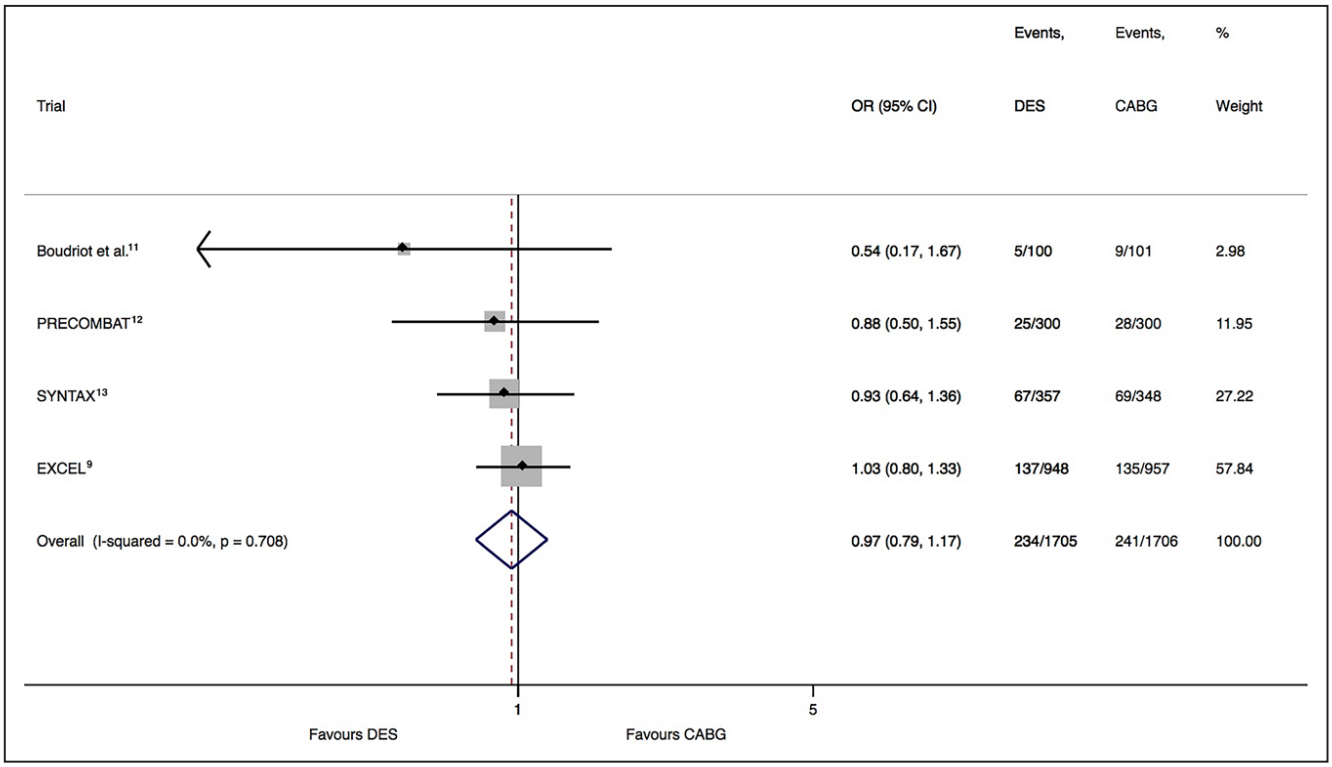

Figure 2. Risk estimates for primary safety end point for percutaneous coronary intervention vs coronary artery bypass grafting (CABG). Forest plot displays summary odds ratio (OR) and 95% confidence intervals (CI) for combined outcome of all-cause death, myocardial infarction (MI), or stroke. DES indicates drug-eluting stent.

in randomized trials to improve survival when compared with optimal medical therapy.[15] Thus, it is imperative when considering alternate revascularization strategies, such as PCI, that the treatment offered does not confer deleterious outcomes. In our study, we demonstrate that there is no difference in the composite outcome of all-cause mortality, MI, or stroke between PCI using DES and CABG. Importantly, the rates of the individual end points of the composite also remain similar between groups, and this equipoise appears regardless of trial follow-up duration. These data imply that PCI using DES for ULMCA disease is not harmful and should be considered an acceptable revascularization option. However, this does not mean that undertaking PCI for ULMCA intervention is not without risk, and suboptimal PCI results may have profound implications for the patient. Previous studies have emphasized that short- and long-term clinical outcomes can be improved when ULMCA PCI procedures are performed in high-volume centers by experienced operators.[16] Ultimately, the decision on which revascularization strategy should be used rests with the patient, who should be fully informed of the risks and potential benefits of each treatment option by a multidisciplinary heart team that understands the local expertise available.[17]

Although we find no difference in the primary safety outcome in our study, we did observe that PCI was associated with significantly higher rates of repeat revascularization (14.2% versus 8.3%). This drove the secondary outcome of clinical effectiveness in favor of CABG. Previous trials comparing PCI using DES with CABG in multivessel coronary artery disease have shown similar findings, with repeat revascularization rates often more than doubled after PCI.[18,19] The beneficial

Table 2. Summary and Individual Trial Clinical Event Rates

	Overall	Boudriot et al[11]	PRECOMBAT[12]	SYNTAX[13]	NOBLE[8]	EXCEL[9]
Safety end point	13.7/14.1	5.0/8.9	8.4/9.6	19.0/20.8	NR	15.4/14.7
Effectiveness end point	23.3/18.2	NR	17.5/14.3	36.9/31.0	29.0/19.0	23.1/19.1
All-cause death	7.4/7.0	2.0/5.0	5.7/7.9	12.8/14.6	12.0/9.0	8.2/5.9
MI	6.0/4.8	3.0/3.0	2.0/1.7	8.2/4.8	7.0/2.0	8.0/8.3
Stroke	2.0/2.2	NR	0.7/0.7	1.5/4.3	5.0/2.0	2.3/2.9
Repeat revascularization	14.2/8.3	14.0/5.9	13.0/7.3	26.7/15.5	16/10	12.9/7.6

Data are presented as percentage treated with PCI/percentage treated with CABG. CABG indicates coronary artery bypass grafting; MI, myocardial infarction; NOBLE, Coronary Artery Bypass Grafting Vs Drug Eluting Stent Percutaneous Coronary Angioplasty in the Treatment of Unprotected Left Main Stenosis; NR, not recorded; PCI, percutaneous coronary intervention; PRECOMBAT, Premier of Randomized Comparison of Bypass Surgery versus Angioplasty Using Sirolimus-Eluting Stent in Patients with Left Main Coronary Artery Disease; and SYNTAX, Synergy Between Percutaneous Coronary Intervention With TAXUS and Cardiac Surgery.

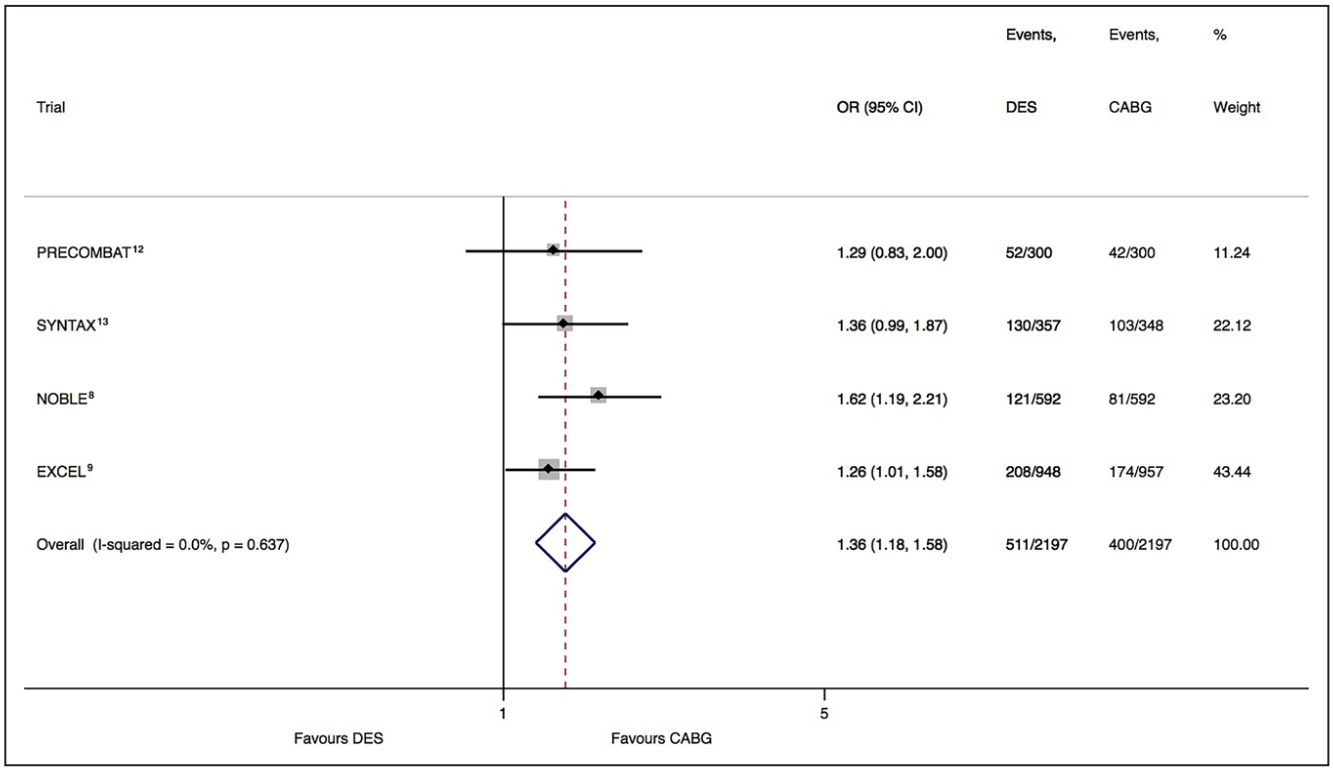

Figure 3. Risk estimates for secondary effectiveness end point for percutaneous coronary intervention vs coronary artery bypass grafting (CABG). Forest plot displays summary odds ratio (OR) and 95% confidence intervals (CI) for combined outcome of all-cause death, myocardial infarction (MI), stroke, or repeat revascularization. DES indicates drug-eluting stent.

effect of CABG in reducing the need for repeat intervention is multifactorial. Graft occlusion, in stark contrast to stent thrombosis, does not necessarily result in clinical symptoms, as the subtended myocardium may be partly supplied through the native vessel. The high use of internal mammary grafts also plays an important role in reducing the need for future revascularization because this conduit almost seems protected from the development of atherosclerosis.[20] Although refinements in DES technology continues to reduce rates of target lesion failure, it is unlikely to ever match the long-term patency rates of an adequately harvested internal mammary graft.

One interventional technique that has proven itself in reducing the need for repeat intervention during DES implantation is use of intravascular ultrasound (IVUS).[21] Although IVUS-guided PCI was frequent (91%) in PRECOMBAT, only 47% of patients underwent pre-PCI IVUS in NOBLE. Use of IVUS during PCI allows for robust measurement of reference vessel dimensions and assessment of lesion characteristics, acting to inform on stent selection and interventional strategy.[22] Stent expansion can also be assessed after implantation, guiding operators on the need for aggressive balloon post-dilatation. Previous studies have shown that DES underexpansion is one of the strongest predictors of restenosis and stent thrombosis.[23] Thus, methods that act to minimize underexpansion are of paramount importance. Meta-analyses have found that IVUS-guided PCI is associated with significantly lower rates of ischemia-driven target lesion revascularization,[24] principally because of larger postinterventional luminal dimension.[25] Although similar gains in stent expansion can be achieved using optical coherence tomography,[26] achieving the blood-free field required for optimal OCT image acquisition can be challenging in ULMCA intervention. Accordingly, operators should give due consideration to IVUS guidance when considering PCI using DES for ULMCA stenosis particularly to reduce the risk of repeat revascularization.

Finally, it is important to appreciate that our results may not necessarily be generalizable to all patients under consideration for ULMCA revascularization. The majority of patients included in the randomized trials presented either with stable angina or with clinically adjudicated unstable angina and the absence of biomarkers indicating myocardial injury. In addition, the predicted operative mortality risk for the cohort was low, as evidenced by the EuroScore values reported by the included trials (2.0%–3.9%). Thus, choice of revascularization strategy is not solely dependent on anatomy and is affected by many other factors including clinical presentation and presence of adverse medical comorbidities. This is most evident in patient presenting with ST-segment elevation MI, where PCI may be preferable as it has the advantage of providing more rapid revascularization, particularly when complicated by cardiogenic shock or ventricular arrhythmias.[27]

Study Limitations

There are some limitations to our analysis that should be considered. First, follow-up data between trials was variable, with 1 trial having follow-up at 12 months, 1 having midterm follow-up at 36 months, and 3 having long-term follow-up at 60 months. Because the benefits of CABG may accumulate over time, the reported pooled results may not adequately estimate a true long-term effect between interventions. Second, the definition of repeat revascularization slightly differed between trials. Ischemia-driven target lesion

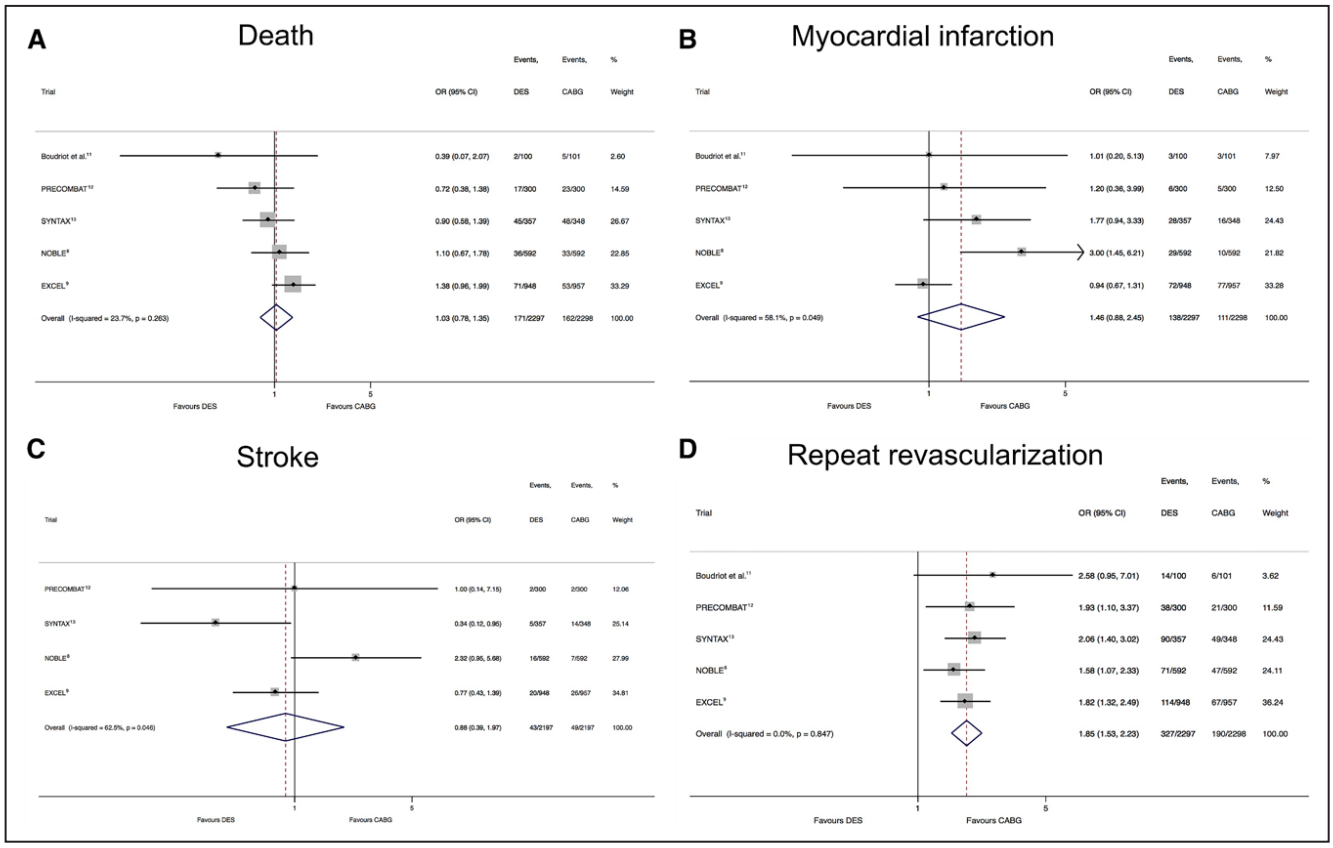

Figure 4. Risk estimates for individual clinical outcomes for percutaneous coronary intervention vs coronary artery bypass grafting (CABG). Forest plot displays summary estimates for (**A**) all-cause death, (**B**) myocardial infarction (MI), (**C**) stroke, and (**D**) repeat revascularization. CI indicates confidence interval; DES, drug-eluting stent; and OR, odds ratio.

revascularization rates were not reported in all trials, which made it difficult to assess the durability of DES results. Third, the included randomized studies used a variety of DES platforms with differing stent designs. Thus, the pooled event rates, including repeat revascularization, may not accurately reflect the performance of any one particular DES. Fourth, ORs were chosen to represent differences in clinical outcomes and have potential to overestimate effect size, particularly when the risk of events is high or when the OR departs from unity. However, the overall clinical event rates and ORs reported were modest and are unlikely to have significantly misrepresented differences between revascularization strategies.[28] Finally, we did not have access to patient-level data and have, therefore, been unable to assess the effect of specific patient or procedural characteristics that may influence clinical end points.

Conclusions

PCI using DES and CABG are equally safe methods of revascularization for patients with significant ULMCA stenosis in patients at low surgical risk. However, CABG is associated with significantly lower rates of repeat revascularization. Multidisciplinary teams should be aware of these results when considering treatment options.

Sources of Funding

This work was supported by the British Heart Foundation and the Academy of Medical Sciences.

Disclosures

None.

References

1. Fajadet J, Chieffo A. Current management of left main coronary artery disease. *Eur Heart J*. 2012;33:36–50b. doi: 10.1093/eurheartj/ehr426.
2. Caracciolo EA, Davis KB, Sopko G, Kaiser GC, Corley SD, Schaff H, Taylor HA, Chaitman BR. Comparison of surgical and medical group survival in patients with left main equivalent coronary artery disease. Long-term CASS experience. *Circulation*. 1995;91:2335–2344.
3. Taggart DP, Kaul S, Boden WE, Ferguson TB Jr, Guyton RA, Mack MJ, Sergeant PT, Shemin RJ, Smith PK, Yusuf S. Revascularization for unprotected left main stem coronary artery stenosis stenting or surgery. *J Am Coll Cardiol*. 2008;51:885–892. doi: 10.1016/j.jacc.2007.09.067.
4. Fihn SD, Gardin JM, Abrams J, Berra K, Blankenship JC, Dallas AP, Douglas PS, Foody JM, Gerber TC, Hinderliter AL, King SB 3rd, Kligfield PD, Krumholz HM, Kwong RY, Lim MJ, Linderbaum JA, Mack MJ, Munger MA, Prager RL, Sabik JF, Shaw LJ, Sikkema JD, Smith CR Jr, Smith SC Jr, Spertus JA, Williams SV; American College of Cardiology Foundation; American Heart Association Task Force on Practice Guidelines; American College of Physicians; American Association for Thoracic Surgery; Preventive Cardiovascular Nurses Association; Society for Cardiovascular Angiography and Interventions; Society of Thoracic Surgeons. 2012 ACCF/AHA/ACP/AATS/PCNA/SCAI/STS Guideline for the diagnosis and management of patients with stable ischemic heart disease: a report of the American College of Cardiology Foundation/American Heart Association Task Force on Practice Guidelines, and the American College of Physicians, American Association for Thoracic Surgery, Preventive Cardiovascular Nurses Association, Society for Cardiovascular Angiography and Interventions, and Society of Thoracic Surgeons. *Circulation*. 2012;126:e354–e471. doi: 110.1161/CIR.0b013e318277d6a0.
5. Kolh P, Windecker S, Alfonso F, Collet JP, Cremer J, Falk V, Filippatos G, Hamm C, Head SJ, Jüni P, Kappetein AP, Kastrati A, Knuuti J, Landmesser U, Laufer G, Neumann FJ, Richter DJ, Schauerte P, Sousa Uva M,

Stefanini GG, Taggart DP, Torracca L, Valgimigli M, Wijns W, Witkowski A; European Society of Cardiology Committee for Practice Guidelines, Zamorano JL, Achenbach S, Baumgartner H, Bax JJ, Bueno H, Dean V, Deaton C, Erol Ç, Fagard R, Ferrari R, Hasdai D, Hoes AW, Kirchhof P, Knuuti J, Kolh P, Lancellotti P, Linhart A, Nihoyannopoulos P, Piepoli MF, Ponikowski P, Sirnes PA, Tamargo JL, Tendera M, Torbicki A, Wijns W, Windecker S; EACTS Clinical Guidelines Committee, Sousa Uva M, Achenbach S, Pepper J, Anyanwu A, Badimon L, Bauersachs J, Baumbach A, Beygui F, Bonaros N, De Carlo M, Deaton C, Dobrev D, Dunning J, Eeckhout E, Gielen S, Hasdai D, Kirchhof P, Luckraz H, Mahrholdt H, Montalescot G, Paparella D, Rastan AJ, Sanmartin M, Sergeant P, Silber S, Tamargo J, ten Berg J, Thiele H, van Geuns RJ, Wagner HO, Wassmann S, Wendler O, Zamorano JL; Task Force on Myocardial Revascularization of the European Society of Cardiology and the European Association for Cardio-Thoracic Surgery; European Association of Percutaneous Cardiovascular Interventions. 2014 ESC/EACTS Guidelines on myocardial revascularization: The Task Force on Myocardial Revascularization of the European Society of Cardiology (ESC) and the European Association for Cardio-Thoracic Surgery (EACTS). Developed with the special contribution of the European Association of Percutaneous Cardiovascular Interventions (EAPCI). *Eur J Cardiothorac Surg*. 2014;46:517–592. doi: 10.1093/ejcts/ezu366.

6. Jang JS, Choi KN, Jin HY, Seo JS, Yang TH, Kim DK, Kim DS, Urm SH, Chun JH, Kang SJ, Park DW, Lee SW, Kim YH, Lee CW, Park SW, Park SJ. Meta-analysis of three randomized trials and nine observational studies comparing drug-eluting stents versus coronary artery bypass grafting for unprotected left main coronary artery disease. *Am J Cardiol*. 2012;110:1411–1418. doi: 10.1016/j.amjcard.2012.06.051.
7. Gargiulo G, Tamburino C, Capodanno D. Five-year outcomes of percutaneous coronary intervention versus coronary artery bypass graft surgery in patients with left main coronary artery disease: an updated meta-analysis of randomized trials and adjusted observational studies. *Int J Cardiol*. 2015;195:79–81. doi: 10.1016/j.ijcard.2015.05.136.
8. Mäkikallio T, Holm NR, Lindsay M, Spence MS, Erglis A, Menown IBA, Trovik T, Eskola M, Romppanen H, Kellerth T, Ravkilde J, Jensen LO, Kalinauskas G, Linder RBA, Pentikainen M, Hervold A, Banning A, Zaman A, Cotton J, Eriksen E, Margus S, Sørensen HT, Nielsen PH, Niemelä M, Kervinen K, Lassen JF, Maeng M, Oldroyd K, Berg G, Walsh SJ, Hanratty CG, Kumsars I, Stradins P, Steigen TK, Fröbert O, Graham ANJ, Endresen PC, Corbascio M, Kajander O, Trivedi U, Hartikainen J, Anttila V, Hildick-Smith D, Thuesen L; Christiansen EH. Percutaneous coronary angioplasty versus coronary artery bypass grafting in treatment of unprotected left main stenosis (NOBLE): a prospective, randomised, open-label, non-inferiority trial [published online ahead of print October 31, 2016]. *Lancet*. doi: 10.1016/S0140-6736(16)32052–9.
9. Stone GW, Sabik JF, Serruys PW, Simonton CA, Généreux P, Puskas J, Kandzari DE, Morice M-C, Lembo N, Brown WMI, Taggart DP, Banning A, Merkely B, Horkay F, Boonstra PW, van Boven AJ, Ungi I, Bogáts G, Mansour S, Noiseux N, Sabaté M, Pomar J, Hickey M, Gershlick A, Buszman P, Bochenek A, Schampaert E, Pagé P, Dressler O, Kosmidou I, Mehran R, Pocock SJ; Kappetein AP; EXCEL Trial Investigators. Everolimus-eluting stents or bypass surgery for left main coronary artery disease [published online ahead of print October 31, 2016]. *N Engl J Med*.
10. Liberati A, Altman DG, Tetzlaff J, Mulrow C, Gøtzsche PC, Ioannidis JP, Clarke M, Devereaux PJ, Kleijnen J, Moher D. The PRISMA statement for reporting systematic reviews and meta-analyses of studies that evaluate health care interventions: explanation and elaboration. *Ann Intern Med*. 2009;151:W65–W94.
11. Boudriot E, Thiele H, Walther T, Liebetrau C, Boeckstegers P, Pohl T, Reichart B, Mudra H, Beier F, Gansera B, Neumann FJ, Gick M, Zietak T, Desch S, Schuler G, Mohr FW. Randomized comparison of percutaneous coronary intervention with sirolimus-eluting stents versus coronary artery bypass grafting in unprotected left main stem stenosis. *J Am Coll Cardiol*. 2011;57:538–545. doi: 10.1016/j.jacc.2010.09.038.
12. Ahn JM, Roh JH, Kim YH, Park DW, Yun SC, Lee PH, Chang M, Park HW, Lee SW, Lee CW, Park SW, Choo SJ, Chung C, Lee J, Lim DS, Rha SW, Lee SG, Gwon HC, Kim HS, Chae IH, Jang Y, Jeong MH, Tahk SJ, Seung KB, Park SJ. Randomized trial of stents versus bypass surgery for left main coronary artery disease: 5-year outcomes of the PRECOMBAT study. *J Am Coll Cardiol*. 2015;65:2198–2206. doi: 10.1016/j.jacc.2015.03.033.
13. Morice MC, Serruys PW, Kappetein AP, Feldman TE, Ståhle E, Colombo A, Mack MJ, Holmes DR, Choi JW, Ruzyllo W, Religa G, Huang J, Roy K, Dawkins KD, Mohr F. Five-year outcomes in patients with left main disease treated with either percutaneous coronary intervention or coronary artery bypass grafting in the synergy between percutaneous coronary intervention with taxus and cardiac surgery trial. *Circulation*. 2014;129:2388–2394. doi: 10.1161/CIRCULATIONAHA.113.006689.
14. Higgins JP, Thompson SG, Deeks JJ, Altman DG. Measuring inconsistency in meta-analyses. *BMJ*. 2003;327:557–560. doi: 10.1136/bmj.327.7414.557.
15. Yusuf S, Zucker D, Peduzzi P, Fisher LD, Takaro T, Kennedy JW, Davis K, Killip T, Passamani E, Norris R. Effect of coronary artery bypass graft surgery on survival: overview of 10-year results from randomised trials by the Coronary Artery Bypass Graft Surgery Trialists Collaboration. *Lancet*. 1994;344:563–570.
16. Xu B, Redfors B, Yang Y, Qiao S, Wu Y, Chen J, Liu H, Chen J, Xu L, Zhao Y, Guan C, Gao R, Généreux P. Impact of operator experience and volume on outcomes after left main coronary artery percutaneous coronary intervention. *JACC Cardiovasc Interv*. 2016;9:2086–2093. doi: 10.1016/j.jcin.2016.08.011.
17. Head SJ, Kaul S, Mack MJ, Serruys PW, Taggart DP, Holmes DR Jr, Leon MB, Marco J, Bogers AJ, Kappetein AP. The rationale for Heart Team decision-making for patients with stable, complex coronary artery disease. *Eur Heart J*. 2013;34:2510–2518. doi: 10.1093/eurheartj/eht059.
18. Farkouh ME, Domanski M, Sleeper LA, Siami FS, Dangas G, Mack M, Yang M, Cohen DJ, Rosenberg Y, Solomon SD, Desai AS, Gersh BJ, Magnuson EA, Lansky A, Boineau R, Weinberger J, Ramanathan K, Sousa JE, Rankin J, Bhargava B, Buse J, Hueb W, Smith CR, Muratov V, Bansilal S, King S 3rd, Bertrand M, Fuster V; FREEDOM Trial Investigators. Strategies for multivessel revascularization in patients with diabetes. *N Engl J Med*. 2012;367:2375–2384. doi: 10.1056/NEJMoa1211585.
19. Serruys PW, Morice MC, Kappetein AP, Colombo A, Holmes DR, Mack MJ, Ståhle E, Feldman TE, van den Brand M, Bass EJ, Van Dyck N, Leadley K, Dawkins KD, Mohr FW; SYNTAX Investigators. Percutaneous coronary intervention versus coronary-artery bypass grafting for severe coronary artery disease. *N Engl J Med*. 2009;360:961–972. doi: 10.1056/NEJMoa0804626.
20. Otsuka F, Yahagi K, Sakakura K, Virmani R. Why is the mammary artery so special and what protects it from atherosclerosis? *Ann Cardiothorac Surg*. 2013;2:519–526. doi: 10.3978/j.issn.2225-319X.2013.07.06.
21. Hong SJ, Kim BK, Shin DH, Nam CM, Kim JS, Ko YG, Choi D, Kang TS, Kang WC, Her AY, Kim YH, Kim Y, Hur SH, Hong BK, Kwon H, Jang Y, Hong MK; IVUS-XPL Investigators. Effect of intravascular ultrasound-guided vs angiography-guided everolimus-eluting stent implantation: the IVUS-XPL randomized clinical trial. *JAMA*. 2015;314:2155–2163. doi: 10.1001/jama.2015.15454.
22. McDaniel MC, Eshtehardi P, Sawaya FJ, Douglas JS Jr, Samady H. Contemporary clinical applications of coronary intravascular ultrasound. *JACC Cardiovasc Interv*. 2011;4:1155–1167. doi: 10.1016/j.jcin.2011.07.013.
23. Fujii K, Carlier SG, Mintz GS, Yang YM, Moussa I, Weisz G, Dangas G, Mehran R, Lansky AJ, Kreps EM, Collins M, Stone GW, Moses JW, Leon MB. Stent underexpansion and residual reference segment stenosis are related to stent thrombosis after sirolimus-eluting stent implantation: an intravascular ultrasound study. *J Am Coll Cardiol*. 2005;45:995–998. doi: 10.1016/j.jacc.2004.12.066.
24. Elgendy IY, Mahmoud AN, Elgendy AY, Bavry AA. Outcomes with intravascular ultrasound-guided stent implantation: a meta-analysis of randomized trials in the era of drug-eluting stents. *Circ Cardiovasc Interv*. 2016;9:e003700. doi: 10.1161/CIRCINTERVENTIONS.116.003700.
25. Jang JS, Song YJ, Kang W, Jin HY, Seo JS, Yang TH, Kim DK, Cho KI, Kim BH, Park YH, Je HG, Kim DS. Intravascular ultrasound-guided implantation of drug-eluting stents to improve outcome: a meta-analysis. *JACC Cardiovasc Interv*. 2014;7:233–243. doi: 10.1016/j.jcin.2013.09.013.
26. Ali ZA, Maehara A, Généreux P, Shlofmitz RA, Fabbiocchi F, Nazif TM, Guagliumi G, Meraj PM, Alfonso F, Samady H, Akasaka T, Carlson EB, Leesar MA, Matsumura M, Ozan MO, Mintz GS, Ben-Yehuda O; Stone GW. Optical coherence tomography compared with intravascular ultrasound and with angiography to guide coronary stent implantation (ILUMIEN III: OPTIMIZE PCI): a randomised controlled trial [published online ahead of print October 30, 2016]. doi: 10.1016/S0140-6736(16)31922–5.
27. Lee MS, Bokhoor P, Park SJ, Kim YH, Stone GW, Sheiban I, Biondi-Zoccai G, Sillano D, Tobis J, Kandzari DE. Unprotected left main coronary disease and ST-segment elevation myocardial infarction: a contemporary review and argument for percutaneous coronary intervention. *JACC Cardiovasc Interv*. 2010;3:791–795. doi: 10.1016/j.jcin.2010.06.005.
28. Davies HT, Crombie IK, Tavakoli M. When can odds ratios mislead? *BMJ*. 1998;316:989–991.

SUPPLEMENTAL MATERIALS

Percutaneous coronary intervention with drug-eluting stents versus coronary artery bypass grafting for unprotected left main coronary artery stenosis: a meta-analysis of randomized trials

Nitesh Nerlekar MBBS, MPH, Francis J. Ha BMedSci, Kunal P. Verma MBBS, Martin R. Bennett MD, PhD, James D. Cameron MBBS, MD, MEngSc Ian T. Meredith MBBS, PhD, and Adam J. Brown MD, PhD

Table of Contents

Table S1. Example search strategy (Medline)

#	Searches	Results
1	Exp Stents/ or exp Drug-Eluting Stents/	62948
2	Exp Percutaneous Coronary Intervention/	43031
3	Exp Coronary Artery Bypass/	48744
4	Coronary Stenosis/su [Surgery]	2414
5	Coronary Artery Disease/su [Surgery]	6566
6	Left main.mp.	8819
7	1 or 2	91144
8	3 or 4 or 5	52405
9	6 and 7 and 8	903

Table S2. Study characteristics

Trial	Location	Period	F/U, months	Center	No. of patients	Registration no.
Boudriot et al.[1]	Germany	2003-2009	12	Multicenter	201	NCT00176397
PRECOMBAT[2]	South Korea	2004-2009	60	Mulitcenter	600	NCT00422968
SYNTAX[3]	Europe and United States	2005-2007	60	Multicenter	705	NCT00114972
NOBLE[4]	Europe	2008-2015	60	Multicenter	1184	NCT01496651
EXCEL[5]	United States	2010-2016	36	Multicenter	1905	NCT01205776

EXCEL, Evaluation of the Xience Everolimus-Eluting Stent Versus Coronary Artery Bypass Surgery for Effectiveness of Left Main Revascularization; F/U, Follow up; NOBLE, Coronary Artery Bypass Grafting Vs Drug Eluting Stent Percutaneous Coronary Angioplasty in the Treatment of Unprotected Left Main Stenosis; PRECOMBAT, Premier of Randomized Comparison of Bypass Surgery versus Angioplasty Using Sirolimus-Eluting Stent in Patients with Left Main Coronary Artery Disease; SYNTAX, Synergy Between Percutaneous Coronary Intervention With TAXUS and Cardiac Surgery.

Table S3. Cochrane Review of bias

	Random Sequence Generation (selection bias)	**Allocation concealment** (selection bias)	**Blinding of participants and personnel** (performance bias)	**Blinding of outcome assessment** (detection bias)	**Incomplete outcome data** (attrition bias)	**Selective reporting** (reporting bias)	**Overall judgment**
Boudriot et al.	*Low*	*Low*	*High*	*Low*	*Low*	*Low*	*Low*
SYNTAX	*Low*	*Low*	*High*	*Low*	*Low*	*Low*	*Low*
PRECOMBAT	*Low*	*Low*	*High*	*Low*	*Low*	*Low*	*Low*
NOBLE	*Low*	*Low*	*High*	*Low*	*Low*	*Low*	*Low*
EXCEL	*Low*	*Low*	*High*	*Low*	*Low*	*Low*	*Low*

Table S4. Study inclusion/exclusion criteria and endpoints

Trial	Main inclusion criteria	Main exclusion criteria	Primary endpoint	Secondary endpoint
Boudriot et al.	Patients aged 18 to 80 years with ULMCA (stenosis ≥50%) with or without additional multi-vessel CAD	MI <48 hours requiring immediate intervention, additional valvular heart disease requiring surgery, previous surgical treatment for coronary artery or valvular disease, severe peripheral arterial disease, significant carotid stenosis requiring treatment, renal dysfunction requiring dialysis, any disease with limited life expectancy, overt congestive heart failure, and contraindication to antiplatelet therapy	Freedom from composite of all-cause death, MI, and the need for repeat revascularization within 12 months	Each individual component of the primary endpoint
PRECOMBAT	Patients older than 18 years of age with a diagnosis of stable angina, unstable angina, silent ischemia, or non-ST-segment elevation MI.	Any previous PCI within 1 year, previous bypass surgery, acute MI within 1 week, ejection fraction <30%, cardiogenic shock, any stroke with a persistent neurological deficit or any cerebrovascular accident within 6 months	MACCE as a composite of all-cause death, MI, stroke or ischemia-driven TVR after randomisation	Individual components of the primary endpoint; composite of all-cause death, MI, or stroke; clinically driven TVR; ST
SYNTAX	Patients with ULMCA and/or 3VD and ≥50% target vessel stenosis with MI (stable, unstable, silent)	Prior PCI or CABG, acute MI, concomitant cardiac valve disease requiring surgical therapy (reconstruction or replacement)	MACCE as a composite of all-cause death, MI, cerebrovascular accident/stroke, and repeat revascularization	Individual components of the primary endpoint; Quality of Life
NOBLE	Patients with stable, unstable angina pectoris or ACS; significant lesion of ULMCA ostium, mid-shaft and/or bifurcation with no more than three additional non-complex PCI lesions;	ST-elevation MI within 24 hours; CABG clearly better treatment option (ULMCA stenosis and >3, or complex additional coronary lesions); patient is too high risk for CABG	Composite of all-cause death, non-procedurally related MI, stroke and repeat revascularization (PCI or CABG)	Individual components of the primary endpoint; composite of all-cause death, stroke or MI; definite ST/symptomatic graft occlusion; CCS angina score; NYHA functional class; duration of admission for index treatment

	patient eligible to be treated by CABG and by PCI			
EXCEL	Patients ≥18 years of age with ULMCA with angiographic diameter stenosis ≥70%	Prior PCI of left main trunk, PCI of any other (non-left main) coronary artery lesions within one year prior to randomisation, CABG at any time; need for any concomitant cardiac surgery other than CABG; non-cardiac comorbidities with life expectancy <3 years	Composite of all-cause death, MI, or stroke	Individual components of the primary endpoint; revascularization (all, ischemia-driven and non-ischemia-driven); disability following stroke event; composite of all-cause death, MI, or stroke; composite of all-cause death, MI, stroke, or ischemia-driven revascularization; ST; bleeding complications; elapsed times: randomisation to procedure, procedure to discharge, procedure to return to work and ICU days; major adverse events: composite of all-cause death, MI, stroke, TIMI major or minor bleeding, transfusion of ≥2 units of blood, major arrhythmia, unplanned coronary revascularization for ischemia, any unplanned surgery or therapeutic radiologic procedure, renal failure, sternal wound dehiscence, infection requiring antibiotics for treatment, intubation for >48 hours, post-pericardiotomy syndrome

3VD, Triple-vessel disease; ACS, Acute coronary syndrome; CAD, Coronary artery disease; CABG, Coronary artery bypass grafts; CCS, Canadian Cardiovascular Society; MACCE, Major adverse cardiac and cerebrovascular events; MI, Myocardial infarction; NYHA, New York Heart Association; ICU, Intensive Care Unit; PCI, Percutaneous coronary intervention; ST, Stent thrombosis; TIMI, Thrombolysis in myocardial infarction; TVR, Target vessel revascularization; ULMCA, Unprotected left main coronary artery

Table S5. Definition of outcomes

Boudriot et al.
Major adverse cardiovascular events: all-cause death, myocardial infarction and the need for repeat revascularization within 12 months
Myocardial infarction: increase in CK-MB activity >3 times ULN after PCI and >5 times after CABG with standard electrocardiographic criteria applied
Stent thrombosis: defined in accordance with the Academic Research Consortium definitions[6]
Repeat revascularization: any revascularization by CABG or PCI within 12 months

SYNTAX
Major adverse cardiac and cerebrovascular events: all-cause death, cerebrovascular event, documented myocardial infarction, repeat revascularization (PCI and/or CABG)
Cerebrovascular event: any acute event related to the impairment of the cerebral circulation that lasts more than 24 hours and results in irreversible brain damage or permanent body impairment. Strokes may be further classified as ischemic or hemorrhagic based on imaging studies. The definitive evaluation for the absence or presence of CVA was conducted and confirmed in both revascularization arms by a local neurologist.
Myocardial infarction: a definitive diagnosis of MI is made based on the following:

- within the first 7 days post intervention (PCI or CABG) – either new, abnormal Q waves and 1 ratio of peak CK-MB/peak total CK>10% or new, abnormal Q-waves and 1 plasma level of CK-MB 5x ULN
- 7 day after any intervention procedure (PCI or CABG) – either new, abnormal Q waves or enzyme changes defined as more than 10% of the ratio of peak CK-MB/peak total CK on one or more than one sample (if no ratio is available – one or more than 1 plasma level of CK-MB 5x upper limit for normal)

Repeat revascularization: any revascularization by CABG or PCI

PRECOMBAT
Myocardial infarction:

- Within the first 48 hours after procedure (CABG or PCI) – the presence of new Q waves in at least 2 or more contiguous leads, or new LBBB and one plasma level of CK-MB 5x upper limit for normal
- More than 48 hours after the procedure (CABG or PCI) – typical rise and gradual fall of troponin or more rapid rise and fall of CK-MB for detecting myocardial necrosis with at least one of the following:
    - Ischemic symptoms or atypical symptoms of ischemia;
    - Development of pathologic Q waves on the ECG, or new LBBB; AND
    - Enzyme changes defined as one or more than one plasma level of CK-MB above upper level of normal

Stent thrombosis: occurrence of any of the following defined by the Academic Research Consortium Definitions[6]:

1. Definite stent thrombosis – clinical presentation of acute coronary syndrome with angiographic confirmation of thrombus or occlusion or pathologic confirmation of acute thrombosis
2. Probable stent thrombosis – Unexplained death within 30 days or target vessel MI without angiographic confirmation of thrombosis or other identified culprit lesion
3. Possible stent thrombosis – unexplained death after 30 days

Stent thrombosis can be Acute (≤1 day post-procedure), Sub-acute (>1 day and ≤30 days post-procedure), Late (>30 days and ≤1-year post-procedure) or Very Late (>1 year post-procedure)

Cerebrovascular accident: defined as sudden onset of vertigo, numbness, aphasia, or dysarthria to vascular lesions of the brain such as hemorrhage, embolism, thrombosis, or rupturing aneurysm, that persisted >24 hours

Repeat coronary vascularization: any subsequent PCI procedure or CABG surgery, as determined by the patient's physician to be clinically indicated.

Target lesion revascularization: any repeat PCI or bypass surgery of the lesion was treated during the index procedure. A target lesion revascularization will be considered ischemia-driven if the target lesion diameter stenosis is ≥50% by QCA and any of the following occur:

- The patient had a positive functional study corresponding to the area served by the target lesion;
- Ischemic ECG changes at rest in a distribution consistent with the target vessel; or
- Ischemic symptoms referable to the target lesion

Target vessel revascularization: Any PCI of the target vessel or bypass surgery of the target vessel. The target vessel consists of the target lesion(s) plus any additional lesions in the main epicardial coronary artery or branches containing the target lesion (LAD, LCX or RCA)

Thrombocytopenia: Nadir platelet count <100,000 cells/mm^3 in a patient with a baseline platelet count >100,000 cells/mm^3. Further divided into mild (50,000 - <100,000 cells/mm^3), moderate (20,000 - <50,000 cells/mm^3), or severe (<20,000 cells/mm^3, or requiring platelet transfusion)

NOBLE

Cardiac death: any death due to a suspected cardiac cause (MI, low-output heart failure, fatal arrhythmia), unwitnessed death and death of unknown cause. All procedure-related deaths, including those related to concomitant treatment, were classified as cardiac death.

Non-procedure-related myocardial infarction: a rise in biochemical markers exceeding the decision limit for myocardial infarction (99^{th} percentile including <10% CV) with at least one of the following:

1. Ischemic symptoms
2. ECG changes indicative of ischemia (ST segment elevation or depression)
3. Development of a pathologic Q-wave with no relation to a PCI procedure

Procedural myocardial infarction: diagnosis of procedural MI for both PCI and CABG patients was based on CK-MB elevations when available. Patients needed to have stable angina pectoris as the clinical indication OR a normal baseline CK-MB, TnI, TnT, or highly-sensitive TnT, to be assessable for procedural MI. Diagnosis required a CK-MB value above 10 x URL or ULN to establish the diagnosis. The diagnosis could also be placed by the combination of a CK-MB value above 5 x URL or ULN, AND one or more of the following:

1. New pathological Q waves in at least 2 contiguous leads or new persistent non-rate-related LBBB
2. Angiographically documented graft or native coronary artery occlusion or new severe stenosis with thrombosis and/or diminished epicardial flow
3. Imaging evidence of new loss of viable myocardium or new regional wall motion abnormality

Repeat revascularization: any new PCI or CABG operation performed during follow-up. If an index revascularization was attempted or successful, any subsequent revascularization was counted as repeat revascularization.

Target lesion revascularization: repeat revascularization by PCI of any target segment treated during the index procedure. A target lesion segment was defined as a stented or balloon treated segment and its 5 mm margin

Definite stent thrombosis: defined in accordance with the Academic Research Consortium definitions[6]

Symptomatic graft occlusion: diagnosis of symptomatic graft occlusion required it to be detected during a clinically indicated coronary angiography

Stroke: Ischemic or hemorrhagic cerebrovascular event verified by CT or MRI brain

EXCEL

Post-procedure myocardial infarction: defined as the occurrence within 7 hours after either PCI or CABG of either:

- CK-MB >10x URL OR
- CK-MB >5x URL plus
    - New pathological Q-waves in at least two contiguous leads or new persistent non-rate-related LBBB, or
    - Angiographically documented graft or native coronary artery occlusion or new severe stenosis with thrombosis and/or diminished epicardial flow, or
    - Imaging evidence of new loss of viable myocardium or new regional wall motion abnormality

Spontaneous myocardial infarction: defined as the occurrence >72 hours after any PCI or CABG of:

- The rise and/or fall of cardiac biomarkers (CK-MB or troponin) >1x URL PLUS
    - ECG changes indicative of new ischemia [ST-segment elevation or depression, in the absence of other causes of ST-segment changes such as left ventricular hypertrophy or bundle branch block] or
    - Development of pathological Q waves (≥0.04 seconds in duration and ≥1 mm in depth) in ≥2 contiguous precordial leads or ≥2 adjacent limb leads) of the ECG, or
    - Angiographically documented graft or native coronary artery occlusion or new severe stenosis with thrombosis and/or diminished epicardial flow, or
    - Imaging evidence of new loss of viable myocardium or new regional wall motion abnormality

Stroke: the rapid onset of a new persistent neurologic deficit attributed to an obstruction in cerebral blood flow and/or cerebral hemorrhage with no apparent non-vascular cause (e.g., trauma, tumour, or infection). A vascular neurologist or stroke specialist determined whether a stroke had occurred and determined the stroke severity using the NIHSS TIA/stroke questionnaire. Available neuroimaging studies was considered to support the clinical impression and to determine if there was a demonstrable lesion compatible with an acute stroke. Strokes were classified as ischemic, hemorrhagic, or unknown. Four criteria must be fulfilled to diagnose stroke:

1. Rapid onset of a focal/global neurological deficit with at least one of the following: change in level of consciousness, hemiplegia, hemiparesis, numbness or sensory loss affecting one side of the body, dysphasia/aphasia, hemianopia, amaurosis fugax, other new neurological sign(s)/symptom(s) consistent with stroke; and
2. Duration of a focal/global neurological deficit ⩾24 hours or <24 hours if any of the following conditions exist:
    a. At least one of the following therapeutic interventions:
        i. Pharmacologic (i.e., thrombolytic drug administration)
        ii. Non-pharmacologic (i.e., neurointerventional procedure such as intracranial angioplasty)
    b. Available brain imaging clearly documents a new hemorrhage or infarct
    c. The neurological deficit results in death
3. No other readily identifiable non-stroke cause for the clinical presentation (e.g., brain tumour, trauma, infection, hypoglycaemia, other metabolic abnormality, peripheral lesion, or drug side effect). Patients with non-focal global encephalopathy will not be reported as a stroke without unequivocal evidence based upon neuroimaging studies.

4. Confirmation of the diagnosis by a neurology or neurosurgical specialist and at least one of the following:
    a. Brain imaging procedure (at least one of the following):
        i. CT scan
        ii. MRI scan
        iii. Cerebral vessel angiography
    b. Lumbar puncture (i.e., spinal fluid analysis diagnostic of intracranial hemorrhage)

Ischemia-driven revascularization:

A coronary revascularization procedure may be either a CABG or PCI. The coronary segments revascularized will be sub-classified as:

- Target lesion: a lesion revascularized in the index procedure (or during a planned or provisional staged procedure)
- Target vessel: the target vessel is defined as the entire major coronary vessel proximal and distal to the target lesion including upstream and downstream branches and the target lesion itself
- Target vessel non-target lesion: the target vessel non-target lesion consists of a lesion in the epicardial vessel/branch/graft that contains the target lesion; however, this lesion is outside of the target lesion by at least 5 mm distal or proximal to the target lesion determined by QCA
- Non-target vessel: for the purposes of this trial, the only possible non-target vessel would be the RCA and its major branches that were not treated by either PCI or CABG at the index procedure (unless either the LAD or LCX is occluded at baseline and no attempt was made to revascularize these territories by either PCI or CABG)

All revascularization events will be adjudicated as either ischemia-driven or non-ischemia-driven. Revascularization will be considered ischemia-driven if the diameter stenosis of the revascularized coronary segment is ≥50% by QCA and any of the following criteria for ischemia are met:

- A positive functional study corresponding to the area served by the target lesion; or
- Ischemic ECG changes at rest in a distribution consistent with the target vessel; or
- Typical ischemic symptoms referable to the target lesion; or
- IVUS of the target lesion with a MLA of ≤4 mm2 for non-left main lesions or ≤6 mm2 for left main lesions. If the lesions are de novo (i.e., not restenotic), the plaque burden must also be ≥60%; or FFR of the target lesion ≤0.80

CABG, Coronary artery bypass grafts; CK, Creatine-kinase; CK-MB, Creatine-kinase MB; CT, Computed tomography; CVA, Cerebrovascular accident; ECG, Electrocardiogram; FFR, Fractional flow reserve; IVUS; Intravascular ultrasound; LAD, Left anterior descending; LBBB, Left bundle branch block; LCX, Left circumflex artery; MLA, Minimal Lumen area; MRI, Magnetic Resonance Imaging; MI, Myocardial Infarction; NIHSS, National Institutes of Health Strokes Scale; PCI, Percutaneous coronary intervention; QCA, Quantitative coronary angiography; RCA, Right coronary artery; TIA, Transient ischemic attack; TnI, Troponin-I; TnT, Troponin-T; ULN, Upper limit of normal; URL, Upper reference limit

Table S6. Sensitivity analysis

Studies included	Outcome	Subgroup	OR	95% CI	I^2	p-value	P-interaction
SYNTAX EXCEL	Death, MI, stroke	Diabetics	0.92	0.60-1.42	17.2%	0.78	0.84
		Non-Diabetic	0.99	0.76-1.28	0%	0.99	
PRECOMBAT SYNTAX	Death, MI, stroke, revascularization	Diabetics	1.46	0.90-2.36	0%	0.18	0.51
		Non-Diabetics	1.20	0.88-1.64	0%	0.16	
PRECOMBAT EXCEL	Death, MI, stroke	Syntax <22	0.78	0.50-1.21	0%	0.26	0.006
		Syntax ≥22	1.64	1.22-2.20	68%	0.002	

Table displays results stratified by Diabetic group and SYNTAX score with at least 2 studies reporting outcomes. Results are pooled OR by random-effects modelling.

MI, myocardial infarction; OR, odds ratio

Figure S1. Risk estimates at 1-year follow up

Forest plot displays summary odds ratio (OR) and 95% confidence intervals (CI) for A) Safety endpoint of all-cause death, MI and stroke; and B) Efficacy-safety endpoint of all-cause death, MI, stroke and repeat revascularization.

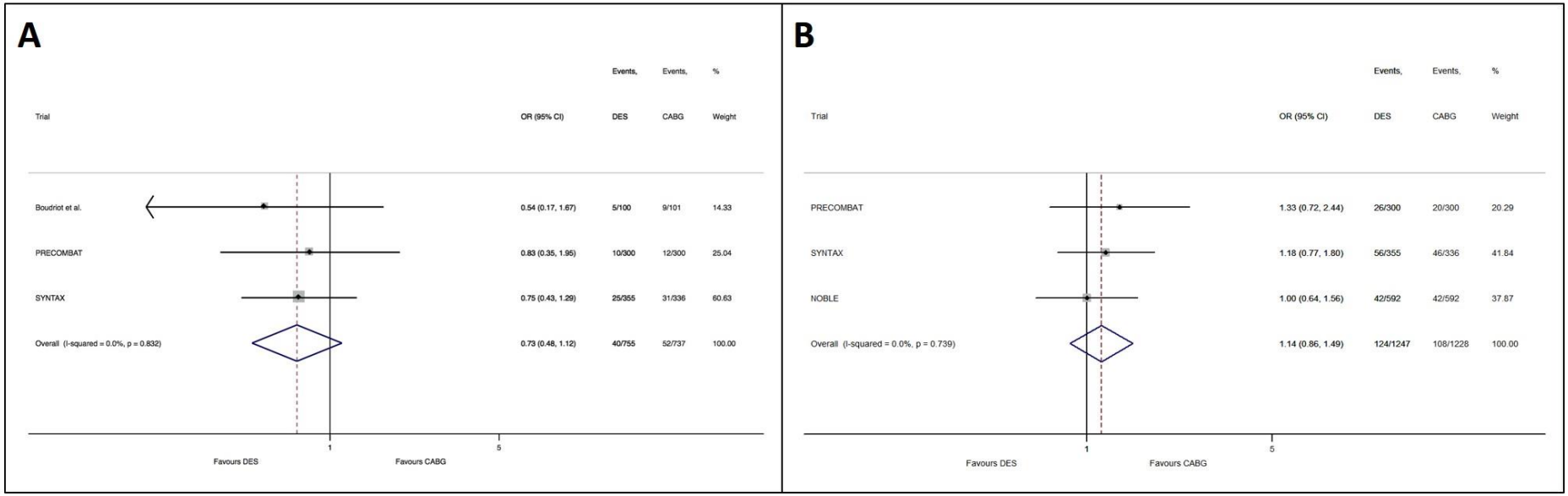

CABG, coronary artery bypass grafting, DES, drug-eluting stent; MI, myocardial infarction,

Figure S2. Risk estimates by stent generation

Forest plot displays summary estimates (odds ratios and 95% confidence intervals) of studies using early generation DES vs. new generation DES compared to CABG. A) Safety endpoint of death, MI or stroke. B) Efficacy-safety endpoint of death, MI, stroke or revascularization. p-value for interaction is displayed as heterogeneity between groups.

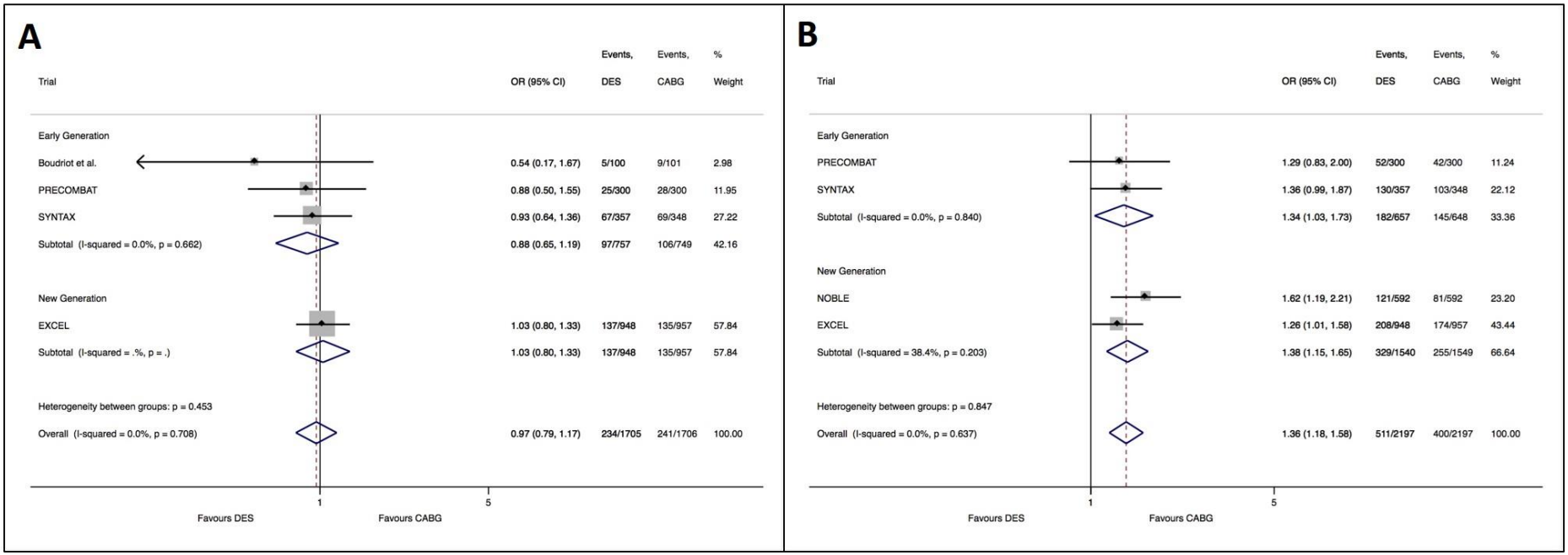

CABG, Coronary artery bypass grafts; DES, Drug eluting stent;

Figure S3: Risk estimates by follow-up duration

Forest plot displays summary estimates (odds ratios and 95% confidence intervals) of studies by short-term (12-months), mid-term (36-months) and long-term (60-months) follow-up. A) Safety endpoint of all-cause death, MI or stroke. B) Efficacy-safety endpoint of all-cause death, MI, stroke or revascularization. P-value for interaction is displayed as heterogeneity between groups.

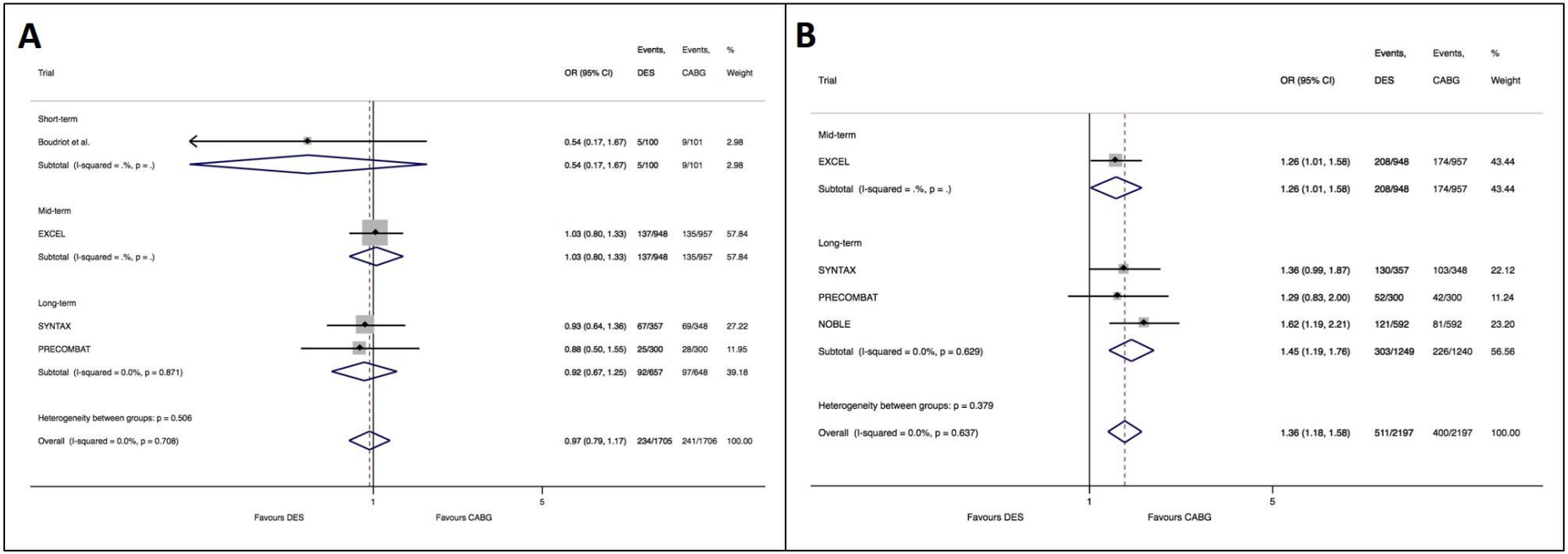

CABG, Coronary artery bypass grafts; DES, Drug eluting stent;

Figure S4. Funnel plot for visual estimation of publication bias

A) Safety endpoint of all-cause death, MI, stroke. B) Efficacy-safety endpoint of all-cause death, MI, stroke or revascularization.

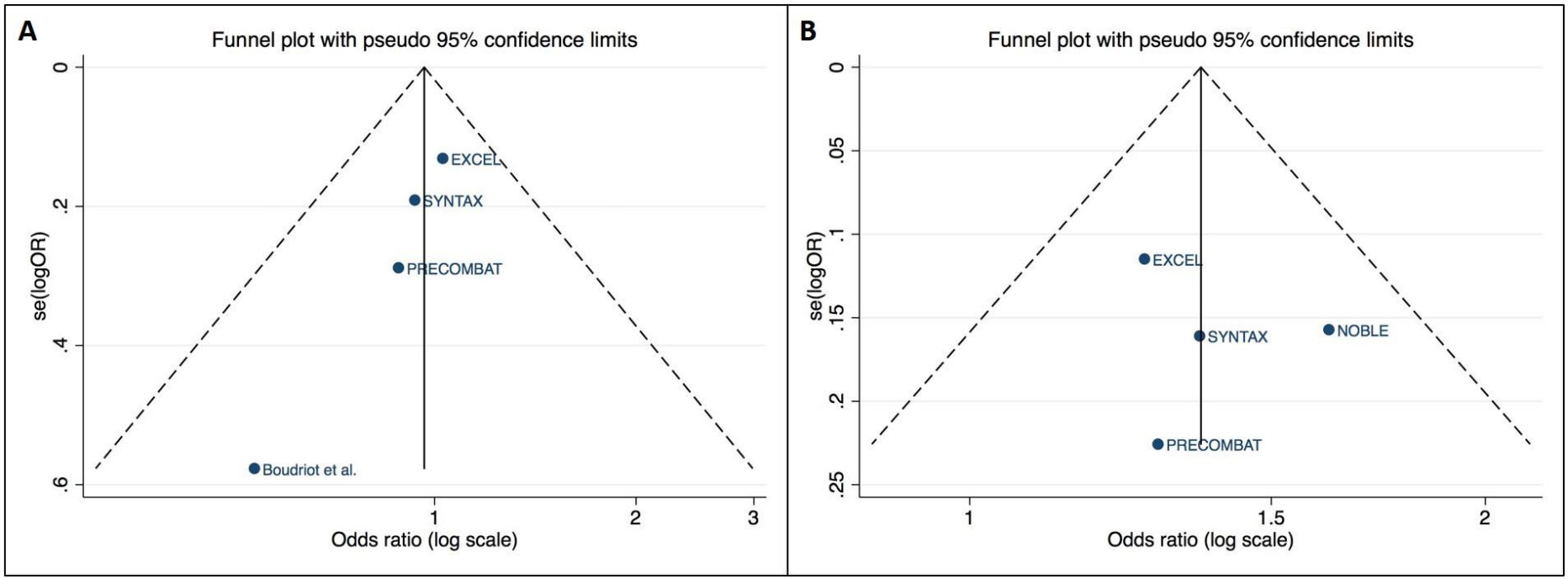

References

1. Boudriot E, Thiele H, Walther T, Liebetrau C, Boeckstegers P, Pohl T, Reichart B, Mudra H, Beier F, Gansera B, Neumann FJ, Gick M, Zietak T, Desch S, Schuler G and Mohr FW. Randomized comparison of percutaneous coronary intervention with sirolimus-eluting stents versus coronary artery bypass grafting in unprotected left main stem stenosis. *Journal of the American College of Cardiology*. 2011;57:538-45.

2. Ahn JM, Roh JH, Kim YH, Park DW, Yun SC, Lee PH, Chang M, Park HW, Lee SW, Lee CW, Park SW, Choo SJ, Chung C, Lee J, Lim DS, Rha SW, Lee SG, Gwon HC, Kim HS, Chae IH, Jang Y, Jeong MH, Tahk SJ, Seung KB and Park SJ. Randomized Trial of Stents Versus Bypass Surgery for Left Main Coronary Artery Disease: 5-Year Outcomes of the PRECOMBAT Study. *Journal of the American College of Cardiology*. 2015;65:2198-206.

3. Morice MC, Serruys PW, Kappetein AP, Feldman TE, Stahle E, Colombo A, Mack MJ, Holmes DR, Choi JW, Ruzyllo W, Religa G, Huang J, Roy K, Dawkins KD and Mohr F. Five-year outcomes in patients with left main disease treated with either percutaneous coronary intervention or coronary artery bypass grafting in the synergy between percutaneous coronary intervention with taxus and cardiac surgery trial. *Circulation*. 2014;129:2388-94.

4. Mäkikallio T, Holm NR, Lindsay M, Spence MS, Erglis A, Menown IBA, Trovik T, Eskola M, Romppanen H, Kellerth T, Ravkilde J, Jensen LO, Kalinauskas G, Linder RBA, Pentikainen M, Hervold A, Banning A, Zaman A, Cotton J, Eriksen E, Margus S, Sørensen HT, Nielsen PH, Niemelä M, Kervinen K, Lassen JF, Maeng M, Oldroyd K, Berg G, Walsh SJ, Hanratty CG, Kumsars I, Stradins P, Steigen TK, Fröbert O, Graham ANJ, Endresen PC, Corbascio M, Kajander O, Trivedi U, Hartikainen J, Anttila V, Hildick-Smith D, Thuesen L and

Christiansen EH. Percutaneous coronary angioplasty versus coronary artery bypass grafting in treatment of unprotected left main stenosis (NOBLE): a prospective, randomised, open-label, non-inferiority trial. *The Lancet*.

5. Stone GW, Sabik JF, Serruys PW, Simonton CA, Généreux P, Puskas J, Kandzari DE, Morice M-C, Lembo N, Brown WM, Taggart DP, Banning A, Merkely B, Horkay F, Boonstra PW, van Boven AJ, Ungi I, Bogáts G, Mansour S, Noiseux N, Sabaté M, Pomar J, Hickey M, Gershlick A, Buszman P, Bochenek A, Schampaert E, Pagé P, Dressler O, Kosmidou I, Mehran R, Pocock SJ and Kappetein AP. Everolimus-Eluting Stents or Bypass Surgery for Left Main Coronary Artery Disease. *New England Journal of Medicine*. 2016.

6. Cutlip DE, Windecker S, Mehran R, Boam A, Cohen DJ, van Es G-A, Gabriel Steg P, Morel M-a, Mauri L, Vranckx P, McFadden E, Lansky A, Hamon M, Krucoff MW and Serruys PW. Clinical End Points in Coronary Stent Trials. *A Case for Standardized Definitions*. 2007;115:2344-2351.

EuroIntervention 2017;12:1632-1642

Intravascular ultrasound guidance improves clinical outcomes during implantation of both first- and second-generation drug-eluting stents: a meta-analysis

Nitesh Nerlekar[1], MBBS, MPH; Caitlin J. Cheshire[1], MBBS; Kunal P. Verma[1], MBBS; Abdul-Rahman Ihdayhid[1], MBBS; Liam M. McCormick[1], MBBS, MD; James D. Cameron[1], MBBS, MD; Martin R. Bennett[2], MD, PhD; Yuvaraj Malaiapan[1], MBBS, MD; Ian T. Meredith[1], MBBS, PhD; Adam J. Brown[1,2]*, MD, PhD

1. Monash Cardiovascular Research Centre, Monash University and MonashHeart, Monash Health, Clayton, Victoria, Australia; 2. Division of Cardiovascular Medicine, University of Cambridge, Cambridge, United Kingdom

This paper also includes supplementary data published online at: http://www.pcronline.com/eurointervention/110th_issue/266

KEYWORDS

- coronary angioplasty
- drug-eluting stent
- intravascular ultrasound
- meta-analysis
- percutaneous coronary intervention

Abstract

Aims: Our aim was to assess whether intravascular ultrasound (IVUS) improves clinical outcomes during implantation of first- and second-generation drug-eluting stents (DES). IVUS guidance is associated with improved clinical outcomes during DES implantation, but it is unknown whether this benefit is limited to either first- or second-generation devices.

Methods and results: MEDLINE, EMBASE and PubMed were searched for studies comparing outcomes between IVUS- and angiography-guided PCI. Among 909 potentially relevant studies, 15 trials met the inclusion criteria. The primary endpoint was MACE, defined as death, myocardial infarction, target vessel/lesion revascularisation (TVR/TLR) or stent thrombosis (ST). Summary estimates were obtained using Peto modelling. In total, 9,313 patients from six randomised trials and nine observational studies were included. First-generation DES were implanted in 6,156 patients (3,064 IVUS-guided and 3,092 angiography-guided) and second-generation in 3,157 patients (1,528 IVUS-guided and 1,629 angiography-guided). IVUS guidance was associated with a significant reduction in MACE (odds ratio [OR] 0.73, 95% CI: 0.64-0.85, p<0.001), across both first- (OR 0.79, 95% CI: 0.67-0.92, p=0.01) and second-generation DES (0.57, 95% CI: 0.43-0.77, p<0.001). For second-generation DES, IVUS guidance was associated with significantly lower rates of cardiac death (OR 0.33, 95% CI: 0.14-0.78, p=0.02), TVR (OR 0.47, 95% CI: 0.28-0.79, p=0.006), TLR (OR 0.61, 95% CI: 0.42-0.90, p=0.01) and ST (OR 0.31, 95% CI: 0.12-0.78, p=0.02). Cumulative meta-analysis highlighted progressive temporal benefit towards IVUS-guided PCI to reduce MACE (OR 0.60, 95% CI: 0.48-0.75, p<0.001).

Conclusions: IVUS guidance is associated with a significant reduction in MACE during implantation of both first- and second-generation DES platforms. These data support the use of IVUS guidance in contemporary revascularisation procedures using second-generation DES.

**Corresponding author: Monash Cardiovascular Research Centre and MonashHeart, Monash Health, Clayton, Victoria 3168, Australia. E-mail: ajdbrown@me.com*

SUBMITTED ON 21/09/2016 - REVISION RECEIVED ON N/A - ACCEPTED ON 22/09/2016

DOI: 10.4244/EIJ-D-16_00769

Introduction

Percutaneous coronary intervention (PCI) and stenting is an established therapeutic option for patients with stable angina and confers prognostic advantage when performed in the context of acute coronary syndromes. However, recurrent major adverse cardiovascular events (MACE) following successful stenting remains an ongoing clinical problem. Although the introduction and widespread uptake of the drug-eluting stent (DES) contributed to significant reductions in the need for repeat revascularisation, ~20% of patients will re-present with further symptoms within five years following PCI[1]. Thus, strategies that can improve clinical outcomes are of great importance.

Intravascular ultrasound (IVUS) use during PCI is known to impact on interventional strategy by providing important information on target lesion and reference vessel characteristics. Following stent deployment, IVUS can accurately quantify stent expansion and strut apposition, and may identify stent edge-related complications not always apparent on angiography[2]. Although previous meta-analyses have shown that IVUS-guided DES implantation is associated with a significant reduction in MACE, the results were either predominantly based on studies in first-generation DES[3,4] or were limited to randomised trials[5]. However, the majority of PCI procedures performed worldwide use second-generation DES, often in "off-label" indications, where the role of IVUS remains uncertain.

We sought to assess whether the clinical benefit of IVUS-guided DES implantation is maintained in second-generation devices by performing a systematic review and meta-analysis, stratified by DES generation.

Editorial, see page 1564

Methods

DATA SOURCES AND SEARCH STRATEGY

A keyword search was performed through the MEDLINE, EMBASE and PubMed databases for the period January 2000 to May 2016. Keywords using Medical Subject Heading included: "intravascular ultrasound", "ultrasound, intravascular", "percutaneous coronary intervention", "drug-eluting stents", "coronary artery disease", "coronary angioplasty" and "coronary angiography" with no limits set **(Online Table 1)**. The reference lists of selected articles were also reviewed for relevant citations. Abstract lists of major international conferences were also manually searched to identify other potential sources of data. Conferences included were the European Society of Cardiology, EuroPCR, American College of Cardiology Scientific Sessions, American Heart Association Scientific Sessions and Transcatheter Cardiovascular Therapeutics. The study was registered with the PROSPERO international register (CRD42016037632) and adhered to the PRISMA statement[6].

STUDY SELECTION

Two investigators (A.J. Brown and N. Nerlekar) independently conducted the literature search, and two further investigators (C.J. Cheshire and K.P. Verma) performed data extraction for study demographics, design, angiographic characteristics and clinical outcomes. Randomised clinical trials, observational and registry studies were included. Other specific inclusion criteria required reported clinical outcomes at a minimum of six months, comparison of IVUS- and angiography-guided strategies and differentially reported outcomes for first- and second-generation stents. For observational studies, matched propensity data were included in the final analysis, where available. First (or early)-generation stents were defined as either paclitaxel (e.g., TAXUS™; Boston Scientific, Marlborough, MA, USA) or sirolimus (e.g., CYPHER®; Cordis, Johnson & Johnson, Miami Lakes, FL, USA) eluting, durable polymer, metallic stents with thick strut design, while second (or new)-generation stents were defined as either zotarolimus (Endeavor®; Medtronic, Minneapolis, MN, USA) or everolimus (XIENCE V®; Abbott Vascular, Santa Clara, CA, USA, or PROMUS™; Boston Scientific, Marlborough, MA, USA) eluting, durable polymer, metallic platforms with a strut thickness <100 µm. A.J. Brown and N. Nerlekar verified extracted data and discrepancies for included studies. Where studies included both stent generations, corresponding authors were contacted to provide individual outcomes if available. The remaining studies with mixed stent platforms were excluded. The risk of bias within individual studies was assessed according to the Cochrane Collaboration Assessment **(Online Table 2)**.

CLINICAL ENDPOINTS

The primary endpoint of this study was MACE, with secondary endpoints including cardiac death, non-fatal myocardial infarction (MI), target lesion revascularisation (TLR), target vessel revascularisation (TVR), and stent thrombosis. The definition of MACE differed slightly across trials, but generally included death, MI and TVR. Two studies included cardiac and non-cardiac death[7,8], while seven reported cardiac death[9-15] and four all-cause death[16-19]. Six studies used TLR instead of TVR[8,13,14,17-19], while stent thrombosis was included as part of MACE in two studies[12,13]. MACE could not be calculated from the reported data of two studies[20,21], but these studies contributed to individual clinical endpoints. Trial-specific definitions of MACE were used in the analysis. MI was defined as either Q-wave or non-Q-wave MI. Stent thrombosis was defined as definite or probable according to the Academic Research Consortium[22].

STATISTICAL ANALYSIS

Statistical analysis was performed by using STATA MP 13.0 (StataCorp LP, College Station, TX, USA). Outcomes were analysed using a Peto model as a small number of events were expected, especially in randomised controlled trials. Sensitivity analysis was also performed using a DerSimonian and Laird random effects model and inverse variance method with a fixed model which did not differ from the Peto model. Summary statistics are reported as a pooled odds ratio (OR) with 95% confidence intervals (CI) between first- and second-generation DES for the outcome of MACE. Further sensitivity analysis was also performed comparing only RCTs between first- and second-generation stents. Additional subgroup analysis was performed to evaluate summary statistics for various components of MACE (all-cause death, cardiac death, MI, TVR, TLR and stent thrombosis). Finally, we performed

a cumulative meta-analysis to evaluate the impact of publication date on the summary odds ratios and to assess temporal trends in effect size. Statistical heterogeneity was quantified with the I^2 statistic. Heterogeneity was quantified as low, moderate or high based on I^2 values of 25%, 50% and 75%, respectively[23]. Publication bias was assessed by the Harbord test between first- and second-generation studies[24]. A two-sided p-value of <0.05 was considered significant.

Results

A total of 909 publications were reviewed, with 32 studies selected for potential inclusion and further evaluation. Of these studies, 17 were excluded as they included bare metal stents or their reported outcomes included both first- and second-generation DES[25-42]. The authors of two studies provided individualised outcome data stratified by DES generation and these were included[8,11]. This resulted in 15 studies meeting the predefined inclusion criteria **(Figure 1)**.

Six studies in the analysis were randomised controlled trials, including the HOME DES IVUS study[17], the AVIO trial[10], the RESET trial[12], the IVUS-XPL trial[14], CTO-IVUS[15] and one randomised trial of unprotected left main coronary artery stenting in the elderly[19]. The other nine were observational studies assessing the use of IVUS in specific lesion subsets, including left main coronary artery stenting[7,8,20], bifurcation PCI[11,18,21] or chronic total occlusions[13], while two were consecutive patient registries[9,16]. Baseline characteristics of the included studies are presented in **Table 1**.

Of the 9,313 patients included, 6,156 received a first-generation DES and 3,157 received a second-generation DES. For first-

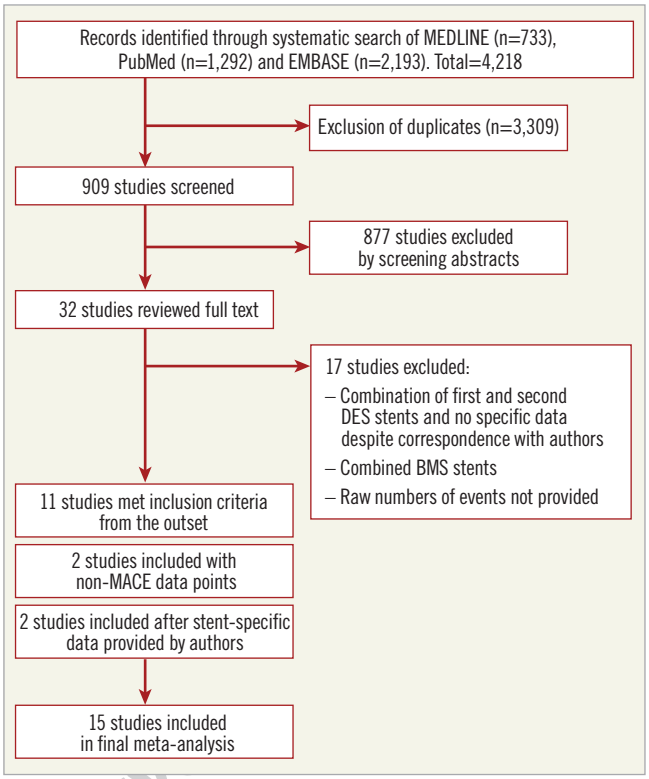

Figure 1. *Flow diagram of study. Flow diagram illustrating the identification and screening of eligible studies. BMS: bare metal stent; DES: drug-eluting stent; MACE: major adverse cardiovascular events*

Table 1. Characteristics of included studies and patients.

Study	Year	Design	DES type	Sample (n)	Age (years)	Male (%)	Diabetes mellitus (%)	Hyperlipidaemia (%)	HTN (%)	Smoker (%)	Previous PCI (%)	Previous MI (%)	Previous CABG (%)	LVEF (%)
Agostoni et al	2005	Observational	1st	24/34	62/64	62/73	37/29	29/30	58/59	17/21	50/21	37/50	NA	52/44
Roy et al	2008	Observational	1st	884/884	66/66	69/70	36/34	86/87	82/82	21/21	27/24	43/41	23/22	47/48
MAIN-COMPARE	2009	Observational	1st	145/145	64/65	70/70	34/34	29/30	59/59	19/21	26/26	7/8	NA	61/61
Kim et al	2010	Observational	1st	473/285	59/60	73/72	20/22	28/35	43/46	36/36	10/7	52/64	0.2/0.4	60/59
HOME DES IVUS	2010	RCT	1st	105/105	59/60	73/71	42/45	63/66	67/71	40/35	17/14	37/32	14/10	NA
MATRIX	2011	Observational	1st	548/548	65/64	74/74	32/31	84/82	82/81	11/12	44/42	30/34	16/16	NA
COBIS	2011	Observational	1st	487/487	62/62	67/67	32/33	35/35	60/58	22/23	NA	9/8	NA	60/59
Chen et al	2013	Observational	1st/2nd	324/304	63/65	81/75	19/18	33/35	67/61	45/41	18/17	15/12	0/0	61/60
RESET	2013	RCT	2nd	269/274	63/64	66/55	32/30	61/62	61/66	22/17	NA	1/3	NA	55/54
AVIO	2013	RCT	1st	142/142	64/64	82/77	24/27	71/77	70/67	34/31	NA	30/26	NA	55/56
ESTROFA-LM	2014	Observational	1st/2nd	415/355	NA	NA	NA	NA	NA	NA	NA	NA	NA	NA
K-CTO	2014	Observational	2nd	201/201	62/62	77/77	30/31	42/43	58/60	29/31	21/20	11/10	NA	NA
CTO-IVUS	2015	RCT	2nd	201/201	61/61	81/81	35/34	NA	63/64	35/34	15/16	8/8	2/3	57/57
IVUS-XPL	2015	RCT	2nd	700/700	64/64	69/69	36/37	67/65	65/63	22/26	11/10	5/4	3/2	63/62
Tan et al	2015	RCT	1st	61/62	77/76	62/69	34/30	NA	41/47	44/47	NA	16/21	NA	55/53

Values are mean or % and presented as intravascular ultrasound (IVUS)-guided/angiography-guided. AVIO: angiography vs. IVUS optimisation; CABG: coronary artery bypass grafting; COBIS: Korean Coronary Bifurcation Stent registry; CTO-IVUS: chronic total occlusion InterVention with drUg-eluting Stents guided by IVUS; ESTROFA-LM: comparison of paclitaxel-eluting stents (TAXUS) and everolimus-eluting stents (XIENCE) in left main coronary artery disease; HOME-DES IVUS: long-term health outcome and mortality evaluation after invasive coronary treatment using drug eluting stents with or without the IVUS guidance; HTN: hypertension; IVUS-XPL: effect of intravascular ultrasound-guided vs. angiography-guided everolimus-eluting stent implantation; K-CTO: Korean Chronic Total Occlusion registry; LVEF: left ventricular ejection fraction; MAIN-COMPARE: revascularisation for unprotected left MAIN coronary artery stenosis: COMparison of Percutaneous coronary Angioplasty versus surgical REvascularization; MATRIX: comprehensive assessment of sirolimus-eluting stents in complex lesions; MI: myocardial infarction; NA: not applicable; PCI: percutaneous coronary intervention; RCT: randomised controlled trial; RESET: real safety and efficacy of a 3-month dual antiplatelet therapy following zotarolimus-eluting stent implantation

generation DES, 3,064 patients underwent IVUS-guided PCI and 3,092 angiography-guided PCI, while for second-generation DES 1,528 patients underwent IVUS-guided PCI and 1,629 angiography-guided PCI. Angiographic and procedural characteristics of the included studies are presented in **Table 2**. Data on IVUS-guided PCI for first-generation DES were available for eleven studies[7-11,16-21], while data on IVUS-guided PCI for second-generation DES were available from six studies[8,11-15].

MAJOR ADVERSE CARDIOVASCULAR EVENTS

Thirteen of the included studies reported the incidence of MACE. The summary OR for all studies was 0.73 (95% CI: 0.64-0.85, p<0.001) in favour of IVUS-guided PCI **(Figure 2)**. There was no evidence of statistical heterogeneity between studies (I^2=0%). The beneficial effect of IVUS-guided PCI was observed for both first-generation (OR 0.79, 95% CI: 0.67-0.92, p=0.01, I^2=0%) and second-generation DES (OR 0.57, 95% CI: 0.43-0.77, p<0.001, I^2=0%). No difference was noted with inverse variance and random-effects modelling **(Online Figure 1)**, and there was no significant interaction between first- and second-generation stent groups (p=0.06). The potential for publication bias was assessed statistically by the Harbord test, which demonstrated no evidence of small study effects, either in first-generation (p=0.08) or in second-generation DES studies (p=0.73). Sensitivity analysis limited to randomised trials was consistent with these findings, with IVUS-guided PCI associated with reduced MACE in both first-generation (OR 0.62, 95% CI: 0.41-0.93, p=0.02, I^2=0.0%) and second-generation DES (OR 0.49, 95% CI: 0.34-0.72, p<0.001, I^2=0.0%) **(Online Figure 2, Online Figure 3)**.

CARDIAC DEATH AND MYOCARDIAL INFARCTION

The incidence of cardiac death was reported in nine studies, while ten studies reported the incidence of MI. IVUS-guided PCI was associated with a significant reduction in the risk of cardiac death (OR 0.55, 95% CI: 0.36-0.83, p=0.005, I^2=0%). This benefit appeared limited to second-generation DES (OR 0.33, 95% CI: 0.14-0.78, p=0.02, I^2=0%), with no clear benefit in first-generation DES (OR 0.64, 95% CI: 0.39-1.04, p=0.07, I^2=0%) **(Figure 3)**. IVUS-guided PCI was also associated with a significant reduction in the risk of MI (OR 0.67, 95% CI: 0.50-0.90, p=0.01, I^2=8.6%). IVUS-guided PCI did not appear to reduce the risk of MI in second-generation DES (OR 0.82, 95% CI: 0.45-1.49, p=0.65, I^2=13.3%), but did for first-generation DES (OR 0.63, 95% CI: 0.45-0.89, p=0.007, I^2=13.6%).

Table 2. Angiographic and procedural characteristics.

Study	Year	Left main %	LAD %	RCA %	LCx %	Multi-vessel PCI %	Bifurcation PCI %	CTO PCI %	Predilation n	Post-dilation n	Kissing balloon %	Mean lesion length mm	Mean stent length mm	Mean stent diameter mm	Mean number of stents	GP IIb/IIIa, %
Agostoni et al	2005	100/100	0/0	0/0	0/0	NA	70/50	NA	50/62	92/76	40/45	7.5±3.1/ 7.3±3.1	27.0±14.0/ 23.0±12.0	3.2±0.4/ 3.2±0.3	1.5±0.5/ 1.4±0.5	46/23
Roy et al	2008	2/2	33/33	34/34	25/23	NA	NA	NA	71/59	31/17	NA	NA	20.7±6.4/ 20.1±6.9	3.1±0.4/ 3.1±1.8	1.5±0.8/ 1.5±0.9	18/18
MAIN-COMPARE	2009	100/100	0/0	0/0	0/0	0/0	NA	NA	NA	NA	NA	NA	35.2±23.8/ 35.6±22.7	NA	1.2±0.5/ 1.2±0.6	NA
Kim et al	2010	NA	NA	NA	NA	NA	29/34	100/100	3/3	NA	NA	NA	25.0±14/ 21±10	34.0±19.0/ 26.0±14.0	NA	1.4±0.7/ 1.2±0.5	4/3
HOME DES IVUS	2010	3/4	56/54	29/24	11/15	15/17	NA	NA	74/77	33/0	NA	18.1±7.3/ 17.6±6.7	23.6 /22.1	NA	1.3/1.3	20/16
MATRIX	2011	3/3	51/51	29/28	38/38	NA	NA	NA	54/70	43/34	NA	17.5±9.6/ 17.9±9.3	23.3±12.0/ 23.8±12.2	3.1±0.4/ 3.0±0.4	NA	8/8
COBIS	2011	4/4	83/83	4/4	13/13	46/47	100/100	NA	100/100	NA	53/34	NA	NA	NA	NA	4/4
Chen et al	2013	42/27	40/61	4/3	14/9	NA	100/100	NA	NA	NA	95/93	NA	NA	NA	NA	3/7
RESET	2013	0/0	62/68	23/20	15/13	41/38	NA	0/0	NA	55/45	1/2	29.6/30.6	32.4/32.3	NA	NA	NA
AVIO	2013	0/0	53/49	NA	NA	NA	23/27	14/18	NA	88/68	NA	27.4±15.9/ 25.5±15.0	23.9±6.7/ 23.2±6.5	3.0±0.4/ 2.9±0.4	NA	NA
ESTROFA-LM	2014	100/100	0/0	0/0	0/0	NA	NA	NA	NA	NA	NA	NA	NA	NA	NA	NA
K-CTO	2014	0/0	44/34	NA	16/25	NA	NA	100/100	NA	NA	NA	26.7±12.9/ 26.9±18.0	44.9±21.2/ 37.3±20.6	3.0±0.4/ 2.8±0.4	1.7±0.8/ 1.4±0.7	NA
CTO-IVUS	2015	0/0	42/47	44/37	14/16	10/8	NA	100/100	NA	51/41	NA	36.3±17.1/ 35.5±17.0	43.6±18.7/ 41.5±17.6	2.9±0.5/ 2.9±0.4	1.7±0.8/ 1.6±0.7	4/4
IVUS-XPL	2015	0/0	65/60	21/25	14/15	NA	NA	NA	NA	76/57	NA	34.7±10.8/ 35.2±10.5	39.3±13.1/ 39.2±12.3	NA	1.3±0.5/ 1.3±0.5	NA
Tan et al	2015	100/100	0/0	0/0	0/0	0/0	40/42	0/0	NA	23/9	NA	NA	21.5±6.4/ 18.2±4.9	3.4±0.1/ 3.4±0.1	NA	NA

Values are %, mean±standard deviation and presented as IVUS/no IVUS. CTO: chronic total occlusion; GP IIb/IIIa: glycoprotein IIb/IIIa inhibitor; LAD: left anterior descending artery; LCx: left circumflex artery; RCA: right coronary artery; TIMI: Thrombolysis In Myocardial Infarction

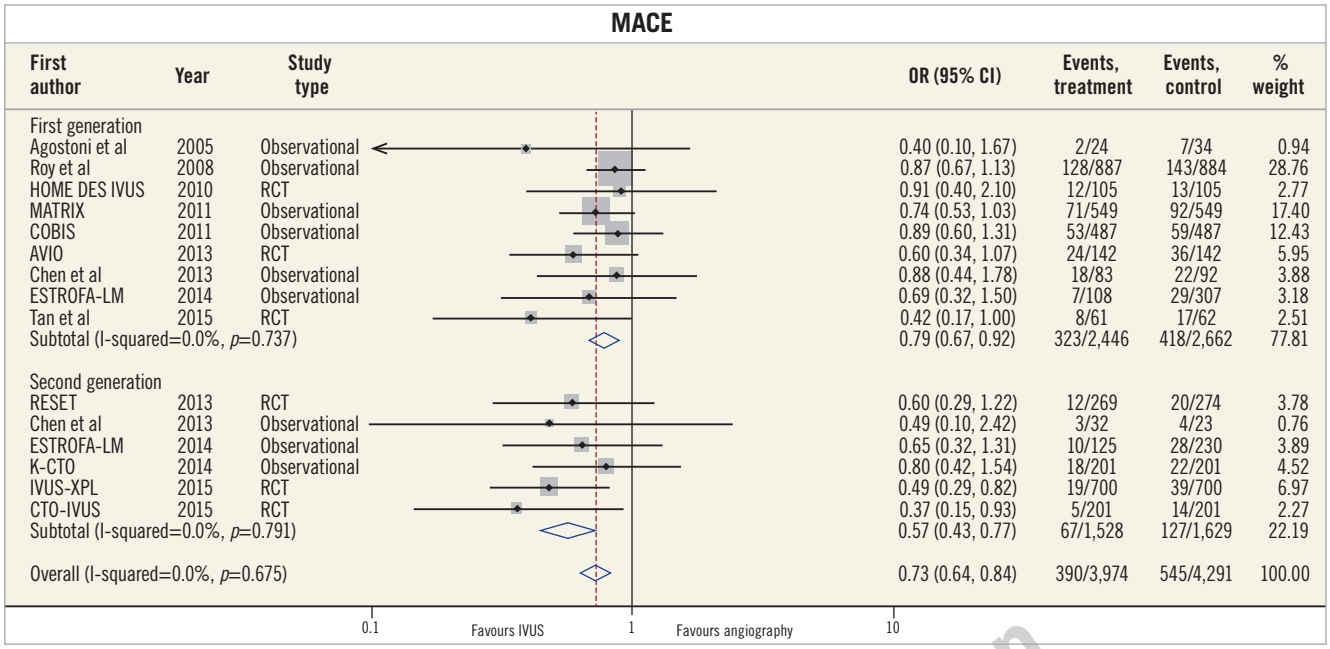

Figure 2. *MACE for IVUS-guided versus angiography-guided PCI stratified by DES generation. The incidence and odds ratios (OR) for major adverse cardiovascular events (MACE) following both intravascular ultrasound (IVUS)-guided and angiography-guided drug-eluting stent (DES) implantation. The benefit of IVUS-guided PCI is consistent across both first- and second-generation DES. CI: confidence interval; RCT: randomised controlled trial*

OTHER CLINICAL ENDPOINTS

Seven studies reported the incidence of TVR and eight studies reported the incidence of TLR. Overall, IVUS-guided PCI significantly reduced the risk of TVR (OR 0.79, 95% CI: 0.64-0.98, p=0.04, I^2=23.2%) and TLR (OR 0.66, 95% CI: 0.52-0.84, p<0.001, I^2=0.0%) **(Figure 4)**. Although IVUS-guided PCI reduced the incidence of both TVR and TLR in second-generation DES, only TLR was reduced in first-generation DES **(Table 3)**. IVUS-guided PCI significantly reduced the risk of ST across both first- (OR 0.56, 95% CI: 0.40-0.79, p<0.001, I^2=0.0%) and second-generation DES (OR 0.31, 95% CI: 0.12-0.78, p=0.02, I^2=0.0%).

CUMULATIVE META-ANALYSIS

Finally, we performed a cumulative meta-analysis on the whole cohort, assessing for temporal trends in the effectiveness of IVUS-guided PCI **(Figure 5)**. Until the end of 2011 (total of 4,111 patients), the summary OR was 0.83 (95% CI: 0.69-0.99, p=0.04). However, after this date there was an incremental progressive trend towards a greater beneficial effect of IVUS-guided PCI to reduce MACE (total of 4,154 patients), with a summary OR of 0.60 (95% CI: 0.48-0.75, p<0.001).

Discussion

Our results demonstrate that IVUS-guided DES implantation is associated with a significant reduction in MACE, when compared with angiography-guided PCI. Importantly, the benefit of an IVUS-guided PCI strategy applies across both first- and second-generation DES. In second-generation DES, IVUS guidance reduces the incidence of cardiac death and clinical endpoints related to DES failure. Finally, we show a temporal and progressive improvement in clinical outcomes for IVUS-guided DES implantation. These results should continue to encourage the use of IVUS-guided PCI and reinforce that clinical benefits are maintained independent of DES type.

Previous meta-analyses have reported that IVUS-guided DES implantation is associated with significantly lower rates of MACE, with an OR of between 0.60 and 0.75[3-5]. However, these three reports included studies using a mixture of DES types and there remains uncertainty on the clinical utility of an IVUS-guided strategy in newer platforms. Here we show that an IVUS-guided second-generation DES implantation is associated with an ~40% relative risk reduction of MACE, when compared with an angiography-guided strategy. Importantly, the majority of the benefit we observed for IVUS guidance with second-generation DES was in clinical endpoints of stent failure, including TVR, TLR and ST (relative risk reductions of 55%, 46% and 80%, respectively). Based on these data, we find that the number needed to treat using IVUS to prevent one MACE event during second-generation DES implantation is ~30 (95% CI: 19.7-57.0). Cost-effectiveness analyses are now required to assess whether the current threshold for IVUS use is appropriate or whether operators should be expanding use to more "routine" cases.

Our results also suggest that there has been a continual temporal improvement in the reported clinical outcomes for studies assessing the role of IVUS guidance during DES implantation. Although definitive mechanisms underlying this observation cannot be

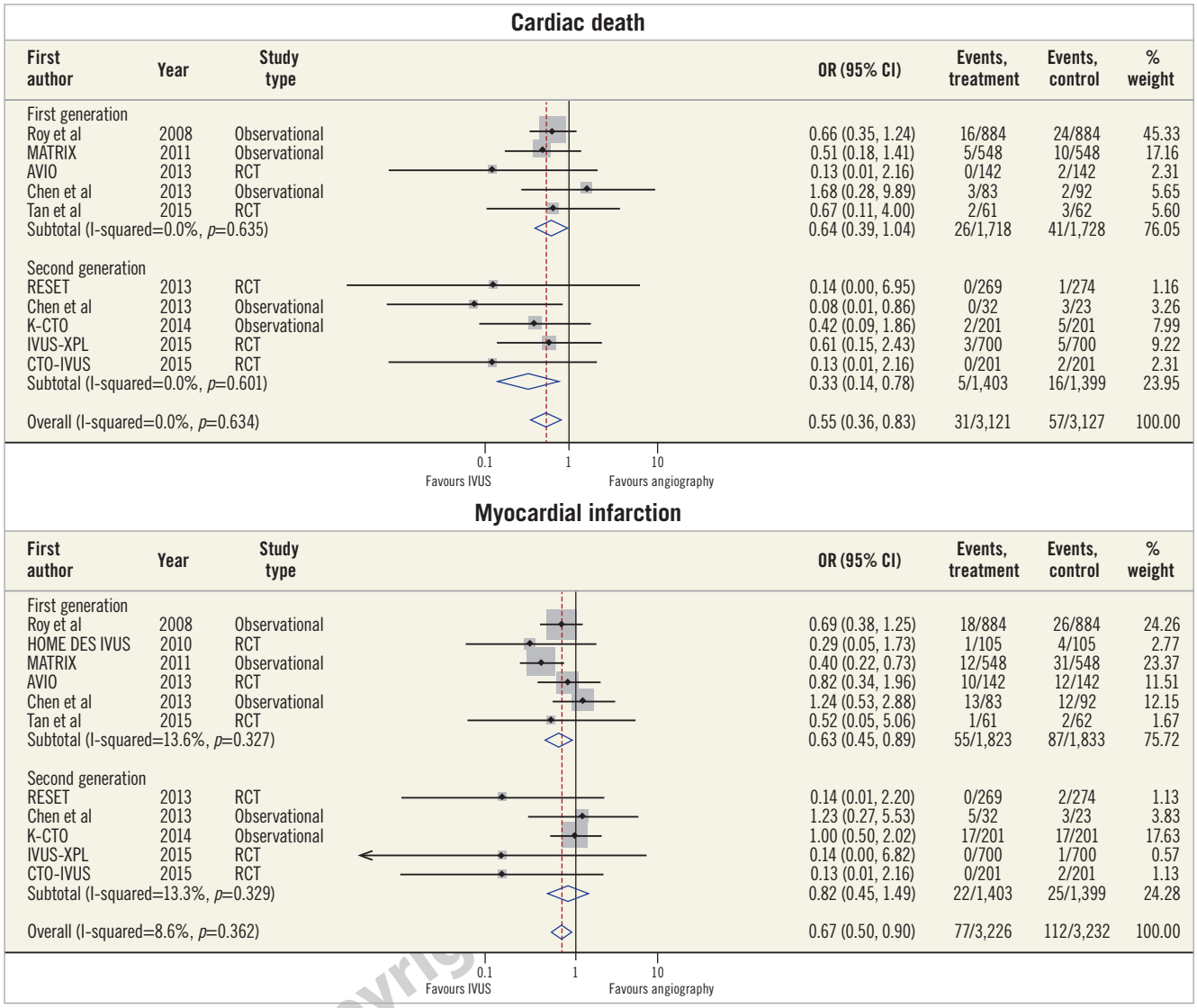

Figure 3. *Summary plot for clinical endpoints of cardiovascular mortality and myocardial infarction. The incidence and odds ratios (OR) for cardiac death (A) and myocardial infarction (B) following both intravascular ultrasound (IVUS)-guided and angiography-guided drug-eluting stent (DES) implantation, stratified by drug-eluting stent generation. CI: confidence interval; RCT: randomised controlled trial*

Table 3. Summary estimates for clinical endpoints following IVUS-guided and angiography-guided DES implantation.

	First-generation DES					Second-generation DES				
	Event rate (%) IVUS/ angiography-guided PCI	OR	95% CI	*p*-value	I^2 (%)	Event rate (%) IVUS/ angiography-guided PCI	OR	95% CI	*p*-value	I^2 (%)
MACE	13.2/15.7	0.79	0.67-0.92	0.01	0.0	4.4/7.8	0.57	0.43-0.77	<0.001	0.0
Cardiac death	1.5/2.4	0.64	0.39-1.04	0.07	0.0	0.3/1.1	0.33	0.14-0.78	0.02	0.0
MI	3.0/4.7	0.63	0.45-0.89	0.007	13.6	1.6/1.7	0.82	0.45-1.49	0.65	13.3
TVR	9.2/10.3	0.88	0.70-1.11	0.29	0.0	2.8/5.9	0.47	0.28-0.79	0.006	3.7
TLR	5.6/7.9	0.70	0.51-0.95	0.02	0.0	3.8/6.0	0.61	0.42-0.90	0.01	30.5
ST	2.4/4.2	0.56	0.40-0.79	<0.001	0.0	0.2/1.0	0.31	0.12-0.78	0.02	0.0

DES: drug-eluting stent; IVUS: intravascular ultrasound; MACE: major adverse cardiovascular events; MI: myocardial infarction; OR: odds ratio; ST: stent thrombosis; TLR: target lesion revascularisation; TVR: target vessel revascularisation

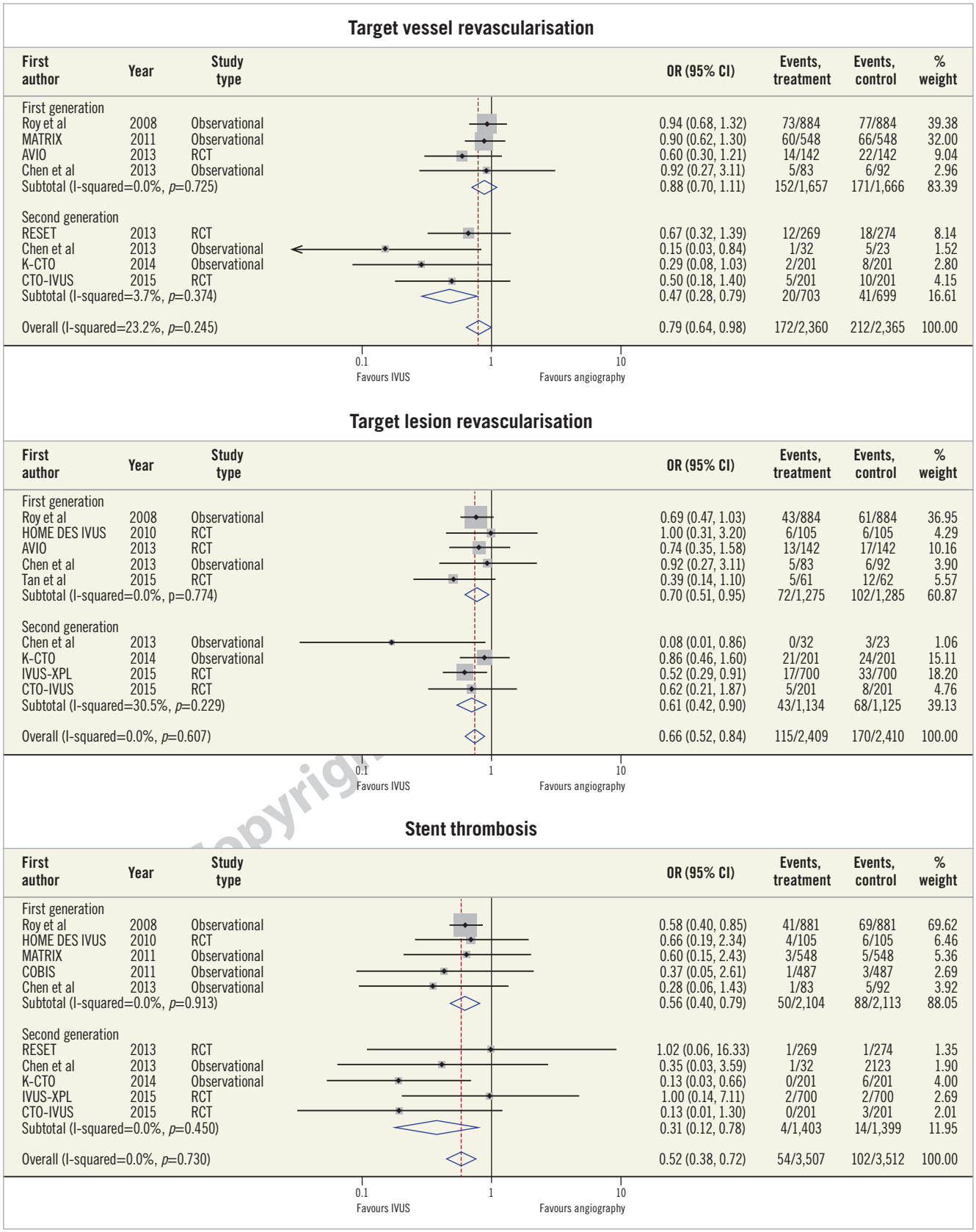

Figure 4. *Summary plot for stent-specific endpoints of target vessel/lesion revascularisation and stent thrombosis. The incidence and odds ratios (OR) for target vessel revascularisation (A), target lesion revascularisation (B) and stent thrombosis (C) following both intravascular ultrasound (IVUS)-guided and angiography-guided drug-eluting stent (DES) implantation, stratified by drug-eluting stent generation. CI: confidence interval; RCT: randomised controlled trial*

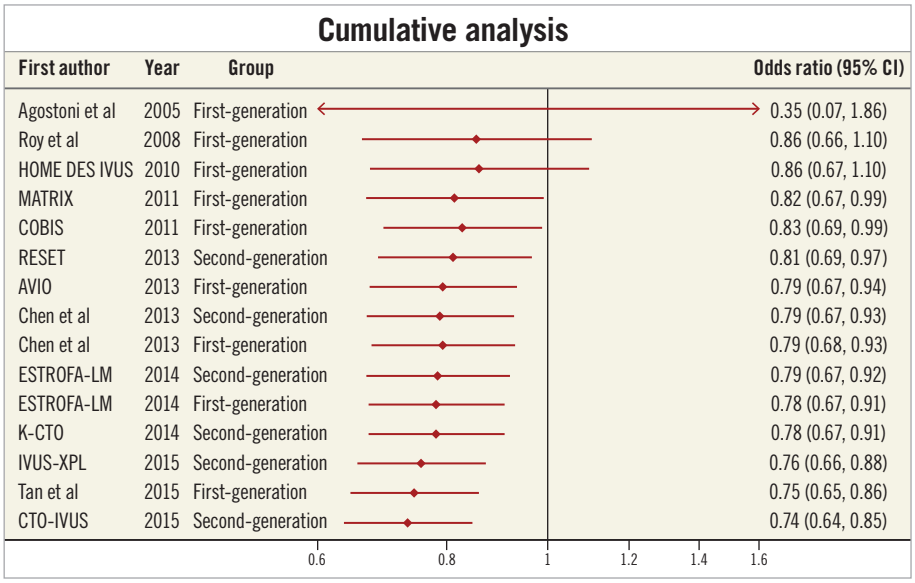

Figure 5. *Cumulative meta-analysis by year of study publication. Cumulative meta-analysis with odds ratios for major adverse cardiovascular events (MACE) by year of study publication showing a continual and progressive benefit of IVUS-guided DES implantation.*

provided by the current analysis, this evolutionary effect may be a consequence of operators becoming increasingly aware of what constitutes optimal stent deployment. The use of IVUS allows operators to evaluate stent expansion quantitatively, with under-expansion independently associated with repeat revascularisation and ST[43]. Additionally, the continual improvement in IVUS catheter technology and image resolution now makes it easier for operators to identify small edge-related complications of PCI, including inflow/outflow dissections and geographical miss of plaque, which have potential to impact on long-term prognosis[2,44]. Further trials that refine our definitions of IVUS-guided optimal stent deployment are now required to ensure treatment benefits are consistent across interventional institutions.

Limitations

There are some limitations to this study that should be highlighted. Firstly, the definitions of MACE differed among studies. However, the clinical benefit of IVUS-guided PCI was observed across all study endpoints and we observed no statistical heterogeneity for the outcome of MACE among studies. Secondly, we were unable to obtain trial-specific DES outcomes for 17 studies identified by our systematic search criteria, and inclusion of these data may have affected the final results. Third, most studies in the current analysis were observational studies. In an effort to ensure that our results were robust, we used propensity-matched data when available, with a sensitivity analysis limited to randomised controlled trial data showing similar findings.

Conclusions

IVUS guidance is associated with a significant reduction in MACE when utilised during PCI with both first- and second-generation DES platforms. These data should support the use of IVUS-guided PCI for contemporary revascularisation procedures, especially in patient and lesion subsets that are known to have a worse clinical prognosis.

Impact on daily practice

IVUS-guided PCI is known to improve clinical outcomes during implantation of DES, particularly in the treatment of complex lesion subsets. However, there remains uncertainty as to whether this beneficial effect is limited to first-generation DES platforms. These data suggest that IVUS guidance is associated with a significant reduction in adverse events during implantation of both first- and second-generation DES, supporting IVUS use during the contemporary procedures performed in daily clinical practice.

Acknowledgements

The authors would like to thank Dr Jose M. de la Torre Hernandez, Dr Nai-Liang Tian and Prof. Shao-Lian Chen for providing unpublished study data included in this manuscript.

Funding

L. McCormick is supported by a Robertson Family Research Cardiologist Fellowship.

Conflict of interest statement

I. Meredith has acted on the Scientific Advisory Board of Boston Scientific. The other authors have no conflicts of interest to declare.

References

1. Ellis SG, Stone GW, Cox DA, Hermiller J, O'Shaughnessy C, Mann T, Turco M, Caputo R, Bergin PJ, Bowman TS, Baim DS;

TAXUS IV Investigators. Long-term safety and efficacy with paclitaxel-eluting stents: 5-year final results of the TAXUS IV clinical trial (TAXUS IV-SR: Treatment of De Novo Coronary Disease Using a Single Paclitaxel-Eluting Stent). *JACC Cardiovasc Interv.* 2009;2:1248-59.

2. McDaniel MC, Eshtehardi P, Sawaya FJ, Douglas JS Jr, Samady H. Contemporary clinical applications of coronary intravascular ultrasound. *JACC Cardiovasc Interv.* 2011;4:1155-67.

3. Jang JS, Song YJ, Kang W, Jin HY, Seo JS, Yang TH, Kim DK, Cho KI, Kim BH, Park YH, Je HG, Kim DS. Intravascular ultrasound-guided implantation of drug-eluting stents to improve outcome: a meta-analysis. *JACC Cardiovasc Interv.* 2014;7:233-43.

4. Ahn JM, Kang SJ, Yoon SH, Park HW, Kang SM, Lee JY, Lee SW, Kim YH, Lee CW, Park SW, Mintz GS, Park SJ. Meta-analysis of outcomes after intravascular ultrasound-guided versus angiography-guided drug-eluting stent implantation in 26,503 patients enrolled in three randomized trials and 14 observational studies. *Am J Cardiol.* 2014;113:1338-47.

5. Elgendy IY, Mahmoud AN, Elgendy AY, Bavry AA. Outcomes With Intravascular Ultrasound-Guided Stent Implantation: A Meta-Analysis of Randomized Trials in the Era of Drug-Eluting Stents. *Circ Cardiovasc Interv.* 2016;9:e003700.

6. Moher D, Liberati A, Tetzlaff J, Altman DG; PRISMA Group. Preferred reporting items for systematic reviews and meta-analyses: the PRISMA statement. *Ann Intern Med.* 2009;151:264-9, W64.

7. Agostoni P, Valgimigli M, Van Mieghem CA, Rodriguez-Granillo GA, Aoki J, Ong AT, Tsuchida K, McFadden EP, Ligthart JM, Smits PC, de Jaegere P, Sianos G, Van der Giessen WJ, De Feyter P, Serruys PW. Comparison of early outcome of percutaneous coronary intervention for unprotected left main coronary artery disease in the drug-eluting stent era with versus without intravascular ultrasonic guidance. *Am J Cardiol.* 2005;95:644-7.

8. De la Torre Hernandez JM, Alfonso F, Sanchez Recalde A, Jimenez Navarro MF, Perez de Prado A, Hernandez F, Abdul-Jawad Altisent O, Roura G, Garcia Camarero T, Elizaga J, Rivero F, Gimeno F, Calviño R, Moreu J, Bosa F, Rumoroso JR, Bullones JA, Gallardo A, Fernandez Diaz JA, Ruiz Arroyo JR, Aragon V, Masotti M; ESTROFA-LM Study Group. Comparison of paclitaxel-eluting stents (Taxus) and everolimus-eluting stents (Xience) in left main coronary artery disease with 3 years follow-up (from the ESTROFA-LM registry). *Am J Cardiol.* 2013;111:676-83.

9. Claessen BE, Mehran R, Mintz GS, Weisz G, Leon MB, Dogan O, de Ribamar Costa J Jr, Stone GW, Apostolidou I, Morales A, Chantziara V, Syros G, Sanidas E, Xu K, Tijssen JG, Henriques JP, Piek JJ, Moses JW, Maehara A, Dangas GD. Impact of intravascular ultrasound imaging on early and late clinical outcomes following percutaneous coronary intervention with drug-eluting stents. *JACC Cardiovasc Interv.* 2011;4:974-81.

10. Chieffo A, Latib A, Caussin C, Presbitero P, Galli S, Menozzi A, Varbella F, Mauri F, Valgimigli M, Arampatzis C, Sabate M, Erglis A, Reimers B, Airoldi F, Laine M, Palop RL, Mikhail G, Maccarthy P, Romeo F, Colombo A. A prospective, randomized trial of intravascular-ultrasound guided compared to angiography guided stent implantation in complex coronary lesions: the AVIO trial. *Am Heart J.* 2013;165:65-72.

11. Chen SL, Ye F, Zhang JJ, Tian NL, Liu ZZ, Santoso T, Zhou YJ, Jiang TM, Wen SY, Kwan TW. Intravascular ultrasound-guided systematic two-stent techniques for coronary bifurcation lesions and reduced late stent thrombosis. *Catheter Cardiovasc Interv.* 2013;81:456-63.

12. Kim JS, Kang TS, Mintz GS, Park BE, Shin DH, Kim BK, Ko YG, Choi D, Jang Y, Hong MK. Randomized comparison of clinical outcomes between intravascular ultrasound and angiography-guided drug-eluting stent implantation for long coronary artery stenoses. *JACC Cardiovasc Interv.* 2013;6:369-76.

13. Hong SJ, Kim BK, Shin DH, Kim JS, Hong MK, Gwon HC, Kim HS, Yu CW, Park HS, Chae IH, Rha SW, Lee SH, Kim MH, Hur SH, Jang Y; K-CTO Registry. Usefulness of intravascular ultrasound guidance in percutaneous coronary intervention with second-generation drug-eluting stents for chronic total occlusions (from the Multicenter Korean-Chronic Total Occlusion Registry). *Am J Cardiol.* 2014;114:534-40.

14. Hong SJ, Kim BK, Shin DH, Nam CM, Kim JS, Ko YG, Choi D, Kang TS, Kang WC, Her AY, Kim YH, Hur SH, Hong BK, Kwon H, Jang Y, Hong MK; IVUS-XPL Investigators. Effect of Intravascular Ultrasound-Guided vs Angiography-Guided Everolimus-Eluting Stent Implantation: The IVUS-XPL Randomized Clinical Trial. *JAMA.* 2015;314:2155-63.

15. Kim BK, Shin DH, Hong MK, Park HS, Rha SW, Mintz GS, Kim JS, Kim JS, Lee SJ, Kim HY, Hong BK, Kang WC, Choi JH, Jang Y; CTO-IVUS Study Investigators. Clinical Impact of Intravascular Ultrasound-Guided Chronic Total Occlusion Intervention With Zotarolimus-Eluting Versus Biolimus-Eluting Stent Implantation: Randomized Study. *Circ Cardiovasc Interv.* 2015;8:e002592.

16. Roy P, Steinberg DH, Sushinsky SJ, Okabe T, Pinto Slottow TL, Kaneshige K, Xue Z, Satler LF, Kent KM, Suddath WO, Pichard AD, Weissman NJ, Lindsay J, Waksman R. The potential clinical utility of intravascular ultrasound guidance in patients undergoing percutaneous coronary intervention with drug-eluting stents. *Eur Heart J.* 2008;29:1851-7.

17. Jakabcin J, Spacek R, Bystron M, Kvasnák M, Jager J, Veselka J, Kala P, Cervinka P. Long-term health outcome and mortality evaluation after invasive coronary treatment using drug eluting stents with or without the IVUS guidance. Randomized control trial. HOME DES IVUS. *Catheter Cardiovasc Interv.* 2010;75:578-83.

18. Kim JS, Hong MK, Ko YG, Choi D, Yoon JH, Choi SH, Hahn JY, Gwon HC, Jeong MH, Kim HS, Seong IW, Yang JY, Rha SW, Tahk SJ, Seung KB, Park SJ, Jang Y. Impact of intravascular ultrasound guidance on long-term clinical outcomes in patients treated with drug-eluting stent for bifurcation lesions: data from a Korean multicenter bifurcation registry. *Am Heart J.* 2011;161:180-7.

19. Tan Q, Wang Q, Liu D, Zhang S, Zhang Y, Li Y. Intravascular ultrasound-guided unprotected left main coronary artery stenting in the elderly. *Saudi Med J.* 2015;36:549-53.

20. Park SJ, Kim YH, Park DW, Lee SW, Kim WJ, Suh J, Yun SC, Lee CW, Hong MK, Lee JH, Park SW; MAIN-COMPARE Investigators. Impact of intravascular ultrasound guidance on long-term mortality in stenting for unprotected left main coronary artery stenosis. *Circ Cardiovasc Interv.* 2009;2:167-77.

21. Kim SH, Kim YH, Kang SJ, Park DW, Lee SW, Lee CW, Hong MK, Cheong SS, Kim JJ, Park SW, Park SJ. Long-term outcomes of intravascular ultrasound-guided stenting in coronary bifurcation lesions. *Am J Cardiol.* 2010;106:612-8.

22. Cutlip DE, Windecker S, Mehran R, Boam A, Cohen DJ, van Es GA, Steg PG, Morel MA, Mauri L, Vranckx P, McFadden E, Lansky A, Hamon M, Krucoff MW, Serruys PW; Academic Research Consortium. Clinical end points in coronary stent trials: a case for standardized definitions. *Circulation.* 2007;115:2344-51.

23. Higgins JP, Thompson SG, Deeks JJ, Altman DG. Measuring inconsistency in meta-analyses. *BMJ.* 2003;327:557-60.

24. Harbord RM, Egger M, Sterne JA. A modified test for small-study effects in meta-analyses of controlled trials with binary endpoints. *Stat Med.* 2006;25:3443-57.

25. Patel Y, Depta JP, Patel JS, Masrani SK, Novak E, Zajarias A, Kurz HI, Lasala JM, Bach RG, Singh J. Impact of intravascular ultrasound on the long-term clinical outcomes in the treatment of coronary ostial lesions. *Catheter Cardiovasc Interv.* 2016;87:232-40.

26. de la Torre Hernandez JM, Baz Alonso JA, Gomez Hospital JA, Alfonso Manterola F, Garcia Camarero T, Gimeno de Carlos F, Roura Ferrer G, Recalde AS, Martínez-Luengas IL, Gomez Lara J, Hernandez Hernandez F, Pérez-Vizcayno MJ, Cequier Fillat A, Perez de Prado A, Gonzalez-Trevilla AA, Jimenez Navarro MF, Mauri Ferre J, Fernandez Diaz JA, Pinar Bermudez E, Zueco Gil J; IVUS-TRONCO-ICP Spanish study. Clinical impact of intravascular ultrasound guidance in drug-eluting stent implantation for unprotected left main coronary disease: pooled analysis at the patient-level of 4 registries. *JACC Cardiovasc Interv.* 2014;7:244-54.

27. Maluenda G, Lemesle G, Ben-Dor I, Collins SD, Syed AI, Torguson R, Kaneshige K, Xue Z, Suddath WO, Satler LF, Kent KM, Lindsay J, Pichard AD, Waksman R. Impact of intravascular ultrasound guidance in patients with acute myocardial infarction undergoing percutaneous coronary intervention. *Catheter Cardiovasc Interv.* 2010;75:86-92.

28. Youn YJ, Yoon J, Lee JW, Ahn SG, Ahn MS, Kim JY, Yoo BS, Lee SH, Choe KH. Intravascular ultrasound-guided primary percutaneous coronary intervention with drug-eluting stent implantation in patients with ST-segment elevation myocardial infarction. *Clin Cardiol.* 2011;34:706-13.

29. Biondi-Zoccai G, Sheiban I, Romagnoli E, De Servi S, Tamburino C, Colombo A, Burzotta F, Presbitero P, Bolognese L, Paloscia L, Rubino P, Sardella G, Briguori C, Niccoli L, Franco G, Di Girolamo D, Piatti L, Greco C, Capodanno D, Sangiorgi G. Is intravascular ultrasound beneficial for percutaneous coronary intervention of bifurcation lesions? Evidence from a 4,314-patient registry. *Clin Res Cardiol.* 2011;100:1021-8.

30. Ahmed K, Jeong MH, Chakraborty R, Ahn Y, Sim DS, Park K, Hong YJ, Kim JH, Cho KH, Kim MC, Hachinohe D, Hwang SH, Lee MG, Cho MC, Kim CJ, Kim YJ, Park JC, Kang JC; Other Korea Acute Myocardial Infarction Registry Investigators. Role of intravascular ultrasound in patients with acute myocardial infarction undergoing percutaneous coronary intervention. *Am J Cardiol.* 2011;108:8-14.

31. Patel Y, Depta JP, Novak E, Yeung M, Lavine K, Banerjee S, Lin CH, Zajarias A, Kurz HI, Lasala JM, Bach RG, Singh J. Long-term outcomes with use of intravascular ultrasound for the treatment of coronary bifurcation lesions. *Am J Cardiol.* 2012;109:960-5.

32. Park KW, Kang SH, Yang HM, Lee HY, Kang HJ, Cho YS, Youn TJ, Koo BK, Chae IH, Kim HS. Impact of intravascular ultrasound guidance in routine percutaneous coronary intervention for conventional lesions: data from the EXCELLENT trial. *Int J Cardiol.* 2013;167:721-6.

33. Hur SH, Kang SJ, Kim YH, Ahn JM, Park DW, Lee SW, Yun SC, Lee CW, Park SW, Park SJ. Impact of intravascular ultrasound-guided percutaneous coronary intervention on long-term clinical outcomes in a real world population. *Catheter Cardiovasc Interv.* 2013;81:407-16.

34. Ahn JM, Han S, Park YK, Lee WS, Jang JY, Kwon CH, Park GM, Cho YR, Lee JY, Kim WJ, Park DW, Kang SJ, Lee SW, Kim YH, Lee CW, Kim JJ, Park SW, Park SJ. Differential prognostic effect of intravascular ultrasound use according to implanted stent length. *Am J Cardiol.* 2013;111:829-35.

35. Yoon YW, Shin S, Kim BK, Kim JS, Shin DH, Ko YG, Choi D, Jeon DW, Kwon H, Jang Y, Hong MK; RESET Investigators. Usefulness of intravascular ultrasound to predict outcomes in short-length lesions treated with drug-eluting stents. *Am J Cardiol.* 2013;112:642-6.

36. Witzenbichler B, Maehara A, Weisz G, Neumann FJ, Rinaldi MJ, Metzger DC, Henry TD, Cox DA, Duffy PL, Brodie BR, Stuckey TD, Mazzaferri EL Jr, Xu K, Parise H, Mehran R, Mintz GS, Stone GW. Relationship between intravascular ultrasound guidance and clinical outcomes after drug-eluting stents: the assessment of dual antiplatelet therapy with drug-eluting stents (ADAPT-DES) study. *Circulation.* 2014;129:463-70.

37. Gao XF, Kan J, Zhang YJ Zhang JJ, Tian NL, Ye F, Ge Z, Xiao PX, Chen F, Mintz G, Chen SL. Comparison of one-year clinical outcomes between intravascular ultrasound-guided versus angiography-guided implantation of drug-eluting stents for left main lesions: a single-center analysis of a 1,016-patient cohort. *Patient Prefer Adherence.* 2014;8:1299-309.

38. Yazici HU, Agamaliyev M, Aydar Y, Goktekin O. The impact of intravascular ultrasound guidance during drug eluting stent implantation on angiographic outcomes. *Eur Rev Med Pharmacol Sci.* 2015;19:3012-7.

39. Singh V, Badheka AO, Arora S, Panaich SS, Patel NJ, Patel N, Pant S, Thakkar B, Chothani A, Deshmukh A, Manvar S, Lahewala S,

Patel J, Patel S, Jhamnani S, Bhinder J, Patel P, Savani GT, Patel A, Mohamad T, Gidwani UK, Brown M, Forrest JK, Cleman M, Schreiber T, Grines C. Comparison of inhospital mortality, length of hospitalization, costs, and vascular complications of percutaneous coronary interventions guided by ultrasound versus angiography. *Am J Cardiol.* 2015;115:1357-66.

40. Magalhaes MA, Minha S, Torguson R, Baker NC, Escarcega RO, Omar AF, Lipinski MJ, Chen F, Suddath WO, Satler LF, Pichard AD, Waksman R. The effect of complete percutaneous revascularisation with and without intravascular ultrasound guidance in the drug-eluting stent era. *EuroIntervention.* 2015;11:625-33.

41. Tian NL, Gami SK, Ye F, Zhang JJ, Liu ZZ, Lin S, Ge Z, Shan SJ, You W, Chen L, Zhang YJ, Mintz G, Chen SL. Angiographic and clinical comparisons of intravascular ultrasound- versus angiography-guided drug-eluting stent implantation for patients with chronic total occlusion lesions: two-year results from a randomised AIR-CTO study. *EuroIntervention.* 2015;10:1409-17.

42. Nakatsuma K, Shiomi H, Morimoto T, Ando K, Kadota K, Watanabe H, Taniguchi T, Yamamoto T, Furukawa Y, Nakagawa Y, Horie M, Kimura T; CREDO-Kyoto AMI investigators. Intravascular Ultrasound Guidance vs. Angiographic Guidance in Primary Percutaneous Coronary Intervention for ST-Segment Elevation Myocardial Infarction - Long-Term Clinical Outcomes From the CREDO-Kyoto AMI Registry. *Circ J.* 2016;80:477-84.

43. Fujii K, Carlier SG, Mintz GS, Yang YM, Moussa I, Weisz G, Dangas G, Mehran R, Lansky AJ, Kreps EM, Collins M, Stone GW, Moses JW, Leon MB. Stent underexpansion and residual reference segment stenosis are related to stent thrombosis after sirolimus-eluting stent implantation: an intravascular ultrasound study. *J Am Coll Cardiol.* 2005;45:995-8.

44. Calvert PA, Brown AJ, Hoole SP, Obaid DR, West NE, Bennett MR. Geographical miss is associated with vulnerable plaque and increased major adverse cardiovascular events in patients with myocardial infarction. *Catheter Cardiovasc Interv.* 2016;88:340-7.

Supplementary data

Online Table 1. Systematic search strategy for MEDLINE database.

Online Table 2. Risk of bias summary in accordance with Cochrane Collaboration methods.

Online Figure 1. MACE for IVUS-guided versus angiography-guided PCI stratified by DES generation using random-effects model and inverse variance method.

Online Figure 2. MACE for IVUS-guided versus angiography-guided PCI in randomised controlled trials stratified by DES generation using Peto model.

Online Figure 3. MACE for IVUS-guided versus angiography-guided PCI in randomised controlled trials stratified by DES generation using random-effects model and inverse variance method.

The supplementary data are published online at: http://www.pcronline.com/eurointervention/110th_issue/266

Supplementary data

Online Table 1. Systematic search strategy for MEDLINE database.

	Searches	Results
1	exp ultrasonography, interventional/ or intravascular ultrasound.mp.	20,537
2	exp percutaneous coronary intervention/	42,534
3	exp drug-eluting stents/	7,972
4	exp coronary artery disease/	48,706
5	exp angioplasty, balloon, coronary/	34,179
6	exp coronary angiography/	55,312
7	2 or 5	42,534
8	1 or 6	72,926
9	3 and 4 and 7 and 8	733

Online Table 2. Risk of bias summary in accordance with Cochrane Collaboration methods.

	Random sequence generation (selection bias)	Allocation concealment (selection bias)	Blinding of participants and personnel (performance bias)	Blinding of outcome assessment (detection bias)	Incomplete outcome data (attrition bias)	Selective reporting (reporting bias)	Overall judgement
Agostoni et al	High	High	High	Unclear	Low	Low	High
Roy et al	High	High	High	Low	Low	Low	Moderate
MAIN-COMPARE	High	High	High	Unclear	Low	Low	High
Kim et al	High	High	High	Low	Unclear	Low	High
HOME DES IVUS	High	Unclear	High	Unclear	Low	High	High
MATRIX	High	High	High	Low	Low	Low	High
COBIS	High	High	High	High	High	Low	High
Chen et al	High	High	High	Low	Low	Low	High
RESET	Low	Unclear	High	Unclear	Low	Low	Low
AVIO	High	Low	High	Low	Low	Low	Moderate
ESTROFA-LM	High	High	Low	Low	Low	Low	Low
K-CTO	High	High	High	Low	Low	Low	High
CTO-IVUS	Low	Unclear	Unclear	Low	Low	Low	Low
IVUS-XPL	Low	Low	High	Low	Low	Low	Low
Tan et al	High	Unclear	High	Unclear	Unclear	High	High

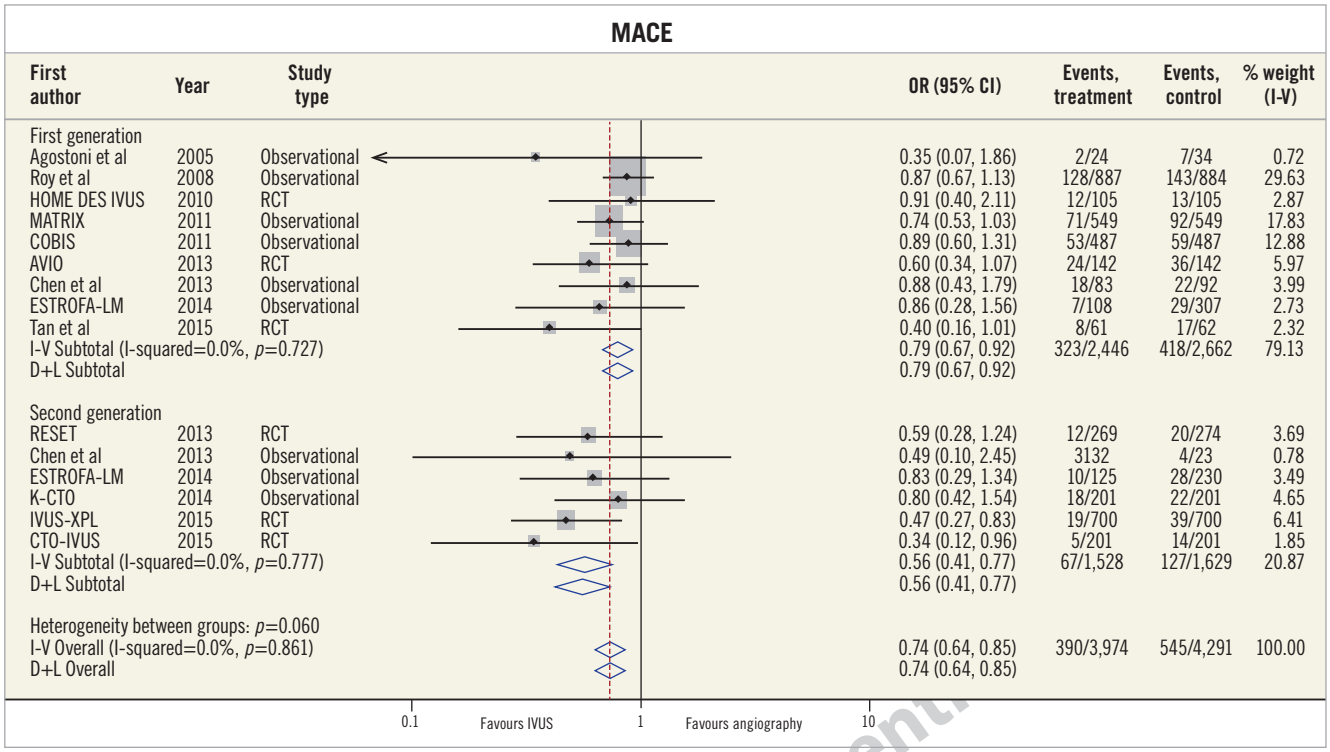

Online Figure 1. *MACE for IVUS-guided versus angiography-guided PCI stratified by DES generation using random-effects model and inverse variance method.*

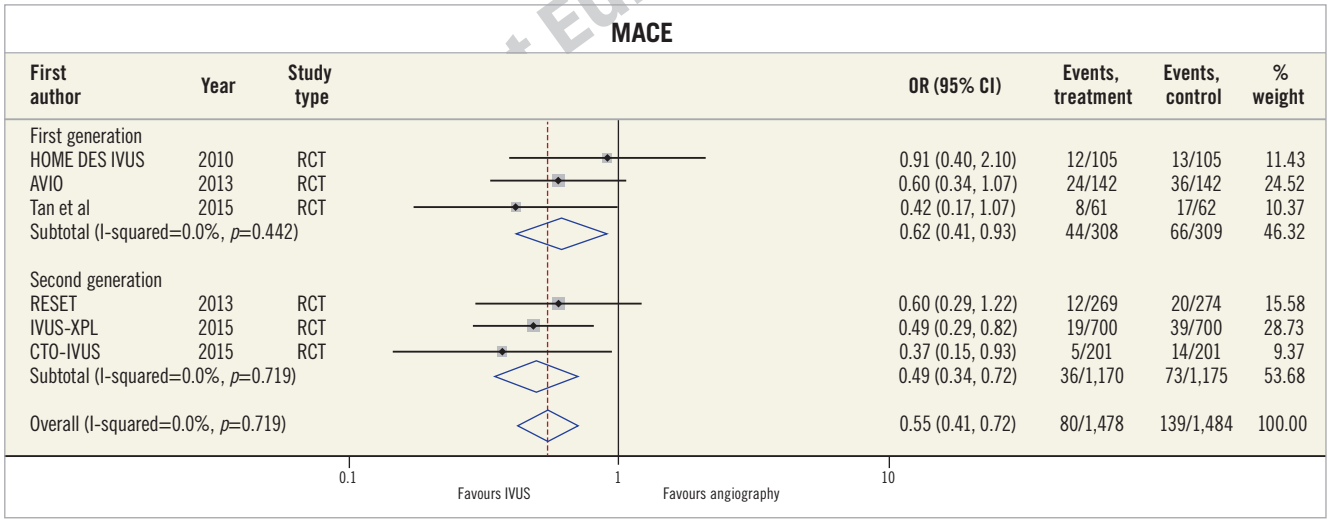

Online Figure 2. *MACE for IVUS-guided versus angiography-guided PCI in randomised controlled trials stratified by DES generation using Peto model.*

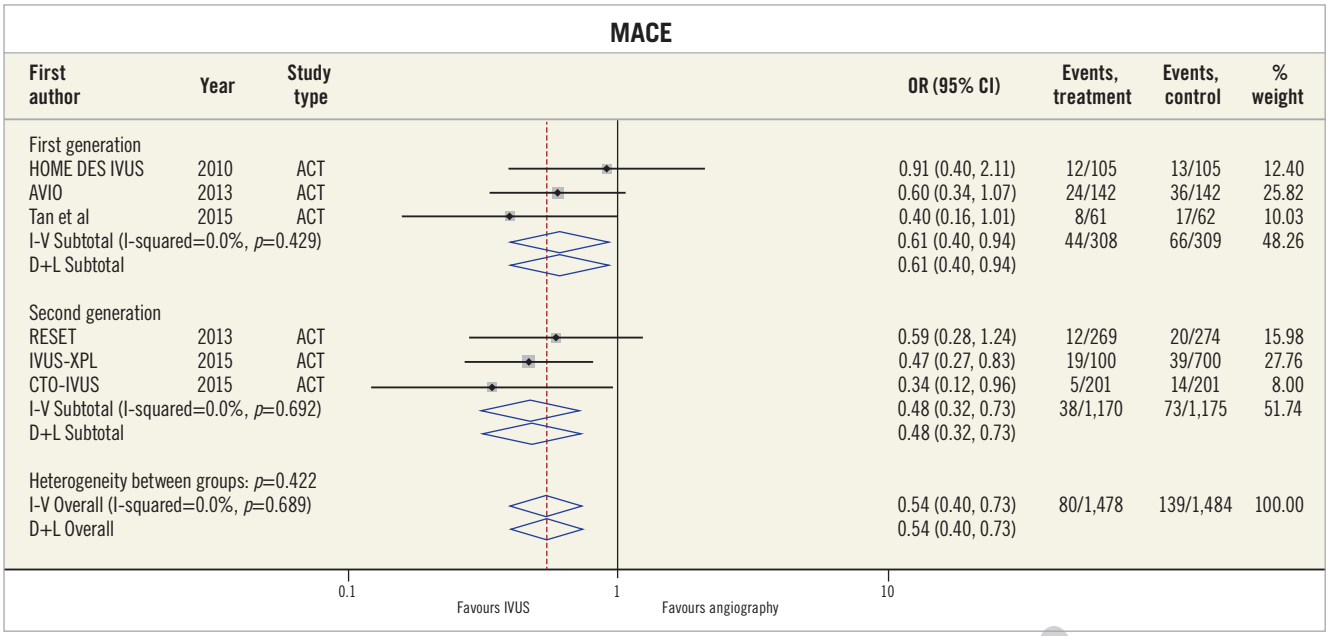

Online Figure 3. *MACE for IVUS-guided versus angiography-guided PCI in randomised controlled trials stratified by DES generation using random-effects model and inverse variance method.*

Original Article

Impact of heart rate on diagnostic accuracy of second generation 320-detector computed tomography coronary angiography

Nitesh Nerlekar[1], Brian S. Ko[1], Arthur Nasis[1], James D. Cameron[1], Michael Leung[1], Adam J. Brown[1], Dennis T. L. Wong[1], Philip J. Ngu[1], John M. Troupis[1,2], Sujith K. Seneviratne[1]

[1]Monash Cardiovascular Research Centre, Department of Medicine (Monash Medical Centre) Monash University and Monash Heart, Monash Health, 246 Clayton Road, Clayton, 3168 VIC, Australia; [2]Department of Diagnostic Imaging, MMC, Southern Health, Melbourne, Australia

Contributions: (I) Conception and design: N Nerlekar, A Nasis, BS Ko; (II) Administrative support: JD Cameron, SK Seneviratne; (III) Provision of study material or patients: None; (IV) Collection and assembly of data: N Nerlekar, AJ Brown, PJ Ngu; (V) Data Analysis and interpretations: N Nerlekar, M Leung, DT Wong, JM Troupis, SK Seneviratne; (VI) Manuscript writing: All authors; (VII) Final approval of manuscript: All authors.

Correspondence to: Dr Nitesh Nerlekar. MonashHeart, MonashHealth, 246 Clayton Road, Clayton, VIC 3168, Australia.
Email: nitesh.nerlekar@monashhealth.org.

Objective: To assess the impact of elevated heart rate (HR) on the diagnostic accuracy and image quality of second-generation 320-detector computed tomography coronary angiography (320-CTCA).

Methods: Consecutive patients with suspected coronary disease referred for invasive coronary angiography (ICA) were prospectively recruited and underwent 320-CTCA. Pre-scan beta-blockers were administered if native HR>80 bpm and post-scan cohorts stratified by traditional (HR ≤60 bpm) and elevated HR (61–80 bpm). A wider phase window was used for the elevated HR group (30–80%). 320-CTCA and ICA were analyzed by independent readers blinded to other data. Significant disease was defined as ≥50% visual stenosis on ICA. Uninterpretable segments by 320-CTCA were considered to be significant on an intention-to-diagnose principle. Image quality was assessed by 5-point Likert score.

Results: Of 107 patients studied (1,662 segments), there was no significant difference in sensitivity, specificity, positive and negative predictive value between patients with HR ≤60 bpm (n=55) *vs.* HR 61–80 bpm (n=52): 97%, 88%, 95%, 94% *vs.* 100%, 88%, 95%, 100%; Receiver operator characteristic-area under the curve 0.93 *vs.* 0.94, P=0.82). Overall per-patient diagnostic accuracy was 96% in both groups with no significant difference in interpretable segments (Likert ≥2) or median radiation dose (2.4 mSv *vs.* 2.7 mSv, P=0.35). Only 4/1,662 (0.2%) segments were uninterpretable by motion artefact in the whole cohort.

Conclusions: In patients with HR >60 and up to 80bpm, second generation 320-CTCA provides comparably adequate diagnostic accuracy to HR ≤60 without significantly impacting upon overall segmental evaluability.

Keywords: Multi-detector CT; 320 row CT coronary angiography; diagnostic accuracy; sensitivity; specificity; positive predictive value; negative predictive value; image quality

Submitted Dec 05, 2016. Accepted for publication Jan 20, 2017.
doi: 10.21037/cdt.2017.03.05
View this article at: http://dx.doi.org/10.21037/cdt.2017.03.05

Introduction

The high diagnostic accuracy of 320 detector-row computed tomography coronary angiography (320-CTCA) in patients with suspected coronary artery disease (CAD) has been demonstrated in multiple single-centre trials, when compared with invasive coronary angiography (ICA) (1-4). In contrast with traditional 64-detector CT, 320-CTCA enables complete acquisition of the coronary tree in a single gantry rotation. However, 320-CTCA using first generation scanners requires strict heart rate (HR) control (≤60 beats per minute) due to a limited effective temporal resolution

of 175msec, which is similar to traditional 64-detector systems (5). To achieve strict HR control, negative chronotropes (most commonly beta-blockers) are often administered via oral or intravenous route. This may increase patient length of stay, time to 320-CTCA, and may be contraindicated in a proportion of patients (6-10).

Imaging at higher HR (11-14) is often associated with motion artifacts resulting in suboptimal image quality (15). It is also associated with increased radiation exposure due to requirement for multiple gantry rotations (13), or wider padding around a mid-diastolic phase.

Second generation 320-CTCA has an effective temporal resolution of 137.5 msec with half-segment reconstruction. This has the potential to image the entire coronary tree at elevated HR with a single gantry rotation at 0.5mm slice collimation with complete 16 cm cranio-caudal coverage. Recent studies using second-generation 320-CTCA have demonstrated superior image quality at varying HR (11) and lower radiation dose (12) when compared with first-generation scanners (14). Data on the diagnostic performance in comparison to ICA at low and high HR is lacking. This study's primary aim is to evaluate the diagnostic accuracy of second-generation 320-CTCA compared to ICA in patients with traditionally controlled (HR ≤60 bpm) and elevated HR (61–80 bpm). The secondary aim is to determine the impact of HR control on image quality and radiation exposure.

Methods

Study population

Consecutive patients referred for clinically mandated ICA to a tertiary referral centre (Monash Heart, Monash Medical Centre, Melbourne, Australia) between November 2012 and March 2014 for evaluation of suspected CAD were prospectively screened. Patients were excluded if they had known obstructive CAD as determined on invasive angiography (≥50% stenosis), coronary artery bypass grafting, previous coronary stenting, advanced atrioventricular block, atrial or ventricular arrhythmia, decompensated heart failure, steroid-dependent asthma or renal insufficiency (eGFR <60 mL/min/1.73 m^2).

All patients gave written consent prior to inclusion in the study. After informed consent, all eligible patients who did not fulfill exclusion criteria underwent research 320-CTCA within one week of ICA. No patients required intervention between ICA and 320-CTCA. The institutional review board approved the study and all recruited patients provided signed informed consent.

ICA protocol and interpretation

ICA was performed via standard techniques by either radial or femoral approach at operator discretion. ICA images were visually evaluated by an interventional cardiologist blinded to clinical data and CTCA results by visual stenosis grade. Coronary segments were classified according to the modified American Heart Association 17-segment model (16) and significant stenosis was defined as ≥50% reduction of maximal coronary luminal diameter.

320-CTCA protocol and interpretation

Upon arrival in the CTCA department, HR was evaluated. Patients with baseline HR ≤80 bpm underwent 320-CTCA acquisition at their native HR; for patients with HR >80 bpm, 25 mg oral metoprolol or 5 mg oral ivabradine was administered with repeat dosing at 30-minute intervals to allow imaging to be performed at HR ≤80 bpm. On-table intravenous metoprolol was administered if the HR increased above >80 bpm. All studies were performed on a second-generation 320-detector row system (AquilionOne VISION, Toshiba Medical Systems, Tokyo, Japan). Nitroglycerin 400 µg sublingually was administered 1 minute before contrast injection. A bolus of 75 mL of 100% Iohexal (Omnipaque 350) was administered at 6 mL/s followed by a 50 mL normal saline chaser. Scanning was manually triggered when peak contrast enhancement in the left ventricle was observed with no enhancement in the right ventricle. Scans were performed via an axial technique with detector collimation of 320 mm × 0.5 mm and no requirement for table movement due to 16 cm cranio-caudal coverage. Tube current was determined with the use of automatic exposure control (SUREExposure3D, Toshiba medical systems) on the basis of X-ray attenuation on anterior-posterior and lateral scout images and the reconstruction kernel. Tube potential was manually set by the radiographer with default at 100 kVp and adjusted to 120 or 135 kVp when the automatic tube current selected was maximum. Gantry rotation time was 275 msec with effective temporal resolution of 137.5 msec. Scans were performed with prospective electrocardiographic triggering using 70–85% of the phase window at HR <70 bpm and 30–80% when HR >70 bpm. Image acquisition was restricted to single beat acquisition (multi-beat acquisition

was not performed). Images were reconstructed with a 512 × 512 matrix, 0.5 mm thick sections and 0.25 mm increments using kernel FC43, iterative reconstruction with adaptive iterative dose reduction 3D (AIDR3D, Toshiba Medical Systems) standard and asymmetric cone beam reconstruction (17). Mean effective radiation exposure was derived from the dose-length product multiplied by a conversion co-efficient for the chest (DLP × 0.014 mSv/mGy) (18).

CTCA images were visually assessed by consensus by two CT trained cardiologists. Readers were blinded to clinical and ICA datasets. Reconstructed images were reviewed on a computer-based platform (Vitrea FX 2.0, Vital Images, Minnetonka, Minnesota) with the best phase chosen for interpretation. Quantification was performed according to standardized 17-segment model (16) for all segments ≥1.5 mm diameter. Significant stenosis was defined as ≥50% reduction of the maximal luminal diameter. Image quality was assessed at per-segment level according to a previously published 5-point Likert score (19): 1=poor, impaired image quality limited by excessive noise or poor vessel wall definition; 2=adequate, reduced image quality with poor vessel wall definition or excessive image noise, limitations in low contrast resolution remain evident; 3=good, impact of image noise, limitations of low contrast resolution and vessel margin definition are minimal; 4=very good, good attenuation of vessel lumen and delineation of vessel walls, relative image noise is minimal, coronary wall definition and low contrast resolution well maintained and 5=excellent, excellent attenuation of the vessel lumen and clear delineation of the vessel walls, limited perceived image noise. If the segment was described as poor, the predominant artifact was identified as calcification, motion or noise. Non-interpretable segments were regarded as containing severe stenosis.

Statistical analysis

Continuous variables are reported as mean ± standard deviation or median with interquartile range. Normality of variables was assessed visually by plotting histograms and statistically by the Shapiro-Wilk test. Variables were compared using a Student t-test, Mann-Whitney or Kruskal Wallis as appropriate. Categorical variables were compared with a chi-square or Fishers exact test. Interobserver agreement between CT readers was measured the Cohen κ test with the scale: κ<0.2 indicates poor agreement, 0.21–0.40 fair agreement, 0.41–0.60 moderate agreement, 0.61–0.80 good agreement, 0.81–1.00 excellent agreement (12). Diagnostic accuracy of 320-CTCA compared to ICA are presented as sensitivity, specificity, positive predictive value (PPV) and negative predictive values (NPV); with precision expressed as 95% confidence intervals as well as by receiver operator characteristic (ROC) analysis comparison and chi-square test (20). Computation of confidence limits for vessels and segments were calculated by generalized estimating equations to account for within-patient clustering (21). Assessment of the Likert score of image quality probability according to HR group was evaluated by ordered logistic regression. Binary logistic regression was performed to assess the image quality difference between high and low HR groups against interpretable (Likert >2) *vs.* non-interpretable segments. Study analysis was performed on an intention-to-diagnose principle (3) to represent 'real-world' practices. A P value <0.05 was considered statistically significant. Statistical analysis was performed using Stata 14/MP (StataCorp, College Station, Texas, USA).

Results

Patient population

Of 885 consecutive patients undergoing ICA, 107 met inclusion criteria for study participation (*Figure 1*). During scan acquisition, 55 patients (Group 1) met traditional rate control criteria with HR ≤60 bpm and 52 (Group 2) had elevated HR from 61–80 bpm. The mean HR in Group 1 was 52±5 bpm compared to 69±8 bpm in Group 2 (P<0.001). The range of heart rate in the study was from minimum 37 bpm to maximum 80bpm. Twenty-nine patients required rate control medication due to baseline HR >80 bpm with 17 patients in Group 1 (31%) and 12 in Group 2 (21%), P=0.25. Baseline demographics and 320-CTCA scan parameters are shown in *Tables 1* and *2* respectively.

Invasive angiography

There were 215 significant stenoses identified with 110 in Group 1 and 105 in Group 2 (P=0.93). Single vessel disease was present in 36 patients, double vessel disease in 28 patients and triple vessel disease in 10 patients in the entire cohort. There were no complications related to ICA.

Diagnostic accuracy

Disease prevalence

There was a high prevalence of significant CAD (≥50%

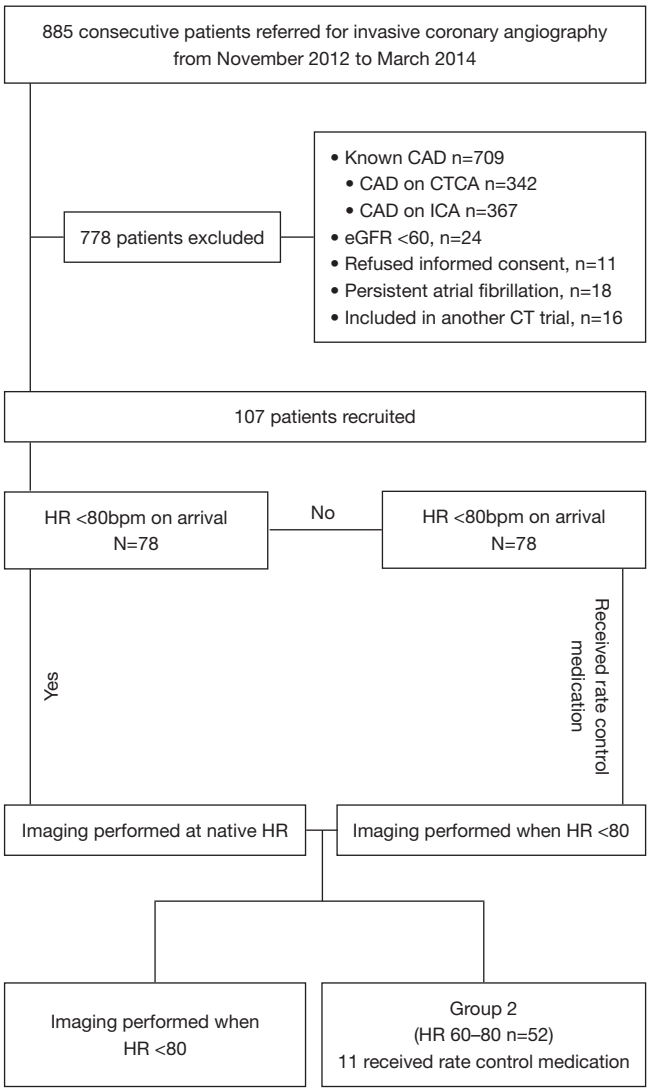

Figure 1 Group selection. CTCA, computed tomography coronary angiography; CAD, coronary artery disease; ICA, invasive coronary angiography; eGFR, estimated glomerular filtration rate; HR, heart rate.

Table 1 Baseline clinical demographics

Characteristic	Group 1 (HR ≤60) (n=55)	Group 2 (HR 60–80) (n=52)	P value
Age (y)	63±10	63±9	0.99
BMI (m/kg)^2	28.5±4.3	28.3±5	0.81
Males	36 (65%)	32 (62%)	0.35
Hypertension	34 (62%)	30 (55%)	0.47
Hyperlipidaemia	24 (44%)	25 (48%)	0.76
Diabetes	10 (18%)	12 (23%)	0.59
Smoker	24 (44%)	23 (44%)	0.93
Family history of IHD	26 (47%)	24 (44%)	0.78
Baseline beta blocker	23 (42%)	19 (37%)	0.58

Values are mean ± SD or n (%). BMI, body mass index; IHD, ischaemic heart disease

Table 2 320-CTCA scan parameters

Parameter	Group 1 (HR ≤60) (n=55)	Group 2 (HR 60–80) (n=52)	P value
Acquisition heart rate (bpm), (mean ± SD)	52±5	69±8	<0.001
Received rate control medication, n (%)	17 (31%)	12 (23%)	0.36
Tube current (mA), (mean ± SD)	590±191	568±178	0.57
Tube Voltage, kVp, median (IQR)	100 (100–120)	100 (100–120)	0.51
Radiation dose (mSv), median (IQR)	2.45 (1.62–3.24)	2.70 (1.58–4.39)	0.35

stenosis in any coronary segment) with per-patient prevalence in Group 1 in 39/55 (70.9%) on ICA *vs.* 37/55 (67.2%) on 320-CTCA (P=0.68). In Group 2 the prevalence of significant disease was 35/52 patients (67.3%) on ICA *vs.* 34/52 (65.3%) on 320-CTCA (P=0.84).

Per-segment analysis

In Group 1,855 segments were evaluated by 320-CTCA and 807 segments in Group 2. At a per-segment level in Group 1 *vs.* Group 2, there was no significant difference in the sensitivity (89% *vs.* 84%, P=0.78), specificity (95% *vs.* 96%, P=0.54), PPV (73% *vs.* 76%, P=0.57) and NPV (98% *vs.* 97%, P=0.28) (*Table 3*). Overall per-segment accuracy was 94% in both groups.

Per-vessel analysis

There were 220 vessels analysed in Group 1 and 208 in Group 2. Overall accuracy was 92% in the Group 1 and 95% in Group 2. There was no significant difference in sensitivity (94% *vs.* 98% P=0.92), specificity (91% *vs.* 94%, P=0.35), PPV (81% *vs.* 86% p=0.32) or NPV (97% *vs.* 99% P=0.37) between groups.

Table 3 Diagnostic accuracy parameters of 320-CTCA

Classification	Group	Disease prevalence (%)	Sensitivity (%)	P value	Specificity (%)	P value	Positive predictive value (%)	P value	Negative predictive value (%)	P value	Accuracy (%)
Per patient, n=107	Group 1, (HR≤60), n=55	69	97 (86–100) (37/38)	>0.99	88 (64–99) (15/17)	1.00	95 (83–99) (37/39)	0.96	94 (70–100) (15/16)	0.37	96 (85–99) (52/55)
	Group 2, (HR 60–80), n=52	67	100 (90–100) (34/34)		88 (64–99) (15/17)		95 (81–99) (34/36)		100 (78–100) (15/15)		96 (87–100) (50/52)
Per vessel, n=428	Group 1, (HR≤60) n=220	28	94 (84–98) (58/62)	0.92	91 (86–95) (144/158)	0.35	81 (69–89) (58/72)	0.32	97 (93–99) (144/148)	0.37	92 (87–95) (202/220)
	Group 2, (HR 60–80), n=208	28	98 (91–100) (57/58)		94 (89–97) (137/146)		86 (76–94) (57/66)		99 (96–100) (137/138)		95 (91–98) (198/208)
Per segment, n=1,662	Group 1, (HR ≤60), n=855	13	89 (81–94) (95/107)	0.78	95 (93–97) (712/748)	0.54	74 (64–80) (95/128)	0.57	98 (97–99) (712/724)	0.28	94 (93–96) (807/855)
	Group 2, (HR 60–80), n=807	13	84 (76–90) (90/107)		96 (94–97) (671/700)		76 (67–83) (90/119)		97 (96–99) (671/688)		94 (92–95) (761/807)

Diagnostic parameter values represented by parameter percentage and respective 95% confidence intervals with raw numbers for parameter calculation below.

Per-patient analysis

The overall per-patient diagnostic accuracy across all 107 patients was 96%. There was no significant difference in accuracy parameters in the Group 1 *vs.* Group 2. Sensitivity was 97% *vs.* 100% (P>0.99), specificity 88% *vs.* 88% (P>0.99), PPV 95% *vs.* 95% (P=0.96) and NPV 94% *vs.* 100% (P=0.37).

ROC analysis at a per-patient level found no difference in diagnostic accuracy between groups (Group 1 0.93 *vs.* Group 2 0.94, P=0.82).

Image quality

The interobserver agreement between readers was excellent (κ=0.84). Of 1,662 segments evaluated on 320-CTCA, 1,632 (98%) were interpretable (defined as Likert score ≥2). There was a significant difference in image quality between groups, with median Likert score 4 (IQR 3–4) in Group 1 *vs.* 4 (IQR 3–4) in Group 2 (P<0.01) with a larger proportion of 'adequate' (Likert score=2) segments in the Group 2 (73 *vs.* 21 in Group 1, P<0.01) (*Table 4*).

Ordered logistic regression demonstrated a decrease in image quality, with increasing Likert score for each unit increase in HR (β coefficient –0.371 (95% CI: –0.56, –0.17, P<0.001) with reducing probabilities across all levels of Likert score. However when assessed according to interpretable *vs.* non-interpretable segments, there was no significant difference in the log odds of higher image quality in Group 1 *vs.* Group 2 (β coefficient –0.19 (95% CI: –1.00, 0.61, P=0.64) (*Table 4*).

There was no difference in the number of poor or non-interpretable segments between groups (P=0.13) with assessment of the best CT phase. Of these 30 poor/non-interpretable segments in the entire cohort, 4 were due to motion artefact: 2 in controlled HR group (in the right posterior descending artery and posterolateral ventricular branch in the same patient) *vs.* 2 in elevated HR group: (in the mid left anterior descending artery and first diagonal branch in two different patients). The remaining segmental non-interpretability was due to severe calcium burden.

Radiation dose

There was no significant difference in median radiation

Table 4 Analysis of image quality between groups

Parameter	Group 1, (HR ≤60), (n=855)	Group 2, (HR 60–80), n=807	P value
Median Likert Score [IQR]	4 [3, 4]	4 [3, 4]	<0.01
Likert score			
Uninterpretable	2 (0.2%)	6 (0.7%)	0.13
(I) Poor	9 (1.0%)	13 (1.6%)	0.32
(II) Adequate	21 (2.4%)	73 (9.0%)	<0.01
(III) Good	258 (30.2%)	242 (30.0%)	0.93
(IV) Very good	446 (52.2%)	380 (47.1%)	0.04
(V) Excellent	119 (13.9%)	93 (11.5%	0.14
Predicted probabilities			
(I) Poor	0.014	0.019	
(II) Adequate	0.035	0.049	
(III) Good	0.281	0.347	
(IV) Very good	0.527	0.481	
(V) Excellent	0.144	0.104	
Ordinal logistic regression β coefficient	–0.371 (95% CI: –0.57, –0.17)		<0.01
Binary logistic regression β coefficient (interpretable *vs*. non-interpretable)	–0.19 (95% CI: –1.00, 0.61)		0.64

Predicted probabilities as based on ordinal logit. Ordinal logistic regression co-efficient as based on ordinal outcome variable Likert 1 to 5. Binary logistic regression coefficient as based on non-interpretable (Likert <2) *vs*. interpretable (Likert ≥2) segments.

dose between groups [2.45 (IQR 1.62–3.24) mSv in Group 1 *vs.* 2.70 (IQR 1.58–4.39) mSv in Group 2 (P=0.35)] (*Table 2*). When stratified by HR of ≤60, 61–70 and 71–80 bpm, there was no difference in radiation dose (2.45 *vs.* 2.24 *vs.* 3.51 mSv, P=0.31). There remained no difference when the lowest cohort of HR (≤60 bpm) *vs.* the highest (71–80 bpm) were compared, P=0.10.

Discussion

We evaluated the diagnostic accuracy of second generation 320-CTCA in 107 consecutively enrolled patients with suspected CAD. Our results demonstrate that second generation 320-CTCA preserves diagnostic accuracy with HR up to 80bpm compared to traditional HR controlled patients ≤60 bpm. Diagnostic accuracy was preserved despite the high prevalence of obstructive CAD (67%) and diagnostic performance is similar to previously reported results in first generation 320-detector scanners (21). Our results do not advise liberal avoidance of heart rate control prior to CTCA, but rather serve as reassuring data in patients in whom rate control can be challenging or contraindicated. The results also demonstrate that image quality, and radiation dose may not be significantly compromised using the second generation scanner.

This is the first reported study of diagnostic accuracy in second generation 320-scanners. Previous studies have focused primarily on image quality and radiation exposure. Notably patients in this study underwent a scan protocol in which the acquisition window was widened when HR was elevated to allow for multiple phase reconstruction and evaluation. This obviated the need for 2 beat scans using multi-segment reconstruction which has described as a limitation in previous studies (22). Furthermore the AIDR 3D algorithm was incorporated into our protocol which may improve spatial resolution and reduce image noise to enhance image quality and lower radiation dose (23).

Surprisingly our findings indicate a comparable radiation dose in scans acquired during high and controlled heart rates. This may be secondary to the use of higher tube current and

lower tube potential (24) to achieve sub-millisievert radiation dose scans (12). Furthermore, the faster gantry rotation speed of 275 ms, allowing near isophasic imaging of the coronary tree avoids the need for multiple rotations. However, as mentioned our study utilized an increased phase window when HR >70 bpm to maximize phase capture. We did not find a difference in radiation dose across stratified HR cohorts, although there was clearly a numerical difference in those with HR >70 bpm at 3.51 *vs.* 2.45 mSv in those with HR <60 bpm, but this did not achieve statistical significance. Narrowing the phase window would further reduce radiation dosing although this requires confirmation with prospective testing.

Various Likert scoring systems have been used to report image quality in CTCA with recent studies comparing first and second generation quality differences, but not within scanner differences based on heart rate (11,14). These scoring systems have generally been described in terms of means, however the use of mean values representing an ordinal scale that is likely to be non-normally distributed data is hard to interpret. We have reported medians to reflect the skewed distribution of Likert score, and additionally performed ordered logistic regression to better reflect statistical parameters of image quality. These methods demonstrate that increasing heart rate reduces the probability of achieving excellent image quality; however the difference in image scores between interpretable and non-interpretable segments is not significant.

The impact of reducing image quality with increasing heart rate, whilst not affecting overall stenosis severity, may have implications at a lesion level when analysing plaque characteristics. Therefore, pending further study, optimal heart rate control is necessary for plaque composition analysis.

In patients requiring HR control prior to 320-CTCA beta-blockers are most commonly used, however their use is contraindicated in chronic obstructive or reactive airways disease, and are avoided in those with hypotension (8). Up to 16% of patients presenting for CTCA have such contraindications (6,7,9,10) whilst up to 50% will have an elevated HR (7,10). Even with the addition of beta-blockade, up to 44% of patients may not be able to reach suggested target HR for protocol acceptable imaging (7). The demonstration of an ability of second-generation 320-CTCA to accurately scan patients with HR up to 80 bpm may not only result in less requirement for beta-blockade, but also increased clinical service delivery and efficiency.

Limitations

We acknowledge certain limitations to our study: this is a single-centre study of a selected and non-randomized patient population with vendor specific software and may not be generalizable to scanners with lower temporal resolution. Additionally, the study was reported by highly experienced cardiologists and therefore results may not be applicable to lower volume centres. The two groups are based on HR at presentation with subsequent beta-blockade if dictated by study protocol, providing two convenience samples rather than randomized groups. The relatively small numbers in each group may have resulted in a type II error with regards to no difference in radiation dose between groups. Furthermore, we excluded patients who had persistent atrial fibrillation. This is because our aim was to assess the influence of heart rate alone on diagnostic accuracy, without R-R interval variability. Finally, we did not assess plaque composition and only luminal stenosis which may impact lesion-level characterization.

Conclusions

In patients with suspected CAD, second-generation 320-CTCA (Aquilion ONE) provides good overall diagnostic accuracy despite reduced image quality in patients with HR up to 80bpm. There is a small, non-significant increase in radiation dose with patients at higher heart rates. Future study is required to assess plaque level characterization at elevated heart rates, as well as assess the potential improvement in departmental efficiency with a lower requirement for pre-scan beta-blockade.

Acknowledgements

None.

Footnote

Conflicts of Interest: The authors have no conflicts of interest to declare.

Ethical Statement: This study has been approved by the local human research ethics committee and therefore performed in accordance with the ethical standards laid down in the 1964 Declaration of Helsinki and its later amendments. All persons gave their informed consent prior to inclusion in the study.

References

1. Dewey M, Zimmermann E, Deissenrieder F, et al. Noninvasive coronary angiography by 320-row computed tomography with lower radiation exposure and maintained diagnostic accuracy: comparison of results with cardiac catheterization in a head-to-head pilot investigation. Circulation 2009;120:867-75.
2. de Graaf FR, Schuijf JD, van Velzen JE, et al. Diagnostic accuracy of 320-row multidetector computed tomography coronary angiography in the non-invasive evaluation of significant coronary artery disease. Eur Heart J 2010;31:1908-15.
3. Nasis A, Leung MC, Antonis PR, et al. Diagnostic accuracy of noninvasive coronary angiography with 320-detector row computed tomography. Am J Cardiol 2010;106:1429-35.
4. Kerl JM, Schoepf UJ, Zwerner PL, et al. Accuracy of coronary artery stenosis detection with CT versus conventional coronary angiography compared with composite findings from both tests as an enhanced reference standard. Eur Radiol 2011;21:1895-903.
5. Abbara S, Arbab-Zadeh A, Callister TQ, et al. SCCT guidelines for performance of coronary computed tomographic angiography: a report of the Society of Cardiovascular Computed Tomography Guidelines Committee. J Cardiovasc Comput Tomogr 2009;3:190-204.
6. de Graaf FR, Schuijf JD, van Velzen JE, et al. Evaluation of contraindications and efficacy of oral Beta blockade before computed tomographic coronary angiography. Am J Cardiol 2010;105:767-72.
7. Maffei E, Palumbo AA, Martini C, et al. "In-house" pharmacological management for computed tomography coronary angiography: heart rate reduction, timing and safety of different drugs used during patient preparation. Eur Radiol 2009;19:2931-40.
8. Mahabadi AA, Achenbach S, Burgstahler C, et al. Safety, efficacy, and indications of beta-adrenergic receptor blockade to reduce heart rate prior to coronary CT angiography. Radiology 2010;257:614-23.
9. Roberts WT, Wright AR, Timmis JB, et al. Safety and efficacy of a rate control protocol for cardiac CT. Br J Radiol 2009;82:267-71.
10. Shapiro MD, Pena AJ, Nichols JH, et al. Efficacy of pre-scan beta-blockade and impact of heart rate on image quality in patients undergoing coronary multidetector computed tomography angiography. Eur J Radiol 2008;66:37-41.
11. Tomizawa N, Maeda E, Akahane M, et al. Coronary CT angiography using the second-generation 320-detector row CT: assessment of image quality and radiation dose in various heart rates compared with the first-generation scanner. Int J Cardiovasc Imaging 2013;29:1613-8.
12. Chen MY, Shanbhag SM, Arai AE. Submillisievert median radiation dose for coronary angiography with a second-generation 320-detector row CT scanner in 107 consecutive patients. Radiology 2013;267:76-85.
13. Pelliccia F, Pasceri V, Evangelista A, et al. Diagnostic accuracy of 320-row computed tomography as compared with invasive coronary angiography in unselected, consecutive patients with suspected coronary artery disease. Int J Cardiovasc Imaging 2013;29:443-52.
14. Wong DT, Soh SY, Ko BS, et al. Superior CT coronary angiography image quality at lower radiation exposure with second generation 320-detector row CT in patients with elevated heart rate: a comparison with first generation 320-detector row CT. Cardiovasc Diagn Ther 2014;4:299-306.
15. Uehara M, Takaoka H, Kobayashi Y, et al. Diagnostic accuracy of 320-slice computed-tomography for detection of significant coronary artery stenosis in patients with various heart rates and heart rhythms compared with conventional coronary-angiography. Int J Cardiol 2013;167:809-15.
16. Austen WG, Edwards JE, Frye RL, et al. A reporting system on patients evaluated for coronary artery disease. Report of the Ad Hoc Committee for Grading of Coronary Artery Disease, Council on Cardiovascular Surgery, American Heart Association. Circulation 1975;51:5-40.
17. Van der Molen AJ, Joemai RM, Geleijns J. Performance of longitudinal and volumetric tube current modulation in a 64-slice CT with different choices of acquisition and reconstruction parameters. Phys Med 2012;28:319-26.
18. Hausleiter J, Meyer T, Hermann F, et al. Estimated radiation dose associated with cardiac CT angiography. JAMA 2009;301:500-7.
19. Leipsic J, Labounty TM, Heilbron B, et al. Adaptive statistical iterative reconstruction: assessment of image noise and image quality in coronary CT angiography. AJR Am J Roentgenol 2010;195:649-54.
20. Ropers U, Ropers D, Pflederer T, et al. Influence of heart rate on the diagnostic accuracy of dual-source computed tomography coronary angiography. J Am Coll Cardiol 2007;50:2393-8.
21. Li S, Ni Q, Wu H, et al. Diagnostic accuracy of 320-slice computed tomography angiography for detection of

coronary artery stenosis: meta-analysis. Int J Cardiol 2013;168:2699-705.
22. Gang S, Min L, Li L, et al. Evaluation of CT coronary artery angiography with 320-row detector CT in a high-risk population. Br J Radiol 2012;85:562-70.
23. Irwan RN, S; Blum, A. AIDR 3D - Reduces Dose and Simultaneously Improves Image Quality. Toshina Med Syst 2011:1-8.</bok>
24. Wong DT, Ko BS, Cameron JD, et al. Transluminal attenuation gradient in coronary computed tomography angiography is a novel noninvasive approach to the identification of functionally significant coronary artery stenosis: a comparison with fractional flow reserve. J Am Coll Cardiol 2013;61:1271-9.

Cite this article as: Nerlekar N, Ko BS, Nasis A, Cameron JD, Leung M, Brown AJ, Wong DT, Ngu PJ, Troupis JM. Seneviratne SK. Impact of heart rate on diagnostic accuracy of second generation 320-detector computed tomography coronary angiography. Cardiovasc Diagn Ther 2017;7(3):296-304. doi: 10.21037/cdt.2017.03.05

Accepted: 19 June 2016

DOI: 10.1111/ctr.12796

ORIGINAL ARTICLE

WILEY Clinical TRANSPLANTATION
The Journal of Clinical and Translational Research

Feasibility of exercise stress echocardiography for cardiac risk assessment in chronic kidney disease patients prior to renal transplantation

Nitesh Nerlekar[1] | William Mulley[2] | Hassan Rehmani[3] | Satish Ramkumar[3] | Kevin Cheng[1] | Sheran A. Vasanthakumar[1] | Hashrul Rashid[1] | Timothy Barton[1] | Arthur Nasis[1] | Ian T. Meredith[1] | Stuart Moir[1] | Philip M. Mottram[1]

[1]Monash Cardiovascular Research Centre, Department of Medicine (Monash Medical Centre), Monash University and Monash Heart, Monash Health, Clayton, Australia

[2]Department of Nephrology, Monash Medical Centre and Department of Medicine, Monash University, Clayton, Australia

[3]Department of Medicine, Monash Health, Clayton, Australia

Correspondence
Dr Nitesh Nerlekar, MBBS, Monash Cardiovascular Research Centre, Department of Medicine (Monash Medical Centre), Monash University and Monash Heart, Monash Health, Clayton, Australia.
Email: [redacted]

Abstract

Background: Pharmacologic stress testing is utilized in preference to exercise stress echocardiography (ESE) for cardiac risk evaluation in potential renal transplant recipients due to the perceived lower feasibility of ESE for achieving adequate workload and target heart rate (THR) in this population.

Methods: Consecutive patients referred for cardiac risk evaluation prior to potential kidney transplantation were evaluated. All patients attempted ESE before pharmacologic testing was considered. Treadmill ESE utilized BRUCE protocol to maximum capacity. THR was defined as >85% of the maximum predicted heart rate (220-age). Functional capacity was assessed by metabolic equivalents (METs) and the rate pressure product (RPP).

Results: Of 535 patients (349 male, age 56±11), 372(70%) reached THR. Mean METs were 10±3 with 531(99%) achieving ≥4 METs and 87% ≥7 METs. Mean RPP was 25 821±5820 bpm×mm Hg (83% achieving >20 000 bpm×mm Hg). On multivariate analysis, independent predictors of failure to reach THR were rate-control medication and diabetes; failure to reach 7 METs: females, diabetics, age≥65, and previous cardiac disease; failure to reach RPP>20 000: rate-control medication. There were 97% of ESE completed to physiologic endpoints.

Conclusion: In unselected potential renal transplant candidates, cardiac assessment by ESE is well tolerated, with 9-in-10 exercising to satisfactory functional capacity. ESE should be considered a feasible alternative to pharmacologic testing in this population.

KEYWORDS
exercise testing, feasibility, renal transplant, stress echocardiography

1 | INTRODUCTION

There is an avoidance of exercise stress modalities for pre-operative cardiac risk evaluation in potential renal transplant recipients due to a perception that patients with chronic kidney disease (CKD) are unable to exercise adequately and fail to reach target heart rates (THR).[1] However, it is not just THR that determines test interpretation, but also the exercise capacity or functional capacity. Therefore, it is recommended that patients exercise to a symptom-limited endpoint rather than just to a specified THR to truly test cardiovascular fitness.[2] Recent guidelines recommend assessment of functional capacity as the first step in the risk evaluation for non-cardiac surgery with a

specified cutoff of 4 metabolic equivalents (METs).[3] These guidelines are not specific to CKD; however, there is evidence in this population that less than 6-minute exercise duration (~7 METS) portends a poor prognosis.[4] Therefore, 7 METs may be a more appropriate threshold to consider. The majority of the literature assesses pharmacologic stress modalities (nuclear myocardial perfusion or dobutamine stress echocardiography); however, exercise stress in general is cheaper, more tolerable, devoid of radiation exposure, and quicker to perform. Furthermore, there is evidence to suggest that exercise induces a greater myocardial stress than pharmacologic alternatives due to achievement of a higher rate pressure product,[5] another important marker of functional capacity. We sought to evaluate the feasibility of ESE in a large cohort of consecutive patients with CKD and the influence of clinical predictors on achievement of markers of functional capacity.

2 | METHODS

We evaluated the exercise stress echocardiograms (ESE) and clinical parameters of consecutively referred patients from 2008 to 2014. Our institutional protocol was that all patients referred for stress echocardiography attempt ESE unless obvious exclusions to exercise such as musculoskeletal or rheumatologic disease affecting mobility, use of a gait aid or prior amputation. All remaining patients underwent a 40-m gait assessment, and the final decision on physiologic vs pharmacologic testing was at the discretion of the supervising cardiologist.

Clinical data were collated from the patients' medical records, and all efforts made across medical record platforms to ensure complete variable collection.

All tests were performed according to American Society of Echocardiography guidelines.[2] ESE was performed utilizing the BRUCE protocol to assess functional capacity with exercise not ceased when THR (≥85% maximum predicted heart rate [220-age]) was attained, but continued to patient exhaustion, that is, symptom-limited test. Baseline and stress imaging of the myocardium was performed using parasternal long and short axes: apical four-chamber, two-chamber, and long-axis views.

Metabolic equivalents were calculated by computer generated algorithm according to the BRUCE protocol. A threshold of 7 METs was considered to be the target capacity in analysis. Rate pressure product (RPP) was calculated as the product of peak systolic blood pressure and peak heart rate. An RPP threshold of 20 000 bpm×mm Hg was considered to be the target capacity in analysis.

Results are reported as means±SD with chi-square and t-tests for differences as appropriate. Pearson's correlation was performed between continuous variables after establishing Gaussian distribution. Univariate binary logistic regression was used to assess predictors of achieving THR, 7 METs, or RPP of 20 000. Each model tested the same set of predictors: sex, quartiles of age, hypertension, diabetes, smoking status, dyslipidemia, quartiles of body mass index, previous cardiac disease, left ventricular hypertrophy, current dialysis, and current rate-control therapy. Multivariate logistic regression was performed including all variables with a *P*-value <.20 on univariate testing. Categorical interactions between variables considered (*P*-value cutoff of .10) to have biologic plausibility were tested and the model refitted. Model fit was assessed using the Hosmer–Lemeshow goodness-of-fit test. There were no significant interactions in this study. A *P*-value of <.05 was considered significant in the final model.[6] Statistical analysis was performed using Stata MP 13.1 (StataCorp, College Station, TX, USA).

The study was approved by the local human research ethics committee.

3 | RESULTS

3.1 | ESE results

There were 602 patients referred for cardiac risk evaluation. Upfront dobutamine testing was performed in 46 patients due to amputation or being wheelchair bound (11), vision impairment (3), chronic musculoskeletal pain (18), chronic neurologic illness including previous strokes (10) and diabetic foot complications (4). There were 10 patients where the reason for not performing ESE was not documented. This left 11 (2%) who underwent dobutamine testing due to failed ESE at discretion of the referring physician. Therefore, a total of 535 (98%) patients suitable for ESE were able to successfully complete the test. Cohort baseline demographics are displayed in Tables 1 and 2.

There were 372 (70%) patients who reached THR. In the total cohort, 216 of 535 patients (40%) were on concurrent rate-control therapy (beta-blockers or non-dihydropyridine calcium channel blockers) of whom 45 (21%) had ceased their medication >48 hours prior to the test which may therefore reclassify them as patients

TABLE 1 Baseline demographics

Age	56±10
Sex, male (n, %)	348 (65%)
BMI	27±5
Hypertension (n, %)	473 (88%)
Hyperlipidemia (n, %)	259 (48%)
Smoker (n, %)	127 (24%)
Diabetes (n, %)	205 (38%)
Previous ischemic heart disease (n, %)	166 (31%)
Current rate-control medication use (n, %)	216 (40%)
Hemodialysis (n, %)	301 (56%)
Peritoneal dialysis (n, %)	100 (19%)
Cause of kidney disease	
Diabetes (n, %)	165 (31%)
IgA (n, %)	80 (15%)
Reflux (n, %)	43 (8%)
Other GN (n, %)	110 (20%)
Polycystic kidney disease (n, %)	63 (12%)
Vasculitis (n, %)	23 (4%)
Miscellaneous (n, %)	51 (10%)

TABLE 2 Echocardiographic parameters

Baseline echo abnormality (n, %)	273 (51%)
Left ventricular hypertrophy (n, %)	148 (28%)
Concentric remodeling (n, %)	75 (14%)
Concentric hypertrophy (n, %)	23 (4%)
Eccentric hypertrophy (n, %)	50 (9%)
Regional hypokinesis with normal EF	39 (7%)
Regional hypokinesis with reduced EF	39 (7%)
Globally reduced EF <55%	31 (6%)
Moderate or greater valvular dysfunction	16 (3%)
Resting heart rate (bpm)	80±14
Peak heart rate (bpm)	146±22
Rate pressure product (bpm×mm Hg)	25 854±5830
Achieved target heart rate (n, %)	372 (70%)
Hypertensive response to exercise (n, %)	101 (19%)
Inducible ST-segment changes (n, %)	74 (14%)

who were effectively not on rate control. When analysis was redefined as patients not on a rate-control agent or who had rate-control medication ceased for >48 hours (n=365, 68%) against those who were on rate-control agents or rate-control medication ceased for <48 hours (n=170, 32%), there remained 372 (70%) patients who reached THR.

In contrast, there were 530 (99%) patients who achieved ≥4 METs (Fig. 1). Further stratification by METs demonstrated 66 (12%) achieved between 4 and <7 METs, 182 (34%) between 7 and <10 METs, and 282 (53%) ≥10 METs with just 5 patients <4 METs. Cumulatively, this represents 465 (87%) of patients achieving ≥7 METs, with the cohort achieving an average of 10±3 METs (Fig. 1).

The average exercise duration was 7 minutes 54 seconds±2 minutes 36 seconds. Exercise duration was very strongly correlated with METs, r=.96, P<.001. The mean rate pressure product was 25 854±5830 mm Hg×bpm with 448 (83%) achieving an RPP>20 000 mm Hg×bpm. RPP was weakly correlated with METs, r=.27, P<.001.

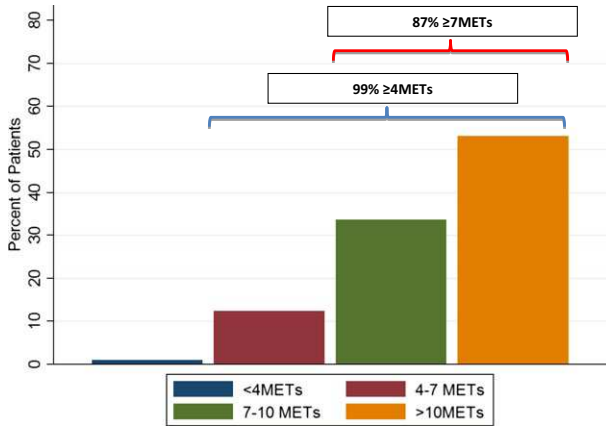

FIGURE 1 Percent of patients stratified by METs achieved. Text boxes above bars demonstrate proportions achieving ≥4 METs (blue parenthesis) and ≥7 METs (red parenthesis)

3.2 | Tolerability

The majority of patients ceased the test for appropriate physiologic indications such as dyspnea, fatigue, or musculoskeletal discomfort (n=517, 97%). Six had inducible chest pain, three complained of dizziness, six were ceased due to significant hypertension, one complained of severe nausea, and one with a fall in systolic blood pressure <90 mm Hg.

There was one major arrhythmic event requiring test cessation due to development of a broad complex tachyarrhythmia later confirmed to be aberrant conduction with no further management required, and two were ceased due to poor treadmill technique. No patient required emergency management or admission (Table 3).

3.3 | Predictors of exercise performance

Univariate and multivariate binary logistic regression analysis using predefined clinical variables (as defined in the methods section above) to predict achievement of reaching THR, METs, and RPP>20 000 mm Hg×bpm are displayed in Tables 4–6.

Patients with diabetes (OR 0.45, 95% CI 0.30–0.48, P<.001) or those on current rate-control therapy (OR 0.34, 95% CI 0.23–0.51, P<.001), representing 56% of the whole cohort, were significantly less likely to achieve THR after adjustment for other clinical factors (Table 5). There were no significant factors in predicting a failure to achieve 4 METs; however, there were only 5 patients that achieved <4 METs. However, in predicting achievement of intermediate functional capacity (>7 METs), females (OR 0.29, 95% CI 0.15–0.55, P<.001), those in the highest age quartile (≥65 years old, OR 0.30, 95% CI 0.13–0.71, P=.003), diabetics (OR 0.31, 95% CI 0.18–0.57, P<.001), and those with a history of previous cardiac disease (OR 0.35, 95% CI 0.18–0.66, P=.001) were all significantly less likely to achieve 7 METs (Table 4). The only independent predictor of failure to achieve an RPP>20 000 bpm×mm Hg was current rate-control therapy (OR 0.58, 95% CI 0.23–0.51, P=.03) (Table 6).

4 | DISCUSSION

We have described data on a protocol of upfront exercise testing in potential renal transplant recipients in preference to pharmacologic testing as a means of challenging contemporary notions that exercise is not a feasible stress modality.[1] Our results have demonstrated several

TABLE 3 Indications for test cessation

Dyspnoea (n, %)	74 (14%)
Fatigue (n, %)	315 (59%)
Musculoskeletal pain (n, %)	128 (24%)
Chest pain (n, %)	6 (1%)
Hypertension (n, %)	6 (1%)
Dizziness (n, %)	3 (0.5%)
Nausea (n, %)	1 (0.1%)
Hypotension (n, %)	1 (0.1%)
Arrhythmia (n, %)	1 (0.1%)

TABLE 4 Univariate and multivariate logistic regression analysis for achievement of 7 METs

		Univariate			Multivariate		
	Mean METs	Odds ratio	95%	*P*-value	Odds ratio	95%	*P*-value
Sex (male reference)	9.86±2.75	0.61	0.36–1.01	.05	0.29	0.15–0.55	<.001*
Age quartiles							
Q1 (18–50)	10.93±2.85	Reference					
Q2 (51–57)	9.72±2.48	1.45	0.54–3.86	.46	1.81	0.63–5.14	.27
Q3 (58–64)	9.18±2.55	0.50	0.23–1.08	.08	0.53	0.23–1.25	.15
Q4 (65–75)	8.24±2.50	0.23	0.11–0.49	<.001	0.30	0.13–0.71	.003*
Diabetes	8.57±2.56	0.32	0.19–0.53	<.001	0.31	0.18–0.57	<.001*
Hypertension	9.49±2.77	0.82	0.36–1.90	.65			
Hyperlipidemia	9.33±2.77	0.72	0.43–1.19	.20	1.24	0.68–2.26	.78
Smoking	9.54±2.72	0.91	0.67–1.24	.55			
Previous IHD	8.77±2.68	0.36	0.21–0.60	<.001	0.35	0.18–0.66	.001*
BMI							
Q1 (13.5–22.9)	10.55±2.96	Reference					
Q2 (22.9–25.9)	10.43±2.59	1.93	0.79–4.74	.15	2.20	0.84–5.70	.11
Q3 (26–29.8)	9.11±2.65	0.63	0.31–1.28	.20	0.73	0.33–1.59	.42
Q4 (29.9–49.4)	8.28±2.15	0.57	0.28–1.14	.11	0.66	0.31–1.41	.28
LVH	9.04±2.60	0.82	0.48–1.42	.49			
Current dialysis	9.45±2.71	1.02	0.58–1.83	.96			
Current rate control	9.28±2.86	0.77	0.45–1.29	.32			

IHD; ischemic heart disease; BMI; body mass index; LVH; left ventricular hypertrophy; METs; metabolic equivalents. See text for details regarding variable selection.
*Significant *P*-value of <.05.

TABLE 5 Univariate and multivariate logistic regression analysis for achievement of target heart rate (≥85% maximum predicted heart rate response)

	Univariate			Multivariate		
	Odds ratio	95%	*P*-value	Odds ratio	95%	*P*-value
Sex	0.61	0.36–1.01	.05	0.85	0.56–1.31	.47
Age quartiles						
Q1 (18–50)	Reference					
Q2 (51–57)	0.98	0.59–1.63	.93			
Q3 (58–64)	1.11	0.67–1.83	.93			
Q4 (65–75)	1.34	0.78–2.31	.29			
Diabetes	0.44	0.30–0.64	<.001	0.45	0.30–0.48	<.001*
Hypertension	0.76	0.42–1.41	.39			
Hyperlipidemia	1.07	0.74–1.56	.70			
Smoking	0.87	0.69–1.10	.25	0.99	0.77–1.27	.93
Previous IHD	0.66	0.45–0.98	.04	0.82	0.54–1.26	.38
BMI						
Q1 (13.5–22.9)	Reference					
Q2 (22.9–25.9)	0.97	0.57–1.65	.91			
Q3 (26–29.8)	0.85	0.50–1.43	.54			
Q4 (29.9–49.4)	0.79	0.47–1.33	.38			
LVH	0.76	0.51–1.13	.18	0.81	0.53–1.24	.34
Current dialysis	0.77	0.50–1.19	.23	0.64	0.40–1.00	.05
Current rate control	0.33	0.22–0.49	<.001	0.34	0.23–0.51	<.001*

IHD, ischemic heart disease; BMI, body mass index; LVH, left ventricular hypertrophy. See text for details regarding variable selection.
*Significant *P*-value of <.05.

TABLE 6 Univariate and multivariate logistic regression analysis for achievement of rate pressure product >20 000 mm Hg×bpm

	Mean RPP (×1000)	Univariate			Multivariate		
		Odds ratio	95%	*P*-value	Odds ratio	95%	*P*-value
Sex (male reference)	25 552	1.00	0.62–1.63	.98			
Age quartiles							
Q1 (18–50)	26 857	Reference					
Q2 (51–57)	25 608	0.67	0.35–1.29	.23	0.74	0.38–1.46	.39
Q3 (58–64)	26 091	0.83	0.41–1.66	.60	0.88	0.43–1.82	.73
Q4 (65–75)	24 543	0.54	0.28–1.04	.07	0.67	0.32–1.37	.27
Diabetes	25 014	0.60	0.38–0.93	.03	0.66	0.41–1.08	.10
Hypertension	25 769	0.97	0.47–2.00	.94			
Hyperlipidemia	25 707	0.98	0.62–1.55	.94			
Smoking	26 434	1.15	0.84–1.57	.37			
Previous IHD	24 902	0.73	0.45–1.18	.20	0.96	0.57–1.63	.89
BMI							
Q1 (13.5–22.9)	26 111	Reference					
Q2 (22.9–25.9)	25 862	1.19	0.59–2.39	.63	1.27	0.62–2.58	.52
Q3 (26–29.8)	26 080	0.88	0.45–1.70	.70	1.00	0.50–1.99	.99
Q4 (29.9–49.4)	25 311	0.64	0.34–1.21	.18	0.70	0.37–1.34	.28
LVH	26 109	0.80	0.49–1.31	.38			
Current dialysis	25 516	0.60	0.34–1.08	.09	0.58	0.31–1.06	.08
Current rate control	25 552	0.59	0.37–0.94	.03	0.58	0.36–0.95	.03*

IHD, ischemic heart disease; BMI, body mass index; LVH, left ventricular hypertrophy; RPP, rate pressure product. See text for details regarding variable selection.
*Significant *P*-value of <.05.

important conclusions: firstly, that almost all independently functioning patients can attempt an ESE unless there are clear exclusions such as neurologic or rheumatologic premorbid conditions. Secondly, there are very few patients (0.2%) who require follow-up pharmacologic testing after an ESE. Thirdly, almost all patients (99%) will achieve satisfactory exercise capacity (≥4 METs) and only slightly less (87%) achieve a level regarded as intermediate or good functional capacity (≥7 METs). Fourthly, while there are factors such as diabetes, previous cardiac disease, and concurrent rate-control therapy that independently influence the achievement of 7 METs or an RPP>20 000 mm Hg×bpm, the average achieved METs among these patients is still high enough to maintain diagnostic confidence. Finally, ESE is very well tolerated with most patients completing the test to physiologic endpoints and no patients requiring emergency medical attention.

Functional capacity is an important marker of perioperative cardiovascular risk, and its assessment is recommended in the evaluation of patients prior to non-cardiac surgery.[7] The lack of functional capacity assessment is a limitation of pharmacologic testing which is generally recommended if <4 METs are achieved or functional capacity is unknown.[7] Furthermore, it has been demonstrated that potential renal transplant recipients who are unable to exercise or have a reduced treadmill exercise time also have reduced long-term survival.[4]

Previous studies in potential renal transplant recipients have demonstrated that only 7–53% achieve THR with exercise[8,9] hence its avoidance in this group of patients. However, pharmacologic studies have also had a high "non-diagnostic" rate, with THR achieved in only 30–66% of cohorts.[10,11] This high incidence of non-diagnostic studies can result in challenging decision-making regarding perioperative risk and often results in further downstream invasive testing and possible delay to renal transplantation.[4] With exercise, however, THR is not the only parameter evaluated; the functional capacity (METs) and the RPP provide both diagnostic and prognostic information, particularly in the approach to perioperative cardiac assessment.[7]

The recommendation for undergoing intermediate risk surgery, such as renal transplantation, is that patients are able to achieve >4 METs.[12] By encouraging patients to exercise to their maximal capacity, we found that 99% of patients achieved or exceeded this target during ESE with just 5 patients not meeting this level. However, no data exist on the use of a 4 METs cutoff for patients with CKD, and accordingly, we used a 7 METs threshold which generally represents approximately 6 minutes of exercise on the BRUCE protocol. Nearly 9 in 10 patients achieved this threshold and the overall cohort mean of 10 METs in our study which was achieved by 53% is regarded as excellent functional capacity[7] and guidelines suggest most of these patients will not require any further testing and may proceed directly to surgery.[7] Even patients receiving renal replacement therapy, a group felt to have a lower exercise tolerance, demonstrated high achievement of mean METs (9.45±2.71), and did not impact upon prediction of exercise capacity. Patients with diabetes are also considered higher risk and while there was an independent, statistically significant influence on achieving 7 METs, these patients still achieved an average of 8.57±2.56 METs which is regarded as very good exercise capacity.

RPP is a marker of myocardial stress, reflecting myocardial oxygen consumption, and has been shown to predict mortality in stress testing[13] and can be used as an alternative, or additional parameter in test interpretation. Our results demonstrated 83% achieving an acceptable threshold of RPP functional capacity (>20 000 bpm×mm Hg), and only current use of rate-control therapy influenced a failure to reach this target. Generally, a much higher RPP is obtained with exercise stress over pharmacologic stress, and therefore, a previous report has suggested that ESE is preferable to dobutamine stress echo for quantification of inducible ischemic burden.[5]

It is important that screening tests are well tolerated by patients to maximize applicability. We have demonstrated that ESE was very well tolerated with 97% of tests completed to physiologic endpoints. There were no major complications requiring hospital admission, and only one significant arrhythmia that was subsequently found to be benign. Of importance, only 2 (0.03%) tests were ceased due to poor technique. The reported adverse event rates in patients undergoing dobutamine studies, including those for perioperative risk assessment, ranges from 3% to 19%, which therefore limits its widespread applicability compared to ESE,[14] and this is reflected in our low rate of adverse events.

Pharmacologic testing will often require significant preparation for the patient including requiring an additional person to accompany them home, intravenous cannulation which is often challenging in CKD patients with scant venous access, longer post-test observation, and possible requirement for additional equipment and supervising staff that increase the overall test duration and cost. Although we did not measure the time taken for each test, it is intuitive that ESE is faster and cheaper and as we have demonstrated, very well tolerated which would make it an ideal upfront strategy in these patients.

Several studies have limited their recruitment to either patients with diabetes or patients requiring renal replacement therapy, whereas we chose to study unselected patients to better represent a real-world analysis. This is of relevance given there are several different guidelines available that describe recommendations for pre-transplant testing. Out cohort comprises all-comers, some of whom may not necessarily have required pre-transplant testing however were still referred. Further study in a similar vein stratified by guideline recommendation would be of interest.

4.1 | Limitations

We acknowledge several limitations to our study which include being subject to all the potential biases of a retrospective analysis. Additionally, this represents a feasibility study and the impact on diagnostic accuracy, revascularization, and future prognosis needs prospective evaluation.

5 | CONCLUSION

In patients with CKD undergoing pre-transplant cardiovascular risk assessment, exercise stress is feasible with most patients demonstrating satisfactory functional capacity. As treadmill exercise time is also an independent marker of perioperative risk and prognosis, ESE should be considered a viable alternative to pharmacologic stress in these patients.

AUTHORS' CONTRIBUTIONS

Timothy Barton, Philip M. Mottram, and Nitesh Nerlekar: Involved in article conception; Hassan Rehmani, Satish Ramkumar, Kevin Cheng, Sheran A. Vasanthakumar, and Hashrul Rashid: Collected data; Nitesh Nerlekar, Timothy Barton, Stuart Moir, and Philip M. Mottram: Involved in data analysis and interpretation; Nitesh Nerlekar, Kevin Cheng, William Mulley, Stuart Moir, and Philip M. Mottram: Drafted the article; William Mulley, Philip M. Mottram, Arthur Nasis, and Ian T. Meredith: Performed critical revision of the article; Nitesh Nerlekar and Hassan Rehmani: Performed statistical analysis, and finally all authors approved the article.

CONFLICT OF INTEREST

The authors have no disclosures or conflicts of interest.

REFERENCES

1. Workgroup KD. K/DOQI clinical practice guidelines for cardiovascular disease in dialysis patients. *Am J Kidney Dis*. 2005;(4 Suppl 3): S1–153.
2. Pellikka PA, Nagueh SF, Elhendy AA, Kuehl CA, Sawada SG. American Society of E. American Society of Echocardiography recommendations for performance, interpretation, and application of stress echocardiography. *J Am Soc Echocardiogr*. 2007;20:1021–1041.
3. Wijeysundera DN, Duncan D, Nkonde-Price C, et al. Perioperative beta blockade in noncardiac surgery: a systematic review for the 2014 ACC/AHA guideline on perioperative cardiovascular evaluation and management of patients undergoing noncardiac surgery: a report of the American College of Cardiology/American Heart Association Task Force on Practice Guidelines. *Circulation*. 2014;130:2246–2264.
4. Patel RK, Mark PB, Johnston N, et al. Prognostic value of cardiovascular screening in potential renal transplant recipients: a single-center prospective observational study. *Am J Transplant*. 2008;8:1673–1683.
5. Rallidis L, Cokkinos P, Tousoulis D, Nihoyannopoulos P. Comparison of dobutamine and treadmill exercise echocardiography in inducing ischemia in patients with coronary artery disease. *J Am Coll Cardiol*. 1997;30:1660–1668.
6. Hosmer DW, Lemeshow S, Sturdivant RX. *Applied Logistic Regression*. New York: Wiley; 2013.
7. Fleisher LA, Fleischmann KE, Auerbach AD, et al. ACC/AHA guideline on perioperative cardiovascular evaluation and management of patients undergoing noncardiac surgery: executive summary: a report of the American College of Cardiology/American Heart Association Task Force on Practice Guidelines. *Circulation*. 2014;24:2215–2245.
8. Morrow CE, Schwartz JS, Sutherland DE, et al. Predictive value of thallium stress testing for coronary and cardiovascular events in uremic diabetic patients before renal transplantation. *Am J Surg*. 1983;146:331–335.
9. Sharma R, Pellerin D, Gaze DC, et al. Dobutamine stress echocardiography and the resting but not exercise electrocardiograph predict severe coronary artery disease in renal transplant candidates. *Nephrol Dial Transpl*. 2005;20:2207–2214.

10. Tita C, Karthikeyan V, Stroe A, Jacobsen G, Ananthasubramaniam K. Stress echocardiography for risk stratification in patients with end-stage renal disease undergoing renal transplantation. *J Am Soc Echocardiogr*. 2008;21:321–326.
11. Cai Q, Serrano R, Kalyanasundaram A, Shirani J. A preoperative echocardiographic predictive model for assessment of cardiovascular outcome after renal transplantation. *J Am Soc Echocardiogr*. 2010;23:560–566.
12. Poldermans D, Bax JJ, Boersma E, et al. Guidelines for pre-operative cardiac risk assessment and perioperative cardiac management in non-cardiac surgery. *Eur Hear J*. 2009;30:2769–2812.
13. Marwick TH, Case C, Poldermans D, et al. A clinical and echocardiographic score for assigning risk of major events after dobutamine echocardiograms. *J Am Coll Cardiol*. 2004;43:2102–2107.
14. Mertes H, Sawada SG, Ryan T, et al. Symptoms, adverse effects, and complications associated with dobutamine stress echocardiography. Experience in 1118 patients. *Circulation*. 1993;88:15–19.

How to cite this article: Nerlekar, N., Mulley, W., Rehmani, H., Ramkumar, S., Cheng, K., Vasanthakumar, S. A., Rashid, H., Barton, T., Nasis, A., Meredith, I. T., Moir, S. and Mottram, P. M. (2016), Feasibility of exercise stress echocardiography for cardiac risk assessment in chronic kidney disease patients prior to renal transplantation. Clinical Transplantation, 30: 1209–1215. doi: 10.1111/ctr.12796

showed that patients who received the 300-mg dose of canakinumab had a total cancer mortality that was lower by 51% than those who received placebo and a lung-cancer mortality that was lower by 77%.[1] The incidence of fatal infection was nearly twice as high in the pooled canakinumab groups as in the placebo group, a finding similar to that observed with the interleukin-1 receptor antagonist anakinra.[2] The accompanying editorial by Harrington[3] discussed the safety risk of interleukin-1β blockade.

Interleukin-1β is driven by multiple inflammasomes. As an alternative to inhibition of interleukin-1β, precise inhibition of a single inflammasome, NLRP3, is likely to be safer. NLRP3 is implicated in diseases of aging, such as atherosclerosis and neurodegenerative disorders. Selective NLRP3 inhibition will leave other inflammasomes to respond to infection. In addition, at the onset of severe infection, an orally available small molecule could be withdrawn, whereas canakinumab cannot. NLRP3 activation also drives interleukin-18, the clinical targeting of which is also safe.[4]

CANTOS has advanced our understanding of the clinical relevance of interleukin-1β and the NLRP3 inflammasome. This trial will drive the development and commercialization of an entirely new class of drugs.

Luke A. O'Neill, Ph.D., F.R.S.

Trinity College Dublin
Dublin, Ireland
[redacted]

Matthew A. Cooper, Ph.D.

University of Queensland
Brisbane, QLD, Australia

Dr. O'Neill reports being the co-founder, the chief scientific officer, and a shareholder of Inflazome, which is developing drugs that target inflammasomes; and Dr. Cooper, being the co-founder, the chief executive officer, and a shareholder of Inflazome. No other potential conflict of interest relevant to this letter was reported.

1. Ridker PM, MacFadyen JG, Thuren T, et al. Effect of interleukin-1β inhibition with canakinumab on incident lung cancer in patients with atherosclerosis: exploratory results from a randomised, double-blind, placebo-controlled trial. Lancet 2017;390:1833-42.
2. Cabral VP, Andrade CA, Passos SR, Martins MF. Hkerberg YH. Severe infection in patients with rheumatoid arthritis taking anakinra, rituximab, or abatacept: a systematic review of observational studies. Rev Bras Reumatol Engl Ed 2016;56:543-50.
3. Harrington RA. Targeting inflammation in coronary artery disease. N Engl J Med 2017;377:1197-8.
4. McKie EA, Reid JL, Mistry PC, et al. A study to investigate the efficacy and safety of an anti-interleukin-18 monoclonal antibody in the treatment of type 2 diabetes mellitus. PLoS One 2016;11(3):e0150018.

DOI: 10.1056/NEJMc1714635

TO THE EDITOR: The trial by Ridker et al. examined canakinumab in a cohort of patients with established coronary artery disease. Although the reduction in cardiovascular events was significant (hazard ratio, 0.85), the disconcerting results included an increased risk of fatal infection and no mortality benefit. In addition, the drug is expensive ($200,000 per year). The accompanying editorial calls for alternative, more cost-effective antiinflammatory agents without the associated risk of fatal infection.

In a prospective, randomized, secondary-prevention trial, colchicine, an ancient[1] but inexpensive antiinflammatory drug with pleiotropic effects including the targeting of neutrophils, resulted in a reduced rate of recurrent cardiovascular events (hazard ratio, 0.29) without an increase in fatal infection.[2] In light of this finding, it is surprising that this agent was not acknowledged by the authors, because at face value, it seems to fulfill the requirements suggested in the editorial. Although studies of colchicine thus far have been predominantly investigator-initiated and smaller in size, it is to be hoped that ongoing research will confirm the initial promising results with this drug.

Nitesh Nerlekar, M.B., B.S., M.P.H.
Richard W. Harper, M.B., B.S.

Monash University
Melbourne, VIC, Australia
[redacted]

No potential conflict of interest relevant to this letter was reported.

1. Nerlekar N, Beale A, Harper RW. Colchicine — a short history of an ancient drug. Med J Aust 2014;201:687-8.
2. Nidorf SM, Eikelboom JW, Budgeon CA, Thompson PL. Low-dose colchicine for secondary prevention of cardiovascular disease. J Am Coll Cardiol 2013;61:404-10.

DOI: 10.1056/NEJMc1714635

THE EDITORIALIST REPLIES: O'Neill and Cooper as well as Nerlekar and Harper provide commentary on the recent report on CANTOS and the accompanying editorial. Both letters point to the observation of an increased risk of serious

Confusion regarding the meaning of the term *left ventricular filling pressure* given the nonequivalence of left ventricular end-diastolic pressure and mean left atrial pressure

Sato et al[1] have compared the ability of algorithms from the 2009 and 2016 American Society of Echocardiography (ASE) and European Association of Cardiovascular Imaging (EACI) diastolic function guidelines to predict elevation of left ventricular (LV) end-diastolic pressure (LVEDP). The study group was 460 consecutive patients who underwent echocardiography and left heart catheterization within a 24-hour period, and an *elevated LVEDP* was defined as >16 mm Hg. One of the study conclusions was that the 2016 recommendations were superior to the 2009 recommendations in detecting and grading elevated LVEDP. However, the appropriateness of the use of LVEDP rather than left atrial (LA) pressure/pulmonary capillary wedge pressure (PCWP) in this study requires further consideration, particularly as the ASE and EACI 2016 guidelines specifically make the points that LVEDP and LA pressure are not the same and that the Doppler variables which correlate with LVEDP are different to those that correlate with LA pressure. Moreover, the use of LVEDP by Sato et al is at variance with a recently published study by Andersen et al which also assessed the accuracy of the 2016 guideline predictions but where pressures were a mixture of PCWP and LV preA pressure.[2] Also divergent between the studies of Sato et al and Andersen et al was that >16 mm Hg was used as the cutoff for an abnormal LVEDP in the former study, whereas >12 mm Hg was used as the cutoff for an abnormal PCWP (and LV preA pressure) in the latter study. A PCWP cutoff of >12 mm Hg was in fact the basis of the 2016 ASE and EACI guidelines,[3] whereas a PCWP >12 mm Hg and an LVEDP >16 mm Hg were the separate cutoffs recommended for a diagnosis of elevation proposed by the European Society of Cardiology in 2007.[4]

Sato et al do attempt to address the appropriateness of their use of LVEDP in the discussion of their paper. However, after suggesting that LVEDP was chosen because "it is directly responsible for LV preload," the authors go on to say that "pulmonary capillary wedge and left atrial pressure closely follow LVEDP" and "preference of one versus the other marker of LV filling pressure is of little relevance." An attempt to justify the equivalence of LVEDP and PCWP by the authors using a subset of their study group who also had right heart catheterization was reported, in which PCWP and LVEDP were found to be correlated with an r value of 0.82. However, not only does an r value of 0.82 not support that 2 variables are interchangeable, but closer inspection of the LVEDP versus PCWP scatter plot reveals a substantial spread of points around the regression line. Moreover, the regression line does not represent the line of unity, and superimposing a line of unity on the scatter plot demonstrates that the LVEDP is in fact systematically, although not uniformly, higher than the PCWP.

Although mean LA pressure is indeed very closely related to LVEDP in the normal young adult and can be similar to the LVEDP in the presence of heart disease, it has been known for more than 50 years that the LVEDP can be higher than the LA pressure in the setting of an abnormal left ventricle and a substantial LA contribution to LV filling.[5] Indeed, in the original description of this phenomenon by Braunwald et al, the LVEDP was higher than the mean LA pressure in all subjects; the pressure difference ranged from 1 to 18 mm Hg, and the average pressure difference was 9 mm Hg.[6] Inspection of the data of Sato et al shows that LVEDP exceeded the PCWP in the majority of subjects and in some subjects by >10 mm Hg. That LVEDP and PCWP cannot be assumed to be equivalent in an individual is of vital importance given that an increase in LVEDP is not only a more sensitive marker than LA pressure for LV dysfunction, but the combination of a normal mean LA pressure and a high LVEDP is a contraindication to diuretic use even in the setting of dyspnoea.[5] That there is a substantial degree of atrial contribution to LV filling and thus likely a discrepancy between the LVEDP and PCWP can be determined simply in an individual subject using the transmitral A wave as a guide to the extent of the atrial contribution.

Finally, 2 methodological points: First, any pressure measurement requires a zero reference point, and to enable comparison between studies, this zero point needs to be the same; however, whereas Anderson et al do describe their zero reference point method,[2] Sato et al make no mention of a zero reference point in their methods section.[1] Second, fasting prior to catheterization, as was the protocol for the study of Sato et al, can lead to dehydration, in which case LA pressure and LVEDP measurements may both underestimate their levels in the nonfasting state.[5]

Am Heart J 2018;e1–e2.
0002-8703

http://dx.doi.org/10.1016/j.ahj.2017.08.025

Nitesh Nerlekar, MB, BS
Roger E. Peverill, MB, BS, PhD
Monash Cardiovascular Research Centre
MonashHeart and Department of Medicine (School of Clinical Sciences at Monash Health)
Monash University and Monash Health
Clayton
Victoria, Australia
E-mail: [redacted]

References

1. Sato K, Grant ADM, Negishi K, et al. Reliability of updated left ventricular diastolic function recommendations in predicting elevated left ventricular filling pressure and prognosis. Am Heart J 2017;189:28-39.

2. Andersen OS, Smiseth OA, Dokainish H, et al. Estimating left ventricular filling pressure by echocardiography. J Am Coll Cardiol 2017;69(15):1937-48.
3. Nagueh SF, Smiseth OA, Appleton CP, et al. Recommendations for the evaluation of left ventricular diastolic function by echocardiography: an update from the American Society of Echocardiography and the European Association of Cardiovascular Imaging. J Am Soc Echocardiogr 2016;29(4):277-314.
4. Paulus WJ, Tschope C, Sanderson JE, et al. How to diagnose diastolic heart failure: a consensus statement on the diagnosis of heart failure with normal left ventricular ejection fraction by the Heart Failure and Echocardiography Associations of the European Society of Cardiology. Eur Heart J 2007;28:2539-50.
5. Peverill RE. "Left ventricular filling pressure(s)"—ambiguous and misleading terminology, best abandoned. Int J Cardiol 2015;191: 110-3.
6. Braunwald E, Frahm CJ. Studies on Starling's law of the heart IV. Observations on the hemodynamic functions of the left atrium in man. Circulation 1961;3:566-71.

2. The LGE pattern can have both a subendocardial and a sub-epicardial distribution with areas of completely normal-appearing myocardium in between segments of LGE.
3. The chronic phase usually has basal thinning of the left ventricle.

As pointed out by Dr. Aneja, the guidelines appropriately advise the insertion of an implantable cardioverter defibrillator in a cohort such as that detailed in our study (4), in additional to other therapy that may modify the arrhythmic substrate (5). Indeed, experience from this institution and others have shown that once a patient is confirmed to have a high probability of having cardiac sarcoidosis by imaging, clinicians often choose to utilize implantable cardioverter defibrillator therapy for preemptive prevention of sudden cardiac death from serious arrhythmias (5).

Tomas G. Neilan, MD*
Raymond Kwong, MD, MPH
*Department of Cardiology
Massachusetts General Hospital
[redacted]
Boston, Massachusetts 02114
E-mail: [redacted]

http://dx.doi.org/10.1016/j.jcmg.2015.05.016

Please note: Both authors have reported that they have no relationships relevant to the contents of this paper to disclose.

REFERENCES

1. Neilan TG, Farhad H, Mayrhofer T, et al. Late gadolinium enhancement among survivors of sudden cardiac arrest. J Am Coll Cardiol Img 2015;8:414–23.

2. Watanabe E, Kimura F, Nakajima T, et al. Late gadolinium enhancement in cardiac sarcoidosis: characteristic magnetic resonance findings and relationship with left ventricular function. J Thorac Imaging 2013;28:60–6.

3. Patel MR, Cawley PJ, Heitner JF, et al. Detection of myocardial damage in patients with sarcoidosis. Circulation 2009;120:1969–77.

4. Epstein AE, Dimarco JP, Ellenbogen KA, et al. ACC/AHA/HRS 2008 guidelines for device-based therapy of cardiac rhythm abnormalities: executive summary. Heart Rhythm 2008;5:934–55.

5. Osborne MT, Hulten EA, Singh A, et al. Reduction in (1)(8)F-fluorodeoxyglucose uptake on serial cardiac positron emission tomography is associated with improved left ventricular ejection fraction in patients with cardiac sarcoidosis. J Nucl Cardiol 2014;21:166–74.

CT Coronary Angiography in Kidney Transplantation Candidates

We read with interest the study by Winther et al. (1) who conclude that rather than stress testing, either coronary computed tomographic angiography (CTA) alone or combined with single-photon emission computed tomography (SPECT) should be considered in kidney transplantation candidates. We believe that such a conclusion is premature and warrants consideration of several important issues.

Firstly, coronary CTA is recommended for symptomatic patients at low to intermediate risk of coronary artery disease (CAD) (2). Chronic kidney disease (CKD) patients have a high prevalence of CAD with 37% to 53% having obstructive stenosis on invasive coronary angiography (ICA) (3). The major utility of coronary CTA lies in its ability to exclude obstructive CAD due its high negative predictive value, but has low specificity for detecting obstructive CAD and increases ICA rates compared to a stress testing strategy. In this study, ICA revealed only a 22% incidence of obstructive CAD which may represent a lower risk cohort possibly explained by the low rate of diabetes (33%) which is the most significant predictor of CAD in CKD (4). Furthermore, despite the low CAD prevalence, there was a 29% false positive rate on coronary CTA in part driven by an 18% rate of uninterpretable segments. Therefore, the results of this study may not be generalizable to all potential transplant recipients and may underestimate the false positive rate in higher risk CKD patients.

Secondly, there is no clear association between asymptomatic CAD and prognosis in CKD patients and controversy exists regarding the management of CAD in this population. Screening should only be performed if the result changes management with subsequent improved outcomes. The presence of CAD may result in omission from transplantation listing (5) yet it is unclear whether CAD in CKD impacts survival. Contemporary data suggests no association with reduced survival after observation for up to 4 years (3). There remains equipoise regarding management: if patients are suitable for revascularization, delays to transplantation result from the need for antiplatelet therapy or rehabilitation if surgery is performed. Therefore, if an initial coronary CTA screening strategy is employed, the diagnosis of CAD may result in unnecessary transplantation delay with unintentional harmful effects.

Thirdly, Winther et al. (1) suggest a hybrid approach with coronary CTA and SPECT to improve the low specificity of coronary CTA alone in detecting myocardial ischemia. A drawback of this approach is a high radiation dose, which is not reported in this study. Stress echocardiography provides a radiation-free alternative with superior specificity and more accurate assessment of left ventricular ejection fraction, an independent predictor of survival (3).

Finally, it is not a diagnostic test that influences outcome but its ability to lead to appropriate intervention (medical therapy ± revascularization). Although Winther et al. (1) have shed light on the diagnostic accuracy of coronary CTA in CKD patients, no data is provided regarding any intervention or effect on prognosis of a coronary CTA-guided diagnostic approach. Therefore, we believe it is premature to promote an initial coronary CTA diagnostic strategy until results of future research becomes available that investigates the influence of intervention on coronary CTA findings to improve outcomes.

Nitesh Nerlekar, MBBS*
Arthur Nasis, MBBS, PhD
*Monash Heart
Monash Medical Centre
246 Clayton Road
Clayton 3168
Victoria, Australia
E-mail: [redacted]

http://dx.doi.org/10.1016/j.jcmg.2015.06.026

Please note: Both authors have reported that they have no relationships relevant to the contents of this paper to disclose.

REFERENCES

1. Winther S, Svensson M, Jorgensen HS, et al. Diagnostic performance of coronary CT angiography and myocardial perfusion imaging in kidney transplantation candidates. J Am Coll Cardiol Img 2015;8:553–62.

2. Liew GY, Feneley MP, Worthley SG. Appropriate indications for computed tomography coronary angiography. Med J Australia 2012;196:246–9.

3. Lentine KL, Costa SP, Weir MR, et al. Cardiac disease evaluation and management among kidney and liver transplantation candidates: a scientific statement from the American Heart Association and the American College of Cardiology Foundation: endorsed by the American Society of Transplant Surgeons, American Society of Transplantation, and National Kidney Foundation. Circulation 2012;126:617–63.

4. de Albuquerque Seixas E, Carmello BL, Kojima CA, et al. Frequency and clinical predictors of coronary artery disease in chronic renal failure renal transplant candidates. Ren Fail 2015;37:597–600.

5. Patel RK, Mark PB, Johnston N, et al. Prognostic value of cardiovascular screening in potential renal transplant recipients: a single-center prospective observational study. Am J Transplant 2008;8:1673–83.

THE AUTHORS REPLY:

We thank Drs. Nerlekar and Nasis for their interest in our paper. We compared the diagnostic accuracy of coronary computed tomographic angiography (CTA) and single-photon emission computed tomography (SPECT) against invasively verified obstructive coronary artery disease (CAD) in kidney transplantation candidates (1).

We agree that our study explores the utility of coronary CTA beyond the conventional area of indications. Currently, coronary CTA is used in the general population to rule out CAD in patients with a pre-test risk of obstructive CAD between 15% and 50%, which is comparable to the prevalence of CAD in kidney transplantation candidates (2). Furthermore, CTA is a rapidly developing technique and recent developments enable combined evaluation of coronary arteries and aorta/pelvic vessels using a single contrast dose. The fact that many hospitals are already using CTA for pre-transplantation evaluation of pelvic vessel facilitates primary coronary evaluation without use of supplementary noninvasive test and with only little extra contrast media and radiation dose.

Despite the fact that coronary CTA was performed in all patients without pre-test selections, we demonstrated that coronary CTA is a reliable test with high sensitivity, high negative predictive value, and similar positive predictive value to diagnose obstructive CAD compared to SPECT. A strategy with pre-test exclusion of patients with a high irregular heart rate or a high calcium score would also have increased the specificity in our study.

We agree with Drs. Nerlekar and Nasis that the evidence of an association between asymptomatic CAD and prognosis in this cohort is lacking. It might be due to bias in retrospective study designs, low sensitivity of noninvasive stress tests, and the inability of invasive coronary angiography to detect nonobstructive CAD. Nonetheless, De Lima et al. (3) demonstrated a prognostic value by invasive coronary angiography in an almost similar population and interestingly also by risk factors but not by SPECT or stress echocardiography. Even so, noninvasive stress tests are currently recommended as diagnostic tools in all guidelines. In general, coronary CTA has an excellent prognostic value for future coronary events, but we agree that specific data for patients with chronic kidney disease are needed (2).

Coronary evaluation of transplantation candidates will remain controversial as long as no studies have firmly demonstrated that the potential benefit outweighs the risk. In the meantime, we believe that CTA can substitute for the stress test and have a pivotal role as an initial evaluation tool in kidney transplantation candidates.

Simon Winther, MD, PhD*
My Svensson, MD, PhD
Hanne Skou Jørgensen, MD
Kirsten Bouchelouche, MD, DMSc
Lars Christian Gormsen, MD, PhD
Birgitte Bang Pedersen, MD, PhD

International Journal of Cardiology 209 (2016) 7–8

Contents lists available at ScienceDirect

International Journal of Cardiology

journal homepage: www.elsevier.com/locate/ijcard

Correspondence

Percutaneous closure of three atrial septal defects with three interleaved atrial septal occluders in an adult patient

Nitesh Nerlekar *, Om Narayan, James Sapontis, Michael Stokes, Sheran A. Vasanthakumar, Philip M. Mottram, Richard W. Harper

[a] Monash Cardiovascular Research Centre, Department of Medicine Monash Medical Centre, Monash University, Southern Health, 246 Clayton Road, Clayton, 3168, VIC, Australia
[b] MonashHeart, 246 Clayton Road, Clayton, 3168, VIC, Australia

ARTICLE INFO

Article history:
Received 31 December 2015
Accepted 5 January 2016
Available online 12 January 2016

Keywords:
Atrial septal defect
Percutaneous closure

A 28-year-old previously well female underwent transthoracic echocardiogram for evaluation of worsening dyspnoea. She had significant right-sided chamber enlargement with left to right inter-atrial shunting noted on colour Doppler. Follow up transoesophageal echocardiogram (TEE) demonstrated three separate secundum type atrial septal defects (ASDs) spanning the entire atrial septum: A large central ASD (18 mm), a smaller superior ASD (10 mm) and a third inferoposterior ASD (13 mm) (Panel A). Given the extensive nature of the defects, her symptoms and right heart dysfunction, surgical ASD closure was recommended. The patient strongly opposed surgical closure and due to persisting dyspnoea and worsening right ventricular function, it was decided to attempt percutaneous closure. (See Fig. 1.)

The procedure was performed under general anaesthesia with TEE guidance. Venous access was obtained with three right-sided 8-French venous sheaths. Each ASD was sized with balloon inflation to observe for residual leak. Due to the separate locations of the ASDs with significant residual shunting after balloon sizing, it was felt that three devices would be required to adequately seal the septum.

As previously recommended [1] the smallest defects were attempted for closure first with the aim of sandwiching the device within the larger defect sequentially. However, this manoeuvre resulted in an altered profile that would not allow interleaving of the discs as the septal tissue was too flimsy. Therefore the largest central defect was crossed instead with an 18 mm Occlutech device (Occlutech, Helsingbord, Sweden) and partially deployed. This essentially created a firm 'pseudo-septum' for which to then attach the other two devices. On a second sheath, a 13 mm Occlutech device was then pulled down across the inferoposterior ASD. The RA disc of this device was opened below the LA disc of the central device in order to capture the LA disc (of the central device) within it. The same technique was utilised for the superior ASD device (12 mm Occlutech) whereby the RA disc of this device was again opened below the LA disc of the central device to capture this disc within it.

All devices remained partially deployed and re-assessment by 2D and 3D TEE was used to confirm that the inferoposterior device had septal tissue posteriorly; the central device LA disc was sandwiched between the inferoposterior and superior device discs (encompassing the RA disc of both); and the superior device discs straddled the aortic rim (Panel B–D). There was no interference to the aortic root or mitral valve, and caval and pulmonary vein flow was not compromised. No residual peri-device leak was noted. Follow up transthoracic imaging at one month demonstrated stable device positioning with complete symptom resolution and no residual shunt.

There are very few reports of using three or more ASD closure devices, the majority of which have been in a paediatric setting [2,3] or performed as staged sequential procedures [4]. In an era of expanded use of transcatheter techniques that are preferable to open surgical intervention, this case highlights an alternative method that is feasible with the necessary and complementary use of TEE imaging to guide successful intervention.

Conflict of interest

The authors have no disclosures or conflicts of interest.

References

[1] Q. Cao, W. Radtke, F. Berger, W. Zhu, Z.M. Hijazi, Transcatheter closure of multiple atrial septal defects. Initial results and value of two- and three-dimensional transoesophageal echocardiography, Eur Heart J 21 (2000) 941–947.
[2] M.T. Bramlet, M.H. Hoyer, Single pediatric center experience with multiple device implantation for complex secundum atrial septal defects, Catheter Cardiovasc Interv 72 (2008) 531–537.
[3] C. Arcidiacono, G. Gaio, G. Butera, M. Carminati, Percutaneous closure of multiple secundum atrial septal defects using 3 amplatzer atrial septal occluder devices: evaluation by live transthoracic 3-dimensional echocardiography, Circ Cardiovasc Imaging 1 (2008) e15–e16.
[4] Y. Kijima, T. Akagi, K. Nakagawa, Y. Takaya, H. Oe, H. Ito, Three-dimensional echocardiography guided closure of complex multiple atrial septal defects, Echocardiography 31 (2014) E304–E306.

* Corresponding author at: Monash Heart, Monash Medical Centre, 246 Clayton Road, Clayton, 3168, VIC, Australia.
E-mail address: [redacted]

http://dx.doi.org/10.1016/j.ijcard.2016.01.116

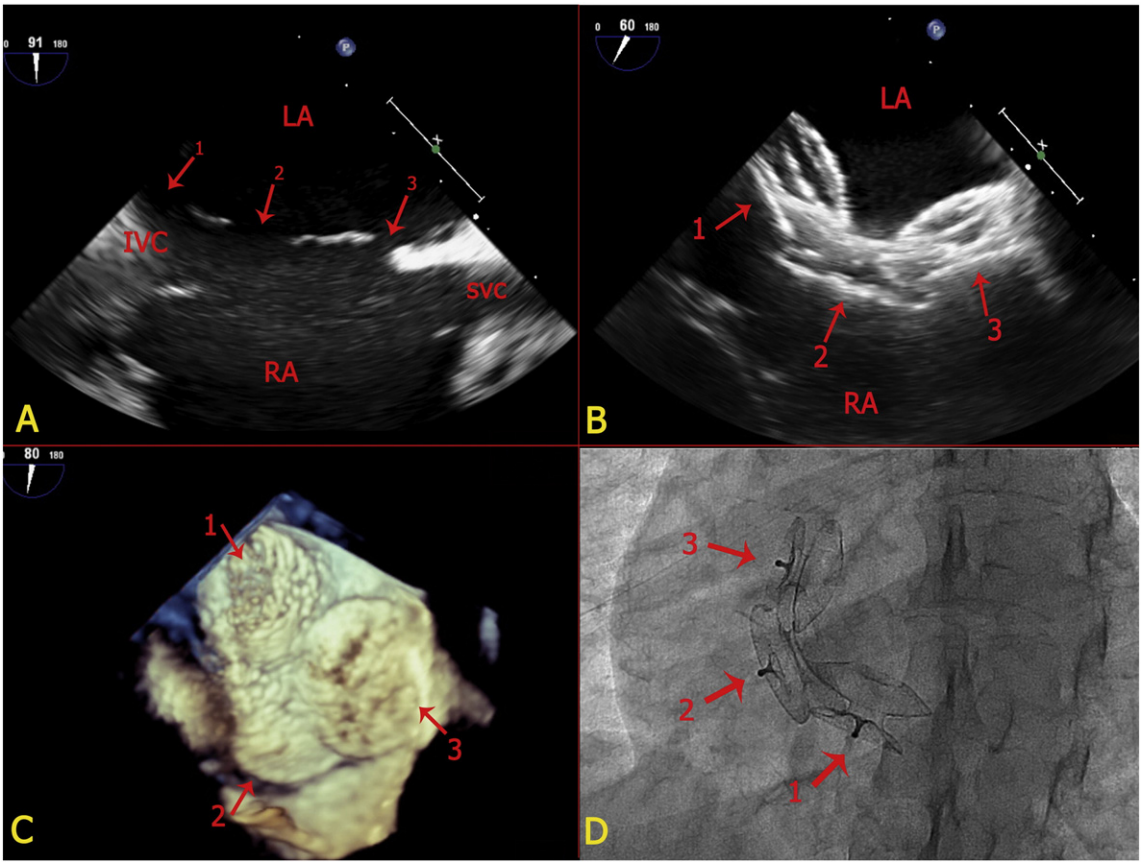

Fig. 1. A) Mid-esophageal bicaval view pre-procedure. B) Post deployment 2D image in the mid-esophageal bicaval view. C) Post-deployment 3D reconstruction of the atrial septum as seen from the left atrial side. D) Fluoroscopic cine image as seen from left anterior oblique-caudal view. 1—inferoposterior ASD, 2—central ASD, 3—superior ASD. LA — Left atrium, RA — Right atrium, SVC — Superior vena cava, IVC — inferior vena cava.

MRI in Patients with Cardiac Implantable Electronic Devices

Rahul G. Muthalaly, MBBS, MPH • Nitesh Nerlekar, MBBS, MPH • Yin Ge, MD • Raymond Y. Kwong, MD, MPH • Arthur Nasis, MBBS, MD, PhD

From the Monash Cardiovascular Research Centre, Monash University and MonashHeart, Monash Health, Clayton, Victoria, Australia (R.G.M., N.N., A.N.); and Cardiovascular Division, Brigham and Women's Hospital and Harvard University, 75 Francis St, Boston, MA 02115 (R.G.M., Y.G., R.Y.K.). Received February 1, 2018; revision requested March 12; final revision received May 30; accepted June 1. **Address correspondence to** R.G.M. (e-mail: *rahul.muthalaly@gmail.com*).

R.G.M. supported by Doctors in Training research grant from Avant Mutual and a research grant from Monash Health. N.N. supported by National Heart Foundation of Australia and National Health and Medical Research Council. These funding bodies had no role in the preparation of this manuscript.

Conflicts of interest are listed at the end of this article.

Radiology 2018; 289:281–292 • https://doi.org/10.1148/radiol.2018180285 • Content codes: MR CA

Indications for MRI have grown considerably in recent years. However, many patients with cardiac implantable electronic devices are denied imaging due to physician misinterpretation of the risks associated with MRI. This review discusses the theoretical basis for the perceived risk by exploring preclinical literature. It then presents a detailed examination of the true rates of adverse events in clinical studies across both MR nonconditional (legacy) and MR conditional devices. Indeed, many of these adverse events are rare, nonexistent, and/or clinically insignificant in the wealth of published data. The authors then address image quality and the constituents of a safety checklist that institutions should consider when performing MRI in patients with a cardiac implantable electronic device. Lastly, the authors conclude with an overview of future directions for advancement in the field.

Online supplemental material is available for this article.

Online SA-CME • *See www.rsna.org/learning-center-ry*

Learning Objectives:

After reading the article and taking the test, the reader will be able to:

- Identify the potential complications of MRI in patients with a cardiac implantable electronic device (CIED)
- Recognize factors that impart a higher risk for patients with CIED undergoing MRI
- Describe the important components of a safe protocol for subjecting patients with CIED to MRI

Accreditation and Designation Statement

The RSNA is accredited by the Accreditation Council for Continuing Medical Education (ACCME) to provide continuing medical education for physicians. The RSNA designates this journal-based SA-CME activity for a maximum of 1.0 *AMA PRA Category 1 Credit™*. Physicians should claim only the credit commensurate with the extent of their participation in the activity.

Disclosure Statement

The ACCME requires that the RSNA, as an accredited provider of CME, obtain signed disclosure statements from the authors, editors, and reviewers for this activity. For this journal-based CME activity, author disclosures are listed at the end of this article.

MRI is the standard imaging modality for an increasing number of medical conditions owing to its excellent spatial resolution, tissue characterization, and lack of ionizing radiation. However, MRI in the presence of a cardiac implantable electronic device (CIED) still causes trepidation owing to concerns regarding the interaction between electromagnetic fields and the CIED. Denial of MRI services is particularly consequential as 50%–75% of patients with a CIED are estimated to require an MRI during their lifetime (1).

Early reports of deaths associated with MRI in patients with permanent pacemakers (PPMs) and implantable cardioverter defibrillators (ICDs) resulted in an inflexible classification of absolute contraindication to CIED for MRI among clinicians, institutions, and professional associations (2,3). However, these deaths occurred during unmonitored MRI examinations and were thus inconclusive regarding etiology. In at least three cases, the deaths were presumed related to spontaneous fatal arrhythmia (3).

The American Society for Testing and Materials uses three specific terms to delineate the safety of products in an MRI environment: MR safe, MR conditional, and MR unsafe (Table 1) (4). No PPMs or ICDs have been declared MR safe by the Food and Drug Administration (FDA). *MR nonconditional* is a term used in the 2017 Heart Rhythm Society guidelines, which refers to objects that have not been declared MR conditional or safe (5). *MR unsafe* refers to objects known to pose a risk in all MRI environments. *MR conditional* denotes an item that poses no hazards in a specified MRI environment with specified conditions of use. The first MR conditional CIED system was approved by the FDA in 2011 (6).

The 2017 Heart Rhythm Society guidelines provide the most up-to-date recommendations for performance of MRI in CIED (5). They make a class I (strong) recommendation for MRI with MR conditional systems only in the context of a standardized institutional workflow. For MR nonconditional systems, they make a class IIa (moderate) recommendation that it is reasonable to perform MRI in the absence of fractured, epicardial, or abandoned leads. However, research suggests persistent reluctance among clinicians and institutions to perform MRI

Abbreviations

CIED = cardiac implantable electronic device, FDA = Food and Drug Administration, ICD = implantable cardioverter defibrillator, POR = power-on reset, PPM = permanent pacemaker, SAR = specific absorption rate

Summary

This review details the current evidence regarding the performance of MRI in patients with cardiac implantable electronic devices.

Essentials

- The presence of a pacemaker or implantable cardioverter defibrillator has traditionally been a contraindication for MRI.
- In the past 10 years, evidence has proven concern for serious adverse events to be overstated, with large studies showing limited and manageable side effects.
- Newer MR conditional devices are now commonly implanted, but patients with older MR nonconditional devices can usually undergo MRI safely with proper precautions.
- Future work will focus on MR safe devices that have no conditions on their use and on further exploration of the safety of leadless device designs.

in patients with MR nonconditional CIEDs (7,8). Experience and technology have advanced rapidly, and these perspectives need to be modified accordingly (9,10).

This review provides a brief summary of the basis for MRI interaction with CIEDs followed by a discussion of the current clinical evidence regarding both MR conditional and MR nonconditional products (11,12). Finally, we discuss the elements of an institutional checklist and outline evolving areas in the field.

Interaction between MRI Units and Implantable Devices

MRI utilizes a static magnetic field that orients hydrogen protons along the axis of the imager–this field is described in tesla and ranges from 0.5 to 10.5 T, about 140 000 times the strength of the Earth's magnetic field (for 7-T imagers). Separate gradient coils vary the magnetic field locally across different sections of the body. Once the atoms align, energy in the form of a specific radiofrequency pulse causes the magnetic vector to deflect. When the radiofrequency pulse is removed, the magnetic vector returns to its resting state, which causes a signal to be produced. For a full explanation of MRI technology, readers are referred to one of many high-quality review articles (13).

The MR imager produces three electromagnetic fields, which can interfere with CIED: the static magnetic field (measured in tesla), the radiofrequency field (measured by specific absorption rate [SAR] in watts per kilogram), and the pulsed gradient field (measured in tesla per meter per second). The hypothetical consequences of these fields interacting with CIED are discussed below and summarized in Table 2.

Mechanical Displacement

Concern about CIEDs in MRI was initially driven by the concern of mechanical displacement of the device due to the static magnetic field acting on the ferromagnetic components of CIEDs (14). Ferromagnetic components are present in the batteries and reed switches (a magnetically activated switch that places the device in "magnet mode") of CIEDs. The effect of the magnetic field on ferromagnetic components has been assessed both in vitro and through symptoms of pulling or movement in patients. However, concern regarding displacement has proven unjustified for PPMs made after 1995, because the ferromagnetic content of these devices is so low that they only experience forces within the range of gravity (15,16). ICDs have a higher ferromagnetic content and consequently generate forces that are marginally higher than gravity, yet, these are still unlikely to be clinically significant (15). It is important to note that CIED lead tips are unaffected by static magnetic fields as they have no ferromagnetic materials. This negates the possibility of the lead becoming dislodged and failing to capture (17).

Device Reprogramming

MRI can reprogram CIEDs in two main ways. First, the static magnetic field can activate the reed switch. The reed switch is normally used to reset the pacemaker into an asynchronous pacing mode and disable antitachyarrhythmia function in response to a magnet being placed on the patient's skin (magnet mode). Activation of the reed switch prevents interference with CIED function during electrocautery surgery. Additionally, pacemakers can undergo power-on reset (POR). PORs are electrical resets designed for safety in the event of battery depletion or circuit malfunction. PORs typically reset the device to inhibited pacing (pacing mode VVI). POR and reed switch activation are detected by interrogating the pacemaker after the MRI and/or noticing changes in the patient's vital signs during imaging.

Reed Switch Closure

A reed switch "closes" in a magnetic field causing current to flow through it. PPMs contain reed switches that, when closed, set the pacemaker to a preprogrammed function. This is typically asynchronous (pacing mode VOO) pacing. In asynchronous pacing, the device paces the ventricle at a preprogrammed rate continuously. In addition, the reed switch suspends antitachyarrhythmia therapies for ICDs. The static magnetic field is capable of closing reed switches. In asynchronous mode with antitachyarrhythmia therapies off, devices will not detect a ventricular arrhythmia, spontaneous or MRI induced, and will not treat the arrhythmia (18). There is also a theoretical danger of competitive pacing between the heart's intrinsic rhythm and the preprogrammed asynchronous pacing. This can lead to proarrhythmia due to R-on-T phenomena in patients who have a high heart rate. Reed switches are unpredictable in the static field strengths produced by clinical MRI, with half of them initially closing and then reopening later during the imaging (19–21). For this reason, most protocols disable the magnet response when reprogramming the CIED prior to MRI so that the static field does not activate the reed switch (22).

Power-On Reset

A POR is a specific type of reprogramming that reverts the device to factory default settings when battery voltage falls below a critical level or damage to the circuits is detected. This is a failsafe feature. The settings to which the device reverts vary by

Table 1: Definitions Related to Cardiac Implantable Electronic Devices and MRI

Term	Definition
MR safe	Objects that pose no known hazards in all MRI environments
MR conditional	Objects that pose no hazards in a specified MRI environment with specified conditions of use
MR unsafe	Objects known to pose a risk in all MRI environments
MR nonconditional	A term used in the 2017 Heart Rhythm Society guidelines that refers to objects that have not been declared MR conditional or MR safe
Asynchronous pacing	A pacing mode where the device delivers stimuli at preset intervals independent of intrinsic cardiac signals
Inhibition pacing	A pacing mode where the device only delivers stimuli when no intrinsic cardiac signals are sensed
Antitachyarrhythmia therapies	Therapies delivered by a device that can terminate arrhythmias. Types of therapy include antitachycardia pacing and defibrillation
Pacing capture threshold	The minimum electrical stimulus needed to consistently depolarize or "capture" the myocardium. This is measured in volts (V)
Lead impedance	A measure of the opposition to current flow through the device's leads. Decreased lead impedance increases the drain on the battery. This is measured in ohms (Ω)
Sensing amplitude	A measure of a device's ability to detect cardiac signals. This is measured in millivolts (mV)

manufacturer. Many devices reset to inhibition pacing, with antitachyarrhythmia therapy on, where the device will initiate therapies for life-threatening arrhythmias. This is problematic when electrical induction in the leads causes inappropriate sensing of induction as intrinsic cardiac activity and results in inhibition of required pacing. Additionally, in patients needing high intrinsic heart rates (such as children), the factory default may not provide the required cardiac output. However, devices are usually easy to reprogram after the MRI following a POR event.

Induction of Currents and Changes in the Electrocardiogram

The gradient magnetic and radiofrequency fields can electromagnetically couple with leads to induce electric currents through the "antenna effect." These currents can alter the recorded electrogram, stimulate dangerous arrhythmias, and permanently interfere with ICD function (23,24). Induced currents can result in inhibition of pacing due to the device perceiving an intrinsic underlying rhythm on the electrogram (25). Furthermore, the induced artifactual current can be interpreted as ventricular arrhythmia with subsequent attempts to initiate antitachyarrhythmia therapy in ICDs (26). However, ICD therapy usually fails as the capacitor cannot charge due to "saturation" in the static magnetic field (27). Thus, the ICD may drain its battery while continuously attempting to charge a saturated capacitor.

There is a potential for induced currents to be substantial enough to cause life-threatening arrhythmia through rapid pacing. This potential was demonstrated in vitro by Erlebacher et al, who showed atrial pacing rates of 800 ppm due to the radiofrequency field detected on pacemaker interrogation (25). This was later replicated in a swine study, where a stable tachycardia of 200 beats per minute was induced for 10 seconds during 1.5-T MRI (28). Again, due to ICD therapy being impaired by the static magnetic field, an MRI-induced arrhythmia may not be treated by the ICD and result in battery drainage. Thus, most protocols call for the disabling of antitachyarrhythmia sensing and therapies to circumvent the problem of unnecessary shock or battery depletion.

Heating Effects

Another consequence of the radiofrequency field is deposition of heat energy, particularly at the lead tips, which can result in myocardial tissue damage. At an SAR of 4.0 W/kg–below most clinical scans, tissue heating in the absence of foreign materials (such as CIEDs) does not exceed 0.7°C (29). However, energy absorption changes in the presence of conducting materials. This makes temperatures difficult to predict. Consequences of myocardial tissue damage include changes in pacing threshold with subsequent loss of capture (where the pacing signal no longer depolarizes the myocardium), re-entrant arrhythmia induction, and myocardial perforation. Thus, these consequences are typically investigated in vitro by measuring temperature directly and in vivo by interrogating the pacemaker and measuring serum biomarkers of myocardial damage such as troponin. There are many variables in determining the degree of heating, including lead location and design, presence of abandoned leads, position in the imager, power and duration of the radiofrequency field, and rate of blood flow (28,30–32). In vitro phantom studies using "worst-possible" conditions have demonstrated severe heating at lead tips, with a maximal temperature of 88.8°C, though this was in a temporary pacing lead (33,34). Most in vitro studies demonstrate much milder heating in the range of 0.5°C or less (35). In a swine model, direct lead tip temperature measurements increased by up to 20.4°C (28). These temperatures were associated with changes in lead impedance. Despite this, there were no elevations in troponin or evidence of thermal injury at histologic examination. The absence of thermal injury around the lead tip has been demonstrated in other animal studies (36). In humans, there have been negligible effects on post-MRI troponin levels, with very few subjects experiencing increases in troponin above the normal limit (20,37). However, pacing capture thresholds before and after imaging undergo minor alterations, presumably due to MRI-induced thermal injury (38). Importantly, threshold changes are rarely clinically significant, and those that occur are usually temporary and do not require pacemaker reprogramming.

Table 2: Electromagnetic Fields Used in MRI, the Most Commonly Studied Field Strengths, Potential Effects on CIEDs, and Event Rates from In-Human Clinical Studies

Electromagnetic Field Type	Commonly Studied Strength	Effect on CIEDs	In-Human Event Rates*
Static magnetic field	1.5 T	Mechanical displacement; Device reprogramming	0 to 0.2% experience symptoms (31,32); 100% "magnet-mode" activation in reed-switch devices (25). 0 to 10.4% power-on reset rate (12,36)
Radiofrequency and gradient magnetic field	2.0 W/kg and 200 T/m/sec	Tissue heating; Induction of current	Up to 37% of leads with minor parameter changes. Almost none clinically significant (27); 13.5% have ventricular ectopy during scan. No sustained ventricular arrhythmias (45). 0 to 7% of devices record artifact as arrhythmia during scan (31,47)

Note.—CIED = cardiac implantable electronic devices.

* These event rates are derived from studies in experienced centers with appropriate protocols.

Clinical Studies of MR Nonconditional Devices

Pacemakers

Early clinical studies of MR nonconditional devices that were not specifically designed for the MRI environment (also known as legacy devices) began in the mid-1990s with single-digit sample sizes (39). These studies used low static field strengths (0.5 T) and limited imaging to nonthoracic regions (34,39,40). Additionally, these studies excluded pacemaker-dependent patients, those with recent (less than 3 months) implants, and those with abandoned or surgical epicardial leads. The early results were reassuring, with most events being reed-switch activation (magnet-response) and minor changes in lead parameters or battery voltage. Importantly, no major complications such as induced arrhythmias or inappropriate pacing inhibition were seen.

After these early reassurances, researchers in the mid-2000s conducted studies with larger numbers of patients. They also included thoracic and cardiac MR examinations, higher magnetic field strengths, and cardiac resynchronization devices (38,41). Again, the most common complications observed were clinically insignificant lead parameter and battery voltage changes, occasional symptoms around the implant site (such as vibration), activation of reed switches, and, uncommonly, PORs (Table 3) (20,38,41).

The MagnaSafe registry of 1500 MRI examinations and the Nazarian et al cohort of 2103 MRI examinations in patients with CIED constitute the largest studies to date with MR nonconditional devices (9,10). MagnaSafe demonstrated a remarkable lack of adverse events in its 1000 PPM MRI examinations, with no deaths, generator failures, lead failures, or loss of myocardial capture. The only complications seen in the pacemaker cohort were low rates of minor lead parameter changes (ranging from 0.8% to 16.4% depending on the parameter), spontaneously reverting atrial fibrillation, and PORs. It is notable that the MagnaSafe registry excluded thoracic MRI examinations, where energy absorption by the CIED is thought to be the greatest. However, low rates of adverse effects were observed in the Nazarian et al cohort that contained 257 thoracic scans (10,37). In Nazarian et al cohort of 880 patients with PPMs, one examination was terminated due to inappropriate inhibition in response to electromagnetic interference resulting in temporary bradycardia (10). There were no clinical consequences. Sommer et al attempted to relate change in lead impedance after MRI to myocardial injury by measuring troponin I levels. They found no overall increase in troponin levels after MRI (20). A lack of troponin increase after MRI has subsequently been observed by other investigators (26,37,42–45). Cohen et al were the first, to our knowledge, to include a control group that did not undergo MRI (46). They found that device parameter changes occur even without exposure to electromagnetic fields. The results of Cohen et al suggest baseline variation in CIED parameters, as opposed to myocardial injury, as a possible explanation for observed pre- and post-MRI differences (46). Thus, CIED parameter changes, while not unusual, should not be considered a clinically significant adverse event of MRI in CIED patients.

Symptoms of pulling, heating, vibration, and palpitations have been reported during MRI in patients with CIED. Very few correlate with clinical events, although the MRI examination may be stopped due to apprehension. In the MagnaSafe and Nazarian cohorts combined, only five instances of symptoms were experienced out of 3603 examinations (0.1%) (9,10). One of these patients experienced a pulling sensation associated with POR of the device and thus, the MRI was aborted. However, this patient had an old ICD implant from 1999. These devices are more prone to displacement due to their higher ferromagnetic content. The majority of literature has shown low or no symptom rates during MRI (20,44,47–49).

Reed switch activation is a largely accepted fact of MRI in devices that are not fitted with newer magnetic field–resistant Hall sensors. As discussed above, reed switch activation creates problems as the device will pace at a preprogrammed rate and fail to deliver therapies for potentially life-threatening arrhythmias. Thus, most protocols call for disabling of magnet response, which means that activation of a reed switch will have no effect. The inevitability of reed switch activation is reflected in the literature with an almost 100% occurrence and resultant pacing at the preprogrammed magnet-response rate if this setting cannot be disabled (10,20,40,50). One case series by Heatlie et al

Table 3: Summary of Major Studies of MRI Effects in MR Nonconditional Cardiac Implantable Electronic Devices

A: Pacemaker Studies with > 40 Patients

Year	First Author	No. of Patients with Pacemakers	Safety Findings
2000	Sommer (34)	44	Reed switch closure and minor battery voltage changes
2004	Martin (38)	54	Vibration and palpitations, reed switch closure and 37% with PCT change but only 9.4% with > 1 V change
2006	Nazarian (41)	31	Reed switch closure
2006	Sommer (20)	82	Reed switch closure, 8.5% with POR, 3.1% had PCT increase > 1 V, minor decrease in impedance and minor decrease in battery voltage
2008	Naehle (42)	44	Minor decreases in battery voltage and 16% with POR
2009	Mollerus (54)	52	Minor decrease in sensing amplitude and 7 patients with significant ectopy
2009	Naehle (59)	47	Minor decrease in PCT (0% > 1 V), minor impedance changes and a minor decrease in battery voltage
2010	Mollerus (47)	105	1 POR and a minor decrease in sensing amplitude
2010	Strach (85)	114	Reed switch closure
2012	Cohen (46)	109 with ICD or PPM	Reed switch closure
2013	Friedman (61)	171	Minor change in PCT, sensing amplitude and frequent ventricular ectopy during scans
2014	Kaasaleinen (86)	62	Reed switch closure and minor change in lead impedance
2014	Muehling (45)	356	Reed switch closure and 10.4% with POR
2015	Higgins (51)	196	3.5% with POR
2015	Sheldon (26)	40	2.5% with POR, 1 patient with artifact sensed as VF
2015	Shenthar (65)	177	Minor PCT changes and minor lead impedance changes
2016	Bertelson (83)	137	None
2016	Camacho (56)	74	3 patients with symptoms but no sequelae, electromagnetic noise in 7.1%
2017	Russo (9)	818	5 patients with spontaneously reverting AF, 6 patients with POR
2017	Nazarian (10)	880	8 PORs, reed switch closure, inhibition of pacing in pacing dependent patient, lead parameter changes not requiring revision/reprogramming, battery drainage

B: ICD Studies with > 20 Patients

Year	Author	No. of Patients with ICDs	Safety Findings
2006	Nazarian (41)	24	Reed switch closure
2010	Mollerus (47)	22	1 POR, 1 ICD arrhythmia log erased and minor decrease in sensing amplitude
2012	Cohen (46)	109 with ICD or PPM	Reed switch closure
2016	Camacho (56)	39	3 patients with symptoms but no sequelae, electromagnetic noise in 7.1%
2016	Dandamudi (64)	29	1 patient with chest pain
2017	Russo (9)	428	1 generator failure requiring replacement, 1 induced AF
2017	Nazarian (10)	629	1 POR, lead parameter changes, 1 pulling sensation in chest, reed switch closure, battery drainage

Note.—PCT = pacing capture threshold, POR = power-on reset, VF = ventricular fibrillation, ICD = implantable cardioverter defibrillator, AF = atrial fibrillation.

reported a patient inappropriately pacing at maximum voltage output at a rate of 100 ppm during cardiac MRI (48).

POR is a more sinister reprogramming complication of CIED during MRI. The reported rates of POR range from 0% to 16% (10,20,26,38,42,43,45,51,52). POR seems to be associated with older devices manufactured before 2002 (43,51). In most of these cases, the devices are reset to an inhibition mode (usually VVI). In VVI mode, the devices pace at the manufacturer's default rate, rarely causing clinical incident. However, the potential for lethal events does exist in pacing-dependent patients who experience POR and have pacing inhibited by inappropriate sensing of electromagnetic interference. In 2009, Gimbel et al described unexpected asystole in a pacemaker-dependent patient undergoing 3-T MRI of the head (53). Pacing resumed when the gradient field was removed, and the patient survived. This occurred in a pacemaker released in 2005, which is against the

trend that only devices older than 2002 are affected by POR. Thus, it is recommended that continuous electrocardiography, if available, and pulse oximetry should always be performed for pacemaker-dependent patients undergoing MRI. This allows identification of cases of inappropriate inhibition of pacemaker function.

There are no records of MRI-induced ventricular arrhythmia aside from ventricular ectopy (54). All of the sustained arrhythmias have been atrial fibrillation and/or flutter, with the MagnaSafe registry reporting six episodes of 1500 MR examinations (9). Furthermore, only one patient did not have a prior history of atrial fibrillation/flutter and it spontaneously resolved within 48 hours.

Implantable Cardioverter Defibrillators

There was initially greater concern in introducing ICDs to the MRI environment owing to their larger size and higher ferromagnetic content. However, after the early successes of MR nonconditional PPMs, testing began in 2004 with small cohorts of patients (55). ICDs were suspected to be associated with more displacement, greater battery voltage change, and the potential for inappropriate tachyarrhythmia sensing and therapies than PPMs. To reduce this, tachyarrhythmia sensing and therapies were disabled before the MRI examination (37,41).

Regarding ICD displacement, there have been no major lead or implant complications in ICD studies to date. Minor symptoms over the implant site have been reported at a rate similar to that of PPMs (10,56).

Inappropriate sensing of electromagnetic noise by the ICD as a shockable rhythm (usually ventricular fibrillation) is well documented. In one example, Burke et al found that nine of 14 patients with ICDs undergoing MRI recorded electromagnetic noise as fast ventricular tachycardia or ventricular fibrillation (57). None of these patients had clinical sequelae because the ICD therapies were programmed off. Burke et al found no difference in the energy required to terminate ventricular fibrillation before and after MRI, suggesting no interference with shock delivery. Other studies have found much lower rates of noise misinterpretation and, in the cases that do occur, they are clinically insignificant owing to appropriate pre-MRI programming (26,58,59). The importance of appropriate programming is highlighted by a case from the MagnaSafe registry (9). In that case, tachycardia therapy was not disabled during pre-MRI reprogramming. After MRI, the ICD could no longer be interrogated or reprogrammed and thus required immediate generator replacement. Retrospective evaluation determined that the device had interpreted MRI signals as ventricular fibrillation and had made repeated failed attempts to charge the capacitor, though no shocks were delivered due to capacitor saturation. Thus, after correct programming the risk of inappropriate sensing and therapy is extremely low.

Battery depletion has also proved to be a low-risk event. Most studies observe transient changes from before to after MRI, with a full recovery in many during follow-up (59,60). In the MagnaSafe registry, 7.2% of ICDs had an immediate battery voltage decrease of 0.04 V or greater; however, only 4.2% had persistent changes at 3–6-month follow-up, with a similar pattern observed in the Nazarian cohort (10). For perspective, at beginning of life a CIED battery will usually have 2.8 V of output. At approximately 2.0–2.4 V, the elective replacement indicator will be triggered, which leaves 6 months before the generator will begin to malfunction.

Contraindications to Imaging

Prior studies of patients with CIEDs have had strict exclusion criteria that developed from the theoretical risks as previously discussed. Previously discussed contraindications include patients with recent implants, epicardial and abandoned leads, high SARs, serial MRI examinations, pacemaker dependency, and thoracic imaging. Next, we examine current evidence in relationship to previously described contraindications.

Recent Implants

Time after implantation has been considered an exclusion criterion. Recent implantation of a CIED ranges from 6 weeks to 3 months (37,59). The purpose of a waiting period after implantation was to allow the lead tips to establish a fibrous sheath in the myocardium, thereby reducing the likelihood of lead dislodgement. Friedman et al prospectively compared outcomes in eight examinations of early pacemaker implants (< 6 weeks; range, 7–36 days) versus 211 examinations of older implants (mean, 1150 days) (61). They observed no major complications or troponin increase in any of the patients, nor any difference in lead parameters at 104 days follow-up. Comparable results were seen in 80 newly implanted leads in the MagnaSafe registry. These results are reassuring for those patients requiring urgent MRI after device implantation (9).

Epicardial and Abandoned Leads

Epicardial and abandoned leads were traditionally excluded from studies due to preclinical research demonstrating unpredictable heating in vivo. However, Higgins et al performed a retrospective review of 35 examinations in patients with abandoned leads undergoing head or spine MRI (62). Within 7 days of follow-up, they observed no symptoms or arrhythmias in these patients. In 10 of the patients who had their generators reconnected for clinical reasons, the largest capture threshold increase was 0.7 V in a ventricular lead. The authors concluded that there were no clinically significant sequelae from the MRI on the abandoned leads. Horwood et al found similar results in a cohort of 12 abandoned leads, which included three epicardial leads (63). Despite this observational data indicating limited risk, most studies still preclude patients with abandoned leads (56,64).

There is limited experience and literature regarding permanent surgical epicardial leads and thus, it is not possible to determine their safety. Temporary postsurgical epicardial leads that have been partially removed are not considered abandoned leads and are not considered contraindications to MRI (5).

High SARs

Most large prospective studies have placed limits on the radiofrequency field (measured in SAR). This was due to preclinical work that suggested a correlation between SAR and potential complications (29). Mollerus et al investigated this in a prospective study of 127 examinations with no SAR restrictions (me-

Table 4: MR Conditional Devices Approved by the U.S. Food and Drug Administration

Manufacturer	Pacemakers	Defibrillators/CRT	Leads
Biotronik (ProMRI)	Eluna 8 (DR-T and SR-T) Entovis (DR-T and SR-T) Edora 8 (DR-T and SR-T)	Iforia (VR-T DX and DR-T) Iperia (VR-T DX, DR-T and HF-T) Inventra (VR-T DX and HF-T) Intica (DX and CRT DX) Ilivia (VR-T, DR-T and HF-T)	Setrox S (53,60) Solia S (45,53,60) Corox OTW Sentus ProMRI Protego (ICD) Linoxsmart (ICD) Plexa ProMRI (ICD)
Boston Scientific (ImageReady)	Accolade MRI Essentio MRI Vitalio MRI Proponent MRI Advantio Formio Ingenio	Emblem MR imaging *S*-ICD Resonate HF/X4/EL Perciva and Perciva HF Vigilant ×4/EL Autogen Mini/EL/X4 Dynagen EL/Mini/X4 Inogen Mini/EL/X4 Origen Mini/EL/X4 Charisma ×4	Ingevity MR imaging Endotak Reliance DF4 (ICD) Fineline II Acuity ×4
Medtronic (SureScan)	Advisa MRI (DR and SR) Revo MRI Micra Transcatheter Pacer	Visia AF MRI VR Evera MRI XT DR Evera MRI S DR and VR Amplia MRI Quad CRT-D Amplia MRI CRT-D Complia MRI Quad CRT-D	5086 MRI 5076 6947M (ICD) 6935M (ICD) 4196 (CRT) 4296 (CRT) 4396 (CRT) 4298 (CRT) 4398 (CRT) 4598 (CRT)
Sorin	None available in United States	None available in United States	None available in Unites States
St Jude Medical/Abbott	Assurity MRI	Ellipse MRI	Tendril MRI LPA1200M Durata 7120Q and 7122Q (ICD) Optisure LDA220Q and LDA210Q (ICD)

Note.—Data received from representatives of each company and by examining their online materials. ICD = implantable cardioverter defibrillator, CRT = cardiac resynchronization therapy.

dian SAR, 2.5 W/kg; interquartile range, 1.3–3.2 W/kg) in both PPMs and ICDs (47). They found that SAR poorly predicted safety outcomes for these patients. At present, many studies continue to impose SAR limits, usually to less than 2.0 W/kg, to limit heating and electromagnetic induction (45,65). However, the recently published Nazarian et al cohort removed SAR restrictions during recruitment owing to a lack of evidence for harm beyond normal SAR limits in non-CIED patients (10).

Serial MRI Examinations

Little was known about the effect of serial MRI examinations on CIED function. The underlying concern was an assumption that cumulative minor effects could become clinically significant. Naehle et al performed a retrospective review of 47 patients with PPM who had undergone at least two examinations (including thoracic examinations) at 1.5 T (59). The study included three patients who underwent more than 10 examinations. They found that changes in capture thresholds, impedance, and battery voltage were not clinically significant even after 10-plus examinations. Junttilla et al furthered this by examining serial cardiac MRI examinations in ICD patients with a follow up of 370 days (60). They observed no meaningful change in lead parameters. Similar results were found by Nazarian et al, where there was an association with changes in lead impedance and capture thresholds, but no other variables (10).

Pacemaker Dependency

Pacemaker dependency comes with a higher risk during MRI due to potential inappropriate inhibition of pacemaker activity with resultant asystole. For this reason, many studies excluded pacemaker-dependent patients. One study reported a decrease in pacing rate from 90 ppm to 50 ppm, resulting in hypotension in a pacemaker-dependent patient who underwent POR. This patient had an ICD system that was on advisory–a notification from the device company that there is an increased risk to patient safety from the device (63). While there is now much experience with pacemaker-dependent patients, careful monitoring is mandated during MRI to avoid potential catastrophe in the form of inappropriately inhibited pacing after a POR.

Thoracic and Cardiac MRI

Experience with thoracic and cardiac imaging has been restricted based on a belief that greater energy deposition would result in worse outcomes. There are minor differences in long-

term battery voltage when imaging the thorax or heart (50). However, most studies including thoracic and cardiac MRI examinations have had a safety profile equivalent to that of extrathoracic MRI (10,37,38,49). The main issue with thoracic and cardiac imaging is the MRI artifact over the area of interest. This is particularly evident on balanced steady-state free precession sequences, as discussed below (44).

Clinical Studies of MR Conditional Devices

MR conditional devices are those that have been designed and approved for use in the MRI environment under specific conditions. A list of all FDA-approved MR conditional PPMs and ICDs is shown in Table 4. Typical MRI examination conditions include static field strength, SAR, and imaging field of view. To achieve a designation as MR conditional, the generator must be paired as a unit with leads that have been tested for MRI safety. MR conditional PPMs and ICDs have been available since the FDA approval of the first system in 2011 (6).

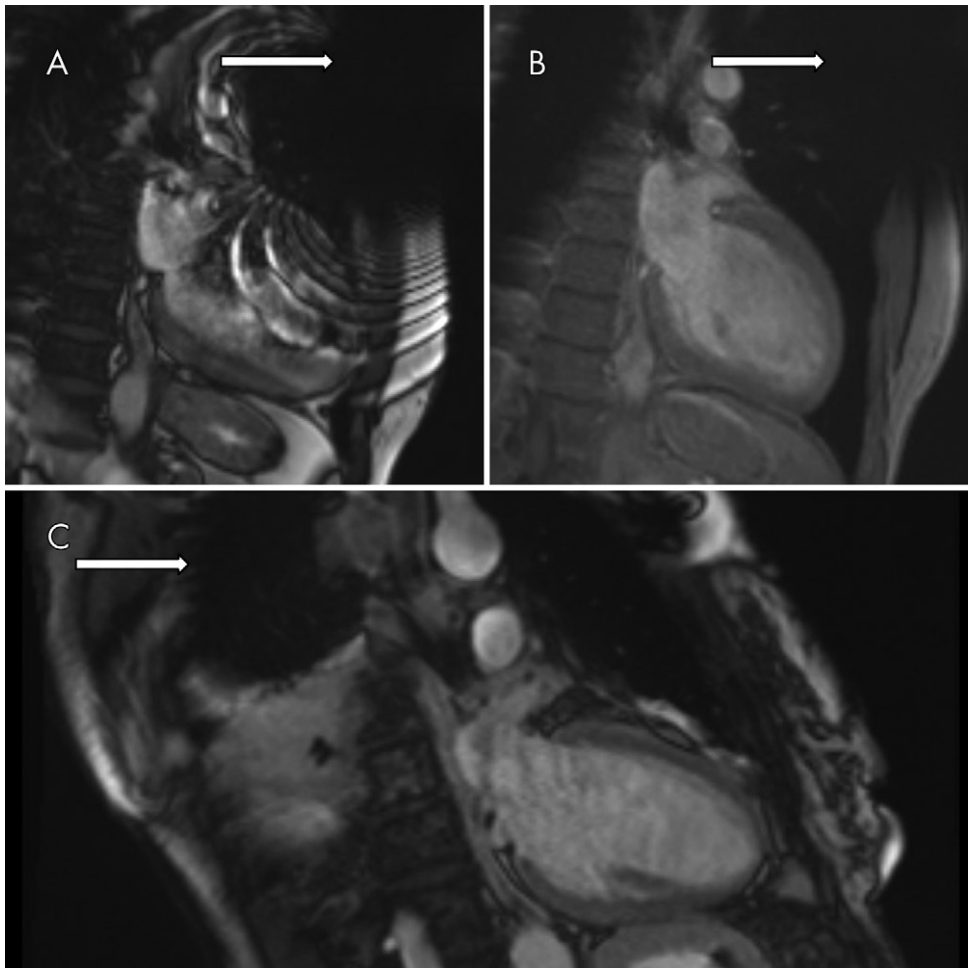

Figure 1: *A, B,* Images in a 61-year-old man with a Medtronic Evera MRI XT single-chamber implantable cardiac defibrillator. *C,* Image in a 55-year-old woman with a Medtronic Revo MRI Surescan dual-chamber pacemaker. Images obtained with a Siemens Magnetom Aera 1.5-T unit. Arrows = artifacts caused by an implantable cardiac defibrillator in a two-chamber plane of the left ventricle: *A,* balanced steady-state free precession sequence with signal loss and banding artifacts, *B,* gradient-echo sequence (same patient as in *A*), and, *C,* balanced steady-state free precession sequence in a right-sided implant, with the generator farther away from the heart.

CIEDs undergo multiple alterations to be MR conditional devices. These include lead modification to reduce lead tip heating, circuitry shielding to prevent POR, reduction of ferromagnetic materials, changing the reed switch to a "Hall sensor" (which has predictable behavior in a magnetic field), and updated software. Newer software aids reprogramming and, in some instances, automatically changes to MRI mode when a strong magnetic field is detected.

The first MR conditional PPM to undergo clinical testing was the Medtronic SureScan system (Medtronic, Minneapolis, Minn) consisting of the EnRhythm generator paired with CapSureFix 5086 MRI leads. In a prospective randomized controlled trial of 464 patients, Wilkoff et al showed no significant difference between the group undergoing MRI and the control group (66). This pattern has continued for all other clinically tested MR conditional PPMs and ICDs, including studies that removed restrictions on thoracic imaging (67–74). Notably, there was initial concern regarding the safety of the specially designed Medtronic CapSureFix 5086 MRI leads. These leads demonstrated unusually high rates of pericarditis, perforation, and tamponade compared with other modern active fixation leads. This was most likely due to their rigid design (75,76). Shortly after this, the older and safer Medtronic 5076 leads were retrospectively declared MR conditional due to their demonstrated safety in a randomized trial (65). None of the other MR conditional leads have displayed the safety concerns seen with the CapSureFix 5086 leads since (67,70).

Image Quality

The most important factor that affects image quality is the anatomic region being imaged. Nonthoracic imaging (imaging with a field of view above C7 and below T12) results in virtually no artifact from CIEDs (34,41,50,52,77). If a thoracic or cardiac imaging is being performed, artifacts will be present from the CIED.

ICDs show larger areas of MRI artifact than do PPMs due to their bulkier design and greater use of ferromagnetic components (49,63,64). Some studies have shown distortion up to 12

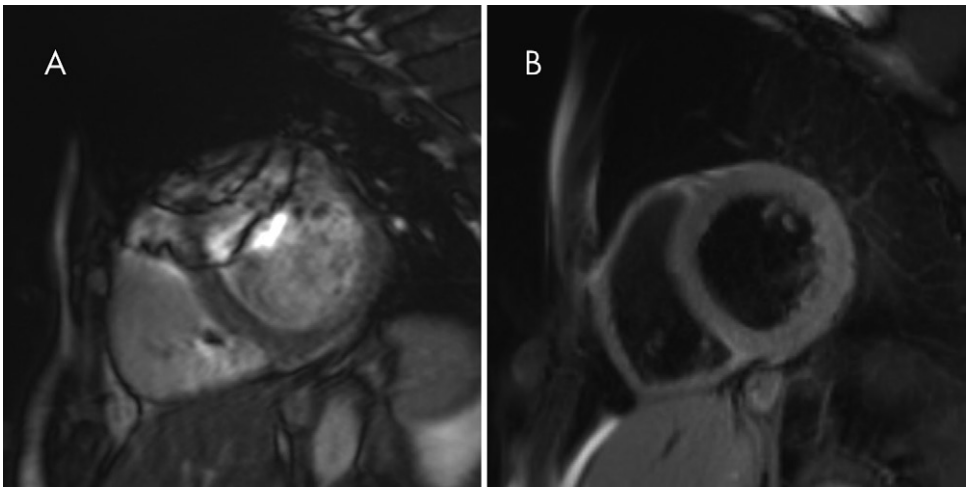

Figure 2: Images in a 61-year-old man with a Medtronic Evera MRI XT single-chamber implantable cardiac defibrillator imaged with a Siemens Magnetom Aera 1.5-T unit. Basal short-axis images acquired with, *A*, balanced steady-state free precession sequence and, *B*, spin-echo sequence (in this case T2 weighted), which is less sensitive to susceptibility artifacts.

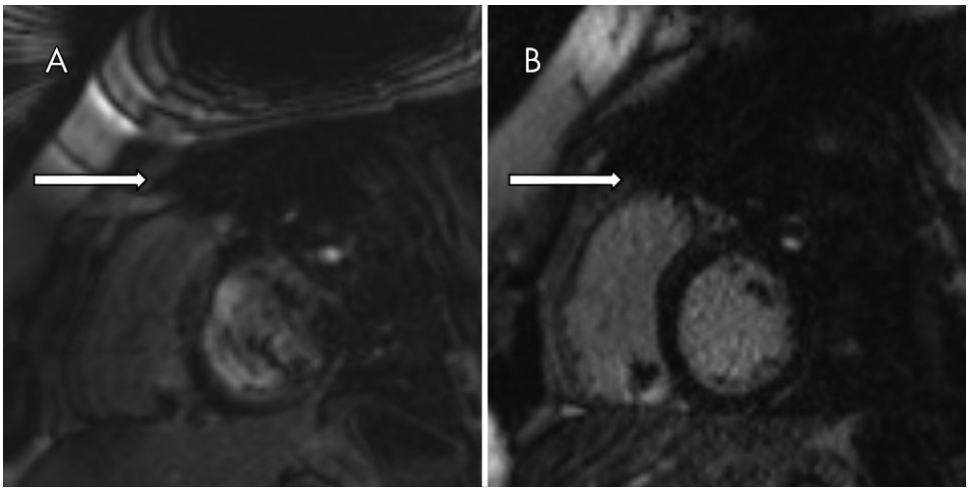

Figure 3: Images in a 28-year-old woman with a Medtronic Evera MRI XT single-chamber implantable cardiac defibrillator imaged with a Siemens Magnetom Aera 1.5-T unit. Short-axis delayed enhancement images with artifacts (arrow) acquired with, *A*, balanced steady-state free precession sequence and, *B*, gradient-echo sequence.

cm away from the generator (78). Leads have a small amount of artifact and do not usually obscure diagnostic quality, even for cardiac MRI (44).

The position of the device also affects the image quality (Fig 1). For cardiac MRI, left-sided devices create more artifact and lead to reduced diagnostic accuracy. In a study of 32 patients, 100% of studies with right-sided devices had diagnostic quality but only 35% of studies with left-sided devices were diagnostic (44,79). In general, right ventricular studies are of higher quality than those of the left ventricle (80).

For cardiac and thoracic MRI, balanced steady-state free precession images exhibit more artifact than do gradient-echo sequences (Figs 2, 3). Therefore, gradient echo should be used to maximize image quality (49,78). For balanced steady-state free precession sequences, frequency-scout acquisition may help to reduce image artifact by adjustment of the receiver center frequency (72). In the presence of artifact, imaging in perpendicular image planes to the generator and using reduced echo time and fast spin-echo sequences may improve image interpretation.

Overall, about 90% of thoracic and cardiac MRI examinations are described as diagnostic (49,56,63). Under worst-case conditions (left-sided ICD and balanced steady-state free precession acquisition) about 50% of studies are reported to have acceptable image quality (78).

Guidelines and Protocols

The 2017 Heart Rhythm Society consensus statement on MRI in CIED is the most up-to-date guideline document available (5). MRI in pacemaker-dependent patients is allowed with the proviso of temporary pacing facilities and a CIED-trained physician in place. The guidelines recommend against the performance of MRI in systems with fractured, epicardial, or abandoned leads. Recently implanted devices are considered reasonable if clinically warranted. A simplified flowchart adapted from the Heart Rhythm Society guidelines is shown in Figure 4.

For MR conditional devices, the FDA provides the conditions required to meet the conditional requirements. This information can be found on the individual manufacturer's website and varies depending on the model of CIED being imaged. Additionally, information regarding the latest FDA approvals can be found on the FDA website under "Device Approvals, Denials and Clearances" (81).

It is the opinion of the authors that every center performing MRI in CIED patients should have a checklist in place with associated adverse event monitoring. The use of a checklist is supported by a class I (strong) recommendation from the Heart Rhythm Society guidelines (5). A copy of the sample checklist provided in the Heart Rhythm Society guidelines is provided in Figure E1 (online). A standard checklist minimizes the potential for harm and improves safe access to a vital modality. Common elements of a standardized checklist include a system for referral and screening of CIED

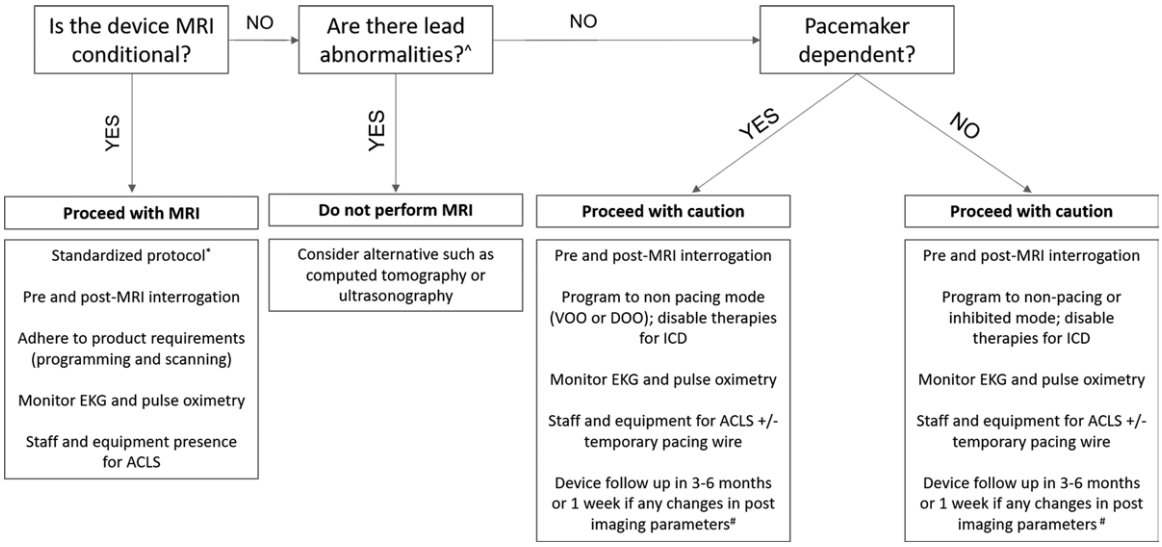

Figure 4: Checklist for treatment of patients referred for MRI with implantable electrical device. Adapted from the Heart Rhythm Society 2017 guidelines see for detailed information (5). ^Fractured, abandoned, or epicardial leads. *All departments should have standardized prebooking checklists and liaison with cardiology electrophysiology departments for patient suitability and device evaluation if possible. #Capture threshold increase more than 1.0 V, sensing drop more than 50%, pacing dependence change more than 50 Ω, shock impedance change more than 5 Ω. ACLS = advanced cardiac life support, EKG = electrocardiography, ICD = implantable cardiac defibrillator.

patients needing MRI, assessment and programming of the CIED before and after the imaging, requirements for monitoring during the imaging, and follow-up at regular intervals to ensure long-term safety (Fig 5). In centers where electrophysiology support staff are not available, device company representatives may be available to help with reprogramming MR conditional devices. In the case of MR nonconditional devices, electrophysiological consultation should be obtained prior to the MRI examination (5).

Future Directions

New MR conditional devices are frequently released with improved designs to limit the interference of MRI. Additionally, there are encouraging early experiences with leadless pacemakers and limited monitoring of patients during MRI.

Leadless pacemakers are new devices that contain the entire pacing system in a small bullet-shaped case that sits in the ventricle. This allows pacing without the use of a generator and pacing leads that run from the generator to the endocardium. Reassuring preclinical data and early case reports of patients with the Micra (Medtronic) leadless pacemaker have emerged leading to a retrospective FDA classification of MR conditional at 1.5 T and 3 T (82). Preclinical data have demonstrated less torque and heating of the Micra compared with a standard pacemaker. A case series of 15 patients with the Micra system undergoing MRI showed no adverse events (82). The Nanostim (St Jude Medical, St Paul, Minn) leadless pacemaker has received CE mark approval in Europe for MR conditional labeling but awaits FDA approval. Larger prospective datasets may validate these systems as being safer than conventional PPMs.

New research has also attempted to lessen the burden of performing MRI in CIED patients. Bertelsen et al, in a study of 207 patients, challenged the need for monitoring in nonpacemaker-dependent patients (83). In that study, they used no additional monitoring of vital signs or symptoms and observed no adverse events in patients undergoing MRI. It is

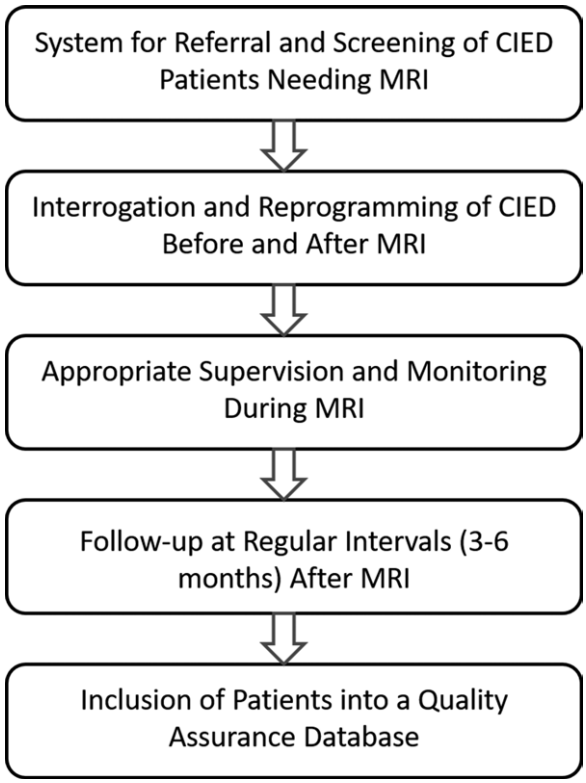

Figure 5: Flowchart shows the essential considerations for an institution when designing a checklist for MRI of implantable cardiac device. *As described in text, dependent on the patient's device and dependence on device. CIED = cardiac implantable electronic device.

important to note that vital sign monitoring is still required in pacemaker-dependent patients to detect asystole caused by POR and subsequent inappropriate inhibition due to electromagnetic interference (53).

With increasing use of 3-T and 7-T MRI systems, data are also required regarding the safety of CIED at these field strengths as most of the contemporary data relate to 1.5-T units. Furthermore, we await the improvement of pacing methods that do not rely on conductive materials, such as optogenetics (84). These are in early stages of development but may one day provide an MR-safe method of pacing and defibrillation.

Conclusion

Significant clinical data have been accumulated to show MRI can be safely performed in the presence of CIEDs, when monitored appropriately. Clinicians should be aware of the risks and safety measures needed to minimize potential harm. Due to the rapidly expanding body of research, committee guidelines must be updated regularly to reflect the current knowledge and prevent patients being denied a potentially vital diagnostic tool. Lastly, institutions should be making efforts to enact a safe checklist and monitor adverse events for contribution to the worldwide understanding of the MRI risk profile.

Disclosures of Conflicts of Interest: **R.G.M.** Activities related to the present article: disclosed no relevant relationships. Activities not related to the present article: received doctors in training research grant from Avant Mutual, a grant from Monash Health, Melbourne, Victoria, and payment from Brigham and Women's Hospital for travel expenses. Other relationships: disclosed no relevant relationships. **N.N.** disclosed no relevant relationships. **Y.G.** disclosed no relevant relationships. **R.Y.K.** disclosed no relevant relationships. **A.N.** disclosed no relevant relationships.

References

1. Kalin R, Stanton MS. Current clinical issues for MRI scanning of pacemaker and defibrillator patients. Pacing Clin Electrophysiol 2005;28(4):326–328.
2. Avery JK. Loss prevention case of the month: not my responsibility! J Tenn Med Assoc 1988;81(8):523.
3. Irnich W, Irnich B, Bartsch C, Stertmann WA, Gufler H, Weiler G. Do we need pacemakers resistant to magnetic resonance imaging? Europace 2005;7(4):353–365.
4. American Society for Testing and Materials. Standard practice for marking medical devices and other items for safety in the magnetic resonance environment. Contract No.: F2503-05. West Conshohocken, Pa: American Society for Testing and Materials International, 2005.
5. Indik JH, Gimbel JR, Abe H, et al. 2017 HRS expert consensus statement on magnetic resonance imaging and radiation exposure in patients with cardiovascular implantable electronic devices. Heart Rhythm 2017;14(7):e97–e153.
6. United States Food and Drug Administration. Revo MRI SureScan pacing system- 090013. Silver Spring, Md: United States Food and Drug Administration, 2011.
7. Sabzevari K, Oldman J, Herrey AS, Moon JC, Kydd AC, Manisty C. Provision of magnetic resonance imaging for patients with "MR-conditional" cardiac implantable electronic devices: an unmet clinical need. Europace 2017;9(3):425–431.
8. Nazarian S, Reynolds MR, Ryan MP, Wolff SD, Mollenkopf SA, Turakhia MP. Utilization and likelihood of radiologic diagnostic imaging in patients with implantable cardiac defibrillators. J Magn Reson Imaging 2016;43(1):115–127.
9. Russo RJ, Costa HS, Silva PD, et al. Assessing the risks associated with MRI in patients with a pacemaker or defibrillator. N Engl J Med 2017;376(8):755–764.
10. Nazarian S, Hansford R, Rahsepar AA, et al. Safety of magnetic resonance imaging in patients with cardiac devices. N Engl J Med 2017;377(26):2555–2564.
11. Shinbane JS, Colletti PM, Shellock FG. MR in patients with pacemakers and ICDs: defining the issues. J Cardiovasc Magn Reson 2007;9(1):5–13.
12. Shinbane JS, Colletti PM, Shellock FG. MR imaging in patients with pacemakers and other devices: engineering the future. JACC Cardiovasc Imaging 2012;5(3):332–333.
13. Berger A. Magnetic resonance imaging. BMJ 2002;324(7328):35.
14. Shellock FG, Tkach JA, Ruggieri PM, Masaryk TJ. Cardiac pacemakers, ICDs, and loop recorder: evaluation of translational attraction using conventional ("long-bore") and "short-bore" 1.5- and 3.0-Tesla MR systems. J Cardiovasc Magn Reson 2003;5(2):387–397.
15. Luechinger R, Duru F, Scheidegger MB, Boesiger P, Candinas R. Force and torque effects of a 1.5-Tesla MRI scanner on cardiac pacemakers and ICDs. Pacing Clin Electrophysiol 2001;24(2):199–205.
16. Shellock FG, O'Neil M, Ivans V, et al. Cardiac pacemakers and implantable cardioverter defibrillators are unaffected by operation of an extremity MR imaging system. AJR Am J Roentgenol 1999;172(1):165–170.
17. Irnich W. Risks to pacemaker patients undergoing magnetic resonance imaging examinations. Europace 2010;12(7):918–920.
18. Pavlicek W, Geisinger M, Castle L, et al. The effects of nuclear magnetic resonance on patients with cardiac pacemakers. Radiology 1983;147(1):149–153.
19. Luechinger R, Duru F, Zeijlemaker VA, Scheidegger MB, Boesiger P, Candinas R. Pacemaker reed switch behavior in 0.5, 1.5, and 3.0 Tesla magnetic resonance imaging units: are reed switches always closed in strong magnetic fields? Pacing Clin Electrophysiol 2002;25(10):1419–1423.
20. Sommer T, Naehle CP, Yang A, et al. Strategy for safe performance of extrathoracic magnetic resonance imaging at 1.5 tesla in the presence of cardiac pacemakers in non-pacemaker-dependent patients: a prospective study with 115 examinations. Circulation 2006;114(12):1285–1292.
21. Hayes DL, Holmes DR Jr, Gray JE. Effect of 1.5 tesla nuclear magnetic resonance imaging scanner on implanted permanent pacemakers. J Am Coll Cardiol 1987;10(4):782–786.
22. Nazarian S, Halperin HR. How to perform magnetic resonance imaging on patients with implantable cardiac arrhythmia devices. Heart Rhythm 2009;6(1):138–143.
23. McIntyre WF, Michael KA, Baranchuk A. Electromagnetic interference induced by magnetic resonance imaging. Can J Cardiol 2010;26(2):e64.
24. Tandri H, Zviman MM, Wedan SR, Lloyd T, Berger RD, Halperin H. Determinants of gradient field-induced current in a pacemaker lead system in a magnetic resonance imaging environment. Heart Rhythm 2008;5(3):462–468.
25. Erlebacher JA, Cahill PT, Pannizzo F, Knowles RJ. Effect of magnetic resonance imaging on DDD pacemakers. Am J Cardiol 1986;57(6):437–440.
26. Sheldon SH, Bunch TJ, Cogert GA, et al. Multicenter study of the safety and effects of magnetic resonance imaging in patients with coronary sinus left ventricular pacing leads. Heart Rhythm 2015;12(2):345–349.
27. Roguin A, Schwitter J, Vahlhaus C, et al. Magnetic resonance imaging in individuals with cardiovascular implantable electronic devices. Europace 2008;10(3):336–346.
28. Luechinger R, Zeijlemaker VA, Pedersen EM, et al. In vivo heating of pacemaker leads during magnetic resonance imaging. Eur Heart J 2005;26(4):376–383; discussion 325–327.
29. Duru F, Luechinger R, Scheidegger MB, Lüscher TF, Boesiger P, Candinas R. Pacing in magnetic resonance imaging environment: clinical and technical considerations on compatibility. Eur Heart J 2001;22(2):113–124.
30. Nordbeck P, Fidler F, Weiss I, et al. Spatial distribution of RF-induced E-fields and implant heating in MRI. Magn Reson Med 2008;60(2):312–319.
31. Mattei E, Triventi M, Calcagnini G, et al. Complexity of MRI induced heating on metallic leads: experimental measurements of 374 configurations. Biomed Eng Online 2008;7(1):11.
32. Langman DA, Goldberg IB, Finn JP, Ennis DB. Pacemaker lead tip heating in abandoned and pacemaker-attached leads at 1.5 Tesla MRI. J Magn Reson Imaging 2011;33(2):426–431.
33. Achenbach S, Moshage W, Diem B, Bieberle T, Schibgilla V, Bachmann K. Effects of magnetic resonance imaging on cardiac pacemakers and electrodes. Am Heart J 1997;134(3):467–473.
34. Sommer T, Vahlhaus C, Lauck G, et al. MR imaging and cardiac pacemakers: in-vitro evaluation and in-vivo studies in 51 patients at 0.5 T. Radiology 2000;215(3):869–879.
35. Shellock FG, Fischer L, Fieno DS. Cardiac pacemakers and implantable cardioverter defibrillators: in vitro magnetic resonance imaging evaluation at 1.5-tesla. J Cardiovasc Magn Reson 2007;9(1):21–31.
36. Roguin A, Zviman MM, Meininger GR, et al. Modern pacemaker and implantable cardioverter/defibrillator systems can be magnetic resonance imaging safe: in vitro and in vivo assessment of safety and function at 1.5 T. Circulation 2004;110(5):475–482.
37. Mollerus M, Albin G, Lipinski M, Lucca J. Cardiac biomarkers in patients with permanent pacemakers and implantable cardioverter-defibrillators undergoing an MRI scan. Pacing Clin Electrophysiol 2008;31(10):1241–1245.
38. Martin ET, Coman JA, Shellock FG, Pulling CC, Fair R, Jenkins K. Magnetic resonance imaging and cardiac pacemaker safety at 1.5-Tesla. J Am Coll

Cardiol 2004;43(7):1315–1324.
39. Gimbel JR, Johnson D, Levine PA, Wilkoff BL. Safe performance of magnetic resonance imaging on five patients with permanent cardiac pacemakers. Pacing Clin Electrophysiol 1996;19(6):913–919.
40. Vahlhaus C, Sommer T, Lewalter T, et al. Interference with cardiac pacemakers by magnetic resonance imaging: are there irreversible changes at 0.5 Tesla? Pacing Clin Electrophysiol 2001;24(4 Pt 1):489–495.
41. Nazarian S, Roguin A, Zviman MM, et al. Clinical utility and safety of a protocol for noncardiac and cardiac magnetic resonance imaging of patients with permanent pacemakers and implantable-cardioverter defibrillators at 1.5 tesla. Circulation 2006;114(12):1277–1284.
42. Naehle CP, Meyer C, Thomas D, et al. Safety of brain 3-T MR imaging with transmit-receive head coil in patients with cardiac pacemakers: pilot prospective study with 51 examinations. Radiology 2008;249(3):991–1001.
43. Boilson BA, Wokhlu A, Acker NG, et al. Safety of magnetic resonance imaging in patients with permanent pacemakers: a collaborative clinical approach. J Interv Card Electrophysiol 2012;33(1):59–67.
44. Naehle CP, Kreuz J, Strach K, et al. Safety, feasibility, and diagnostic value of cardiac magnetic resonance imaging in patients with cardiac pacemakers and implantable cardioverters/defibrillators at 1.5 T. Am Heart J 2011;161(6):1096–1105.
45. Muehling OM, Wakili R, Greif M, et al. Immediate and 12 months follow up of function and lead integrity after cranial MRI in 356 patients with conventional cardiac pacemakers. J Cardiovasc Magn Reson 2014;16(1):39.
46. Cohen JD, Costa HS, Russo RJ. Determining the risks of magnetic resonance imaging at 1.5 tesla for patients with pacemakers and implantable cardioverter defibrillators. Am J Cardiol 2012;110(11):1631–1636.
47. Mollerus M, Albin G, Lipinski M, Lucca J. Magnetic resonance imaging of pacemakers and implantable cardioverter-defibrillators without specific absorption rate restrictions. Europace 2010;12(7):947–951.
48. Heatlie G, Pennell DJ. Cardiovascular magnetic resonance at 0.5T in five patients with permanent pacemakers. J Cardiovasc Magn Reson 2007;9(1):15–19.
49. Buendía F, Cano Ó, Sánchez-Gómez JM, et al. Cardiac magnetic resonance imaging at 1.5 T in patients with cardiac rhythm devices. Europace 2011;13(4):533–538.
50. Nazarian S, Hansford R, Roguin A, et al. A prospective evaluation of a protocol for magnetic resonance imaging of patients with implanted cardiac devices. Ann Intern Med 2011;155(7):415–424.
51. Higgins JV, Sheldon SH, Watson RE Jr, et al. "Power-on resets" in cardiac implantable electronic devices during magnetic resonance imaging. Heart Rhythm 2015;12(3):540–544.
52. Halshtok O, Goitein O, Abu Sham'a R, Granit H, Glikson M, Konen E. Pacemakers and magnetic resonance imaging: no longer an absolute contraindication when scanned correctly. Isr Med Assoc J 2010;12(7):391–395.
53. Gimbel JR. Unexpected asystole during 3T magnetic resonance imaging of a pacemaker-dependent patient with a 'modern' pacemaker. Europace 2009;11(9):1241–1242.
54. Mollerus M, Albin G, Lipinski M, Lucca J. Ectopy in patients with permanent pacemakers and implantable cardioverter-defibrillators undergoing an MRI scan. Pacing Clin Electrophysiol 2009;32(6):772–778.
55. Coman JA, Martin ET, Sandler DA, Ryan Thomas J. 1147-210 Implantable cardiac defibrillator interactions with magnetic resonance imaging at 1.5 tesla. J Am Coll Cardiol 2004;43(5):A138.
56. Camacho JC, Moreno CC, Shah AD, et al. Safety and quality of 1.5-T MRI in patients with conventional and MRI-conditional cardiac implantable electronic devices after implementation of a standardized protocol. AJR Am J Roentgenol 2016;207(3):599–604.
57. Burke PT, Ghanbari H, Alexander PB, Shaw MK, Daccarett M, Machado C. A protocol for patients with cardiovascular implantable devices undergoing magnetic resonance imaging (MRI): should defibrillation threshold testing be performed post (MRI). J Interv Card Electrophysiol 2010;28(1):59–66.
58. Buendía F, Sánchez-Gómez JM, Sancho-Tello MJ, et al. Nuclear magnetic resonance imaging in patients with cardiac pacing devices. Rev Esp Cardiol 2010;63(6):735–739.
59. Naehle CP, Strach K, Thomas D, et al. Magnetic resonance imaging at 1.5-T in patients with implantable cardioverter-defibrillators. J Am Coll Cardiol 2009;54(6):549–555.
60. Junttila MJ, Fishman JE, Lopera GA, et al. Safety of serial MRI in patients with implantable cardioverter defibrillators. Heart 2011;97(22):1852–1856.
61. Friedman HL, Acker N, Dalzell C, et al. Magnetic resonance imaging in patients with recently implanted pacemakers. Pacing Clin Electrophysiol 2013;36(9):1090–1095.
62. Higgins JV, Gard JJ, Sheldon SH, et al. Safety and outcomes of magnetic resonance imaging in patients with abandoned pacemaker and defibrillator leads. Pacing Clin Electrophysiol 2014;37(10):1284–1290.
63. Horwood L, Attili A, Luba F, et al. Magnetic resonance imaging in patients with cardiac implanted electronic devices: focus on contraindications to magnetic resonance imaging protocols. Europace 2017;19(5):812–817.
64. Dandamudi S, Collins JD, Carr JC, et al. The safety of cardiac and thoracic magnetic resonance imaging in patients with cardiac implantable electronic devices. Acad Radiol 2016;23(12):1498–1505.
65. Shenthar J, Milasinovic G, Al Fagih A, et al. MRI scanning in patients with new and existing CapSureFix Novus 5076 pacemaker leads: randomized trial results. Heart Rhythm 2015;12(4):759–765.
66. Wilkoff BL, Bello D, Taborsky M, et al. Magnetic resonance imaging in patients with a pacemaker system designed for the magnetic resonance environment. Heart Rhythm 2011;8(1):65–73.
67. Wollmann CG, Steiner E, Vock P, Ndikung B, Mayr H. Monocenter feasibility study of the MRI compatibility of the Evia pacemaker in combination with Safio S pacemaker lead. J Cardiovasc Magn Reson 2012;14(1):67.
68. Gimbel JR, Bello D, Schmitt M, et al. Randomized trial of pacemaker and lead system for safe scanning at 1.5 Tesla. Heart Rhythm 2013;10(5):685–691.
69. Wollmann CG, Thudt K, Kaiser B, Salomonowitz E, Mayr H, Globits S. Safe performance of magnetic resonance of the heart in patients with magnetic resonance conditional pacemaker systems: the safety issue of the ESTIMATE study. J Cardiovasc Magn Reson 2014;16(1):30.
70. Bailey WM, Rosenthal L, Fananapazir L, et al. Clinical safety of the ProMRI pacemaker system in patients subjected to head and lower lumbar 1.5-T magnetic resonance imaging scanning conditions. Heart Rhythm 2015;12(6):1183–1191.
71. Savouré A, Mechulan A, Burban M, Olivier A, Lazarus A. The Kora pacemaker is safe and effective for magnetic resonance imaging. Clin Med Insights Cardiol 2015;9:85–90.
72. Awad K, Griffin J, Crawford TC, et al. Clinical safety of the Iforia implantable cardioverter-defibrillator system in patients subjected to thoracic spine and cardiac 1.5-T magnetic resonance imaging scanning conditions. Heart Rhythm 2015;12(10):2155–2161.
73. Gold MR, Sommer T, Schwitter J, et al. Full-body MRI in patients with an implantable cardioverter-defibrillator: primary results of a randomized study. J Am Coll Cardiol 2015;65(24):2581–2588.
74. Kypta A, Blessberger H, Hoenig S, et al. Clinical safety of an MRI conditional implantable cardioverter defibrillator system: a prospective Monocenter ICD-Magnetic resonance Imaging feasibility study (MIMI). J Magn Reson Imaging 2016;43(3):574–584.
75. Elmouchi DA, Rosema S, Vanoosterhout SM, et al. Cardiac perforation and lead dislodgement after implantation of a MR-conditional pacing lead: a single-center experience. Pacing Clin Electrophysiol 2014;37(1):4–10.
76. Rickard J, Taborsky M, Bello D, et al. Short- and long-term electrical performance of the 5086MRI pacing lead. Heart Rhythm 2014;11(2):222–229.
77. Gimbel JR. Magnetic resonance imaging of implantable cardiac rhythm devices at 3.0 tesla. Pacing Clin Electrophysiol 2008;31(7):795–801.
78. Schwitter J, Gold MR, Al Fagih A, et al. Image quality of cardiac magnetic resonance imaging in patients with an implantable cardioverter defibrillator system designed for the magnetic resonance imaging environment. Circ Cardiovasc Imaging 2016;9(5):e004025.
79. Kaasalainen T, Kivistö S, Holmström M, et al. Cardiac MRI in patients with cardiac pacemakers: practical methods for reducing susceptibility artifacts and optimizing image quality. Acta Radiol 2016;57(2):178–187.
80. Schwitter J, Kanal E, Schmitt M, et al. Impact of the Advisa MRI pacing system on the diagnostic quality of cardiac MR images and contraction patterns of cardiac muscle during scans: Advisa MRI randomized clinical multicenter study results. Heart Rhythm 2013;10(6):864–872.
81. Device approvals, denials and clearances. Silver Spring, Md: U.S. Food and Drug Administration, 2017. https://www.fda.gov/MedicalDevices/ProductsandMedicalProcedures/DeviceApprovalsandClearances/default.htm. Accessed February 2, 2018.
82. Soejima K, Edmonson J, Ellingson ML, Herberg B, Wiklund C, Zhao J. Safety evaluation of a leadless transcatheter pacemaker for magnetic resonance imaging use. Heart Rhythm 2016;13(10):2056–2063.
83. Bertelsen L, Petersen HH, Philbert BT, Svendsen JH, Thomsen C, Vejlstrup N. Safety of magnetic resonance scanning without monitoring of patients with pacemakers. Europace 2017;19(5):818–823.
84. Nussinovitch U, Gepstein L. Optogenetics for in vivo cardiac pacing and resynchronization therapies. Nat Biotechnol 2015;33(7):750–754.
85. Strach K, Naehle CP, Mühlsteffen A, et al. Low-field magnetic resonance imaging: increased safety for pacemaker patients? Europace 2010;12(7):952–960.
86. Kaasalainen T, Pakarinen S, Kivistö S, et al. MRI with cardiac pacing devices: safety in clinical practice. Eur J Radiol 2014;83(8):1387–1395.

The evolving role of cardiac magnetic resonance imaging in the assessment of cardiovascular disease

Michael B Stokes, Nitesh Nerlekar, Stuart Moir, Karen S Teo

Background

Imaging of the heart is important in the diagnosis and follow-up of a broad range of cardiac pathology. The authors discuss the growing role of cardiac magnetic resonance imaging (CMR) in cardiology practice and its relevance to primary healthcare.

Objective

In this article we discuss the advantages of CMR over other imaging modalities, and give a brief description of the common CMR techniques and cardiac pathologies where CMR is especially useful.

Discussion

CMR provides specific advantages over other cardiac imaging modalities when evaluating pathology in congenital heart disease, cardiac masses, cardiomyopathies, and in some aspects of ischaemic and valvular heart diseases. The strength of CMR in these pathologies includes its precise anatomical delineation of structures, characterisation of myocardial tissue, and accurate, reproducible measurements of blood volume and flow. CMR is used in inpatient and outpatient settings, and is available primarily in major hospitals.

Cardiac imaging

A number of imaging modalities are used by clinicians in the assessment and care of patients with cardiovascular disease. Echocardiography is the first-line cardiac imaging investigation for many cardiac conditions. It is widely available, provides structural and functional information, and reliably reports the required clinical information in the majority of cases. However, the limitations of echocardiography include difficulty obtaining ultrasound images in specific patients and differentiating specific pathologies (eg cardiac infiltration versus hypertrophy). Delineation of the endocardial border can also be challenging with echocardiography when measuring ventricular volumes used to calculate ejection fraction.[1] Cardiac computed tomography (CT) and nuclear cardiac perfusion studies are modalities used predominantly in the investigation of ischaemic heart disease.

Cardiac magnetic resonance imaging (CMR) has grown as an imaging modality

Box 1. Advantages and disadvantages of CMR compared with imaging modalities

Advantages

- Improved image quality
- No ionising radiation
- Accurate ejection fraction measurement
- Investigation for suspected myocarditis that cannot be confirmed on echocardiography
- Assessment of newly diagnosed cardiomyopathy with diagnostic and prognostic advantages over echocardiography
- Assessment of myocardial viability and perfusion in work-up for coronary artery bypass surgery
- Assessment of congenital heart disease

Disadvantages

- Cost and accessibility
- Contraindicated in patients with metallic implants (eg aneurysm clips, neurostimulators, implanted pacemakers/defibrillators), metal retained fragments in eyes or gunshot injuries
- May be unsuitable for patients with claustrophobia
- A specific cut-off weight for patients varies among individual MRI scanners. Large abdominal and shoulder girths may limit the physical ability of patients to fit in an MRI scanner
- Gadolinium is contraindicated in significant renal disease (eGFR <30 mL/minute)

CMR, cardiac magnetic resonance imaging; eGFR, estimated glomerular filtration rate; MRI, magnetic resonance imaging

to provide additive and complementary information to echocardiography.
It provides high-quality, cross-sectional images that enable accurate anatomical delineation. It also enables highly reproducible measurement of ventricular volumes and myocardial mass, and quantifies flow across heart valves.[1,2]
CMR can assess myocardial structure and assist in the diagnosis of cardiac masses. Sophisticated electrocardiogram (ECG) gating and respiratory motion suppression methods are used to ensure the acquisition of high-quality images. CMR can overcome patient-specific limitations, such as obesity, presence of respiratory disease, or presence of soft tissue, lungs and/or scar tissue following cardiac surgery, which can limit the ability to obtain high-quality echocardiographic images.[3,4]

Advantages and disadvantages of CMR

Box 1 summarises the advantages and disadvantages of CMR.

There is now an increasing number of cardiac devices that are considered MRI-conditional. Patients in whom these devices have been implanted can have CMR performed with appropriate safety precautions and device checks.[5]

Techniques in CMR

A number of MRI sequences are used in CMR studies. These are tailored in each individual study for a particular pathology or the assessment of a specific aspect of cardiac function:

- still-frame images that delineate cardiac structures and great vessels in the assessment of congenital heart disease
- high-quality moving images that measure cardiac volumes and myocardial mass, and visualise regional wall motion abnormalities, which may indicate underlying ischaemic heart disease (Figure 1)
- velocity flow imaging that directly measures blood flow in assessment of valvular abnormalities, such as calculation of regurgitant volumes in aortic regurgitation[6]
- others
  - quantification of myocardial iron content: used in patients with beta-thalassemia major, where iron chelation therapy is introduced or intensified to prevent the development of heart failure[7]
  - myocardial fibrosis estimates in cardiomyopathy[8]
  - myocardial oedema detection: indicative of myocarditis or recent myocardial injury.[9]

Gadolinium use in CMR

Gadolinium is an intravenous contrast agent used in CMR. It is a useful adjunct in CMR to aid the diagnosis of specific cardiac pathologies. Delayed or late myocardial enhancement imaging (where images are acquired 10–20 minutes after gadolinium administration), allows assessment for specific patterns of uptake (Figure 2).[10]
Gadolinium is contraindicated in patients with significant renal disease (estimated glomerular filtration rate <30 mL/minute) as it increases the risk of developing the rare, progressive skin condition called nephrogenic systemic fibrosis.[11]

Pathologies where CMR can be considered

Aortic and valvular disease

CMR visualises the aortic course and precisely measures aortic dimensions. It is advantageous in patients who require repeated interval imaging, avoiding the repeated exposure to ionising radiation that occurs with CT. Aortic coarctation, bicuspid aortic valve disease and aortopathies (eg Marfan syndrome) may result in progressive aortic enlargement and the severity may influence the timing of surgical intervention. Flow velocity–encoded mapping enables more accurate quantification of the severity of valvular lesions.[6]

Pericardial constriction or pericarditis

Assessment of the pericardium on CMR by measuring pericardial thickness, detection of pericardial inflammation and/or masses,

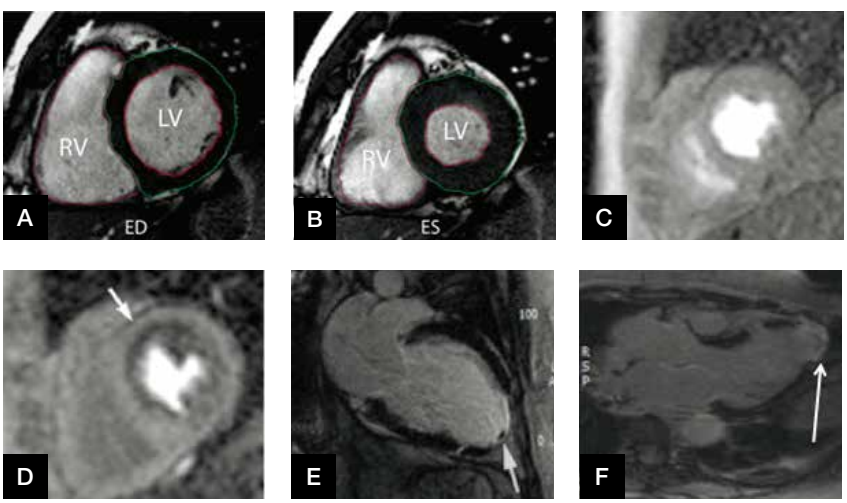

Figure 1. Utility of CMR in ischaemic heart disease and measurement of ventricular volumes on short axis CMR images

A and B. Short axis imaging allowing LV and RV end diastolic, and end systolic volume measurement. C and D. A positive adenosine stress perfusion study with no rest perfusion defect at rest (image C), while the stress image (image D) shows a subendocardial perfusion defect in the anterior and anteroseptal walls (arrowed). This corresponded to a significant left anterior descending (LAD) artery stenosis at coronary angiography. E and F. Detection of LV apical thrombus and transmural late gadolinium enhancement indicative of full thickness apical infarction
CMR, cardiac magnetic resonance imaging; LV, left ventricle; RV, right ventricle

and assessment of pericardial effusion can provide important additive information to echocardiography. Interventricular interdependence (indicative of constrictive physiology) can be detected by visualising movement of the interventricular septum during respiration.[12]

Cardiomyopathy

CMR is important in the diagnostic work-up and management of newly diagnosed cardiomyopathy because it can accurately measure ejection fraction, calculate myocardial mass, and detect scar tissue, fibrosis and oedema.[10]

In hypertrophic cardiomyopathy (HCM), CMR-measured septal wall thickness is a prognostic indicator of sudden death. The burden of myocardial fibrosis on CMR is also an emerging marker of risk in HCM. Information obtained through a CMR study in a patient with HCM may directly impact upon the decision for a patient to undergo placement of an implantable cardiac defibrillator (Figure 3).[13]

Variable patterns of late gadolinium uptake can indicate myocardial infiltration (eg cardiac amyloidosis, sarcoidosis), myocardial scar and viability (in ischaemic heart disease), and myocardial fibrosis (in non-ischaemic cardiomyopathy).[10]

ARVC is a rare but important cause of sudden cardiac death in athletes and young people.[14] It is characterised by ventricular arrhythmias and fibrous or fibro-fatty replacement of the myocardium that typically involves the right ventricle (RV). There are complex diagnostic criteria for the diagnosis of ARVC, which includes cardiac imaging. CMR has significant benefits over echocardiography in the assessment of the right heart in this condition and is therefore the imaging modality of choice, and in the screening of relatives of those diagnosed with ARVC.[15]

Ischaemic heart disease

CMR is useful in ischaemic heart disease (IHD) in the following settings:

- distinguishing ischaemic versus non-ischaemic aetiology of a newly diagnosed cardiomyopathy[16]
- detection of complications following myocardial infarction, such as detection of left ventricular (LV) thrombus (when suspected in large left anterior descending artery territory myocardial infarction)
- assessment of myocardial viability prior to potential revascularisation[16]
- detection of ischaemia: CMR imaging is combined with dobutamine or a vasodilator such as adenosine, which allows the detection of LV wall segments that become ischaemic (with reduced wall motion) with stress or define a myocardium 'at risk.'[17,18]

Myocarditis

In suspected myocarditis, CMR is extremely useful. It allows detection of inflammatory hyperaemia, oedema and myocyte necrosis. Clinically, this may have an impact on the decision to perform endomyocardial biopsy or the indication for corticosteroid therapy.[9] CMR may identify myocarditis in more than 30% of patients with chest pain, elevated troponin levels and normal coronary arteries. This has important long-term therapeutic implications.[19]

Congenital heart disease and pulmonary hypertension

The ability of CMR to calculate accurate right ventricular volumes and provide optimal imaging planes for the assessment of RV size has a growing role in assessment, prognostication and for monitoring treatment efficacy in pulmonary arterial hypertension.[20] Congenital heart disease encompasses a broad range of cardiac pathologies, and CMR can provide accurate data regarding ventricular size

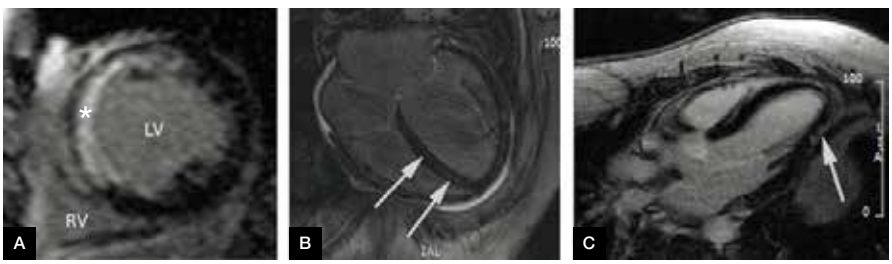

Figure 2. Patterns of late gadolinium enhancement

*A. LGE image showing subendocardial enhancement of the anterior and anteroseptal walls (marked with *) corresponding to a LAD territory myocardial infarction. B. Mid-wall LGE in dilated cardiomyopathy. C. Sub-epicardial LGE in myocarditis or sarcoidosis*
LAD, left anterior descending; LGE, late gadolinium enhancement

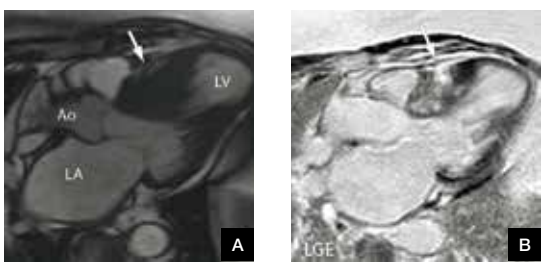

Figure 3. Hypertrophic cardiomyopathy on CMR

A. Significant septal hypertrophy
B. Corresponding patchy mid-wall myocardial fibrosis (indicated by LGE) post-gadolinium administration in a patient with hypertrophic cardiomyopathy
Ao, aorta; CMR, cardiac magnetic resonance imaging; LA, left atrium; LGE, late gadolinium enhancement; LV, left ventricle

and function, the follow-up of previous surgery, and the assessment and quantification of shunts. CMR overcomes many of the limitations of a transthoracic echocardiogram (TTE) in this setting. Three-dimensional magnetic resonance angiography (3D-MRA) provides excellent anatomical assessment of the great vessels, vascular abnormalities and vascular shunts.

Accessibility of CMR

CMR is generally accessed through a cardiologist and it is normal practice for echocardiography to be performed first. In each major Australian city, there are a small number of CMR services that are usually attached to the cardiology department of major public hospitals. A Medicare rebate for CMR can be accessed for congenital heart disease, aortic disease and for the assessment of cardiac masses in Australia.[21] When a patient does not meet the Medicare requirements, the individual CMR service may fund the scan or patients may pay an out-of-pocket fee, which may vary between departments. Some private health insurance companies may provide a rebate for inpatient CMR testing.

Future directions

New CMR techniques are constantly undergoing research and validation that includes further development of sequences that characterise myocardial tissue content. Techniques that allow for single acquisition-based measurements of ventricular volumes, and evaluation of valvular and aortic disease, may assist in reducing the scan times required for CMR studies.[22,23]

Conclusion

CMR is primarily used as a complementary tool to other imaging modalities, such as echocardiography, in the investigation and diagnosis of specific cardiac diseases. Current availability of CMR is limited by the expense of the study, a limited number of indications with a Medicare rebate, and the time and resources required for an individual CMR study. However, the number of CMR studies being performed in Australia will inevitably increase with improved MRI techniques, increased clinical utility and wider availability.

Authors

Michael B Stokes MBBS FRACP, Cardiac Imaging Fellow, Department of Cardiology, Royal Adelaide Hospital, North Terrace, Adelaide, SA. mbstokes83@gmail.com

Nitesh Nerlekar MBBS FRACP, Cardiac Imaging Fellow and PhD Student, Monash Heart, Monash Health, Clayton, Vic

Stuart Moir MBBS PhD FRACP, Consultant Cardiologist and Lead of Cardiac MRI, Monash Heart, Monash Health, Clayton, Vic

Karen S Teo MBBS PhD FRACP, Consultant Cardiologist, Department of Cardiology, Royal Adelaide Hospital, North Terrace, Adelaide, SA

Competing interests: None.

Provenance and peer review: Not commissioned, externally peer reviewed.

References

1. Bellenger NG, Burgess MI, Ray SG, at al. Comparison of left ventricular ejection fraction and volumes in heart failure by echocardiography, radionuclide ventriculography and cardiac magnetic resonance. Are they interchangeable? Eur Heart J 2000;21:1387–96.
2. Teo KS, Carbone A, Piantadosi C, et al. Cardiac MRI assessment of left and right ventricular parameters in healthy Australian normal volunteers. Heart Lung Circ 2008;17(4):313–17.
3. Saeed M, Van TA, Krug R, Hetts SW, Wilson MW. Cardiac MR Imaging: Current status and future directions. Cardiovasc Diagn Ther 2015;5(4):290–310.
4. Hamilton-Craig CR, Slaughter RE, Maki JH. Cardiovascular magnetic resonance from basics to clinical applications. Appl Radiol 2010;39(11):42–53.
5. Van Der Graaf AWM, Phagirath P, Gotte MJW. MRI and cardiac implantable electronic devices: Current status and required safety conditions. Netherlands Heart J 2014;22:269–76.
6. Cawley PJ, Maki JH, Otto C. Valvular heart disease: Changing concepts in disease management. Cardiac magnetic resonance imaging for valvular heart disease. Circulation 2009;119:468–78.
7. Pennell DJ. T2* Magnetic resonance: Iron and gold. JACC: Cardiovasc Imaging 2008;1(5):579–81.
8. Jellis CL, Kwon DH. Myocardial T1 mapping: Modalities and clinical applications. Cardiovasc Diagn Ther 2014;4(2):126–37.
9. Friedrich MG, Marcotte F. Cardiac magnetic reasonance assessment of myocarditis. Circ Cardiovasc Imaging 2013;6:833–39.
10. Parsai C, O'Hanlon R, Prasad SK, Mohiaddin RH. Diagnostic and prognostic value of cardiovascular magnetic resonance in non-ischaemic cardiomyopathies. J Cardiovasc Magn Reson 2012;14:54.
11. The Royal Australian and New Zealand College of Radiologists. Guidelines for use of gadolinium-containing MRI contrast agents in patients with renal impairment. Sydney: RANZCR, 2013.
12. Verhaert, D, Gabriel RS, Johnston D, Lytle BW, Desai MY, Klein AL. The role of multimodality imaging in the management of pericardial disease. Circ Cardiovasc Imaging 2010;3(3):333–43.
13. Maron MS, Maron BM. Clinical impact of contemporary cardiovascular magnetic resonance imaging in hypertrophic cardiomyopathy. Circulation 2015;132:292–98.
14. Sen-Chowdhry S, Lowe MD, Sporton SC, McKenna W. Arrhythmogenic right ventricular cardiomyopathy: clinical presentation, diagnosis, and management. Am J Med 2004;117(9):685–95.
15. Riele ASJM, Tandri H, Bluemke DA. Arrhythmogenic right ventricular cardiomyopathy: Cardiovascular magnetic resonance update. J Cardiovasc Magn Reason 2014;16:50.
16. McCrohon JA, Moon JCC, Prasad SK, et al. Differentiation of heart failure related to dilated cardiomyopathy and coronary artery disease using gadolinium-enhanced cardiovascular magnetic resonance. Circulation 2003;108: 54–59.
17. Kim RJ, Wu E, Rafael A, et al. The use of contrast-enhanced magnetic resonance imaging to identify reversible myocardial dysfunction. N Engl J Med 2000;343:1445–53.
18. Nagel E, Lehmkuhl HB, Bocksch W, et al. Noninvasive diagnosis of ischemia-induced wall motion abnormalities with the use of high-dose dobutamine stress MRI: Comparison with dobutamine stress echocardiography. Circulation 1999;99(6):763.
19. Assomull RG, Lyne JC, Keenan N. The role of cardiovascular magnetic resonance in patients presenting with chest pain, raised troponin, and unobstructed coronary arteries. Eur Heart J 2007;28:1242–49.
20. Bradlow WM, Gibbs JSR, Mohiaddin RH. Cardiovascular magnetic reasonance in pulmonary hypertension. J Cardiovasc Magn Reson 2012;14:6.
21. Department of Health. Medicare Benefits Schedule book category 5. Canberra: DoH, 2013. Available at www.mbsonline.gov.au/internet/mbsonline/publishing.nsf/Content/85A357DC1CD8BA24CA257D6600087FAD/$File/201407-Cat5.pdf [Accessed 30 June 2016].
22. Claus P, Omar AM, Pedrizzetti G, Sendgupta PP, Nagel E. Tissue tracking technology for assessing cardiac mechanics: Principles, normal values, and clinical applications. JACC Cardiovasc Imaging 2015;8(12):1444–60.
23. Dyverfeldt P, Bissell M, Barker AJ, Bolger AF, Carlhall CJ, Ebbers T. 4D flow – Cardiovascular magnetic resonance consensus statement. J Cardiovas Magn Reson 2015;17:72.

correspondence **afp@racgp.org.au**